

RENDICONTI *Online* della *Società Geologica Italiana*

Volume 35, Supplemento n. 2 - Luglio 2015

Il Pianeta Dinamico: sviluppi e prospettive a 100 anni da Wegener
Congresso congiunto SIMP-AIV-SoGeI-SGI

Firenze, 2-4 Settembre 2015



ABSTRACT BOOK

Edited by

**Cesare B., Giordano G., Monaco C., Vaselli O., Avanzinelli R.,
Bonazzi P., Cappelletti P., Carosi R., Cidu R., Cioni R., Cosentino
D., Frondini F., Princivalle F., Viccaro M.**



ROMA
SOCIETÀ GEOLOGICA ITALIANA
2015

www.socgeol.it

RENDICONTI *Online della Società Geologica Italiana*, è un periodico quadrimestrale della Società Geologica Italiana. Esce nei mesi di Dicembre, Aprile ed Agosto.

The RENDICONTI *Online della Società Geologica Italiana* is a journal of the Italian Geological Society. It is published every four months in December, April and August.

Direttore responsabile e Redattore (*Editor-in-Chief*): Domenico CALCATERRA (Napoli).

Responsabili editoriali (*Editorial Managers*): Fabio Massimo PETTI (SGI - Roma), Alessandro ZUCCHARI (SGI - Roma).

Comitato di redazione (*Associate Editors*):

Alessandra ASCIONE (Napoli), Domenico COSENTINO (Roma TRE - Roma), Corrado CENCETTI (Perugia), Gianfranco CIANCETTI (Pavia), Massimo CIVITA (Torino), Piero FARABOLLINI (Camerino), Fabrizio GALLUZZO (ISPRA - Roma), Massimo MATTEI (Roma TRE - Roma), Carmelo MONACO (Catania), Paolo MOZZI (Padova), Mariano PARENTE (Napoli), Dario SLEJKO (OGS - Trieste), Iole SPALLA (Milano).

La SOCIETÀ GEOLOGICA ITALIANA fu fondata il 29 settembre 1881, eretta ad Ente Morale con Regio Decreto del 17 Ottobre 1885. La Segreteria è ospitata dal Dipartimento di Scienze della Terra della Sapienza, Università di Roma, Piazzale Aldo Moro, 5 - 00185 Roma, Italy.

The SOCIETÀ GEOLOGICA ITALIANA was founded in Bologna on September 29th, 1881. It was recognized as non-profit corporation with the Royal Decree of October 17th, 1885. The secretary office is hosted by the Dipartimento di Scienze della Terra of the Sapienza University, Piazzale Aldo Moro, 5 - 00185 Roma, Italy.

Contatti (*Contacts*): Tel. +39-06-4959-390; Fax +39-06-4991-4154; e-mail: info@socgeol.it

Sito web (*Society Web Site*): www.socgeol.it

Codice Fiscale (*Income Tax Number*): 80258790585; Conto corrente postale (*Postal giro account*): 350009.

CONSIGLIO DIRETTIVO 2015 (*Council Members for 2015*):

Elisabetta Erba - *President*, Alessandro ZUCCHARI - *General Secretary*, Marco PETITTA - *Treasurer*, Domenico CALCATERRA (*EiC of the ROL*), William Cavazza (*EiC of the IJG - BSGI*), Giovanni CAPPONI, Domenico COSENTINO, Sandro CONTICELLI, Stefano DALLA, Carlo DOGLIONI, David GOVONI, Massimo MATTEI, Vincenzo MORRA, Fabio Massimo PETTI.

REVISORI DEI CONTI 2015 (*Financial Auditors 2015*):

Andrea BILLI, Davide SCROCCA, Gian Paolo CAVINATO

SEZIONI DELLA SOCIETÀ GEOLOGICA ITALIANA (*Italian Geological Society Sections*):

Marine Geology: Francesco CHIOCCI - *Chair*

Planetary Geology: Gaetano D'ACHILLE - *Chair*

Hydrogeology: Giovanni BARROCU - *Chair*

Carbonate Geology: Gloria CIARAPICA, Antonio PRATURLON - *Chairs*

Geo-informatics: Chiara D'AMBROGI - *Chair*

Structural Geology: Carmelo MONACO - *Chair*

Young Geologists: Federico FAMIANI - *Chair*

Environmental Geology: Leo ADAMOLI - *Chair*

Himalayan Geology: Rodolfo CAROSI - *Chair*

GeoSed: Simonetta CIRILLI - *Chair*

History of Geosciences: Alessio ARGENTIERI, Marco PANTALONI - *Chairs*

Geothics and Geological Culture: Silvia PEPOLONI - *Chair*

Petroleum Geology: Pierluigi VECCHIA - *Chair*

Forensic Geology: Eva SACCHI - *Chair*

Geological Cartography: Stefano CATALANO, Laura CRISPINI - *Chairs*

La Società Geologica Italiana è affiliata alla European Geosciences Union (EGU).

The Società Geologica Italiana is affiliated to the European Geosciences Union (EGU).

QUOTA ASSOCIATIVA 2015 (*Association Fees 2015*): socio sostenitore (*supporter fellow*) € 100, socio ordinario (*ordinary fellow*) € 93; socio senior (*senior fellow*) € 68, socio junior (*junior fellow*) € 68; studente (*student*) € 36; Istituzioni (*Institutions*) € 300.

Iscrizione alla pagina (*Subscription at*): http://www.socgeol.it/284/quota_sociale.html or at

http://www.socgeol.it/285/pagamento_tramite_carta_di_credito.html

La Società Geologica Italiana detiene il copyright degli articoli, dei dati, delle figure e di tutto il materiale pubblicato.

Papers, data, figures, maps and any other material published are covered by the copyright own by the Società Geologica Italiana.

DISCLAIMER: The Società Geologica Italiana, the Editors (Chief, Associates), and the Publisher are not responsible for the ideas, opinions, and contents of the papers published; the authors of each paper are responsible for the ideas, opinions and contents published.

La Società Geologica Italiana, i curatori scientifici (Chief, Associates), e la Casa Editrice non sono responsabili delle opinioni espresse e delle affermazioni pubblicate negli articoli: l'autore/i è/sono il/i solo/i responsabile/i.

RENDICONTI *Online*
della
Società Geologica Italiana

Volume 31, Supplemento n. 2 - Luglio 2015

**Il Pianeta Dinamico:
sviluppi e prospettive a 100 anni da Wegener**

Congresso congiunto SIMP-AIV-SoGeI-SGI

Firenze, 2-4 Settembre 2015

Abstract Book

Edited by

**Cesare B., Giordano G., Monaco C., Vaselli O., Avanzinelli R.,
Bonazzi P., Cappelletti P., Carosi R., Cidu R., Cioni R., Cosentino
D., Frondini F., Princivalle F., Viccaro M.**



ROMA
SOCIETÀ GEOLOGICA ITALIANA
2015
www.socgeol.it



Il Pianeta Dinamico

Congresso congiunto SIMP-SGI-So.Ge.I-AIV

Firenze, 2-4 settembre 2015

PRESIDENTI DEL CONGRESSO

Bernardo Cesare (SIMP) - Guido Giordano (AIV) - Carmelo Monaco (SGI) - Orlando Vaselli (SoGel)

COMITATO SCIENTIFICO

Riccardo Avanzinelli (Firenze) - Paola Bonazzi (Firenze) - Piergiulio Cappelletti (Federico II, Napoli) - Rodolfo Carosi (Torino) - Bernardo Cesare (Padova) - Rosa Cidu (Cagliari) - Raffaello Cioni (Firenze) - Domenico Cosentino (Roma Tre) - Francesco Frondini (Perugia) - Francesco Princivalle (Trieste) - Orlando Vaselli (Firenze) - Marco Viccaro (Catania)

COMITATO ORGANIZZATORE e LOGISTICA

Maria Laura Balestrieri (IGG-CNR, Firenze) - Luca Bindi (UniFI) - Eleonora Braschi (IGG-CNR, Firenze) - Marco Bonini (IGG-CNR, Firenze) - Francesco Capecchiacci (UniFI) - Bernardo Carmina (UniPI) - Sandro Conticelli (UniFI - IGG-CNR, Firenze) - Giacomo Corti (IGG-CNR, Firenze) - Francesco Di Benedetto (UniFI) - Lorenza Fascio (SIMP) - Lorella Francalanci (UniFI - IGG-CNR, Firenze) - Giovanna Moratti (IGG-CNR, Firenze) - Fabio Petti (SGI) - Marco Pistolesi (UniFI) - Giovanni Pratesi (UniFI) - Alba Patrizia Santo (UniFI) - Franco Tassi (UniFI) - Simone Tommasini (UniFI) - Orlando Vaselli (UniFI - IGG-CNR, Firenze) - Alessandro Zuccari (SGI)

PLATINUM SPONSORS



Thermo
SCIENTIFIC



ENTE
CASSA DI RISPARMIO
DI FIRENZE

GOLD SPONSORS



SILVER SPONSORS



SOMMARIO

Plenary lectures	4
Sessione S1. Mountain building processes: from surface to deep Earth.....	12
Sessione S2. Mantle processes and crustal genesis in extensional environments.....	35
Sessione S3. The cycles of volatiles: fluxes and processes from the oceans, down to the mantle and backward to the Earth surface	56
Sessione S4. The subduction factory - a key element in the Earth s dynamics.....	78
Sessione S5. Subduction and exhumation of continental lithosphere: implications on orogenic architecture, environment and climate.....	101
Sessione S6. Experimental and Computational Methods in Mineralogy and Geochemistry	119
Sessione S7. Microstructures: key to the interpretation of processes	145
Sessione S8. Magma chamber dynamics and timescales of volcanic processes.....	161
Sessione S9. The role of GMPV disciplines in the definition of volcanic hazards.....	186
Sessione S10. Field studies in modern volcanology	197
Sessione S11. Mineralogy	215
Sessione S12. Mantle mineralogy.....	254
Sessione S13. Characterization and use of geomaterials for sustainable industry and the environment.....	264
Sessione S14. Environmental mineralogy and geochemistry: natural environment versus human activities.....	284
Sessione S15. The geosciences for Cultural Heritage and Archeometry: consolidated and innovative approaches	323
Sessione S16. Fluid geochemistry in volcanic, geothermal and seismic areas	360
Sessione S17. From Rocks to Stars (The Nuclear History of the Galaxy as Written in Solar System Solids).....	373
Sessione S18. Geological, geophysical and geochemical prospection for economic geology and geothermal resources	394
Sessione S19. Global pollutants: from mercury to POPs.....	419
Sessione S20. Multidisciplinary contributes to the understanding of active geodynamic processes.....	435
Sessione S21. Open Poster Session	460

In coda al volume elenco alfabetico dei riassunti per sessione ed elenco degli autori

PLENARY LECTURES

The Metamorphosis of Melt Inclusions from Interesting Artifact to Valuable Geochemical Tool

Bodnar R.J.

Department of Geosciences, Virginia Tech, Blacksburg, VA 24061 USA.

Corresponding email: rjb@vt.edu

Keywords: Fluid inclusions, Melt inclusions.

Fluid (FI) and melt inclusions (MI) have been known at least since the time of Sorby (1958). Many of the melt inclusions that Sorby described in his classic paper are from locations in Italy that continue to be the focus of modern melt inclusion studies, and include descriptions of glassy MI in nepheline from Vesuvius and crystallized MI (Sorby referred to these as “stone cavities”) in quartz from a trachyte from the island of Ponza. Although the presence of FI and MI in rocks had been known for at least a century, it was not until the middle of the last century that researchers began to apply inclusions in earnest to constrain physical and chemical processes. And, the development of our understanding of how to apply FI and MI have followed similar paths, albeit offset temporally by about a quarter century. In the 1950s researchers began to use FI to study hydrothermal processes, but the methodology and interpretations were often questionable, and this led some well-known researchers to question the validity of fluid inclusions. For example, Kennedy (1950) wrote that “*It is our fundamental assumptions in the use of vacuoles [fluid inclusions] in geologic thermometry that need revision*” in discussing the observation that fluid inclusions often indicated a different P-T history compared to other geothermobarometers. Skinner (1953) also reported that “*When evidence from liquid inclusions is at variance with other lines of geologic evidence, as is often the case, it would seem pertinent to consider the possibility that the vacuoles indicate later and different conditions from those operative at the time of formation*”. The lack of confidence in fluid inclusions by the scientific community resulted because most practitioners did not consider the potential that FI could “change” after formation to record results not indicative of the original trapping conditions but, rather, conditions experienced by the FI and the host rock long after the inclusions formed. It took many years of careful research to recognize that such processes occur and to develop an effective protocol to recognize and test FI that have reequilibrated – today this protocol is often referred to as Sorby’s (or Roedder’s) Rules.

Much of the early data and interpretations from melt inclusion studies are now known to be of questionable quality because early workers did not recognize or consider the many possible mechanisms that could alter MI compositions and microthermometric behavior. Starting in about the 1970s, early practitioners such as Anderson (1974), Clocchiatti (1975) and Roedder (1979) began to establish protocols for studying MI, especially methods for recognizing changes that MI experience after trapping in a magma system and during cooling to ambient conditions, either in a plutonic body or in an eruptive volcanic unit. These advances in our understanding of the processes that might alter MI occurred in parallel with significant advances in analytical techniques that provided tools such as the ion microprobe, micro-FTIR, laser ablation ICPMS, Raman spectroscopy, and others, as well as the introduction of high temperature microscope heating stages and improved microscope optics. These advances made it possible to determine not only the major element chemistry of MI, but also the minor and trace element compositions, including the important volatile components, as well as to observe and measure temperatures of phase changes during heating of MI from room temperature to the homogenization temperature. These advances combined allow us today to apply MI within a rigorously constrained framework to determine the pre-eruptive physical and chemical environment of magmatic systems.

- Anderson A.T., Jr. 1974. Evidence for a picritic, volatile-rich magma beneath Mt. Shasta, California. *Journal of Petrology*, 15, 243-267.
- Clocchiatti R. 1975. Les inclusions vitreuses des cristaux de quartz. Étude optique, thermo-optique et chimique. Applications géologiques. [Glass (melt) inclusions in quartz. Optical, microthermometric and chemical study. Geologic applications] *Memoires de la Société Géologique de France*, LIV, 122, 1–96 [in French].
- Kennedy G.C. 1950. “Pneumatolysis” and the liquid inclusion in geologic thermometry. *Economic Geology* 45, 533-547.
- Roedder E. 1979. Origin and significance of magmatic inclusions. *Bulletin de Mineralogie*, 102, 467-510.
- Skinner B.J. 1953. Some considerations regarding liquid inclusions as geologic thermometers. *Economic Geology* 48, 541-550.
- Sorby H.C. 1858. On the microscopic structures of crystals, indicating the origin of minerals and rocks. *The Quarterly journal of the Geological Society of London*, 14(1), 453-500.

Volcanic ash and civil aviation: a new perspective

Bonadonna C.

Department of Earth Sciences, University of Geneva, Geneva, Switzerland

Corresponding email: Costanza.Bonadonna@unige.ch

Keywords: volcanic ash, civil aviation.

Worldwide, there are about 20 volcanoes erupting at any given time, posing a potential hazard to aviation. Since 1973 there have been 120 reported aviation incidents due to volcanic ash, including 26 cases of very severe engine damage and 9 incidents of in-flight engine failure. Several recent eruptions (such as Eyjafjallajökull 2010, Iceland, and Cordón Caulle 2011, Chile) are a stark reminder of the need to plan for, and be able to respond effectively to, future eruptions to minimize disruption to air transport and to protect human safety.



Figure 1. Volcanic plume associated with the 2010 eruption of Eyjafjallajökull volcano, Iceland (photograph by J. Eliasson).

As a consequence of the severe disruption to air traffic generated by the April-May 2010 eruption of Eyjafjallajökull volcano in Iceland (Fig. 1), it became clear that the tephra-dispersal community needed to improve monitoring and forecasting methodologies and to provide a more robust and reliable response to societal needs. In particular, an integrated strategy was urgently needed, based on collaboration between the volcanological and meteorological communities and the International Civil Aviation Organization (ICAO) in order to ensure that both the scientific knowledge and aviation safety aspects were considered. As a result, a new multidisciplinary international scientific community able to work together on a better description of both the source term and the transport and sedimentation of volcanic particles naturally developed.

This diverse community gathered at the Geneva Headquarters of the World Meteorological Organization (WMO) on 18-20 October 2010 for the 1st IUGG-WMO workshop to promote stronger interactions between the volcanological and the operational forecasting communities. The resulting outcomes served as a road-map for on-going research. A consensual document was produced together with a document summarizing the results of a model-benchmark exercise carried out before the workshop, a document summarizing critical features of the main Volcanic Ash Dispersal and Transport Models (VATDMs) and a document summarizing the main data-acquisition techniques available at that time (<http://www.unige.ch/hazards/Workshop.html>).

A great deal of scientific progress has been made since 2010 to improve characterisation of volcanic eruptions and to understand sensitivities and uncertainties in ash dispersal modelling and forecasting as a result of increased multidisciplinary collaboration. In particular, a large number of projects and consortia were funded worldwide that

cover multiple aspects of ash dispersal, ranging from the expansion of ground-based remote sensing networks and capabilities for the characterization of far-field ash clouds to the real-time characterization of the source. However, more recent volcanic ash crises (i.e. Grimsvötn 2011, Iceland; Cordón Caulle 2011, Chile) have demonstrated how specific needs remain (e.g. accurate description of the source term) and posed new challenges (e.g. re-suspension of deposited volcanic ash). A significant challenge in the rapid operationalization of scientific achievements was also evident.

Three years after our first gathering, the 2nd IUGG-WMO workshop (18-20 November 2013) aimed at consolidating the multidisciplinary community established in 2010 and at optimizing the scientific and operational advances. The workshop was sponsored by WMO, the University of Geneva, the British Geological Survey, the Met Office (UK), the International Union of Geodesy and Geophysics and the International Association of Volcanology and Chemistry of the Earth's Interior. Priorities to maximise national and international cooperation and advancement of scientific research were identified. These include the need for systematic ground and space-borne monitoring, increased integration of observations with forecast models and further opportunities to share knowledge and experience across the community (see Consensual Document and additional material at <http://www.unige.ch/hazards/Workshop2.html>).

The work presented and the discussions held at the 2nd IUGG-WMO workshop show that the whole ash-aviation community, from research to operations, is working together to build the most capable system for aviation safety. The resulting outcomes provide the next steps for the community to move forward. In particular, a systematic combination of geophysical monitoring, field observations and numerical modelling based on a large multi-disciplinary effort represents a significant step forward towards a better understanding and description of tephra dispersal both for real-time forecasting and long-term hazard assessment.

Plate tectonics: a polarized self-organized chaotic system

Doglionì C.¹

1. Dipartimento di Scienze della Terra, Università Sapienza – Roma

Corresponding email: carlo.doglionì@uniroma1.it

Keywords: Mainstream of plates, Asymmetric plate margins, Westward drift, Plate tectonics mechanisms

Plates do not move randomly, but they rather follow a sort of mainstream, which is “westerly” polarized and responsible for a number of asymmetries at plate boundaries (Doglionì, 1993; 1994; Scoppola et al., 2006; Crespi et al., 2007; Cuffaro and Doglionì, 2007; Doglionì et al., 2003; 2007; 2009; 2015; Garzanti et al., 2007; Panza et al., 2010; Riguzzi et al., 2010; Doglionì & Panza, 2015). Deviations from the main flow have been analyzed in terms of plate subrotations, i.e., plates having two contemporaneous poles of rotation (Cuffaro et al., 2008). The velocity of the so-called westward drift of the lithosphere in the hotspot reference frame depends on the depth of the last residence of volcanic plume tracks (Fig. 1).

However, wet spots and last residence of the magma chamber supplying the Pacific hotspots support an asthenospheric location for most of plumes (Bonatti, 1990; Rychert et al., 2013) used to infer plate motion relative to the mantle. The shallower the plume magma chamber within the decollement zone in the low-velocity layer, the faster the rotation of the lithosphere relative to the underlying mantle (Doglionì et al., 2015). Regardless the speed of the net rotation, rift and subduction zones show asymmetries that depend on their polarity relative to the “westerly” directed mainstream and related “tectonic equator” (Fig. 2).

W-directed subduction zones provide three times larger volumes of lithosphere recycling into the convecting mantle, hence determining asymmetric mantle convection as well. Moreover, contrary to the narrow subduction zones, mantle uplift should be slower and widely diffused (Doglionì & Anderson, 2015). The heat dissipation from the Earth’s interior fuels convection, and perpetuating the low viscosity in the low-velocity layer it allows decoupling at the lithosphere base. However, the astronomical torque exerted by the horizontal component of the solid Earth tide delivers a large amount of energy that is added to the system. The energy provided both by mantle convection and by tides may explain the steady state dissipation distributed all over the planet (Fig. 3), as suggested by stationary plate motions derived from GPS data and the Gutenberg-Richter law of earthquakes frequency. Therefore, the vibration generated by tides (Doglionì et al., 2011) and mantle convection driven from the top are combined to produce the self-organized chaotic system which can be ascribed to plate tectonics (Riguzzi et al., 2010), thus explaining why plates move faster at low latitude relative to the tectonic equator.

Bonatti E. 1990. Not so hot “hot spots” in the oceanic mantle. *Science*, 250, 107-111.

Doglionì C. 1993. Geological evidence for a global tectonic polarity. *J. Geol. Soc. London*, 150, 991-1002.

Doglionì C. 1994. Foredeeps versus subduction zones. *Geology*, 22, 3, 271-274.

Doglionì C., Carminati E. & Bonatti E. 2003. Rift asymmetry and continental uplift. *Tectonics*, 22, 3, 1024.

Scoppola B., Boccaletti D., Bevis M., Carminati E. & Doglionì C. 2006. The westward drift of the lithosphere: a rotational drag? *Bull. Geol. Soc. Am.*, 118, 199–209.

Crespi M., Cuffaro M., Doglionì C., Giannone F. & Riguzzi F. 2007. Space geodesy validation of the global lithospheric flow. *Geophys. J. Int.*, 168, 491-506.

Cuffaro M. & Doglionì C. 2007. Global Kinematics in the deep versus shallow hotspot reference frames. In: Foulger, G.R., and Jurdy, D.M., eds., *Plates, plumes, and planetary processes*, *Geol. Soc. Am. Spec. Pap.*, 430, 359–374.

Doglionì C., Carminati E., Cuffaro M. & Scrocca D. 2007. Subduction kinematics and dynamic constraints. *Earth Sci. Rev.*, 83, 125-175.

Garzanti E., Doglionì C., Vezzoli G. & Andò S. 2007. Orogenic Belts and Orogenic Sediment Provenances. *J. Geol.*, 115, 315–334.

Doglionì C., Tonarini S. & Innocenti F. 2009. Mantle wedge asymmetries along opposite subduction zones. *Lithos*, 113, 179-189.

Panza G. Doglionì C. & Levshin A. 2010. Asymmetric ocean basins. *Geology*, 38, 1, p. 59–62, doi: 10.1130/G30570.1.

Riguzzi F., Panza G., Varga P. & Doglionì C. 2010. Can Earth’s rotation and tidal despinning drive plate tectonics? *Tectonophysics*, 484, 60–73.

Doglionì C., Ismail-Zadeh A., Panza G., Riguzzi F. 2011. Lithosphere-asthenosphere viscosity contrast and decoupling. *Phys. Earth Planet. Int.*, 189, 1-8.

Carminati E. & Doglionì C. 2012. Alps Vs. Apennines: The paradigm of a tectonically asymmetric Earth. *Earth Sci. Rev.*, 112, 67-96.

Cuffaro M., Caputo M. & Doglionì C. 2008. Plate sub-rotations. *Tectonics*, 27, TC4007.

- Doglioni C., Carminati E., Crespi M., Cuffaro M., Penati M. & Riguzzi F. 2015. Tectonically asymmetric Earth: From net rotation to polarized westward drift of the lithosphere. *Geoscience Frontiers*, 6, 3, 401–418.
- Doglioni C., & Anderson D.L., 2015. Top driven asymmetric mantle convection. In *The Interdisciplinary Earth: A volume in honor of Don L. Anderson*. GSA-AGU, Sp. Publ.
- Doglioni C. & Panza G.F. 2015. Polarized plate tectonics. *Advances in Geophysics*, 56, 3, 1-167.
- Rychert C.A., Laske G., Harmon N. & Shearer P.M. 2013. Seismic imaging of melt in a displaced Hawaiian plume. *Nature Geosci.*, 6, 657-660.

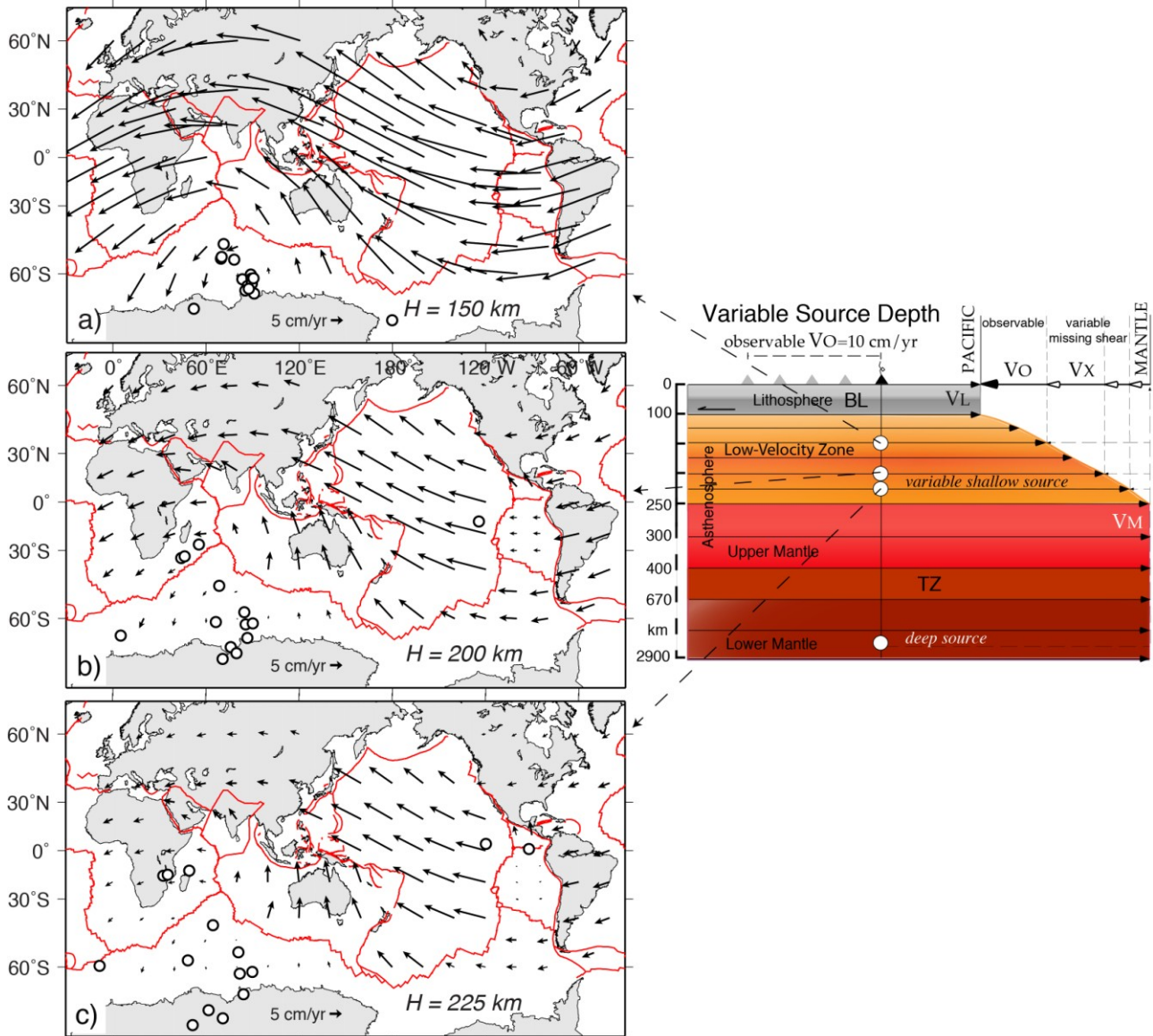


Fig. 1. Plate kinematics computed assuming a hot spot reference frame “anchored” in the asthenosphere, i.e., within the decoupling zone. The faster decoupling and “westward” drift of the lithosphere (>1 Ma) occurs if the volcanic tracks are fed from a depth of about 150 km, (a), within the LVZ since the surficial age-progressive volcanic track does not record the entire decoupling between the lithosphere and the mantle beneath the LVZ. Computations made considering the two other deeper depths of magmatic sources at 200 and 225 km, (b) and (c), would provide a slower westward drift. An even deeper source (2800 km) would make the net rotation very slow, about 0.2 and 0.4 Ma. Note the clustering of the poles of rotation (open circles) in the southern Indian Ocean. The clustering increases as the source of the volcanic trails shallows. Slightly modified after Doglioni et al. (2015).

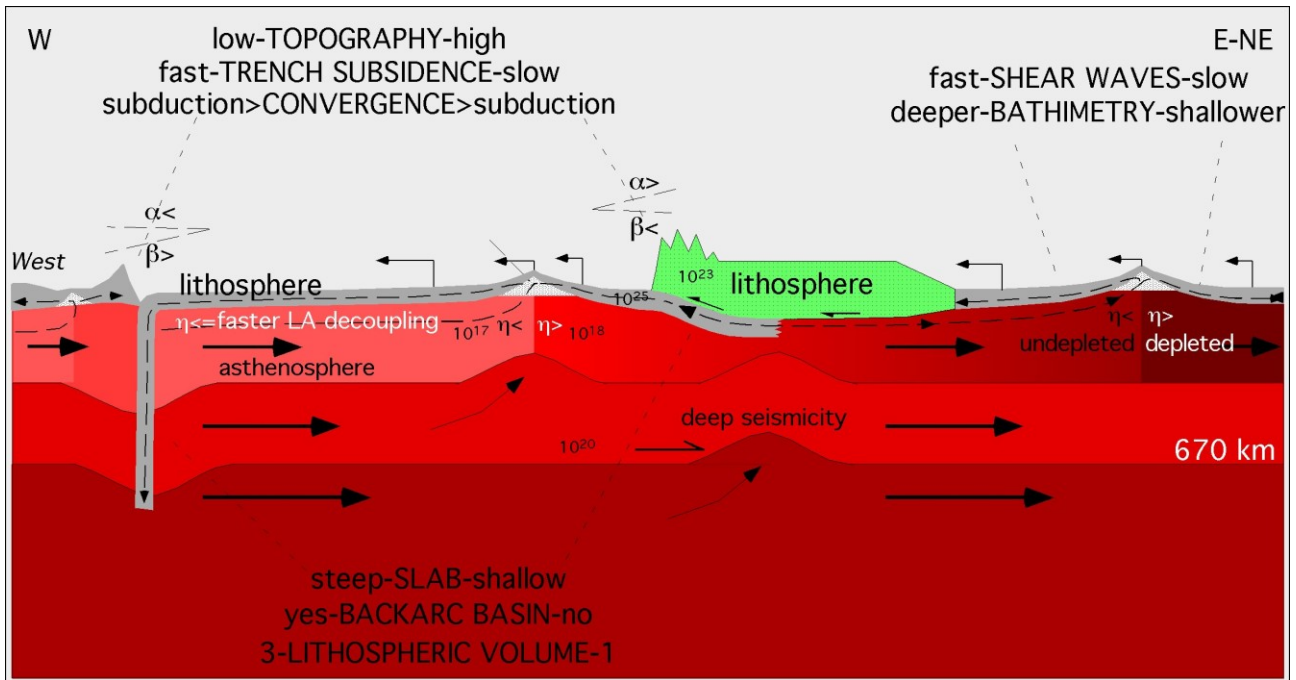


Fig. 2. Main asymmetries at plate boundaries supporting a “westerly” polarized flow of the lithosphere relative to the underlying mantle (after Carminati & Doglioni 2012).

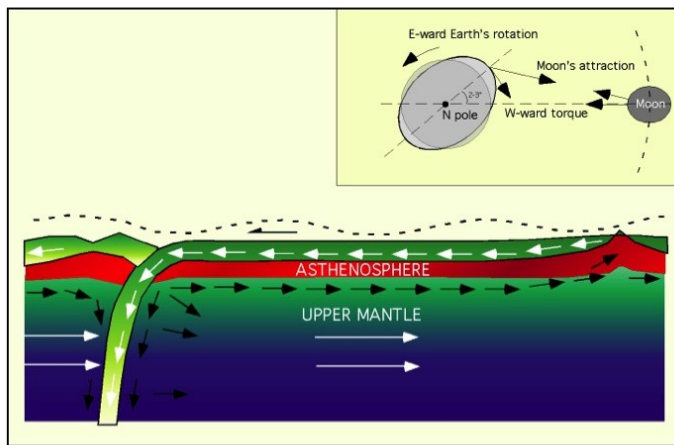


Fig. 3. The westward drift of the lithosphere relative to the mantle can be generated by the torque exerted by the misalignment of the excess of mass of the Earth’s bulge with respect to the Earth-Moon gravitational alignment. This motion is consistent with the presence of a hot, low-viscosity layer at the base of the lithosphere, within the low-velocity zone (LVZ) in the uppermost asthenosphere. The tidal oscillation of the lithosphere facilitates the decoupling. Mantle convection appears polarized due to the oscillating westerly directed tidal drag. The horizontal component of the body tide can slowly but steadily shift the lithosphere relative to the underlying mantle. Therefore, plate tectonics can be a combination of mass transfer within the planet, but polarized by the astronomical tuning (after Doglioni & Panza, 2015).

Mineralogy and Crystal Chemistry: Past, Present and Future

Nancy L. Ross

Department of Geosciences, Virginia Tech., USA.

Corresponding email: nross@vt.edu

Keywords: Mineralogy, Crystal Chemistry.

In the early decades of the 20th century, the three pioneers W. L. Bragg, V. M. Goldschmidt and L. Pauling (BGP) formulated a number of the concepts and fundamentals of oxide crystal chemistry that have since been used to establish much of the basis for understanding the structures of crystals and their properties. With the advent of the single crystal diffractometer and the computer and computer software in the late 1950s, a large number of oxide crystal structures have since been determined, providing a wealth of different structure types, accurate bond length and angle data that have been used to advance our understanding of the crystal chemistry of materials. The bulk of these structures have been found to conform with many of the BGP concepts regarding the sizes of the ions and the types and linkages of the cation containing coordination polyhedra. However, unraveling the total response of crystal structures to changes in temperature, pressure or composition in order to understand the relationship between structure and properties is often very challenging. This is especially true for framework materials such as feldspars and perovskites in which several levels of structural response interact. Hazen and Finger (1982) developed a polyhedral approach to describe changes of crystal structures under high pressure, high temperature and with variable composition which predicts that the structural response of framework structures is dominated by the tilting of “rigid” polyhedral units. In the 1990’s, Dove et al. (1995) and Hammonds et al. (1996) further developed a “rigid unit” model that has extended our understanding of the structure and thermodynamics of framework minerals. However, polyhedral deformation and compression appears to play a role in the compression of all frameworks that have been studied to sufficient precision. For example, high-pressure single-crystal X-ray diffraction studies of orthorhombic ABO₃ perovskites suggest that the pressure-induced change in the bond-valence sums at the two cation sites within any given perovskite is equal. With this assumption, Zhao et al. (2004) developed a model based on the bond valence concept (Brown and Altermatt 1985) that predicts the relative compressibilities of the cation sites in perovskites that control the tilts between the octahedral units of the structure under pressure. The polyhedral compression plays an important role in the high-pressure behavior of framework minerals by modifying the detailed compression patterns away from the exact rigid-unit mode. In addition, polyhedral deformation under pressure may also serve to select which of the many rigid unit modes present in these structures is actually used for compression. Recently, there has been recent interest in extending these studies to encompass hybrid framework materials, including metal-organic frameworks. Spencer et al. (2009) reported the pressure-dependent structural evolution of a three-dimensional zinc-imidazolate (ZnIm) framework and found that it undergoes a phase transition to a previously unknown phase between 0.543(5)-0.847(5) GPa. The room-temperature bulk modulus for ZnIm is estimated to be 14 GPa, substantially lower than the bulk moduli for the corresponding inorganic frameworks. Since this study, a variety of novel phase transitions and unusual mechanical properties have been reported in other hybrid frameworks at high pressure. These high precision structural studies not only clarify the stability of hybrid frameworks at high pressure, but they also elucidate the mechanisms responsible for anomalous properties such as extreme negative linear compressibility.

- Brown I.D., Altermatt D. 1985. Bond-valence parameters obtained from a systematic analysis of the Inorganic Crystal Structure Database. *Acta Cryst.* 8., 41, 244-241 .
- Dove M.T., Heine V, Hammonds K.D. 1995. Rigid unit modes in framework silicates. *Mineral. Mag.* 59, 629 -639.
- Hammonds, K.D., Dove, M.T., Giddy, A.P., Heine, V., Winkler, B. 1996. Rigid-unit phonon modes and structural phase transitions in framework silicates. *Am. Mineral.* ,81, 1057- 1709.
- Hazen R.M., Finger L.W. 1982. *Comparative Crystal Chemistry*. John Wiley and Sons, New York.
- Spencer E.C., Angel R.J., Ross N.L., Hanson B.E., Howard J.A.K. 2009. Pressure-Induced Cooperative Bond Rearrangement in a Zinc Imidazolate Framework: A High-Pressure Single-Crystal X-Ray Diffraction Study. *J. Amer. Chem. Society*, 131:4022-4026.
- Zhao J., Ross N.L., Angel R.J. 2004. A new view of the high-pressure behaviour of GdFeO₃-type perovskites. *Acta Cryst.* B60: 263-271.

SESSION S1

Mountain building processes: from surface to deep

CONVENORS

Laura Crispini (Univ. Genova)

Chiara Montomoli (Univ. Pisa)

Giorgio Pennacchioni (Univ. Padova)

Metamorphic and structural constrains for the exhumation of (U)HP - metaophiolites from the Susa Valley, Western Alps

Balestro G., Borghi A.*, Compagnoni R., Cossio R., Gattiglio M. & Ghignone S.

Dipartimento di Scienze della Terra, Università di Torino

Corresponding email: alessandro.borghi@unito.it

Keywords: Meta-ophiolite, eclogite facies, western Alps.

High and ultra-high pressure metamorphic rocks have a crucial role in the construction of geodynamic models concerned with convergent plate margins. They offer the possibility of constructing P-T-t trajectories, and thus constrain the evolution of orogenic belts.

In this work, new structural and metamorphic data were collected in the Susa Valley, wherein Zermatt-Saas-like meta-ophiolite units (i.e., the Internal Piedmont Zone, IPZ) are tectonically overlain by Combin-like meta-ophiolite units (i.e., the External Piedmont Zone, EPZ). The IPZ and EPZ record different metamorphic P-T peaks and are separated by a hundreds of meters thick shear zone (Susa Shear Zone, SSZ). The SSZ drove exhumation of the IPZ until coupling with the EPZ, and is characterized by two main mylonitic events. The younger one (ME2) develops a pervasive mylonitic foliation, with top to W extensional sense of shear, which wraps various-scale lithons wherein an older mylonitic foliation (ME1) developed under HP conditions (about 17 kbar) and characterized by top to E sense of shear, is preserved.

In the IPZ four tectono-metamorphic events developed under variables metamorphic conditions. The first event (M1) shows UHP conditions, defined by the occurrence of microdiamonds (detected by micro-Raman spectroscopy analyses) included in Grt, Omp and Rt. The paragenesis is completed by Zo+Pg pseudomorphoses after Lws. For this relict metamorphic event P of about 33 kbar (microdiamonds occurrence) and T of 650 °C (Grt-Cpx geothermometers, and Zr contents in the Rt) were inferred. After the P peak, the IPZ was exhumed along the subduction channel following a near isothermal decompression path, up to the development of the second metamorphic event, which still occurred under eclogitic conditions (14-16 kbar and 580-600 °C). This event is correlated with firstly exhumation along the SSZ (ME1). Following a retrograde and decompressional trajectory the IPZ was then re-equilibrated under greenschist facies conditions (M3, 5 kbar and 450-500 °C), that is related to the D2 main regional deformation phase. The last metamorphic event (M4) is defined by a rise of T up to about 550 °C, with formation of new stable paragenesis (Bt, Ep, Olig, Hbl-Prg, Ms) that partially replaced the previous. This late heating was registered also by SSZ mylonites, with formation of stable minerals in these metamorphic conditions developed along the shear planes (ME2). The inferred P-T path suggests that during the exhumation of the IPZ different processes occurred. A first fast exhumation stage mainly driven by buoyancy forces in a compressional regime from the base of the orogenic wedge towards shallow crustal level can be related to major cooling and was mainly controlled by E-verging compressional stage along the SSZ. Finally, a rapid unroofing of the hanginwall by W-directed extensional movement along the SSZ was responsible for the later heating.

Crustal melting from amphibolite- to granulite-facies conditions: the perspective of melt inclusions

Bartoli O.^{*1}, Acosta-Vigil A.¹, Cesare B.¹, Remusat L.², Tajcmanova L.³, Walle M.³, Heinrich C.³ & Poli S.⁴

1. Dipartimento di Geoscienze, Università di Padova. 2. IMPMC – UMR CNRS 7590, Sorbonne Universités, IRD, Muséum National d'Histoire Naturelle, Paris, France. 3. Department of Earth Sciences, ETH, Zurich, Switzerland. 4. Dipartimento di Scienze della Terra, Università di Milano.

Corresponding email: omar.bartoli@unipd.it

Keywords: Crustal anatexis, melt inclusion, nanogranites.

Being trapped by growing peritectic phases at suprasolidus conditions, MI in migmatites and granulites represent a window into the pre-peak anatexis history of partially melted terranes, and may provide a wealth of microstructural and compositional information on crustal anatexis. The crustal footwall of the Ronda peridotites (S Spain) consists of an inverted metamorphic sequence with migmatites and mylonites at the top. Mylonites represent strongly deformed former diatexites. To shed light on the nature and mechanisms of melting, a detailed microstructural and geochemical study has been conducted on primary MI hosted in peritectic garnet of i) metatexites at the bottom of the migmatitic sequence and ii) mylonites close to the contact with the mantle rocks. Both metatexites and mylonites have compositions corresponding to peraluminous greywackes. Phase equilibria modeling shows that metatexites and mylonites underwent anatexis under amphibolite- and granulite facies conditions, respectively (660-700 °C, 4.5-5 kbar and 820-830 °C, 5.5-6.0 kbar). Clusters of MI in the metatexites are rounded and preferentially located at the core of small garnet crystals, whereas these clusters may have a sigmoidal to spiral-like shape in garnets of mylonites. MI are small (2-10 µm) and show a variable degree of crystallization ranging from totally glassy to fully crystallized (i.e., nanogranites). The latter consist of Qtz+Pl+Kfs+Bt+Ms aggregates (often modal Kfs > Pl in mylonites). Piston cylinder remelting experiments led to the complete rehomogenization of nanogranites in metatexites at the conditions inferred for anatexis: 700 °C and 5 kbar. Rehomogenized nanogranites in metatexites and glassy MI in mylonites are all leucogranitic and peraluminous and differ from those of coexisting leucosomes and from melts calculated by phase equilibria modeling at the inferred P–T conditions. Systematic compositional variations have been observed between MI in metatexites and mylonites. MI produced under amphibolite-facies conditions show higher H₂O and Na₂O/K₂O, lower FeO and higher concentrations of the trace elements controlled by feldspars: Sr and Ba. MI formed under granulite-facies conditions have higher concentrations of trace elements controlled by biotite (Cs, Rb and FRTE e.g. Zn, Sc) and accessory minerals (HFSE e.g. Zr, U, Th). Leucosomes show anomalously high contents of Ca, Sr and Ba which are not consistent with primary melts produced at higher T than melt inclusions. The MI in metatexites and mylonites are interpreted to record the composition of the anatexis melts produced from a peraluminous greywacke 1) on, and immediately after crossing, the fluid-saturated solidus of this metasedimentary rock, and 2) during syn-kinematic anatexis via biotite dehydration melting at increasing temperature, respectively.

From rift-inherited hyper-extension to orogenesis: De-coding the axial zone of the Alpine belt

Beltrando M.*¹, Manatschal G.², Mohn G.³, Dal Piaz G.V.⁴, Vitale Brovarone A.⁵ & Masini E.⁶

1. Dipartimento di Scienze della Terra, Università di Torino. 2. IPGS-CNRS-EOST, Strasbourg, France.
3. GEC, Université de Cergy-Pontoise, France. 4. Accademia delle Scienze di Torino.
5. IMPMC-CNRS, Paris, France. 6. TOTAL, CSTJF, France.

Corresponding email: marco.beltrando@unito.it

Keywords: Rift inheritance, hyper-extension, subduction dynamics.

The relative role of rift-inherited hyper-extension and subduction/collisional dynamics in establishing the lithostratigraphic associations and overall architecture of orogenic belts has been investigated in the Western Alps and Corsica. This case study was selected to test existing models involving complex subduction/exhumation dynamics to account for seemingly chaotic mixing of continental crust and serpentized mantle rocks in high-pressure metamorphic units.

The methodology developed to assess the role of rift-inheritance in multiply deformed/metamorphosed tectono-metamorphic units stems from recent advances in the understanding of hyper-extended domains in present day magma-poor rifted margins, where the crustal architecture displays transitional features between typical oceanic and continental domains. In these areas, slivers of hyper-extended continental crust or pre-rift sediments may rest as extensional allochthons upon serpentized mantle, while syn- and post- rift sediments seal the extension-related lithostratigraphy. Following multi-stage orogeny-related deformation and metamorphism, this rift-related lithostratigraphic architecture can erroneously be ascribed to complex subduction dynamics, partly due to the sliver-like appearance of continental basement. However, the partial preservation of rift-related lithostratigraphic associations may still be assessed by (1) the consistency of the lithostratigraphic architecture over large areas, based on the continuity of key surfaces (i.e. base of early post-rift sediments) across the orogeny-related macro-structures, (2) the presence of clasts of basement rocks in the neighboring meta-sediments, indicating the original proximity of the different lithologies, (3) evidence of brittle deformation in continental basement and ultramafic rocks pre-dating Alpine metamorphism, indicating that they were juxtaposed by fault activity prior to the deposition of post-rift sediments, and (4) the similar Alpine tectono-metamorphic evolution of ophiolites, continental basement and meta-sediments.

The partial preservation of rift-related relationships despite subduction to (U)HP conditions indicates that the association of serpentinites and continental basement, which in the Western Alps has often been ascribed to chaotic counter-flow in a subduction channel, may also be an inherited feature from the rifting history. Within this context, the high-pressure Alpine tectono-metamorphic units were probably detached from the downgoing lithosphere along a hydration front that is typically observed in present-day distal margins.

The relationship between the architecture of the Jurassic rifted margins and the distribution/extent of Alpine metamorphism indicates that the axial zone of the Western Alps, which records multi-stage deformation and high pressure metamorphism, originated from the hyper-extended rifted margins of the European and Adriatic and from the intervening magma-poor ridge system. Relative plate motion during Cretaceous-Tertiary inversion was largely accommodated at the transition between hyper-extended domains, floored by extremely thinned crust or hydrated subcontinental mantle, and proximal domains consisting of thicker continental crust. As a result, distal hyper-extended margins were preferentially subducted, whereas the proximal domains underwent relatively minor deformation and metamorphism. The final stage of continent-continent collision was achieved following subduction of the distal European margin, when the European necking zone reached the subduction zone.

3D modelling and balancing of post-metamorphic brittle deformation in the Austroalpine-Penninic collisional wedge of the NW Alps

Bistacchi A.*¹, Gouffon Y.², Monopoli B.³, Massironi M.⁴, Sartori M.⁵ & Dal Piaz G.V.⁶

1. Dipartimento di Scienze dell'Ambiente e del Territorio e di Scienze della Terra, Università di Milano-Bicocca. 2. Swiss Geological Survey, SWISSTOPO. 3. Land Technology & Services, Padova. 4. Dipartimento di Geoscienze, Università di Padova. 5. Section of Earth and Environmental Sciences, University of Geneva, Suisse. 6. Accademia delle Scienze di Torino.

Corresponding email: andrea.bistacchi@unimib.it.

Keywords: NW Alps, Austroalpine-Penninic collisional wedge, 3D geological modelling.

We know since the beginning of the 20th century, thanks to mapping and structural studies by the Italian Regio Servizio Geologico (Franchi et al., 1908) and by Argand (1909; 1911; 1916), that the Austroalpine-Penninic collisional wedge of the NW Alps is spectacularly exposed across the Aosta Valley and Valais ranges (Italy and Switzerland). In the 150th anniversary of the first ascent to Ruskin's "most noble cliff in Europe" - the Cervino/Matterhorn (Whymper, July 14th 1865), first described in a geological profile by Giordano (1869) and in a detailed map by Gerlach (1869; 1871), we see the conclusion of very detailed mapping projects carried out in the last years over the two regions, with collaborative efforts across the Italy-Switzerland border, constellated by 4000 m-high peaks. These projects have pictured with an unprecedented detail the geology of this complex region, resulting from pre-Alpine events, Alpine subduction- and collision-related ductile deformations, and finally late-Alpine brittle deformations from the Oligocene to the Present. Based on this dataset, we use up-to-date technology to undertake a 3D modelling study aimed at: i) reconstructing the 3D geometry of the principal tectonic units, ii) detecting and unravelling problems and incongruences in the 2D geometrical models proposed in the literature, iii) modelling the kinematics of the Oligocene and Miocene fault networks using 2D and 3D balancing and palinspastic restoration techniques. The results of this study, which are preliminarily presented here, will open new opportunities to study the collision- and subduction-related nappe architecture and kinematics with younger deformations removed, and will eventually lead (with additional studies) to a step-by-step retrodeformation supported by modern technologies, following the path traced by Argand at the beginning of the 20th century.

Argand E. 1909. L'exploration géologique des Alpes pennines centrales. Bull. Soc. Vaudoise Sci. Nat., 45, 217-276.

Argand A. 1911. Les nappes de recouvrement des Alpes pennines et leurs prolongements structuraux. Mat. Carte Géol. Suisse, 31, 25.

Argand A. 1916. Sur l'arc des Alpes occidentales. Eclogae Geol. Helv., 14, 145-191.

Franchi S., Mattiolo E., Novarese V., Stella A. & Zaccagna D. 1908. Carta geologica delle Alpi Occidentali alla scala 1:400.000. Regio Ufficio Geologico, Roma.

Gerlach H. 1869. Die Penninischen Alpen. N. Denkschr. Schweiz. Natf. Ges., 23, 132.

Gerlach H. 1871. Das Suedwestliche Wallis. Beitrage Geol. Karte Schweiz, 9, 175.

Giordano F. 1869. Sulla orografia e sulla geologica costituzione del Gran Cervino. Atti R. Acc. Sci. Torino, 4, 304-321.

The role of the mechanical anisotropy on deformation and failure mode of phyllosilicate-rich mylonitic fabric: new insights from rock deformation laboratory experiments

Bolognesi F.¹, Vinciguerra S.^{*2-3}, Bistacchi A.¹ & Dobbs M.³

1. Dipartimento di Scienze dell'Ambiente e del Territorio e di Scienze della Terra, Università di Milano-Bicocca. 2. Dipartimento di Scienze della Terra, Università di Torino. 3. British Geological Survey, Environmental Science Centre, Nottingham, UK.

Corresponding email: sergiocarmelo.vinciguerra@unito.it

Keywords: Mechanical anisotropy, rock deformation, phyllosilicate-rich mylonitic fabric.

It is assumed that the mechanical anisotropy of phyllosilicate-rich mylonitic rocks control the enucleation and propagation of fractures and faults with non-Andersonian geometry. To this aim the mechanical anisotropy and failure mode of phyllosilicate-rich (~30%) mylonites from the Grandes Rousses Massif (Helvetic-Dauphinois Domain, French Alps) has been investigated. 12 uniaxial (UCS) at 0 and 90° and 25 triaxial (TXT) tests varying the σ_1 /schistosity angle from 0 to 90° and at confining pressures of 60 and 120 MPa were carried out at constant strain rate of $6 \cdot 10^{-6} \text{ s}^{-1}$. Microseismicity in terms of acoustic emissions (AE) are measured during the rock deformation experiments. High strength and failure mode characterized by both low-angle segments along schistosity and high-angle ones cutting quartz-feldspar layers are evidenced by UCS tests carried out at 90°. At 0° on the contrary lower strength and axial splitting along schistosity is observed. For TXT tests maximum strength is achieved at 0°, at 45° minimum strength is observed with values around 50% and a significant strength anisotropy. The “process zone” develops mainly along schistosity for tests at 20-70°, whilst Andersonian shear fractures are observed at 0-20° and 70-90°. Microstructural observations further suggest that biotite foliation may have a primary role in the enucleation, propagation and coalescence of microcracking during dilatant failure. Foliated rocks are found in a wide range of σ_1 /schistosity angles and, because the failure mode is controlled by the slip along the schistosity, a significant deviation from the prediction of Anderson's theory is observed depending upon the angle to σ_1 at which new macroscopic fault zones enucleate. AE mirror the mechanical behaviour with higher rate occurrence related to higher mechanical damage.

Acquisition of morpho-structural data by the use of aerial lidar and proximal sensing in the southern end of Monte Altissimo syncline (Apuan Alps, Italy)

Carmignani L.*¹, Massa G.¹, Salvini R.¹, Pieruccioni D.¹⁻², Tufarolo E.¹, Conti P.¹, Mancini S.³ & Lorenzoni V.³

1. Centro di Geotecnologie, Università di Siena. 2. Dipartimento di Scienze Chimiche e Geologiche, Università di Cagliari. 3. Studio di Geologia Monte Altissimo, Seravezza (LU)

Corresponding email: diegopieruccioni@hotmail.it

Keywords: Proximal sensing, airborne lidar, polydeformed structures.

A new interpretation of the tectonic evolution of the southern end of Monte Altissimo syncline is given in this study on the basis of new information acquired through traditional geo-structural survey and photo-interpretation of data derived from airborne lidar and optical proximal sensing. The high spatial resolution and the geometric accuracy of the data led to the creation of digital geo-referenced products and, through the creation of 3D models with decimeter accuracy, the digitization of new morpho-structural elements. The study area is known in the geology of Apuan Alps because is studied since late nineteenth century by several authors among which Zaccagna (1932), Giglia (1967), and Meccheri et al. (2007). The interest in this zone is also increased by the presence of precious marbles cultivated by the Henraux company since 1821. The Monte Altissimo syncline has an approximately North-South trend for about ten kilometres in the Apuan Alps tectonic window (Northern Apennines). In the area of interest, the syncline is characterized by a core consisting of the Marbles Formation (Hettangian). The syncline flanks consist of carbonate formations with aged between Noricum and Hettangian (Megalodont Marbles, *Seravezza* Breccias and *Grezzoni* dolomites), that overlay the Hercynian basement. The tectonic evolution of the Apuan metamorphic complex is polyphasic, characterized by ductile and fragile deformation, and connected with the tertiary evolution of the orogenic Apennine wedge. In the area the following elements are particularly evident:

- i) the deformation geometries in low metamorphic state (green schists facies), produced by the compressional tectonic regime, which led to the structuring of the Monte Altissimo large isoclinal syncline with an East vergency;
- ii) the effects of the retro-deformation, created during ductile regime and low grade metamorphism, probably contemporary to the final stages of the orogenic wedge building, which develops a kilometric synform/antiform structure with a West vergency;
- iii) a subsequent deformative phase characterized by significant shear zones and low angle normal faults connected to the left and right transfer systems which overlaps the previous fold systems.

These systems of faults and shear zones represent a novelty in geological knowledge of the area that have been studied thanks to availability of a low altitude photogrammetric survey acquired through the multi-parametric vehicle developed by the Centre of Geotechnology of Siena University.

Giglia G. 1967. Geologia dell'Alta Versilia settentrionale (Tav. M. Altissimo). Mem. Soc. Geol. It., 6, 67-95.

Meccheri M., Bellagotti E., Berretti G., Conti P., Dumas F., Mancini S. & Molli G. 2007. The Mt. Altissimo marbles (Apuan Alps, Tuscany): commercial types and structural setting. Boll. Soc. Geol. It., 126, 25-35.

Zaccagna D. 1932. Descrizione Geologica delle Alpi Apuane, Memorie Descrittive della Carta Geologica d'Italia, Vol. XXV. Servizio Geologico d'Italia, Roma, 440 pp.

In-sequence shearing within the Greater Himalayan Sequence in Central Himalaya: deformation and metamorphism by crustal accretion from the Indian plate

Carosi R.*¹, Montomoli C.² & Iaccarino S.²

1. Dipartimento di Scienze della Terra, Università di Torino. 2. Dipartimento Scienze della terra, Università di Pisa.

Corresponding email: rodolfo.carosi@unito.it

Keywords: Exhumation, tectonic discontinuities, metamorphic discontinuities, Himalaya.

The Greater Himalayan Sequence (GHS) is the main metamorphic unit of the Himalayas, stretching for over 2400 km, bounded to the South by the Main Central Thrust (MCT) and to the North by the South Tibetan Detachment (STD) whose contemporaneous activity controlled its exhumation between 23 and 17 Ma (Godin et al., 2006).

Several shear zones have been recognized within the GHS, usually regarded as out of sequence thrusts. In the GHS in Central Himalaya we identified a tectonic and metamorphic discontinuity, above the MCT, with a top-to-the SW sense of shear (Higher Himalayan Discontinuity: HHD) (Carosi et al., 2010; Montomoli et al., 2014). U-Th-Pb *in situ* monazite ages provide temporal constraint of initiation of the HHD at 27-25 Ma, older than the Main Central Thrust, and continuing up to 17 Ma. Data on the P and T evolution testify that HHD zones affected the tectono-metamorphic evolution of the belt and different P and T conditions have been recorded in the hanging-wall and footwall of the HHD. The correlation of the HHD with several other discontinuities recognized in the GHS led to propose that it is a main tectonic feature running for several hundreds kilometers, documented at the regional scale and dividing the GHS in two different portions.

The occurrence of even more structurally higher contractional shear zone in the GHS (above the HHD): the Kalopani shear zone in the Kali Gandaki valley, points out to an even more complex deformation pattern within the metamorphic core. Recent U-Th-Pb *in situ* monazite ages of the Kalopani s.z. point to a ~ 36-38 Ma age of the exhumation of the higher portion of the GHS.

The most popular models for the exhumation of the GHS (i.e. extrusion and channel flow), based on the MCT and STD contemporaneous activities, are not able to explain the occurrence of the HHD and of other older in-sequence shear zones. Any model of the tectonic and metamorphic evolution of the GHS should account for the occurrence of the tectonic and metamorphic discontinuities within the GHS and its consequences on the metamorphic paths and on the assembly of Himalayan belt.

- Carosi R., Montomoli C., Rubatto D. & Visonà D. 2010. Late Oligocene high-temperature shear zones in the core of the Higher Himalayan Crystallines (Lower Dolpo, Western Nepal). *Tectonics*, 29, TC4029, doi:10.1029/2008TC002400.
- Godin L., Grujic D., Law, R. D. & Searle, M.P. 2006. Channel flow, ductile extrusion and exhumation in continental collision zones: an introduction. *Geol. Soc. London Sp. Pub.*, 268, 1-23.
- Montomoli C., Carosi R., Iaccarino S. 2014. Tectono-metamorphic discontinuities in the Greater Himalayan Sequence and their role in the exhumation of crystalline units. In: Mukherjee S., Carosi R., Mukherjee B., Robinson D. & van Der Beek P. Eds., *Tectonics of Himalayas*. *Geol. Soc. London Sp. Pub.*, 412, in press.

The Au-transporting hydrothermal fluid of the shear syntectonic vein of Dorn, northern Victoria Land (Antarctica)

Garofalo P.S.¹, Crispini L.², Gundlach-Graham A.³, Günther D.³ & Capponi G.²

1. Dipartimento di Biologia, Geologia, Ambiente. Università di Bologna. 2. Dipartimento di Scienze della Terra dell'Ambiente e della Vita, Università di Genova. 3. Department of Chemistry and Applied Biosciences, Trace Element and Microanalysis Group ETH Zurich, Switzerland.

Corresponding email: paolo.garofalo@unibo.it

Keywords: Orogenic gold deposits, Fluid inclusions, LA-ICP-TOFMS.

The quartz-carbonate vein of Dorn is a gold-mineralized, composite shear zone, crosscutting metabasalts of the Glasgow Formation (Bowers Terrane, northern Victoria Land, Antarctica). The established key geological features of this vein (Crispini et al., 2011) show that a) its occurrence is close to a regional tectonic lineament (Leap Year Fault); b) the vein is located within a Barrovian metamorphic sequence; c) the shear zone mineral assemblage is made mostly by quartz and carbonates, and the modal abundance of sulphides (pyrite, arsenopyrite) is quite low; d) a carbonate-sericite-albite-sulphide hydrothermal alteration is well developed adjacent to the vein and postdates Barrovian metamorphism; e) there is a poorly developed mineral and metal zoning within the vein. All points a-e listed above fit the well described characteristics of orogenic gold deposits (Garofalo et al., 2014), and indeed the Dorn vein was interpreted as an orogenic gold vein based on these arguments (cf. Crispini et al., 2011).

In this communication, we will report on a database of fluid inclusion properties from the Dorn vein and will provide a comparison between these properties and those determined in fluid inclusions from economic orogenic veins of other belts. Our dataset determines the properties of the late vein fluid, which formed euhedral quartz crystals within late-stage druses. It combines panchromatic cathodoluminescence imaging of the host quartz, microthermometric determinations, vapour/liquid ratios determined via spindle stage measurements, and chemical analyses of individual inclusions from a prototype Laser Ablation-Inductively Coupled Plasma-Time of Flight Mass Spectrometry (LA-ICP-TOFMS).

Preliminary results show that the fluid inclusions from the euhedral quartz contain an aqueous-carbonic (H₂O-NaCl-CO₂) fluid, in which CO₂ is the main molecular component. The vapour/liquid ratios of individual fluid inclusion assemblages are extremely variable, suggesting heterogeneous entrapment of the vein fluid (phase separation). The bulk salinity of this fluid in individual assemblages is between <1 and 9 mass% NaCl_{eq}, in line with the evidence for heterogeneous entrapment. The temperatures of total homogenization are determined between ~200 and 300 °C, but peak at 280-290 °C. All these properties are consistent with a genesis from an orogenic environment.

Crispini L., Federico L., Capponi G. & Talarico F. 2011. The Dorn gold deposit in northern Victoria Land, Antarctica: Structure, hydrothermal alteration, and implications for the Gondwana Pacific margin: *Gondwana Res.*, 19, 128-140.
Garofalo P.S., Fricker M.B., Guenther D., Bersani D. & Lottici P.P. 2014. Physical-chemical properties and metal budget of Au-transporting hydrothermal fluids in orogenic deposits. In: Garofalo P. S. & Ridley J.R. Eds., *Gold-transporting hydrothermal fluids in the Earth's crust*. *Geol. Soc. Sp. Publ.*, 402, 71-102.

Pressure-temperature-time-deformation path of kyanite-bearing migmatitic paragneiss in the Kali Gandaki valley (Central Nepal): Evidence for Late Eocene-Early Oligocene melting

Iaccarino S.*¹, Montomoli C.¹⁻², Carosi R.³, Massonne H.-J.⁴, Langone A.⁵ & Visonà D.⁶

1. Dipartimento di Scienze della Terra, Università di Pisa. 2. Istituto di Geoscienze e Georisorse, CNR, Pisa. 3. Dipartimento di Scienze della Terra, Università di Torino. 4. Institut für Mineralogie und Kristallchemie, Universität Stuttgart, Germany. 5. Istituto di Geoscienze e Georisorse, CNR, Pavia. 6. Dipartimento di Geoscienze, Università di Padova.

Corresponding email: iaccarino@dst.unipi.it

Keywords: Kyanite-bearing migmatite, *in situ* geochronology, pseudosection modelling.

Kyanite-bearing migmatitic paragneiss of the lower Greater Himalayan Sequence (GHS) in the Kali Gandaki transect (Central Himalaya) was investigated. In such paragneisses, Carosi et al. (2014) found crystallized melt inclusions (“nanogranite”) in garnet. These inclusions suggest the presence of a “high-Ca” melt.

In spite of the intense shearing, it was still possible to obtain fundamental information for the understanding of processes active during orogenesis. Using a multidisciplinary approach, including meso- and microstructural observations, pseudosection modelling (with PERPLE_X), trace element thermobarometry (e.g. Zr-in-rutile) and *in situ* monazite U-Th-Pb geochronology, we constrained the pressure-temperature-time-deformation (P-T-t-D) path of the studied rock, located in a structural key position.

The migmatitic gneiss has experienced protracted prograde metamorphism after the India-Asia collision (50-55 Ma) from ~ 43 Ma to 28 Ma. During the late phase (36-28 Ma), the gneiss underwent high-pressure melting at “near peak” conditions (710-720 °C/1.0-1.1 GPa) leading to kyanite-bearing leucosomes. In the time span of 25-18 Ma, the rock experienced decompression and cooling associated with pervasive shearing reaching P-T conditions of 650-670°C and 0.7-0.8 GPa, near the sillimanite-kyanite transition. This time span is somewhat older than previously reported for this event in the study area. Taking the migmatitic gneiss as representative of the GHS, these data demonstrate that this unit underwent crustal melting at depths of 35 km (~ 1 GPa) in the Eocene-Early Oligocene, clearly before the widely accepted Miocene decompressional melting related to its extrusion. In general, kyanite-bearing migmatite, as reported here, could be potentially linked to the production of “high-Ca” granitic melts found along the Himalayan belt.

Carosi R., Montomoli C., Langone A., Cesare B., Turina A., Iaccarino S., Fascioli L., Visonà D., Ronchi A. & Rai S.M. 2014. Eocene partial melting recorded in peritectic garnets from kyanite-gneiss, Greater Himalayan Sequence, central Nepal. *Geol. Soc. London*, 412, doi:10.1144/SP412.1.

Tectonometamorphic evolution of the Massa Unit in Punta Bianca area (Northern Apennines, Italy)

Iaccarino S., Montomoli C. & Papeschi S.*

Dipartimento di Scienze della Terra, Università di Pisa.

Corresponding email: s.papeschi@gmail.com

Keywords: Metamorphism, geothermobarometry, structural analysis.

The Northern Apennine (Italy) is characterized by the occurrence of low-grade metamorphic units derived from the Adria plate margin, which are the lowermost tectonic units of the apenninic nappe-pile. They are commonly referred to as the Tuscan Metamorphic Units and they comprise the Apuane and Massa units. These units, including basement rocks of Hercynian age and a Mesozoic-Tertiary sequence, were affected by a polyphase tectonic history, during which they reached peak metamorphic conditions and were subsequently exhumed to the surface. New quantitative data about the structural and metamorphic evolution of the Massa Unit cropping out in the Punta Bianca area will be presented. Three main ductile tectonic phases, followed by two brittle and brittle-ductile tectonic events have been recognized. The first tectonic phase (D_1) was related to continental collision and northeastward thrusting. The second tectonic phase (D_2) was linked to the main exhumation stage of the metamorphic rocks, achieved during syn-orogenic extension. The later D_3 phase was related to a renewal of the compressive tectonics. In addition an episode of ductile to brittle NE-thrusting (D_4) is documented before the main event of high-angle normal faulting (D_5). Finite strain analyses were performed on metabreccias and metabasalts with deformed strain-markers (clasts and vesicles), demonstrating that the D_2 phase occurred under general flattening. A study of progressive deformation was performed on vein sets developed in different moments during the tectonic history, allowing to reconstruct a more detailed tectonic evolution and to understand the complex relationships between structural elements formed during different moments of the tectonometamorphic evolution of the area. Microstructural analyses were combined with petrographic studies to reconstruct the P-T path. Synkinematic recrystallization of white micas + chlorite + quartz + albite \pm epidote in metapelites has been recognized along both S_1 and S_2 foliations, developed parallel to F_1 and F_2 folds axial planes respectively.

Electron microprobe X-Ray maps and chemical points highlighted different compositions of white micas and chlorite recrystallized along both S_1 and S_2 foliations. Temperature estimations constrained D_1 phase at 330 ± 10 °C and D_2 phase at 350 ± 5 °C while decreasing pressure values have been detected from D_1 (0.6-0.8 GPa) to D_2 (0.5-0.6 GPa).

Unusual interpretation of the compositional heterogeneity of potassic white mica in low-grade metapsammopelites from Punta Bianca, Tuscany, by integrating petrography, mineral chemistry and thermodynamic modelling

Lo Pò D.*¹, Braga R.¹ & Massonne H.-J.²

1. Dipartimento di Scienze Biologiche, Geologiche e Ambientali, Università di Bologna.
2. Institut für Mineralogie und Kristallchemie, Universität Stuttgart, Germany.

Corresponding email: deborah.lopo@unibo.it

Keywords: Potassic white mica, pseudosection, Northern Apennines.

Potassic white-mica is a widespread phase in very low- to medium-grade metamorphic sediments. It is a fabric-forming mineral, which changes composition in response to P - T variation and contains radiogenic isotopes useful for age dating. For these reasons potassic white-mica is an important source of microstructural, thermobarometric and geochronological information in metapsammopelites. Potassic white-mica from sub greenschist- and greenschist-facies metapsammopelites commonly shows a large compositional spread, for instance, in terms of Si contents, which are frequently P -sensitive. Thus, a large spread of Si in potassic white-mica may indicate large P variations. However, the partial chemical re-equilibration of detrital micas could result in the preservation of a chemical signature unrelated to the actual metamorphic evolution.

We present a petrological study of phyllites from the Variscan basement at Punta Bianca (Northern Apennines, Italy). An integrated approach involving microstructural analysis, X-ray mapping and thermodynamic modelling was carried out to investigate the reasons of the observed white mica compositional heterogeneity. The Punta Bianca phyllites, which are believed to be the result of Alpine and Variscan metamorphism of pre-Carboniferous shales, show the mineral assemblage Fe-chlorite + potassic white-mica + quartz + minor paragonite + accessories. The main foliation is a spaced foliation (S_2) consisting of alternating layers of white mica + chlorite and quartz. Locally, folded relics of an earlier foliation containing white mica and chlorite are preserved within the quartz-rich layers. In addition, large flakes of white mica and chlorite (up to 20 μm thick and 200 μm long) oriented nearly perpendicular to the main foliation can be found in these layers. White mica aligned along S_2 and perpendicular to S_2 (i.e. pre- S_2) is always muscovite-phengite with Si contents per double formula unit (pdfu) between 6.05 and 6.51.

A P - T isochemical phase diagram, calculated for one phyllite, indicates that large potassic white-mica with high Si contents around 6.5 pdfu should occur at pressures higher than 14 kbar in a carpholite-bearing paragenesis. This is in disagreement with the P - T conditions obtained for the main schistosity-forming stage (5-9 kbar and 300-400 °C). The large phengite flakes show a grain-size which is not compatible with the HP - LT conditions suggested by the thermodynamic modelling. Thus, they were interpreted as detrital grains. The compositional heterogeneity of potassic white mica is due to the mechanical re-orientation of detrital grains and early metamorphic micas along S_2 without complete adjustment of their chemistry to the new P - T conditions for the studied Punta Bianca phyllite.

Mountain building processes at oblique subduction zones: clue from 3D numerical models

Malatesta C.*¹, Gerya T.², Crispini L.¹, Federico L.¹ & Capponi G.¹

1. DISTAV, Università di Genova. 2. Institute of Geophysics, ETH-Zurich, Switzerland.

Corresponding email: cristina.malatesta@unige.it

Keywords: Balanced accretion-erosion regime, mountain building, oblique subduction.

Despite subduction zones have been studied for a long time by previous workers, several topics remain still highly debated. Some of them result particularly attractive, such as the accretion or erosive behaviour of the margin, the relationship “subducting slab vs overriding plate deformation”, the role of the upper plate in a subduction system and the evolution of topography on the overriding plate. At oblique subduction zones, the simultaneous action of a trench-normal and a trench-parallel component of convergence produces a complex geological setting, with an equally complex deformational pattern of the upper plate; to give new clue about these important topics, we produced 3D numerical models simulating an oblique convergence between plates.

The numerical code we use solves thermo-mechanical equations with finite differences method and marker-in-cell techniques, combined with a multigrid approach. We mainly simulate intraoceanic subduction processes starting 100-km far from the continental margin; the Pacific-style oceanic crust is layered with a 5 km-thick layer of gabbro overlain by a 3 km-thick layer of basalt. A 1 km-thick sediment layer seals the sequence. We apply velocity vectors on the lateral boundaries of the model; vectors form an angle of 45° with the initial starting point of subduction (weak zone in the lithosphere), producing the oblique convergence. We observe that the accretionary or erosive behaviour of the margin mostly depends on the degree of obliquity of subduction: high oblique subductions favor the formation along the same margin of both erosional and balanced accretion/erosion regimes (Gerya and Meilick, 2011), whereas a small trench-parallel component of velocity promotes the occurrence of a predominant accretion/erosion regime.

Moreover, we observed different behaviours of the upper plate and in particular two main sectors along the plate margin, i.e. a) a sector with mostly stable trench and shortening upper plate, and b) a sector with retreating trench and extending upper plate. The first behaviour (a) occurs where sediment amount in the trench is low causing the indentation of the forearc upper plate and the formation of a topographic relief that is later gradually eroded; here tiny slices of upper plate crust are buried only during the first stages of subduction. The second behaviours (b) occurs where sediment amount increases in the trench and the upper plate crust is dragged downwards into the trench, showing a “plane” topography of the forearc region.

Finally, we will discuss the applicability of our models to natural cases of mountain belt, that developed along the oblique subduction zone of the South-American margin.

Gerya T.V. & Meilick F.I. 2011. Geodynamic regimes of subduction under an active margin: effects of rheological weakening by fluids and melts. *J. Metamorph. Geol.*, 29, 7-31.

The high-pressure Fe-Mn metacherts of the Aosta valley: a key to the metamorphic evolution of the Piemonte Nappe

Martin S.*¹, Tumiati S.², Godard G.³, Toffolo L.¹ & Nestola F.¹

1. Dipartimento di Geoscienze, Università di Padova. 2. Dipartimento di Scienze della Terra "A. Desio", Università di Milano. 3. Institut de Physique du Globe de Paris, Université Paris Diderot, France.

Corresponding email: silvana.martin@unipd.it

Keywords: Fe-Mn metacherts, Piemonte nappe, high-pressure metamorphism.

The Piemonte nappe (Italian Western Alps) is a composite system of various units composed of metaophiolites and metasediments. The Fe-Mn metacherts are common in the Piemonte nappe, and are usually transposed with mafic and ultramafic rocks derived from the Tethys oceanic floor and re-equilibrated at different metamorphic conditions. This nappe comprehends at least two lithologically different units, the Zermatt Saas and Combin-Tsatè units, characterized by eclogite-facies and blueschist/greenschist-facies metamorphism, respectively. Recent studies suggest that other tectonic units could be recognized in this nappe, on the basis of the characteristics of the metacherts associated to the metaophiolites. In particular, the minerals and fluid inclusions preserved in the Mn-rich garnet of the metacherts have been proven to be a powerful tool for highlight differences in metamorphic evolution.

Mn-rich metacherts typically include spessartine garnets. The eclogite-facies spessartine garnet from Cignana (Valtournanche) is also pyrope-rich and encloses coesite and diamond (Frezzotti et al., 2014), indicating UHP conditions. The eclogite-facies metacherts of Praborna (Saint-Marcel), besides many other Mn minerals, show garnets of complex compositions (spessartine, calderite, grossular, andradite, and minor pyrope endmembers), Mn-rich omphacite (violan) and the pyroxmangite, indicating HP conditions (Tumiati et al., 2014). The Castelstrutto metacherts (Piemonte nappe), transposed with metaophiolites, also show layers rich in spessartine garnet associated with quartz, white mica and titanite. This mineral assemblage indicates blueschist/eclogite-facies conditions. Metacherts of the Piemonte nappe at Varenche (Saint-Barthélémy valley) show a blueschist/greenschist-facies metamorphism. Other metacherts from the Piemonte nappe, i.e. Lago Nero (Val di Susa), Lago Blu (Val Varaita), Val Chisone and Queyras (Briançon zone), where garnet can include prograde sursassite, show a very low-T blueschist imprint (Martin & Lombardo, 1995).

Alpine metacherts are exceptionally interesting rocks, capable to record the composition of the Tethyan sediments, the hydrothermal processes occurred on the ocean floor and the conditions of the subduction process during Alpine orogenesis.

Frezzotti M.-L., Huizenga J.-M., Compagnoni R. & Selverstone J. 2014. Diamond formation by carbon saturation in C–O–H fluids during cold subduction of oceanic lithosphere. *Geochim. Cosmochim. Acta*, 143, 68-86.

Martin S. & Lombardo B. 1995. Sursassite, spessartine, piemontite in Fe-Mn metacherts from Lago Bleu, upper Val Varaita (western Alps). *Boll. Mus. Reg. Sci. Nat. Torino*, 13, 103-130.

Tumiati S., Godard G., Martin S., Malaspina N. & Poli S. 2014. Ultra-oxidized rocks in subduction mélanges? Decoupling between oxygen fugacity and oxygen availability in a Mn-rich metasomatic environment. *Lithos*, doi:10.1016/j.lithos.2014.12.008.

Structural and petrological features of the central-eastern Nepalese Himalaya

Mosca P.*¹, Groppo C.¹⁻², Rapa G.² & Rolfo F.¹⁻²

1. Istituto di Geoscienze e Georisorse, CNR, Torino. 2. Dipartimento di Scienze della Terra, Università di Torino.

Corresponding email: p.mosca@csg.to.cnr.it

Keywords: Himalaya, central-eastern Nepal, geological setting.

The metamorphic core of the central-eastern Nepalese Himalaya (from the Sikkim border to Langtang) consists of the Greater Himalayan Sequence (GHS), bounded to the north by the South Tibetan Detachment System (STDS) and overlying the Lesser Himalayan Sequence (LHS) along the Main Central Thrust zone (MCTZ) to the south. This contribution presents the main geological features of this region and discusses them in the regional tectonic scenario. The GHS can be divided into a lower (GHS-L) and an upper (GHS-U) portion (e.g. Mosca et al., 2014). The GHS-L is mainly made of Grt ± St ± Ky -bearing two-micas schist, associated to two-micas quartzitic gneiss and phylladic micaschist and shows evidence of partial melting in the uppermost levels. The GHS-U consists of Grt + Bt + Kfs + Ky/Sil anatectic paragneiss and Kfs + Bt + Sil ± Grt paragneiss with Qtz + Sil nodules, intruded upsection by networks of leucogranitic and pegmatitic dikes. Calc-silicate rocks are widespread through the whole GHS. The LHS is typically represented by low-grade quartz-sericite schists and phyllite, intercalated with massive quartzite (± Grt, ± Ctd), and passing upsection to strongly mylonitic orthogneiss. Even if the whole metamorphic core shows a pervasively distributed ductile shear, the MCTZ identifies a several km-thick shear zone characterized by a top-to south ductile shearing and roughly centred on the GHS-L. The MCTZ is internally imbricated, resulting in the juxtaposition of rocks characterized by different P-T evolutions and T/depth gradients. Evidences of late extension can be identified in the MCTZ and particularly in the upper GHS-U. The overall geometries of calculated P-T paths and the regional structural framework suggest that from a petrological point of view the Channel Flow model is a suitable way to explain the main processes operating during the exhumation of the high-grade rocks between the MCTZ and the STDS (Rolfo et al., 2014). However, a more detailed knowledge of the relationship between kinematic and timing of shear zones and their associated metamorphism is needed to constrain this – as well as any other - type of model.

Mosca P., Groppo C. & Rolfo F. 2014. The geology between Khimti Khola and Likhu Khola valleys: a field trip along the Numbur Cheese Circuit (central-eastern Nepal Himalaya). In: Montomoli C., Carosi R., Law R., Singh S. & Man Rai S. Eds., Geological field trips in the Himalaya, Karakoram and Tibet. *J. Virtual Explorer*, 47, DOI:10.3809/jvirtex.vol.2014.047.

Rolfo F., Groppo C. & Mosca P. 2014. Petrological constraints of the "Channel Flow" model in eastern Nepal. In: Mukherjee S., Carosi R., van der Beek P.A., Mukherjee B.K. & Robinson D.M. Eds., *Tectonics of the Himalaya*. Geol. Soc. London Sp. Publ., 412, doi:10.1144/SP412.4.

Preliminary new stratigraphic, biostratigraphic and structural data on the Boeotian Flysch (Boeotia and Parnassus, central Greece)

Nirta G.¹, Montanari D.², Moratti G.*², Papini M.¹, Piccardi L.², Carras N.³, Catanzariti R.⁴, Moraiti E.³ & Valleri G.¹

1. Dipartimento di Scienze della Terra, Università di Firenze. 2. Istituto di Geoscienze e Georisorse, C.N.R. Firenze. 3. Institute of Geology and Mineral Exploration, Athens, Greece. 4. Istituto di Geoscienze e Georisorse, C.N.R. Pisa.

Corresponding email: giovanna.moratti@cnr.it

Keywords: Boeotian Flysch, biostratigraphy, structural evolution.

Ophiolitic rocks crop out along the Dinaric-Hellenic collisional belt arranged as discontinuous large bodies encompassing more than 1000 km in length along the orogen. The current position of these rocks onto the Adria continental crust is commonly regarded as the consequence of Early Jurassic convergence between Adria and Eurasia which eventually led to intraoceanic subduction and finally to westward obduction of portions of the Western Tethys oceanic lithosphere onto the Adria continental margin, with strong impact on its sedimentary and structural evolution. Obduction led to flexure of the underlying lithosphere that progressively controlled sedimentation into deep basins facing the advancing ophiolite slab. Basin deepening and accumulation of ophiolite-bearing mass flow deposits marked progressive ophiolite emplacement onto the Adria continental margin. The older, and well-developed, ophiolite-derived clastic sediments in the continental margin environment are represented by the so-called Boeotian Flysch of Late Jurassic-Early Cretaceous age. Sedimentary hiatuses, syn-sedimentary deformations and high facies variability characterizing this succession can be interpreted as the beginning of deformation in the Basins facing the advancing ophiolitic thrust sheet. A detailed knowledge of the age, stratigraphy and deformation history of this syn-tectonic flysch deposit allows definition of the chronology of the early phases of continental stage of obduction and the following continental collision between Adria and Eurasia. This paper reports preliminary new data on biostratigraphy, stratigraphy and structural evolution concerning the Boeotian Flysch cropping out in the key outcrops of Levadia and Amfiklia areas (Boeotia and Parnassus, Central Greece). These new data obtained for the Boeotian flysch succession provide a more accurate definition of the obduction mechanism at the Jurassic-Cretaceous transition in the eastern continental margin of the Adria plate.

High-pressure metamorphism in Antarctica as marker of different palaeo-subduction zones: a review between history and scientific research

Palmeri R.*¹, Di Vincenzo G.², Godard G.³, Sandroni S.¹, Talarico F.^{1,4} & Ricci C.A.^{1,4}

1. Museo Nazionale dell'Antartide - Sezione Scienze della Terra, Università di Siena. 2. Istituto di Geoscienze e Georisorse, CNR, Pisa. 3. Institute de Physique du Globe, Paris Sorbonne, France. 4. Dipartimento di Scienze Fisiche, della Terra e dell'Ambiente, Università di Siena.

Corresponding email: rosaria.palmeri@unisi.it

Keywords: Antarctica, Gondwana, High-Pressure rocks.

After the emergence of the plate tectonics theory in the 1960's, the high-pressure (HP) and ultrahigh-pressure (UHP) metamorphic rocks appeared to be typical of subduction zones, where the oceanic or continental lithosphere is submitted to the high-*P* low-*T* gradient necessary to their formation. Nowadays, when HP/UHP rocks delineate a trail within an orogenic belt, they are considered as the markers of a palaeo-subduction zone that has evolved into a suture zone during a continental collision. Hence, HP/UHP metamorphic rocks are useful for reconstructing the evolution of the past continents and orogenies. Antarctica is a continent to which applying this approach is difficult as its geological knowledge is incomplete, mostly because of the ice sheet that covers 98% of its surface. Notwithstanding this difficulty, Antarctica has been considered a key piece (Du Toit, 1937) for every reconstruction of the continents since the Archaean Eon, particularly the Rodinia and Gondwana supercontinents. Antarctica resulted from a collage of different terranes assembled at some stages in the geological past (Boger, 2011). It includes old Archean nuclei onto which were accreted Proterozoic terranes in the course of several collisional orogenies, as the Grenvillian (~1300–900 Ma) and Pan-African (~600–500 Ma) orogens, as well as during the subduction-accretion orogens that took place more recently at the palaeo-Pacific margin of Gondwana/Antarctica, from the Cambro-Ordovician (Ross–Delamerian orogen) to the Cretaceous-Cenozoic (Andean orogen) times. These events have generated eclogite and other HP/UHP metamorphic rocks, to which little attention has been paid till now (Godard & Palmeri, 2013).

Here, we focus our attention on the Cambro-Ordovician Ross–Delamerian orogen at northern Victoria Land (NVL) and on the Pan-African/Grenvillian orogens at the Shackleton Range (SR) and Dronning Maud Land (DML). At Lanterman Range (NVL), well-preserved eclogite-facies rocks were discovered during the 1993-94 Italian expedition (Ricci et al., 1996). They represent the only known HP/UHP record of the Antarctic palaeo-Pacific margin of Gondwana. At SR and DML, new data on mafic–ultramafic rocks suggest that HP metamorphism developed before granulite/amphibolite-facies stages. New data testify to HP metamorphism in the ophiolite sequence of SR, attributed to the Pan-African orogen (Talarico et al., 1999), whereas at DML, the HP conditions may reflect either Grenvillian or Pan-African orogenic activity.

Boger S.D. 2011. Antarctica, before and after Gondwana. *Gondwana Res.*, 29, 335-371.

Du Toit A.L. 1937. Our wandering continents an hypothesis of continental drifting. Oliver & Boyd Eds., Edinburgh.

Godard G. & Palmeri R. 2013. High-pressure metamorphism in Antarctica from the Proterozoic to the Cenozoic: a review and geodynamic implications. *Gondwana Res.*, 23, 844-864.

Ricci C.A., Talarico F., Palmeri R., Di Vincenzo G. & Pertusati P.C. 1996. Eclogite at the Antarctic palaeo-Pacific active margin of Gondwana (Lanterman Range, northern Victoria Land, Antarctica). *Antarctic Sci.*, 8, 277-280.

Talarico F., Kleinschmidt G. & Henjes-Kunst F. 1999. An ophiolitic complex in the northern Schackleton Range, Antarctica. *Terra Antarctica*, 6, 292-315.

HP/UHP metamorphic and structural evolution of subducted rodingites from the upper Valtournanche, Western Alps, Italy

Rebay G.*¹, Zanoni D.² & Spalla M.I.²

1. Dipartimento di Scienze della Terra e dell'Ambiente, Università di Pavia.
2. Dipartimento di Scienze della Terra "A. Desio", Università di Milano.

Corresponding email: gisell.rebay@unipv.it

Keywords: HP/UHP rodingites, structural and metamorphic evolution, Zermatt-Saas.

Rodingites associated with serpentinites are usually derived from metasomatic ocean floor processes. Even if rodingitisation can also happen in subduction environments, re-structuration and metamorphic transformations involving rodingites within a convergent system are generally neglected. Former studies on rodingites from the Alpine belt described rodingitic mineral assemblages as metasomatic relicts, until Dal Piaz (1967) pointed out that rodingites were widely re-equilibrated during Alpine HP metamorphic evolution together with their country rocks.

Multiscale structural and petrologic analyses were combined to define the HP mineral assemblages in the boudinaged rodingites of the upper Valtournanche, embodied in HP/UHP partly de-hydrated serpentinites of Zermatt-Saas Zone. On the basis of different parageneses and their modal amount, three types of rodingite are distinguished: epidote-, garnet-chlorite-clinopyroxene-, and vesuvianite-bearing rodingites (Zanoni et al., 2012). They derive from ocean floor metasomatism of former gabbro dykes intruded in mantle rocks. Serpentinites and rodingites record 3 syn-metamorphic stages of ductile deformation after the ocean floor history. D1 and D2 developed under HP to UHP conditions and D3 under lower pressure conditions. Syn-D2 assemblages in rodingites are interpreted as developed under the same HP/UHP conditions already inferred in serpentinites (2.5 ± 0.3 GPa and 600 ± 20 °C, Rebay et al., 2012): Ep2, Cpx2, Mg-Chl2, Sph1, \pm Grt2, \pm Tr1 in Ep-bearing rodingites; Mg-Chl2, Grt2, Cpx2, \pm Ves2, \pm opaque minerals, in Grt-Chl-Cpx-bearing rodingites; Ves2, Mg-Chl2, Cpx2, Grt2, \pm Sph1, \pm Ep1 in Ves-bearing rodingites. Thermodynamic modelling in Ep- and Grt-Chl-Cpx-bearing rodingites confirms the P-T range inferred in the associated serpentinites. Pre-D1 Cr-rich spinel and cm-sized Cpx porphyroclasts are interpreted as igneous relicts, whereas Cr-rich garnet and Cr-Ti-Ca-rich vesuvianite as developed during oceanic metasomatism. Distinct chemical compositions characterise the same minerals recrystallised during the Alpine subduction.

Multiscale structural analysis shows that the dominant structural and metamorphic imprint of the Valtournanche eclogitised rodingites developed during the Alpine subduction and that, in the favourable bulk composition (Ca-rich), vesuvianite is stable up to the estimated P-climax metamorphic conditions.

Dal Piaz G.V. 1967. Le "granatiti" nelle serpentine delle Alpi occidentali italiane. Mem. Soc. Geol. Ital., 6, 267-313.

Rebay G., Spalla M.I. & Zanoni D. 2012. Interaction of deformation and metamorphism during subduction and exhumation of hydrated oceanic mantle: insights from the Western Alps. J. Metam. Geol., 30, 687-702.

Zanoni D., Rebay G., Bernardoni J. & Spalla M.I. 2012. Using multiscale structural analysis to infer high-/ultrahigh-pressure assemblages in subducted rodingites of the Zermatt-Saas Zone at Valtournanche. J. Virtual Expl., 41, paper 6.

Cold subduction processes in the western Himalaya (Ladakh, NW India): petrological constraints from lawsonite-blueschist facies metasediments

Rolfo F.*¹, Groppo C.¹, Sachan H.K.² & Rai S.K.²

1. Dipartimento di Scienze della Terra, Università di Torino. 2. Wadia Institute of Himalayan Geology, Dehra Dun, India.

Corresponding email: franco.rolfo@unito.it

Keywords: Lawsonite-blueschist facies metamorphism, cold subduction processes, western Himalaya.

High pressure metamorphic rocks are scanty in the Himalayan collisional orogen. Beside rare eclogite (Lombardo & Rolfo, 2000), few blueschist occur along the Yarlung-Tsangpo Suture (ITS), i.e. the suture marking the India-Asia collision. Save for a recent paper on blueschist from the far eastern Himalaya (Ao & Bhowmik, 2014), modern petrologic studies on the relatively more abundant blueschist from the western Himalaya are still lacking.

The best occurrence of blueschist in the western Himalaya is that of the Shergol ophiolitic mélange, which outcrops over a distance of 250 km along the ITS. Blueschist lithologies are heterogeneous and dominated by volcanoclastic sequences rich in mafic material with subordinate interbedding of metasediments. Prior to this study, P-T estimates based on conventional thermobarometry suggested $T = 350\text{-}420\text{ }^{\circ}\text{C}$ and $P = 9\text{-}11\text{ kbar}$ (Honegger et al., 1989).

West of the village of Tringo, blueschist facies metasediments are particularly abundant and suitable for petrologic modeling. They show the typical Lws-blueschist (LBS) facies assemblage $\text{Qtz} + \text{Phe} + \text{Lws} + \text{Na-Amp} + \text{Grt}$. Lws and strongly zoned Grt porphyroblasts overgrow the main foliation defined by high-celadonite Phe ($\text{Si} \geq 3.83\text{ a.p.f.u.}$). Petrologic results obtained from pseudosection calculations in the MnNCKFMASH model system constrain peak-P-T conditions to $430\text{-}470\text{ }^{\circ}\text{C}$, $18\text{-}19\text{ kbar}$, i.e. at significantly higher P than previously estimated. The following exhumation still occurred in the LBS-facies field, allowing the preservation of Lws.

Petrologic modeling also suggests a very moderate effect of Fe^{3+} in the system, as well as significant addition of H_2O near peak conditions to allow Lws formation.

According to the reconstructed P-T evolution, the Shergol blueschists are the result of cold subduction along a very low to low thermal gradient ("early" prograde: ca. $5\text{ }^{\circ}\text{C}/\text{km}$; "late" prograde: ca. $7\text{-}8\text{ }^{\circ}\text{C}/\text{km}$). Such a low geothermal gradient was followed also during exhumation, in order to preserve lawsonite in the studied lithologies. This P-T evolution is consistent with a mature subduction zone system in an intra-oceanic subduction setting, as also suggested by Ao & Bhowmik (2014) for blueschist from the far eastern Himalaya.

- Ao A. & Bhowmik K. 2014. Cold subduction of the Neotethys: the metamorphic record from finely banded lawsonite and epidote blueschists and associated metabasalts of the Nagaland Ophiolite Complex, India. *J. Metam. Geol.*, 32, 829-860.
- Honegger K., Le Fort P., Mascle G. & Zimmerman J.L. 1989. The blueschists along the Indus Suture Zone in Ladakh, NW Himalaya. *J. Metam. Geol.*, 7, 57-72.
- Lombardo B. & Rolfo F. 2000. Two contrasting eclogite types in the Himalayas: implications for the Himalayan orogeny. *J. Metam. Geol.*, 30, 37-60.

Lawsonite-bearing HP metabasite associated with eclogite in the Voltri Massif (Ligurian Alps, Italy): constraints for the geodynamic evolution

Scarsi M.* & Malatesta C.

Dipartimento di Scienze della Terra dell'Ambiente e della Vita, Università di Genova.

Corresponding email: marco.scarsi@edu.unige.it

Keywords: Lawsonite blueschist, exhumation, Voltri Massif.

Lawsonite-bearing HP metamorphic rocks have been reported throughout the Alpine orogen and their importance has been broadly highlighted in literature (Brovarone et al., 2014 and references therein).

Moreover the occurrence of Lws-bearing HP metamorphic rocks associated with eclogite facies rocks could give important constraints on the coupling mechanisms between different tectono-metamorphic slivers in subduction zones and on the interaction with fluids along the subducting slab.

In this work, we present a detailed study of the field and metamorphic features of an area at the eastern border of the Voltri Massif (Ligurian Alps, Italy) characterized by Lws-bearing blueschist metabasite associated with eclogite. The Voltri Massif occurs at the eastern end of the Western Alps and in the study area is characterized by ocean-, continental- and mantle-derived slices of tectometamorphic units involved in the Alpine orogeny.

We focus on a newly discovered plurimetric lens of Lws-bearing HP metabasite, accompanied by metasediment, embedded in a highly sheared serpentinite that separates the metabasite lens from an eclogite lens and small slices of metamorphic dolostones.

The Lws-bearing metabasite displays a mylonitic texture and shows alternating green and blue layers, most likely reflecting a compositional layering. The associated metasediment is a Gln-bearing qtz-calcschist and serpentinite shows a pervasive mylonitic texture with abundant carbonate.

The preliminary structural study pointed out the occurrence of at least three synmetamorphic deformational events, responsible for the formation of compositional layering and of the mylonite, with multiple schistositys and shear bands.

The main mylonitic foliation in the metabasite, appears to be parallel to the compositional layering and is defined by a composite fabric with syn-kinematic $\text{Agt} \pm \text{Grt} + \text{Rt} + \text{opaque}$ minerals, representing the peak metamorphic assemblage; some relics of Di are preserved along the foliation.

The peak metamorphic assemblage is synkinematically replaced by $\text{Gln} + \text{Ep} + \text{Ttn} + \text{Grt} + \text{Lws} + \text{opaque}$ minerals. A subsequent retrogressive stage is associated to the syn-kinematic growth of $\text{Alb} + \text{Ep} + \text{Chl}$ replacing former minerals.

The structural features and architecture of the study area together with the different metamorphic characteristics of the associated tectometamorphic slices supply information and clue for the geodynamic evolution of this sector of the Alpine orogen.

Brovarone V.A., Picatto M., Beyssac O., Lagabrielle Y. & Castelli D. 2014. The blueschist-eclogite transition in the Alpine chain: P-T paths and the role of slow-spreading extensional structures in the evolution of HP-LT mountains belts. *Tectonophysics*, 615-616, 96-121.

The Silurian beds of the Calabria-Peloritani Southern Subterrane (southern Italy)

Somma R.*¹, Navas-Parejo P.², Martín-Algarra A.³, Rodríguez-Cañero R.³, Sanchez-Navas A.⁴,
Cambeses A.⁴, Scarrow J.H.⁴ & Perrone V.⁵

1. Dipartimento di Scienze dell'Ambiente, della Sicurezza, del Territorio, degli Alimenti e della Salute (S.A.S.T.A.S.), Università di Messina. 2. Estación Regional del Noroeste, Instituto de Geología UNAM, Hermosillo, Mexico. 3. Departamento de Estratigrafía y Paleontología, Universidad de Granada, España. 4. Departamento de Mineralogía y Petrología, Universidad de Granada, España. 5. Dipartimento di Scienze della Terra, della Vita e dell'Ambiente, Università di Urbino

Corresponding email: rsomma@unime.it

Keywords: Variscan Intra-Alpine terranes, Calabria-Peloritani Terrane, Silurian.

Recent lithostratigraphic, conodont biostratigraphic, and geochronological analyses have been carried out in several Variscan Intra-Alpine terranes preserved in the Calabria-Peloritani Terrane of southern Italy (Navas-Parejo et al., 2009a, 2009b; Somma et al., 2013). Particularly, in the Peloritani Mts. (NE Sicily), three main formations have been conscientiously dated in the Longi-Taormina Unit basement (from base to top): the Castelmola Formation, the Lower Pizzo Leo Formation, and the Upper Pizzo Leo Formation (Somma et al., 2013). The lowermost formation is formed by marine fine-grained siliciclastic beds hosting calc-alkaline volcanites. Recent geochronological analyses performed on these volcanites, using Zircon SHRIMP U-Pb dating, indicated an early Silurian age (Martín-Algarra et al., 2014). The intermediate formation is also volcano-clastic and is composed of analogous marine siliciclastic beds but with intercalations of alkaline volcanites. Recent lithostratigraphic correlations and conodonts findings indicated a Silurian age for this formation (Rodríguez-Cañero et al., 2013). The uppermost formation is constituted by pelagic carbonates with minor fine-grained siliciclastic intercalations. The age of the Upper Pizzo Leo Fm, based on conodonts, ranges from the late Silurian to the Early Devonian. The present research allowed: *i*) to reconstruct the stratigraphic record from the Silurian up to the Early Devonian, notwithstanding the effects of Variscan metamorphism and Alpine tectonics; and *ii*) to evidence that the oldest Palaeozoic beds ever dated in this sector of the Variscan Intra-Alpine terranes are Silurian in age.

- Martín-Algarra A., Somma R., Navas-Parejo P., Rodríguez-Cañero R., Sanchez-Navas A., Cambeses A., Scarrow J.H. & Perrone V. 2014. The geodynamics of northern Gondwana: evidence from Paleozoic volcanic-sedimentary evolution of the Calabria-Peloritani terrane, southern Italy. *Gondwana* 15, Madrid (Spain) 14-18 July 2014, 107.
- Navas-Parejo P., Rodríguez-Cañero R., Somma R., Martín-Algarra A. & Perrone V. 2009a. The Frasnian Upper Kellwasser event and a lower Famennian stratigraphic gap in Calabria (southern Italy). *Palaeobio. Palaeoenv.*, 89, 111-118. DOI 10.1007/s12549-009-0006-4.
- Navas-Parejo P., Somma R., Martín-Algarra A., Perrone V. & Rodríguez-Cañero R. 2009b. First record of Devonian orthoceratid-bearing limestone in southern Calabria (Italy). *Comptes Rendus Palevol.*, 8, 365-373. DOI: 10.1016/j.crpv.2009.01.001.
- Rodríguez-Cañero R., Navas-Parejo P., Somma R., Martín-Algarra A. & Perrone V. 2013. First finding of upper Silurian and Lower Devonian conodonts from the Peloritani Mountains (NE Sicily, southern Italy). *Boll. Soc. Paleont. It.*, 52, 1-9. DOI: 10.4435/BSPI.2013.15.

Mantle-cover sequence in the Western Alps metaophiolites: a key to recognize remnants of an exhumed Oceanic Core Complex (OCC)

Tartarotti P.*¹, Festa A.², Benciolini L.³ & Balestro G.²

1. Dipartimento di Scienze della Terra "Ardito Desio", Università di Milano. 2. Dipartimento di Scienze della Terra, Università di Torino. 3. Dipartimento di Chimica, Fisica e Ambiente, sezione Georisorse e Territorio, Università di Udine.

Corresponding email: paola.tartarotti@unimi.it

Keywords: Western Alps ophiolites, ophicarbonated breccia, Oceanic Core Complex.

Alpine ophiolites represent the sutured Jurassic Tethys ocean interposed between the European and African plates. They mostly consist, similarly to modern oceanic lithosphere at slow spreading ridges, of mantle peridotites intruded by gabbros sealed by basaltic lavas and sediments (e.g., Lagabrielle & Cannat, 1990). A true sheeted dike complex has never been recognized. In modern slow spreading ridge systems, mantle rocks and gabbros are commonly exposed at the seafloor along detachment shear zones which exhume Oceanic Core Complexes (OCC). In the hangingwall of detachment faults, syn-tectonic sediments bearing mafic/ultramafic breccias unconformably rest atop mantle rocks or ophicarbonated breccias. In the southern Aosta valley, the Mount Avic serpentinite massif is interpreted as a fossil OCC (Fontana et al., 2013), as attested by the occurrence of ophicarbonated breccias (Tartarotti et al., 1998 and refs.). In the nearby Champorcher valley a primary mantle-cover sequence is tentatively reconstructed. Here, massive to mylonic serpentinite pass upward to ophicarbonated breccias covered by carbonate-rich serpentinitic metarenites and by a chaotic rock unit on which calcschists, embedding cm-sized clasts of actinolite/tremolite-schists, rest unconformably. The chaotic rock unit has a block-in-matrix fabric with rounded to irregularly-shaped blocks of serpentinite, cm-to several dm in size, randomly distributed within a matrix of foliated impure marbles and calcschists. The internal fabric of this metasedimentary succession is well consistent with mass-transport processes related to an active tectonic setting in which mantle rocks were progressively and continuously exhumed by faulting. This mantle-cover sequence may represent part of the Mount Avic OCC documenting, as for Balestro et al. (2015) for the Monviso meta-ophiolite Complex, one of the first examples of remnants of OCCs preserved in exhumed eclogitic ophiolites. The correct interpretation of this mantle-cover sequence is crucial for better interpreting intra-oceanic processes that controlled the Tethys ocean floor evolution during the Jurassic extensional stage.

Balestro G., Festa A. & Tartarotti P. 2015. Tectonic significance of different block-in-matrix structures in exhumed convergent plate margins: examples from oceanic and continental HP rocks in Inner Western Alps (northwestern Italy). *Intern. Geol. Rev.*, 57, 581-605, doi:10.1080/00206814.2014.943307.

Fontana E., Tartarotti P., Panseri M. & Buscemi S. 2013. Geological map of the Mount Avic massif (Western Alps ophiolites): Is it a fossil Oceanic Core Complex? *Rend. Online SGI*, 29, 237.

Lagabrielle Y. & Cannat M. 1990. Alpine Jurassic ophiolites resemble the modern central Atlantic basement. *Geology*, 18, 319-322.

Tartarotti P., Benciolini L. & Monopoli B. 1998. Breccie serpentinitiche nel massiccio ultrabásico del Monte Avic (falda Ofiolitica Piemontese): possibili evidenze di erosione sottomarina. *Atti Tic. Sci. Terra*, 7, 73-86.

The Cogne magnetite-bearing ultramafic body (NW Italian Alps): a metasomatized slice of oceanic lithosphere

Toffolo L., Martin S.* & Nimis P.

Dipartimento di Geoscienze, Università di Padova.

Corresponding email: silvana.martin@unipd.it

Keywords: Cogne, magnetite, metasomatism.

The Cogne magnetite deposit (Valle d'Aosta, Italy) is hosted by a 2.5 km long serpentinite lens, which is part of the Piemonte ophiolite nappe (NW Alps). Both the tectonometamorphic history of the Cogne serpentinite and the origin of the magnetite are not exhaustively understood. The Cogne serpentinite lens, which outcrops on the sides of the Montzalet, is embedded between a calcschist sequence on the hangingwall and meta-dolostones on the footwall, to which it is juxtaposed by a tectonic contact (Elter, 1971). The serpentinite and the calcschists belong to the blueschist Aouilletta Unit, while the meta-dolostones belong to the greenschist Cogne Unit (Dal Piaz et al., 2010).

The Cogne mine exploited two pure magnetite (Cr, V, Ti in traces) orebodies: (i) Liconi-Colonna-Costa del Pino and (ii) Larsinaz, which outcrop respectively S-SE and W of the Montzalet. They show heterogeneous parageneses: in (i), magnetite is associated with antigorite, carbonates (calcite, magnesite, dolomite), prograde olivine, brucite (\pm lizardite \pm Ti-clinohumite \pm diopside and andradite); in (ii), magnetite occurs in antigorite-only or diopside-rich (\pm lizardite \pm chlorite \pm antigorite) rocks crosscut by frequent veins of diopside (\pm chlorite \pm antigorite). Another serpentinite outcrop is located on the western side of the Montzalet, ca. 300 m above (ii), in the niche of Truc Cretetta post-glacial landslide: here magnetite is associated with diopside (\pm lizardite \pm olivine \pm Ti-clinohumite) and locally with chalcopyrite.

Petrographic and chemical data suggest the following sequence of events: (1) early seafloor alteration of peridotites, which originated lizardite pseudomorphs after olivine and pyroxene together with minor magnetite; (2) a subsequent hydrothermal metasomatic event, responsible for the deposition under static conditions of abundant magnetite coexisting with chlorite (\pm uraninite; \pm calcite \pm brucite, in site (i); \pm andradite, in site (ii)) and, later, with diopside (\pm chlorite \pm antigorite); (3) prograde subduction metamorphism, which caused the replacement of lizardite by antigorite and successively the stabilization of olivine at the expense of antigorite.

Further studies will be aimed at constraining the physico-chemical characteristics of the metasomatizing fluid/s and to evaluate the conditions of alpine metamorphism.

Dal Piaz G.V., Gianotti F., Monopoli B., Pennacchioni G., Tartarotti P. & Schiavo A. 2010. Note illustrative della Carta Geologica d'Italia alla scala 1:50.000 Chatillon F. 91. Ispra-Servizio Geologico d'Italia, Treviso, 152 p.

Elter G. 1971. Schistes lustrés et ophiolites de la zone piémontaise entre Orco et Doire Baltée (Alpes Graies). Hypothèse sur l'origine des ophiolites. Géol. Alpine, 47, 147-169.

SESSIONE S2

Mantle processes and crustal genesis in extensional environments

CONVENORS

Elisabetta Rampone (Univ. Genova)

Paola Tartarotti (Univ. Milano)

Alberto Zanetti (CNR Pavia)

The Oligo-Miocene alkaline volcanism of Bahariya (Western Desert, Egypt)

Agostini S.^{*1}, Ronca S.², Bellon H.³, Luciani N.² & Lustrino M.²

1. Istituto di Geoscienze e Georisorse, C.N.R. Pisa. 2. Dipartimento di Scienze della Terra, Sapienza Università di Roma. 3. Faculté des Sciences et Techniques, Université de Bretagne Occidentale, Brest, France.

Corresponding email: s.agostini@igg.cnr.it

Keywords: African Plate, alkali basalts, isotope geochemistry.

Late Oligocene-Early Miocene volcanic rocks around the Bahariya Oasis in the Western Desert, Egypt occur as basaltic lava flows, subvolcanic sills and necks in an area of approximately 1800 km². Five new K-Ar age cluster in a relatively narrow range from 23.9 to 20.7 Ma. Bahariya rocks are mildly alkaline basic in terms of silica content (SiO₂ ranging from 48.4 to 51.4 wt.%), with total alkali content ranging from 4.9 to 5.9 wt.%, and variable amounts of normative nepheline. The samples are essentially sodic (Na₂O-K₂O > 2) and can be classified as alkali basalts, hawaiites or mugearites. Only the samples from one locality (Qala Siua) can be classified as K-trachybasalts. Samples are usually porphyritic, with phenocryst assemblage made by olivine + clinopyroxene + plagioclase, and the same minerals along with alkali feldspar, ilmenite, Ti-magnetite, and eventually intersertal glass in the groundmass. Samples from Qala Siua can be distinguished also by their petrography, being plagioclase present only in the groundmass. All the samples have slightly fractionated REE patterns with (La/Yb)_N ≈ 10-18, and no Eu anomaly. Primitive mantle-normalized patterns are bell-shaped, with positive Nb and Ta anomalies, which are more pronounced of Qala Siua samples, and small troughs for Zr and Hf.

The ¹⁴³Nd/¹⁴⁴Nd initial isotopic ratios are high and constant (≈ 0.51295 for all the samples), whereas some variations are revealed by ⁸⁷Sr/⁸⁶Sr ratios, which are around 0.7028 for two samples, and 0.7036 for the most evolved sample of Bahariya volcanic field. The ²⁰⁶Pb/²⁰⁴Pb isotope ratios vary from 19.19 to 19.31 and are negatively correlated with the SiO₂ content.

Summing up, all the petrographic, geochemical and isotopic characters of studied rocks, are typical of within plate magmas, sourced in a depleted asthenospheric mantle unaffected by any subduction imprint. Their composition fully overlap the field of the other rocks of the Circum-Mediterranean anorogenic Cenozoic igneous rocks (CiMACI Province). Their relationships with coeval extensional faulting, characterized by NE directed faults, may indicate that these magmas were erupted in an incipient intracontinental rift, with no geochemical evidence for the involvement of any deeper mantle sources.

Rethinking mantle heterogeneity: insights into mantle geology

Armienti P.¹ & Gasperini D.²

1. Dipartimento di Scienze della Terra, Università di Pisa. 2. Datageo SrL, Navacchio, Pisa.

Corresponding email: pietro.armienti@unipi.it

Keywords: Chaos, mantle, mantle components.

The Earth's mantle structure is here investigated by extending methods of non-linear analysis to the geochemical composition of Ocean Island Basalts. The intrinsic geochemical organization of the mantle is reflected by mutual distribution of isotope and immobile trace element ratios in their mantle sources, showing the systematic occurrence of strange attractors. In fact, even if we cannot directly convert a compositional difference in the space of geochemical compositions into a distance in the Euclidean space, it is possible to well recognize the correspondence (= isomorphism) between geometric structures and chemical features in the OIB mantle source. In other words, recurrent intervals of geochemical variability have to match specific physical domains, and a chaotic signal in the compositional space is necessarily related to the spatial organization of chaotic mantle regions. This supports the evidence for a chaotic mantle, bridging the discrepancy between geochemical and geophysical views of mantle composition, and overcomes the impasse of the twenty years-old theories on mantle reservoirs. The underlying mechanisms can be easily modeled by means of image analysis that allows to simplify calculations and bring to direct analogues of the hypothesized structures. Our results confirm that the vertical scale of mantle heterogeneity is similar to its horizontal organization, as revealed by MORB sampled at ridge axes, and reinforces the conclusion that this structure is inherited from an ancient convection regime, probably affecting the whole mantle scale.

Microstructural variations in lower crustal oceanic troctolites: an indicator of melt-rock interactions (Erro Tobbio, Ligurian ophiolites, Italy)

Basch V.¹, Ferrando C.², Rampone E.*¹, Ildefonse B.², Crispini L.¹ & Godard M.²

1. DISTAV, Università di Genova. 2. Géosciences Montpellier, Université Montpellier 2, France.

Corresponding email: basch.valentin@edu.unige.it

Keywords: Oceanic lithosphere, troctolites, melt-rock reaction.

The interaction between an olivine-rich crystal mush and a melt by reactive porous flow is an important process in the formation of the lower oceanic crust and in the evolution of the composition of MORBs. It is still a matter of debate whether this matrix reacting with the incoming melt is formed by previous fractional crystallization of primitive melts, or represents an earlier mantle-derived olivine matrix. In order to address this issue, we studied field relationships, microstructural features, crystallographic preferred orientations and grain misorientation distribution (measured by EBSD mapping) in troctolites, plagioclase wehrlites and olivine gabbros from the Erro-Tobbio ophiolitic mantle unit (Ligurian Alps, Italy). In the studied area, a hectometre-scale body of troctolites intrudes the mantle peridotites with interfingering contacts. Subsequent intrusions of olivine-gabbro lenses and dykes crosscut both peridotites and troctolites (Borghini et al., 2007). Within the troctolite body, we distinguished different generations of troctolite having the same modal composition (olivine + interstitial plagioclase and clinopyroxene), but showing different microstructural features. The host troctolite exhibits predominant granular texture and compositional layering. Olivine displays intracrystalline high-temperature deformation microstructures (dislocation creep) consistent with the activation of the main high temperature slip system (010)[100], thus possibly recording a mantle signature. The second generation of troctolite occurs in discrete, decametre-size pseudo-tabular bodies (discordant to the host troctolite layering), and sills. They display textural heterogeneity, with olivine varying from granular to hopper to dendritic shape (harrisitic troctolite). The olivine crystals within the dendritic part of the harrisitic troctolite have quite distinct structural features with respect to the host troctolites, shown by an unusual preferred orientation of the [001] axes and a poor preferred orientation of the [100] axes. Olivines in the granular part display structural characteristics similar to those observed in the gabbro intrusions, with relatively strong preferred orientations of [010] and [001], consistent with magmatic flow. The interpretation of these structural variations reflecting different origin and formation processes within the troctolite body (mantle vs. magmatic origin of the olivine, melt-rock interactions) still has to be confirmed on a larger number of study cases, and by geochemical signatures. The microstructural and deformation study will be combined with in situ chemical analyses of the minerals to better constrain the variability induced by melt-rock interactions.

Borghini G., Rampone E., Crispini L., De Ferrari R. & Godard M. 2007. Origin and emplacement of ultramafic–mafic intrusions in the Erro-Tobbio mantle peridotite (Ligurian Alps, Italy). *Lithos*, 94, 210-229.

Major and trace element variability within the troctolite-olivine gabbro association of the Pineto ophiolite (Corsica)

Berno D.*¹, Sanfilippo A.¹, Tribuzio R.¹ & Zanetti A.²

1. Dipartimento delle Scienze della Terra e dell'Ambiente, Università di Pavia. 2. Istituto di Geoscienze e Georisorse, C.N.R. Pavia.

Corresponding email: davide.berno01@universitadipavia.it

Keywords: Troctolites, pineto, aggregation.

Mantle melting is believed to be near fractional, with melts continuously extracted from the mantle at different pressures (Johnson et al., 1990). This process generates a wide spectrum of parental melt compositions. Since MORBs are compositionally uniform, these diverse melts must be mixed together before they may erupt on the seafloor, a process generally referred to as “aggregation” (Grove et al., 1992). Wherever this process occurs within the mantle or in the lower crust has not been established yet. This study aims to investigate the chemical heterogeneity of the lowermost sector of the oceanic crust forming the Pineto gabbroic sequence (Corsica). This sequence exposes a unique 1.5 km-thick transect of the lower oceanic crust formed at the Jurassic Ligurian-Piedmontese basin and may represent the plutonic foundation of a fossil (ultra-)slow-spreading centre (Sanfilippo & Tribuzio, 2013).

We characterized whole rock and mineral major and trace element compositions of three olivine-rich troctolites (olivine Fo₈₈₋₈₉, plagioclase An₆₈₋₇₂), nine troctolites (olivine Fo₈₄₋₈₈, plagioclase An₆₅₋₇₃) and three olivine-gabbros (olivine Fo₈₁₋₈₄, plagioclase An₆₃₋₆₅). We showed that the shape of whole-rock REE and incompatible elements patterns are controlled by modal compositions. For instance, troctolites have plagioclase-like patterns with low REE amounts and a substantial positive Eu anomaly, whereas the whole-rock REE concentrations and the Eu anomaly increase and decrease, respectively, with increasing modal clinopyroxene. No correlation exists between the incompatible element compositions of clinopyroxene, plagioclase and olivine and the host rock-type. In addition, plagioclase shows significant variations in the LREE/MREE fractionation with the incompatible elements content. These preliminary data allow us to infer that fractional crystallization from similar parental melts was not the main process governing the chemical evolution of the lowermost oceanic crust at the Pineto sequence.

Grove T.L., Kinzler R.J. & Bryan W.B. 1992. Fractionation of mid-ocean ridge basalt (MORB). In: Morgan J.P., Blackman D.K. & Sinton J.M. Eds., *Mantle Flow and Melt Generation at Mid-Ocean Ridges*. Geophys. Monogr. Ser. AGU, 71, 281-311.

Johnson K.T.M., Dick H.J.B. & Shimizu N. 1990. Melting in the oceanic upper mantle: an ion-microprobe study of diopsides in abyssal peridotites. *J. Geophys. Res.*, 95(B3), 2661-2678.

Sanfilippo A. & Tribuzio R. 2013. Building of the deepest crust at a fossil slow-spreading centre (Pineto gabbroic sequence, Alpine Jurassic ophiolites). *Contrib. Mineral. Petrol.*, 165, 705-721.

Partial melting experiments on a natural pyroxenite at 1 and 1.5 GPa: insights on the role of secondary-type pyroxenite in basalt generation

Borghini G.*¹, Fumagalli P.¹ & Rampone E.²

1. Dipartimento di Scienze della Terra "A. Desio", Università di Milano. 2. DISTAV, Università di Genova.

Corresponding email: giulio.borghini@unimi.it

Keywords: Pyroxenite partial melting, experimental petrology, upper mantle.

The role of pyroxenite components in the origin of basaltic magmas from different geological settings remains a debated argument (e.g. Lambert et al., 2013). Recent models of basalt petrogenesis proposed that a secondary generation of pyroxenite forms when mafic components in the mantle encounter early melting and their melts react with the host peridotite (e.g. Lambert et al., 2012). New hybrid rocks with a large range of major element composition are thus formed in the mantle before this latter encounters large batch of melting. So far, this type of pyroxenite has been not yet experimentally investigated and the composition of their partial melts is still unknown. In this work, starting from an excellent natural example (Borghini et al., 2013), we performed partial melting experiments at 1 and 1.5 GPa to derive the extent and composition of melts produced by moderate to high melting degree of a secondary-type pyroxenite. Starting material has been obtained by complete melting of rock powder in a furnace at 1500 °C (at FMQ fO_2) and rapid quench in dry ice. The resulting glass has $X_{Mg} = 0.83$, $SiO_2 = 47.3$ wt.%, $CaO = 14.4$ wt.%, $Al_2O_3 = 10.1$ wt.% and $Na_2O = 0.3$ wt.%. A layer of carbon vitreous spheres ($d < 125$ μm) is used to favor melt trapping. Coherent element partitioning and mass balance support approach to equilibrium. Crystal size increases with T from 1-10 μm in subsolidus experiments up to about 80 μm in near-liquidus runs. At 1 GPa, a subsolidus clinopyroxene + orthopyroxene + olivine + spinel assemblage is stable at 1180 °C and trace amount of glass appears at 1200 °C. At 1.5 GPa, about 5% of modal garnet is present in the subsolidus assemblage at 1230 °C and it disappears after about 7% of melting degree at 1250 °C. At both pressures, orthopyroxene is rapidly exhausted within 10% of partial melting. At increasing T, spinel and later clinopyroxene are consumed and olivine remains as liquidus phase. Pyroxenite GV10 starts to melt at 70-100 °C less than peridotite MM3 (e.g. Falloon et al., 2008), at 1 and 1.5 GPa respectively, and it encounters very high melting degrees (about 90%) within a T range of 100-130 °C, when the melt fraction of MM3 peridotite is only around 20%. Melts produced after low melting degrees (< 8%) are silica- and alumina-rich, with X_{Mg} ranging 0.53-0.63. SiO_2 drastically decreases once orthopyroxene disappears from the liquidus. X_{Mg} and CaO increase and Al_2O_3 , Na_2O and TiO_2 contents decrease with increasing T. FeO is rather homogeneous and slightly higher in 1.5 GPa experiments. High-CaO melts are produced at near-liquidus T ($CaO > 15$ wt.%). Experimental results of this work are used to estimate the contribution of secondary pyroxenite through a simple model of basalt generation from a peridotite-pyroxenite mixed source.

- Borghini G., Rampone E., Zanetti A., Class C., Cipriani A., Hofmann A.W. & Goldstein S.L. 2013. Meter-scale Nd isotopic heterogeneity in pyroxenite-bearing Ligurian peridotites encompasses global-scale upper mantle variability. *Geology*, 41, 1055-1058.
- Falloon T.J., Green D.H., Danyushevsky L.V. & McNeill A.W. 2008. The composition of near-solidus partial melts of fertile peridotite at 1 and 1.5 GPa: implications for the petrogenesis of MORB. *J. Petrol.*, 49, 591-613.
- Lambert S., Laporte D., Provost A. & Schiano P. 2012. Fate of pyroxenite-derived melts in the peridotitic mantle: Thermodynamic and experimental constraints. *J. Petrol.*, 53, 451-476.
- Lambert S., Laporte D. & Schiano P. 2013. Markers of the pyroxenite contribution in the major-element compositions of oceanic basalts: Review of the experimental constraints. *Lithos*, 160, 14-36.

Multiple origins of pyroxenites in the upper mantle: from nature to experiments

Borghini G.

Dipartimento di Scienze della Terra "Ardito Desio", Università di Milano.

Corresponding email: giulio.borghini@unimi.it

Keywords: Pyroxenites, mantle heterogeneity, melt-rock reaction.

Pyroxenites are today considered diffuse lithological heterogeneities in the upper mantle and an essential component in petrological and geochemical models for melt generation at mid oceanic ridges (MORB) and oceanic islands (OIB). Since the first models of two-components mantle that invoked the presence of stirred recycled crust in the mantle source (Allegre & Turcotte, 1986), an increasing attention has been devoted to study the pyroxenites, thus inciting the debate on their origin and possible involvement in basalt production. Direct information on pyroxenites concerned petrological studies on samples from ultramafic massifs, mantle xenoliths and rare abyssal peridotites. These studies showed their large range in major and trace element compositions and contributed to define their different origins, spanning from magmatic to metamorphic processes, which can be more or less erased by later metamorphism, metasomatism or partial melting. Trace element and isotopic models have emphasized the role of pyroxenites in basalt generation because lower solidus temperature and higher melt productivity with respect to peridotites are expected to amplify their contribution in mantle melting (Hirschmann & Stolper, 1996). This encouraged several experimental studies to investigate partial melting of pyroxenitic/mafic components, and their results showed that much of compositional variability in oceanic basalts is explainable by the presence of pyroxenite in the mantle source (Lambart et al., 2013). Geochemical models on the origin of MORB and OIB have been based on mixed pyroxenite-peridotite mantle sources. Observations on pyroxenite-peridotite sequences from ultramafic massifs evidenced different generations of pyroxenite veins and dikes thus suggesting that the upper mantle can experience multiple episodes of formation and/or modification of pyroxenites. Recent experimental and thermodynamical studies have underlined that the interaction between pyroxenite-derived melts and host peridotites plays a crucial role in originating different generations of pyroxenites (Lambart et al., 2012). Further work is therefore requested to better define the origin of this type of pyroxenites, evaluate their role in basalt generation and study the ability of pyroxenitic melts to rise through the mantle. Some mantle sequences from Alpine-Apennine ophiolites represent excellent study cases to investigate the petrologic evolution of pyroxenite-peridotite associations (Montanini et al., 2012; Borghini et al., 2013). In light of recent models, field-based and experimental petrological studies of these rocks contribute to enlarge our knowledge on mechanisms of upper mantle modification via pyroxenite-peridotite interaction.

Allegre C.J. & Turcotte D.L. 1986. Implications of a two-component marble-cake mantle. *Nature*, 323, 123-127.

Borghini G., Rampone E., Zanetti A., Class C., Cipriani A., Hofmann A.W. & Goldstein S.L. 2013. Meter-scale Nd isotopic heterogeneity in pyroxenite-bearing Ligurian peridotites encompasses global-scale upper mantle variability. *Geology*, 41, 1055-1058.

Hirschmann M.M. & Stolper E.M. 1996. A possible role for garnet pyroxenite in the origin of the garnet signature in MORB. *Contrib. Mineral. Petrol.*, 124, 185-208.

Lambart S., Laporte D., Provost A. & Schiano P. 2012. Fate of pyroxenite-derived melts in the peridotitic mantle: Thermodynamic and experimental constraints. *J. Petrol.*, 53, 451-476.

Lambart S., Laporte D. & Schiano P. 2013. Markers of the pyroxenite contribution in the major-element compositions of oceanic basalts: Review of the experimental constraints. *Lithos*, 160, 14-36.

Montanini A., Tribuzio R. & Thirlwall M. 2012. Garnet clinopyroxenite layers from the mantle sequences of the Northern Apennine ophiolites (Italy): Evidence for recycling of crustal material. *Earth Planet. Sci. Lett.*, 351, 171-181.

Isotopic evidence for an enriched lithospheric component in the mantle source of the Freetown Layered Complex (Sierra Leone)

Callegaro S.*¹, Marzoli A.¹, Bertrand H.², Blichert-Toft J.², Reisberg L.³, Cavazzini G.⁴, Zanetti A.⁵, Jourdan F.⁶, Davies J.⁷, Parisio L.¹, Bouchet Bert Manoz R.² & Schaltegger U.⁷

1. Dipartimento di Geoscienze, Università di Padova. 2. Université Lyon 1 et Ecole Normale Supérieure de Lyon, Laboratoire de Géologie de Lyon, France. 3. Centre de Recherches Pétrographiques et Géochimiques (CRPG/CNRS), Vandoeuvre-les-Nancy Cedex, France. 4. Istituto di Geoscienze e Georisorse - Laboratorio di Geocronologia, CNR Padova. 5. Istituto di Geoscienze e Georisorse, CNR Pavia. 6. Department of Applied Geology, Curtin University, Bentley, Australia. 7. Section des Sciences de la Terre, Université de Genève, Switzerland.

Corresponding email: sara.callegaro@unipd.it

Keywords: Mafic layered intrusion, Central Atlantic Magmatic Province, isotopes.

The tholeiitic intrusive rocks (from olivine gabbros to anorthosites) of the Freetown Layered Complex (FLC; ca. 1000 km³) intrude the Pan-African coastal belt of Sierra Leone (Rokelide orogen) on the Atlantic rim of the West African Craton (Archean). The complex is cut by coast-parallel high-Ti basaltic dykes attributed to the Central Atlantic Magmatic Province (CAMP). Radiogenic isotope dating (U-Pb on baddeleyite: 198.794 ± 0.048/0.071/0.22 Ma and ⁴⁰Ar/³⁹Ar on plagioclase: 201.7±0.7 and 202.3±2.3 Ma) and trace element crystal chemistry show that, similarly to the dykes, the FLC was formed by high-Ti tholeiites intruding during the peak of CAMP volcanic activity (ca. 201 Ma; Marzoli et al., 2011). This classifies the FLC as a rift-related intrusion associated with the late Triassic opening of the Central Atlantic, during the early stages of Pangea breakup. The Sr-Nd-Hf-Pb-Os isotope compositions (the first for the FLC and, for Hf, also the first for CAMP; ⁸⁷Sr/⁸⁶Sr_{200Ma} = 0.70311-0.70651; ¹⁴³Nd/¹⁴⁴Nd_{200Ma} = 0.51152-0.51259; ¹⁷⁶Hf/¹⁷⁷Hf_{200Ma} = 0.28206-0.28290; ²⁰⁶Pb/²⁰⁴Pb_{200Ma} = 16.614-17.850, ²⁰⁷Pb/²⁰⁴Pb_{200Ma} = 15.549-15.611; ²⁰⁸Pb/²⁰⁴Pb_{200Ma} = 36.945-37.936; ¹⁸⁷Os/¹⁸⁸Os_{200Ma} = 0.1295-0.1319) of these tholeiites reveal enriched signatures, typical of the Dupal-flavored (Hart, 1984) basalts of the Atlantic region and extending the field of previously studied high-Ti CAMP rocks from Brazil, Guyana, and Liberia. In particular, low ²⁰⁶Pb/²⁰⁴Pb coupled with high ²⁰⁷Pb/²⁰⁴Pb require the contribution from an ancient source, likely metasomatized sub-continental lithospheric mantle, to the parent magma of the FLC. We estimated that addition of 1-4% of lamproitic melts derived from the enriched lithosphere to a predominantly asthenospheric melt suffices to explain the observed enriched isotopic characteristics. Furthermore, the signatures shown by some outlier samples, together with evidence of disequilibrium at the mineralogical scale, indicate assimilation of up to 10% lower crustal granulites. In addition to shedding new light on the formation of the CAMP high-Ti rocks restricted to the proximity of the West African and Amazonian (South American) cratons, the data of this study also suggest a shallow, lithospheric origin of the Dupal anomaly and extend the occurrence of this signature further north of its previously known distribution. Lithospheric domains trapped during the breakup of Pangea may be at the origin of the enriched signatures shown by many Atlantic basalts.

Hart S.R. 1984. A large-scale isotope anomaly in the Southern Hemisphere mantle. *Nature*, 309, 753-757.

Marzoli A., Jourdan F., Puffer J.H., Cuppone T., Tanner L.H., Weems R.E., Bertrand H., Cirilli S., Bellieni G. & De Min A. 2011. Timing and duration of the Central Atlantic magmatic province in the Newark and Culpeper basins, eastern U.S.A. *Lithos*, 122, 175-188.

Olivine-gabbros and olivine-rich troctolites origin through melt-rock reaction in oceanic spreading lithosphere: an experimental study up to 0.7 GPa

Francomme J.E., Fumagalli P.* & Borghini G.

Dipartimento di Scienze della Terra "A. Desio", Università di Milano.

Corresponding email: patrizia.fumagalli@unimi.it

Keywords: Melt-rock reactions, troctolites, oceanic lithosphere.

Olivine-gabbros and troctolites are thought to originate at mantle-crust transition and they were traditionally considered the result of fractional crystallization processes. However, on the basis of peculiar microstructures and mineral chemistry observed on natural samples from mid-ocean ridge settings, as well as in ophiolitic rocks, recent petrological studies have emphasized that they rather result by partial dissolution of replacive mantle dunite and infiltration of basaltic melts (e.g. Drouin et al., 2010; Sanfilippo et al., 2013). Extensive melt-rock reaction and melt impregnation significantly affect not only the physical and chemical properties at mantle-crust transition, but also control the evolution of migrating melts (e.g. Lissenberg et al., 2013). The aim of this study is to provide experimental constraints on the origin of olivine-rich troctolites and olivine-gabbros by melt-rock reaction performing reactive dissolution and crystallization experiments at pressure ≤ 0.7 GPa. Experiments are carried out in single stage and end-loaded piston-cylinders using salt-Pyrex-MgO assemblies. Two experimental strategies are exploited: i) powder-to-powder experiments, where a fine powder ($<10 \mu\text{m}$) of San Carlos olivine (Fo₉₀) mixed to 10% of basaltic glass powder is juxtaposed against a basaltic melt within a graphite-lined platinum capsule, and ii) dunite infiltration runs, where pre-sintered (1 GPa, 1100 °C for 48 hours) polished dunite rods in contact with basaltic glass powder are charged in graphite-lined molybdenum capsule. Two MORB-type glasses have been selected and modeled in complex chemical system: a primitive basalt (XMg = 0.74, SiO₂ = 48.25 wt.%, CaO = 11.90 wt.%, Na₂O = 1.80 wt.%), and an evolved basalt (XMg = 0.62, SiO₂ = 47.70 wt.%, CaO = 13.80 wt.%, Na₂O = 2.28 wt.%). Powder-to-powder experiments have been run at 1300 °C, at 0.5 and 0.7 GPa, for 24 hours in order to favor isothermal dissolution; then runs have been step cooled down to 1150 °C at a rate of 10 °C/min in order to promote in situ crystallization of interstitial melts. They resulted in a sequence of plagioclase-bearing dunite, olivine-rich troctolite and olivine gabbro developed from the dunite layer towards the melt side of the run charge. A pilot dunite infiltration experiment run at 0.7 GPa, 1250 °C shows an extensive melt-rock reaction with the formation of new olivine and reacted melt. Microtextures are in general well comparable with those observed in natural samples. Preliminary mineral chemistry suggests systematic variations along the melt-rock interface from the dunite layer towards the melt side of the charge, shedding light to the reactive process responsible for the formation of olivine rich troctolites and olivine gabbros.

Drouin M., Ildefonse B. & Godard M. 2010. A microstructural imprint of melt impregnation in slow-spread lithosphere: olivine-rich troctolites from the Atlantis Massif (Mid-Atlantic Ridge 30°N, IODP Hole U1309D). *Geochem. Geophys. Geosyst.*, 11, Q06003, doi:10.1029/2009GC002995.

Lissenberg C.J. & Dick H.J.B. 2008. Melt-rock reaction in the lower ocean crust and its implications for the genesis of midocean ridge basalt. *Earth. Planet. Sci. Lett.*, 271, 311-325.

Sanfilippo A., Dick H.J.B. & Ohara Y. 2013. Melt-Rock Reaction in the Mantle: Mantle Troctolites from the Parece Vela Ancient Back-Arc Spreading Center. *J. Petrol.*, 54, 861-885.

Comparing the Cana Brava and Niquelândia complexes: different contamination and fractionation processes in coeval intrusions

Giovanardi T.*¹, Girardi V.A.V.¹, Correia C.T.¹, Sinigoi S.², Tassinari C.C.G.¹ & Mazzucchelli M.³

1. Instituto de Geociências, Universidade de São Paulo, Brazil. 2. Dipartimento di Matematica e Geoscienze, Università di Trieste. 3. Dipartimento di Scienze Chimiche e Geologiche, Università di Modena e Reggio Emilia.

Corresponding email: tommaso.giovanardi@gmail.com

Keywords: Layered complex, contamination, Brazil.

Contamination processes during the intrusion in the crust of mantle-derived melt which produced huge layered complexes are recognized in almost all the layered complexes (e.g. Val Sesia magmatic system). However, the contamination does not always occur (e.g. Finero mafic complex) or occurred in different intrusions with different modalities.

The Niquelândia and Cana Brava complexes (Goiás, central Brazil) are part of a 300 km long, North-trending belt of mafic-ultramafic massifs outcropping in the Brasília Belt. Among the three complexes forming the belt (together with the Barro Alto one), the Cana Brava complex is the less known while the Niquelândia complex is the better known. The intrusion of the complexes occurred during a continental rift in the lower crust and the parent melt compositions were estimated to be MORB-like.

Notwithstanding these, the stratigraphy of the two complexes is different: the Niquelândia complex shows anorthositic rocks forming the so-called Upper Sequence while the Cana Brava complex is similar to the Niquelândia Lower Sequence.

New U-Pb SHRIMP-II analyses on zircons from 4 samples from the Cana Brava complex provided for concordia ages between 798.7 ± 2.2 Ma and 779.3 ± 1.3 Ma. These ages constrain the Cana Brava intrusion at 800-780 Ma, similarly to the intrusion ages estimated in literature for the Barro Alto and Niquelândia complexes.

Literature data suggests that the Niquelândia complex suffered crustal contamination as a late event during its growth only locally and in the Lower Sequence. The contamination enriched the melt in incompatible elements (e.g. LREE and Ba) and affected the Rb-Sr and Sm-Nd isotopes.

New bulk-rock major and trace elements analyses from the Cana Brava complex show strong enrichments for the most incompatible elements at the top of the complex which suggest, together with the occurrence of xenoliths, that the parent melt was affected by crustal contamination. Rb-Sr and Sm-Nd isotopic analyses confirm this hypothesis, showing an increasing contamination trend along the stratigraphy ($^{87}\text{Sr}/^{86}\text{Sr}(790)$ between 0.708243-0.736590 and $\epsilon\text{Nd}(790)$ between 1.71 and -8.47 from the bottom to the top). This suggests a continuous contamination process during the complex growth.

The comparison of the two complexes evidenced a different development of the contamination processes.

AlphaMELTS models for the Niquelândia and Cana Brava complexes provide evidences of different fractionation of the parent melts, thus suggesting that the different development of crustal contamination is led to the fractionation processes and a different melt compositions.

Financial Support: FAPESP projects 2011/50307-0 and 2013/19519-6.

Gabbroic dykes in the Finero Phlogopite-Peridotite Massif: evidence for melt-peridotite interactions at mantle conditions and igneous sapphirine formation by auto-metasomatism

Giovanardi T.*¹, Zanetti A.², Morishita T.³, Langone A.², Dallai L.⁴ & Mazzucchelli M.⁵

1. Instituto de Geociências, Universidade de São Paulo, Brazil. 2. Istituto di Geoscienze e Georisorse, CNR, Pavia. 3. Frontier Science Organization, Kanazawa University, Japan. 4. Istituto di Geoscienze e Georisorse, CNR, Pisa. 5. Dipartimento di Scienze Chimiche e Geologiche, Università di Modena e Reggio Emilia.

Corresponding email: tommaso.giovanardi@gmail.com

Keywords: Sapphirine, Finero, rock-melt interaction.

The Finero Phlogopite Peridotite (FPP: Ivrea-Verbano Zone, western Alps, Italy) is a mantle sequence completely recrystallized by several events of melt migration. Literature studies provide evidence that a main metasomatic event induced the pervasive crystallisation of Amphibole-Phlogopite-bearing mineral assemblages (harzburgites and pyroxenites; Amph, Phl), as well as the formation of dunite bodies. These lithologies have similar geochemical compositions characterised by strong crustal components, as testified by enrichment in K, Mg, H₂O, LREE and LILE and depletion in HREE and HSFE, radiogenic Sr and Pb, and unradiogenic Nd. Besides, the FPP shows bands, veins or pockets with variable mineral assemblages, but usually rich in Apatite (Ap) and Carbonates (Crb).

Late gabbroic dyke swarms, different from all the other lithologies and containing Sapphirine (Spr), were recently described (Giovanardi et al., 2013). These dykes were formed by multi-stage magma intrusions via hydraulic-fracturing, characterised by early crystallisation of Amph ± Ap ± Phl (i.e. the Early Amph Zone) followed by segregation at the vein core of Plagioclase ± Amph ± Crb (the Leucocratic Zone). Spr occurred in a reaction zone placed between them. Another reaction zone occurs at the contact between the host peridotite and the vein, being characterised by the complete replacement of peridotite Olivine by secondary Orthopyroxene (the Opx Zone).

The occurrence of Spr only in the Late Amph Zone was possibly interpreted as i) direct magmatic crystallization from an evolved Al-rich melt or ii) crystallization by auto-metasomatic process with interaction between the Early Amph Zone with the most evolved melt segregating the Leucocratic Zone.

A new study on the Spr-bearing gabbroic dykes of the FPP allowed us: i) to constrain the occurrence of local (up to 8 cm from the veins) melt interaction with the host harzburgite, which provides high δ¹⁸O, Al, Mg, K, H₂O, locally associated to pronounced enrichments in U, Th, LILE and LREE, which unravels different degrees of contamination by host rock; ii) to provide new evidence supporting the Spr formation by auto-metasomatic process, after reaction of the first cumulates (i.e. the Early Amph Zone) with the most evolved melt which crystallized the Leucocratic Zone; iii) to give new constraints on the nature of the gabbroic dykes parent melts. The formation of the Opx Zone within the host peridotite and the cumulus crystallization of hydrous phases (i.e. Amph and Phl) suggest to a silica-saturated, hydrous evolved melt as parent melt of the gabbroic dykes. The L/MREE-enriched convex-upward patterns of the Amph, point to an alkaline geochemical affinity of the parent melts.

Giovanardi T., Morishita T., Zanetti A., Mazzucchelli M. & Vannucci R. 2013. Igneous sapphirine as a product of melt-peridotite interactions in the Finero Phlogopite-Peridotite Massif, Western Italian Alps. *Eur. J. Mineral.*, 25, 17-31.

New insights into the evolution of the Finero Mafic Complex, north-eastern Ivrea-Verbano Zone

Langone A.¹, Zanetti A.*¹, Renna M.R.², Tiepolo M.³, Mazzucchelli M.⁴ & Giovanardi T.⁵

1. Istituto di Geoscienze e Georisorse, C.N.R. Pavia. 2. Dipartimento di Fisica e Scienze della Terra, Università di Messina. 3. Dipartimento di Scienze della Terra "A. Desio", Università di Milano. 4. Dipartimento di Scienze Chimiche e Geologiche, Università di Modena e Reggio Emilia. 5. Institute of Geology and Geophysics, Chinese Academy of Sciences, Beijing, P.R.C.

Corresponding email: alberto.zanetti9@gmail.com

Keywords: Ivrea-Verbano Zone, Finero Complex, magmatic underplating.

The Finero Mafic Complex outcrops in the northern sector of the Ivrea-Verbano Zone (IVZ, Southern Alps). It occurs at the flank of an antiform which core is constituted by mantle peridotites, and it consists of mafic/ultramafic rocks subdivided in three units: a) the Layered Internal Zone (LIZ), in tectonic contact with the mantle unit; b) the Amphibole Peridotite (Amph-Pd); c) the External Gabbro (EG), which is in tectonic contact with the Variscan crystalline basement (Rivalenti et al., 1984; Siena & Coltorti, 1989). Recent studies point to a Middle Triassic emplacement age for the EG unit (Zanetti et al., 2013), suggesting that it is unrelated to the Permian Mafic Complex of the central IVZ. Owing to the lack of a detailed petrochemical characterisation of the FMC, we performed new major (EMP) and trace element (LA-ICPMS) analyses on representative samples from the LIZ and Amph-Pd. The LIZ mainly consists of hornblende-gabbros; anorthosites and garnet hornblendites with minor pyroxenites. The Amph-Pd is mostly made up of Amph-bearing harzburgites and dunites with minor pyroxenites. Locally, Amph-rich veins with a variable thickness from a few cm to about 1 m crosscut the magmatic layering. Olivine (Fo₈₇₋₈₂) only occurs in the peridotites from Amph-Pd, whereas amphibole and clinopyroxene are common throughout the entire sequence. The Mg# of Cpx and Amph tends to increase from the LIZ towards the upper part of the Amph-Pd whereas the Al₂O₃ content in Cpx and Amph is up to 11 and 18 wt.%, respectively and show an opposite trend. In garnet-free pyroxenites and hornblendites from LIZ, Amph and Cpx have slightly LREE-depleted patterns with flat HREE (at 2xCI in Cpx) and marked positive Eu, Sr, Pb and U anomalies. Similar features are shown by the Cpx and Amph from the associated gabbros, but they are strongly depleted in HREE indicating chemical equilibration with garnet. Cpx and Amph from the Amph-bearing peridotites (Amph-Pd) have instead LREE-enriched spoon-shape patterns with HREE contents comparable with those of the LIZ lithologies, being also characterised by Eu, Sr and U enrichments. The LILE enrichments and fractionation can be reconciled by an interaction dominated by ion exchange chromatographic-type process with strongly LILE-enriched melts: the composition of the latter is recorded by the amphibole-dominated lithologies. The new data suggest that the LIZ with a clear crustal signature. Instead, the trace element variations in the Amph-Pd cannot be explained via a closed-system evolution, pointing to the presence of significant changes in the composition of the uprising mantle melts.

Rivalenti G., Rossi A., Siena F. & Sinigoi S. 1984. The layered series of the Ivrea-Verbano igneous complex, Western Alps, Italy. *Tscher. Miner. Petrog. Mitt.* 33, 77-99.

Siena F. & Coltorti M. 1989. The petrogenesis of a hydrated mafic-ultramafic complexes and the role of amphibole fractionation at Finero Italian western Alps. *N. Jb. Miner. Mh.*, 6, 255-274.

Zanetti A., Mazzucchelli M., Sinigoi S., Giovanardi T., Peressini G. & Fanning M. 2013. SHRIMP U-Pb Zircon Triassic Intrusion Age of the Finero Mafic Complex (Ivrea-Verbano Zone, Western Alps) and its Geodynamic Implications. *J. Petrol.*, 54, 2235-2265.

Oceanization starts from below during continental rupturing in the Red Sea

Ligi M.*¹, Bonatti E.¹⁻², Bosworth W.³, Cai Y.², Cipriani A.²⁻⁴, Palmiotto P.¹, Ronca S.⁵, Sanfilippo A.⁶ & Seyler M.⁷

1. Istituto di Scienze Marine, C.N.R. Bologna. 2. Lamont Doherty Earth Observatory, Columbia University, New York, USA. 3. Apache Egypt Companies, Cairo, Egypt. 4. Dipartimento di Scienze Chimiche e Geologiche, Università di Modena e Reggio Emilia. 5. Dipartimento di Scienze della Terra, Sapienza Università di Roma. 6. Dipartimento di Scienze della Terra e dell'Ambiente, Università di Pavia. 7. UFR des Sciences de la Terre, Université Lille 1, France.

Corresponding email: marco.ligi@bo.ismar.cnr.it

Keywords: Continental rupturing, seafloor spreading initiation, magmatism and mantle related processes.

The role of magmatism in continental rupturing and in the birth of a new ocean are not well understood. Continental rupture can take place with intense and voluminous volcanism, as in the Southern Red Sea/Afar Rift or in a relatively amagmatic mode, as in the Northern Red Sea rift. Within the Red Sea system, magnetic anomalies show a south to north time progression of the initial emplacement of oceanic crust. Mantle upwelling and melting may be affected by the south-north decreasing opening rate of the Red Sea and by the influence of the Afar plume, also decreasing from south to north. The tholeiitic basalts of the Red Sea spreading system contrast with the extensive Cenozoic basaltic lava fields occurring in the western part of the Arabian peninsula and forming one of the largest alkali basalt provinces in the world. In order to establish possible relationship between the Red Sea rift evolution and the widespread intraplate alkali volcanism of the western Saudi Arabia, field work was carried out on lava fields lying along the 25°N parallel, for over 150 km far from the shoreline. Samples from the Lunayyir, Ishara, al Kura and Khaybar volcanic fields, covering the full range of chemical diversity (olivine basalt, hawaiite, mugearite, benmoreite and trachyte) and spanning over a 20 Ma interval, were selected for chemical analyses. We attempt a comparison of the geochemistry of igneous rocks from western Arabia dykes and volcanic fields with those from the Red Sea axis and from the islands of Zabargad and Brothers in the northern Red Sea, that represent basaltic melts injected into the thinned continental crust before continental rupturing and initiation of seafloor spreading. The origin of the western Arabia igneous rocks and their relationship with rifting processes in the Red Sea have been assessed. Gabbros from the Brothers and Zabargad islands suggest that continental break up in the northern Red Sea, a relatively non-volcanic rift, is preceded by intrusion of oceanic-type basaltic melts that crystallize at progressively shallower crustal depths as rifting progresses towards continental break-up. A seismic reflection profile running across the central part of the southern Thetis basin shows a ~5 km wide reflector below the axial neovolcanic zone that marks the roof of a magma chamber or melt lens located ~3.5 km below the seafloor. The presence of a few kilometers deep subrift magma chamber soon after the initiation of oceanic spreading implies the crystallization of lower oceanic crust intrusives as a last step in a sequence of basaltic melt intrusion from pre-oceanic continental rifting to oceanic spreading. Thus oceanic crust accretion in the Red Sea rift starts at depth before continental break up, emplacement of oceanic basalt at the sea floor, and development of Vine-Matthews magnetic anomalies, pointing to a rift model, where the lower continental lithosphere has been replaced by upwelling asthenosphere before continental rupturing.

Melt/rock interaction: case study from Mt. Pollino ophiolites (Basilicata, Southern Italy)

Mazzeo F.C.*¹⁻², Zanetti A.³, D'Antonio M.², Petrosino P.² & Aulinas M.⁴

1. Dipartimento di Fisica "E.R. Caianiello", Università di Salerno. 2. Dipartimento di Scienze della Terra, dell'Ambiente e delle Risorse, Università di Napoli "Federico II". 3. Istituto di Geoscienze e Georisorse, CNR Pavia. 4. Departamento de Geoquímica, Petrología i Prospecció Geològica, Universitat de Barcelona, España.

Corresponding email: famazzeo@unisa.it

Keywords: Serpentinized peridotites, melt/rock interaction, mantle refertilisation.

The petrologic evolution of mantle peridotites during ocean formation is characterized by several episodes of refertilisation due to melt migration after large degree of partial melting. This feature is recognizable also in the Mt. Pollino (Calabria-Basilicata boundary, Southern Italy) ophiolite which represents well preserved oceanic lithosphere fragments of the Ligurian Tethys. This ophiolite includes serpentinized peridotites (Cpx-poor lherzolite; modal Cpx less than 6%) consisting mainly of serpentine and other phyllosilicates such as talc and chlorite. Some samples are characterized by porphyroclasts of olivine and orthopyroxene, varying from anhedral to subhedral. Spinels occur as disseminated skeletal grains sometimes with evident signs of resorption, and as inclusions in olivine. Clinopyroxene is present as large crystals with clear signs of deformation and alteration along the traces of cleavage (Cpx I) or as small, less deformed and exolved grains at the rim of large porphyroclasts (Cpx II). Some samples (Type-1) have lower MgO, highest Al₂O₃ and CaO values, and are less depleted in LREE, while other samples (Type-2) show opposite characteristics. Cpx crystals are diopside. CaO contents overlap in both Types (21.6-23.6 wt.%). Al₂O₃ content of Cpx is higher in Type-1 peridotites (3.3-5.1 wt.%) compared to that of Type-2 peridotites (2-3 wt.%). Moreover, in Type-1 peridotite the Al₂O₃ content allows us to divide the Cpx into two groups. The first shows higher Al₂O₃ contents (Cpx I = 4.4-5.1 wt.%) than those measured in the second group (Cpx II = 3.2-3.9 wt.%). REE contents of Cpx are about 8-12xCI in the MREE and HREE region where the patterns are almost flat (Gd_N/Lu_N = 0.66-1.58). Conversely, the LREE contents are considerably depleted, with a significant difference in Type-1 peridotites between Cpx II (La_N/Nd_N = 0.01-0.06) and Cpx I (La_N/Nd_N = 0.09-0.21). Very similar to the Cpx II are the LREE contents of Cpx Type-2 peridotites (La_N/Nd_N = 0.04-0.21). Both Types of Mt. Pollino peridotites show evidence of significant partial melting; however, the degree of partial melting based on REE concentrations of Cpx (4-6%) is much lower than that recorded by spinel composition (10-20%). The discrepancy between these two estimates allows us to interpret the Mt. Pollino peridotites as the result of a reactive melt/rock interaction with MORB melts after an earlier melt extraction, which determined the re-enrichment of LREE in Cpx. However, the geochemical data indicate different petrologic evolution histories for these peridotites. Type-2 peridotites testify an interaction between the peridotitic matrix and N-MORB melts obtained from a 4% partial melting degree of a DMM source. Type-1 peridotites have been affected by a multistage refertilization, through at least two events. The first event is similar to that recognized in Type-2 peridotites, while the second event was driven by N-MORB melts similar to those obtained from 2-3% partial melting degree of a DMM source.

Highly siderophile elements and Os isotope compositions of recycled mantle pyroxenites in the Ligurian mantle section (N Apennine, Italy)

Montanini A.*¹, Luguët A.², Van Acken D.² & Tribuzio R.³⁻⁴

1. Dipartimento di Fisica e Scienze della Terra, Università di Parma. 2. Steinmann Institut für Geologie, Mineralogie und Paläontologie, Universität Bonn, Germany. 3. Dipartimento di Scienze della Terra e dell'Ambiente, Università di Pavia. 4. Istituto di Geoscienze e Georisorse, C.N.R. Pavia.

Corresponding email: alessandra.montanini@unipr.it

Keywords: Mantle pyroxenite, HSE, Os isotope.

Mantle pyroxenites derived by crustal recycling are believed to be significant components of OIB-MORB sources. The presence of a recycled pyroxenite component may contribute to the radiogenic ¹⁸⁷Os and ¹⁸⁶Os signatures within the sources of oceanic basalts. However, the highly siderophile element (HSE) signatures of mantle pyroxenites are not well constrained. Here, we present HSE (Os, Ir, Pt, Pd, Re) and ¹⁸⁷Os compositions of thirteen garnet pyroxenites and two lherzolites from the External Ligurian ophiolites.

This pyroxenite-peridotite sequence includes Mg-rich, Al-poor garnet websterites and three types of garnet clinopyroxenites that were distinguished on the basis of trace elements and Nd-Hf isotopes. Type-A and Type-B are strongly LREE-depleted and show flat and HREE-enriched whole-rock patterns, respectively. Type-C have moderate LREE depletion and lower HREE contents than Type-A-B. Small to distinct Eu positive anomalies characterize Type-A and Type-C garnet clinopyroxenites. The garnet clinopyroxenites have heterogeneous mafic crustal precursors that experienced a long-lived evolution of recycling into the mantle (1.5-1.0 Ga). The different garnet clinopyroxenite types originated by crystallization of eclogite-derived melts that did not experience significant interaction with the host peridotites. The garnet websterites are interpreted as reactions products between eclogite-derived melts and peridotites, yielding hybrid, second-stage pyroxenites with a crustal geochemical fingerprint.

The Ligurian peridotites show flat CI-chondrite-normalised HSE patterns, in agreement with their lithophile major and trace element composition close to PM. All the pyroxenites are variably depleted in Os and Ir and enriched in the incompatible HSE (Pt, Pd and Re) with respect to host peridotites. Os and Ir abundances and Re/Os ratios are broadly correlated with Al₂O₃ and Mg# values. Type-A pyroxenites exhibit lower low Os, Ir, and higher Pt, Pd concentrations and flatter Pd-Re segments than the associated Type-B pyroxenites. Type-C pyroxenites show variable HSE compositions. They have Os-Ir contents similar or higher than Type-B pyroxenites, whereas the Pd-Re segments range from flat to negatively sloping. Pt-Pd enrichment is observed in two out of four Type-C pyroxenites. The Mg-rich websterites have HSE patterns similar to Type-A but are significantly enriched in Os and Ir by a factor of ca. 10.

The External Ligurian mantle sequence shows centimetre- to metre-scale Os isotopic heterogeneity. The initial ¹⁸⁷Os/¹⁸⁸Os ratios recalculated for the age of the partial melting event inferred from Nd-Hf isotope systematics (220 Ma) are unradiogenic to slightly radiogenic in the peridotites (0.124-0.134) and vary from moderately to highly radiogenic in the pyroxenites (0.149-2.190), corresponding to gOs of +17 to +1628. The Mg-rich websterites have the least radiogenic Os isotope composition observed in the pyroxenite suite.

We show that recycled mantle pyroxenites display a wide range of highly siderophile elements signatures and Os isotope ratios, which may be related to heterogeneity of crustal protoliths, age of recycling, interaction with the host peridotites and late-stage melt percolation during exhumation. Recycled pyroxenites likely contribute to geochemical and isotopic heterogeneities of the Earth's mantle and may partly explain the wide range of ¹⁸⁷Os-¹⁸⁶Os isotopic signatures in OIBs and MORBs.

The Iherzolite-pyroxenite-hornblendite association from St. Lucia (Corsica): evidence for refertilization of subcontinental mantle

Montanini A.*¹, Tribuzio R.²⁻³, Zanetti A.³ & Zibra I.⁴

1. Dipartimento di Fisica e Scienze della Terra, Università di Parma. 2. Dipartimento di Scienze della Terra e dell'Ambiente, Università di Pavia. 3. Istituto di Geoscienze e Georisorse, C.N.R. Pavia. 4. Geological Survey of Western Australia, Department of Mines and Petroleum, Australia.

Corresponding email: alessandra.montanini@unipr.it

Keywords: Mantle geochemistry, refertilization, Corsica.

The St. Lucia nappe from Alpine Corsica includes a lower crustal section exhumed along the European rifted margin of the Ligurian Tethys (Beltrando et al., 2013). The lower crustal rocks consist of a High Grade Mafic Complex and a Granitoid Complex of Early Permian age. The base of the Mafic Complex is associated with up to 50-m thick mantle slices formed by mylonitic spinel-bearing Iherzolites and mm- to cm-thick pyroxenite and hornblendite layers elongated concordantly with the foliation of the host rocks. These rocks represent a unique occurrence of subcontinental lithospheric mantle in Corsica.

The mylonite microstructure in the Iherzolites is characterized by aligned porphyroclasts of pyroxene + spinel in a fine-grained polyphase matrix composed of olivine + pyroxenes + spinel. Relics of an older low-strain spinel tectonite predating the mylonite deformation are locally preserved as Opx porphyroclasts mantled by neoblastic Cpx + Opx + spinel. Major element compositions of olivine, Cpx and spinel porphyroclasts of the Iherzolites attest a fertile geochemical signature. The pyroxenites include (i) Opx-poor websterites with disseminated Cr-poor spinel, kaersutite and accessory Fe-Ni sulphides, (ii) Cr-rich spinel clinopyroxenites. Pyroxenites have fine-grained granoblastic texture with Al-rich Cpx porphyroclasts displaying high TiO₂ in the websterites (~1.0 - 1.5 wt.%) and lower contents (~0.5 wt.%) in the clinopyroxenites. The peridotites show lower Fo values in olivine, increasing TiO₂ contents in Cpx, decreasing Cr# in spinel and crystallization of Ti-rich amphibole over a distance < 2 cm from the websterite contact. Spinel-facies mylonite recrystallization in both Iherzolites and websterites occurred at ~850-900 °C. The hornblendites are made up of K₂O-rich kaersutite + Ti-rich phlogopite + ilmenite. The Cpx porphyroclasts from the Iherzolites show heterogeneous trace element compositions pointing to four different geochemical signature: Type 1 Cpx is markedly LREE-depleted (CeN/SmN down to 0.05) with nearly flat MREE-HREE at 8-10 times chondrite; Type 2 Cpx is moderately LREE-depleted (CeN/SmN = 0.31-0.49) and Type 3 has nearly flat LREE; Type 4 Cpxs are weakly LREE depleted, peak at MREE and show a slight HREE depletion with respect to MREE (GdN/YbN = 1.1-1.6) and variable HREE (e.g. YbN = 7-12). The websterite Cpxs display convex-upward REE patterns and higher concentrations of incompatible trace element. The Cpx from the clinopyroxenites is very similar to Type 4 Cpx from the Iherzolites. Kaersutite from the hornblendites are enriched in Rb, Ba, U, Nb, Ta, LREE and depleted in HREE with respect to the websterite ones.

The peridotite protoliths are interpreted as residua after low degrees of fractional melting of spinel facies DM. Type 4 Cpx from the peridotite reflect equilibrium with infiltrating MORB-type melts, which most likely produced also the clinopyroxenite layers. Computed melts in equilibrium with Cpx and kaersutite from the websterites and the hornblendites suggest transitional to alkaline affinity. This study shows that the St. Lucia mantle slices underwent injections of melts with MORB to alkaline affinity forming different kinds of magmatic layers, which were associated with a metasomatic imprint in the ambient peridotite.

Beltrando M., Zibra I., Montanini A. & Tribuzio R. 2013. Crustal thinning and exhumation along a fossil magma-poor distal margin preserved in Corsica: a hot rift to drift transition. *Lithos*, 168-169, 99-112.

Modelling the petrogenesis of the Ethiopian-Yemeni picrite-basalt CFB association: inferences on mantle heterogeneities and plume processes

Natali C.*, Beccaluva L., Bianchini G., Savo A. & Siena F.

Dipartimento di Fisica e Scienze della Terra, Università di Ferrara

Corresponding email: ntclcd@unife.it

Keywords: CFB, picrites, Afar plume.

The Oligocene Northern Ethiopian-Yemeni LIP, represented by a CFB plateau extending ca. 700 km in diameter, is characterized by a well-defined zonal arrangement with increasing plume-related physico-chemical features of erupted magmas, such as thermal regime, incompatible element enrichment and specific Sr-Nd-Pb-He isotopic fingerprint, from the periphery to the central plateau area (Beccaluva et al., 2009). Two CFB volcanic piles in the Lalibela district (Northern Ethiopia, ca. 2 km thick) and in the Manakhah section (Northern Yemeni plateau, ca. 1 km thick) which erupted close to the Oligocene Afar plume axis, are similarly characterized by very high-Ti transitional basalts and picrites (HT2, Beccaluva et al., 2009; 2011) that account for ca. 13% (40,000 km³) of the total Ethiopian-Yemeni CFB lavas. These magmas are characterized, in addition to the extremely high TiO₂ content (3-6 wt.%) by a high MgO content (mostly between 8 and 18 wt.%), and show striking compositional analogies with those from the Karoo province and the Siberian meimechites (Ellam & Cox, 1991; Heinonen et al., 2014). Petrological modelling based on whole rock FeO-MgO and Ol composition (Herzberg et al., 2007) indicates that some of picrites (MgO 16-17 wt.%) are near-primary magmas with olivine phenocrysts up to Fo 90.4. Calculation shows that the primary melts have picrite composition MgO 19.8-20.7 wt.% and were generated by polybaric melting in the pressure range 3-4 GPa at a potential temperature of 1570 °C. Together with high-MgO lavas from Hawaii and Gorgona, these are the highest temperatures of any OIB and LIP lavas. The available data suggest that HT2 magma sources necessarily require the involvement of specific high-Ti (and Fe) deep-seated sublithospheric components which were entrained and remobilized by the rising plume.

- Beccaluva L., Bianchini G., Natali C. & Siena F. 2009. Continental Flood Basalts and Mantle Plumes: a Case Study of the Northern Ethiopian Plateau. *J. Petrol.* 50, 1377-1403.
- Beccaluva L., Bianchini G., Ellam R.M., Natali C., Santato A., Siena F. & Stuart M.F. 2011. Peridotite xenoliths from Ethiopia: inferences on mantle processes from Plume to Rift settings. In: Beccaluva L., Bianchini G., Wilson M. Eds., *Volcanism and evolution of the African Lithosphere*. Geol. Soc. Am. Sp. Paper, 478, 77-104.
- Ellam R.M. & Cox K.G. 1991. An interpretation of Karoo picrite basalts in terms of interaction between asthenospheric magmas and the mantle lithosphere. *Earth Planet. Sci. Lett.* 105, 330-342.
- Heinonen J.S., Carlson R.W., Riley T.R., Luttinen A.V. & Horan M.F. 2014. Subduction-modified oceanic crust mixed with a depleted mantle reservoir in the sources of the Karoo continental flood basalt province. *Earth Planet. Sci. Lett.* 394, 229-241.
- Herzberg C., Asimow P.D., Arndt N., Niu Y., Leshner C.M., Fitton J.G., Cheadle M.J. & Saunders A.D. 2007. Temperatures in ambient mantle and plumes: Constraints from basalts, picrites and komatiites. *Geochem. Geophys. Geosys.*, 8, doi:10.1029GC001390.

Preliminary study on polymorphs of serpentine present in the ophiolites from La Rocchetta (Taro Valley, Eastern Ligurian Apennines, Italy)

Petriglieri J.R.^{1,2}, Salvioli-Mariani E.², Costa S.², Mantovani L.², Tribaudino M.²,
D'Alessio D.^{*2}, Bersani D.² & Lottici P.P.²

1. Laboratoire PPME, Université de la Nouvelle Calédonie, Noumea, Nouvelle Calédonie.
2. Dipartimento di Fisica e Scienze della Terra, Università di Parma.

Corresponding email: jasminerita.petriglieri@studenti.unipr.it

Keywords: Serpentine polymorphs, Raman Spectroscopy, ophiolites.

The ultramafic rocks of La Rocchetta outcrop in the Taro Valley, south of Mt. Penna and Mt. Aiona. These ophiolite complexes belong to the External Ligurid Units of the Northern Apennines and appear as large olistoliths within Cretaceous-Eocene sedimentary melange ("Complessi di base", Upper Cretaceous).

The peridotites of the External Ligurid ophiolites consist of fertile spinel lherzolite partially re-crystallized to plagioclase facies. They are intensely serpentinized but some bodies of kilometric size with preserved original textures and associations are retained.

The Mt. Rocchetta outcrop consists of serpentinites and peridotites of the Mt. Aiona Subunit. It probably was tectonically overlapped by the Casanova Complex and was subjected to a strong erosion. Indeed, its ultramafic rocks are less serpentinized and transformed than those intercalated and reworked of the Complex of Casanova. The Subunit of Mt. Aiona mainly consists of serpentinites and peridotites, subordinately gabbro and cumulitic peridotites. Relicts of fresh lherzolite with clinopyroxene, orthopyroxene, Mg-olivine and accessory Cr-spinel and plagioclase are present (Casnedi et al., 1993).

This work focuses on the identification and characterization of the polymorphs of the serpentine family present in these ophiolites. The introduction of micro-Raman spectroscopy, combined with the traditional analytical techniques – optical microscopy, SEM-EDS, XRD – has allowed to recognize the main minerals of the serpentine group directly on the sample, preserving their textural environments at micrometric scale. Raman peaks observed in the high wavenumber spectral range 3550-3850 cm⁻¹, associated with OH stretching vibrations, allowed the discrimination of all the varieties (Auzende et al., 2004). Because of their fine-grained distribution and sub-microscopically intergrown, especially in the fibrous veins, the characterization of these minerals has usually proved to be complex. In fact, many of the later fibrous veins of La Rocchetta ultramafic complex are mainly constituted, in contrast to the expectations, by the lamellar polymorphs of the group, instead by the fibrous one. This new analytical strategy shows how these different phases are much more intimately intermixed at a microscopic scale, than expected.

Auzende A.L., Daniel I., Reynard B., Lemaire C. & Guillot F. 2004. High-pressure behavior of serpentine minerals: a Raman spectroscopic study. *Phys. Chem. Minerals*, 31, 269-277.

Casnedi R., Galbiati B., Vernia L. & Zanzucchi G. 1993. Note descrittive della cartageologica delle ofioliti del gruppo di M. Penna e M. Aiona (Appennino Ligure-Emiliano). *Atti Tic. Sci. Terra*, 36, 231-268.

Geochemical evolution of mantle sources during continental rifting: the volcanism of the Red Sea

Pinarelli L.*¹, Mattash M.A.², Vaselli O.¹⁻³, Minissale A.¹ & Tassi F.¹⁻³

1. Istituto di Geoscienze e Georisorse, C.N.R. Firenze. 2. Geological Survey and Mineral Resources Board, Ministry of Oil and Minerals, Sana, Yemen. 3. Dipartimento di Scienze della Terra, Università di Firenze.

Corresponding email: lapina@igg.cnr.it

Keywords: Red Sea, geochemistry, mantle components.

Rift formation is a crucial topic in global tectonics. The Red Sea is part of the Afro-Arabian rift system, the world's largest active continental rift system. It is an exemplary case of a young rifting process that developed shortly after the arrival of a mantle plume at shallow depth, i.e. the Afar triangle. The mantle plume signature was indicated by the Ethiopian-Yemeni continental flood basalt sequences in the Late Eocene to Middle Miocene. The onset of continental rifting began ~22 Ma ago and encompassed the whole length of the present-day Red Sea basin and Gulf of Aden. The oceanic stage of the Red Sea, associated with the onset of seafloor spreading and production of oceanic crust, started about 5 Ma ago. In the late Oligocene-early Miocene up to the present time, large volumes of flood basalts emplaced at discrete eruptive centres along the western margin of the Arabian plate from the Gulf of Aden to the Mediterranean area. These plateau basalts are concentrated on the Arabian side of the Red Sea without matching counterparts on the Nubian plate, and represent one of the largest areas worldwide of predominantly alkali-olivine basalts.

Basaltic rocks from the Red Sea display systematic along-axis geochemical and isotope variation patterns. In the central Red Sea basin, associated with the current mid-ocean ridge, a N-MORB mantle component is prevalent. In both northern and southern sectors of the basin, basalts determined a mixing trend between a depleted component and a reservoir with prevailing HIMU component. The strongest HIMU signature is present at 17°N, where the site of the initial spreading is set. The sub-aerial magmas from the southern restricted extremity of the trough, along with continental flood basalts from the Cenozoic Yemen Volcanic Province, defined a mixing trend between N-MORB and a reservoir with dominant EM (I+II) component, geochemically and isotopically similar to the Arabia Lithospheric Mantle.

The geographical distribution of geochemical signatures is mostly consistent with a narrow mantle plume controlled by direct flow of asthenosphere beneath a pre-existing flexure in the continental lithosphere. The main asthenospheric source for the Red Sea volcanism lies eccentric to its axis and coincident with a north-south thermal line. At the place of initial seafloor spreading, 17°N, basalts show the strongest HIMU signature. From there, symmetric rift propagation, both northward and southward, away from the maximum mantle upwelling, is reflected by symmetric decreasing of the HIMU signature. Interaction with lithospheric mantle in both southern and northern restricted extremity of the trough produced the EM signature to the north (basalts from 25 to 26°N), to the south (the volcanic islands) and in the Yemen continental flood basalts.

Role of melt-mantle interactions on the composition of MORB: the case of Re-Os isotopes

Sanfilippo A.^{*1-2}, Morishita T.² & Senda R.³

1. Dipartimento di Scienze della Terra e dell'Ambiente, Università di Pavia. 2. Institute of Science and Engineering, Kanazawa University, Kakuma, Japan. 3. Japan Agency for Marine-Earth Science and Technology, Yokosuka, Japan.

Corresponding email: alessio.sanfilippo@unipv.it

Keywords: Re-Os isotopes, melt-rock reactions, troctolites.

One axiom of mantle geochemistry is that magmas produced by partial melting at mantle conditions attain the chemical equilibrium with their solid residue. This requires that Mid-Ocean Ridge Basalts (MORB) must preserve the same isotopic composition of the abyssal peridotites sampled at ocean floor. However, using MORB as proxy for their source composition neglects the evidences that parental MORBs can extensively interact with the shallow mantle during their ascent (Niu et al., 1997), a process that likely obliterates the composition of the parental melt (Collier & Kelemen, 2010). In this contribution, we propose that interactions between the abyssal mantle and melts migrating through it might have shaped the Os isotope composition of primitive troctolites from the southernmost area of the Central Indian Ridge. The radiogenic Os signature of these samples was likely produced by the selective assimilation of radiogenic interstitial sulphides from the reacted mantle. This mechanism is able to generate melts mimicking the entire Os isotope variability of MORB, without the need to invoke a component different than abyssal peridotites in their mantle source.

Collier M.L. & Kelemen P.B. The case for reactive crystallization at mid-ocean ridges. *J. Petrol.*, 51, 1913-1940.

Niu Y., Langmuir C.H. & Kinzler R.J. The origin of abyssal peridotites: A new perspective. *Earth Planet. Sci. Lett.*, 152, 251-265.

Olivine from replacive mantle bodies reveals modes of partial melting of the MORB mantle source

Sanfilippo A.*¹⁻², Tribuzio R.¹⁻², Ottolini L.² & Hamada M.³

1. Dipartimento di Scienze della Terra e dell' Ambiente, Università di Pavia. 2. Istituto di Geoscienze e Georisorse, CNR, Pavia.
3. Japan Agency for Marine-Earth Science and Technology, Yokosuka, Japan.

Corresponding email: alessio.sanfilippo@unipv.it

Keywords: Olivine, dunite, partial melting.

There is a general consensus that melts erupted on the seafloor are not in equilibrium with the residual mantle under low-pressures (Stolper, 1980). To preserve the original geochemical signature, the primitive melts must rise without re-equilibrating with surrounding peridotite. This may be accomplished by replacive mantle dunites (Kelemen et al., 1995). These rocks represent the main pathways for the extraction of the primitive mantle-derived melts and are expected to preserve the chemical characteristics of the parental melts acquired upon mantle melting. This contribution discusses the chemistry of olivine from MORB-type replacive mantle dunites exposed at the Lanzo South Massif. Three different analytical techniques were used to obtain a complete picture of the chemistry of olivine from these rocks, by coupling Laser Ablation and Secondary Ion Mass Spectrometry with Fourier Transform Infrared Spectroscopy. Minor (Ni, Mn and Co) and trace (Sc, V, Ti, Zr, Y and HREE) element compositions of the dunite olivines are consistent with formation by interaction between shallow peridotites and MORB-type melts (Piccardo et al., 2007). Chemical differences between the different dunite bodies led us to propose that the melts extracted through these high-permeability conduits were melt batches not fully aggregated after their formation in the asthenospheric source. Positive correlations among the concentrations of Ni, Mn, Co, Sc and V indicate equilibration with melts produced under different pressure conditions (Sanfilippo et al., 2014). New determinations of H, Li and B in the dunite olivines are consistent with this idea and suggest the involvement of a garnet-bearing component in the source of MORB. The chemistry of olivine from replacive mantle conduits is thus a powerful tool to explore the mode of partial melting of the MORB mantle, preserving a chemical heterogeneity not entirely documented in erupted melts.

- Kelemen P.B., Shimizu N. & Salters V. 1995. Extraction of mid-ocean ridge basalt from the upwelling mantle by focussed flow of melt in dunite channels. *Nature*, 375, 747-753.
- Piccardo G.B., Zanetti A., Poggi E., Spagnolo G. & Muntener O. 2007. Melt/peridotite interaction in the Southern Lanzo peridotite: field, textural and geochemical evidence. *Lithos*, 94, 181-209.
- Sanfilippo A., Tribuzio R. & Tiepolo M. 2014. Mantle-crust interaction in the oceanic lithosphere: constraints from minor and trace elements in olivine. *Geoch. Cosmoch. Acta*, 141, 423-439.
- Stolper E. 1980. A phase diagram for mid-ocean ridge basalts: Preliminary results and implications for petrogenesis. *Contrib. Mineral. Petrol.*, 74, 13-27.

SESSION S3

The cycles of volatiles: fluxes and processes from the oceans, down to the mantle and backward to the Earth surface

CONVENORS

Giovanni Chiodini (INGV Napoli)

Elisabetta Erba (Univ. Milano)

Stefano Poli (Univ. Milano)

Microbial biogeomorphology in extreme surface environments fed by hot and cold springs and its implications

Barbieri R.* & Cavalazzi B.

Dipartimento di Scienze Biologiche, Geologiche e Ambientali, Università di Bologna.

Corresponding email: roberto.barbieri@unibo.it

Keywords: Biogeomorphology, hydrothermalism, microbes.

The interactions between organisms and physical environments lead to landforms that are the direct expression of biological activity across different scales. Because of their ubiquity and ability to interact with rock/mineral surfaces, microbes are important geologic agents and their effects can be observed in a wealth of extreme surface environments since the Archean. Critical settings in which microbes play primary roles in processes such as mineral precipitation, sediment trapping, and weathering include those typified by hot and cold springs. Here the production in large areas of biofilms and biological structures by prokaryotes (such as cyanobacterial filaments) and eukaryotes (such as diatoms) - strictly depending on physical factors that may include the chemistry of water springs, thermal gradients, UV radiation and oxidative processes - can impact on the development and stabilization of surface morphologies with some fossilization potential. Examples can be found from hydrothermal travertines in the complex array of interactions between the extracellular polymeric substances of the microbial slimes, the bacterial and diatom cells that they host, and sediment/mineral component.

Compared to deep marine hydrothermal sites, those from subaerial areas represent an obvious facilitation for observation of the phenomena mediated by hot/cold springs. Because the hydrothermal systems sustain a variety of biospaces since the dawn of our planet, and it is assumed that they were also present on the surface of Mars (as in the Gusev Crater, the site currently explored by the NASA rover Curiosity), the significance of these natural systems is potentially enormous for i) the identification and the measure of diversity of the microorganisms involved in Earth surface processes and landforms, and ii) the search of traces of Martian life and habitable environments.

Biogenic carbonate paleofluxes as proxy for $p\text{CO}_2$ during the Aptian

Bottini C.* & Erba E.

Dipartimento di Scienze della Terra "A. Desio", Università di Milano.

Corresponding email: cinzia.bottini@unimi.it

Keywords: Biogenic carbonate fluxes, nannofossils, Aptian.

Coccolithophores are phytoplanktonic algae which produce a calcitic exoskeleton (coccosphere) and are extremely important primary producers playing a direct role on the equilibrium of the organic and inorganic carbon cycle. Laboratory experiments on living coccolithophores documented decreased biocalcification and partial production of deformed/malformed coccoliths in some species as a consequence to increased surface-water acidification associated with elevated CO_2 concentrations. A similar response is registered during geological intervals of super-greenhouse climate and profound environmental perturbations. Specifically, malformed coccoliths were identified during the early Aptian Oceanic Anoxic Event (OAE) 1a characterized by emission of large amount of CO_2 , widespread organic matter burial in oxygen-depleted oceans, paralleled by a decrease in total nannofossil carbonate paleofluxes. The OAE 1a was also accompanied by a geologically rapid warming and input of biolimiting metals in the oceans associated with multiple volcanic phases of the Ontong Java Plateau (OJP). The late Aptian was instead characterized by intervals of intense sub-aerial volcanism of the Kerguelen Plateau (KP) province and resulted to be coeval with interludes of relatively cool conditions.

The aim of this study is to reconstruct the biogenic carbonate production of calcareous nannoplankton during the Aptian and detect if and how biocalcification of coccolithophores was affected by fluctuating $p\text{CO}_2$ prior, during and after the construction of the OJP and KP. Specifically, we present quantitative analyses of nannofossil micrite in thin sections and reconstructed nannofossil calcite paleofluxes in three drill sites: the Cismon core (Northern Italy), Piobbico core (Central Italy) and DSDP Site 463 in the mid-Pacific Mountains. The data obtained revealed a drastic reduction in nannoplankton calcification starting in the latest Barremian related to a decrease in the rock-forming nannoconids ("nannoconids decline") that culminated with the "nannoconids crisis" just prior to OAE 1a. At the end of OAE 1a, nannofossil biocalcification increased again, but it never reached pre-anoxia values. In the late Aptian, nannofossil paleofluxes reached high values only during the *Nannoconus truittii* acme, followed by a final collapse across the Aptian/Albian boundary interval.

The variations in nannoplankton carbonate production are interpreted as the adaptive response to perturbed surface-water conditions that favoured small and less calcified forms and caused false extinctions among heavily calcified nannoconids. The correlation between reduced biocalcification rates and intervals of intense volcanism, suggests that mid-Cretaceous nannoplankton biocalcification and nannofossil paleofluxes were strongly controlled by excess volcanogenic CO_2 . Following this observation, we propose calcite paleofluxes as proxy for reconstructing past atmospheric CO_2 and provide possible scenarios of paleo CO_2 concentrations delivered by OJP and KP volcanism and interplay with climate changes.

Chemistry and fluxes of major and trace element from worldwide passive degassing volcanoes: a critical review

Calabrese S.*¹, D'Alessandro W.², Aiuppa A.¹ & Parello F.¹

1. Dipartimento di Scienze della Terra e del Mare, Università di Palermo. 2. INGV, Palermo.

Corresponding email: sergio.calabrese@gmail.com

Keywords: Trace elements, passive degassing volcanoes, fluxes.

Volcanic emissions represent one of the most important natural sources of trace elements (e.g. As, Cd, Cu, Hg, Pb, Sb, Tl and Zn) into the atmosphere, sequentially influencing the hydrosphere, lithosphere and biosphere. The human health hazard during episodic volcanic eruptions generally follows from deposition of coarse and fine particles (2.5-10 and < 2.5 µm) that produces effects such as asthma and lung and respiratory disease. Regarding passive degassing volcanoes, the harmful effects of fluorine fumigation are known both for vegetation (foliar necrosis) and human/animals (fluorosis), but only a few studies have been focused on the effects of potentially toxic trace elements. From a review published work on the metal output from active worldwide volcanoes, 52 publications (the first dating back to the 70's) were identified, 13 of which on Etna and the others from some of the world most active volcanoes: Mt. St. Helens, Stromboli, Vulcano, Erebus, Merapi, White Island, Kilauea, Popocatepetl, Galeras, Indonesian arc, Satasuma and Masaya. In general, the review shows that available information is scarce and incomplete. We compiled a database both for concentrations and fluxes of 59 chemical elements (major and trace), which allowed us to constrain the compositional and output range. In this study we also present unpublished results from Etna (Italy), Turrialba (Costa Rica), Nyiragongo (Democratic Republic of Congo), Mutnovsky and Gorely (Kamchatka), Aso Asama and Oyama (Japan). Concentrations of major and trace elements were obtained by direct sampling of volcanic gases and aerosols on filters. Sulfur and halogens were collected by using filter-packs methodology, and analyzed by ion chromatography. Untreated filters for particulate were acid digested and analyzed by ICP-OES and ICP-MS. Sulfur to trace element ratios were related to sulfur fluxes to indirectly estimate elemental fluxes. Etna confirms to be one of the greatest point sources in the world. Nyiragongo results to be an additional large source of metals to the atmosphere, especially considering its persistent state of degassing from the lava lake. Turrialba and Gorely also have high emission rates of trace metals considering the global range. Only Mutnovsky volcano show values which are sometimes lower than the range obtained from the review, consistent with its dormant (fumarolic) stage of activity.

The accurate estimation of individual and global volcanic emissions of trace metals is still affected by a high level of uncertainty. The latter depends on the large variability in the emission of the different volcanoes, and on their changing stage of activity. Moreover, only few of the potential sources in the world have been directly measured. This preliminary work highlights the need to expand the current dataset including many other active volcanoes for better constraining the global volcanic trace metal fluxes.

Sulfur degassing from LIPs estimated through clinopyroxene/melt S partition coefficient: synchrotron analyses and experimental constraints

Callegaro S.*¹, Baker D.R.², Marzoli A.¹, De Min A.³ & Geraki K.⁴

1. Dipartimento di Geoscienze, Università di Padova. 2. Department of Earth and Planetary Sciences, McGill University, Montreal, Canada. 3. Dipartimento di Matematica e Geoscienze, Università di Trieste. 4. Diamond Light Source, Harwell Science and Innovation Campus, UK.

Corresponding email: sara.callegaro@unipd.it

Keywords: Volcanic degassing, sulfur, partition coefficient.

In the geologic past, Large Igneous Provinces (LIPs) prompted severe environmental upheavals through massive degassing of volcanic SO₂ and CO₂. The delineation of LIPs' climatic impacts hinges on estimates of magmatic gas burdens, which are still scarce and based only on melt inclusions, which yield potentially biased results (Baker, 2008). We recently presented (Callegaro et al., 2014) a new approach for sulfur quantification in basaltic magmas, based on S equilibrium partitioning between pyroxene and melt. The partition coefficient (K_D) was obtained on experimental augites and basaltic glasses by micro-XRF (Diamond synchrotron, UK) and ion microprobe (WHOI, USA) analyses. Subsequent measures of S in natural augite crystals by *in-situ* micro-XRF allowed calculation of the S dissolved in the equilibrium melts of three LIPs. We showed that the amount of S in the basalts correlates positively with the severity of the LIPs' aftermath as recorded in the geological/paleontological record. Recently, we performed new piston cylinder experiments (800 or 1000 MPa, at 1000-1350 °C), to investigate how the composition, oxidation state and water content of melts affect the cpx/melt K_D , with the aim of extending the applicability of this new method to a broader spectrum of igneous rocks. Using andesite and dacite glass powders doped with pyrrhotite, and a Mid Ocean Ridge Basalt, anhydrous and hydrous (ca. 5 wt.% H₂O) experiments were performed at different oxygen fugacities (around 3 log units above and below the fayalite-magnetite-quartz buffer). Preliminary results showed that cpx/melt K_D correlates with melt SiO₂, whereas it does not vary significantly with the H₂O content. The clinopyroxene crystal chemistry has a strong effect on S partitioning, i.e. cpx/melt K_D is negatively correlated with the Mg# (calculated with either total or Fe²⁺) of the cpx. Notably, cpx/melt K_D s at FMQ-2, where a sulfide species dominates in the melt, are significantly higher than at FMQ+2, where a sulfate species dominates. These observations suggest that S²⁻ presumably replaces O in the crystal structure and is probably associated with Fe²⁺.

Baker D.R., 2008. The fidelity of melt inclusions as records of melt composition. *Contrib. Mineral. Petrol.*, 156, 377-395.

Callegaro S., Baker D.R., De Min A., Marzoli A., Geraki K., Bertrand H., Viti C. & Nestola F. 2014. Microanalyses link sulfur from large igneous provinces and Mesozoic mass extinctions. *Geology*, 42, 895-898.

Diffuse CO₂ Earth degassing in Italy: a globally relevant study case

Cardellini C.*¹, Chiodini G.², Frondini F.¹ & Caliro S.³

1. Dipartimento di Fisica e Geologia, Università di Perugia. 2. Istituto Nazionale di Geofisica e Vulcanologia, Bologna
3. Istituto Nazionale di Geofisica e Vulcanologia, Osservatorio Vesuviano, Napoli.

Corresponding email: carlo.cardellini@unipg.it

Keywords: CO₂ earth degassing, CO₂ flux, carbon budget.

Central and southern Italy are affected by an active and intense process of CO₂ Earth degassing as revealed by numerous studies focussed on CO₂ fluxes from point emission and soil diffuse degassing, and on the carbon dissolved by the groundwater. Regional scale studies, based on carbon mass balance of groundwater, highlighted the presence of two large CO₂ degassing structures that, for magnitude, shape and geochemical-isotopic features, can be related to a regional scale process of uprising of deeply derived fluids. Central and southern are also characterised by the presence of many cold gas emissions where deeply derived CO₂ is released by both vents and soil diffuse degassing, where soil CO₂ fluxes are order of magnitude higher than the biogenic CO₂ fluxes and are generally associated to tectonic structures. Both direct CO₂ expulsion and carbon-rich groundwater are different manifestations of a large scale regional process. The released gases show a roughly E-W compositional-isotopic trend, revealing the possible occurrence of common deep source of fluids and the occurrence of more “shallow”, i.e., crustal, processes contributing to the geochemical variability. Quantitative estimates provided i) a regional CO₂ flux of about 9 Mt/y based on the carbon dissolved in groundwaters and ii) a flux of about 1.4 Mt/y by the measured gas emissions, which are only a minor part of the existing. Summing this two estimates the CO₂ flux from the region results globally relevant, being from 2 to 10% of the estimated present-day global CO₂ discharge from subaerial volcanoes. Besides the magnitude of the process, interesting links between the CO₂ degassing and the seismicity of the region and a strict correlation between the input of deep CO₂-rich fluids in to the regional aquifers and the heat flux in the Apennine region have been highlighted. The studies performed in Italy on “non-volcanic” CO₂ degassing, together with global distribution of evidences of earth degassing, suggest that a better quantitative knowledge of CO₂ fluxes from non-volcanic, tectonically active areas worldwide, would contribute to better constrain the global CO₂ budget. To support this goal, a new global database of gas emissions (MaGa) is under development, starting from the Italian experience.

Tithonian Nannofossil Calcification Events and the Shatsky Rise Plateau emplacement: is there a relationship?

Casellato C.E.* & Erba E.

Dipartimento di Scienze della Terra "A. Desio", Università di Milano.

Corresponding email: cristina.casellato@unimi.it

Keywords: Volatiles, nannoplankton, Late Jurassic.

Ocean fertility and chemistry, climatic conditions and pCO₂ are controlling factors of nannoplankton abundance and diversity. Earth degassing associated with igneous-tectonic activity triggers major variations in CO₂ that may induce ocean acidification hampering biocalcification including a general suppression of coccolithophores. It is most plausible that construction of large oceanic igneous provinces affected the marine ecosystem at global scale, triggering fluctuations in calcareous nannoplankton biodiversity and abundance.

The latest Jurassic was a crucial time for nannoplankton evolution: a rapid diversification took place, with a rise in abundance of several taxa and a consequent major increase in biogenic calcite (= pelagic micrite) production. Interestingly, it was also the time of emplacement of the Shatsky Rise Plateau in the Pacific Ocean.

Were there any linkages between calcareous nannoplankton evolution and this major geologic event? High-resolution chronology of paleobiological and geological events is crucial for assessing potential causal links between emplacement of volcanic provinces and ecosystem perturbations possibly driving evolutionary processes. We selected a few sections from Tethys and Atlantic Oceans with a high-resolution bio-magnetostratigraphic framework, to gain nannofossil calcite palaeofluxes. The appearances of several new taxa and consecutive abundance increases in the Tithonian resulted in discrete intervals of elevated micrite production, named nannofossil calcification events (NCE). A first NCE 1 occurred in the Early Tithonian (nannofossil Zones NJT15-NJT16a, magnetochrons CM22n-CM20r) and a second NCE 2 occurred across the Jurassic/Cretaceous boundary (nannofossil Zones NJT17-NK1; magnetochrons CM19-CM18).

Tithonian NCEs suggest the establishment of paleoenvironmental conditions ideal for nannoplankton diversification and their spread through the photic zone. Cooler and arid climate and stable oligotrophic oceanic conditions under low CO₂ levels favored the appearance and rapid evolution of heavily calcified taxa producing NCEs. While the causes of the Tithonian cooler climate and stable oceanic conditions remain elusive, we notice that the interruption between NCE 1 and NCE 2, a discrete interval of suppressed nannoplankton calcification, correlates with the construction phase of the huge TAMU Massif within the Shatsky Rise province (nannofossil subzone NJT16b, magnetochron CM20n). When the history of the southern Shatsky Rise is considered, we see a possible link with the onset of a major origination episode in calcareous nannoplankton during the Tithonian. Perhaps, magmas especially rich in biogeochemically important elements from the mantle might be crucial for biota evolution. However, excess volcanogenic CO₂ during the paroxysmal construction phase of the TAMU Massif apparently hampered nannoplankton calcification possibly under some ocean acidification, although in absence of extinctions.

The Toarcian Oceanic Anoxic Event and the emplacement of the Karoo-Ferrar Large Igneous Province: calcareous nannoplankton evidence trace major climate and paleoceanographic changes

Casellato C.E.* & Erba E.

Dipartimento di Scienze della Terra "A. Desio", Università di Milano.

Corresponding email: cristina.casellato@unimi.it

Keywords: Toarcian Oceanic Anoxic Event, calcareous nannoplankton, Karro-Ferrar Large Igneous Province.

The Early Jurassic was punctuated by a huge speciation episode of calcareous nannoplankton (Pliensbachian-Early Toarcian) and the Toarcian Oceanic Anoxic Event (T-OAE). The latter is associated to a global climatic-oceanographic perturbation, marked by a C-isotopic anomaly, coeval with the emplacement of the Karoo-Ferrar Large Igneous Province (LIP).

We quantitatively investigated calcareous nannofossils through the uppermost Pliensbachian-lower Toarcian at Colle di Sogno (Southern Alps) to reconstruct paleoecological affinities and paleoceanographic conditions preceding, during and following the T-OAE.

Results indicate that the latest Pliensbachian was characterized by the highest nannofloral abundances, with the large and higher calcified forms dominating (*Schizosphaerella*, *M. jansae*). A first change is registered across the Pliensbachian/Toarcian boundary with a decline of *Schizosphaerella* and an increase of small coccoliths/nannoliths. The major shift in nannoplankton assemblages is at the onset of the T-OAE: abundances are halved, with a dramatic drop of heavily calcified forms (*Schizosphaerella*, *M. jansae*) paralleled by the increase of small and less calcified coccoliths (*Lotharingius*, *Biscutum*) that show relatively high abundances through the T-OAE. The interval following the T-OAE sees the partial recovery of *Schizosphaerella*, while coccoliths decrease and *M. jansae* disappears.

Principal Component Analysis implemented nannofossil paleoecological and paleoenvironmental reconstructions. Stable oligotrophic conditions favourable to calcification at low CO₂ levels promoted the proliferation of deep-dwelling and high-calcified *Schizosphaerella* in the latest Pliensbachian. During the Early Toarcian enhanced continental run-off introduced terrigenous material favouring the intermediate-dweller *M. jansae* and the low-salinity adapted *Calyculus*. The "Schizosphaerella decline" interval may imply initial ocean acidification that magnified during the T-OAE, concomitant with higher nutrient concentrations stimulating mesotrophic low-calcified coccolith producers. After the T-OAE, the partial recovery of calcareous nannoplankton indicates still perturbed conditions. We infer that the observed nannofossil variations are due to a combination of fertility, changes in surface water salinity and calcification failure under high CO₂ levels, a scenario compatible with variations in atm-CO₂ triggered by the emplacement of Karoo-Ferrar LIP. The CO₂ degassing during the LIP construction may have triggered climate change, accelerated hydrological cycle and weathering, which in turn drove changes in nannofloras. The latest Pliensbachian-Early Toarcian nannoplankton speciation episode is testified by high rates of appearances without extinctions: although dramatic changes in nannofloral communities are recorded, the perturbations associated to the T-OAE may had also some positive effects on evolution, stimulating calcification of new coccolith morphologies.

Geochemical characterization of the fluids circulating in the Kizildag ophiolitic body (Turkey)

D'Alessandro W.*¹, Yuce G.², Italiano F.¹, Bellomo S.¹ & Gulbay A.H.³

1. INGV, Palermo. 2. Department of Geological Engineering, Hacettepe University, Ankara, Turkey
3. Eskişehir Osmangazi Üniversitesi, Turkey.

Corresponding email: walter.dalessandro@ingv.it

Keywords: Serpentinization, abiotic methane, hydrogen.

The large Kizildag ophiolitic body (~ 1000 km²) outcrops in the Hatay region (southern Turkey). It belongs to the peri-Arabian ophiolite belt that includes the Troodos (Cyprus), Baër-Bassit (Syria) and Semail (Oman) ophiolites in the eastern Mediterranean region which are the remnants of the Southern Tethys oceanic lithosphere. The study of ultramafic rocks and especially their hydration products (serpentinites) received great impulse in recent years. In particular serpentines play an important role in the C cycle and are considered as a possible candidate for the origin of life on the Earth.

Until now 6 groups of hyperalkaline springs and 1 cold gas seep have been sampled in the area. Apart from several water samples, analysed for major ions, trace elements and water isotopes, also 23 gas samples (dry seeps, bubbling and dissolved gases) were analysed for their chemical (He, Ne, Ar, O₂, N₂, H₂, CO, CH₄, C₂-C₅ hydrocarbons and CO₂) and isotopic composition (He, C and H).

All gas samples were characterized by low CO₂ contents (generally < 1000 ppm) and variable H₂ and CH₄ contents (from < 5 up to 605,000 ppm and from 36 to 942,000 ppm respectively). $\delta D-H_2 < -700\text{‰}$ indicate low formation temperatures (< 50 °C). $\delta^{13}C-CH_4$ of ~ -5 ‰ and C₁/(C₂+C₃) ratios < 100 indicates a purely abiogenic origin for CH₄ in the dry seeps while values as low as ~ -30‰ and C₁/(C₂+C₃) ratios > 1000 in some of the bubbling gases could indicate a partial biogenic contribution.

Further geochemical and microbiologic studies should help us to understand the biotic or abiotic processes that are responsible of the high variability in the H₂ and CH₄ concentrations of these fluids.

Gas manifestations of Greece: Catalogue, geochemical characterization and gas hazard definition

Daskalopoulou K.*¹, D'Alessandro W.², Kyriakopoulos K.³, Calabrese S.¹ & Parello F.¹

1. INGV, Palermo. 2. Department of Geology & Geo-environment, National & Kapodistrian University of Athens, Greece.
3. Dipartimento di Scienze della Terra e del Mare, Università di Palermo.

Corresponding email: kdaskalopoulou@hotmail.com

Keywords: Geochemical characterization, gas hazard, Greece.

Like other geodynamically active areas, Greece is affected by a large number of geogenic gas manifestations. These occur either in form of point sources (fumaroles, mofettes, bubbling gases) or as diffuse emanations.

We produced a first catalogue of the geogenic gas manifestations of Greece also considering few literature data. Collected samples were analysed for their chemical (He, Ne, Ar, O₂, N₂, H₂, H₂S, CO, CH₄ and CO₂) and isotopic composition (He, C and N).

Most of the sampled gas manifestation are found along the South Aegean active volcanic arc (32 sites) and in the majority they belong to the CO₂ dominated group. Very few gas manifestations, N₂- or CH₄- dominated, are found along the most external units of the Hellenides orogen (Apulia domain - W and SW Greece), where generally compressive or transpressive tectonic prevails. On the contrary, gas manifestations (mainly CO₂- dominated) are widespread along northern Greece (28 sites) and along Sperchios basin - north Evia graben (12 sites) which are characterised by extensional tectonic.

Geogenic gases, apart from having important influences on the global climate, could have strong impact on human health. Gas hazard is often disregarded because fatal episodes are often not correctly attributed. Geodynamic active areas release geogenic gases for million years over wide areas and the potential risks should not be disregarded.

A preliminary estimation of the gas hazard has been made for the last 20 years considering the whole population of Greece. In this period at least 2 fatal episodes with a total of 3 victims could be certainly attributed to CO₂. This would give a risk of $1.3 \cdot 10^{-8}$ fatality per annum. Such value, probably underestimated, is much lower than most other natural or anthropogenic risks. Nevertheless this risk, being unevenly distributed along the whole territory, should not be overlooked and better constrained in areas with high density of gas manifestations and high soil gas fluxes.

Environmental consequences of Ontong Java Plateau and Kerguelen Plateau volcanism: Climate and ocean variability under excess CO₂

Erba E.* & Bottini C.

Dipartimento di Scienze della Terra "A. Desio", Università di Milano.

Corresponding email: elisabetta.erba@unimi.it

Keywords: Large igneous provinces, climate change, ocean dynamics.

The mid-Cretaceous was marked by emplacement of large igneous provinces (LIPs) that formed gigantic oceanic plateaus, affecting ecosystems on a global scale, with biota forced to face excess CO₂ resulting in climate and ocean perturbations. Construction of Ontong Java Plateau (OJP) and Southern Kerguelen Plateau (SKP) are radiometrically dated and correlate with paleoenvironmental changes, suggesting causal links between LIPs and ecosystem responses. Aptian biocalcification crises and recoveries are largely coeval with C, Pb, and Os isotopic anomalies, trace metal fluxes, global anoxia, and climate changes.

In the latest Barremian-earliest Aptian intermediate temperatures characterized the pre-Oceanic Anoxic Event (OAE) 1a interval, followed by a maximum warming (of ca. 2 °C) during the first phase of anoxia under intense volcanic activity of the OJP. A short-lived cooling episode interrupted the major warming, following a rapid increase in weathering rates. Early Aptian greenhouse or super-greenhouse conditions were followed by prolonged cooling during the late Aptian when OJP and SKP developed, respectively. The lowest temperatures (ca. -5 °C relative to Barremian climate), combined with low fertility, were reached in the middle-late Aptian. The prolonged cooling that correlates with formation of the SKP, was followed by progressive warming across the Aptian/Albian boundary.

Massive volcanism occurring at equatorial versus high paleolatitudes and submarine versus subaerial settings triggered very different climate responses but similar disruptions in the marine carbonate system. Excess CO₂ arguably induced episodic ocean acidification that was detrimental to marine calcifiers, regardless of hot or cool conditions. Global anoxia was reached only under extreme warming, whereas cold conditions kept the oceans well oxygenated even at times of intensified fertility. The environmental disruptions attributed to the OJP did not trigger a mass extinction: rock-forming nannoconids and benthic communities underwent a significant decline during OAE 1a, but recovered when paroxysmal volcanism finished. Extinction of many planktonic foraminiferal and nannoplankton taxa, including most nannoconids, and most aragonitic rudists in latest Aptian time was likely triggered by severe ocean acidification.

Upgraded dating of paleoceanographic events, improved radiometric ages of the OJP and SKP, and time-scale revision are needed to substantiate the links between magmatism and paleoenvironmental perturbations.

The effects of excess CO₂ on calcareous nannoplankton biocalcification: the case history of the latest Cenomanian Oceanic Anoxic Event 2

Faucher G.*, Erba E. & Bottini C.

Dipartimento di Scienze della Terra "Ardito Desio", Università di Milano.

Corresponding email: giulia.foucher@unimi.it

Keywords: CO₂, OAE 2, coccoliths.

The latest Cenomanian Oceanic Anoxic Event 2 (OAE 2, ~ 94 Ma) represents a profound perturbation of the ocean-atmosphere system caused by natural CO₂ emissions related to the emplacement of the Caribbean Plateau inducing climate change, ocean fertilization and acidification. This study was performed on pelagic sediments from five localities: Eastbourne (Sussex, United Kingdom), Clot de Chevalier (France), Novara di Sicilia (Sicily, Italy) and two Western Interior sections (Pueblo, Colorado and Cuba, Kansas, USA). These five sections have been chosen based on availability of integrated stratigraphy. In fact, they all have a good time control, especially C isotopic stratigraphy and biostratigraphy, that offers the opportunity to correlate data from the different localities, discriminating between local, regional and global changes.

The work was aimed at the identification of possible changes in coccolith size/shape as a response to paleoenvironmental perturbations associated with Oceanic Anoxic Event 2 (OAE 2). Biometric analyses were performed on selected coccolith species *Biscutum constans* and *Watznaueria barnesiae* across the Cenomanian – Turonian time interval. For each species, length and width of coccoliths have been measured on digitally captured images. The data collected document a decrease in size of *B. constans* observed in all sections during OAE 2, interpreted as due to excess CO₂ that might have induced species-specific dwarfism. On the other hand, any changes in size of *W. barnesiae* were detected, suggesting that this taxon was less sensitive to stressed environmental conditions.

The comparison of our morphometric data with those available for the early Aptian OAE 1a and latest Albian OAE 1d, indicates that *B. constans* repeatedly underwent size reduction and malformation possibly suggesting that the same paleoenvironmental factors controlled calcification of *B. constans* during OAEs. The analyses also pointed out a progressive reduction of the mean size of *B. constans* through time, with generally larger specimens in the early Aptian, intermediate in the late Albian and smaller in the Cenomanian-Turonian boundary interval, here potentially ascribed to different degrees of paleoenvironmental changes. The data available for OAE 1a, OAE 1d and OAE 2 suggest that ocean chemistry related to the amount of CO₂ concentrations, played a central role in coccolith secretion by *B. constans*. We speculate that, even if different degrees (and maybe types) of paleoenvironmental perturbations were acting during the Cretaceous OAEs, biocalcification of specific coccoliths reacted analogously with dwarfism when threshold conditions of excess CO₂ and warming were reached.

OH incorporation in quartz in lithium-bearing systems at high pressure

Frigo C.* & Stalder R.

Institute of Mineralogy and Petrography, University of Innsbruck, Austria.

Corresponding email: corinne.frigo@uibk.ac.at

Keywords: OH-defects, quartz, high pressure.

Hydrogen is a common impurity in quartz either as molecular water in fluid inclusions either as OH point defects in its structure. Because of its wide occurrence in a broad variety of rocks, numerous studies on fluid inclusions and trace elements in natural and synthetic quartz have been performed for applications to geothermobarometry. On the other hand, several studies focused on hydrogen incorporation as OH point defects mainly for interpreting its influence on the physicochemical properties of quartz. Recent experiments on hydrogen incorporation in quartz exhibit a pressure dependent OH incorporation behaviour that may be used as information source of the formation conditions (Stalder & Konzett, 2012; Baron et al., 2015). In this work, quartz crystals were grown from a spodumene-granite starting material (i.e., a Li-rich system) with 13-26 wt.% water at 900-1050°C and 5-20 kbar in a piston cylinder apparatus. The quenched run products were analyzed by IR spectroscopy and electron microprobe and consisted of a free aqueous fluid, quartz, and amorphous quench material. BSE images of the run products showed quartz crystals included in water saturated melt and revealed that the grain size of quartz increases with pressures. Preliminary results for Al-concentration in quartz cluster around 200-300 ppm for most selected crystals, but may reach values up to 1600 ppm. IR absorption spectra revealed absorption features that can be assigned to AlOH- (3310, 3378 and 3430 cm^{-1}), LiOH- (3483 cm^{-1}) and (4H)Si-defects (3583 cm^{-1}). Both AlOH- and LiOH-defects exhibited a negative correlation with pressures between 5 and 15 kbar, where LiOH basically dropped to zero. Two additional experiments were performed with progressively higher spodumene concentration at 10 kbar to investigate the saturation level of LiOH-defects in quartz. A positive trend between LiOH-defect in quartz (from 1 ppm to 4 ppm) and spodumene content (between 2% and 20%) in the starting material suggests that the system was not saturated with respect to spodumene. Saturation may be reached earlier at lower pressure, as LiOH incorporation at 5 kbar is comparably high (6.5 ppm) even at low Li-contents in the system. Therefore, further piston cylinder experiments, e.g., 1) at 5 kbar and moderate Li-content and 2) at 10 kbar and higher spodumene concentration are required. Furthermore, a smaller amount of AlOH-defects in quartz within a Li-richer system was observed. Such result might depend on a preferred coupled incorporation of Li^+ and Al^{3+} by forming a “dry” defect. To prove this hypothesis, further electron microprobe and LA-ICP-MS analyses are required.

Baron M.A., Stalder R., Konzett J. & Hauzenberger C.A. 2015. OH-point defects in quartz in B- and Li-bearing systems and their application to pegmatites. *Phys. Chem. Min.*, 42, 53-62.

Stalder R. & Konzett J. 2012. OH defects in quartz in the system quartz-albite-water and granite-water between 5 and 25 kbar. *Phys. Chem. Min.*, 39, 817-827.

Interaction between geosphere and biosphere in geothermal soil at Pantelleria Island, Italy

Gagliano A.L.¹, D'Alessandro W.*¹, Tagliavia M.², Franzetti A.³, Parello P.⁴ & Quatrini P.⁵

1. Istituto Nazionale di Geofisica e Vulcanologia, Palermo. 2. Istituto per l'Ambiente Marino Costiero, C.N.R. Capo Granitola. 3. Dipartimento di Scienze dell'Ambiente e del Territorio e di Scienze della Terra, Università di Milano-Bicocca. 4. Dipartimento di Scienze della Terra e del Mare, Università di Palermo. 5. Dipartimento di Scienze e Tecnologie Biologiche Chimiche e Farmaceutiche (STEBICEF), Università di Palermo.

Corresponding email: walter.dalessandro@ingv.it

Keywords: Geothermal areas, methane, methanotrophs.

Every day tons of gases, including CH₄, are released in to the atmosphere from geothermal areas, increasing the global warming effect. Total CH₄ emissions strictly depend by the co-evolution of the geosphere and biosphere in extreme environments. In fact, geofluids drive the chemical differentiation of soils, and feed the microbiota that often acts a natural filter. Although the interdependence of biota and abiotic factors is intuitive, knowledge on how they interact, in these environments, is still scarce. Our aim is to better understand how the soil microbial communities of two close geothermal sites (FAV1 and FAV2) at Pantelleria respond to different geochemical conditions. Pantelleria Island is an active volcanic system, hosting a high energy geothermal system. Top-soil and soil gases were sampled at the most exhalative area, Favara Grande. The sites were similar in the main components of the hydrothermal gas (CH₄, H₂, CO₂) and surface temperature, but different in soil chemistry (in particular, pH, NH₄⁺, H₂O, sulphur). Site FAV2 showed milder condition (higher pH, lower amount of NH₄⁺, sulphur, H₂O content) than site FAV1. Soil gases, from a vertical profile, suggested that these differences were due to a lowering of the hydrothermal flux velocity in deeper layers at milder site, that leads to the depletion of the soluble species (such as H₂S and NH₃) in the hydrothermal gases when they reach the surface. Conversely, the hydrothermal flux was still sustained up to the surface at site FAV1. These conditions created two totally different environments for the microbiota thriving in these sites. As reported in Gagliano et al. (2014), FAV2 showed high CH₄ consumption and FAV1 was totally inactive although both were characterized by high CH₄ emissions. Next-Generation Sequencing (NGS) techniques were applied to describe the two bacterial communities. The FAV2 bacterial community was characterized by an extraordinary diversity of methanotrophs, with 40% of the 16S gene sequences assigned to *Methylocaldum*, *Methylobacter* (Gammaproteobacteria) and *Bejerickia* (Alphaproteobacteria); conversely, a community of thermo-acidophilic chemolithotrophs (*Acidithiobacillus*, *Nitrosococcus*) dominates at FAV1, in the absence of methanotrophs. FAV1 physical-chemical factors (e.g. temperature and pH), cannot be considered limiting for methanotrophy. Our results suggest that hydrothermal flux, determining abundant availability of high energy electron donors and acceptors, and controlling the temperature, creates more energetically favourable conditions for chemolithotrophs at site FAV1. Thus chemolithotrophs take over methanotrophs at FAV1, suggesting a previously unrecognized competition between chemolithotrophy and methanotrophy.

Gagliano A.L., D'Alessandro W., Tagliavia M., Parello F. & Quatrini P. 2014. Methanotrophic activity and diversity of methanotrophs in volcanic geothermal soils at Pantelleria (Italy). *Biogeosciences*, 11, 5865-5875.

Inside the volatile content of Antarctic mantle responsible for the Cenozoic basic alkaline magmatism of Northern Victoria Land (Antarctica)

Giacomoni P.P.*¹, Coltorti M.¹, Bonadiman C.¹, Ferlito C.², Pelorosso B.¹ & Ottolini L.³

1. Dipartimento di Fisica e Scienze della Terra, Università di Ferrara. 2. Dipartimento di Scienze Biologiche, Geologiche e Ambientali, Università di Catania. 3. Istituto di Geoscienze e Georisorse, CNR, Pavia.

Corresponding email: pierpaolo.giacomoni@unife.it

Keywords: Melt inclusions, volatiles, Antarctica.

The Trans-Antarctic Rift represents the most extended continental break up on the Earth. Notwithstanding the origin of the related magmatism and the nature of its mantle sources are still poorly understood, especially if the focus is addressed to the volatiles species. To this aim the petrologic features of the basic lavas are compared with those of olivine-hosted melt inclusions (MI) and the volatile contents of these latter are compared with those analyzed in amphibole from mantle xenoliths of the same area. Three distinct localities provided olivine-phyric basalts, while in two other localities amphibole-bearing mantle xenoliths are found.

Lavas are olivine-phyric (up to 15 %vol) with minor clinopyroxene and plagioclase in a glassy to microcrystalline plagioclase-dominated groundmass; opaque minerals are mostly magnetites and subordinately ilmenites. Samples are basanites (42.41-44.8 SiO₂ wt.%; 3,11-6,19 Na₂O+K₂O wt.%) and basalts (44.91-48.73 SiO₂ wt.%; 2.81-4.55 Na₂O+K₂O wt.%).

Olivine-hosted melt inclusions (MI) were analyzed for major element and volatiles (H₂O, CO₂, S, F, and Cl) after HT (1300 °C) and HP (6 kbar) homogenization at Reensealer Polytecnic Institute (New York-USA). Volatile content in MI and amphiboles has been determined by SIMS at Woods Hole Oceanographic Institute (Massachusetts-USA) and at the IGG-CNR laboratory of Pavia.

MI are compositionally comparable to host lavas but show a wider variability. Two compositionally distinct populations can be identified, sometimes coexisting in the same sample: a high-Fe-Ti-K and a low-Fe-Ti-K groups.

The H₂O content ranges from 0.70 wt.% to 2.64 wt.% and CO₂ from 25 ppm to 341 ppm (H₂O/(H₂O+CO₂)~ 1, mol%). At comparable H₂O contents few samples show a remarkable higher CO₂ values (1322 ppm to 3905 ppm) with a H₂O/(H₂O+CO₂) down to 0.88. F and Cl content varies from 1386 to 10 ppm and from 1336 to 38 ppm respectively. Concentration of volatiles show a good correlation with alkalis, especially with K₂O.

Assuming a partial melting degree able to reproduce the major element composition of basanites and basalts (from 3 to 7%) the volatile content of the mantle source was calculated. Accordingly, the estimated amount of volatiles is as follows: 790-1850 ppm of H₂O, 120-273 ppm of CO₂, 42-97 ppm of F and 40-93 ppm of Cl. These estimates were then compared with the volatile content measured in mantle amphibole and in NAMs from the two localities nearby. In order to obtain the water content measured in MI, these latter appear enriched in Cl with respect to the content observed in the amphiboles. This disagreement can be due to: i) mantle amphiboles are not representative of those present in the magma sources, ii) phlogopite may be also present in the magma source, although it is absent in the xenoliths. In both cases this study indicate an anomalous K and Cl enrichment in the lithospheric mantle domain of NVL.

Electron microprobe U-Th-Pb dating of monazite inclusions in apatite: geochronological clues to fluid-rock interaction during Permian hornfels formation in the Monte Sabiona contact aureole

Mair P. *, Zöll K. & Tropper P.

Institute of Mineralogy and Petrography, University of Innsbruck, Austria.

Corresponding email: philipp.mair@uibk.ac.at

Keywords: Metamorphic fluids, Apatite solubility, U-Th-Pb dating of monazite.

The Klausen Diorite is part of the Permian calc-alkaline plutonic association consisting of Brixen Granodiorite, Ifinger Granite, Kreuzberg Granite and Cima d'Asta Granitoid as the most prominent members. They all intruded into the polymetamorphic basement of the Southalpine Brixen Quartzphyllite. The Klausen dioritcomplex – the common local name is Klausenite - is located to the south of the Brixen Granodiorite in the eastern part of the Southalpine. The main focus of the research conducted in the course of this work is the monastery-mountain Säben near to Klausen, a small town in South Tyrol (Italy). During the Permian (278 Ma) the diorite intruded into the Brixen Quartzphyllites. The pressure conditions of this intrusion range from 0.3 GPa to 0.55 GPa, which corresponds to a depth of 8 to 17 km. The solidus temperature was between 840 °C and 890 °C (opx-cpx-geothermometer). The intrusion formed a small, about 140 to 180 m wide, contact aureole at the locality of Säben. The aureole can be divided into four different zones based upon mineralogical, mineral chemical and textural features. The entire area is characterized by late-stage hydrothermal alteration. In the 20 m wide innermost area (zone IV) the mineral paragenesis cordierite, biotite, plagioclase, quartz and spinel occurs. After 20 m from the contact spinel disappears. The extension of Zone III stretches from 20 to 40 m. In this zone cordierite, biotite, plagioclase, quartz and sillimanite occur. The rocks of zone III and IV also show typical hornfels textures. After 40 m sillimanite disappears. Zone II is characterized by the loss of the typical hornfels textures. The rocks are macroscopically predominated by quartzphyllites and to paragneisses. White micas occur in this zone. This zone can be distinguished from the non-contact-metamorphic quartzphyllites only by the chemical composition of plagioclase, which becomes more calcic ($X_{An} = 0.25 - 0.10$). F-apatite shows newly-formed monazite in this zone as well due to dissolution and reprecipitation processes. In zone I (>140 m from the contact) X_{An} in plagioclase approaches zero, which corresponds to the chemical composition of albite in the non-contact-metamorphic quartzphyllites. Electron microprobe U-Th-Pb dating of monazite inclusions in apatite yielded Permian ages ranging from 252.2 Ma to 298.9 Ma. Based on these data the age of the contact metamorphic overprint is 278.4 ± 12.1 Ma. Geothermometry revealed a decrease (two-feldspar-, Ti-in-biotite, Na-in-cordierite, Pseudosection and Schreinemaker's analysis) in temperature from 760-720 °C in the innermost aureole (zone IV) to 540-450 °C in the outermost aureole (zone I).

Geochemical and petrographic characterization of basalts and rhyolites of Fantale's area (Ethiopia)

Minissale S.*¹ & Ferlito C.²

1. Dipartimento di Scienze della Terra, dell'Ambiente e delle Risorse, Università di Napoli "Federico II". 2. Dipartimento di Scienze Geologiche, Biologiche e Ambientali, Università di Catania.

Corresponding email: silvia.minissale@unina.it

Keywords: Ethiopia, volatiles, differentiation.

Understanding the causes that influence petrogenetic and geodynamic processes in continental rifts such as the East African Rift System (EARS) is an important issue in volcanology. One of the most intriguing petrological aspects of the EARS products is the lack of rocks with intermediate composition, compared with the abundances of products with more basic compositions and the relative abundance of acidic products.

In this study, we have carried out a petrographic, geochemical and thermodynamic characterizations of some Quaternary basalts and rhyolites, collected at the Main Ethiopian Rift (MER), within the volcano-tectonic segments of Gedemsa, Doffen; Fantale-Metehara. In particular, we focused on the volcanic rocks outcropping at Fantale volcano: its products present, at thin section scale, not easily explainable resorption textures of labradoritic plagioclase phenocrysts inside the trachitic glass.

Textures and zoning of plagioclase could be an effective tool for understanding the dynamics and kinetics of magmatic processes, due to the high sensitivity that plagioclase has to pressure and volatiles content changes. The rocks analyzed by optical and electronic microscope, show high Cl content in rhyolitic samples (> 1500 ppm) and a low Cl content in basaltic ones (< 200 ppm). Moreover alkali enrichments were testified by Na-rich in plagioclase resorption zones and by observed K-rich whole rock compositions with respect to MELTS simulations. The petrological features of the magma involved evidences the role played by volatiles in chemical evolution control within a magmatic system. In fact volatiles (H₂O, CO₂, Cl-complexes) easily migrate through the magmatic system, with a transfer efficiency mostly depending on partial pressure gradients and on the microfracture systems. This migration can involve the transfer of metallic elements such as K, Na, Ti, Fe, which have a particular affinity with H₂O and halogens, due to the crucial role of halogens as complexing agents. The data allowed us to envisage a differentiation induced by volatiles which may be derived from the mantle rich in H₂O and CO₂, able to carry Cl-complexes. This differentiation, along with partial melting processes, can originate respectively alkali-enrichments and silica-enrichments, alternatively to traditionally employed models, such as crystal fractionation or assimilation, which are normally used to explain the occurrence of evolved volcanites in extensional tectonic settings. The mechanism has been highlighted only to Fantale volcano, but further data and improvements of the model might help to better constrain the role of volatiles in the MER and in other continental rifts.

Preliminary data on natural CO₂ emissions from Nurra karst terrain (NW Sardinia, Italy)

Sanna L.*, Arca A., Casula M. & Duce P.

Istituto di Biometeorologia, CNR, Sassari

Corresponding email: sanna@ibimet.cnr.it

Keywords: Carbon dioxide, cave breathing, Earth degassing.

The Mesozoic carbonate platform of NW Sardinia (Italy) pertains to the historical region of Nurra and since 1999 to the Regional Natural Park of Porto Conte. The area is also part of the Fluxnet project, a global network that coordinates the analysis of the net ecosystem carbon balance by direct measurement of gas exchanges across canopy-atmosphere interface using micrometeorological flux tower.

The carbonate terrains of this sector host well-developed cave systems. The karst aquifer has a high dissolved carbon and the underground atmosphere is often characterised by anomalous level of carbon dioxide that has never been investigated before. As geological diffusive background emission over the carbonate outcrop was previously neglected, this study is aimed to assess the magnitude of the CO₂ outgassing from caves to outside atmosphere.

An environmental monitoring programme has been carried out in the Monte Doglia cave, a 100 m-deep vertical shaft located at 320 m asl and 2 km far from the coast. It opens in an area where a significant part of the surface is bare rock. The soil cover, where it exists, rarely exceeds 20 cm in thickness and consists of fine red, sandy material. The natural vegetation consists mainly of shrubs.

The cave is monitored with multiple meteorological sensors that record continuously air CO₂ and microclimatic parameters. Carbon dioxide concentration is measured at -10 m depth from the entrance by an infrared spectrometer (NDIR technology, range 0-10,000 ppm).

Preliminary data indicate periodic oscillations of cave air CO₂ levels ranging from 500 ppm to 1600 ppm, punctuated by events that provide clues to ventilation and degassing mechanisms. These gas plumes reach concentration >10,000 ppm. This huge CO₂ content is hidden when a prevailing advective-renewal of cave air is established. Ventilation occurs via density driven flow and by wind across the entrance. Subsurface airflow in unsaturated zones can be also induced by atmospheric pressure fluctuations, topographic effects, water table oscillations and meteoric water infiltration. About the origin of this CO₂-rich gas, examples of volatiles escapes along faults have been documented in Sardinia. They have been related to mantle-derived fluxes associated to Quaternary volcanism. Other non-volcanic degassing involved on natural CO₂ emissions from Nurra karst terrain might derive from carbonate rock weathering, oxidation of sulphur deposits and surface processes. Future stable isotopes analyses will be devoted to clarify these points.

Finally, by considering the density of cave entrances and the contribution of numerous fractures widespread in the karst terrain, the temporal CO₂ pattern of Nurra region provides evidence that the amounts of carbon that might be released from subsurface atmosphere in the vadose zone could be noticeable at both local and regional scale.

The role of altered ultramafic rocks in subduction-zone volatile recycling

Scambelluri M.

Dipartimento di Scienze della Terra, Ambiente e Vita, Università di Genova.

Corresponding email: marco.scambelluri@dipteris.unige.it

Keywords: Subduction, volatiles, serpentinite.

Volatile transfer from surface reservoirs to the deep mantle via subduction causes refertilization of the earth's mantle, magnetism at convergent plate margins and changes the physico-chemical properties of slabs and mantle wedges. Though much attention has been paid to mafic oceanic crust and sediments, the hypothesis that serpentinitized mantle rocks are vital to the global cycles of H₂O, CO₂, halogens and fluid-mobile elements (FME) has gained ground. Shallow uptake and subduction transport of volatiles by serpentinites can be established by field and geochemical studies of samples recrystallized at increasing subduction P-T conditions. Serpentinites host up to 13 wt.% water and derive from hydration of mantle rocks in several tectonic settings. Historically, serpentinitization is attributed to seawater-driven alteration of mid-ocean ridge mantle. More recent works document mantle serpentinitization at convergent margins, either along bend-faults in outer rise settings, or in the forearc mantle by uprising subduction fluids. Compared to abyssal serpentinites, the halogen, noble gas and FME compositions of serpentinites from convergent margins suggest involvement of sediments present above bend-faults, or in subduction channels. This makes the subduction serpentinites reliable markers of exchange with circulating slab fluids and traps of fluid-transported sediment- and crust-derived components. The studies performed hitherto thus show that serpentinites are major sinks of H₂O, C, Cl, I, Br and FME: serpentine breakdown to 150-200 km subduction depths provides a means to deliver the above elements to arcs. Significant retention of such elements in de-serpentinitized high-pressure peridotites enables transfer of volatile anomalies beyond the subarc settings.

Concerning carbon, the occurrence of ophicarbonates in modern oceans, in non-subducted and in high-pressure ophiolites (blueschist, eclogite-facies) indicates that ultramafic rocks fix carbon at low P-T conditions and play a role in the C-subduction cycle. The latter is poorly constrained and contradictory interpretations exist about C residence in subducting plates, its mobility out of slabs and its reactivity with the supra-subduction mantle. Current studies on alpine ophicarbonates show that these rocks grossly preserve the pre-subduction C isotope signatures, suggesting scarce C mobility. However, high-pressure rocks from the Ligurian Voltri Massif show that aqueous fluids released by serpentinite trigger breakdown of dolomite in associated marbles and C release to the fluid. Back-reaction of the COH fluid with serpentinite causes carbonation of rock-forming minerals and formation of high-pressure ophicarbonate domains. Carbon remains stored in slab and mantle wedge presumably until subarc heating enhances substantial rock decarbonation.

Oxygen isotope analysis of serpentine minerals by SHRIMP: analytical developments and geological applications

Scicchitano M.R.*¹, Rubatto D.¹, Hermann J.¹, Padrón-Navarta J.A.² & Shen T.³

1. Research School of Earth Sciences, ANU, Canberra, Australia. 2. Géosciences Montpellier, CNRS-UM. 2, Montpellier, France.
3. School of Earth and Space Sciences, Peking University, Beijing, China.

Corresponding email: mari.scicchitano@anu.edu.au

Keywords: Oxygen isotopes, ion microprobe, serpentinites.

Serpentinites play a crucial role in recycling volatiles and trace elements from ocean floor to mantle through seafloor metamorphism and subduction. Information on the source(s) of fluids that interacted with serpentinites can be obtained using oxygen isotopes.

Fluid-rock interaction can occur at different stages of metamorphism and thus serpentinites commonly preserve complex textures. In order to investigate these stages of metamorphism, *in-situ* analytical techniques able to resolve oxygen isotopic variations recorded at the microscale are necessary. We present the first investigation of oxygen isotopes in serpentine minerals by ion microprobe.

Due to significant instrumental mass fractionation, data obtained with ion microprobes should be corrected by analysing well-characterised reference materials. Reference values for three chemically homogeneous samples of antigorite, chrysotile, and lizardite were obtained by laser fluorination. Analysis for oxygen isotopes using the SHRIMP ion microprobe aimed to assess their reproducibility compared to San Carlos olivine as well as potential matrix bias and crystal orientation effects. The obtained data suggest reproducibility comparable to San Carlos olivine of ca. ± 0.3 - 0.4% (SD at 95% c. l.) for all samples. Crystal orientation effects were identified only in chrysotile and no matrix bias were observed in the investigated compositional range.

The developed standards were used for analysing oxygen isotopic compositions of different serpentine polymorphs in ultrahigh-pressure serpentinites that are enclosed in metapelites from Tianshan (China). The $\delta^{18}\text{O}$ of high-pressure antigorite is $\sim 6.0 \pm 0.4\%$ (σ at 95% c. l.) resulting in a bulk rock $\delta^{18}\text{O}$ of $\sim 4.8\%$. This value is similar to bulk rocks in oceanic serpentinites and suggests that serpentinitization most likely occurred during seafloor alteration. Despite the observation of crystal orientation effects in chrysotile, the highest $\delta^{18}\text{O}$ values measured in late chrysotile veins are comparable to those obtained in antigorite and allow to exclude interaction with fluids derived from the surrounding metasediments. The developed technique was also used to analyse oxygen isotopic compositions of serpentine and olivine in a partly serpentinitized dunite from the Nuasahi massif (India). The $\delta^{18}\text{O}$ value of lizardite is $\sim 4.9 \pm 0.3\%$ (σ at 95% c. l.) and is comparable with the $\delta^{18}\text{O}$ value of $\sim 5.3 \pm 0.3\%$ measured in olivine cores. These values are typical of mantle compositions and different from those measured in olivine rims ($\delta^{18}\text{O} \sim 2.8 \pm 0.3\%$; σ at 95% c. l.), thus suggesting that a secondary fluid might be involved in late olivine formation.

Silicate dissolution boosts the CO₂ content of deep fluids

Tumiati S.*¹, Tiraboschi C.¹, Pettke T.², Recchia S.³, Ulmer P.⁴ & Poli S.⁵

1. Dipartimento di Scienze della Terra "A Desio", Università di Milano. 2. Institut für Geologie, Universität Bern, Switzerland. 3. Dipartimento di Scienza e Alta Tecnologia, Università dell'Insubria. 4. Institut für Geochemie und Petrologie, ETH Zürich, Switzerland.

Corresponding email: simone.tumiati@unimi.it

Keywords: Volatiles, dissolution, subduction.

Carbon dioxide released at arc volcanoes exceeds what is currently thought to be removable from the subducting slab through devolatilization reaction. To overcome this inconsistency, further processes have been proposed, such as dissolution of carbonates, upwelling of carbonated slab materials and/or carbonatitic melts. With few exceptions, estimates of CO₂ released from the slab due to fluid-rock interactions are based on thermodynamic modeling, where fluids are treated as if they are mixtures of the neutral species H₂O, CO₂, CO, CH₄ and H₂, neglecting all other dissolved species. Here we present experimental data on graphite-saturated H₂O-CO₂ fluids, synthesized at high-pressure and temperatures in equilibrium either with forsterite + enstatite or quartz, and analyzed both for solutes and volatiles. At 1 GPa and 800-900 °C, the dissolution of either forsterite + enstatite or quartz leads to CO₂ contents in the fluid up to +40 mol% compared to estimates retrieved by conventional thermodynamic models of ternary COH fluids. Our results suggest that the interaction of deep carbon-bearing fluids with these silicates, occurring for example in subduction mélanges, and in particular incongruent dissolution reactions exert a major role in controlling the fluid composition, enhancing the CO₂ content towards unpredicted values. We suggest that SiO₂, in the form of dissolved aqueous species, is the major component able to buffer the CO₂ content of GCOH deep fluids. Therefore, in rock-fluid systems the use of simple fluid models based on mixing of neutral COH species, as found in popular thermodynamic modeling packages, is not recommended because the presence of dissolved solutes could introduce unconstrained uncertainties in the estimated fluid composition. In particular, mass balances performed with these methods could largely underestimate the amount of CO₂ released at subduction zones due to fluid-rock interactions, with profound consequences to the global CO₂ cycle.

On the complexity of volatile fluxes in subducting oceanic slabs

Vitale Brovarone A.*¹, Chu X.², Martin L.A.J.³ & Ague J.J.²

1. IMPMC-CNRS, Paris, France. 2. Department of Geology and Geophysics, Yale University, New Haven, USA.
3. CCFS-CMCA, University of Western Australia.

Corresponding email: alberto.vitale-brovarone@impmc.upmc.fr

Keywords: Volatile fluxes, subduction, new C and H₂O fluxes.

Subducted oceanic lithosphere recycles volatile reservoirs into the deep mantle or back to the atmosphere at volcanic arcs. Establishing the actual volatile budgets of subducting slabs is challenging, and most attempts oversimplify the complexity of natural systems. Early works considered a rather limited number of representative lithologies, and simple metamorphic processes in closed systems. More recently, attention has been paid on open systems and fluid-rock interactions that cannot be easily reproduced experimentally, and their role on the recycling of specific volatile elements (H, C, S...) or species. Modern computational models now predict new processes and fluxes that deeply modify, or even reverse previous budgets. In general, our current knowledge of volatile recycling in subducting slabs is still limited, or even confusing.

A considerable number of papers in recent years have highlighted the importance of natural samples of exhumed high-pressure rocks in order to identify and quantify new volatile fluxes in subducting slabs where open systems and fluid-rock interactions are common, and their contribution to larger budgets. In line with these studies, here we present examples of new volatile fluxes occurring in natural subducted systems such as metasediments and metabasalts in the metamorphic complex of Alpine Corsica. These include, among others, interplay between water, and inorganic and organic C fluxes at various depths into subduction zones. The interaction between the generated fluxes and other slab-forming rocks generates new, unpredicted reservoirs, which will in turn generate new fluxes under changing boundary conditions. These results demonstrate how premature large-scale slab budgets may be and provide hints for new field-based studies and numerical simulations.

SESSION S4

The subduction factory - a key element in the Earth

CONVENORS

Gianluca Bianchini (Univ. Ferrara)

Daniele Castelli (Univ. Torino)

Nadia Malaspina (Univ. Milano Bicocca)

Constraining slab recycling under Vesuvius volcano from combined U-series and non-traditional stable isotope (Mo, $^{238}\text{U}/^{235}\text{U}$) data

Avanzinelli R.*¹, Casalini M.¹, Elliott T.² & Conticelli S.¹

1. Dipartimento di Scienze della Terra, Università di Firenze. 2. Bristol Isotope Group, University of Bristol, UK.

Corresponding email: riccardo.avanzinelli@unifi.it

Keywords: Vesuvius volcano, U-series disequilibria, non-traditional stable isotopes.

The fate of deeply subducted oceanic crust and overlying sediments is of great importance for its role in the generation of magmas in subduction-related geodynamic settings. Italian volcanoes, and Vesuvius in particular, are good laboratories to investigate these processes due to their strong enrichment in K and incompatible trace element that requires a significant amount of sediment material recycled into the mantle. Volcanic rocks from Vesuvius display ubiquitous ^{238}U excesses (up to 27%), a feature that is unusual in such enriched subduction-related magmas. In addition they have among the highest ($^{231}\text{Pa}/^{235}\text{U}$) and ($^{226}\text{Ra}/^{230}\text{Th}$) reported for arc rocks. These characteristics require a recent addition of a high-U component to the mantle beneath the Italy. In order to constrain the origin and nature of this slab-related component we present new data on non-traditional stable isotopes (Mo, $^{238}\text{U}/^{235}\text{U}$) on both volcanic rocks and possible sedimentary end-members. Non-traditional isotope systems such as Mo and $^{238}\text{U}/^{235}\text{U}$ are sensitive to redox-related isotopic fractionation on the Earth's surface, hence they may provide key information on the type of material recycled from the subducting slab to the mantle wedge.

The combined use of these different isotope systematics will provide a wider picture of the mechanism and timescales of the processes occurring from slab subduction to magmas generation and ascent above subduction zones.

Carbon budget in Calatrava and Tallante xenoliths: insights on sources and petrogenetic processes

Bianchini G.* & Natali C.

Dipartimento di Fisica e Scienze della Terra, Università di Ferrara.

Corresponding email: bncglc@unife.it

Keywords: Carbon, isotopes, xenoliths.

We present elemental and isotopic analyses of carbon (C) carried out on mantle xenoliths from the Calatrava and Tallante volcanic districts (Spain). The C content of peridotite xenoliths from Calatrava, previously studied by Bianchini et al. (2010), generally range between 1100 and 5500 ppm, with up to 2.9 wt.% C in a single sample. The associated isotopic composition ($\delta^{13}\text{C}$) of most samples varies between -26.1 to -15.2 ‰, whereas the carbon-rich outlier displays a distinctly less negative C isotopic composition (-6.2‰) that conforms with a typical “mantle signature” (Deines, 2002). The C content of xenoliths from Tallante previously studied by Bianchini et al. (2011), varies from 600 to 1000 ppm in anhydrous peridotites, to 1500 ppm in an amphibole bearing peridotite; higher C content of 4000 ppm have been recorded in the felsic vein crosscutting a peridotite composite xenolith previously studied by Bianchini et al. (2015). The associated isotopic composition ($\delta^{13}\text{C}$) varies between -20.1 to -22.4 ‰ in peridotites, whereas the mentioned felsic vein displays the value of -11.9‰. In both xenolith suites a correlation is observed between the carbon contents and the respective $\delta^{13}\text{C}$ values suggesting that analogous fractionation processes affected vast domains of the Iberian lithospheric mantle. Noteworthy, in the Tallante xenolith suite $\delta^{13}\text{C}$ values approaching the notional “mantle signature” are never recorded. The less negative isotopic composition recorded by Tallante xenoliths approaches that of the carbonate matrix of the xenolith-bearing volcanoclastic deposit (-9.8‰). On the whole, the available data suggest that the carbon of the studied xenoliths, host lavas and carbonate volcanoclastic matrices is juvenile, mostly originated deep in the mantle, and influenced by multiple episodes of degassing, that ultimately led to extremely explosive volcanic eruptions. Differences between the two suites are possibly related to distinct geodynamic settings, as the Tallante mantle section was interested by supra-subduction metasomatic fluids/melts that didn't occur at Calatrava.

Bianchini G., Beccaluva L., Bonadiman C., Nowell G.M., Pearson D.G., Siena F. & Wilson M. 2010. Mantle metasomatism by melts of HIMU piclogite components: new insights from Fe-Iherzolite xenoliths (Calatrava Volcanic District, Central Spain). *Geol. Soc. London Sp. Publ.*, 337, 107-124.

Bianchini G., Beccaluva L., Nowell G.M., Pearson D.G. & Siena F. 2011. Mantle xenoliths from Tallante (Betic Cordillera): insights into the multi-stage evolution of the south Iberian lithosphere. *Lithos*, 124, 308-318.

Bianchini G., Braga R., Langone A., Natali C. & Tiepolo M. 2015. Metasedimentary and igneous xenoliths from Tallante (Betic Cordillera, Spain): Inferences on crust–mantle interactions and clues for post-collisional volcanism magma sources. *Lithos*, 220-223, 191-199.

Deines P. 2002. The carbon isotope geochemistry of mantle xenoliths. *Earth-Science Reviews*, 58, 247-278.

Geologic and petrographic study of the veins in the metabasites of the ultra-high pressure Lago di Cignana Unit (upper Valtournenche, western Alps)

Borghini A.¹, Ferrando S.¹ & Groppo C.*¹⁻²

1. Dipartimento di Scienze della Terra, Università di Torino. 2. Istituto di Geoscienze e Georisorse, CNR, Torino.

Corresponding email: chiara.groppo@unito.it

Keywords: Fluid-rock interaction, subduction zones, ultra-high pressure Lago di Cignana Unit.

The ultra-high pressure Lago di Cignana Unit (LCU), which consists of coesite-eclogite facies metabasics and metasediments, is among the best examples of deeply subducted oceanic crust worldwide. This contribution is a petrographic study of veins, and of their relative chronology, occurring in metabasites, in order to distinguish the events of fluid circulation occurred during the metamorphic evolution of the LCU. A detailed petrographic characterization of the different generations of veins occurring in the LCU metabasites is, in fact, still missing, except for some information on few quartz-bearing vein types studied by van der Klauw et al. (1997), most of them associated to the late greenschist facies retrogression.

The hosting metabasites are mainly represented by eclogite (Omp + Grt + ex-Lws ± Gln ± Phe ± Cb ± Qtz + Rt), variably retrogressed eclogite (characterized by the pervasive growth of green-blue Amp + Czo/Ep ± Ab) and minor prasinite. Layers and pods of omphacite and garnetite, locally occurring in fresh eclogites, have been interpreted as primary compositional layering in the protolith (i.e. not related to fluid circulation). The observed mineral assemblages allowed to constrain the tectono-metamorphic evolution, which is characterized by a HP prograde stage, an UHP peak stage (coesite-bearing eclogite facies) often coinciding to the development of the main foliation (Sp_{ec1}), followed by several retrograde stages under Lws-blueschists, Ep-blueschist, blueschist/greenschist and greenschist –facies conditions.

Concerning the evidence of fluid circulation, the following vein types have been recognised:

- syn-Sp_{ec1} veins (UHP eclogite facies): Omp+Gln veins; Qtz+ex-Lws veins;
- post-Sp_{ec1} veins (UHP eclogite facies): Qtz (ex-Coe) -bearing veins with selvages enriched in Omp, Gln and Grt; Qtz+Omp+Gln+ex-Lws veins;
- post-Sp_{ec1} veins (Lws-eclogite/blueschist facies): Grt+Gln+Whm+Qtz veins; Gln+Grt veins; Gln+Grt+ex-Lws veins; Qtz+Gln+Whm veins; Whm veins; Qtz+Cb+ex-Lws veins; Qtz+Cb+Gln±ex-Lws veins; Qtz veins with selvages enriched in Whm and Gln;
- post-Sp_{ec1} veins (Ep-eclogite facies): Qtz+Ep+Gln veins; Zo+Qtz veins; Qtz+Zo/Czo veins; Ep+Whm+Grt veins;
- post-Sp_{ec1} veins (Ep-blueschist facies): Qtz+Czo+Ttn veins;
- post-Sp_{gs} veins (greenschist facies): Ep+Ab; Ep+blue-green Amp+Ab+Chl veins.

The obtained results allowed to reconstruct in detail the relative chronology of fluid circulation in the oceanic crust during subduction and the following exhumation, providing a quite more complex picture than previously suggested in the literature. This study has therefore important implications for the understanding of the nature of the fluids circulating in the subducting slab, and of the fluid mobility in subduction zones.

van der Klauw S.N., Reinecke T. & Stöckert B. 1997. Exhumation of ultrahigh-pressure metamorphic oceanic crust from Lago di Cignana, Piemontese zone, western Alps: the structural record in metabasites. *Lithos*, 41, 79-102.

As, Sb and B-Sr-Pb isotopes in Voltri serpentinites: evidences of fluid-mediated mass transfer in subduction zones

Cannaò E.*¹, Scambelluri M.¹, Agostini S.² & Tonarini S.²

1. Dipartimento di Scienze della Terra, Ambiente e Vita, Università di Genova. 2. Istituto di Geoscienze e Georisorse, C.N.R. Pisa.

Corresponding email: enrico.cannaò@unige.it

Keywords: Serpentinites, interaction, subduction processes.

Fluid-mediated mass transfer between different geochemical reservoirs can be traced by B, Sr and Pb isotopic systems and fluid-mobile elements, like As and Sb. As proposed by many authors, these geochemical interactions can be used as proxy for element recycling at convergent margins. Serpentinites are important lithology for tectonic and chemical processes in subduction zones and play a key role in slab-mantle interface domains. Here, we focus on the Voltri Massif case-study (Ligurian Western Alps), where oceanic serpentinites and associated mafic rocks underwent Alpine subduction and high pressure metamorphism. The texture of these ultramafic rocks allows to distinguish between undeformed and mylonitic serpentinite domains. Field relationships highlight that the undeformed rocks are enclosed in the deformed ones. Metamorphic olivine overgrew antigorite-bearing structures and locally crystallized in dehydration veins as the result of partial serpentinite dewatering at eclogite-facies conditions. Undeformed rocks are characterized by high $\delta^{11}\text{B}$ (up to +30‰) and low Sr and Pb isotopic ratios (0.7053-0.7069 of $^{87}\text{Sr}/^{86}\text{Sr}$ and 18.131-18.205 of $^{206}\text{Pb}/^{204}\text{Pb}$) and low contents in As and Sb (0.1 and 0.01 ppm, respectively). In contrast, mylonitic serpentinites display lower values of $\delta^{11}\text{B}$ (down to +18‰), high radiogenic enrichment in Sr and Pb isotopes (up to 0.7105 of $^{87}\text{Sr}/^{86}\text{Sr}$ and up 18.725 of $^{206}\text{Pb}/^{204}\text{Pb}$) and enrichment in As and Sb (1.3-0.39 ppm, respectively). Based on the field occurrence, the preserved undeformed domains record the oceanic stage, whereas mylonitic serpentinites reset their B-Sr-Pb isotopic signature and As and Sb and trace the interaction with sediment-derived fluids. The undeformed domains could represent the compositions of the starting materials allowing an understanding of fluid and deformation-mediated trace element exchange during interaction processes. The ability of serpentinites to retain incompatible elements allow mylonitic serpentinites to increase their budget up to 150% of B, 1000% of As and 7600% of Sb with respect to the undeformed rocks. The geochemical imprint shown by mylonitic serpentinites can be acquired along bend-faults near the trench prior to its entrance in subduction: these can act as major site for infiltration of fluids with sedimentary signature providing the geochemical anomalies observed in the mylonitic rocks. Another key scenario for hydration of ultramafic rocks are the subduction channel domains, where slices of slab and wedge materials can be accreted to the slab-mantle interface and undergo hydration by uprising slab fluids (originated by sediment). The geochemical features of the Voltri serpentinites documented here underline the key role of serpentinites in the mass transfer processes to depth. Their capacity to retain fluid-mobile elements during interaction processes has important consequence in the recycling of elements via fluids during the antigorite-out reaction.

Non-traditional isotope tracers ($^{238}\text{U}/^{235}\text{U}$ and $^{98}\text{Mo}/^{95}\text{Mo}$) of subduction processes in the Central-Mediterranean magmatism

Casalini M.^{*1-2}, Avanzinelli R.¹, Elliott T.³, Tommasini S.¹ & Conticelli S.¹

1. Dipartimento di Scienze della Terra, Università di Firenze. 2. Dipartimento di Scienze della Terra, Università di Pisa.
3. School of Earth Science, University of Bristol, UK.

Corresponding email: martina.casalini@unifi.it

Keywords: Non-traditional isotopes, subduction, potassic/ultrapotassic rocks.

Non-traditional isotope systems such as Mo and $^{238}\text{U}/^{235}\text{U}$ are notably fractionated by redox-related processes on the Earth's surface. Such distinctive signatures may be carried into the mantle wedge via subduction and provide valuable tracers of components involved in magma genesis. Thus we measured Mo isotopes and $^{238}\text{U}/^{235}\text{U}$ on a suite of central-western Mediterranean calc-alkaline to ultra-potassic rocks (both silica-oversaturated and under-saturated). The studied rocks are associated with destructive plate margins, showing strong depletions in Nb and Ta, highly radiogenic Sr isotopes and most notably extreme enrichment in incompatible trace elements with respect to other volcanic arcs. These features have been long related to recycling of sedimentary material of different compositions into their mantle sources, making these rocks particularly suitable to investigate the role and nature of recycled sediments in subduction related magmatism. The data show an extremely wide spread of $^{98}\text{Mo}/^{95}\text{Mo}$ values, especially for the silica under-saturated products, that is significantly larger than any volcanic rocks suites reported so far. Smaller variations have been measured for $^{238}\text{U}/^{235}\text{U}$.

We discuss the isotope composition of the studied volcanic rocks and possible sedimentary end-members with the aim of constraining the lithology of the recycled sediments as well the mechanism of element transport from the slab to the mantle (i.e. fluids vs. melts).

Is there a new UHP unit in the Southern Dora-Maira Massif? Insights from metasomatic Coe-Ctd-Gln-Grt-talcschists used for ancient quern-stones (III c. AD)

Castelli D.*¹, Groppo C.¹, Ferrando S.¹, Elia D.², Meirano V.² & Facchinetti L.²

1. Dipartimento di Scienze della Terra, Università di Torino. 2. Dipartimento di Studi Storici, Università di Torino.

Corresponding email: daniele.castelli@unito.it

Keywords: Ultra-high pressure metamorphism, metasomatic Coe-Ctd-Gln-Grt-talcschists, thermodynamic modellin.

Peculiar Coe-Ctd-Gln-Grt-talcschists have been used to make at least six quern-stones, unearthed in the ruins of a *villa rustica* belonging to the Roman imperial period and located at Costigliole Saluzzo, Western Alps (Elia & Meirano, 2012).

The Coe-bearing Ctd+Grt±Gln-talcschists consist of Tlc, Grt, Ctd, Qtz ± Gln, late Mg-Chl and accessory Rt, Ap and Py. Grt occurs as strongly zoned porphyroblasts with a reddish core (Alm₇₂₋₇₉Prp₇₋₉Sps₉₋₁₂Adr₈₋₁₀), a pink mantle (Alm₇₆₋₈₂Prp₈₋₁₃Sps₁₋₇Adr₆₋₈) and a colourless rim (Alm₇₄₋₈₁Prp₁₂₋₂₀Sps₁₋₀Adr₄₋₇). Ctd inclusions occur in the Grt core, and relict Coe, partially inverted to Qtz, is preserved in the Grt mantle and rim. The bluish-green Ctd is slightly zoned (X_{Mg} from 0.29 in the core to 0.38 in the rim) and it is partially replaced by a greenish Mg-Chl. Bluish to colourless Gln is also slightly zoned (X_{Mg} from 0.70 in the core to 0.76 in the rim) and it seems in equilibrium with zoned Ctd, Grt mantle and rims, and with talc ($X_{Mg} = 0.86-0.88$).

The transition from an Fe-rich to a Mg-rich assemblage suggest that these talcschists originated by Mg-metasomatism of a former Fe-rich metapelitic protolith. Preliminary thermodynamic modelling applied on the Mg-rich metasomatic assemblage (Grt rim + Ctd rim + Gln rim + Tlc + Coe) tightly constrained peak P-T conditions at $T < 600$ °C and $P > 28$ kbar.

Although the field occurrence of these Coe+Ctd+Grt±Gln-talcschists is still unknown, these results clearly show that these rocks cannot belong to the UHP Brossasco-Isasca Unit (BIU), whose peak P-T conditions are at significantly higher T and P (730 °C, 40-43 kbar) (Castelli et al., 2014). The occurrence of Coe relics at the transition between Grt core and mantle indicates that the Mg-metasomatic event likely occurred at UHP conditions. A mechanism similar to that constrained for the well-known pyrope-bearing whiteschists of the UHP BIU (Ferrando et al., 2009), i.e. influx of Atg-derived fluids along shear zones during subduction, can be envisaged. Therefore, this finding opens the challenging hypothesis of the existence of a further, still unmapped, UHP Unit in the Southern Dora-Maira Massif that also experienced UHP fluid influx from underlying serpentinites.

- Castelli D., Compagnoni R., Lombardo B., Angiboust S., Balestro G., Ferrando S., Groppo C., Hirajima T. & Rolfo F. 2014. Crust-mantle interactions during subduction of oceanic & continental crust. *Geol. Field Trips*, 6, 1-73.
- Elia D. & Meirano V. 2012. La villa di Costigliole Saluzzo (CN). Contributo alla conoscenza del territorio piemontese in età romana. *Orizzonti. Rassegna di Archeologia*, XIII, 43-65.
- Ferrando S., Frezzotti M.L., Petrelli M. & Compagnoni R. 2009. Metasomatism of continental crust during subduction: the UHP whiteschists from the Southern Dora-Maira Massif (Italian Western Alps). *J. Metamorph. Geol.*, 27, 739-756.

Late Miocene ultrapotassic rocks from NE Algeria (Constantine) in the framework of the circum-Mediterranean lamproites

Colombi F.*¹, Chalal Y.², Agostini S.³ & Lustrino M.¹

1. Dipartimento di Scienze della Terra, Sapienza Università di Roma. 2. Université Houari Boumediene, Alger, Algeria
3. Istituto di Geoscienze e Georisorse, CNR, Pisa.

Corresponding email: francesco.colombi89@gmail.com

Keywords: Lamproites, ultrapotassic, Mediterranean.

A petrographic, mineralogical, geochemical and isotopic study of late Miocene (11-9 Ma) volcanic rocks from the Kef Hahouner volcanic body, situated ~50 km NE of Constantine (NE Algeria) has been undertaken in this study. The body shows a steeply-dipping dike-like shape, several ten of meters thick, which has been traced for about 1.2 km. This outcrop is one of the easternmost outcrops of Cenozoic igneous rocks of Maghreb, where ~1200 km-long and ~50 km wide volcanic and plutonic belt runs parallel to the coast from Morocco to Tunisia.

Two small outcrops of volcanic rocks around Constantine have been classified as quartz-normative lamproites in literature (Kaminskiy et al., 1993). These rocks have been the subject of study because they were considered the source rocks of small diamonds found in N Algeria. Recently Godard et al. (2014) identified the sources of these diamonds to more ancient rocks, unrelated to the Miocene volcanic activity.

These rocks are characterized by an anhydrous paragenesis, with feldspar and Mg-rich olivine representing the most abundant phases. Pyroxenes are confined to the groundmass only, together with plagioclase, alkali feldspar and opaque minerals. On the basis of petrography and the TAS diagram these rocks are classified as shoshonite and latite. They can be defined as ultrapotassic since are characterized by $K_2O > 3$ wt.%, $K_2O/Na_2O > 2.5-3.0$, $MgO > 3-4$ wt.%, $SiO_2 < 55-57$ wt.% and $SiO_2/K_2O < 15$. According to their normative mineralogy they range from silica-oversaturated to silica-saturated. All the investigated samples show a multi-element pattern enriched in LILE (e.g., Cs, Rb, Ba) and LREE (e.g., $La/Yb = 37-59$), with peaks at Pb and troughs in Nb and Ta, resulting in high LILE/HFSE ratios, all geochemical signatures of orogenic (arc-type) magmas. These rocks show initial isotopic values of $^{87}Sr/^{86}Sr$ (0.70874-0.70961), $^{143}Nd/^{144}Nd$ (0.51222-0.51223), $^{206}Pb/^{204}Pb$ (18.54-18.60), $^{207}Pb/^{204}Pb$ (15.62-15.70) and $^{208}Pb/^{204}Pb$ (38.88-39.16).

The Constantine volcanic rocks show multi-element pattern and extreme Sr, Nd and Pb isotopic compositions similar to the other circum-Mediterranean lamproites. Nevertheless, the abundant presence of plagioclase and the relatively Al-rich character, the Constantine volcanic rocks cannot be defined as lamproites, being these latter peralkaline, Ca- and Al-poor magmas. At least a significant portion of the circum-Mediterranean rocks classified as lamproites should be better defined as “normal” potassic to ultrapotassic volcanic rocks.

New geochemical data on submarine volcanics from the Pontine Archipelago (Tyrrhenian Sea, Italy)

Conte A.M.*¹, Perinelli C.², Bianchini G.³, Natale C.³, Martorelli E.⁴ & Chiocci F.L.²

1. Istituto di Geoscienze e Georisorse, CNR, Roma. 2. Dipartimento di Scienze della Terra, Sapienza Università di Roma. 3. Dipartimento di Fisica e Scienze della Terra, Università di Ferrara. 4. Istituto di Geologia Ambientale e Geoingegneria, CNR, Roma.

Corresponding email: aidamaria.conte@uniroma1.it

Keywords: Western Pontine Islands, submarine volcanic rocks, orogenic environment.

In the framework of the spatial-temporal distribution and compositional variability of Plio-Quaternary magmatic products emplaced in the Tyrrhenian and surrounding regions, the magmatism of the Western Pontine Islands (WPI - Ponza, Zannone, Palmarola) is still matter of debate, due to the complex geological setting in which the islands formed. The magmatism of WPI offers the opportunity to investigate the origin of calcalkaline and alkaline-peralkaline magmas in a complex basin undergoing extension within an overall collisional geodynamic setting. Previous studies defined that: 1) Pliocene volcanic episodes are represented by silica-rich, high-K calcalkaline volcanic units at Ponza and Zannone islands; 2) Pleistocene volcanic episodes are represented by intermediate to highly evolved (K-trachytes to peralkaline trachytes and rhyolites) shoshonitic rocks cropping out in SE Ponza and Palmarola islands.

According to Conte & Dolfi (2002) the magmatism of WPI was related to magmas similar to the less evolved mafic-intermediate calcalkaline and shoshonitic magmas occurring nearby Campanian Volcanic District, which variously interacted with crustal materials. Other Authors proposed different scenarios, relating the WPI magmatism: i) to sources influenced by the change of geodynamic setting from subduction-related to intraplate (Cadoux et al., 2005) or ii) to the framework of the whole Italian magmatism resulting by a mixture of a ~FOZO mantle component and minor upper crustal contamination (Cadoux et al., 2007). Paone (2013) emphasized the occurrence of widespread anatexic processes for Pliocene and Pleistocene rhyolites.

In this contribution we present new data on dredged samples from the submarine part of the archipelago that extends the dataset currently available from subaerial rocks. Noteworthy, the new samples include relatively undifferentiated rocks (andesites, latites), which weren't known in the WPI magmatic associations. In this framework, on the basis of new major/trace element and Sr-Nd isotopic data we propose that the WPI magmas formed in coherent subduction-related environment from mantle derived melts variously affected by crustal contamination during differentiation in shallow level magma chambers.

Cadoux A., Pinti D.L., Aznar C., Chiesa S. & Gillot P. 2005. New chronological and geochemical constraints on the genesis and geological evolution of Ponza and Palmarola Volcanic Islands (Tyrrhenian Sea, Italy). *Lithos*, 81, 121-151.

Cadoux A., Blichert-Toft J., Pinti D.L. & Albarède F. 2007. A unique lower mantle source for Southern Italy volcanics. *Earth Plan. Sci. Lett.*, 259, 227-238.

Conte, A.M. & Dolfi, D. 2002. Petrological and geochemical characteristics of Plio-Pleistocene Volcanics from Ponza Island (Tyrrhenian Sea, Italy). *Mineral. Petrol.*, 74, 75-94.

Paone A. 2013. Petrogenesis of trachyte and rhyolite magmas on Ponza Island (Italy) and its relationship to the Campanian magmatism. *J. Volcanol. Geotherm. Res.*, 267, 15-29.

Tracing carbon sources and mobility in subduction zones: an approach using carbon contents and isotopes in orogenic Ulten Zone peridotites

Förster B.*¹, Bianchini G.², Natali C.², Aulbach S.³ & Braga R.¹

1. Dipartimento di Scienze Biologiche, Geologiche e Ambientali, Università di Bologna. 2. Dipartimento di Fisica e Scienze della Terra, Università di Ferrara. 3. Institut für Geowissenschaften, Goethe-Universität, Frankfurt am Main, Germany.

Corresponding email: bibiana.forster2@unibo.it

Keywords: Mantle wedge-derived orogenic peridotites, carbon contents and isotopes, Ulten Zone.

The fate of carbon (C) in subduction-related environments is still under debate and of particular importance for unravelling the origin and cycling of carbon within the Earth's mantle. Mantle wedge-derived orogenic peridotites of the Ulten Zone (UZ) tectonic unit (Eastern Alps, Italy) have been captured by a subducting crustal slab and subsequently exhumed during the Late Paleozoic Variscan orogeny (Scambelluri et al., 2006). Besides common hydrous metasomatic phases (Marocchi et al., 2007), metasomatic dolomite has been optically detected in only a few samples in UZ peridotites (Sapienza et al., 2009). However, samples that are dolomite-free on thin-section scale have been shown to be compositionally indistinguishable from dolomite-bearing varieties (Sapienza et al., 2009). Thus, these rocks represent a natural laboratory to study the sources, storage and recycling of carbon in subduction-modified lithospheric mantle.

We will present a systematic study of whole-rock (WR) C-content and C-isotopic compositions of UZ peridotites combined with their detailed petrography. Preliminary C-analyses have been carried out at the University of Ferrara using EA-IRMS. The peridotite samples investigated so far cover a wide range of mineral assemblage, grain size, texture and retrogression and do not contain optically detectable carbonate. Nevertheless, these samples display homogeneous C-concentrations (0.06 wt.% to 0.08 wt.%), likely residing in dolomite. The associated C-isotopic composition is light relative to the primitive mantle (~ -5 ‰) and characterized by high variability ($\delta^{13}\text{C}$ from -17.17 ‰ to -11.12 ‰, relative to PDB).

While these results confirm the presence of carbonate as an accessory phase in UZ peridotites and indicate that carbon, if mobilized from the subducting slab, can be stored within the mantle wedge, the isotope systematics require a recycling model that considers complex C-fractionation processes related to fluid-rock interaction and/or devolatilization.

By integrating petrographic information with elemental and isotopic signatures, we aim to unravel the different carbon sources and the processes involved in the transfer of carbon to the mantle wedge in collisional subduction zone settings.

Marocchi M., Hermann J. & Morten L. 2007. Evidence for multi-stage metasomatism of chlorite-amphibole peridotites (Ukten Zone, Italy): Constraints from trace element compositions of hydrous phases. *Lithos*, 99, 85-104.

Sapienza G.T., Scambelluri M. & Braga R. 2009. Dolomite-bearing orogenic garnet peridotites witness fluid-mediated carbon recycling in a mantle wedge (Ukten Zone, Eastern Alps, Italy). *Contrib. Mineral. Petrol.*, 158, 401-420.

Scambelluri M., Hermann J., Morten L. & Rampone E. 2006. Melt- versus fluid-induced metasomatism in spinel to garnet wedge peridotites (Ukten Zone, Eastern Italian Alps): clues from trace element and Li abundances. *Contrib. Mineral. Petrol.*, 151, 372-394.

Dolomite evolution from HP to UHP conditions: the impure Cal-Dol marbles from Dora-Maira Massif (Italian Western Alps)

Ferrando S.*¹, Groppo C.¹⁻², Frezzotti M.L.³, Castelli D.¹, Compagnoni R.¹ & Proyer A.⁴

1. Dipartimento di Scienze della Terra, Università di Torino. 2. Istituto di Geoscienze e Georisorse, C.N.R. Torino.
3. Dipartimento di Scienze dell'Ambiente e del Territorio e di Scienze della Terra, Università di Milano-Bicocca.
4. Department of Geology, University of Botswana, Gaborone, Botswana.

Corresponding email: simona.ferrando@unito.it

Keywords: Carbon dissolution, thermodynamic modelling, fluid inclusions.

During deep and cold subduction, carbon dissolution is a relevant mechanism for carbon transfer from the slab into the mantle. The ultra-high pressure (UHP; 730 °C and 4.0-4.5 GPa) impure Cal-Dol-marbles from the Dora-Maira Massif are studied to investigate the poorly known evolution of dolomite during deep subduction.

Dolomite constitutes pre-kinematic porphyroclasts showing four stages of growth, coupled with chemical variations and distinct included mineral assemblages, depending on bulk-rock composition: I) a pre-Alpine inner core; II) a HP prograde-Alpine outer core, concentrically overgrowing the inner core; III) an UHP inner rim asymmetrically overgrowing the partly resorbed core; IV) an UHP early-retrograde outer rim that asymmetrically overgrows the inner rim in sharp discontinuity.

To explain the growth of dolomite through prograde, peak, and early retrograde metamorphism, a chemically simple marble (Cal, Dol, Cpx, Ol, and retrograde Atg, Tr, Mg-Chl) has been studied in detail. To predict the production-consumption of dolomite by metamorphic reactions along the P-T path, mixed-volatile P-T grids modelled in the simple CMS-H₂O-CO₂ system have been calculated. T/P-X(CO₂) petrogenetic grids and pseudosections, and mixed-volatile P-T grids predict the prograde (1.7 GPa, 550 °C) growth of Dol II in equilibrium with Cpx and Ol through the breakdown of Atg+Arg. The subsequent HP-UHP evolution is predicted in the Cpx+Fo+Dol+Arg stability field in equilibrium with a dominantly aqueous COH fluid (0.0003 < X(CO₂) < 0.0008). According to thermodynamics, only HP prograde growth of Dol II is due to metamorphic reactions, whereas growth of peak Dol III and early-retrograde Dol IV cannot be induced by simple isochemical metamorphic reactions.

A possible explanation for these microstructures comes from the abundant primary H₂O+chloride±Cal+Dol+Tlc+Tr fluid inclusions present in the Alpine Cpx. The relatively-broad Raman peaks of minerals, the presence of molecular water in the crystallographic structure of Tlc, and the constant occurrence of Cl in the hydrous minerals indicate that these minerals have a poor crystallinity due to their precipitation from a saline (salinity > 26.3 wt.% of NaCl_{eq}) aqueous solution.

The growth of Dol III and Dol IV is interpreted as due to dissolution/precipitation episodes in saline aqueous fluids. Kinetics of Dol dissolution in aqueous fluids is poorly known, and experimental and thermodynamic data under HP conditions are still lacking. Data on calcite indicate that dissolution at HP is enhanced by a prograde increase in both P and T, by high salinity in aqueous fluids, and/or low pH conditions. In the studied marble, the prograde P-T path and the occurrence of free high-saline fluids represent favourable conditions i) for the inferred dissolution-precipitation processes of the stable dolomite in a closed system; ii) for possible migration of the dissolved carbonate, if the system would have been open during subduction.

Ultrahigh-pressure metamorphism in accretionary orogens – the contribution of tectonic erosion to the subduction factory

Gilotti J.A.*, Petrie M.B. & McClelland W.C.

Department of Earth and Environmental Sciences, University of Iowa, USA.

Corresponding email: jane-gilotti@uiowa.edu

Keywords: Accretionary orogens, subduction erosion, ultrahigh-pressure metamorphism.

Evidence for ultrahigh-pressure (UHP) metamorphism of continental material in Pacific-type accretionary orogens is growing, and must be considered as input to the subduction factory. Possible examples – such as the Qinling terrane (Bader et al., 2013) and the Tianshan orogen (Liu et al., 2014), China – contain coherent slices of continental arc crust that have seen UHP conditions and imply that the base of the arc was eroded in the subduction channel. Another potential candidate for ultrahigh-pressure metamorphism formed by subduction erosion of the overriding plate is found in the Yukon-Tanana terrane of the western North American Cordillera. The Yukon-Tanana terrane is interpreted as a continental arc built on a peri-Laurentian substrate that experienced subduction on both sides before it was accreted back on to western North America in the Mesozoic. Eclogites are found as layers and lenses in quartzofeldspathic schist derived from both igneous and sedimentary protoliths, and metamorphosed during the Permian. In the St. Cyr area, slices of eclogite-bearing crust up to 30 km long and 1-2 km thick have been mapped. Isochemical thermodynamic models combined with mineral chemistry and modes from eclogite document metamorphism in the coesite stability field (Petrie, 2014). Si = 3.3-3.4 atoms per formula unit in phengite from the host schists indicate that they also record eclogite-facies metamorphism. U-Pb zircon ages of 331-337 Ma from metatolitic intrusions fit with the Klinkit stage of arc-construction (Petrie et al., in press), and U-Pb detrital zircon spectra show that the surrounding metasedimentary rocks are also derived from the Yukon-Tanana composite arc. Subduction erosion is a challenging process to recognize in the rock record, but given that over half of modern subduction zones are erosional, it may play a fundamental role in UHP metamorphism and recycling of continental crust into the mantle.

- Bader T., Franz L., Ratschbacher L., de Capitani C., Webb A., Yang Z., Pfänder J., Hofman M. & Linnemann U. 2013. The Heart of China revisited: II Early Paleozoic (ultra)high-pressure and (ultra)high-temperature metamorphic Qinling orogenic collage. *Tectonics*, 32, 922-947.
- Liu X., Su W., Gao J., Li J., Jiang T., Zhang X. & Ge X. 2014. Paleozoic subduction erosion involving accretionary wedge sediments in the South Tianshan Orogen: evidence from geochronological and geochemical studies of eclogites and their host metasediments. *Lithos*, 210-211, 89-110.
- Petrie M.B. 2014. Evolution of eclogite facies metamorphism in the St. Cyr klippe, Yukon-Tanana terrane, Yukon, Canada. Iowa City, University of Iowa, Ph.D. Thesis, 168 p.
- Petrie M.B., Gilotti J.A., McClelland W.C. & van Staal C. in press. Geologic setting of eclogite-facies assemblages in the St. Cyr klippe, Yukon-Tanana terrane, Yukon, Canada. *Geoscience Canada*.

Blueschist-facies boudinage and veining: implications for deformation processes and fluid flow in subduction zones

Malatesta C.*, Federico L., Crispini L. & Capponi G.

DISTAV, Università di Genova

Corresponding email: cristina.malatesta@unige.it

Keywords: Blueschist veining, subduction zone, brittle deformation.

Fluids in subduction zones strongly influence rheology, seismogenesis, and interaction between lithologies: understanding their occurrence and path at high-pressure (HP) conditions could thus give new hints on processes acting at these complex settings.

We therefore studied a blueschist-facies mafic mylonite occurring at the contact between two metaophiolitic HP units of the Western Alps (the eclogitic Voltri Unit and the blueschist Montenotte Unit, Ligurian Alps). This mylonite is characterized by fine-grained and ultra-fine-grained domains with similar mineralogical composition; we observed a symmetric chocolate tablet foliation boudinage evolving into several sets of veins and locally into breccia horizons. Both in boudin necks, in veins and in breccia matrix a Na-amphibole-rich assemblage grows, suggesting that all the above structures formed during a progressive deformation in blueschist facies metamorphism within the same structural level.

Four sets of veins cut the mylonite: i) syntaxial shear veins filled by Na-am fibers + minor Ep and Spn; ii) syntaxial composite veins with Na-am + Fe-ox infill growing during the first opening stage and Qtz + Ap + Wmca + Fe-ox growing during the second; iii) unitaxial composite veins including Na-am + minor Ep + Fe-ox forming during a first stage and Ab + Ep + Na-am + Wmca + Ap + Fe-ox during the second; iiiii) veins filled by Fe-rich Ep + Chl + Ab + Spn + Fe-ox forming in localized domains.

A progressive chemical and mineralogical variation occurs in the wall-rock approaching the veins: Na, Mg and Si content increase whereas Ca and K decrease, as reflected by a higher abundance of albite and Fe-oxydes and the nucleation of paragonite.

The brittle deformation concentrates in some ultra-fine-grained horizons and pods, where the vein network becomes more pervasive and the boudins are progressively disrupted up to brecciation. Such breccia is characterized by monogenic clasts of the enclosing mylonite, with size ranging from less than 1 cm to some cm, often sub-rectangular in shape. The breccia is clast-supported, with a high clast to matrix ratio; clasts are cemented by abundant interclast synkinematic Na-amphibole and display an incipient internal rotation, testified by the variability of attitude of mylonitic foliation in the different fragments.

We suggest that textural heterogeneities inside the mylonite induce stress perturbations that increase fluid pressure and focus brittle deformation; fluids thus flow into the brittle structures allowing the crystallization of hydrated minerals (Na-amphibole, epidote, micas).

Since we detected evidence of fluid-rock reaction but limited breakdown of hydrous phases in the wall-rock, we propose that fluids mostly derive from an external source.

We discuss the possible mechanisms of brittle failure, the possible fluid flow at HP conditions and the implications for fluid-assisted deformative processes, active inside subduction zones.

Noble gases isotope composition of mantle-derived peridotite xenoliths from Sardinia

Martelli M.*¹ & Bianchini G.²

1. INGV, Palermo. 2. Dipartimento di Fisica e Scienze della Terra, Università di Ferrara.

Corresponding email: mauro.martelli@ingv.it

Keywords: Mantle xenoliths, noble gases, Sardinia.

Peridotite xenoliths entrained in Plio-Pleistocene alkali basalts from north-central Sardinia represent fragments of the uppermost lithospheric mantle and offer the opportunity to investigate the subcontinental upper mantle beneath the central Mediterranean. These rocks range in bulk composition from fertile spinel-lherzolites to residual spinel-harzburgites. Previous studies illustrated that such peridotite samples suffered variable degrees of partial melting followed by enrichment associated to metasomatism, in turn due to fluids rising through the lithosphere. In this study we explore the chemical and isotopic characteristics of noble gases (He, Ne, Ar) retained into fluid inclusions of olivine and orthopyroxene belonging to this peridotitic suite. This approach allows to evaluate the noble gas characteristics of the mantle source without the potential interferences of crustal component additions. Measurements on samples previously characterised for their major, trace elements and Sr-Nd isotopic data have been performed by single-step crushing in ultra-high vacuum. Aim of the study is the identification of the noble gas isotope characteristics of the lithospheric mantle beneath Sardinia and comparison with trace elements and lithophile isotopes. In particular, by means of noble gases we would like to trace the possible involvement of metasomatic volatiles that were scarcely highlighted by lithophile elements. The first set of obtained data are presented and compared with other peridotite samples of the European/Mediterranean mantle xenoliths.

Magma with slab fluid and decompression melting signatures coexisting in the Gulf of Fonseca: evidence from Isla El Tigre volcano (Honduras, Central America)

Mattioli M.*¹, Renzulli A.¹, Agostini S.² & Lucidi R.¹

1. Dipartimento di Scienze della Terra, della Vita e dell'Ambiente, Università di Urbino "Carlo Bo".

2. Istituto di Geoscienze e Georisorse, CNR, Pisa.

Corresponding email: michele.mattioli@uniurb.it

Keywords: Isla El Tigre, Honduras, Central America Volcanic Arc.

Isla El Tigre volcano is located in the Gulf of Fonseca (Honduras) along the secondary line of the Central America Volcanic Front, where there is a significant break in the strike of the volcanic chain. The studied samples of this poorly investigated volcano are sub-alkaline, mafic lavas with calcalkaline affinity (basalts and basaltic andesites) with the typical characters of a volcanic arc magmatism. On the basis of petrographic and geochemical features, two groups of rocks were distinguished. Lavas from the main volcanic edifice (low-MgO samples) are highly porphyritic. They show a significant LILE and LREE enrichment and Nb depletion and have a strong slab signature as well as incompatible element contents similar to those of the main front of the adjacent volcanoes in El Salvador and Nicaragua (e.g. Ba/La up to 80). In contrast, lavas from the parasitic cones show higher MgO content (> 5 wt.%) and lesser HFSE depletion relative to LILE and LREE, with lower Ba/La, Ba/Nb and Zr/Nb ratios. This suggests that mantle-derived magmas were not produced by the same process throughout the activity of the volcano.

The bulk rock geochemistry and Sr–Nd–Pb isotopic data of Isla El Tigre, compared with the other volcanoes of the Gulf of Fonseca and the whole literature data of Central America (main chain and secondary line of Volcanic Front, Behind Volcanic Front and Back-Arc area) suggest this stratovolcano was mainly built by mantle-derived melts driven by fluid-flux melting, while magmas erupted through its parasitic cones have a clear signature of decompression melting, with minor slab contribution. The coexistence of these two different mantle melting generation processes should be linked to the complex geodynamic setting of the Gulf of Fonseca where the volcanic front change direction of ca. 30° and two fundamental tectonic structure of the Chortis block such as the N-S Honduras Depression and the NE-SW Guayape Fault Zone cross each other.

Host-inclusion geobarometry for ultra high pressure metamorphic (UHPM) rocks

Mazzucchelli M.L.*¹, Angel R.J.², Alvaro M.¹, Nimis P.², Domeneghetti M.C.¹ & Nestola F.²

1. Dipartimento di Scienze della Terra e dell'Ambiente, Università di Pavia.

2. Dipartimento di Geoscienze, Università di Padova.

Corresponding email: mattialuca.mazzucchelli01@universitadipavia.it

Keywords: Elastic geobarometry, Host-Inclusion geobarometry, UHPM rocks.

Conventional thermo-barometric methods can be challenged in UHPM terrains as sluggish diffusion may prevent full equilibrium among minerals and re-equilibration on exhumation may erase records of peak conditions achieved during deep subduction.

Minerals trapped as inclusions within other host minerals develop residual stresses on exhumation as a result of the differences between the thermo-elastic properties of the host and inclusion phases. Their elastic behavior provides an alternative geobarometric method independent of chemistry and chemical equilibria. The determination of possible entrapment pressures from this residual stress requires the knowledge of the equations of state (EoS) and the mutual elastic relaxation of the host and inclusion phases. This approach could provide constraints on the prograde and retrograde stress-temperature paths of metamorphic assemblages.

We will present a general solution that relies on the concept of the isomeke, a line in P - T space along which the fractional volume changes of the host and inclusion are the same (Angel et al., 2014a). This allows our solution to be used in combination with any form of equation of state and/or thermal expansion, and is not restricted to linear elasticity or just invertible EoS. Calculations can be performed with Eosfit7c (Angel et al., 2014b).

A key result is that, away from the entrapment isomeke, non-uniform stress fields are developed within the constrained two-phase system. Such stress fields can give rise to either over- or under-pressure with respect to external lithostatic pressure. Thus, for example, quartz inclusions trapped in the cores of garnet during the prograde path of the Kulet whiteschist (e.g Parkinson, 2000) experience pressures lower than the external pressure. By peak conditions of ~3.5 GPa and ~780 °C, the quartz inclusions are calculated as experiencing a peak pressure of only 1.9 GPa, sufficiently low to prevent them entering the stability field of coesite. In order to transform these quartz inclusions into coesite (i.e. enter in the coesite stability field) at the peak temperature, the pair should have experienced a much higher external pressure of about 5.9 GPa. Therefore, the absence of quartz-to-coesite transformation does not necessarily imply that a rock has not undergone UHPM.

This work was supported by ERC starting grant 307322 to Fabrizio Nestola.

Angel R.J., Mazzucchelli M.L., Alvaro M., Nimis P. & Nestola F. 2014a. Geobarometry from host-inclusion systems: The role of elastic relaxation. *Amer. Mineral.*, 99, 2146-2149.

Angel R.J., Alvaro M., Gonzalez-Platas J. 2014b. EosFit7c and a Fortran module (library) for equation of state calculations. *Z. Kristallogr.*, 229, 405-419.

Parkinson C.D. 2000. Coesite inclusions and prograde compositional zonation of garnet in whiteschist of the HP-UHPM Kokchetav massif, Kazakhstan: a record of progressive UHP metamorphism. *Lithos*, 52, 215-233.

Genesis and evolution of the Late Mesozoic magmatism of the High Atlas (Morocco)

Moratti G.*¹, Santo A.P.², Benvenuti M.², Laurenzi M.A.³, Braschi E.¹ & Tommasini S.²

1. Istituto di Geoscienze e Georisorse, C.N.R. Firenze. 2. Dipartimento di Scienze della Terra, Università di Firenze

3. Istituto di Geoscienze e Georisorse, C.N.R. Pisa.

Corresponding email: giovanna.moratti@cnr.it

Keywords: High Atlas, Jurassic-Cretaceous magmatism, radiometric dating.

Two main magmatic events occurred during the Mesozoic evolution of the Atlas System, the first one dated to Late Triassic-Early Liassic (200-195 Ma), tied to the opening of the Central Atlantic Ocean (CAMP - Central Atlantic Magmatic Province - Event), the second dated from Middle-Late Jurassic to Early Cretaceous (~ 165-110 Ma), within which K-Ar ages seem to cluster into two distinct groups, 175-155 Ma and 135-110 Ma. The post-Liassic magmatic rocks, possibly representing the last magmatic phases related to the CAMP event, are specific for the High Atlas domain, with the emplacement of (1) subvolcanic intrusive complexes, often cropping out in the cores of anticlinal ridges, and (2) basaltic lava flows, interbedded in the Middle-Late Jurassic to Early Cretaceous red beds. Their magmatic signatures, ranging from transitional basalt series to weakly/moderately alkaline series, are typical of continental intraplate magmatism and are usually considered as rift-related. In our work, we studied magmatic bodies (1) cropping at the core of anticlines and/or (2) interbedded in the red beds of the High Atlas, in the chain and at its southern front. The relationships observed between the magmatic products (2) and both the stratigraphic succession and structures, faults and folds, point to their possible emplacement as sills and to a development of the magmatism within an active, Jurassic-Cretaceous, compressive stress field. In particular, we present the first results obtained on two mafic magmatic bodies outcropping in correspondence of the South Atlas front. They are intruded at the core of anticlines folding Late Jurassic-Cretaceous rocks, or are interbedded within the vertical Late Jurassic-Cretaceous succession as a sub-effusive body. We present an important first radiometric ⁴⁰Ar-³⁹Ar dating obtained on a lava flow rock sample; the obtained age of 119 Ma, allows us to refer it to the second magmatic event of the High Atlas. We also present preliminary petrographic and geochemical compositional data of collected rock samples that display porphyritic and fluidal textures in the lavas and porphyroid textures with poikilitic crystals set in an ophitic matrix in dykes and sills. The studied rocks display a restricted compositional range, falling across the fields of basalts, trachybasalts and basaltic trachyandesites with alkaline to subalkaline affinity. We report here major and trace elements and isotopic compositions (⁸⁷Sr/⁸⁶Sr and ¹⁴³Nd/¹⁴⁴Nd) obtained on representative lava flow, dyke and sill rock samples.

The contributions of oxidised crustal carbonates to the modification of the explosive, aluminium depleted magmas of the Pollara eruptions of Salina, Italy

Moretti H.C*., Blundy J.D. & Gottsmann J.H.

Department of Earth Sciences, University of Bristol, U.K.

Corresponding email: hm12523@bristol.ac.uk

Keywords: Carbonates, Salina, fassaite.

The Pollara eruptions of Salina, Italy mark the explosive conclusion of activity on this central island in the Aeolian archipelago. Bulk chemistry shows the Lower and Upper Pollara (LPP & UPP) to be relatively depleted in aluminium and sodium, silica saturated, with low iron-enrichment and relatively enriched in potassium, rubidium and barium. These eruptions, especially the UPP, appear to have greater basement assimilation as evidenced by the rubidium enrichment rate.

The LPP, however, appears more calcic and a number of skarn samples suggest assimilation of carbonate may also modify the magma. The skarn assemblage of grossular garnet, magnetite, olivine (Fo₇₁), plagioclase (An₈₇₋₉₉) and hedenbergite is unusual in having a large proportion of fassaite pyroxene. This fassaite has a higher modal proportion of FaTs (Ca.Fe³⁺.Al.SiO₆) and similar CaTs proportion (Ca.Al₂SiO₆) to those found experimentally by Mollo et al. (2010) with 20% carbonate assimilation in a water saturated basalt. Within some crystals the proportion of Fe³⁺ in total iron reaches 100% suggesting extreme oxidation (above the MH buffer).

Cumulate samples from a magma-skarn reaction zone show a lower CaTs proportion but increasing FaTs from core-to-rim. Melt inclusions from these cumulates suggest magma with 4.7 wt.% H₂O ponded at 1.7 kbar and a set from the skarn suggest complete dehydration with CO₂ saturation up to 1 wt.%. This dehydration is proposed to have initiated earlier plagioclase saturation and thus explain the aluminium depletion whilst the fassaite reactions act to balance the usually desilicating reactions of the carbonate.

Microprobe analyses of magmatic amphiboles may evidence this degassing, estimating an overpressure of 30-40 MPA and the CO₂ saturated skarn would explosively destabilise with any injections of fresh water-rich magma.

The absence of similar trends elsewhere on Salina suggest these carbonates are at a previously untapped depth or within a geographically separated basement unit. The higher FaTS component implies a greater degree of oxidisation and equilibrium reactions favour the additional presence of hematite. Studies by Frezzotti et al. (2010) suggest mid to low crustal ponding depths occur throughout the Aeolian Islands and thus it is proposed that an isolated, volcanic, hematite-rich, carbonate atoll is buried within the basement.

Frezzotti M.L., Peccerillo A. & Bonelli R. 2003. Magma ascent rates and depths of crustal magma reservoirs beneath the Aeolian volcanic Arc (Italy): inferences from fluid and melt inclusions in xenoliths. In: De Vivo B. & Bodnar R.J. Eds., *Melt Inclusions in Volcanic Systems: Methods, Applications and Problems*. Elsevier Science. Amsterdam. NL. 175-206.

Mollo S., Gaeta M., Freda C., Di Rocco T., Misiti V. & Scarlato P. 2010. Carbonate assimilation in magmas: A reappraisal based on experimental petrology. *Lithos*, 114, 503-514.

Mantle heterogeneity and crustal contamination in Tertiary extensive magmatism in Southern Rhodopes: geochemical and isotope evidence from Evros volcanic rocks (Greece)

Pinarelli L.*¹, Christofides G.², Pipera K.², Soldatos T.², Koroneos A.² & Pecskey Z.³

1. Istituto di Geoscienze e Georisorse, C.N.R. Firenze. 2. Department of Mineralogy, Petrology and Economic Geology, School of Geology, Aristotle University of Thessaloniki, Greece. 3. ATOMKI Institute of Nuclear Research, Hungarian Academy of Sciences, Debrecen, Hungary.

Corresponding email: lapina@igg.cnr.it

Keywords: Rhodope Massif, Evros volcanics, geochemistry.

The Rhodope Massif (RM) is regarded as an eastern extension of the Alpine-Himalayan orogenic belt, whose tectonic evolution in SE Europe resulted, among other events, in an extensive magmatism. The RM in Greece and surrounding areas was the loci of an intensive Tertiary (Late Eocene - Oligocene - Miocene) intrusive and extrusive magmatic activity, which was younging southward. This magmatism was related with an extensional event that started with block faulting and depressions and the formation of E-W to NNW-SSE aligned volcano-sedimentary basins. It has been interpreted as post-collisional magmatism as a consequence of the underplating of the African plate beneath the Eurasian one. The magmatism is represented by volcano-plutonic associations with rocks of calc-alkaline, high-K calc-alkaline, and shoshonitic affinity that differ significantly in composition, demonstrating a strong dependence on the present thickness of the crust and decreasing crustal input from NW to SE. Moreover, the mantle wedge underlying the area underwent variable degrees of metasomatism induced by fluids or sediment melts released from the subducting and dehydrating oceanic lithosphere. Its melting generated mafic melts with variable enrichment in incompatible elements, having a large range of geochemical signatures from calc-alkaline to lamprophyric.

Among the above volcano-plutonic associations, the Evros Volcanic Rocks (EVR) belong to one of the two largest Tertiary volcanic districts in northern Greece. Most EVR show either calc-alkaline or high-K calc-alkaline characters. The less evolved rocks have mantle normalised trace element patterns with LILE enrichments relative to HFSE and negative spikes of Ta, Nb, and Ti. Their initial Sr and Nd isotope ratios range between 0.70545-0.70773 and 0.51260-0.51242, respectively. These characteristics denote a derivation from a mantle source enriched in incompatible elements and radiogenic isotopes. The EVR show an increase of K₂O and hygromagmaphile elements, and a decrease of compatible elements, as the silica content increase. Despite some scattering in the Harker's diagrams, particularly in the most mafic rocks, the latter show trends with different slopes when compared to those of intermediate-acidic rocks. Besides, mafic rocks have large variations of both Sr and Nd isotope ratios for a restricted range of silica. Vice versa, intermediate-acidic rocks have large variation of silica with smaller variations of isotope ratios. In the (⁸⁷Sr/⁸⁶Sr)_i versus (¹⁴³Nd/¹⁴⁴Nd)_i diagram the EVR arrange along a negative correlation that points to crustal rocks, e.g. gneisses from Southern Rhodope. However, the EVR do not fit a single correlation curve and their distribution is consistent with an evolution by fractional crystallization plus mixing with heterogeneous crustal melts. Some trachydacites, having shoshonitic affinity, show peculiar characteristics, not compatible with a derivation from the basic rocks. They seem to be derived from a geochemically distinct original magma, more strongly enriched in K₂O and incompatible elements.

The subduction of carbonated rocks and Earth degassing at warm convergent margins

Poli S.

Dipartimento di Scienze della Terra "A. Desio", Università di Milano.

Corresponding email: stefano.poli@unimi.it

Keywords: Subduction, carbonate, water.

Ternary carbonates are fundamental mineralogical constituents of the oceanic uppermost lithosphere upon subduction. Calcite and aragonite are common in pelagic sediments as well as in the alteration products of both mafic and ultramafic portions of the oceanic basement; they therefore account for percent level contribution of CO₂ mass input at subduction zones.

Metamorphic reactions are responsible for the formation of (Mg,Fe)-calcite, dolomite-ankerite, magnesite-siderite solid solutions as a function of pressure-temperature conditions and bulk composition. Ternary carbonates coexist with hydrous phases and, eventually, percolating aqueous fluids in a large range of depths, down to at least antigorite breakdown at 150-200 km depth.

More than half a gigaton of CO₂ per year is recycled in the Earth interior at convergent margins. At least 40% of this CO₂ returns to the atmosphere via igneous activity at subduction zones. Experimental and thermodynamic modelling of phase relationships at high pressure indicate that decarbonation or carbonate dissolution in fluids account for only a portion of CO₂ released, and that carbonatitic melts from a subducting crust are feasible only if thermal relaxation occurs at sub-arc depth. I find that H₂O strongly depresses the liquidus surface for ternary carbonates, and promotes the generation of hydrous carbonatitic liquids in a variety of lithologies. These liquids are enriched in calcium and efficiently scavenge volatiles, Si, and secondarily Al, from the slab and represent a potentially significant pathway for slab decarbonation. Such liquids are expected to be extremely mobile and reactive in a percolated mantle wedge, where they generate carbonate pyroxenites, a fertile CO₂ source for magmatism at subduction zones. This process is most effective at warm convergent margins and could correlate with the high CO₂ content of undegassed melts reconstructed for Central America and the northern volcanic zone in the Andes.

The contribution of amphibole from deep arc crust to the Silicate Earth's Nb budget

Tiepolo M.*¹ & Vannucci R.²

1. Dipartimento di Scienze della Terra "A. Desio", Università di Milano.
2. Dipartimento di Scienze della Terra e dell'Ambiente, Università di Pavia.

Corresponding email: massimo.tiepolo@unimi.it

Keywords: Continental crust, Nb-Ta, amphibole.

The continental crust (CC) and the depleted mantle (DM) are generally assumed to be complementary reservoirs within the Earth. Although Nb and Ta are considered refractory lithophile elements, they are depleted relative to other elements with similar geochemical affinity in both the CC and in the upper mantle (Rudnick et al., 2000; Münker et al., 2003). The mixture between CC and upper mantle, in proportions as implied by other trace elements, therefore does not generate the Nb/Ta and Nb/La ratios of chondrites. The latter are commonly assumed to represent the unfractionated Earth (Taylor, 1964). A reservoir with superchondritic ratios for Nb/Ta and Nb/La is thus required in the Earth's system.

Since several decades ago, amphibole has been identified as a potentially important mineral during differentiation of arc magma and in the production of the upper CC. Geochemical evidences suggest cryptic amphibole crystallisation in the deep crust and in turn the presence of a hidden amphibole reservoir (Davidson et al., 2007). This, coupled with the capability of calcic amphibole to give rise to a superchondritic Nb/Ta and Nb/La reservoir (Tiepolo et al., 2007), led us to determine to what extent amphibole-rich ultramafic rocks can account for the Nb (and Nb/Ta, Nb/La as well) imbalance on Earth.

We have considered lower crust mafic and ultramafic amphibole-rich intrusive rocks from collisional settings worldwide. Because CC is considered to have primarily formed in collisional setting these rocks are important for its genetic model. We modelled Nb, Ta and La contents of the hidden Nb reservoir by mass balance calculations between continental crust, depleted mantle and primitive mantle. Modelling shows that amphibole-rich mafic lower crust can solve the so-called Nb paradox if large volumes of materials are returned into the mantle during the Earth's history. A possible mechanism is recycling, particularly in Precambrian times, of eclogites that melted as amphibolites and were later transferred to the eclogite field as a metamorphic reaction.

- Davidson J., Turner S., Handley H., Macpherson C. & Dosseto A. 2007. Amphibole "sponge" in arc crust?. *Geology*, 35, 787-790.
- Münker C., Pfander J.A., Weyer S., Buchl A., Kleine T. & Mezger K. 2003. Evolution of planetary cores and the Earth-Moon system from Nb/Ta systematics. *Science*, 301, 84-87.
- Rudnick R.L., Barth M., Horn I., McDonough W.F. 2000. Rutile-bearing refractory eclogites: Missing link between continents and depleted mantle. *Science*, 287, 278-281.
- Taylor S.R. 1964. Chondritic Earth model. *Nature*, 202, 281-282.
- Tiepolo M., Oberti R., Zanetti A., Vannucci R. & Foley S. 2007. Trace-Element Partitioning Between Amphibole and Silicate Melt. *Rev. Mineral. Petrol.*, 67, 417-452.

Solubility of forsterite, enstatite and magnesite in high-pressure COH fluids

Tiraboschi C.*¹, Tumiati S.¹, Ulmer P.², Pettke T.³ & Poli S.¹

1. Dipartimento di Scienze della Terra, Università di Milano. 2. Department of Earth Sciences, ETH Zurich, Switzerland.
3. Institute of Geological Sciences, University of Bern, Switzerland.

Corresponding email: carla.tiraboschi@unimi.it

Keywords: COH fluids, solubility, mantle minerals.

Fluids play a crucial role in many processes in subduction zones, influencing the melting temperatures and promoting mass transfer from the subducting lithosphere to the overlying mantle wedge. The amount of dissolved species mobilized by high-pressure fluids has been investigated so far mainly in H₂O-only fluids. However, CO₂ is also thought to be a significant volatile species, as carbon is a relevant component in subduction-related fluids. Compared to H₂O-only fluids, the solubility of mantle minerals in high-pressure COH fluids is substantially unexplored. For this reason we choose to experimentally investigate the dissolution of forsterite, enstatite and magnesite in graphite-saturated COH fluids at controlled redox conditions. We conducted experiments at pressures from 1 to 2 GPa and temperatures from 800 to 1100 °C employing a rocking piston cylinder apparatus. Synthetic forsterite, enstatite and natural magnesite were used as starting material. A diamond trap was placed between two layers of mantle minerals to collect fluid and solutes. Carbon-saturated COH fluids were generated starting from oxalic acid anhydrous (H₂C₂O₄), water (doped with 580 ppm of Cs) and graphite. Redox conditions were controlled employing the double capsule technique and nickel-nickel oxide buffer ($\Delta\text{FMQ} = -0.69$ at 800 °C). Thermodynamic calculations predict fluids mainly composed of H₂O and CO₂, characterized by different XCO₂ (= CO₂/H₂O + CO₂) contents as a function of *P* and *T*. We analyzed the fluid and solutes using the cryogenic laser ablation ICP-MS technique. As the temperature reached by the freezing stage (*T* = -35 °C) is not sufficient to freeze CO₂, the analyzed solute content refers to the aqueous part of the COH fluid and has to be scaled to the volatile speciation of the COH fluid, retrieved through thermodynamic modeling.

For what concerned the forsterite + enstatite assemblages, the Si content in the COH fluid ranges from 0.15 mol/kg (*P* = 1 GPa, *T* = 800 °C) to 1.57 mol/kg (*P* = 2 GPa, *T* = 1100 °C), while Mg spans from 0.20 mol/kg (*P* = 1 GPa, *T* = 800 °C) to 1.95 mol/kg (*P* = 2 GPa, *T* = 1100 °C). The enstatite + magnesite assemblages present Si contents ranging from 0.22 to 0.28 mol/kg and Mg from 0.20 to 0.28 mol/kg at *P* = 1.5 GPa and temperatures from 800 to 900 °C. Our results show that Si solubility in COH fluids is lower compared to H₂O-only system (Newton & Manning, 2002). On the other hand, the presence of CO₂ seems to favor the formation of Mg-solutes. Subduction zone fluids can therefore transport a significant amount of solutes, acting as an effective recycling vehicle in the Subduction Factory.

Newton R.C. & Manning C.E. 2002. Solubility of enstatite + forsterite in H₂O at deep crust/upper mantle conditions: 4 to 15 kbar and 700 to 900 °C. *Geochim. Cosmochim. Acta*, 66, 4165-4176.

Are the Mn-rich subduction metasediments of Praborna (Zermatt-Saas Unit) really ultra-oxidized?

Tumiati S.*¹, Godard G.², Martin S.³, Malaspina N.⁴ & Poli S.¹

1. Dipartimento di Scienze della Terra "A. Desio", Università di Milano. 2. Institut de Physique du Globe de Paris, Université Paris Diderot, France.
3. Dipartimento di Geoscienze, Università di Padova. 4. Dipartimento di Scienze dell'Ambiente e del Territorio e di Scienze della Terra, Università di Milano Bicocca.

Corresponding email: simone.tumiati@unimi.it

Keywords: Eclogite, manganese, redox.

The manganese ore of Praborna (Italian Western Alps) is embedded within a metasedimentary sequence belonging to a subduction mélange equilibrated at high-pressure (HP) conditions (ca. 2 GPa) during the Alpine orogenesis. The pervasive veining of the ore and the growth of "pegmatoid"• HP minerals suggest that these Mn-rich rocks strongly interacted with slab-derived fluids during HP metamorphism. These rocks are in textural and chemical equilibrium with the veins and in contact with sulphide- and magnetite-bearing metabasites at the bottom of the sequence. They contain braunite ($\text{Mn}^{2+}\text{Mn}^{3+}_6\text{SiO}_{12}$), quartz, pyroxmangite ($\text{Mn}^{2+}\text{SiO}_3$), and minor hematite, omphacite, piemontite and spessartine-rich garnet. Sulphides are absent in the Mn-rich rocks, whereas sulphates (barite, celestine) occur together with As- and Sb-oxides and silicates. This rock association provides an excellent natural laboratory to constrain the redox conditions in subducting oceanic slab mélanges at HP and fluid-present conditions. Similarly to Fe-bearing minerals, Mn oxides and silicates can be regarded as natural redox-sensors. A thermodynamic dataset for these Mn-bearing minerals is built, using literature data as well as new thermal expansion parameters for braunite and pyrolusite, derived from experiments. Based on this dataset and the observed assemblages at Praborna, thermodynamic calculations show that these mélange rocks are characterized by ultra-oxidized conditions (ΔFMQ up to +12.7) if the chemical potential of oxygen (or the oxygen fugacity $f\text{O}_2$) is accounted for. On the other hand, if the molar quantity of oxygen is used as the independent state variable to quantify the bulk oxidation state, the ore appears only moderately oxidized and comparable to typical subduction-slab mafic eclogites. Such an apparent contradiction may happen in rock systems whenever oxygen is improperly considered as a perfectly mobile component. In the Earth's mantle, redox reactions take place mainly between solid oxides and silicates, because O_2 is a negligible species in the fluid phase. Therefore, the description of the redox conditions of most petrological systems requires the introduction of an extensive variable, namely the oxygen molar quantity ($n\text{O}_2$). As a consequence, the oxygen chemical potential, and thus $f\text{O}_2$, becomes a dependent state variable, not univocally indicative of the redox conditions of the entire rock column of a subduction zone, from the dehydrating oceanic crust to the overlying mantle wedge. On a more general basis, the comparison of $f\text{O}_2$ retrieved from different bulk compositions and different phase assemblages is sometimes challenging and should be undertaken with care. From the study of mélange rocks at Praborna, the distribution of oxygen at subduction zones could be modelled as an oxidation gradient, grading from a maximum in the subducted altered oceanic crust to a minimum in the overlying peridotites of the mantle hanging-wall.

SESSION S5

Subduction and exhumation of continental lithosphere: implications on orogenic architecture, environment and climate

CONVENORS

Rodolfo Carosi (Univ. Torino)

Franco Rolfo (Univ. Torino)

Giuliano Panza (Univ. Trieste)

A geophysical perspective on the lithosphere-asthenosphere system of the Periadriatic region

Brandmayr E.¹, Raykova R.², Romanelli F.^{*1} & Panza G.¹

1. Dipartimento di Matematica e Geoscienze, Università di Trieste.

2. Department of Meteorology and Geophysics, University of Sofia, Bulgaria.

Corresponding email: romanel@units.it

Keywords: Periadriatic region, tomography, lithosphere.

We present a multiscale 3D model of the crust and upper mantle of the Periadriatic region showing how the Adriatic plate, the Northern indent of the African promontory, is involved in the Apennines, Alpine, and Dinarides subduction zones, respectively surrounding its western, northern, and eastern margins.

The model obtained at the scale of $1^{\circ} \times 1^{\circ}$ is analysed along selected sections perpendicular to the orogenic complexes of the study area (Apennines, Alps, Dinarides) and it confirms the existence of deep structural asymmetries between E- and W-directed subduction zones. The asymmetry found between the almost vertical Apenninic subduction and the Alpine-Dinaric subduction, which is in turn characterized by a low dip angle, can be ascribed to an eastward mantle flow taking place in the low velocity zone (LVZ) that characterizes the top of the very shallow asthenosphere beneath the Tyrrhenian basin. The high-resolution model obtained for the Alpine region at a scale of $0.5^{\circ} \times 0.5^{\circ}$ enlightens the extreme variability of the crustal thickness as well the small scale heterogeneities in the upper mantle beneath the study area. The density model clearly shows that the subducting lithosphere turns out to be less dense than the surrounding mantle (Brandmayr et al., 2011). A temperature model of the mantle layers is obtained by means of an advanced conversion technique of VS to temperature that takes in account variable chemical composition and bulk water content (Tumanian et al., 2012 and references therein).

The superposition of different geodynamic mechanisms in the mentioned areas is coherent with the global asymmetry of plate tectonics (Doglioni et al., 2007; Panza et al., 2010), evidence of polarized plate tectonics (Doglioni & Panza, 2015), and supports a passive origin of plate boundaries, contrary to what is usually assumed.

Brandmayr E., Marson I., Romanelli F. & Panza G.F. 2011. Lithosphere density model in Italy: no hint for slab pull. *Terra Nova*, 23, 292-299, doi: 10.1111/j.1365-3121.2011.01012.x.

Doglioni C. & Panza G.F. 2015. Polarized plate tectonics. *Adv. Geophys.*, 56, 1-167.

Doglioni C., Carminati E., Cuffaro M. & Scrocca D. 2007. Subduction kinematics and dynamic constraints. *Earth Sci. Rev.*, 83, 125-175.

Panza G.F., Doglioni C. & Levshin A. 2010. Asymmetric ocean basins. *Geology*, 38, 59-62, doi:10.1130/G30570.1.

Tumanian M., Frezzotti M.L., Peccerillo A., Brandmayr E. & Panza G.F. 2012. Thermal structure of the shallow upper mantle beneath Italy and neighbouring areas: correlation with magmatic activity and geodynamic significance. *Earth Sci. Rev.*, 114, 369-385.

Mechanics of Variably Deformed Basalt in the Osa Mélange, Costa Rica: implications for seismogenesis in the erosive Middle America subduction zone

Clarke A.P.¹, Vannucchi P.¹ & Vinciguerra S.*²⁻³

1. Department of Earth Sciences, Royal Holloway, University of London, UK. 2. Dipartimento di Scienze della Terra, Università di Torino.
3. British Geological Survey, NERC Environmental Council, UK.

Corresponding email: sergiocarmelo.vinciguerra@unito.it

Keywords: Rock deformation, melange mechanics, basalt properties.

The Middle America subduction zone is a textbook example of the subduction erosion tectonic process - accounting for half of modern subduction zones - which causes material from the forearc to be entrained into the plate boundary interface as it migrates upwards. The Osa Peninsula, Costa Rica, lies above the seismogenic portion of this subduction zone and exposes material from the forearc basement - the Osa Mélange - which forms the hanging wall at depth. Offshore Osa Peninsula is uniquely within reach of modern drilling technologies at the depth of seismic nucleation and is the target of the CRISP expedition.

The forearc consists of the Osa Mélange and overlying slope sediments. The mélange is a highly deformed terrane of accreted seamounts and is composed of variably deformed basalt with minor clastic and carbonate sediments, which in turn display a range of structural styles, from flow and injection into cracks in the surrounding basalt to extensive brittle fracturing and brecciation.

The deformation in the basalt varies from being largely undeformed, through moderately fractured hyaloclastite to intensely comminuted basalt displaying grain-by-grain disaggregation. This comminuted basalt forms a mechanical matrix for the stronger material and is observed to flow around these blocks. This is a situation where the basalt - usually considered to be the mechanically stronger lithology - is deformed so that it is weaker than the sedimentary rocks. As such the response of this material to the conditions likely to be found at the plate boundary interface cannot be predicted a priori.

Rock deformation laboratory experiments on the basalt are planned to characterise the physical properties, the deformation style and the failure mode envelopes in conditions close to those at the plate boundary interface. Experimental conditions will span the full range of temperature and pressure present in the mélange. This will be used to define the effect of this prior fabric on subsequent deformation within the plate boundary interface with a focus on whether the deformation is brittle or ductile and how its localisation evolves.

By characterising this plate boundary we can infer the attributes of earthquake nucleation and propagation in pre-deformed rocks and can extrapolate this to other erosive subduction zones around the world.

Competing/collaborative effect between snow-ice load and tectonic forces modulates large earthquakes occurrence

Cocetta F.*¹, Peresan A.¹⁻²⁻³ & Panza G.F.¹⁻³⁻⁴

1. Dipartimento di Matematica e Geoscienze, Università di Trieste. 2. Istituto Nazionale di Oceanografia e di Geofisica Sperimentale, Osservatorio Geofisico Sperimentale, Udine. 3. SAND Group, The Abdus Salam International Centre for Theoretical Physics, Trieste. 4. China Earthquake Administration, Institute of Geophysics, Beijing, China Peoples Republic.

Corresponding email: aperesan@units.it

Keywords: Seismicity, seasonal modulation, snow-ice load.

Tectonic forces responsible for mountain building must overcome, among others, gravity; this suggests the possibility for competing effects of tectonic forces and the load due to snow and ice cover (Heki, 2003; Panza et al., 2011). Compared to other seasonal meteorological phenomena (e.g. rainfall), snow and ice load are characterized by a longer residence time and a relatively more homogeneous distribution over the affected Earth surface. As evidenced by theoretical computations (Heki, 2003) and quantitative analyses of seismicity, they may perturb the stress pattern within the entire crust and possibly deeper in the lithosphere.

Seasonal patterns associated with stress modulation and large earthquake occurrence have been detected in regions characterized by present day mountain building and glacial retreat in the Northern Hemisphere (Panza et al., 2011). In the Himalaya (very recent example, Nepal event of April 25, 2015) and the Alps the seismicity is peaking in spring and summer; opposite behavior - peak in fall and winter - is observed in the Apennines. This diametrical behavior well correlates with the dominant tectonic regime: peak in spring and summer in contraction areas, peak in fall and winter in extensional areas. In this study the analysis of the seasonal effect is extended to several contraction (e.g. Zagros and Caucasus) and extensional regions; counter-examples, from regions where no seasonal modulation is expected (e.g. Tropical Atlantic Ridge), are considered as well. In the Southern Hemisphere, a quantitative study is warranted only in Antarctica, where the Circum-Antarctic ridge, as a whole, reacts to the seasonal thaw on the Antarctic continent.

A quantitative assessment of the statistical significance of the detected seasonal modulation has been carried out for the Antarctica region, as well as for the two extensional areas where no modulation was expected, namely the Pacific and Atlantic ridges. For this purpose, the analysis was repeated considering one hundred randomized catalogues, where origin time was shuffled on random basis (thus destroying any possible seasonal modulation). It is found that the results obtained for the Antarctica differ significantly from those provided by random catalogues (the confidence level being > 99%), whereas in the mid-oceanic ridges results are still compatible with random ones.

Our findings generalize to different seismotectonic settings the observations made about short-term (seasonal) and long-term (secular) modulation of seismicity (Panza et al., 2011), and confirm that snow and ice thaw may cause crustal deformations that modulate seismicity.

Heki K. 2003. Snow load and seasonal variation of earthquake occurrence in Japan. *Earth Planet. Sci. Lett.*, 207, 159-164.

Panza G.F., Peresan A. & Zuccolo E. 2011. Climatic modulation of seismicity in the Alpine-Himalayan mountain ranges. *Terra Nova*, 23, 19-25.

The Ross orogen in northern Victoria Land (Antarctica): new aeromagnetic and gravity perspectives for its geodynamic evolution and crustal architecture

Ferraccioli F.¹, Armadillo E.², Crispini L.² & Capponi G.*²

1. British Antarctic Survey, Cambridge, UK. 2. DISTAV, Università di Genova.

Corresponding email: capponi@dipteris.unige.it

Keywords: Geodynamic evolution, crustal architecture, northern Victoria Land.

The Ross Orogen in East Antarctica is linked to the evolution of the paleo-Pacific active margin of Gondwana. Northern Victoria Land (NVL) contains several key geological records of these active margin processes. Most models depict NVL as a collage of three terranes, the Wilson, Bowers and Robertson Bay terranes (WT, BT, RBT). However, whether these are exotic terranes or merely different components of an evolving and migrating backarc-arc-trench system is still uncertain.

Here we interpret new aeromagnetic, aerogravity and land-gravity compilations, derived from over 2 decades of geophysical exploration, that enable us to trace the subglacial extent of major terrane-bounding and intra-terrane faults in NVL, investigate crustal architecture, and propose an evolutionary model for the active margin of the craton.

Prominent aeromagnetic anomalies lie along the eastern edge of the Wilkes Subglacial Basin. Small exposures of gabbro-diorites within the Prince Albert Mountains further south suggest that these anomalies may be delineating the buried extent of an early-Ross magmatic arc. This arc may have accreted as an exotic element onto the former Neoproterozoic rifted margin of E Antarctica, or may have developed “in situ” upon a pre-existing suture zone.

Magnetic segments of the arc are also identified within the WT. We infer that these may have originally been adjacent or at least closer to each other and that transtension triggered arc boudinage, separating the arc segments in the WT. Such a configuration might be expected in an overall retreating Early Cambrian subduction setting. Extension/transtension in the overriding East Antarctic plate may also have created the accommodation space for the development of thick mid-Cambrian(?) sedimentary basins within the central WT, which are imaged by prominent magnetic lows.

Basin inversion is proposed here for the central WT during a later predominantly transpressional stage (ca 490-460 Ma), that triggered the development of a major pop-up structure within the WT; several buried thrusts of the pop-up can now be traced in enhanced aeromagnetic images.

Regardless of the uncertainties associated with the original position of the terranes, high amplitude magnetic and gravity anomalies suggest that oceanic basement floors the northern BT. Previous geophysical interpretations suggested that oceanic basement may have subsequently been uplifted and obducted onto the margin because of a phase of renewed, but more oblique Cambrian subduction. An alternative explanation that we put forward here is that docking of a microcontinent inferred to underlie part of the RBT occurred, and this facilitated obduction. The latter scenario is particularly intriguing, as it bears similarities with recently proposed geodynamic models for the Tasmanian sector of the Gondwana active margin.

Petrological and geochemical role of fluid phases in orogenic settings

Ferrando S.*¹ & Frezzotti M.L.²

1. Dipartimento di Scienze della Terra, Università di Torino. 2. Dipartimento di Scienze dell'Ambiente e del Territorio e di Scienze della Terra, Università di Milano Bicocca.

Corresponding email: simona.ferrando@unito.it

Keywords: Continental subduction, mantle metasomatism, ultra-high pressure metamorphism.

The fluid phase in orogenic settings has a key role in petrology and geochemistry, with implications for deep carbon cycle. We will present some examples from our research group within the Prin project 2010PMKZX7.

Fluids enhance metamorphic reactions and re-equilibration of mineral assemblages, determine stability field of metamorphic minerals, and are responsible for metasomatism. Sulu quartzites (China) Dora-Maira whiteschists and marbles (Italy), and Karakorum high-pressure xenoliths (China) represent typical examples of fluid-mineral metamorphic evolution in deeply subducted continental rocks from orogenic settings differing on *P/T* gradients.

Trace element compositions of ultra-high pressure fluids from peak multiphase solid inclusions in quartzite (Sulu) and whiteschists (Dora-Maira) are characterized by significant LILE enrichments and HFSE depletions (Frezzotti & Ferrando, 2015). This selective mass transfer from the subducted continental crust to the mantle wedge by fluid flow deeply modifies the geochemistry of peridotites and, consequently, represents a key for understanding the geochemical variations observed in orogenic magmas (Peccerillo & Frezzotti, 2015).

Fluid phases generated during deep subduction are crucial to our understanding for the Earth's deep carbon cycle (Flesia & Frezzotti, 2015). In collisional contexts characterized by relatively high temperatures such as the Himalayan orogen, deep reactions of decarbonation and of graphite oxidation, as evident in Karakorum xenoliths, are the primary mechanisms to produce CO₂ subsequently released into the atmosphere via tectonic discontinuities. In collisional contexts characterized by deep and cold subduction such as the Western Alps, carbon dissolution (Frezzotti et al., 2014) from both oceanic (Lago di Cignana Mn-nodules) and continental (Dora-Maira marbles) crust is an additional relevant mechanism for the transfer of carbon into the mantle, ultimately outgassed by magmatism and tectonics.

Flesia C. & Frezzotti M.L. 2015. The dilemma of the dwarf Earth's CO₂ degassing: irrelevant or crucial? *J. Geochem. Explor.*, 152, 118-122.

Frezzotti M.L. & Ferrando S. 2015. The chemical behavior of fluids released during deep subduction based on fluid inclusions. *Am. Mineral.*, 100, 352-377.

Frezzotti M.L., Huizenga J.M., Compagnoni R. & Selverstone J. 2014. Diamond formation by carbon saturation in C-O-H fluids during cold subduction of oceanic lithosphere. *Geochim. Cosmochim. Acta*, 143, 68-86.

Peccerillo A. & Frezzotti M.L. 2015. Magmatism, mantle evolution and geodynamics at the converging plate margins of Italy. *J. Geol. Soc.*, doi:10.1144/jgs2014-085.

Metamorphic CO₂-producing processes in collisional orogens: case studies from the Himalayas

Groppo C.^{*1-2}, Rolfo F.¹⁻², Castelli D.¹, Mosca P.² & Rapa G.¹

1. Dipartimento di Scienze della Terra, Università di Torino. 2. Istituto di Geoscienze e Georisorse, CNR, Torino.

Corresponding email: chiara.groppo@unito.it

Keywords: Orogenic CO₂ cycle, calc-silicate rocks, phase petrology.

A reliable quantitative estimate of the metamorphic CO₂ flux from collisional orogens, which is fundamental for our understanding of the deep carbon cycle, is still far from being constrained. Beside the limited and incomplete information on the volumes of potential CO₂-source rocks in collisional orogens, one of the major uncertainties is the still poor knowledge of the nature of metamorphic CO₂-producing processes, and of the amount of CO₂ potentially released through these reactions.

Previous studies of metamorphic decarbonation reactions in metacarbonate rocks mainly used simple model reactions between end-members in simplified model systems (e.g. CMAS-HC) and considered Qtz and Cc in excess. However, natural calc-silicate rocks are much more complex than the CMAS-HC model system, because Ca-Mg-Fe solid solutions commonly occur (e.g. Grt, Cpx), as well as K- (e.g. Bt, Mu, Kfs) and Ca-Na (e.g. Pl, Scp) silicates. Moreover, Qtz and/or Cc may be completely consumed during prograde metamorphism. A fully quantitative modeling of calc-silicate rocks thus requires to investigate very complex ³ 6-component systems.

We present two case studies from the Himalayas, discussing the importance of phase petrology for understanding (and quantifying) the metamorphic CO₂-producing processes in collisional orogens.

Phase relations and devolatilization reactions in the 6- and 8-component CFAS-HC and NKCMAS-HC systems are investigated, and applied to high-grade Qtz+Grt+Cpx+Pl (Cc-absent) and Cpx+Cc+Kfs+Scp+Pl+Zo (Qtz-absent) calc-silicate rocks. The CFAS-HC and NKCMAS-HC equilibria involving garnet Ca-Fe solid solution and plagioclase and scapolite Na-Ca solid solutions, respectively, are investigated using: (i) isobaric T-X(CO₂) phase diagram sections, (ii) chemographies or isobaric T-X(CO₂) pseudosections, and (iii) mixed-volatile P-T phase diagram projections. Our results suggest that most of the observed key microstructures in the studied rocks correspond to isobaric univariant or invariant assemblages. A correct interpretation of such assemblages is only possible by combining microstructural observations with modeling of phase relations through mixed-volatile phase diagram projections.

Our study has identified CO₂-producing reactions that have never been considered before, thus underlying the importance of considering solid solutions (e.g. Grt, Pl, Scp) in the modeling of calc-silicate rocks. Our results also demonstrate that Qtz+Grt+Cpx+Pl and Cpx+Cc+Kfs+Scp+Pl+Zo calc-silicate rocks may act as CO₂-source during prograde heating, releasing internal-derived CO₂-rich fluids through Grt, Cpx and Kfs -forming reactions. These reactions, rather than simple (and often unrealistic) model reactions between mineral end-members, should be considered whenever one wants to obtain quantitative and reliable estimates of the CO₂ metamorphic flux from orogenic zones.

Geology and tectono-metamorphic evolution of the Himalayan Metamorphic Core along the Mugu Karnali transect, Western Nepal (Central Himalaya)

Iaccarino S.^{*1}, Montomoli C.¹⁻², Carosi R.³, Massonne H.-J.⁴, Langone A.⁵ & Visonà D.⁶

1. Dipartimento di Scienze della Terra, Università di Pisa. 2. Istituto di Geoscienze e Georisorse, CNR, Pisa. 3. Dipartimento di Scienze della Terra, Università di Torino. 4. Institut für Mineralogie und Kristallchemie, Universität Stuttgart, Germany. 5. Istituto di Geoscienze e Georisorse, CNR, Pavia. 6. Dipartimento di Geoscienze, Università di Padova.

Corresponding email: iaccarino@dst.unipi.it

Keywords: Greater Himalayan Sequence, Himalayan metamorphism, pseudosection modelling.

In this contribution we present new structural and tectono-metamorphic data related to a geological transect along the Mugu Karnali valley (Montomoli et al., 2013) in Western Nepal (Central Himalaya). An almost continuous natural cross-section of the Himalaya metamorphic core is exposed from Lesser Himalaya Sequence (LHS) up to the Everest Series (ES) through the high-grade gneiss of Greater Himalayan Sequence and its leucogranite intrusions. A detailed meso- and micro-structural analysis was carried out along the studied transect. Newly identified high temperature ductile shear zones within the GHS have been mapped. This mapping revealed a possible structural complexity of this unit. We derived P-T conditions and P-T paths for samples from different structural units using different methods (e.g. pseudosections, THERMOCALC Average P-T). It turned out that these (GHS, LHS, ES) units are characterized by different P-T evolutions. *In situ* U-(Th)-Pb monazite geochronology on selected samples allowed us to put temporal constraints in their metamorphic evolution. Integrating our meso- and micro-structural observations with metamorphic data and geochronology data, a strong diachronism in metamorphism and deformation is evident along the studied transect, where different crustal slices attained their characteristics at different time. Coeval activity of basal thrusting at the bottom with normal shearing at the top is not necessarily supported. Our new data point to a much more complex deformational and metamorphic history of the GHS than a one characterized by a single tectonic unit bounded by two faults with opposite sense of shear.

Montomoli C., Iaccarino S., Carosi R., Langone A. & Visonà D. 2013. Tectonometamorphic discontinuities within the Greater Himalayan Sequence in Western Nepal (Central Himalaya): Insights on the exhumation of crystalline rocks. *Tectonophysics*, 608, 1349-1370.

Relations between South Tibetan Detachment System, Tethyan Sedimentary Sequence and High Himalayan granite: a new perspective

Montomoli C.*¹, Carosi R.², Langone A.³, Iaccarino S.¹ & Visonà D.⁴

1. Dipartimento di Scienze della Terra, Università di Pisa. 2. Dipartimento di Scienze della Terra, Università di Torino. 3. Istituto di Geoscienze e Georisorse, C.N.R. Pavia. 4. Dipartimento di Geoscienze, Università di Padova

Corresponding email: chiara.montomoli@unipi.it

Keywords: South Tibetan Detachment, Tethyan Himalayan Sequence, Exhumation.

In the Himalayas the top-to-the-N South Tibetan Detachment System (STDS) is a wide regional shear zone separating the lower high-grade metamorphic rocks of the Greater Himalayan Sequence (GHS) from the overlying Tethyan Himalayan Sequence (THS). Along many sections of the belt STDS is characterized by a lower ductile shear zone, affecting the upper part of the GHS and the amphibolites facies rocks at the bottom of the THS and by an upper brittle fault, above which the very-low-grade to non metamorphic rocks of the THS crop out.

It is commonly assumed that the coeval activity of the STDS and the lower Main Central Thrust (MCT), led to the exhumation of GHS including the High Himalayan granites at the point that their contemporaneous shearing become a paradigm for the Himalayan tectonics. Granites are located in the upper part of the GHS, and in the North Himalayan domes, and intrude mainly in the lower ductile shear zone of the STDS.

By the way, a large undeformed leucogranite cross-cutting the STDS and intruding both the GHS and the THS has been recognized in Western Nepal (Carosi et al., 2013). U-Pb ages pinpoint a crystallization age at ~ 23-24 Ma constraining the youngest shearing event between the two tectonic units (GHS and THS).

Dykes from the upper portion of the granite intrude the low-grade metamorphic rocks of the THS made by biotite-bearing quartzites, impure limestone, metarenites and metapelites, characterized by the metamorphic assemblage of calc + qz + ms + bt ± chl and scapolite. Sedimentary structures are well-preserved and contact metamorphism has been observed within a few meters from the granite contact.

To investigate the depositional age of THS intruded by the granite, detrital zircons have been extracted by two samples and dated using a laser-ablation, inductively coupled, plasma mass spectrometry. CL features and radiometric results confirm a detrital origin of the zircon grains. Age spectra point out that the younger data, indicate a depositional age from Upper Jurassic to Lower Cretaceous. These findings confirm that the ~ 23-24 Ma undeformed granite intruded the THS up to the Cretaceous layers and rule out the occurrence of a tectonic discontinuity between GHS and THS active after ~ 23-24 Ma.

Being the MCT active between 25 and 17 Ma in Western Nepal, our results limit the contemporaneous activity of the MCT and STDS to a short period of time (~1-2 Ma) and thus argue against generally accepted exhumation models of the GHS requiring prolonged contemporaneous activity of the two shear zones.

For western Nepal, we suggest an exhumation model driven by shear zones propagating from N to S allowing the exhumation of different slices starting from the upper portion to the lower one of the GHS.

Carosi R., Montomoli C., Rubatto D. & Visonà D. 2013. Leucogranite intruding the South Tibetan Detachment in western Nepal: implications for exhumation models in the Himalayas. *Terra Nova* 25, 6, 478-489.

Lithospheric V_S models in the Campanian volcanic area

Nunziata C.*, Costanzo M.R. & Mandara R.

Dipartimento di Scienze della Terra, dell'Ambiente e delle Risorse, Università "Federico II", Napoli.

Corresponding email: conunzia@unina.it

Keywords: Campanian volcanic area, Rayleigh waves, lithospheric V_S models.

A comprehensive lithospheric (up to 73 km depth) shear wave velocity (V_S) model of the Campanian volcanic area is proposed by merging the results obtained for the volcanic systems of Roccamonfina, Campi Flegrei (Nunziata & Gericitano, 2012) and Mt. Vesuvius (e.g. Nunziata et al., 2006), in the Neapolitan area (Nunziata, 2010), in the Campanian Plain (e.g. Costanzo & Nunziata, 2014) and those in the Campi Flegrei-Napoli area and in the Gulf of Napoli (PRIN project, PRIN2010PMKZX7). Such models are obtained by the non-linear inversion of group velocity dispersion data of fundamental-mode Rayleigh surface wave, extracted by frequency-time analysis from earthquake recordings and, mostly, from seismic noise cross-correlations between two receivers. In the inversion, local data (up to 7 s) are joined with regional phase (25-80 s) and group (10-150 s) velocity data (Panza et al., 2007).

The main features are a thinned crust (20-25 km) above a low velocity mantle (~ 4.2 km/s) and a sharp increment of V_S (3.7-4.0 km/s), detected below the Campanian Plain and the Gulf of Napoli at 8-10 km depth, relative to metamorphic rocks. At 14-16 km depth a 5-8% V_S reduction is found consistent with the brittle-ductile transition zone identified in the peri-Tyrrhenian area at 10-15 km depth (400 ± 170 °C) (e.g. Viti et al., 1997).

In the northeast of the Gulf of Napoli, toward Mt. Vesuvius, a V_S reduction (8-15%) is observed at 6-8 km depth which can be attributed to partial melting of rocks. At 12-13 km depth, V_S increases to 3.4-3.8 km/s, as below the Campanian Plain and western part of the Gulf of Napoli.

These findings agree with the geodynamic context of the southern Tyrrhenian Sea: stretching of the continental lithosphere, with passive upwelling of asthenosphere, and consequent magmatism and high surface heat flow.

- Costanzo M.R. & Nunziata C. 2014. Lithospheric V_S models in the Campanian Plain (Italy) by integrating Rayleigh wave dispersion data from noise cross-correlation functions and earthquake recordings. *Phys. Earth Planet. Inter.*, 234, 46-59
- Nunziata C. 2010. Low shear-velocity zone in the Neapolitan-area crust between the Campi Flegrei and Vesuvio volcanic area. *Terra Nova*, 22, 208-217
- Nunziata C. & Gericitano F. 2012. V_S crustal models of the Roccamonfina volcano and relationship with Neapolitan Volcanoes (southern Italy). *Int. J. Earth Sci.(Geol Rundsch)*, 101(5), 1371-1383.
- Nunziata C., Natale M., Luongo G. & Panza G.F. 2006. Magma reservoir at Mt. Vesuvius: size of the hot, partially molten, crust material detected deeper than 8 km. *Earth. Planet. Sci. Lett.*, 242, 51-57.
- Panza G.F., Peccerillo A., Aoudia A. & Farina B. 2007. Geophysical and petrological modelling of the structure and composition of the crust and upper mantle in complex geodynamic settings: The Tyrrhenian Sea and surroundings. *Earth-Sci. Rev.*, 80, 1-46.
- Viti M., Albarello D. & Mantovani E. 1997. Rheological profiles in the Central-Eastern Mediterranean. *Ann. Geophys.*, 40(4), 849-864.

Receiver functions analysis to determine crustal structure at the contact of the northern Dinarides and southwestern Pannonian Basin

Orešković J.*¹, Šumanovac F.¹, Hegedűs E.², Kolar S.¹ & Kovács A.C.²

1. Faculty of Mining, Geology and Petroleum Engineering, University of Zagreb.

2. Eötvös Loránd Geophysical Institute of Hungary, Budapest.

Corresponding email: jasna.oreskovic@rgn.hr

Keywords: Dinarides, crustal structure, receiver function modelling.

Passive seismic experiment was carried out at the SW contact of the Dinarides and Pannonian basin to determine the crustal structure and velocity discontinuities. The aim of the experiment was to define the relationship between the Adriatic microplate, which is a part of the African plate, and the Pannonian segment which is a part of the Eurasian plate. Most of the temporary seismic stations were deployed in Croatia along the Alp07 profile – a part of the active-source ALP2002 project (Šumanovac et al., 2009). About 300 km long profile stretches from Istra peninsula, crosses the Dinarides and ophiolite zones and ends at the Drava river, in a WSW-ESE direction. Teleseismic events recorded on 12 short-period and 1 broad-band station along the profile were analysed by P-receiver function method. Three types of characteristic receiver functions have been identified, belonging to Dinaridic, Transitional and Pannonian crusts as defined on the Alp07 profile from the wide-angle refraction and reflection experiment. Three major crustal discontinuities can be identified for the Dinaridic and Transitional types: sedimentary basement, intracrustal discontinuity and Mohorovičić discontinuity; whereas the Pannonian type revealed only two discontinuities. The intracrustal discontinuity was not observed in the Pannonian type, thus pointing to a single-layered crust in the Pannonian basin.

The forward modelling of receiver functions has been performed with initial models based on the refraction velocity model along Alp07 profile. The RF modelling has given S wave velocity models of the crust and upper mantle with Moho depths that agree with the seismic refraction results at the SW end of the profile, i.e. in the area of Pannonian crust. The Pannonian crust is characterised by simple crustal structure and low seismic velocities, with Moho depths between 22 and 26 km. In the Dinarides and its peripheral parts, RF modelling regularly gives greater Moho depths comparing to the Alp07 profile, due to more complex crustal structure. The differences are up to +15 %. The main intracrustal discontinuity can be also followed by the RF modelling and coincide very well with discontinuity on the Alp07 profile (the differences are around 1 km at the majority of stations). The depths of the Moho calculated by the Zhu and Kanamori (2000) method vary within wide limits. The results at the five stations deviate anomalously and have to be rejected, while at the seven stations the Moho depths vary within $\pm 15\%$ around the Moho of the Alp07 profile.

Šumanovac F., Orešković J., Grad M. & ALP 2002 Working Group. 2009. Crustal structure at the contact of the Dinarides and Pannonian basin based on 2-D seismic and gravity interpretation of the Alp07 profile in the ALP 2002 experiment. *Geophys. J. Int.*, 179, 615-633.

Zhu L. & Kanamori H. 2000. Moho depth variation in southern California from teleseismic receiver functions. *J. Geophys. Res.*, 105, 2969-2980.

An incipient lithospheric tear fault beneath Northern Apennines? Insights from geophysical and geological data

Piana Agostinetti N.*¹ & Rosenbaum G.²

1. Geophysics Section, School of Cosmic Physics, Dublin Institute for Advanced Studies, Dublin, Ireland. 2. School of Earth Sciences, The University of Queensland, Brisbane, QLD, Australia.

Corresponding email: piana@cp.dias.ie

Keywords: Tear faults, subduction, Apennines.

Along-strike variations in trench retreat is likely to induce deformations in the subducting lithospheric which can develop in complete lithospheric faulting. Such structures are observed in the central Mediterranean region, where vertical slab tearing has progressively led to the segmentation of the subduction zone and allowed the development of orogenic curvatures (e.g., the Calabrian Orocline). However, the response of the crust and upper mantle to the development of such faults is still debated. Here we present an analysis of the seismic, structural and morphological features associated with a incipient tear fault in the Adria microplate, beneath the northern Apennines. The area investigated correspond to the region where a lineament, the Livorno-Sillaro line, has previously been described as a traverse fault based on the surface geology. We investigated the lithospheric structure using a range of independent high-resolution data. Our results show that the area of the Livorno-Sillaro lineament is defined by a major crustal and upper mantle discontinuity, which can be recognised along a section parallel to the Apennine belt. The width of the discontinuity is typically 10-20 km. We find that this zone is characterised by an anomalously low density of crustal and intermediate earthquakes, and by an abrupt along-strike variations in the spatial distribution of deep crustal earthquakes. The discontinuity is also reflected by a pronounced (~20 km) step in the Moho depth, and in a complex and incoherent pattern of SKS wave splitting. The upper crustal expressions of the Livorno-Sillaro lineament involve a sharp bend in the orientation of the watershed and an abrupt along-strike change in the denudation rates (as reflected in low-temperature cooling ages). Our results confirm the suggestion that the Livorno-Sillaro lineament is a major lithospheric-scale discontinuity that marks the boundary between domains of contrasting rates of trench retreat (with faster rates southwest of the discontinuity). The discontinuity, rather than acting as a seismic fault, is characterised by a weaker, possibly hotter, aseismic zone. We suggest that similar types of structures may play a crucial role in the development of along-strike segmentation of orogenic belts. Ultimately, further tearing along these types of structures could potentially lead to the development of tear-related magmatism and the formation of slab windows.

Post collisional evolution in hot orogens and influence of surface processes

Piccolo A.¹, Faccenda M.*¹, Carosi R.², Visonà D.¹ & Montomoli C.³

1. Dipartimento di Geoscienze, Università di Padova. 2. Dipartimento di Scienze della Terra, Università di Torino.
3. Dipartimento di Scienze della Terra, Università di Pisa

Corresponding email: manuele.faccenda@gmail.com

Keywords: Numerical modelling, continental collision, lithosphere exhumation.

This work investigates the relationship between tectonics and climate, with particular regards to the burial and exhumation processes in orogenic systems. Tectonics, causing high topographic elevations, may interact with the atmospheric circulation and induce local or regional climate changes. Surface processes may be focused in particular areas, redistributing the loading acting on geological units, thus, promoting or muffling several geological processes (Burov & Toussaint, 2007). These relationships can be witnessed in hot orogens, i.e. orogens characterised by large dimensions and high temperatures inducing pervasive partial melting. The partially molten rocks have low density and low viscosity, therefore they readily react to the change in loading induced by surface processes. One of the best examples of hot orogens is the Himalayan range, characterized by the occurrence of pervasive partial melting. The geological evidence is associated with the occurrence of migmatites in the Greater Himalayan Sequence (GHS). The channel flow model proposed by Beaumont et al. (2001) implies a coherent exhumation of the GHS due to the focused monsoonal erosion acting on the southern flank of the Himalayas. However, channel flow model is not consistent with the recent data that demonstrate the presence of several tectono-metamorphic discontinuities within the GHS, indicating a sequential exhumation of different GHS sub-units (Montomoli et al., 2014).

We have numerically simulated the interaction between surface and exhumation processes in post-subduction collisional orogens. Two kinds of collisional orogens are obtained: asymmetric and symmetric. Asymmetric collisional orogens feature the occurrence of a channel flow-like behaviour, high crustal temperatures and exhumation of partially molten rocks, while symmetric orogens features lower crustal temperatures and different patterns of exhumation. The asymmetric models have been chosen to test the influence of surface processes. By taking a fixed value of focused erosion rate, the timing of the focused erosion and sedimentation rate are independently varied. The results give several insights: 1) focused erosion is not a necessary condition for the exhumation of the partially molten rocks; 2) timing of the focused erosion controls the dynamics of the channel flow and, consequently, the exhumation processes; 3) the sedimentation rate may induce first order modifications on the evolution of the orogeny; 4) sequential exhumation of high grade metamorphic sub-units is achieved when the focused erosion is activated at the final stage of the collision.

- Beaumont C., Jamieson R.A., Nguyen M. & Lee B. 2001. Himalayan tectonics explained by extrusion of a low-viscosity crustal channel coupled to focused surface denudation. *Nature*, 414, 738-742.
- Burov E. & Toussaint G. 2007. Surface processes and tectonics: forcing of continental subduction and deep processes. *Global Planetary Change*, 58, 141-164.
- Montomoli C., Carosi R. & Iaccarino S. 2014. Tectonometamorphic discontinuities in the Greater Himalayan Sequence: a local or a regional feature? *Geol. Soc., Sp. Publ.*, 412.

Metamorphic CO₂-source rocks in collisional orogens: a petrographic journey through not-(always) obvious CO₂-producing lithologies in central Himalaya

Rapa G.*¹, Groppo C.¹⁻², Rolfo F.¹⁻², Mosca P.² & Neupane P.K.³

1. Dipartimento di Scienze della Terra, Università di Torino. 2. Istituto di Geoscienze e Georisorse, CNR, Torino
3. Nepal Academy of Science and Technology, Khumaltar, Lalitpur, Nepal.

Corresponding email: giulia.rapa@unito.it

Keywords: metamorphic CO₂-source rocks, collisional orogens, Himalaya.

Decarbonation reactions during regional metamorphism in “large-hot” collisional orogens are an important source of atmospheric CO₂, able to influence global climate through geologic time (Gaillardet & Galy, 2008). The petrologic study of the CO₂-source rocks is consequently the key to successfully investigate the metamorphic CO₂ flux in the past.

This contribution focuses on the distribution and petrographic description of different types of CO₂-source rocks (i.e. calc-silicate rocks) in the archetype of “large-hot” collisional orogens, the Himalaya. Fieldwork performed in central and eastern Nepal highlighted that calc-silicate rocks are widespread in the Greater Himalayan Sequence (GHS) and occur as: dm- to m- thick layers or boudins within medium- to high-grade metapelites in the lower portion of the GHS, vs. tens to hundreds of meter thick layers within anatectic gneisses in the structurally upper GHS.

Three different groups of calc-silicate rocks have been recognized, corresponding to different protolith compositions, and they can be described in terms of relatively complex chemical systems: (i) CFMAS-HC (CaO-FeO-MgO-Al₂O₃-SiO₂-H₂O-CO₂) system, significantly more abundant in the lower GHS; (ii) NCFMAS-HC (Na₂O-CaO-FeO-MgO-Al₂O₃-SiO₂-H₂O-CO₂) and (iii) NKCFMAS-HC (Na₂O-CaO-FeO-MgO-Al₂O₃-SiO₂-H₂O-CO₂) systems, widespread in both the lower and the upper GHS.

In all groups, mineral assemblages vary with increasing metamorphic grade from lower to upper structural levels. The CFMAS-HC assemblages are represented by: (a) Cc+Tr±Qtz±Pl in impure marbles and by (b) Grt+Amp+Qtz+Pl±Zo±Cc (Cpx-absent), (c) Grt+Cpx+Qtz+Pl±Zo±Cc and (d) Cpx+Qtz+Pl±Zo±Cc (Grt-absent) in calc-silicate rocks. The NCFMAS-HC assemblages consist of: (a) Grt+Cpx+Qtz+Scp+Zo±Pl and (b) Cpx+Scp+Zo+Qtz+Pl+Cc (Grt-absent). In the NKCFMAS-HC group the following mineral assemblages can be observed: (a) Cc+Mu+Phl+Qtz±Pl±Tr impure marbles; (b) Mu±Bt+Cc+Qtz+Pl (Kfs, Cpx and Grt-absent) phylladic micashists; (c) Mu+Bt+Zo+Scp+Grt+Qtz+Pl (Kfs and Cpx-absent) micashist; (d) Bt±Mu+Kfs+Scp+Qtz+Pl±Zo (Cpx and Grt-absent), (e) Bt±Kfs±Scp+Qtz+Pl+Czo±Amp±Cpx±Cc (Grt-absent) and (f) Kfs±Bt±Scp+Qtz+Cpx±Zo±Cc (Grt-absent) calc-silicate gneisses and granofelses.

Many of these assemblages, especially those equilibrated at lower temperatures and still containing abundant phyllosilicates, are not easy to be recognized in the field and have been probably considerably overlooked in the past. Most of them do not contain calcite anymore, because it was completely consumed during prograde metamorphism; nevertheless, their role in the orogenic-CO₂ cycle should be considered. Detailed fieldwork and petrographic analysis are therefore indispensable tools to estimate the volumes of potential CO₂-source rocks in collisional orogens.

Gaillardet J. & Galy A. 2008. Himalaya-carbon sink or source? *Science*, 320, 1727-1728.

The subduction of continental lithosphere: insights from multiscale geophysical modelling

Romanelli F.

Dipartimento di Scienze della Terra, Università di Trieste.

Corresponding email: romanel@units.it

Keywords: Surface waves, tomography, lithosphere.

The subduction of continental lithosphere has been demonstrated in the Alps (Panza & Müller, 1979) and it has been recognized in several other collisional belts such as in the Himalaya (e.g. Zhang et al., 2014) and Zagros chain (e.g. Motaghi et al., 2014). Selected 3D models of the crust and upper mantle of these regions, have been obtained assembling cellular models expressed in terms of shear waves velocity (V_S), thickness and density of the layers, to a depth of 350 km. The main features of the structure of the crust and upper mantle in Tibet and its neighboring regions represent a clue to understand the modality of the convergence and collision process between the Indian and Eurasian plates, and the influence of this process on the uplift of the plateau. The high-resolution structures of the lithosphere-asthenosphere system beneath a seismic profile in Iran confirm the presence of crustal roots at the north and south of the Iranian Plateau where it meets the Arabian Plate and Eurasia.

The mechanical properties models are obtained by means of advanced non-linear inversion techniques, such as the "hedgehog" non-linear inversion method of group and phase velocity dispersion curves for the determination of V_S (see Brandmayr et al., 2010 and references therein) and the inversion of gravity data. The "hedgehog" method allows for the definition of a set of structural models without resorting to any a priori model, considering the V_S and the thickness of the layers as independent variables. Given the well-known non-uniqueness of the inverse problem, the representative solution of each cell is determined through the application of optimization algorithms and is also validated with the use of independent geological, geophysical and petrological data, e.g. the distribution of seismicity with depth. The gravimetric inversion has been constrained to the geometry of the layers defined by the V_S model obtained from the inversion of surface wave dispersion data.

Brandmayr E., Raykova R., Zuri M., Romanelli F., Doglioni C. & Panza G.F. 2010. The lithosphere in Italy: structure and seismicity. *J. Virtual Expl.*, 36, paper 1.

Motaghi K., Tatar M., Priestley K., Romanelli F., Doglioni C. & Panza G.F. 2014. The deep structure of the Iranian Plateau, *Gondwana Res.*, in press. doi:10.1016/j.gr.2014.04.009.

Panza G.F. & Mueller S. 1979. The plate boundary between Eurasia and Africa in the Alpine area. *Mem. Soc. Geol. It.*, 33, 43-50.

Zhang X., Teng J., Sun R., Romanelli F., Zhang Z. & Panza G.F. 2014. Structural model of the lithosphere-asthenosphere system beneath the Qinghai-Tibet Plateau and its adjacent areas. *Tectonophysics*, 634, 208-226. doi:10.1016/j.tecto.2014.08.017.

Metamorphic recrystallization related to the circulation of CO₂-rich hydrothermal fluids: the case of the Valdieri marbles (Maritime Alps)

Rossetti P.¹, Barale L.¹, Bertok C.*¹, d'Atri A.¹, Gerdes A.³, Martire L.¹, Piana F.² & Scarrone F.¹

1. Dipartimento di Scienze della Terra, Università di Torino. 2. Istituto Geoscienze e Georisorse, CNR, Torino. 3. Institut für Geowissenschaften, Goethe Universität, Frankfurt am Main, Germany.

Corresponding email: carlo.bertok@unito.it

Keywords: Valdieri Marbles, CO₂-rich hydrothermal fluids, Maritime Alps.

In the Maritime Alps, at the NE border of the Argentera crystalline massif, a kilometre-scale rock body of marbles, quarried in the past as ornamental stones ("Marmi di Valdieri"), occurs within a carbonate succession referable to the Dauphinois domain and consisting of dark marls (Entracque Marl, Middle Jurassic-Berriasian), micritic limestones with breccia beds (Lausa Limestone, Valanginian-early Aptian), dark shales and marls (Marne Nere, Aptian-Cenomanian) and marly limestones (Puriac Limestone, Turonian-Campanian). The Puriac Limestone is unconformably overlain by middle Eocene-lower Oligocene sediments of the Alpine foreland basin.

Recrystallization affects the Lausa Limestone, the Marne Nere, and the lower and middle portions of the Puriac Limestone. The marbles pass gradually to poorly recrystallized rocks in a range of few tens of meters. The Valdieri marbles lower part (corresponding to Lausa Limestone) consists of pure white and grey marbles with rare mm-thick elongated and folded domains strongly enriched in muscovite, K-feldspar, albite and quartz. The upper part (corresponding to Puriac Limestone) is composed of lens-shaped, cm- to dm-thick granoblastic marbles, interlayered with mm-thick anastomosed greenish-purple levels made up of white mica (muscovite-paragonite s.s.), chlorite and epidote.

The Valdieri Marbles are cut by at least two orders of tectonic foliations and deformed by folds, faults and fractures belonging to regional systems well known in the surrounding region. Although most of these meso-structural associations clearly postdate the marbles recrystallization, there are evidences of a syn-genetic shearing during the blastic event, leading to elongation of primary clasts and localized development of metamorphic foliations. The marbles are crossed by mm- to dm-thick veins filled with calcite, quartz and Fe-rich dolomite.

Different types of fluid inclusions occur in the vein minerals:

- early H₂O-CO₂ inclusions showing (at room T) L_{H₂O} ± L_{CO₂} + V_{CO₂} assemblage, often coexisting with CO₂ vapour-rich inclusions, possibly as a result of heterogeneous entrapment;
- late aqueous inclusions, generally showing L_{H₂O} + V_{H₂O} assemblage.

The reported data document that the recrystallization of the Valdieri Marbles was not related to regional metamorphism but to a localized flux of CO₂-rich hydrothermal fluids flowing up from the underlying basement rocks.

Exploitation methods of the metamorphic rock memory in the continental crust of orogenic belts to infer subduction history

Spalla M.I.*¹, Delleani F.¹, Gosso G.¹, Marotta A.M.¹, Rebay G.², Regorda A.¹, Roda M.¹, Zanoni D.¹ & Zucali M.¹

1. Dipartimento di Scienze della Terra "A. Desio", Università di Milano.
2. Dipartimento di Scienze della Terra e dell'Ambiente, Università di Pavia.

Corresponding email: iole.spalla@unimi.it

Keywords: Alps, Canadian Cordillera, PTdt paths.

The narrow axial zone of collisional belts, where ocean closure apparently generates the highest tectonic complexity, paradoxically provides in the petro-structural memory of polydeformed tectonites structural and petrological data critical to undertake on a new physical base the reconstruction of nappe trajectories. As a matter of fact, subduction-collision zones are characterized by repeated coupling and decoupling of lithospheric slices, acting in competition during building up of tectonic units of a metamorphic belt. Contours of these mobile units are transient and can be inferred integrating structural and petrologic analysis. Due to its propensity to be exhumed, continental crust in such a scenario represents the repository of rocks characterised by the longest memory preserving, in the same structural domain, tectonic and metamorphic imprints recorded during superposed subduction cycles. This makes continental crust, repeatedly forged along active margins, a key to unravel significant variations in thermal state and mechanical devices along subduction zones through time. Due to competing amalgamation and disaggregation of lithospheric slices in the construction of the tectonic architecture of subduction-collision belts, the reconstruction of the structural and metamorphic history requires an integrated field and laboratory approach implying geometrical and kinematic analysis of tectonic units, together with a joint reconstruction of quantitative P-T-d-t paths. The inferred translational trajectories and shape changes during P-prograde and P-retrograde paths are characterised by a marked thermo-tectonic connotation that, through the comparison with numerical modelling predictions, can shed light on the still largely unknown aspects (e.g. burial and exhumation of continental crust during oceanic subduction) of the deep dynamics of subduction systems.

LAM U-Pb zircon Early Jurassic exhumation age of the Finero Phlogopite Peridotite (Ivrea-Verbano Zone, Western Alps) and its geodynamic consequences

Zanetti A.*¹, Giovanardi T.², Mazzucchelli M.³, Langone A.¹, Tiepolo T.⁴ & Wu F.-Y.⁵

1. Istituto di Geoscienze e Georisorse, C.N.R. Pavia. 2. Instituto de Geociências, Universidade de São Paulo, Brazil. 3. Dipartimento di Scienze Chimiche e Geologiche, Università di Modena e Reggio Emilia. 4. Dipartimento di Scienze della Terra "A. Desio", Università di Milano. 5. Institute of Geology and Geophysics, Chinese Academy of Sciences, Beijing, P.R.C.

Corresponding email: zanetti@crystal.unipv.it

Keywords: Ivrea-Verbano Zone, lithospheric mantle exhumation, U-Pb zircon ages.

A new LA-ICP-HRMS investigation of transparent zircons, unzoned and smoky at cathodoluminescence (CL), separated from three chromitite layers segregated in mantle dunite bodies belonging to the Phlogopite Peridotite unit (hereafter PP) of the Finero Complex (Ivrea-Verbano Zone, Southern Alps) provides single-spot $^{206}\text{Pb}/^{238}\text{U}$ Lower Jurassic ages between 200 to 180 Ma, with a pronounced peak at ~190 Ma. Relevant exception is represented by two pinky zircons showing relics of zoning at CL, with darker cores that give Triassic ages from 240 to 230 Ma. The presence of continental crust component(s) evidenced by the negative eHf of the zircons, the strict similarity of the trace element contents shown by clinopyroxenes and amphiboles from chromitites and the phlogopite harzburgites and pyroxenites hosting the dunite bodies, as well as the complete to partial disappearance of olivine replaced by orthopyroxene, indicate that the parent melts of the chromitites had a cognate origin with the hydrous LILE-enriched silica-saturated melts responsible of the pervasive metasomatism recorded by the Finero mantle sequence. The combination of our data with those reported in literature for the PP chromitite zircons determines a large age interval ranging from 290 to 180 Ma. However, zircon populations with different U-Pb ages show eHf very similar to that found in this study.

The latter evidence, together with the rejuvenation of the ages with the disappearing of the internal structures suggest that the large age variability is the result of a prolonged residence at mantle/lower crustal depths of the PP, characterised by progressive re-equilibration stages of the U-Pb zircon system.

Thus, it is here proposed that the segregation of the zircon-bearing chromitite layers was related to the pervasive metasomatic event, which occurred at ~290 Ma or before. Successively, the U-Pb zircon system remained virtually unperturbed until Middle Triassic, when the area was affected by at least two main magmatic cycles with tholeiitic to Na-alkaline geochemical affinity associated to tectonic instability. The consequent thermal perturbations induced re-equilibration stages of the chromitite zircons, which ended with the Early Jurassic exhumation documented by the U-Pb ages of chromitite zircons of this study. Our data suggest that the Early Jurassic extensional tectonics was characterised by an important reheating event at 190 Ma, possibly due to lithospheric hyperextension.

Such a scenario considers that the PP unit resided at mantle depths during Early Permian, being possibly emplaced at crustal levels only thanks to trans-lithospheric faults during the Early Jurassic. This evolution is completely different with respect to the present day interpretation of the geodynamic history of the mantle bodies in the Val Sesia area, which are believed to have been emplaced within the continental crust, as part of accretionary prisms, since the end of the Variscan orogeny or before. This evidence confirms that the northernmost part of the Ivrea-Verbano Zone underwent peculiar Paleozoic to Mesozoic geodynamic processes, thus unravelling important additional complexities to the interpretation of the geodynamic evolution of the area now related to the Southern Alps.

SESSION S6

Experimental and Computational Methods in Mineralogy and Geochemistry

CONVENORS

Donato Belmonte (Univ. Genova)

Marco Bruno (Univ. Torino)

Simone Tumiati (Univ. Milano)

A comparison of ternary feldspar-mixing models

Benisek A.*¹, Dachs E.¹ & Kroll H.²

1. Fachbereich Materialforschung und Physik, Universität Salzburg, Austria.
2. Institut für Mineralogie, Westfälische Wilhelms-Universität Münster, Germany.

Corresponding email: artur.benisek@sbg.ac.at

Keywords: Feldspar, activity, thermometry.

Thermodynamic feldspar-mixing models for the $\text{NaAlSi}_3\text{O}_8$ - KAlSi_3O_8 - $\text{CaAl}_2\text{Si}_2\text{O}_8$ system are used in petrological calculations such as, e.g., two-feldspar thermometry and pseudosection calculations. Recently, a mixing model describing ternary high-structural state feldspars was formulated (Benisek et al., 2010), which is based exclusively on calorimetric and volumetric data. When it is compared to mixing models, which are based on phase-equilibrium experiments (e.g., Fuhrman & Lindsley, 1988; Elkins and Grove, 1990), distinct differences are revealed. The calorimetry-based model shows less solubility for both K in Ca-rich plagioclase and Ca in K-rich alkali feldspar. On the other hand, the stability field of Na-rich feldspars is broadened.

The two approaches can best be tested on natural feldspar assemblages, in which both feldspars, plagioclase and alkali feldspar, show exsolution textures (two-perthite rocks). It is to be expected that exsolution preserves the bulk composition of the feldspar grains, because compositional adjustments to cooling occur between exsolved lamellae and host, and not between different grains. The compositional reintegration of lamellae and host thus delivers the original feldspar composition. One of such two-perthite rocks is the Klokken syenogabbro, South Greenland, which was thoroughly investigated by Parsons & Brown (1983). It contains a perthite and a mesoperthite whose bulk compositions should plot on the 970 °C/1kbar isotherm according to melting experiments and petrologic reasoning. Although the 970 °C/1kbar isotherms of the phase-equilibrium-based mixing models plot near the composition of the perthite, they are obviously not consistent with the composition of the mesoperthite. The 970 °C/1kbar isotherm of the calorimetry-based mixing model plots on the compositions of both perthites. Therefore, the calorimetry-based model agrees with the petrologic expectation far better than the phase-equilibrium-based models. Similar analyses were applied to other natural feldspar assemblages delivering the same pattern. The reason for the discrepancies between observed and predicted feldspar compositions when using mixing models based on phase-equilibrium experiments is thought to be connected with disequilibrium states present in these experiments.

Benisek A., Dachs E. & Kroll H. 2010. A ternary feldspar-mixing model based on calorimetric data: development and application. *Contrib. Min. Petrol.*, 160, 327-337.
Elkins L.T. & Grove T.L. 1990. Ternary feldspar experiments and thermodynamic models. *Am. Mineral.*, 75, 544-559.
Fuhrman M.L. & Lindsley D.H. 1988. Ternary feldspar modeling and thermometry. *Am. Mineral.*, 73, 201-215.
Parsons I. & Brown W.L. 1983. A TEM and microprobe study of a two-perthite alkali gabbro: implications for the ternary feldspar system. *Contrib. Mineral. Petrol.*, 82, 1-12.

Nanotribological analysis of frictional anisotropy of crystalline surfaces and its relationship with surface structure studied through atomic force microscopy

Campione M.

Dipartimento di Scienze dell'Ambiente e del Territorio e di Scienze della Terra, Università di Milano Bicocca.

Corresponding email: marcello.campione@unimib.it

Keywords: Atomic force microscopy, nanotribology, surface chemical structure.

Friction forces play a key role in mechanical phenomena occurring on all scales, from the operation of microelectromechanical systems to interplate earthquakes. The study of friction forces is also useful for understanding a large spectrum of physical properties of surfaces. Thanks to the development of nanoscale investigation tools such as scanning probe microscopy, the study of friction and wear phenomena down to the atomic scale is becoming a leading topic within the field of surface physics, and has given rise to the science called nanotribology (Urbakh & Meyer, 2010). We focus here on the anisotropic aspects of nanotribology, related in particular to the surface of crystalline materials such as minerals. Frictional anisotropy is characterized by a dependence of the friction force intensity on the sliding direction and friction force components orthogonal to the sliding direction (Zmitrowicz, 1989). We show how an atomic force microscope can be used to map in two dimensions the frictional anisotropy at the nanoscale and how to carry out data interpretation to unravel the friction- surface structure relationship. As a model system, we analyzed the basal plane of antigorite, which is inherently characterized by marked corrugations, and interpreted the data in terms of constitutive models of anisotropic friction (Campione & Capitani, 2013). The proposed approach unravels unexpected mechanical behaviors which, while consolidating a deeper knowledge of atomic-scale mineral physics, can be now considered the cause of macro-scale phenomena related to seismic anisotropy, slip partitioning, glacial surge, etc.

Campione M. & Capitani G.C. 2013. Subduction-zone earthquake complexity related to frictional anisotropy in antigorite. *Nat. Geosci.*, 6, 847-851.

Urbakh M. & Meyer E. 2010. Nanotribology: the renaissance of friction. *Nat. Mater.*, 9, 8-10.

Zmitrowicz A. 1989. Mathematical descriptions of anisotropic friction. *Int. J. Solids Structures*, 25, 837-862.

The mobility of hydrous carbonate liquids in the mantle: an experimental model

Capizzi L.S.*, Fumagalli P., Poli S. & Tumiati S.

Dipartimento di Scienze della Terra "A. Desio", Università di Milano.

Corresponding email: luca.capizzi@unimi.it

Keywords: CO₂, hydrated fluids, infiltration experiments.

There is much direct and indirect evidence that carbonatitic melts exist in the mantle. Their physical and chemical properties largely differ from the majority of silicate melts. The processes accounting for the mobility of carbonate liquids, their infiltration rates, and their influence on the annealing of mantle peridotites are largely unknown. Although natural carbonate magmas are complex chemical systems, bearing some silica, iron and water, previous work has been performed in simple model systems, which neglect the role of these relevant components. Most volatiles should fractionate in these liquids when moving to shallower levels, contributing to volcanic activity. In this project we will focus on the experimental reproduction of rock textures resulting from the percolation of hydrous carbonate liquids in an olivine-rich lithology at high pressure. The goal of this work is a quantitative assessment of variables controlling the ascent of such liquids in the mantle. For the first time we will study an iron-bearing hydrous system in chemical equilibrium with a model mantle composition. Natural carbonatitic magmas in equilibrium with a peridotitic mantle assemblage are dolomitic in composition. For this reason we use an experimental liquid produced by melting of a mixture of calcite, dolomite, siderite and brucite. Furthermore, the mantle is known to be graphite and/or diamond saturated, so the reactive assembly has a graphite lining to obtain reasonable redox conditions and to prevent iron loss to the Pt capsule. According to phase diagram constraints of Tumiati et al. (2013) a pressure temperature condition of 2.5 GPa and 1100 °C is expected to stabilize a dolomitic hydrous liquid in equilibrium with a peridotitic mantle source. Because this project is intended to shed light on variables controlling transport properties, we perform experiments in time-resolved series at fixed P-T conditions.

Here we report infiltration experiments in a synthetic dunite placed against the hydrous carbonatite reservoir. The dunite was prepared by sintering natural San Carlos olivine crystals sieved to 38 µm in single stage piston cylinder apparatus at 0.8 GPa and 1200 °C for 5 days. The infiltration experiments are realized in an end-loaded piston cylinder apparatus.

BSE images and X-ray mapping at EMP allow a quantification of the dihedral angle between the carbonate liquid and the olivine grains; results are compared to data available for anhydrous systems, in a setup where sodium carbonate was infiltrated in a Fe-free dunite (Hammouda & Laporte, 2000). A measure of the infiltration distance is obtained in experiments where the cylindrical geometry of the assembly is ensured by the usage of stiff and thick Mo capsules. By means of etching techniques we plan to highlight grain boundaries and to perform quantitative image analysis of synthetic infiltrated textures in order to estimate the role of carbonatitic liquids on grain growth and annealing processes.

Hammouda T. & Laporte D. 2000. Ultrafast mantle impregnation by carbonatite melts. *Geology*, 28, 283-285.

Tumiati S., Fumagalli P., Tiraboschi C. & Poli S. 2013. An Experimental Study on COH-bearing Peridotite up to 3.2 GPa and Implications for Crust-Mantle Recycling. *J. Petrol.*, 54, 453-479.

Crystallization kinetics and time-scales of magmatic processes

Carroll M.R.

Scuola di Scienze e Tecnologie - Sezione di Geologia, Università di Camerino.

Corresponding email: michael.carroll@unicam.it

Keywords: Experimental petrology, crystallization kinetics, magma dynamics.

The crystals present in an igneous rock and the observed variations in their dimensions and compositions reflect the integrated pressure (P) -temperature (T) -composition (X) - time (t) history of the sample. Because crystals take a finite time to nucleate and grow (rates depending on undercooling - ΔT , composition, etc), variations in their sizes, size distributions, and compositions can provide insights into magmatic processes and their time-scales. In order to use observed variations in the textures of igneous rocks to gain quantitative insights into the timescales of magmatic processes we require quantitative information on the rates of nucleation (J) and growth (G) as a function of undercooling (ΔT) for the crystals and melts of interest. A number of recent experimental studies involving undercooling induced by changes in Temperature and Pressure (for hydrous magmas) provide the necessary data concerning variation in J and G and aid in interpretation of observed textural variations in natural volcanic samples. In the case of Stromboli, decompression experiments show that microlites and low-An overgrowth rims may form on timescales of hrs to days. Complex textures showing multiple resorption and growth zones indicate that some crystals must be much older. For andesitic magma from Montserrat, studies of Plag growth rates during decompression aid the interpretation of textural variability in samples from this dome-forming eruption, and textural variations can be correlated with differences in dome growth rate (assumed to be related to magma ascent rate). In the case of Campi Flegrei trachytic -phonolitic magmas, studies of alkali feldspar growth rates indicate the possibility of very fast feldspar growth on timescales of hrs, allowing a melt to become more than 50% crystalline in a very short time period, with consequent significant changes in magma physical properties and possibly leading to explosive eruption due to crystallization induced vapor exsolution ("second boiling").

Determining isotopic composition of elements by linearization of exponential instrumental isotope fractionation

Cavazzini G.

Istituto di Geoscienze e Georisorse, C.N.R. Padova

Corresponding email: giancarlo.cavazzini@igg.cnr.it

Keywords: Thermal-ionization mass spectrometry, exponential isotope fractionation, isotope dilution technique.

Exponential isotope fractionation in TIMS can be linearized by binomial expansion. The linearization can be used to model a particular calculation of the isotopic composition of an element with at least three isotopes by ID-MS technique (here applied to strontium single-spike ID).

In the equivalence of the spiking ratio for all the isotopic ratios in a sample-spike mixture, the true values of the mixture can be expressed in terms of the measured values and of the instantaneous relative deviations ξ_1 , ξ_2 , ξ_3 of the measured values of $^{87}\text{Sr}/^{86}\text{Sr}$, $^{84}\text{Sr}/^{86}\text{Sr}$ and $^{88}\text{Sr}/^{86}\text{Sr}$ ratios from the respective true values. The instantaneous relative deviations of the $^{84}\text{Sr}/^{86}\text{Sr}$ and $^{88}\text{Sr}/^{86}\text{Sr}$ ratios can be expressed in terms of the relative deviation of the $^{87}\text{Sr}/^{86}\text{Sr}$ ratio at the same instant, and of increments which are functions of the instantaneous fractionation factor f and of the natural logarithm of the mass ratio $^{84}\text{Sr}/^{87}\text{Sr}$ and $^{88}\text{Sr}/^{87}\text{Sr}$, respectively. A system of two linear equations can therefore be written in the two unknowns ξ_1 and f , which can be solved to calculate the other two relative deviations ξ_2 , ξ_3 .

Since the instantaneous relative deviations can also be expressed as the products between the instantaneous fractionation factor and the natural logarithm of the mass ratio between the isotope at the numerator and the isotope at the denominator, respectively, the pairs ξ_i , $\ln(m_i/m_{86})$ for the three ratios fall on a straight line which passes through the origin, the angular coefficient giving the instantaneous fractionation factor f .

In this calculation, we have used the true values of the isotopic ratios in the sample. Actually, these values are unknowns. Nevertheless, we can scan values for these ratios, generate systems of equations, calculate the relative deviations ξ_1 , ξ_2 , ξ_3 , plot the pairs ξ_i , $\ln(m_i/m_{86})$ to define straight lines, and calculate how far each straight line passes from the origin. We can therefore identify the straight line which passes closest to the origin, and the values of $^{84}\text{Sr}/^{86}\text{Sr}$, $^{87}\text{Sr}/^{86}\text{Sr}$ and $^{88}\text{Sr}/^{86}\text{Sr}$ we have used in that calculation should be the values closest to the respective values in the natural sample.

The isotopic composition of a spike enriched in ^{84}Sr has been determined using the method proposed by Cavazzini (2005). An algorithm has been designed and simulated calculations have been performed, which have shown that the $^{87}\text{Sr}/^{86}\text{Sr}$ of the sample is determined within 0.004 – 0.006% from the true value. The algorithm has been used to determine the isotopic composition of a modern coral (*Cladocora Cespitosa*) and of the NIST standard reference material 611.

Cavazzini G. 2005. A method for determining isotopic composition of elements by thermal ionization-source mass spectrometry: application to Strontium. Int. J. Mass Spectrom., 240, 17-26.

The way from estimated to measured thermodynamic properties: The impact of relaxation calorimetry on petrological calculations

Dachs E.*, Benisek A. & Geiger C.A.

Department of Materials Science and Physics, University of Salzburg, Austria.

Corresponding email: edgar.dachs@sbg.ac.at

Keywords: Relaxation calorimetry, thermodynamics, petrological calculations.

Relaxation calorimetry (RC) is a relatively new experimental method that enables the measurement of low-temperature heat capacities (C_p). Its commercial implementation is the physical properties measuring system (PPMS) from Quantum Design® (Dachs & Bertoldi, 2005). A major advantage of RC is that *small sample amounts in the mg range* can be studied as compared to other calorimetric techniques that require at least several grams of material (e.g. adiabatic calorimetry). RC thus opens up a new field for measuring low-T C_p for the first time on many phases that can only be synthesized in small amounts in high-pressure devices or occurring in nature as small or fine-grained crystals. For handling powdered samples, specific techniques have been developed (Dachs & Benisek, 2011).

The impact of RC on petrologic thermodynamic calculations is twofold:

- **Mineral end-members:** *The standard entropy S° can now be determined* with an accuracy of 0.7-1.0%. Examples that will be discussed include the ultra-high pressure phase TiO₂II (Yong et al., 2013), spessartine (Dachs et al., 2009), and annite (Dachs & Benisek, Eur. J. Mineral., in press).
- **Solid solutions:** PPMS measurements made on solid solutions allow the *calorimetric excess entropy* to be determined. Examples that will be discussed are almandine-spessartine garnets (Dachs et al., 2014) and feldspars (Benisek et al., 2009, 2010a). The thermodynamic data on feldspar enabled the formulation of a new mixing model that is based exclusively on calorimetric and volumetric data (Benisek et al., 2010b).

- Benisek A., Dachs E. & Kroll H. 2009. Excess heat capacity and entropy of mixing in high structural state plagioclase. *Am. Mineral.*, 94, 1153-1161.
- Benisek A., Dachs E. & Kroll H. 2010a. Excess heat capacity and entropy of mixing in the high-structural state (K,Ca)-feldspar binary. *Phys. Chem. Minerals*, 37, 209-218.
- Benisek A., Dachs E. & Kroll H. 2010b. A ternary feldspar-mixing model based on calorimetric data: development and application. *Contrib. Mineral. Petrol.*, 160, 327-337.
- Dachs E. & Benisek A. 2011. A sample-saving method for heat capacity measurements on powders using relaxation calorimetry. *Cryogenics*, 51, 460-464.
- Dachs E. & Bertoldi C. 2005. Precision and accuracy of the heat-pulse calorimetric technique: low-temperature heat capacities of milligram-sized synthetic mineral samples. *Eur. J. Mineral.*, 17, 251-261.
- Dachs E., Geiger C.A., Withers A.C. & Essene E.J. 2009. A calorimetric investigation of spessartine: Vibrational and magnetic heat capacity. *Geochim. Cosmochim. Acta*, 73, 3393-3409.
- Dachs E., Geiger C.A., Benisek A. & Grodzicki M. 2014. Thermodynamic mixing properties and behavior of almandine-spessartine solid solutions. *Geochim. Cosmochim. Acta*, 125, 210-224.
- Yong W., Dachs E., Benisek A. & Secco R. 2013. Heat capacity and entropy of rutile and TiO₂II: thermodynamic calculation of rutile-TiO₂II transition boundary. *Phys. Earth Planet. In.*, 226, 39-47.

Quantifying groundwater changes in evaporitic basins using stable isotopes experimental approaches on hydrated minerals

Gatti E.*¹, Coleman M.¹ & Bustos D.²

1. NASA Jet Propulsion Laboratory, California Institute of Technology, Pasadena, CA, USA.

2. White Sands National Monument, New Mexico, USA.

Corresponding email: emma.gatti@jpl.nasa.gov

Keywords: Stable isotopes, gypsum, water of crystallization.

While the dynamics of groundwater evaporation are well known, it is still challenging to reconstruct the water patterns in areas where water is not available anymore. We selected a specific location in White Sands National Monument (WSNM), New Mexico, to validate a method to extract information from hydrated minerals regarding past groundwater evaporation patterns in evaporitic basins. WSNM has gypsum ($\text{CaSO}_4 \cdot 2\text{H}_2\text{O}$) dunes and crystals precipitated from the evaporation of an ancient lake. Our approach aims to extract the water of crystallization of gypsum and measure its oxygen and hydrogen isotopic compositions, in order to reconstruct the groundwater history of the area. The idea is that as the mother brine evaporates its isotopic composition changes continuously, recorded as water of crystallization in successive growth zones of gypsum. To check if the isotopic composition of the salt could effectively differentiate between distinctive humidity conditions, the methodology was tested first on synthetic gypsum grown under controlled humidity and temperature conditions. T and RH% were maintained constant in a glove box and precipitated gypsum was harvested every 24 hours. d^2H and d^{18}O of water of crystallization from the synthetic gypsum was extracted using a specially developed technique on a TC/EA. The brine was measured using a Gas Bench II for d^{18}O and an H-Device for d^2H on a Thermo Finnigan MAT 253 mass spectrometer. With the method tested, we measured natural gypsum. In order to identify the growth zones we mapped the surface of the crystals using a cathodoluminescence coupled to a scanning electron microscope (CL-SEM). Crystals were then sampled for isotopic analyses. Preliminary results suggest that site-specific groundwater changes can be described by the isotopic variations. We will show that the methodology is a reliable and fast method to quantify hydrological changes in a targeted environment. The study is currently ongoing but the full dataset will be presented at the conference.

Solubility of F-Cl-apatites in KCl-H₂O brines at 800 °C and 1 GPa: Implications for REE transport during high-grade metamorphism

Mair P.*¹, Tropper P.¹, Manning C.² & Harlov D.³

1. Institute of Mineralogy and Petrography, University of Innsbruck, Austria. 2. Department of Earth and Space Sciences, University of California, USA. 3. GeoForschungsZentrum, Telegrafenberg, Potsdam, Germany

Corresponding email: philipp.mair@uibk.ac.at

Keywords: Apatite solubility, experimental petrology, REE mobility.

Chloride-rich brines are increasingly recognized as playing an important role in high P-T metamorphic and magmatic systems (Newton et al., 2010). The origins of these saline, multicomponent fluids are still debated, but experimental evidence suggests that regardless of their origin they are important agents of rock alteration and mass transfer wherever they occur. Apatite (Ca₅(PO₄)₃(OH, F, Cl)) is a ubiquitous accessory mineral in many crustal rocks that is widely used to evaluate petrogenetic processes (Spear et al., 2002) and is also particularly suitable for assessing the role of fluids at high pressures and temperatures, where metasomatic activity is important but poorly understood. Apatite is an important host for LREE, F, and Cl and thus can be used to monitor elemental mass transfer in high P-T settings. Therefore the determination of its solubility in geologic fluids is of utmost geochemical importance. To this end, we have investigated the influence KCl-H₂O aqueous fluids on the solubility behaviour of synthetic F-apatite, synthetic Cl-apatite, and natural Durango F-apatite at 800 C and 1.0 GPa using 3 mm diameter/1cm long Pt capsules arc welded shut and the piston-cylinder apparatus (NaCl setup, cylindrical graphite oven). The experimental results indicate a strong increase in apatite solubility for aqueous fluids with a moderate KCl mole fraction (X_{KCl}). Synthetic F-apatite and synthetic Cl-apatite dissolve congruently. Their solubility increases from 19 and 37 ppm in pure H₂O to 1917 and 2487 ppm, respectively, at $X_{KCl} = 0.4$. Natural Durango F-apatite dissolves incongruently at $X_{KCl} < 0.2$ to monazite + fluid and congruently at $X_{KCl} > 0.2$. The solubility behaviour of both apatites with increasing X_{KCl} indicates the participation of H₂O in the dissolution reaction. In contrast to the NaCl-H₂O system investigated by (Antignano & Manning, 2008), apatite solubilities in the system KCl-H₂O are considerably lower and at all conditions (700 to 900 °C and 0.7 to 2.0 GPa), apatite dissolves incongruently to monazite + fluid.

Antignano A. & Manning C. 2008. Fluorapatite solubility in H₂O and H₂O–NaCl at 700 to 900 °C and 0.7 to 2.0 GPa. *Chem. Geol.*, 251, 112-119.

Newton R.C. & Manning C. 2010. Role of saline fluids in deep-crustal and upper-mantle metasomatism: insights from experimental studies. *Geofluids*, 10, 58-72.

Spear F.S. & Pyle J.M. 2002. Apatite, monazite, and xenotime in metamorphic rocks. In: Kohn M.J., Rakovan J. & Hughes J.M. Eds., *Phosphates: Geochemical, Geobiological, and Materials Importance*. *Rev. Mineral. Geoch.*, 48, 293-335.

Forward modelling of redox equilibria in the Earth mantle: simple versus complex systems

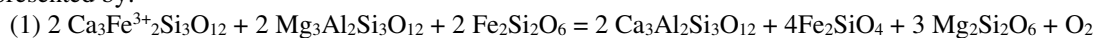
Malaspina N.

Dipartimento di Scienze dell'Ambiente e del Territorio e di Scienze della Terra, Università di Milano Bicocca.

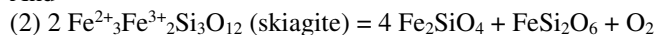
Corresponding email: nadia.malaspina@unimib.it

Keywords: Oxygen fugacity, solid solution model, skiaigite.

Oxygen fugacity (fO_2) is conventionally used in petrology as a variable describing the oxygen chemical potential (μO_2). In multiphase systems fO_2 is classically determined by the distribution of Fe^{3+} in mineral phases. For peridotite mineral assemblages fO_2 can be evaluated from several equilibria involving Fe^{3+} -garnet components, where Fe^{3+} occurs in octahedral coordination. For the olivine + orthopyroxene + Fe^{3+} -garnet assemblage two of these reactions are represented by:



And



Equilibrium (1) by Luth et al. (1990) has been recently experimentally tested by Stagno et al. (2013), while equilibrium (2) was calibrated by Gudmundsson & Wood (1995). Both equilibria have advantages and limits in their applicability. This contribution aims to compare the use of the two oxybarometers in simple and complex natural systems, selecting garnet peridotite samples of well studied suprasubduction mantle from the Sulu belt (China) and Ulten Zone (Italy) as case studies. Solid solution models will be applied to both equilibria in a forward modelling of fO_2 , using the available thermodynamic database of Holland & Powell (2011) for andradite and grossular garnet end-members and that of Malaspina et al. (2009) which combined experimental and thermochemical data for skiaigite. The results suggest that the Sulu and Ulten peridotites apparently record higher fO_2 s (FMQ to FMQ+2) than garnet peridotite xenoliths from the sub-cratonic mantle equilibrated at similar pressure conditions. These results will be also discussed in terms of extensive thermodynamic properties (moles of O_2), demonstrating that fO_2 is not a simple, monotonically increasing function of the quantity of O_2 , and that high μO_2 can be attained by lowering the bulk oxygen proportion in the system. The μO_2 , and therefore its conventional representation in fO_2 space, exhibits a complex variation as a function of the variable phase assemblages developed in metasomatised peridotites.

- Gudmundsson G. & Wood B.J. 1995. Experimental tests of garnet peridotite oxygen barometry. *Contrib. Mineral. Petrol.*, 119, 56-67.
- Holland T. & Powell R. 2011. An improved and extended internally consistent thermodynamic dataset for phases of petrological interest, involving a new equation of state for solids. *J. Metamorph. Geol.* 29, 333-383.
- Luth R.W., Virgo D., Boyd F.R. & Wood B.J. 1990. Ferric iron in mantle-derived garnets; implications for thermobarometry and for the oxidation state of the mantle. *Contrib. Mineral. Petrol.*, 104, 56-72.
- Malaspina N., Poli S. & Fumagalli P. 2009. The oxidation state of metasomatized mantle wedge: insights from C-O-H-bearing garnet peridotite. *J. Petrol.*, 50, 1533-1552.
- Stagno V., Ojwang D.O., McCammon C.A. & Frost D. 2013. The oxidation state of the mantle and the extraction of carbon from Earth's interior. *Nature*, 493, 84-88.

Lower mantle hydrogen partitioning between periclase and perovskite: a quantum chemical modeling

Merli M.*¹, Bonadiman C.², Diella V.³ & Pavese A.^{3,4}

1. Dipartimento di Scienze della Terra e del Mare, Università di Palermo. 2. Dipartimento di Fisica e Scienze della Terra, Università di Ferrara. 3. Istituto per la Dinamica dei Processi Ambientali, C.N.R. Milano. 4. Dipartimento di Scienze della Terra "A. Desio", Università di Milano.

Corresponding email: marcello.merli@unipa.it

Keywords: H₂O-partitioning in lower mantle, *Ab-initio* calculations, periclase.

The partitioning of hydrogen (often addressed to as H₂O) between periclase (*pe*) and perovskite (*pvk*) at lower mantle conditions (24-80 GPa) has been investigated, using quantum mechanics, equilibrium reaction thermodynamics and following two H-incorporation models. One is based on the replacements (MSWV) given by $Mg^{2+} \leftrightarrow 2H^+$ and $Si^{4+} \leftrightarrow 4H^+$; the other relies upon substitutions (MSWA) in terms of $2Mg^{2+} \leftrightarrow Al^{3+} + H^+$ and $Si^{4+} \leftrightarrow Al^{3+} + H^+$. H₂O partitioning between the two mentioned phases is considered in the light of homogeneous (Bulk Silicate Earth; *pvk*: 75% - *pe*:16% modal contents) and heterogeneous (Layered Mantle; *pvk*:78% - *pe*:14% modal contents) mantle geochemical models, which are set up to bear lower and upper bulk H₂O contents (*BWC*) of 800 and 1500 ppm, respectively. The equilibrium constant, ${}_{BWC}K(P,T)_{D,H_2O}^{pe/pvk}$, of the reactions governing the H-exchange between *pe* and *pvk* exhibits an almost negligible dependence on *P*, whereas it is remarkably sensitive to *T*, *BWC* and hydrogen incorporation scheme. Both MSWV and MSWA lead to ${}_{BWC}K(P,T)_{D,H_2O}^{pe/pvk} \leq 1$, which suggests an ubiquitous shift of the exchange reaction towards a H₂O-hosting perovskite. This takes place more markedly in the latter model, thus showing that the H₂O-partitioning is affected by the mechanism of uptake. In general, the larger *BWC*, the smaller is ${}_{BWC}K(P,T)_{D,H_2O}^{pe/pvk}$. Over the *BWC* range of 800-1500 ppm, MSWV leads to a $\langle {}_{BWC}K_{D,H_2O}^{pe/pvk} \rangle$ (average of ${}_{BWC}K(P,T)_{D,H_2O}^{pe/pvk}$ calculated along the lower mantle related *P-T*-paths predicted by the lower mantle geochemical models) that may be ultimately considered as a constant value (0.875). In the case of the MSWA mechanism, $\langle {}_{BWC}K_{D,H_2O}^{pe/pvk} \rangle$ is more sensitive to *BWC* (and LM over BSE), but its values lie in the rather narrow range 0.610-0.780. The concentration ratios (formally named "partition coefficient": $C_{H_2O}^{pe}/C_{H_2O}^{pvk}$), inferred from $\langle {}_{BWC}K_{D,H_2O}^{pe/pvk} \rangle$ range, for MSWV, between 0.60 and 0.49 (*BWC* spanning from 500 to 3000 ppm). In this view, the MSWV partition coefficient is estimated to be 0.56. MSWA, in turn, yields a $C_{H_2O}^{pe}/C_{H_2O}^{pvk}$ -trend having a slightly steeper negative slope ($C_{H_2O}^{pe}/C_{H_2O}^{pvk}$ ratio: 0.6-0.3; *BWC* 500-3000 ppm), but over the interval 800-1500 ppm it may also be considered nearly invariant and as large as 0.47 (average over an interval between 0.43 and 0.51). Combining the results from MSWV and MSWA we propose that, in the *P-T-BWC* range of geochemical interest, the H₂O *pe/pvk* "partition coefficient" lies in the short interval 0.47-0.56. This implies that water always prefers *pvk* than *pe*, but also suggests that even in a lower mantle with low or very low bulk water content, periclase hardly becomes a pure anhydrous phase.

Complexity of CaCO₃ polymorphism

Merlini M.*¹, Sciascia L.², Merli M.², Gatta G.D.¹, Pavese A.¹, Hanfland M.³, Lausi A.⁴ & Plaisier J.⁴

1. Dipartimento di Scienze della Terra "A. Desio", Università di Milano. 2. Dipartimento di Scienze della Terra e del Mare, Università di Palermo. 3. ESRF, Grenoble, France. 4. Elettra - Sincrotrone Trieste S.C.p.A., Basovizza (TS).

Corresponding email: marco.merlini@unimi.it

Keywords: CaCO₃, high pressure, high temperature.

Carbonates may play a fundamental role as carbon repository phases in the Earth's interior. Recent crystal structure determinations by single crystal diffraction technique at high pressure have shown that these phases may adopt very complex structures at pressures corresponding to Earth's upper and lower mantle. Calcite, CaCO₃, transforms to low symmetry phases. Computational studies have confirmed the crystal structure of CaCO₃-VI polymorph (observed experimentally above 15 GPa), and further suggest that this phase may possess a thermodynamic stability at low temperatures, compared to aragonite, in the pressure range 15-60 GPa. The complexity of carbonate structure is also apparent at high temperature, where carbonate groups present rotational and off-plane tilting disorder. This is confirmed by experiments at controlled atmosphere at high temperature, in the CaCO₃-V stability field.

A new methodology to analyse COH fluids in experimental capsules

Miozzi F.*¹, Tumiatì S.¹, Recchia S.², Tiraboschi C.¹ & Poli S.¹

1. Dipartimento di Scienze della Terra, Università di Milano. 2. Dipartimento di Scienze e Alta Tecnologia, Università dell'Insubria.

Corresponding email: francesca.miozziferrini@studenti.unimi.it

Keywords: Mass spectrometry, experimental petrology, thermodynamic modeling.

COH fluids are composed of the volatile species belonging to the C–O–H system, i.e. CO₂, CO, CH₄, H₂, H₂O e O₂. COH fluids influence different surface and deep geological processes, such as devolatilisation reactions and metasomatic processes due to element transport in solution. The determinant factor in these processes is the composition of the COH fluid in terms of volatiles (e.g., the XCO₂ ratio), which varies in function of pressure, temperature and the oxidation state of the system. The composition of natural and synthetic COH fluids can be retrieved using different techniques. Fluid inclusions analysis is classically performed using the heating–freezing stage or by Raman or infra - red spectroscopy. Thermodynamic models (Perple_X; Connolly, 1990) are based on thermodynamic calculations that use equations of state of H₂O and non-polar species (e.g. CO₂, CH₄), and are used to predict the composition of COH fluids in natural systems and in experimental petrology. However, thermodynamic models rely on some assumptions that could be not fulfilled in the system of interest. We develop a new methodology to analytically measure the volatile fluid composition in experimental capsules. The capsules are pierced in a gas-tight vessel and the evolved gases are conveyed to a quadrupole mass spectrometer (QMS), calibrated against standard gas mixtures of known composition. Eight channels, selected in function of the atomic mass/charge ratio, are monitored in our analytical setting. QMS data are then processed using a routine developed in the computation environment Mathematica, which allows generating ternary COH diagrams with the analysed fluid composition and its associated analytical uncertainty. This routine, using the least squares method, transforms the mass/charge data into abundances of volatiles present in the experimental capsule. In order to validate the technique, we performed an experiment at ambient *P* and *T* = 250 °C, with oxalic acid dihydrate as COH fluid source. The consistency of our results with previously published reference data (Morgan et al., 1992) guarantees the reliability of the technique. Therefore, this new analytical technique can be applied to analyse COH fluids in experimental capsules and, in the next future, to give constraints on the composition of COH fluids at *HP–HT* conditions.

Connolly J.A.D. 1990. Multivariable phase diagrams; an algorithm based on generalized thermodynamics. *Am. J. Sci.*, 290, 666-718.

Morgan G.B., Chou I. & Pasteris J.D. 1992. Speciation in experimental COH fluid produced by the thermal dissociation of oxalic acid dihydrate. *Geochim. Cosmochim. Acta*, 56(1), 281-294.

Cross-correlated Scanning Probe Microscopy and Quantum Mechanics investigation of chlorite-glycine interaction at the single molecule level

Moro D.*, Ulian G. & Valdrè G.

Centro di Ricerca Interdisciplinare di Biomineralogia, Cristallografia e Biomateriali, Dipartimento di Scienze Biologiche, Geologiche e Ambientali, Università di Bologna.

Corresponding email: daniele.moro@unibo.it

Keywords: Chlorite, glycine, cross-correlated SPM and QM investigation.

It is well known that the physical and chemical properties of phyllosilicates and hydroxides surfaces can drive mineral-environment surface interactions (Hayati-Ashtiani, 2013; Alencar et al., 2014). Mineral surface properties may control important interaction processes, such as adhesion, aggregation, coagulation, sedimentation, filtration, catalysis, and ionic transport in porous media.

In this work we studied the interaction of the (001) surface of chlorite with the amino acid glycine at the single molecule level by cross-correlating Atomic Force Microscopy (AFM) and *ab initio* quantum mechanics (QM) investigations. Chlorite is particularly interesting and peculiar for the interaction with organic molecules because it presents an alternated stacking of brucite-like (hydrophobic) and talc-like (hydrophilic) layers of different polarities. Brucite-like is positive, whereas talc-like is negative. Furthermore, zeolitic-type Brønsted-Lowry sites on atomic flat surfaces (bi-dimensional systems) were recently discovered in chlorites and modelled by *ab initio* techniques (Valdrè et al., 2011). These sites are known by theoretical analysis to act as potential sites of both molecular adsorption (Stückenschneider et al., 2014) and bond catalysis in zeolites (Phuakkong et al., 2011). The experimental AFM observations show that glycine is stably and selectively adsorbed on the brucite-like layer, organized in monolayers with different patterns. The sizes of single molecules of glycine measured by AFM are in agreement with those calculated by QM. Glycine molecules were found to align both at the edges and on the terraces of the brucitic surface. QM simulations confirmed the AFM observations that glycine molecule is adsorbed with high adsorption energy preferentially with its plane parallel to the (001) brucite-like surface. QM also provided the geometry conformation of the molecule and the bonding scheme between glycine and brucite surface. This kind of data can be very helpful both to biotechnological applications of chlorite and to depict some important processes that might have been occurred in prebiotic environments.

Alencar J.M., Oliveira F.J.V.E., Airoldi C. & Silva Filho E.C. 2014. Organophilic nickel phyllosilicate for reactive blue dye removal. *Chem. Eng. J.*, 236, 332-340.

Hayati-Ashtiani M. 2013. Characterization and surface properties of bentonites in the separation process of iron(III). *Part. Sci. Technol.*, 31, 419-425.

Phuakkong O., Bobuatong K., Pantu P., Boekfa B., Probst M. & Limtrakul J. 2011. Glycine peptide bond formation catalyzed by faujasite. *Chem. Phys. Chem.*, 12, 2160-2168.

Stückenschneider K., Merz J. & Schembecker G. 2014. Molecular interaction of amino acids with acidic zeolite BEA: the effect of water. *J. Phys. Chem. C*, 118, 5810-5819.

Valdrè G., Tosoni S. & Moro D. 2011. Zeolitic-type Brønsted-Lowry sites distribution imaged on clinocllore. *Am. Mineral.*, 96, 1461-1466.

Fluid-rock interaction experiments at supercritical conditions: a tool to investigate geothermal systems

Orlando A.*¹, Ruggieri G.¹, Chiarantini L.¹, Rimondi V.¹ & Borrini D.²

1. Istituto di Geoscienze e Georisorse, CNR, Firenze. 2. Dipartimento di Scienze della Terra, Università di Firenze.

Corresponding email: orlando@igg.cnr.it

Keywords: Fluid-rock interaction experiments, Elba Island, Iceland.

In the framework of Integrated Methods for Advanced Geothermal Exploration (IMAGE) project, fluid-rock interaction experiments were performed with the aim to better understand the mineralogical reactions occurring in different geothermal systems at supercritical conditions. Experiments considered different geological environments represented by two fossil geothermal systems:

1) Elba Island (Italy), assumed an exposed proxy of the high-temperature hydrothermal system active below the presently exploited reservoir of the Larderello-Travale geothermal field;

2) the Geitafell (Iceland) fossil hydrothermal system resembling the supercritical conditions occurring around the intrusive rocks of actively rifting neo-volcanic zones of Iceland.

Experiments evaluated either a metamorphic (Elba) or a magmatic (Iceland) rock reacting with aqueous fluids (with variable salinities and pH) under upper crustal conditions (400-600 °C, 50-130 MPa). They were performed using sealed gold capsules in an externally heated pressure vessel for duration of around 1 week. These P-T conditions were chosen based on microthermometric measurements on fluid inclusions found in rocks of both fossil systems. Furthermore, some experiments were planned in order to sample the liquid phase, besides to solid, at the end of the experiments. In these cases, long capsules were utilised and, at the end of the experiments, the liquid inside them was extracted and diluted with milli-Q water. Solids before and after experiments were characterized through XRD, SEM and EMPA whereas liquids were analysed through LC and ICP-OES.

Experiments results indicate mica and plagioclase from Elban micaschist as the major suppliers to the tourmaline crystallisation when aqueous fluids containing boric acid react with a micaschist. Moreover, mineral chemistry shows a compositional overlapping between natural and synthetic crystals (mainly dravites) in the experiments. Chamosite of micaschist disappears after experiments and its' role in tourmaline formation is currently under investigation. It is thus expectable to find tourmaline-rich rocks in the deep reservoir of Larderello-Travale geothermal system. The quartz-tourmaline veins fragments erupted from San Pompeo 2 geothermal well, which encountered a deep high-temperature pressurized fluid, support this assertion.

Experiments using a basalt produced a palagonitization only at 400 °C whereas modest spilitization and amphibole formation developed mainly at higher temperatures using pure water as a fluid reactant. The high sulphate contents found in the liquids after the experiments disclose the significant S content in glass of the basalt. The utilization of acid fluids and/or Ag₂C₂O₄ (as a CO₂ source) significantly increased the rate of metamorphic reactions but other common alteration minerals, extensively found in active and fossil geothermal fields (e.g. chlorite, garnet, hedenbergite,...) were still not detected through XRD, probably due to kinetic reasons.

Timescale of relaxation of garnet growth zoning via multi-component diffusion modeling: the example of Mammola Paragneiss Complex (Serre Massif-Southern Calabria)

Ortolano G., Visalli R.* & Cirrincione R.

Dipartimento di Scienze Biologiche, Geologiche e Ambientali, Università di Catania.

Corresponding email: rvisalli@unict.it

Keywords: Finite-difference diffusion model, garnet-micaschists, Variscan orogenesis.

Diffusion modeling of the major elemental compositional zonings is a valuable tool to know how long a zoned mineral can resist in chemical disequilibrium with the surrounding matrix at high temperature before the pre-existing composition is modified by diffusion. It allows to derive the timescales of metamorphic processes such as heating and cooling rates, providing information about the burial and exhumation history if mineral diffusion properties, crystal size and temperature are known.

In this study we have investigated millimeter almandine-rich garnet crystals from garnet-micaschists of the Mammola Paragneiss Complex (Serre Massif) (Angi et al., 2010), in order to estimate the timescales of metamorphic events registered in the upper crust section of the Variscan European Belt, using the extent of relaxation of garnet growth zoning by means of a finite-difference diffusion model (Crank, 1975; Storm & Spear, 2005). According to Angi et al. (2010), these rocks highlight a multistage metamorphic evolution consisting of an orogenic cycle partly overprinted by a thermal one, both of them ascribable to the Variscan orogenesis. In particular, the authors recognize a prograde low amphibolite facies evolution ($P = 5.9-7.5$ Kbar; $T = 500-550$ °C) followed by a retrograde *quasi*-adiabatic decompression ($P = 4$ Kbar; $T = 500$ °C), evolving toward a retrograde deep seated shearing stage ($P = 3$ Kbar; $T = 470$ °C). The subsequent post-tectonic progressive emplacement of huge masses of granitoid bodies gave rise then to a gradually distributed thermal metamorphic overprint ($P = 3$ Kbar; $T = 685$ °C), followed by a low pressure cooling path ($P = 1.5$ Kbar; $T = 500$ °C) consistent with the final unroofing stage of the former crystalline basement complex.

In this tangled scenario, relaxation of garnet zoning profiles was modelled taking into account two distinct set of diffusion data (Chakraborty & Ganguly, 1992; Carlson, 2006). Preliminary results obtained with the two distinct data set highlight a timescale of relaxation of the growth zoning around 1-3 My, suggesting prograde and exhumation events to be relatively rapid in this portion of the dismembered southern Hercynian European Belt, presently involved within the internal Alpine sector of the western Mediterranean geodynamics.

- Angi G., Cirrincione R., Fazio E., Fiannacca P., Ortolano G. & Pezzino A. 2010. Metamorphic evolution of preserved Hercynian crustal section in the Serre Massif (Calabria- Peloritani Orogen, southern Italy). *Lithos*, 115, 237–262.
- Carlson W.D. 2006. Rates of Fe, Mg, Mn and Ca diffusion in garnet. *Am. Mineral.*, 91, 1-11.
- Chakraborty S. & Ganguly J. 1992. Cation diffusion in aluminosilicate garnets: experimental determination in spessartine-almandine diffusion couples, evaluation of effective binary diffusion coefficients, and applications. *Contrib. Mineral. Petr.*, 111, 74-86.
- Crank J. 1975. *The Mathematics of Diffusion*, 2nd edition. Clarendon Press, Oxford.
- Storm L.C. & Spear F.S. 2005. Pressure, temperature and cooling rates of granulite facies migmatitic pelites from the southern Adirondack highlands, New York. *J. Metam. Geol.*, 23, 107-130.

Liquids from CaCO₃ in the presence of H₂O and the mobility of carbon in subduction zones

Poli S.* & Da Mommio A.

Dipartimento di Scienze della Terra "A. Desio", Università di Milano.

Corresponding email: stefano.poli@unimi.it

Keywords: Calcite, carbonatite, subduction.

Phase transformations in the system CaCO₃ and in the join CaCO₃ - H₂O have been of primary concern for Earth scientists since the early XIX century. Sir J. Hall successfully investigated the decarbonation reactions and the melting of calcite with water in externally heated gun barrels. Despite two centuries passed, the experimental results on phase transformations in this system are still contradictory. Discrepancy between *ex-situ* and *in-situ* determination of the reaction calcite = aragonite is in the order of 3 GPa at 1200 °C. Experimental data on the melting of calcite with an aqueous fluid differ by 300 °C. Uncertainties on the phase diagram for CaCO₃ and CaCO₃ - H₂O - CO₂ have profound consequences in predicting the fate of altered oceanic crust and of metasedimentary materials re-introduced in the mantle at subduction zones.

Multianvil experiments were performed at 4.2 GPa on model bulk compositions in the system CaO-Al₂O₃-SiO₂-H₂O-CO₂, obtained from calcite, Al(OH)₃ and silica. Stoichiometric proportions are intended to produce at run conditions kyanite + CaCO₃ + a "fluid" or/and a "melt". Al₂SiO₅ saturation prevents the formation of portlandite and dellaite, and offers a basis for modelling liquids formed from impure marbles. Furthermore the usage of Al(OH)₃ in the starting material allows an accurate control of H₂O added.

Aragonite + kyanite + fluid, and minor lawsonite form at 700 °C, replaced by zoisite at 800 °C. At 850 °C and 900 °C, a complex sequence of textural features is observed upon quenching; "chains" and dendrites of CaCO₃ grow nucleating from liquid-solid interface; they are followed by growth of Si-Al-bearing fibres; spheres of silica precipitate from the residual fluid exsolved from the liquid carbonate phase. Textures and composition of quench products vary as a function of silica added. Estimates of liquid – solid proportions, retrieved by image analysis, at known bulk H₂O content, provide constraints for H₂O solubility in CaCO₃ liquid. Chemographic analysis support a continuous transition from dissolution to melting at 4.2 GPa, i.e. the coalescence of the liquidus and the vaporous in wet-carbonate-silicate systems. Hydrous liquids enriched in Ca-carbonate at 850-900 °C are efficient media for scavenging volatiles from the subducted slab and for metasomatizing the mantle wedge.

Multivariate statistical characterization of groundwater chemistry: a case study in a zone affected by hydrothermal circulation (southern Tuscany, Italy)

Russo C.*¹, Bianchi S.², Protano G.¹ & Salleolini M.¹

1. Dipartimento di Scienze Fisiche, della Terra e dell'Ambiente, Università di Siena. 2. Geologo minerario, Via Roma 99 - Follonica (GR).

Corresponding email: russocristoforo@email.it

Keywords: Multivariate statistical techniques, hydrothermal fluids, groundwater.

Multivariate statistical techniques such as principal component (PCA) and cluster analyses, were applied for the interpretation of chemical composition of groundwater in a zone of Colline Metallifere (southern Tuscany, Italy). The aim was to classify groundwater into hydrochemical facies and groups, and to identify the main sources and hydrogeochemical processes governing the spatial and temporal variation of groundwater chemistry. Multivariate statistical analysis involved the main physico-chemical parameters (temperature, pH, electrical conductivity, redox potential) and the major ions (Ca^{2+} , Mg^{2+} , Na^+ , K^+ , HCO_3^- , Cl^- , SO_4^{2-}) of about 200 groundwater samples. Water samples were collected at 5 sites (springs and monitoring wells) from 2004 to 2014, over an area of about 3 km² in the zone of Montioni (Grosseto). This area was affected by a widespread circulation of hydrothermal fluids that altered rocks (silicization and kaolinite alteration) and formed alunite deposits as well as manganese and cinnabar mineralizations. The results of PCA analysis allowed to identify the hydrochemical facies of groundwater (SO_4 -Ca, HCO_3 -Ca and Cl-Na), the contribution of each hydrochemical facies to groundwater chemistry in each collection site, as well as the influence of water table fluctuations. PCA analysis revealed a component characterized by potassium, iron and manganese ions likely related to the alunite deposits and hydrothermal mineralizations present throughout the study area. This feature is important to define the origin of the HCO_3 -Ca and Cl-Na waters. Cluster analysis carried out with the k-means method, categorized the sampling locations into five dissimilar groups, and showed that there were temporal variations of groundwater chemistry within the same group. This study demonstrates that multivariate statistical analysis is a useful and powerful tool for the characterization and interpretation of groundwater chemistry in a zone affected by hydrothermal circulation.

Elastic geobarometry for host-inclusion systems: Pressure release and the role of brittle failure

Rustioni G.*¹, Angel R.J.², Milani S.², Mazzucchelli M.L.¹, Nimis P.², Domeneghetti M.C.¹, Marone F.³, Alvaro M.¹, Harris J.W.⁴ & Nestola F.²

1. Dipartimento di Scienze della Terra e dell'Ambiente, Università di Pavia. 2. Dipartimento di Geoscienze, Università di Padova. 3. Swiss Light Source - Paul Scherrer Institut, Switzerland. 4. Department of Geographical and Earth Sciences, University of Glasgow, U.K.

Corresponding email: greta.rustioni@gmail.com

Keywords: Diamond, inclusion, brittle failure.

Mineral inclusions trapped in host minerals can provide fundamental information about several geological processes at different length and time scales. One of the crucial open questions related to diamond investigation is their statistical vertical distribution in the mantle, which is related to the physical conditions of formation. Traditionally, estimates of the pressures of formation of natural diamonds have been retrieved by chemical thermobarometry of rare mineral inclusions. However, chemical geothermobarometric methods require destructive preparation procedures and the presence of minerals or mineral assemblages that are rarely available in natural diamonds.

Inclusions trapped in diamonds preserve a residual pressure (P_{inc}) due to the contrast in thermoelastic properties between the diamond and the inclusion phase (e.g. Izraeli et al., 1999; Nestola et al., 2012). Such P_{inc} can be used to calculate the entrapment pressure (P_e , at mantle P and T) at which the inclusion has been enclosed in its diamond host (Angel et al., 2014). This in turn allows the depth of formation of the diamond to be estimated. However, “elastic geobarometry” can only be applied within some boundary conditions (Angel et al., 2014) one of which is that the deformation in the pair has been purely elastic. This excludes from analysis inclusions that are surrounded by cracks as the brittle deformation could have caused a partial release of the P_{inc} , thus impairing calculations of the entrapment pressure for many inclusion-bearing diamonds.

Here we show the results of a pilot experiment in which 9 olivine inclusions in 6 diamonds have been investigated by synchrotron X-ray tomographic microscopy (at TOMCAT, Swiss Light Source, PSI) in order to evaluate the status of the brittle failure surrounding the inclusions. Preliminary results showed that at the spatial resolution of our experiments (ca. 1 μm) 90% of the inclusions trapped in our set of diamonds were surrounded by cracks. Single-crystal X-ray diffraction measurements performed on the very same set of inclusions showed a correlation between the size of the cracks and the pressure release. Quantitative modelling of such relationships for several types of mineral inclusions would extend the applicability of the “elastic geobarometry” to a much larger number of natural diamonds, thus leading to much greater statistics in the evaluation of formation pressures for diamonds worldwide.

This work was supported by ERC starting grant 307322 to F. Nestola.

- Angel R.J., Mazzucchelli M.L., Alvaro M., Nimis P. & Nestola F. 2014. Geobarometry from host-inclusion systems: the role of elastic relaxation. *Am. Mineral.*, 99, 2146-2149.
- Izraeli E., Harris J. & Navon O. 1999. Raman barometry of diamond formation. *Earth Planet. Sci. Lett.*, 173(3), 351-360.
- Nestola F., Nimis P., Ziberna L., Longo M., Marzoli A., Harris J.W., Manghnani M.H., Fedortchouk Y. 2011. First crystal-structure determination of olivine in diamond: Composition and implications for provenance in the Earth's mantle. *Earth Planet. Sci. Lett.*, 305, 249-255.
- Seward T.M. & Kerrick D.M. 1996. Hydrothermal CO₂ emission from the Taupo Volcanic Zone, New Zealand. *Earth Planet. Sci. Lett.*, 139, 105-113.

Experimental study on the effect of alkali ratio and oxygen fugacity on Fe redox and viscosity in pantelleritic glasses

Stabile P.*¹, Giuli G.¹, Behrens H.², Knipping J.², Webb S.³, Cicconi M.R.⁴ & Paris E.¹

1. Scuola di Scienze e Tecnologie - Sezione di Geologia, Università di Camerino. 2. Institute of Mineralogy, Leibniz University, Hannover, Germany. 3. Georg-August-Universität, Göttingen, Germany. 4. Department Werkstoffwissenschaften, Lehrstuhl für Glas und Keramik, Universität Erlangen-Nürnberg, Germany.

Corresponding email: paola.stabile@unicam.it

Keywords: Fe redox state, pantelleritic glasses, viscosity.

Iron represents the fourth most common element in the earth crust where it is present in significant portions in two different common oxidation states, Fe³⁺ and Fe²⁺. The relative abundance of different Fe species can affect physical properties of a melt/glass, in particular density, colour and viscosity (Dingwell & Virgo, 1987; Lange & Carmichael, 1987; 1989; Liebske et al., 2003).

The main aim of this study is to investigate the iron speciation in glasses representative of pantelleritic magmas (Scaillet & MacDonald, 2006) depending on the redox conditions, temperature, alkali ratio and water content. This is important to infer their behaviour in natural magmas of the same composition, since still relatively scarce information are available in literature on peralkaline silicic rocks.

For this purpose a XANES spectroscopic study has been performed, in order to acquire information on Fe structural environment in the dry glasses synthesized at ambient pressure and 1250 °C at controlled redox conditions (ranging from 0 to -13.8 log fO₂/bar) and to investigate the temperature and alkali ratio [Na/(Na+K)] effects on iron redox. The increase of Fe²⁺/Fe³⁺ ratio by decreasing the fO₂ of the system has been presented as a straight line with an average slope value of -0.11 ± 0.02, lower than the defined ideal value of -0.25 may be related to the stabilizing effect of the alumina component to ferric iron at the expense of ferrous iron in such systems. This is also documented by high abundance of ferric iron in similar peralkaline alumina silicate melts as trachytes or phonolites (Dickenson & Hess, 1981). But no simple relationship has been found between slope and [Na/(Na+K)] ratio of the glasses studied here.

In terms of coordination number, Fe³⁺ is present in tetrahedral coordination, while divalent iron displays an average coordination number intermediate between 4 and 5. Present data suggest that low [Na/(Na+K)] stabilizes Fe³⁺ in the melt: in fact, the association of tetrahedral Fe³⁺ with charge compensating cations is strongest for K⁺, which is consistent with the lower ferrous ferric iron ratios here observed in the potassium-rich alumina silicates. But in the compositional range examined, the Fe average coordination number does not vary significantly as a function of Na/(Na+K) ratio.

The viscosity of two sets of glasses, both at oxidizing and reducing conditions, has been also studied by a micropenetration technique, to address the influence of iron redox and different [Na/(Na+K)] ratio on viscosity. These data represent an important tool to implement actual viscosity predicting models that still do not take in consideration the influence of iron redox state on viscosity.

- Dickenson M.P. & Hess P.C. 1981. Redox equilibria and the structural role of iron in alumino-silicate melts. *Contrib. Mineral. Petrol.*, 78, 352-357.
- Dingwell D.B. & Virgo D. 1987. The effect of oxidation state on the viscosity of melts in the system Na₂O-FeO-Fe₂O₃-SiO₂. *Geochim. Cosmochim. Acta*, 51, 195-205.
- Lange R.A. & Carmichael I.S.E. 1987. Densities of Na₂O- K₂O-CaO-FeO-Fe₂O₃- Al₂O₃- TiO₂-SiO₂ liquids: new measurements and derived partial molar properties. *Geochim. Cosmochim. Acta*, 51, 2931-2946.
- Lange R.A. & Carmichael I.S.E. 1989. Ferric-ferrous equilibria in Na₂O-FeO-Fe₂O₃-SiO₂ melts: effects of analytical techniques on derived partial molar volumes. *Geochim. Cosmochim. Acta*, 53, 2195-2204.
- Liebske C., Behrens H., Holtz F. & Lange R.A. 2003. The influence of pressure and composition on the viscosity of andesitic melts. *Geochim. Cosmochim. Acta*, 67, 473-485.
- Scaillet B. & MacDonald R. 2006. Experimental constraints on pre-eruption conditions of pantelleritic magmas: Evidence from Eburrú complex, Kenya Rift. *Lithos*, 91, 95-108.

Analysing the Raman vibrational pattern of $\text{Mg}_2\text{Si}_2\text{O}_6$ *Pbca* enstatite: a quantum mechanical approach

Stangarone C.*¹, Tribaudino M.¹, Lottici P.P.¹ & Prencipe M.²

1. Dipartimento di Fisica e Scienze della Terra, Università di Parma. 2. Dipartimento di Scienze della Terra, Università di Torino.

Corresponding email: claudia.stangarone@studenti.unipr.it

Keywords: Orthoenstatite, *ab initio* methods, CRYSTAL14.

Enstatite is a major constituent of natural pyroxenes. It occurs, not only, as a rock forming phase in mafic and ultramafic assemblages of the Earth crust and upper mantle, but also, it is found to be a constituent of planetary bodies and meteorites, where a specific class of undifferentiated chondrites takes its name (Biswas et al., 1980).

Enstatite displays a complex polymorphism, however the orthorhombic phase *Pbca* is by far the most common at ambient condition. It has been subject of extensive studies, both experimental and computational (some examples: Chopelas, 1999; Tribaudino et al., 2002; Lin, 2003; Yu & Wentzcovitch, 2009). Although Raman spectroscopy has extensively been performed, a careful assignment of the observed vibrations is still lacking: orthoenstatite displays 120 Raman active modes and a rather complex spectrum, with significant overlapping of several peaks, which hinders a proper assignment of the Raman modes.

The spectra of orthoenstatite have been computed from first principles by means of CRYSTAL14 (Dovesi et al., 2014), employing the hybrid Hamiltonian WC1LYP (Wu & Cohen, 2006), which is particularly suitable to calculate vibrational frequencies. The calculated Raman spectrum of orthoenstatite, shows excellent agreement with the experimental data from literature (Lin, 2003), with an absolute average difference of 5 cm^{-1} .

Moreover, by exploiting some of the program features, the vibrational pattern has been studied, and every Raman signal has been assigned to a specific pattern of atomic motion (normal mode). Frequency shifts due to temperature or pressure variations have also been investigated and eventually related to structural modifications due to the changes in thermos-baric conditions.

- Biswas, S., Walsh, T., Bart G., Lipschutz, M.E. 1980. Thermal metamorphism of primitive meteorites—XL The enstatite meteorites: origin and evolution of a parent body. *Geochim. Cosmochim. Acta*, 44, 2097-2110.
- Chopelas A. 1999. Estimates of mantle relevant Clapeyron slopes in the MgSiO_3 system from high-pressure spectroscopic data. *Am. Mineral.*, 84, 233-244.
- Dovesi R., Saunders V.R., Roetti C., Orlando R., Zicovich-Wilson C.M., Pascale F., Civalieri B., Doll K., Harrison N.M., Bush I.J., D'Arco P., Llunell M., Causà M. & Noël Y. 2014. CRYSTAL14 User's Manual. University of Torino.
- Lin C. 2003. Pressure induced metastable phase transition in orthoenstatite (MgSiO_3) at room temperature: a Raman spectroscopic study. *J. Solid State Chem.*, 174, 403-411.
- Tribaudino M., Nestola F., Cámara F. & Domeneghetti M.C. 2002. The high- temperature *P21/c-C2/c* phase transition in Fe-free pyroxene ($\text{Ca}_{0.15}\text{Mg}_{1.85}\text{Si}_2\text{O}_6$): Structural and thermodynamic behavior. *Am. Mineral.* 87, 648-657.
- Wu Z. & Cohen R.E. 2006. More accurate generalized gradient approximation for solids. *Phys. Rev. B*, 73, 235116-235121.
- Yu Y.G. & Wentzcovitch R.M. 2009. Low-pressure clino- to high-pressure clinoenstatite phase transition: a phonon-related mechanism. *Am. Mineral.* 94, 461-466.

Carbon-saturated COH fluids speciation at 1 GPa: experimental data versus thermodynamic modeling

Tiraboschi C.*¹, Tumiati S.¹, Recchia S.² & Poli S.¹

1. Dipartimento di Scienze della Terra "A. Desio", Università di Milano. 2. Dipartimento di Scienze e Alta Tecnologia, Università dell'Insubria.

Corresponding email: carla.tiraboschi@unimi.it

Keywords: COH fluids, speciation, experiments.

The quantitative assessment of species in COH fluids is crucial in modelling mantle processes. For instance, H₂O/CO₂ ratio in the fluid phase influences the location of the solidus and of carbonation/decarbonation reactions in peridotitic systems (Wyllie, 1978). In the scientific literature, the speciation of COH fluids has been generally assumed on the basis of thermodynamic calculations using equations of state of simple H₂O-non-polar gas systems (e.g., H₂O-CO₂-CH₄). Only few authors dealt with the experimental determination of high-pressure COH fluid species at different conditions, using diverse experimental and analytical approaches (e.g., piston cylinder + capsule-piercing + gas-chromatography/mass-spectrometry; cold-seal + silica glass capsules + Raman).

We choose to experimentally investigate the volatile speciation of COH fluids through a capsule-piercing quadrupole mass spectrometer device. Experiments were carried out in a rocking piston cylinder apparatus at pressure of 1 GPa and temperatures from 800 to 900 °C. Carbon-saturated fluids were generated through the addition of oxalic acid dihydrate (C₂H₂O₄·2H₂O) and graphite. Single/double capsules, different packing materials (BN and MgO) and oxygen buffers (iron-wustite, nickel-nickel oxide and hematite-magnetite) were used to evaluate the divergence from the thermodynamic speciation model. Moreover, to assess the effect of solutes on COH fluid speciation we also performed a set of experiments adding synthetic forsterite and enstatite to the charge.

Results suggest that fluid speciation can diverge considerably compared to the thermodynamic model depending on the experimental strategy adopted. The assembly seems to strongly control the speciation of the COH fluid in single capsule experiments. In particular, BN imposes reducing conditions on the COH fluid, favouring the formation of H₂O. On the other hand MgO shift the composition toward more oxidizing terms. Double capsule experiments provided similar COH volatile speciation compared to thermodynamic modeling for what concerned the COH-only system. However, in complex COH systems the presence of solutes seems to affect the volatile speciation of the fluid, shifting the composition toward more CO₂-rich terms.

The experimental investigation of high-pressure COH fluids, generated employing the double capsule technique, could therefore represent a valuable tool in addition to thermodynamic models and fluid inclusions analyses.

Wyllie P.J. 1978. The effect of H₂O and CO₂ on planetary mantles. *Geophys. Res. Lett.*, 5, 440-442.

Quantum mechanics simulations of structural and physico-chemical properties of apatites and layer silicates

Ulian G.*, Moro D. & Valdrè G.

Dipartimento di Scienze Biologiche, Geologiche e Ambientali, Università di Bologna.

Corresponding email: gianfranco.ulian2@unibo.it

Keywords: Apatite, muscovite, Density Functional Theory.

Calcium apatites are among the most studied minerals in the biomedical field because of their similarities with natural bone minerals (Dorozhkin, 2009; Corno et al., 2010). The surface biomimetic features of hydroxylapatite (OHAp) are very important to understand organic biomolecular interactions. Furthermore, the knowledge of the high-pressure and high-temperature behaviour of layer silicates is very important in minero-petrological and industrial fields for various genetic and thermobarometric issues and for ceramic/electric applications, respectively (Comodi et al., 2002; Curetti et al., 2006). In both perspectives, there are very few works in literature devoted to the physico-chemical characterization of apatites and layer silicates at atomic scale. Both mineralogical families present interesting challenges to computational mineralogists. Hydroxylapatite presents both anionic and cationic substitutions to stabilize its structure, where the most common defect is the carbonate ion (CO_3^{2-}), in a weight percentage ranging from 3% to 7%. Layered silicate structures are made by tetrahedral-octahedral-tetrahedral (T-O-T) with an empty interlayer (talc and pyrophyllite end members) or with cations between the TOTs (e.g. potassium in muscovite). For this reason, the simulation parameters should be chosen carefully when dealing with layered silicates, because two directions of the mineral are dominated by covalent bonds (within the TOT layers), while the third direction exhibits an interplay of van der Waals forces (between the layers) and strong ionic interactions due to the interlayer cations. In the present study, we show both the surface properties of carbonated hydroxylapatite and the thermo-chemical and thermo-physical properties of the $2M_1$ polytype of muscovite in the 0 – 10 GPa and 0 – 900 K ranges. In both cases, the hybrid DFT/B3LYP density functional has been adopted, adding a correction for dispersive forces and employing the quasi-harmonic approximation for the analysis of muscovite. The results of the analysis can be used (1) for the synthesis of apatite-based biomaterials with tailored surface properties and (2) in the study of the thermodynamic properties of layered silicates at physical conditions that are difficult to obtain during experimental procedures, especially controlled high pressures and temperatures.

Comodi P., Gatta G.D., Zanazzi P.F., Levy D., Crichton W. 2002. Thermal equations of state of dioctahedral micas on the join muscovite-paragonite. *Phys. Chem. Mineral.*, 29, 538-544.

Corno M., Rimola A., Bolis V., Ugliengo P. 2010. Hydroxyapatite as a key biomaterial: quantum-mechanical simulation of its surfaces in interaction with biomolecules. *Phys. Chem. Chem. Phys.*, 12, 6309-6329.

Curetti N., Levy D., Pavese A., Ivaldi G. 2006. Elastic properties and stability of coexisting 3T and 2M(1) phengite polytypes. *Phys Chem. Mineral.*, 32, 670-678.

Dorozhkin S.V. 2009. Calcium Orthophosphates in Nature, Biology and Medicine. *Materials*, 2, 399-498.

Limits in modeling organic carbon-bearing rocks at upper crust and forearc slab conditions

Vitale Brovarone A.

IMPMC-CNRS, Paris, France.

Corresponding email: alberto.vitale-brovarone@impmc.upmc.fr

Keywords: Disordered graphitic C, metasomatism, limits of thermodynamics.

Crustal rocks represent an important reservoir of organic C. Their transformations in deep crustal or subduction environments deeply contribute to the redistribution of global C reservoirs. The implications of deep redistribution of organic C span geophysical explorations, e.g. electrical conductivity of graphite; formation of mantle diamonds; formation of graphite reservoirs of economic significance; C return into the atmosphere and climate change. The stability of organic C reservoirs in rocks submitted to extreme geological environments, e.g. subduction or crustal thickening/thinning is therefore matter of interest in several branches of the Earth Sciences. Several experimental and numerical studies have focused on the fate of organic C under different metamorphic conditions. These studies, however, rely on two crucial assumptions, i) rock evolving in closed systems, i.e. no external buffers, and ii) organic C to be pure graphite. Natural systems do not always fit these two assumptions. Fluid rock interactions, especially in channelized fluid pathways, have been shown to dramatically affect the stability of minerals and rates of fluid-rock interactions. Moreover, under a large range of relevant metamorphic conditions (ca. $250 < T \text{ } ^\circ\text{C} < 650$) organic C is not structurally ordered (i.e. pure graphite) and has chemical radicalization and nanoporosity. Disordered graphitic C is expected to be the dominant organic C fraction at metamorphic conditions characteristic of forearc subducting slabs. An example of the natural organic C-bearing rocks affected by fluid-rock interactions at ca. $450 \text{ } ^\circ\text{C}$ and 1.8 GPa is shown. Petrographic and geochemical data indicate that organic C was removed from the systems at metamorphic conditions at which standard thermodynamic approaches predict graphite stability. Raman spectroscopy on organic C across the reaction zone indicates that only disordered organic C was removed, whereas pure graphitic C (present in the rock as detrital component) was preserved. On one side, these results confirm the thermodynamic stability of graphite under these metamorphic conditions. On the other side, this work indicates that current thermodynamic approaches cannot easily reproduce natural processes at these conditions. The role of disordered organic C is highlighted for generating significant (isotopically light) C fluxes in forearc slabs and upper crust environments.

New micro-furnace for “in situ” high-temperature single crystal X-ray diffraction measurements

Zaffiro G.*¹, Angel R.J.², Alvaro M.¹, Nestola F.², Domeneghetti M.C.¹, Scandolo L.¹, Mazzucchelli M.L.¹, Milani S.²,
Rustioni G.¹ & Marciano C.¹

1. Dipartimento di Scienze della Terra e dell'Ambiente, Università di Pavia. 2. Dipartimento di Geoscienze, Università di Padova.

Corresponding email: gabriele.zaffiro@gmail.com

Keywords: High-temperature device, single-crystal X-ray diffraction, thermal expansion.

High temperature devices for *in situ* single crystal X-ray diffraction measurements have been extensively developed in the past century. Fundamental requirement in any of these devices is that they should provide the most controlled isothermal environment as possible across the entire sample. It is intuitive that in general, thermal gradient across the sample increases as the temperature increases. Even if the small isothermal volume required for single-crystal X-ray diffraction experiments makes such phenomena almost negligible, the design of a furnace should be also aimed to reduce thermal gradients by including a large thermal mass that encloses the sample.

However this solution often leads to complex design that often results in a restricted access to reciprocal space or attenuation of the incident or diffracted intensity (with consequent reduction of the accuracy and/or precision in the lattice parameters determination), a decrease of the thermal stability (i.e. while performing the measurements) and a lack of accuracy and/or precision in the temperature determination.

Here we present a newly developed H-shaped Pt-Pt/Rh resistance microfurnace for *in situ* high-temperature single crystal X-ray diffraction measurements. The compact design of the furnace together with the long collimator-sample-detector distance allows us to perform measurements up to $2\theta = 70^\circ$ with no further restrictions on any other angular movement. The microfurnace is equipped with a water cooling system that allows to maintain a constant thermal gradient that guarantees thermal stability with oscillations smaller than 5 °C in the whole range of operating T (i.e. room-T to 1200 °C). The furnace has been built for the use with a conventional 4-circle Eulerian geometry (i.e. Huber 4-circle diffractometer) equipped with point detector and automated with the SINGLE software (Angel & Finger, 2011) that allows to eliminate the effects of crystal offsets and diffractometer aberrations from the refined peak positions by the 8-position method (King & Finger, 1979). The temperature calibration has been performed iteratively by combining measurements with a standard small diameter (i.e. 0.25 mm) thermocouple mounted in the same conditions as the sample together with the lattice parameters determination of materials with known thermal expansion behavior (i.e. silicon, quartz etc...). This procedure has the main advantage that the temperature calibration can be obtained with a large number of measurements over a large temperature interval (i.e. room-T to 1200 °C) and allows the waiting time for the χ movements to be calibrated as a function of temperature.

This work was supported by ERC starting grant 307322 to Fabrizio Nestola.

Angel R.J. & Finger L.W. 2011. SINGLE: A program to control single-crystal diffractometers. *J. Appl. Crystallogr.*, 44, 247-251.

King H.E. & Finger L.W. 1979. Diffracted beam crystal centering and its application to high-pressure crystallography. *J. Appl. Crystallogr.*, 12, 374-378.

Geobarometry of igneous cumulates and the depth of magma storage zones

Ziberna L.*¹, Green E.C.R.², Schumacher J.¹ & Blundy J.D.¹

1. School of Earth Science, University of Bristol, UK. 2. Institute of Geochemistry and Petrology, ETH Zurich, Switzerland.

Corresponding email: luca.ziberna@bristol.ac.uk

Keywords: Igneous cumulates, geobarometry, phase equilibria.

Revealing the vertical structure of magmatic systems in island arcs is a critical step towards understanding both crust-forming processes and the conditions of magma storage prior to volcanic eruptions. We are investigating these issues using a large collection of cumulate xenoliths from the Lesser Antilles volcanic arc, in combination with a large number of phase equilibria experiments on Lesser Antilles magmas. The petrology of the xenoliths, which are mostly characterised by gabbroic-like mineralogy and occur in almost all the islands of the arc, could potentially reveal the roots of each individual volcanic system and greatly enhance understanding of the overall crustal structure of the arc. However, no geobarometers exist which allow calculation of the pressure of formation (and therefore the depth of provenance) of gabbroic assemblages with acceptable uncertainties. Existing geobarometers show high uncertainties ($1\sigma > 0.3-0.4$ GPa) or show systematic deviations up to 1.0 GPa when compared with phase equilibria experiments. In some cases, the discrepancies are of the same order of magnitude of the whole pressure range under investigation (i.e. 0.0-1.0 GPa). In addition, most of these geobarometers rely on the composition of a single phase and were calibrated independently of each other. This is likely to produce highly inconsistent results where various of these geobarometers must be applied to a set of cumulates characterised by different mineral assemblages.

Multiple-reaction thermobarometry is in principle more reliable. An independent set of reactions is considered using internally consistent thermodynamic models, taking account of correlated uncertainties in the activities of mineral end-members. However, this method requires well-calibrated activity-composition (a-x) relations for numerous phases, including complex solid solution in hornblende. Thanks to the vast collection of natural and experimental data, we can use the Lesser Antilles magmatic suite to refine a set of suitable a-x relations specifically for this purpose. We hope to achieve uncertainties in relative pressures of < 0.1 GPa, sufficient to discriminate the main magma storage zones in the crust. In addition, the adoption of self-consistent thermodynamic models will ensure consistency where different sets of thermobarometers are applied to different mineral assemblages.

SESSION S7

Microstructures: key to the interpretation of processes

CONVENORS

Gaetano Ortolano (Univ. Catania)

Cecilia Viti (Univ. Siena)

Frictional processes in smectite-rich gouges sheared at low to high slip rates

Aretusini S.^{*1}, Mittempergher S.², Gualtieri A.F.² & Di Toro G.¹⁻³

1. Dipartimento di Geoscienze, Università di Padova. 2. Dipartimento di Scienze Chimiche e Geologiche, Università di Modena e Reggio Emilia.
3. School of Earth, Atmospheric and Environmental Sciences, University of Manchester, UK.

Corresponding email: stefano.aretusini@studenti.unipd.it

Keywords: Rotary shear, smectite, friction.

The slipping zones of shallow sections of large landslides and fault zones are often smectite-rich (the most common being the dioctahedral type Montmorillonite). Consequently, similar "frictional" processes might be responsible of the mechanics of large landslides (e.g. the 1963 Vajont slide, Italy) and earthquakes (e.g., 2011 Tohoku Mw 9.0 earthquake, Japan). At present, only rotary shear apparatuses can reproduce simultaneously the large slips (tens to hundreds of meters) and slip rates (meters per second) of these events. Noteworthy, the "frictional" processes responsible for the large weakening during landslides and seismic slip faults remain rather obscure.

Here we present results obtained with the ROTary Shear Apparatus (ROSA) installed at Padua University. Eighty experiments were performed at ambient conditions on (1) smectite-rich standard powders (STx-1b: 61 wt.% Ca-Montmorillonite, 17 wt.% Opal-CT, 1 wt.% Quartz, 21 wt.% amorphous; opal and smectites are aggregated in grains < 100 μm in size), (2) Quartz powders (grain size < 100 μm) and (3) on 80:20 and 40:60 STx-1b:Qtz mixtures (the latter corresponding to 50 and 25 wt.% smectite). A 2-mm thick layer of powder was sandwiched between two hollow (25/15 mm external/internal diameter) stainless-steel cylinders, confined by inner and outer Teflon rings. The powder was sheared for a total slip of 3 m under a normal stress of 5 MPa and slip rates V ranging from 300 μms^{-1} to 1.5 ms^{-1} . In smectite-rich (≥ 50 wt.%) powders, the friction coefficient drastically decreased from ~ 0.8 to ~ 0.2 for $V \geq 0.1$ ms^{-1} ; instead, by increasing the quartz content (≤ 25 wt.% smectite), the friction coefficient decreased monotonically (from ~ 0.8 to ~ 0.6) with slip rate from 300 μms^{-1} to 1.5 ms^{-1} .

The sheared powders were investigated with quantitative X-Ray Powder Diffraction (XRPD) using BGMN software and with Scanning Electron Microscopy (both SEM and FEG-SEM). The Rietveld analysis of both 60 and 50 wt.% smectite-rich gouges showed that the amount of the amorphous fraction (1) increased (from ~ 20 to ~ 40 wt.% and from ~ 10 to ~ 30 wt.%, for 60 and 50 wt.% smectite respectively) while the content of smectite decreased with frictional work (i.e., product of shear stress with displacement), and (2) was higher in the experiments performed at $V \leq 0.1$ ms^{-1} . Instead, production of amorphous material and mineralogical changes were unrelated to the frictional work rate (i.e., product of shear stress with slip rate). Opal-ct content remained constant in all the experiments (~ 20 and ~ 10 wt.%, for 60 and 50 wt.% smectite respectively): as a consequence, the formation of amorphous material resulted from smectite breakdown.

The microstructure of the slipping zones varied with slip rate and smectite content. In experiments performed at $V \leq 0.1$ ms^{-1} with 60 and 50 wt.% smectite, deformation was distributed over ~ 500 mm thick anastomosing bands of ultra-comminuted (amorphous-rich) smectites alternated with less deformed smectite-rich bands. In the latter, quartz grains were rimmed by ultra-comminuted smectites forming "clay cortex aggregates". For $V > 0.1$ ms^{-1} slip localized in a principal ~ 200 mm thick band at the boundary with the sandwiching steel holder and made of "baked-like" smectites. For < 25 wt.% in smectite, if $v \geq 0.1$ ms^{-1} , slip was localized in a 50-100 μm thick band cutting through the undeformed gouge. Only if $v < 0.1$ ms^{-1} the deformation is more diffuse and leads to an extensive comminution of the starting material.

We can interpret the microstructures and mechanical data in terms of conversion of frictional work into energy exchanged for grain size reduction and temperature increase during gouge shearing (energy budget). In smectite-rich mixtures (≥ 50 wt.%), the work and work rate dissipated in the slipping zones are converted (1) at low slip rates ($V < 0.1$ ms^{-1}), into amorphization processes and grain size reduction; (2) at higher slip rates, into frictional heating and slip localization. In smectite-poor mixtures (≥ 75 wt.% quartz), work and work rate are mainly dissipated into grain size reduction, independently of the imposed slip rate. The different energy budgets are due to the higher thermal conductivity of quartz (6 $\text{Wm}^{-1}\text{K}^{-1}$) with respect to smectite (0.5-1 $\text{Wm}^{-1}\text{K}^{-1}$). Given the same experimental conditions, with respect to smectite-rich gouges, the higher thermal conductivity of quartz allows easy heat diffusion resulting in lower temperatures in the slipping zones and in limited frictional weakening.

Alpine re-activation of a late post - Variscan shear-zone: microstructural and petrological investigations (Sila, northern Calabria)

Cirrincione R.¹, Ortolano G.*¹, Pezzino A.¹, Sacco V.¹, Visalli R.¹, Fiannacca P.¹, Punturo R.¹ & Mengel K.²

1. Dipartimento di Scienze Biologiche, Geologiche e Ambientali, Università di Catania.
2. Institut für Endlagerforschung, Clausthal University, Germany.

Corresponding email: ortolano@unict.it

Keywords: Mylonitic microstructures, LPO quartz analysis, Mediterranean geodynamics.

A detailed structural and petrological study has been focused on the Sila Piccola Massif (Northern Calabria), in order to obtain new constraints about the tectono-metamorphic history of the “Castagna Unit” (Dubois & Glangeaud, 1965). This unit represents a pervasively mylonitized continental crust complex, comprised of amphibolite to greenschist facies metamorphic rocks intruded by late Variscan granitoids. Structural investigations highlighted as the pervasive mylonitic fabric (Sm) has obliterated older metamorphic ones, locally preserved as relics in the low strain domains of the metapelite horizons. The relics of these pre-mylonitic fabrics (D1 stage) are represented by a $grt_1+pl_1+bt_1+wm_1+qtz$ assemblage in which garnet exhibits a *quasi*-absent crystal zoning, reflecting a long residence time at deep crust conditions. Field investigations integrated with microstructural data highlight as the mylonitic process (D2 stage) can be subdivided into two different metamorphic events: i) the first one, indicating an early retrograde path (M2a) developed under amphibolite facies conditions ($P = 5.7-6.8$ Kbar; $T = 595$ °C), is characterized by the syn-kinematic growth of $grt_2+pl_2+bt_2+sil+qtz$ observable in the pressure shadows of syn-D1 garnet porphyroclasts; ii) the second one, consistent with a late-retrograde metamorphic overprint (M2b) under greenschist facies conditions ($P = 2-3$ Kbar; $T = 400-500$ °C), is highlighted by the syn-shearing crystal growth of $chl_1+wm_2(Si \text{ a.p.f.u. } 3.15-3.25) +pl_3+qtz$ observed along C-planes. A further mylonitic event (D3; $P = 4-8$ Kbar; $T = 400-500$ °C) appears having developed at higher pressure conditions than the previous one, as testified by the syn-shearing white micas with high phengite content (Si a.p.f.u. 3.25-3.40). The bimodal composition of the white mica arranged along C-planes, points to the occurrence in the same terrains of two different mylonitic processes, probably ascribable to two orogenic cycles developed under different baric regimes. This hypothesis is geologically consistent with the re-activation of a Variscan shear zone during an Alpine shearing event (D3) developed in a HP-LT regime. Such a hypothesis is also supported by quartz LPO analyses indicating the presence of two contrasting senses of shear developed under greenschist facies conditions.

In this scenario, the “Castagna Unit” can be interpreted as an extensional late-to-post Variscan shear zone, locally re-activated during the building of the Alpine edifice. Finally, an asymmetrical folding involving the mylonitic field foliation, suggests a shallower deformative event (D4) linkable to the stacking stages of the Alpine-Appennine tectonic activity in the central Mediterranean area.

Dubois R. & Glangeaud L. 1965. Grandes structures, microstructures et sens des chevauchements de matériel cristallin à l'extrémité méridionale du massif de la Sila (Calabre centrale, Italie). C.R. Somm. Geol. France, 7, 239-240.

Timing of microstructure development along carbonate-bearing faults

Collettini C.*¹, Carpenter B.M.², De Paola N.³, Giorgetti C.¹, Mollo S.², Scuderi M.M.¹, Tesei T.²,
Trippetta F.² & Viti C.⁴

1. Dipartimento di Scienze della Terra, Sapienza Università di Roma. 2. INGV, Roma. 3. Department of Earth Sciences, University of Durham, U.K.
4. Dipartimento di Scienze Fisiche, della Terra e dell' Ambiente, Università di Siena

Corresponding email: cristiano.collettini@uniroma1.it

Keywords: Faults, microstructures, carbonates.

In the last decade we have worked at the characterization of fault zone structure, fault rocks and inferred slip behaviour of carbonate-bearing faults. To pursue these objectives we have integrated field and laboratories studies of exhumed faults. During the seismic cycle, the superimposition of fast and slow slip makes the discrimination between the associated deformation mechanisms challenging, when studying exhumed structures. Here we attempt to classify microstructures into two groups: slow microstructures, SM, that likely formed at low strain rates typical of the interseismic, preseismic and postseismic phases of the seismic cycle, and fast microstructures, FM, that may be associated with the coseismic slip phase.

SM formed predominantly by distributed deformation and pressure solution processes along cataclasites. The latter seem to be favoured by both the presence of clay-rich material within the protolith (e.g. development of smectite rich pressure solution seams) and intense fluid rock interaction with exotic fluids (e.g. talc development from dolostones via an interaction with silica-rich fluids).

Slip localization along thin, < 1 mm, slipping surfaces seems to be a prerequisite to trigger the temperature rise capable of promoting FM that are responsible for dynamic weakening. Dynamic weakening results from a number of thermally activated physicochemical processes that for carbonates may include flash heating, thermal decomposition and/or pressurization, nano-powder lubrication, and viscous flow. The occurrence of relict calcite grains, containing holes and vesicles, and newly formed calcite skeletal crystals point to thermal decomposition. The development in some slipping zones of equiaxial, nanograin aggregates exhibiting polygonal grain boundaries testify localized plastic deformation.

The vast gamut of rock types and associated deformation processes that we have documented with the study of just a single rock type, i.e. carbonates, testifies the importance of multi-scale and interdisciplinary studies for uncovering the secrets preserved within fault rocks.

Microstructures and quartz c-axis patterns of mylonites at the ductile-brittle transition: insights from a crustal scale shear zone (Southern Calabria, Italy)

Fazio E.*, Ortolano G., Cirrincione R., Pezzino A. & Visalli R.

Dipartimento di Scienze Biologiche, Geologiche, Ambientali - Sezione di Scienze della Terra, Università di Catania.

Corresponding email: efazio@unict.it

Keywords: Quartz c-axis pattern, mylonite, shear zone.

Crustal scale shear zones are rooted in the deep crust and evolve over a considerable period of time often highlighting the retrograde trajectory of the orogenic cycle along plate boundaries delineated by strain gradient distribution from kilometer to millimeter scale. Different rock-types are normally involved during their evolution, strongly influencing the strain gradient distribution, mostly controlled by simple/pure shear deformative ratio and by rock rheology contrast. The investigated shear zone (Cirrincione et al., 2010) crops out in the Aspromonte Massif, southern Calabria (Italy), near Montalto. The outcrop is characterized by a pervasive mylonitic foliation (Fm) dipping 60° towards NNW with an average strike of 260° and a stretching lineation (L1) gently NNE dipping which is often obliterated by a secondary sub-horizontal intersection lineation (L2) (Fazio et al., 2010) oriented at about 90° with respect the first one (i.e. roughly E-W). Two lithologies essentially occur: brownish colored paragneiss and leucocratic gneiss. Minor augen gneiss and pegmatites also occur. The repetition of such lithotypes is due to an isoclinal folding phase which followed the main syn-shear deformational episode developed essentially in the ductile regime. Subsequent deformational phase are represented by an asymmetric folding at the ductile-brittle transition evolving to a clear brittle phase responsible of thrust activation. A suite of samples has been collected covering the various rock-types at different strain gradient. Microstructural features are typical of mylonitic rocks with a lot of kinematic indicators like mica fish, domino-type porphyroclasts, S-C-C' foliations, among others, suggesting an average top-to-the-NNE sense of shear in the present day geographic coordinates. Ultramylonites interbedded to mylonites show complex fold patterns resembling microscale sheath folds. Recrystallization of quartz during shear zone activity is mainly developed by subgrain rotation recrystallization (SGR) and minor bulging (BLG). Often an oblique foliation is developed by recrystallized quartz subgrains within layers parallel to the mylonitic foliation. Quartz c-axis patterns revealed simple shear deformation suggesting a dominant basal slip system activation typical of greenschist facies conditions (Passchier & Trouw, 2005).

- Cirrincione R., Fazio E., Heilbronner R., Kern H., Mengel K., Ortolano G., Pezzino A. & Punturo R. 2010. Microstructure and elastic anisotropy of naturally deformed leucogneiss from a shear zone in Montalto (southern Calabria, Italy). *Geol. Soc. London, Sp. Publ.*, 332, 49-68.
- Fazio E., Punturo R. & Cirrincione R. 2010. Quartz c-axis texture mapping of mylonitic metapelite with rod structures (Calabria, southern Italy): Clues for hidden shear flow direction. *J. Geol. Soc. India*, 75, 171-182.
- Passchier C.W. & Trouw R.A.J. 2005. *Microtectonics*. Springer-Verlag Berlin Heidelberg.

Insights on the relationships between felsic granitoids in the Serre Batholith (Calabria, southern Italy) from plagioclase microstructures and compositions

Fiannacca P.*, Lombardo R., Militello G.M. & Cirrincione R.

Dipartimento di Scienze Biologiche, Geologiche e Ambientali, Università di Catania.

Corresponding email: pfianna@unict.it

Keywords: Magma mixing, crystallization, Serre Massif.

The late Variscan granitoids of the Serre Batholith form the middle portion of an entire crustal section exposed in central Calabria. The most felsic rock types consist of two-mica K-feldspar megacrystic granodiorites and granites (BMPG), passing southward to slightly inequigranular two-mica granodiorites and granites (BMG), that grade further south to Bt±Am granodiorites (BAG). A detailed petrographic study has shown the presence of different sub-groups as follows: BAG s.s., BAG proximal to BMG, BMG proximal to BAG, BMG proximal to BMPG, PA (BMPG with Kfs megacrysts <2 cm) and KA (BMPG with Kfs megacrysts >2 cm). Transitional features have been also observed, especially at the BAG-BMG transition. Mixing processes were previously proposed to have been involved in the evolution from BAG (SiO₂ = 65-67 wt.%) to BMG (SiO₂ = 68-74 wt.%); BMPG were instead considered unrelated to the other groups. Since plagioclase is known to record in its internal structure and chemical zoning valuable information on open vs. closed magmatic conditions, Pl crystals from all the subgroups were characterized in detail at the optical microscope and selected Pl grains from three samples (a BMPG, a BMG proximal to BAG and a BAG) were then analyzed at the SEM. The petrographic study highlighted that BAG and BMG proximal to BAG show complex zoning, patchy cores and embayments, while in both BMPG and BMG proximal to BMPG zoning is simple and resorption structures are almost absent. In the Pl from BMPG composition is usually constant from core to rim (An₃₉₋₃₇); normally zoned crystals, with rim compositions down to An₂₇, also occur. BAG and BMG proximal to BAG share many similarities also in terms of Pl compositions. Core compositions in BAG Pl of all sizes is ca. 50% An. Intermediate portions with greater An content (61-72%) characterize large-intermediate crystals; rims are An₂₁₋₃₇ in crystals of all sizes and similar compositions (An₃₀₋₃₇) also occur in random patchy zones of large crystals. Pl from BMG proximal to BAG has mainly andesinic core and intermediate portions showing inverse zoning (An₃₂₋₄₉). Finally, An content is 35-28% in the rim of large crystals and 26-15% in intermediate-small crystals. Acquired data support an independent origin and an undisturbed magmatic evolution in a closed system for porphyritic granitoids and most BMG, as indicated by the Pl regular internal microstructure and composition. Mixing processes may have occurred between BAG and BMG proximal to BAG magmas during the emplacement of the BAG, as suggested by similar/transitional whole rock and Pl compositions and microstructures and by reverse zoning in the core-intermediate portions of the BMG Pl, suggesting interaction with slightly more mafic magmas. BAG also appear to have locally recorded a subsequent intrusion of mafic magma, as suggested by increase of the An content up to bytownitic compositions in Pl intermediate portions in samples characterized by the presence of MME.

Fault zone microstructures from laboratory experiments on calcite/talc binary mixtures

Giorgetti C.*¹, Carpenter B.M.² & Collettini C.¹

1. Dipartimento di Scienze della Terra, Sapienza Università di Roma. 2. INGV, Roma.

Corresponding email: carolina.giorgetti@uniroma1.it

Keywords: Talc/calcite mixtures, rock deformation experiments, friction.

Microstructures derived from rock mechanic experiments give insights into the deformation processes acting in natural fault gauges. Here we present microstructural analyses on structures developed in synthetic faults during laboratory deformation experiments. We sheared different mixtures of talc and calcite as powdered gouges, systematically increasing the talc content. Experiments were conducted at a normal stress of 5 MPa, under saturated conditions and at room temperature. We evaluated the reduction of friction with increasing talc content and, in addition, we performed slide-hold-slide tests, 1-3000 seconds, to measure the amount of frictional healing. At the end of the experiments, we collected samples and made thin sections, in order to assess the deformation mechanisms responsible for the observed mechanical behavior.

SEM investigations on the experimental faults indicate that deformation-induced microstructures are strongly controlled by the amount of talc. Pure calcite sample deforms via cataclastic flow, with grain rotation, translation, frictional sliding at grain contact, and minor amount of grain size reduction. With small amounts of talc, i.e. 5% and 10%, the overall deformation mechanism is cataclastic flow, with talc lamellae scattered in the bulk microstructure, partially coating calcite grains and iso-orienting themselves forming a “proto-foliation”. With the addition of 20% talc, the development of an interconnected network of talc lamellae throughout the sample results in frictional sliding along talc-rich shear planes as the predominant deformation mechanism.

Our microstructural analysis shows that increasing talc content results in a progressive microstructural organization, with maximum localization of deformation attained by the addition of 20% talc. These observations provide key information in interpreting the frictional behavior of talc-bearing fault gouges, with strong implications for the slip behavior of talc-bearing, carbonate faults.

Control of saturant's state upon intergranular adhesion affecting seismic and aseismic near surface site strength response inferred by combined V_p/V_s and Poisson's ratios examination

Hassan B.*¹, Butt S.¹ & Hurich C.²

1. Faculty of Engineering and Applied Science, Memorial University of Newfoundland, Canada.
2. Department of Earth Sciences, Memorial University of Newfoundland, Canada.

Corresponding email: p94bh@mun.ca

Keywords: V_p/V_s fluid effects, Poissons ratio sensitivity, V_p/V_s -Poissons ratio.

Velocities measure sediments/materials resistance to changes in any linear dimension or in shape i.e., V_p and V_s , discretely. They also, in principle, inform of source polarity controlled, compensatory deformation. A linear change in dimensions of an ideal elastic real material with definite geometry since is compensated by a coincident lateral strain when directly stressed, and vice versa. Conservative principles do hold in ideal and/or any non-ideal strain hysteretics. Compensatory effects are imperative to appropriate understanding of material behavior. They might be negligible but noticeable at macro-scale, at near micro-scale however, the variability of infinitesimal deformations are not only unidentifiable, signifying their proportionate magnitudes is not straight forward. Especially when their recurrence and decay aspects varying in magnitudes portend additional information about interactions of material's constituent's properties and any consequent change in them at those scales under cyclical stresses, as in saturated porous media. Advantage of composite V_p/V_s ratio thus lies in empirically quantifying material capability to recover direct deformation compared to shear deformation indirectly. Sensitivity of this ratio, with gravity bias excluded, to changes in adhesion and porosity, and any superimposed gravity allows isolate and infer lithology and pore fluid effects. Such effects have consequential implications upon structural strength of porous granular sediment/material matrix. Poisson's ratio conventionally means ratio of lateral deformation to the direct, in seismic restricted dynamic sense it has the meaning of V_p/V_s e.g., strengths, described response or variability of material deformational susceptibility to direct stress effects compared to those of shearing. Both V_p/V_s and poisson's ratios, so, provide specific "localized" information of control of saturant affected adhesion upon matrix dynamic structural strength behavior in unconsolidated sediments, which velocities alone may not. It is inferred in extended analysis of ultrasonically imaged immiscible displacement through simulated unconsolidated sediment in laboratory experiment (Hassan et al., 2014) that V_p/V_s of dry granular sediments when gas or air saturated could be quite low i.e., $<\sqrt{2}$. Liquid saturation, albeit, raises it to clearly discriminate and fix flow of immiscible saturants type and interfaces spatiotemporally. Poisson's ratios appearing negative provide critical information about higher susceptibility of such granular sediments strength to lateral shear stresses compared to direct, confirming an inherent liability/risk of landslide or liquefaction triggered site failure upon seismic or aseismic stimulation.

Hassan B., Butt S. & Hurich C. 2014. An assessment of S-waves potential for integrated geotechnical and geohydrological characterization and monitoring of near surface unconsolidated sediments for hazard prevention, Congress of SGI-SIMP, Abstracts, 662.

Understanding scale and direction dependent strength susceptibility of fault systems to seismic and aseismic effects by examining lateral and dilatational displacements characteristics using S-waves

Hassan B.*¹, Butt S.¹ & Hurich C.²

1. Faculty of Engineering and Applied Science, Memorial University of Newfoundland, Canada.
2. Department of Earth Sciences, Memorial University of Newfoundland, Canada.

Corresponding email: p94bh@mun.ca

Keywords: S-wave faults characterization, faults(V/H) spectral examination, fault rheology analysis.

Understanding strength susceptibility of near surface strata to seismic and non- and associated aseismic time rated directional stress effects is essential. Structural integrity and functioning, for, supported infrastructure upon direction and polarization dependence of ensuing dynamic loads, in scale and orientation sense is paramount. Response damage appearing as preferential, scale restricted, to either horizontal or vertical displacement is no rarity. Given the context, with results reported in Hassan et al., (2104) in hindsight, commensurating but peculiar renewed insights are presented. The sediment specimen, stack of six slabs (108 x 65 x 65, mm) with five equi-separated parallel fault interfaces was through transmitted by ultrasonic S-waves along the specimen long axis. Equi-incremented cyclical load i.e., 0-900 kg, was applied normal to fault planes in nine successions, and 1 MHz ultrasonic source and receiver, attached mirroring at specimen ends were rotated relative and together 0° through 360° in 30° step at each increment, for a multi-azimuth multi-component type acquisition. For the nature of configuration, S-wave time and stress dependent characteristics of lateral displacements and, non- and associated vertical dilatations are examined to better understand the effect and interplay of a sync-transmission of friction-restricted “slip” and friction-affected “dilatations”. Examination of displacements shows that laterally along interfaces they are stress- and shear-rate dependent while dilatations are only stress-rate dependent. It is inferred dilatations affect a friction reduction, exaggerating a lateral deformation however with stress increment/s friction “healing” type effect frustrates lateral deformation and pronounces/amplifies the dilatation effect across interfaces, occurring at each others expense. Lateral response is inferred visco-elastic marked by hardening-relaxation episode/s however dilatational appears elastic beyond initial “asperity settling”, with stress increments. Lateral relative shear displacements show spectral periodicity, though dilatations resonate uniquely. Spectral ratios, w.r.t. intact standard specimen (A1), examination shows that lateral displacements associated attenuation has a scale and direction dependent nonlinear anisotropic character, dilatational displacement attenuation but remains linear, interestingly. In conclusion, consideration of “scale” and “direction” dependence of fractured near surface and/or bedrock susceptibility to (V/H) deformation by “seasonality” of lateral seismic/aseismic effects for specifying localized site responses is essential. Exploiting S-waves sensitivity appears quite reliable for such realization.

Hassan B., Butt S. & Hurich C. 2014. Investigation of aseismic monitoring of near surface fracture systems by examining S-wave diffraction and interference spectral signature for geo-environmental hazard prognosis in coastal areas. Congress of SGI-SIMP, Abstracts, 642.

Deformation mechanisms of the shallow subduction plate interface of the Sestola Vidiciatico unit, Northern Apennines (Italy)

Mitterpergher S.*, Cerchiari A. & Remitti F.

Dipartimento di Scienze Chimiche e Geologiche, Università di Modena e Reggio Emilia.

Corresponding email: silvia.mitterpergher@gmail.com

Keywords: Megathrust, seismogenetic zone, microstructures.

Exhumed megathrust faults allow to investigate the deformation mechanisms active along subduction plate interfaces at depths far beyond the reach of scientific drilling (so far, < 1 km below sea floor). The Sestola-Vidiciatico Unit (SVU) in the Northern Apennines is interpreted as a subduction channel active during the early Miocene (Vannucchi et al., 2008). The SVU is a tectonic mélangé composed of blocks from the upper plate, overriding the turbidites deposited on top of the subducting plate. Based on previous field and mineralogic studies, the SVU reached temperatures < of 150 °C and depth of about 5 km (Vannucchi et al., 2008).

We characterized one exposure of the contact between the base of the SVU, here composed of green-gray deformed marls, and the foreland turbidites. We performed a mesoscale structural analysis, integrated with a systematic microstructural (optical, cathodoluminescence and Scanning Electron microscopy) and mineralogical (XRPD) characterization of the fault zone rocks.

The contact is lined by a less than 2 m thick fault zone, composed of multiple elongated domains juxtaposed along calcite shear veins. A layer of strongly foliated, dark gray siltstone shows “soft-sediment” deformation along diffuse synthetic shear bands, overprinted by calcite veins either parallel (shear veins) or roughly perpendicular (extensional veins) to the fault. Along the foliation, almost parallel to the fault, stress driven dissolution is pervasive, with shortening and folding of the extensional veins. The overlying block is composed of marls, with foliation planes spaced few centimeters apart, and oriented at low angle (about 15°) to the shear zone. At the microscale, the blocks between foliation planes are nearly undeformed. The foliated marls are cut by low angle normal calcite shear veins, in some cases exploiting foliation planes. A planar shear zone lined by a calcite shear vein and continuous for several tens of meters cuts across all other deformation structures.

The fault rocks within the SVU experienced different deformation styles from the seafloor down to the transition to the seismogenetic zone, which in active settings is thought to occur at about 5 km of depth. We identified relict structures of bulk deformation of poorly lithified sediments, overprinted by localization of the deformation along shear veins. Several features, such as foliation sub-parallel to the fault zone, conjugate normal shear veins, high-angle extensional veins, suggest that the megathrust behaved as a weak fault oriented at high angle to σ_1 .

Vannucchi P., Remitti F. & Bettelli G. 2008. Geological record of fluid flow and seismogenesis along an erosive subducting plate boundary. *Nature*, 451, 600-703.

Strain softening mechanisms in a regional scale shear zone: the Main Central Thrust Zone in the Mt. Makalu area (Eastern Nepal)

Montomoli C.*¹⁻², Iaccarino S.¹, Carosi R.³, Nania L.¹ & Lezzerini M.¹

1. Dipartimento di Scienze della Terra, Università di Pisa. 2. Istituto di Geoscienze e Georisorse, C.N.R. Pisa. 3. Dipartimento di Scienze della Terra, Università di Torino.

Corresponding email: chiara.montomoli@unipi.it

Keywords: Shear zone, Main Central Thrust, Himalaya.

Deformation in mountain belt at middle/deep crustal levels is quite often heterogeneous and localized in high-strain zone, i.e. ductile shear zones, with the development of mylonites. One of the largest worldwide shear zones is exposed in the Himalaya where the Main Central Thrust Zone (MCTZ), a km thick ductile (to brittle) shear zone, tectonically juxtaposes the medium- to high grade metamorphic rocks of the Greater Himalaya Sequence structurally above the low- to medium- grade metamorphic rocks of the Lesser Himalaya Sequence (Hodges, 2000). In this contribution we investigate the processes active during the MCTZ evolution in the Makalu area (Eastern Nepal) where Precambrian orthogneiss, locally known as Num-orthogneiss, are ductile sheared and structural analysis testifies how a progressive transformation from orthogneiss to micaschist, through a transitional zone, is present.

Quantitative textural evolution, bulk-rock major and trace element chemical changes and mineral phases chemical changes have been characterized studying representative samples from “pristine” orthogneiss, transitional zone and micaschist.

Kinematic indicators developed both at the meso and microscales, such as S-C fabric, rotated porphyroclasts and mica fishes point to a top-to the-south sense of shear. Kinematic indicators are progressively much more developed associated with changes of foliation morphology (from a spaced anastomosing schistosity to a continuous) starting from orthogneisses to micaschist.

ICP-MS trace elements data confirm the common protolith origin of the studied rocks. Quantitative modal phase variations have been investigated with image analysis techniques (on BSE-SEM images) pointing to a progressive disappearance of feldspars balanced by increasing of micas. This latter process is assisted by progressive increasing of XMg in white micas and of a transition from biotite to phlogopite. Major and trace elements comparison between less deformed rocks (“pristine orthogneiss”) and higher deformed ones (micaschist) have been computed using the Isocon method (Grant, 2005).

In summary, microstructural and geochemical analyses led to recognize a non-isochemical process of strain softening related to phase transformation (feldspar replaced by micas) enhanced by fluids infiltration and Mg metasomatism, which progressively favoured deformation localization within the MCTZ.

Grant A.J. 2005. Isocon analysis: A brief review of the method and applications. *Phys. Chem. Earth*, 30, 997-1004.

Hodges K.V. 2000. Tectonics of Himalaya and southern Tibet from two perspectives. *Geol. Soc. Am. Bull.*, 112, 324-350.

Development of petrofabric within the Kavala syn-tectonic pluton (NE Greece) and insights for the seismic behaviour of extensional shear zones

Punturo R.*¹, Cirrincione R.¹, Fazio E.¹, Fiannacca P.¹, Kern H.², Mengel K.³, Ortolano G.¹ & Pezzino A.¹

1. Dipartimento di Scienze Biologiche, Geologiche e Ambientali, Università di Catania. 2. Institut für Geowissenschaften, CAU Universität, Kiel, Germany. 3. Institut für Endlagerforschung, Technische Universität Clausthal, Germany.

Corresponding email: punturo@unict.it

Keywords: Petrophysics, seismic anisotropy, granodiorites.

The Kavala granitoid pluton (NE Greece), whose emplacement and deformation took place in the early Miocene, offers a peculiar opportunity for investigating the textural development related to the extensional shearing events which affected the evolution of the southern Rhodope Core Complex. In this view, one important aspect concerns the relationship between progressive deformation, correlated rock fabric and the distribution of seismic properties within the shear zone. To this aim, we studied the microstructural, compositional and petrophysical features of a mylonitic granitoid suite that testifies as deformation occurred at various extents. The main assemblage of sheared granodiorites is given by quartz, K-feldspar, plagioclase, biotite, white mica with subordinate chlorite and allanite. Feldspar porphyroclasts usually are enveloped by ribbon-like quartz and micaceous matrix. S-C-C' foliations developed during the shearing phase are quite common. Calculated and measured seismic properties of mylonite granodiorites pointed out that, despite the average compressional and shear wave velocity as well as density values are similar (average values: $V_p \sim 5.87 \text{ km s}^{-1}$, $V_s \sim 3.4 \text{ km s}^{-1}$, $V_p/V_s = 1.73$ and density = 2.65 g cm^{-3}), the V_p - and V_s -related seismic anisotropy becomes progressively marked from the least to the most deformed mylonite specimen (up to V_p anisotropy = 6.92%). This is due to the dramatic microstructural changes (e.g. mica strong alignment, development of quartz ribbons), which affect the velocity distribution within the mylonitic granitoids, since the highest P- and S-wave velocities become progressively oriented parallel to the foliation plane, whereas the lowest values are localised normal to foliation. The obtained results testify the textural control on the seismic properties and this holds important implications in the behaviour of high strain zones as potential seismic reflectors and on the source of seismic anisotropy. At the same time they provide an important link between microstructures, tectonics and distribution of seismic properties within a shear zone.

Carbonate-clay mixing in cataclasite during fault activity

Smeraglia L.*¹, Billi A.², Carminati E.¹⁻² & Cavallo A.³

1. Dipartimento di Scienze della Terra, "Sapienza" Università di Roma.

2. Istituto di Geologia Ambientale e Geoingegneria, CNR, Roma.

3. INGV, Roma.

Corresponding email: luca.smeraglia@uniroma1.it

Keywords: Fault, cataclasite, carbonate-clay mixing.

Natural faults produce granular wear material, known as gouge or cataclasite, as a function of shear and grinding along the slipping surfaces. The characteristics of fault gouge have been studied extensively in the field, laboratory, and numerical simulations in order to gain a better understanding of fault mechanics (e.g., Marone & Scholz, 1989). However, observations of natural fault gouges in active fault zones can still provide precious information about fault activity and mechanical processes acting during fault evolution. Here, we report detailed microstructural observations (optical and electronic microscopy) on natural fault rocks from the scarp of an active fault in carbonate rocks: the Tre Monti fault, in the Lazio-Abruzzi Apennines. This area is one of the most seismic regions in the Mediterranean area (e.g., L'Aquila Earthquake, Mw 6.3, 2009). We revealed, for the first time in this area, the occurrence within fault cataclasite of very comminute localization zones enriched with exotic material mostly composed of clays of the smectite group, minor biotite/muscovite, quartz, feldspar and other minerals. Clay minerals completely enwrap carbonate particles (<10 µm) and thick clay rich zones show fluid-like structures, carrying small carbonate particles in them. Previous studies in this area considered fault cataclasites to be composed only of carbonate wear material, smeared from pure limestones exposed in the footwall of the faults (Agosta & Kirschner, 2003). Chemical analysis confirmed that allogenic material derives from smearing and infiltration from clay-rich sedimentary sequences (Orbulina Marls Fm. and Flysch deposits.), within the fault zone. Moreover geophysical and geological studies revealed that Orbulina Marls and Flysch deposits occur in the hangingwall of the Tre Monti fault, buried beneath Plio-Pleistocene continental deposits (Cavinato et al., 2002), this evidence confirms our observations. Using field and microstructural data is possible to reconstruct the long-term evolution of a fault. Lithological juxtaposition during time, along a fault plane, can change the mechanical properties and fault strength by mixing of different lithologies progressively involved during fault activity. This mixing could control different deformation mechanism and earthquake potential, both in terms of nucleation and propagation. Further experimental studies will be performed to characterized frictional properties of natural mixture of clay rich fault gouges.

Agosta F. & Kirschner D.L. 2003. Fluid conduits in carbonate-hosted seismogenic normal faults of central Italy. *J. Geophys. Res.*, 108, 2221.

Cavinato G.P., Carusi C., Dall'Asta M., Miccadei E. & Piacentini T. 2002. Sedimentary and tectonic evolution of Plio-Pleistocene alluvial and lacustrine deposits of Fucino basin (central Italy). *Sed. Geol.*, 148, 29-59.

Marone C. & Scholz C.H. 1989. Particle-size distribution and microstructures within simulated fault gouge, *J. Struct. Geol.*, 11, 799-814.

Frictional strength and deformation microstructures of mineralogically controlled Serpentinites

Tesei T.*¹, Viti C.², Mugnaioli E.² & Collettini C.³

1. INGV, Roma. 2. Dipartimento di Scienze Fisiche, della Terra e dell'Ambiente, Università di Siena
3. Dipartimento di Scienze della Terra, Sapienza Università di Roma.

Corresponding email: telemaco.tesei@ingv.it

Keywords: Serpentine, friction, fault.

Serpentinites give insights into large-scale convergent margin processes because they are important constituents of faults in tectonic mélanges associated to subduction and strike-slip settings or in obducted tectonic slivers in collisional orogens (ophiolites), or along oceanic extensional detachments. For these reasons, it is important to understand the frictional properties of serpentine minerals that modulate these tectonic processes.

Friction of the three principal serpentine minerals, namely antigorite, lizardite and chrysotile, has been extensively investigated under a large variety of P-T-strain conditions. Lizardite and antigorite have been always reported to have high friction $\mu > 0.4$, whereas chrysotile has been reported to be frictionally weak $\mu < 0.3$. However, due to the ultrafine association of the different serpentine minerals in massive serpentinites, they cannot be easily separated. Conversely, in our tests, we extracted lizardite and antigorite from almost monomineralic veins from the Monte Fico ophiolitic shear zone (Elba island, Italy). We have tested the frictional properties of these mineralogically controlled serpentinite powders using a biaxial apparatus under various applied normal stresses and water-saturated conditions. Both lizardite and antigorite standards yield extremely low coefficients of friction, i.e. $\mu = 0.15$ and $\mu = 0.16$, respectively. In addition, we ran additional tests on mixed serpentinites, either foliated or massive, to test the role of inherited metamorphic/deformational fabric on the frictional properties.

We suggest that preferred orientation of lizardite and antigorite lamellae in localized shear zones, which mainly deform as non-dilatant Mode II cracks, is the cause of frictional weakness. These zones of isoriented flakes represent the analogue of monomineralic shear veins and coatings commonly found at the edge of massive serpentine bodies or serpentine-rich cataclasites in brittle fault zones. Our data therefore suggest inherent weakness of serpentinite-bearing faults and can explain the apparent weakness of some major tectonic features such as the San Andreas fault.

3D image analysis of deformation bands in porous carbonate grainstones

Zambrano M.^{*1-2}, Tondi E.¹⁻², Mancini L.³, Dinolfo G.⁴, Aibibula N.¹, Arzilli F.³⁻⁵ & Napoli G.⁴

1. Scuola di Scienze e Tecnologie - Sezione di Geologia, Università di Camerino. 2. Reservoir Characterization Project
3. Elettra-Sincrotrone Trieste S.C.p.A., Basovizza (TS). 4. Dipartimento di Scienze della Terra e del Mare, Università di Palermo. 5. Istituto Nazionale di Geofisica e Vulcanologia, Pisa.

Corresponding email: miller.zambrano@unicam.it

Keywords: Deformation bands, grainstones, X-ray computed tomography.

Recent studies based on field and laboratory data have documented the effects of Deformation Bands (DBs) in fluid flow in porous rocks. The hydraulic properties of porous carbonates rocks could change abruptly due to the presence of DBs. The inner structure of DBs could show high variability in terms of textural and petrophysical properties, which have been traditionally assessed with 2D microscopy techniques.

The aim of this work is to perform a quantitative 3D image analysis of the microstructure of DBs hosted in porous carbonate grainstones by using a non-destructive 3D-imaging technique. The experiments consisted of the synchrotron X-ray computed microtomography (micro-CT) characterization of rock samples prepared in small parallelepipeds (4x4x40 mm size) and corresponding to grainstones highly affected by DBs exposed in San Vito Lo Capo peninsula (Sicily, Italy), Favignana Island (Sicily, Italy) and Majella Mountain (Abruzzo, Italy). For the analysis, the data is segmented in two main components porous and solid phases. The properties of interest are porosity, connectivity, a grain and/or porous textural properties, in order to differentiate host rock, DBs and their inner structure.

The preliminary results of the quantitative X-ray micro-CT image analysis indicate trends of porosity and connectivity for host rock, DB and zones therein. San Vito Lo Capo's sample presents the most complex structure of DB, which is composed by three inner zones. Wherein, the porosity and connectivity are reduced from the outer to the inner zone of the DB due to grain compaction, cementation and grain size reduction. For the samples of Favignana Island and Majella Mountain, no differentiated zones within the DBs were found. However, for the Majella Mountain's sample we observed a low porosity zone surrounding the DB that could be the result of water interaction. In general, we noted that the porous space within DB is poorly connected and it is about five times less than in the surrounding host rock. The preliminary results presented in this study and future analysis may be helpful for better understanding the inner structure of deformation bands and their implications to fluid flow in porous carbonates.

Quantitative microstructural analysis of naturally deformed rocks as tool to understand tectono-metamorphic evolution

Zucali M.*¹, Spalla I.¹, Gosso G.¹, Chateigner D.², Ouladdiaf B.³, Tartarotti P.¹, Fontana E.¹, Mancini L.⁴ & Barberini V.⁵

1. Dipartimento di Scienze della Terra "A. Desio", Università di Milano. 2. Ecole Nationale Supérieure d'Ingénieurs de Caen (ENSICAEN), France. 3. Institut Laue Langevin, Grenoble, France. 4. Elettra, Sincrotrone Trieste S.C.p.A. 5. Dipartimento di Scienze Geologiche e Geotecnologie, Università di Milano-Bicocca.

Corresponding email: michele.zucali@unimi.it

Keywords: Shape Preferred Orientation, Lattice Preferred Orientation, geodynamic.

Microstructures are fundamental keys to the interpretation of geological processes at various scales and times. In this contribution we will discuss modern approaches to the quantification of microstructure parameters to investigate active processes, their physical conditions and geodynamic environment.

Two main parts constitute rock fabric: shape preferred orientation (SPO); lattice preferred orientation (LPO).

- The SPO may be quantified by means of **image analysis at 2D or 3D** by combining various orthogonal thin sections or by **X-ray synchrotron micro-tomography** allowing a real 3D investigation over a relatively small sample and permitting a EBSD-like analysis of fitting-ellipsoid orientations.

- The LPO quantification is performed by **neutron diffraction texture analysis** allowing a complete statistical coverage of large volumes of the order of 1 cm³ or by EBSD investigation more suited for localized analysis.

We will show the investigation of various cases of natural rocks from lower and middle crust under convergent and divergent geodynamic regimes, submarine volcanic lavas at IODP Hole at 1256D, turbidite sediments and building stones.

SESSION S8

Magma chamber dynamics and timescales of volcanic processes

CONVENORS

Lorella Francalanci (Univ. Firenze)

Carmelo Ferlito (Univ. Catania)

Guido Giordano (Univ. Roma Tre)

Claudia Romano (Univ. Roma Tre)

Massimo Pompilio (INGV)

Diego Perugini (Univ. Perugia)

Experimental constraints on pre-eruption conditions of the 1631 Vesuvius eruption

Bardeglinu I.¹⁻², Cioni R.^{*3} & Scaillet B.²

1. Dipartimento Scienze Chimiche e Geologiche, Università di Cagliari. 2. ISTO-CNRS, Orleans, France
3. Dipartimento di Scienze della Terra, Università di Firenze.

Corresponding email: raffaello.cioni@unifi.it

Keywords: Vesuvius, experimental petrology, geothermometry.

The knowledge of the range of possible styles of magmatic activity to be expected for a next reactivation at dormant active volcanoes as Somma-Vesuvius is a very challenging task, and a first order information in terms of volcanic hazard assessment and emergency planning. Magma composition and its general physical conditions strongly control the style of volcanic activity, directly influencing magma rheology, volatile content and style of degassing. Experimental petrology conducted on the products of past activity has been used as a tool for revealing the conditions of pre-eruptive magma crystallization, defining the general stability fields of the different mineralogical phases under different conditions of pressure P, temperature T and volatile fugacity (X) in the coexisting fluid phase. Evidence exists that after the famous AD 79 Pompeii eruption, a major change in the shallow magmatic system occurred, marked by the shallowing of the magma reservoir feeding the main eruptions. However, while the products of the AD 472 eruption have been the object of in depth studies aimed at defining PTX magma conditions, the products of the 1631 event are not still well studied in this respect. We present here data on the mineral phase stability for this very important eruption, aimed at fixing the expected range of magma composition and physical properties for this eruptive scenario. About 30 runs on natural tephritic phonolite were performed on an Internally Heated Pressure Vessel under controlled P, T X_{H_2O} and redox conditions. Phases identified include quenched glass (Gl), clinopyroxene (Cpx), leucite (Lc), biotite (Bt), plagioclase (Pl), and fluid (Fl), the latter as voids of 10-100 microns sizes evenly dispersed across the charge. Mineral sizes vary from a few tens of microns (Lc, Bt) down to a few microns (Cpx). In order to constrain pre-eruptive conditions, composition of glass and mineral phases was checked against data collected on natural samples. In particular, the occurrence of Bt in natural samples implies pre-eruptive T below 1000 °C. Experimental results also allowed tracing thermometric relationships based on Gl composition, which implement and improve those already existing.

Investigating heterogeneous magma systems by detailed characterization of the juvenile products: example from the Upper Pumice eruption at Nisyros Volcano (Greece)

Braschi E.*¹, Francalanci L.¹⁻² & Vougioukalakis G.³

1. Istituto di Geoscienze e Georisorse, C.N.R. Firenze. 2. Dipartimento di Scienze della Terra, Università di Firenze
3. Institute of Geology & Mineral Exploration, Athens, Greece.

Corresponding email: leonora.braschi@igg.cnr.it

Keywords: Mingling, Nisyros, pyroclastic deposits.

The last explosive activity on Nisyros Volcano (Dodecanese, Greece) was a sub-Plinian eruption emplacing a moderate volume (Longchamps et al., 2011) of pyroclastic products forming the Upper Pumice (UP) formation (Vougioukalakis, 1993). The deposits are scattered around the island, mainly to the north, where the whole sequence crops out, and are constituted by fallout and grain flow levels, at the base, interlayered with diluted pyroclastic density current (PDC) deposits to the top. The sequence is closed by a lag-breccia unit, overlaid by a final grey ash flow level.

The juvenile material is mainly characterized by white-yellow, quite crystalline pumices with rhyo-dacitic composition, forming more than 90 vol.% of the basal fallout deposit. Some amount (< 4%) of dense, grey, crystalline juvenile lapilli clasts, with rounded, globular shape and less evolved composition (dacite to andesite) are also present, dispersed into the fallout unit and PDCs. They show a large variability in density, crystal content and textures as well as type of contacts with the “host” pumices. In particular, many of them show peculiar dictyotaxitic structures characterized by a loose crystal network. On the contrary, the juvenile material of the lag-breccia is only constituted by dense, gray, crystalline bombs, with crenulate or bread crust surfaces and basaltic-andesite composition. They clearly have microcrystalline, dictyotaxitic textures. The compositional variability of the juveniles, both inside a single unit and along the entire sequence, is also shown by Sr isotopes, which vary from 0.70456 in pumice to 0.70420 in the crystalline bombs.

The presence of different juvenile products, erupted together, but physically separated, with distinct composition and isotopic signature, suggests the presence of two (or more?) variably evolved magmas in the UP reservoir, interacting each other and generating mingling.

We have performed a detailed field study of the UP deposits, with an accurate sampling of the different juvenile material on each different outcrop over the island, from the base to the top of the sequence. The aim is to accurately describe the compositional and textural variability of the erupted juveniles, especially focusing on the characterization of the dense, mafic, crystalline clasts and their relationships with the acid component. This combined approach is of fundamental importance to the understanding of the possible eruption trigger, to the reconstruction of the pre-eruptive conditions of the UP eruption as a possible model for similar context.

Longchamp C., Bonadonna C., Bachmann O. & Skopelitis A. 2011. Characterization of tephra deposits with limited exposure: the example of the two largest explosive eruptions at Nisyros volcano (Greece). *Bull. Volcanol.*, 73, 1337-1352.

Vougioukalakis G. 1993. Volcanic stratigraphy and evolution of Nisyros island. *Bull. Geol. Soc. Greece*, 28, 239-258.

Rheology and crystallization kinetics of the Pozzolane Nere tephriphonolite from Colli Albani volcano (Italy)

Campagnola S., Vona A.*, Romano C. & Giordano G.

Dipartimento di Scienze, Università di Roma Tre.

Corresponding email: alessandro.vona@uniroma3.it

Keywords: Rheology, crystallization kinetics, Colli Albani.

The Pozzolane Nere ignimbrite (PNR) represents one of the largest explosive events in the history of the Colli Albani volcano (407 ka, Vulcano Laziale period). The PNR is tephri-phonolitic in composition and is characterized by a basal scoria fallout deposit with an east-trending axis of dispersion overlain by a radial low aspect ratio ignimbrite, estimated at 30 km³ as bulk volume. High (1250–1569 °C) and low (690–800 °C) temperature viscosity measurements of the dry liquid relative to the fall-out phase were performed by a combination of concentric cylinder (10^{1.0} to 10^{3.6} Pa s) and micropenetration (10^{9.2} to 10^{12.2} Pa s) rheometry. Comparison with literature data reveals that while at high temperature viscosity seems to be strictly related to the polymerization degree of this melt, at low temperatures the dependency is not linear with values of viscosity higher than expected. *Subliquidus* isothermal crystallization experiments and viscosity determinations were carried out at high temperature (1150–1240 °C) in air using a concentric cylinder apparatus at constant shear strain rate (shear rate = 0.1 s⁻¹). Viscosity increases with decreasing temperature and consequent increasing of crystal fraction, that is constituted by almost exclusively leucite varying between $\phi = 0.06 - 0.34$. The inspection of products quenched at the end of the crystallization stage, defined when viscosity reaches constant values, reveals strong evidence of leucite clustering. After the first segment of experiment, performed at constant shear rate, a second stage of experiment at variable shear rate was performed, comprising an up (shear rate = 0.1 s⁻¹ - 0.9 s⁻¹) and a down (shear rate = 0.9 s⁻¹ - 0.1 s⁻¹) shear ramps. At the end of the down-ramp, leucite crystals appear sub-spherical and unclustered. For the same applied shear rate, the viscosity values of the up-ramp are not recovered in the experimental time-scale, indicating time-strain dependent rheology for these suspensions (namely thixotropy). While the down-ramp viscosity results are shown to be in perfect agreement with literature models, discrepancies between the up-ramp data and pre-existing predicting models have been observed. We suggest that this complex behavior is related to the clustering of leucite crystal during the crystallization process. The kinetics of crystallization (in terms of nucleation and growth rates) seems to be strongly affected by viscosity, degree of undercooling and dynamic flow conditions. Any modeling pertaining to tephriphonolite magma flow (either in conduit or subaerial) crystallization and emplacement should take into account the effects of stirring (flow) on the crystallization kinetics, and the influence of crystal clustering (and its disruption) on the velocity of a flowing lava.

Magmatic Processes Revealed by Textural and Compositional Features of Large Anorthoclase Crystals from the Lajes-Angra Ignimbrite (Terceira Island, Azores)

D'Oriano C.*¹, Landi P.², Pimentel A.³ & Zanon V.³

1. Istituto Nazionale di Geofisica e Vulcanologia, Palermo. 2. Istituto Nazionale di Geofisica e Vulcanologia, Pisa
3. Centro de Vulcanologia e Avaliação de Riscos Geológicos, Universidade dos Açores, Portugal.

Corresponding email: claudia.doriano@ingv.it

Keywords: Anorthoclase texture, trace elements, magma mixing.

We have studied the products of the most recent (~21 ka) caldera-forming event produced by Pico Alto volcano (Terceira Island, Azores) in order to reconstruct the pre- and syn-eruptive magmatic conditions. Stratigraphic succession consists of a thin crystal-rich basal layer, overlaid by a fine-grained welded lapilli-tuff layer and an upper partially welded coarse clast-bearing layer. Juvenile clasts are porphyritic comenditic-trachyte, ranging from highly vesicular pumice to dense scoriae. This study has been carried out using a combination of textural and compositional analyses, performed by linking CL (cathodoluminescence) and BSE imaging and *in-situ* major and trace elements analyses of anorthoclase phenocrysts and groundmass glasses. Groundmass glasses are characterized by different degrees of evolution, although remaining within the field of trachytes. Chemical variations reveal that the deposit of the eruption corresponds to a reversed magma chamber, with the most evolved products at base and less evolved products at the top. Mineral assemblage mainly consists of anorthoclase (Ab₆₄₋₇₀, An_{<7} mol%), and less abundant olivine (Fo₂₈₋₄₅), clinopyroxene (En₆₀₋₈₀Fs₂₀₋₄₀), ilmenite and magnetite. Anorthoclases range in size from < 2mm in basal layer, up to 4-5 mm in the partially welded upper layer. Basing on the description of phenocrysts's pattern zoning, two types of anorthoclase phenocrysts have been distinguished. Type 1 phenocrysts occur in all the studied samples with different abundances and are idiomorphic with elongated, rectangular shape, and are either inclusions-free or can include small, rounded glass inclusions with a single shrinkage bubble. Type 2 crystals, present in all samples except for the crystal-rich basal layer, are tabular and often show disequilibrium features, such as embayments and reaction rims. The most of the core of these crystals host irregular pockets, several hundreds of μm large, filled with vesicular glass. The vesicular glass in the pockets is a comendite-trachyte with composition quite similar to that of the matrix glass. CL imaging spectroscopy reveals that type2 crystals are patchy-zoned, with resorbed cores and inclusions-free rims (100-300 μm). LAM-ICP-MS analyses highlighted a large trace-element compositional variation, which is also evident at the scale of the single crystal. Textural and compositional features of the different types of crystals evidence that the history of crystallization of magma feeding the eruption was complex and that the crystals moved within the reservoir being in contact with melts with different degrees of evolution, producing disequilibrium textures and reverse to direct zonings. We suggest that Type 1 crystals are associated with the magma chamber evolution and dynamics which involve equilibrium crystallization on the wall of the chamber, related to chemical and thermal convection. Instead, Type 2 crystals record disequilibrium processes related to refilling of the shallow reservoir and magma mixing. The oscillatory zoning commonly observed in the large rims show that after the main event (or events) of refilling, the crystals experienced repetitive change in the melt-solid equilibrium. Similarly to what we saw in Type 1 anorthoclase, oscillatory zoning is likely related to thermal/chemical convection inside a zoned magma chamber able to moving the crystal through different zones of the chamber. The last event of refilling could be the trigger of the eruption, during which magma depressurization by degassing and vesiculation occurred.

The Lipari-Vulcano volcanic complex: insights into the plumbing system of the last 1000 years

De Rosa R.*¹, Di Salvo S.², Donato P.¹, Francalanci L.², Gioncada A.³, Nicotra E.⁴, Pistolesi M.³,
Viccaro M.⁴, Barca D.¹ & Braschi E.²

1. Dipartimento di Biologia, Ecologia e Scienze della Terra, Università della Calabria. 2. Dipartimento di Scienze della Terra, Università di Firenze.
3. Dipartimento di Scienze della Terra, Università di Pisa. 4. Dipartimento di Scienze Biologiche, Geologiche ed Ambientali, Università di Catania.

Corresponding email: derosa@unical.it

Keywords: Plumbing system, trace elements in minerals, micro-Sr isotopic data.

New whole rock and microanalytical data on mineral phases provide constraints for a comprehensive model of the Lipari-Vulcano plumbing system, at least during the last 1000 years.

The eruptive activity between 1100-1200 AD represents an important phase of the Lipari-Vulcano volcanic complex (LVVC) for several reasons: 1) fairly contemporaneous activity at Vulcanello and Fossa vents at Vulcano island and at Rocche Rosse on Lipari island, along a common N-S alignment; 2) simultaneous eruptions at Lipari and Vulcano at 1230±40 AD; 3) since this date latitic products, associated or not with rhyolitic magmas, have always been erupted with variable eruptive styles and volumes.

Shoshonitic products erupted at Vulcanello at the end of XII century are the least differentiated of the last 1000 years. Whole rock, mineral phase and mineral-hosted melt inclusion data show that latitic products emitted at both islands have several geochemical affinities. In particular, latites show superimposed trends of REE and incompatible elements for whole rock and all mineralogical phases. Whole rocks Sr-Nd isotopic data indicate that Vulcano and Vulcanello latites are intermediate between those of Lipari, with poor Sr-Nd isotope correlation. Micro-Sr isotopic data performed by microdrilling techniques (Micromill + TIMS instruments), on clinopyroxenes, plagioclases and groundmasses belonging to the Pietre Cotte lava flow (1720 AD) and 1888-90 products of La Fossa eruptions show small but consistent variations of Sr isotopes (0.70458-0.70492), which increase from plagioclase core to rim and then groundmass. These variations can indicate: i) mixing with more Sr-radiogenic magmas; ii) crustal contamination; iii) crystal recycling from a crystal mush related to the previous and less Sr-radiogenic activity of Vulcano.

Textural observations and core-to-rim profiles on plagioclases show that dynamics of magma ascent and storage are markedly different in the Fossa and Vulcanello system of Vulcano. Transfer mechanisms are however almost unchanged in each system during the considered timespan. Petrological data suggest that the historical eruptions of Lipari and Vulcano islands could be fed by a common plumbing system at depth, hosting shoshonitic basalts to shoshonites. Shoshonites were erupted only at the end XII-early XIII century AD (e.g. early Vulcanello). Magma ascent occurred through a polibarc storage system allowing the eruption of mafic and prevalently degassed magmas (Vulcanello), but also the repeated storage and differentiation to latites and rhyolites at intermediate and very shallow depth (late Vulcanello, La Fossa and Rocche Rosse at Lipari). Differentiation models suggest that latites can be obtained by AFC process starting from the shoshonite. Latites are the prevalent magmas erupted in historical times and are always involved in the rhyolitic eruptions, indicating the recurrent occurrence of mingling following refilling events.

Understanding the last 3600 years plumbing system evolution of Santorini volcano: contributions by *in-situ* micro-Sr isotope data

Di Salvo S.*¹, Francalanci L.¹, Braschi E.², Avanzinelli R.¹ & Druitt T.H.³

1. Dipartimento di Scienze della Terra, Università di Firenze. 2. Istituto di Geoscienze e Georisorse, C.N.R. Firenze. 3. Laboratoires Magma Et Volcans, Université Blaise Pascal, Clermont-Ferrand, France.

Corresponding email: sara.disalvo@stud.unifi.it

Keywords: Santorini, micro-analyses, enclave.

Petrogenetic processes such as magmas interaction and crustal contamination can be investigated by micro-Sr isotope analyses in minerals because the latter are able to retain the history of physical and chemical changing conditions during their growth. In this light micro-quantity analyses play a key role in the understanding of magmatic system. In particular, analyses of $^{87}\text{Sr}/^{86}\text{Sr}$ on core-rim traverses of minerals give us the chance to understand the dynamics and timescales of magmatic processes during the ascent of magma to the surface. We investigated the plumbing system evolution of the Santorini volcano (Greece) during the last 3.6 ky, after the occurring of the catastrophic, caldera-forming Minoan eruption. In particular, we focused our studies on dacitic lavas of the first and last post-caldera subaerial Kameni activity (46-47 A.D. and 1950 A.D., respectively), also comparing the obtained data with those analyzed in the previous Minoan volcanic products. Basaltic to andesitic magmatic enclaves are included in these lavas and Sr isotopes increase with time in both enclaves and host lavas. We have performed Sr and Nd isotope data of mafic enclaves and textural, compositional and micro-Sr isotope analyses of plagioclase crystals in post-caldera lavas. The isotope data on enclaves have contributed to better define the crustal contamination processes occurring in the mafic magmas feeding the silicic system. Micro-Sr isotopes on plagioclase, analyzed by microdrilling technique, agree with the previously proposed Kameni plumbing system (Conticelli et al. 1998; Francalanci et al. 1998; Petrone et al. 2013) represented by a zoned magma chamber where a resident dacitic magma interacts with small input of mafic magma by mixing and mingling processes. $^{87}\text{Sr}/^{86}\text{Sr}$ values of plagioclase do not largely change within the single eruptive event and generally reflect the respective whole-rock values, except for some xenocrysts in Kameni lavas coming from the mafic enclaves. Our data suggest that the Kameni plagioclases record a short history, indicating small resident time and possible crystallization during the magma ascent. Comparison with micro-Sr isotope data performed on plagioclases of Minoan pumices indicates this system has no relationships with the huge magma reservoir of the previous explosive Minoan activity.

- Conticelli S., Francalanci L., Santo A.P. & Petrone C. 1998. Mineral chemistry data as a contribution to the understanding of the post minoan magmatic system of Santorini, Greece. The European laboratory Volcanoes, Proceedings of the second workshop, Science Research Development EUR 18161 EN, 157-174.
- Francalanci L., Vougioukalakis G., Eleftheriadis G., Pinarelli L., Petrone C., Manetti P. & Christofides G. 1998. Petrographic, chemical and isotope variations in the intracaldera post-minoan rocks of the santorini volcanic field, Greece. The European laboratory Volcanoes, Proceedings of the second workshop, Science Research Development EUR 18161 EN, 175-186.
- Petrone C.M., Francalanci L. & Vougioukalakis G.E. 2013. Mixing, mingling and enclave crumbling in the post-Minoan dacitic magmas of Santorini volcano, Greece. Mineralogical Magazine, 77(5), Goldschmidt 2013 Conference, August, Firenze, Italy, Abstracts, 1959.

Pre-eruptive magmatic processes associated with the historic explosive activity of Kolumbo submarine volcano, Santorini, Greece: a petro-chemical study on the emitted products

Fantozzi I.*¹, Petrone C.M.², Vougioukalakis G.³, Braschi E.⁴ & Francalanci L.¹

1. Dipartimento di Scienze della Terra, Università di Firenze. 2. Department of Earth Sciences, The Natural History Museum of London, UK. 3. Institute for Geology and Mineral Exploration (IGME), Athens, Greece.
4. Istituto di Geoscienze e Georisorse, CNR, Firenze.

Corresponding email: iacopo.fantozzi@gmail.com

Keywords: Mixing, kolumbo, submarine.

Kolumbo submarine volcano, located 7 km northeast of Santorini in the Aegean Sea, last erupted in 1650 AD with submarine and subaerial explosive activity. Twenty-eight samples of pumices, lavic lithic and mafic enclaves were collected during two submarine expeditions in 2006 and 2010 from the main cone and some secondary cones. All samples mainly belong to the 1650 AD eruption. Petrography, mineral chemistry and whole rock geochemistry (major and trace elements, Sr and Nd isotopes) have been undertaken on all samples with the final aim of understanding magma evolutionary processes and triggering mechanism of the 1650 AD eruption.

Rhyolitic pumices and mafic enclaves, with basaltic andesite composition, represent the juvenile components emitted during the eruption, whilst lithics represent samples of lavas emitted during previous unknown eruptions and having variable compositions (andesite to rhyodacite). Pumices are heterogeneous in color, density and texture ranging from highly vesicular white pumices to low vesicular grey lithotypes. Banded white - dark grey pumices are also present.

Plagioclase, biotite, orthopyroxene and amphibole are the main mineral phases of the pumices, whilst plagioclase, clinopyroxene, amphibole and rare olivine are found in the mafic enclaves.

Sr and Nd isotopes indicate that magmas, in the plumbing system of Kolumbo, evolved through processes of crustal assimilation coupled with fractional crystallization (AFC).

Geochemical and isotopic analyses indicate, however, that not all magmas are cogenetic, recognizing at least two different groups. The 1650 AD rhyolitic magmas cannot be derived by AFC from the rhyodacitic magmas of lithic, suggesting the presence of different reservoirs in the plumbing system of Kolumbo. In addition, our data indicate that mafic magmas have undergone compositional changes in time. Indeed, the most mafic lithic lavas have lower incompatible trace elements contents and $^{87}\text{Sr}/^{86}\text{Sr}$, and higher values of $^{143}\text{Nd}/^{144}\text{Nd}$ in respect with the 1650 AD mafic magma.

The presence of banded pumices and mafic enclaves clearly point out to mixing and mingling processes. Matrix glasses composition also support the evidence of mixing processes. Indeed grey glasses show intermediate compositions between white and black zones both for isotopes and major and trace elements. Several inputs of mafic magmas are supported by compositional changes of mafic magmas. Early arrivals mixed with rhyolitic magma, creating the banded pumices, whereas only mingling processes are recognized toward the end of the eruption as testified by the mafic enclaves.

The most likely hypothesis suggests that the plumbing system of Kolumbo is composed of two magma chambers maybe located at different depth.

The 1650 AD explosive eruption was fed from the shallower magma chamber where mixing/mingling processes, possibly triggering the eruption, took place.

Magma dynamics of the 2000 Miyakejima eruption inferred from textural analysis of erupted products

Garozzo I.*¹, Romano C.¹, Giordano G.¹, Geshi N.² & Vona A.¹

1. Dipartimento di Scienze - Sezione geologia, Università di Roma Tre. 2. AIST, Geological Survey of Japan.

Corresponding email: ileana.garozzo@uniroma3.it

Keywords: Volcanic ash, textural analysis, eruptive dynamics.

Miyakejima Volcano is a basaltic-andesite stratovolcano active from ~10.000 years, located on the north of the Izu-Bonin arc. During the last 600 years the volcano has been characterized mainly by flank fissure activity, with explosive phreatomagmatic eruptions on the coastal areas. In the last century, the activity became more frequent and regular with intervals of 20 to 70 years (1940, 1962, 1983 and 2000). The last activity started on 27 June 2000, with a minor submarine eruption on the west coast of the volcano, and proceeded with six major summit eruptions from July 8 to August 29. The eruptions led to the formation of a collapse caldera ~1.6 km across. The total erupted tephra represents only 1.7% in volume of the caldera and it is mainly constituted by fine-grained volcanic ash. In order to improve the understanding on the triggering and dynamics of this explosive eruption, we carried out a detailed investigation of the erupted materials with particular attention to the textural features of juvenile pyroclasts (Vesicle and Crystal Size Distributions). The stratigraphic record can be divided into six fall units, corresponding to the six summit eruptions, although juvenile materials were identified only in 4 units (unit 2, 4, 5, 6). We selected about 100 juvenile grains sampled from the bottom to the top of each level, to be analyzed by scanning electron microscopy. The study of juvenile morphological features allowed us to recognize the existence of two characteristic morphotypes, showing marked differences in their external morphologies and internal textures (from poorly to highly crystallized and vesiculated clasts). The distribution of these morphotypes is non-homogeneous along the eruptive sequence indicating changes of dynamics during magma ascent. Juveniles do not show features inherited from the interaction with external water. Vesicle Volume Distributions of the selected ash grains show that the two types of pyroclasts experienced different nucleation and growth processes. Also the Vesicles Number Densities (VNDs) vary of about one order of magnitude in the different populations (from 10^7 to 10^8 cm⁻³), with values comparable with those commonly related to sub-Plinian and Plinian eruptions. Data from the CSD analysis show perfect agreement with the measured VNDs (crystal population densities increasing with VNDs), suggesting a link between the degassing history and the syn-eruptive crystallization. Insights on the eruptive dynamics leading to this high - energetic eruption are presented in the light of the results of the textural analysis.

Textural and chemical zoning of clinopyroxene and plagioclase as a tool to calculate the thermobarometric constraints of Mt. Etna feeding system

Giacomoni P.P.*¹, Coltorti M.¹, Ferlito C.² & Mollo S.³

1. Dipartimento di Fisica e Scienze della Terra, Università di Ferrara. 2. Dipartimento di Scienze Biologiche, Geologiche e Ambientali, Università di Catania. 3. INGV, Laboratorio HT-HP, Roma.

Corresponding email: pierpaolo.giacomoni@unife.it

Keywords: Phenocrysts zoning, geothermobarometry, feeding system.

Clinopyroxene (Cpx) and plagioclase (Plg) are common phenocrysts in lavas at Mt. Etna volcano (Sicily, Italy) and best candidates to describe physico-chemical processes occurring along the entire path of magma ascent.

This study investigates the stability fields of Cpx and Plg and their dependence on the intensive variables of the magmatic system: pressure (P), temperature (T), volatile contents (H₂O) and oxygen fugacity (fO₂). Thus, we have analysed mineral chemical and textural zoning and defined the P-T-H₂O path of magmas through thermobarometric, hygrometric and oxybarometric calculations.

Both Cpx and Plg show core-to-rim compositional variations and dissolution-regrowth processes. The textures of Cpx can be classified in five types: i) normal zoning or oscillatory; ii) Fe-rich rim; iii) Sieved core; iv) Reverse zoned; v) Reverse zoned with dusty rim. Plg textures and zoning were divided in two groups as a function of textures observed at the core (simple rounded, sieved, dusty) and at the rim (dusty, melt inclusion alignments).

P estimates indicate that the early nucleation of Cpx cores started at 1.1 GPa with the majority of crystals forming between 600 and 400 MPa and proceeding up to shallow levels (< 100 MPa). Cpx with Fe-rich rim (Type ii) formed at < 400 MPa, while reverse zoning and dusty rim occurred between 400 and 800 MPa. The comparison between Cpx and Plg dissolution-regrowth textures suggests that most of these processes occurred between 4 and 8 km b.s.l.

As a whole, the feeding system appears continuous and vertically extended where mantle-derived magmas with variable water contents (0.4 to 3.6 wt.%) crystallize Cpx in an oxidized system (av. +1.5 QFM). Plg nucleation and growth is driven by volatile loss and mixing between degassed and undegassed magmas.

Calderas and magma reservoirs

Giordano G.*¹ & Cashman K.²

1. Dipartimento di Scienze, Università Roma Tre. 2. School of Earth Sciences, University of Bristol, UK.

Corresponding email: guido.giordano@uniroma3.it

Keywords: Magma reservoirs, calderas, ignimbrites.

Large caldera-forming eruptions have long been a focus of both petrological and volcanological studies; traditionally, both have assumed that eruptible magma is stored within a single long-lived melt body. Over the past decade, however, advances in analytical techniques have provided new views of magma storage regions, many of which provide evidence of multiple melt lenses feeding a single eruption, and/or rapid pre-eruptive assembly of large volumes of melt. These new petrological views of magmatic systems have not yet been fully integrated into volcanological perspectives of caldera-forming eruptions. We discuss the implications of syn-eruptive melt extraction from complex, rather than simple, reservoirs and its potential control over eruption size and style, and caldera collapse timing and style. Implications extends to monitoring of volcanic unrest and eruption progress under conditions where successive melt lenses may be tapped. We conclude that emerging views of complex magma reservoir configurations provide exciting opportunities for re-examining volcanological concepts of caldera-forming systems.

Experimental determination of major and trace element diffusivities in natural silicate melts: application to magma mixing and determination of timescales of volcanic eruptions

González-García D.*¹, Zezza A.¹, Vetere F.¹, Behrens H.², Morgavi D.¹, Petrelli M.¹ & Perugini D.¹

1. Dipartimento di Fisica e Geologia, Università di Perugia. 2. Institut für Mineralogie, Leibniz Universität Hannover, Germany.

Corresponding email: diego.gonzalez@studenti.unipg.it

Keywords: Eruption timescales, magma mixing, diffusion.

Magma mixing has been recognized as a key process in the generation of the wide compositional variety of igneous rocks in the Earth and in the triggering of some highly explosive volcanic eruptions. When two magmas of contrasting composition interact, mass exchange by diffusion starts between them, a process that can potentially shed light into the time extent of magma interaction processes in magma chambers prior to eruptions. Previous experimental works coupled with diffusion modeling have demonstrated their potential when applied to eruptions in Campi Flegrei.

In order to achieve these goals, a set of diffusion coefficient data for major and trace elements in silicate melts is necessary, which can be applied to problems involving natural melts. However, the currently available set of data, while voluminous, is not systematic and shows a wide disparity in experiment conditions and melt composition, a significant part of which are synthetic. As an example, in the rare earth element group only La has diffusion data in basaltic compositions.

In the present research we aim at obtaining a consistent dataset of diffusion coefficients in a range of P-T-X(H₂O) conditions in natural silicate melts. A set of diffusion couple experiments will be carried out, using a shoshonite (Vulcanello lava platform) and a rhyolite (Pietre Cotte lava flow, Vulcano) as starting materials, in both dry and water-bearing conditions. Glass cylinders of the previously powdered and melted samples are subject to pressure of 3 kb and temperature of 1200 °C during times ranging from 2 to 8 hours, followed by a rapid quench. The diffusion profiles are then analyzed by IR spectroscopy, EPMA and LA-ICP-MS to obtain H₂O, major and trace element abundances, respectively.

High-resolution geochemical mapping of volcanic ash: Constraining of end-member proportions for syn-eruptive magma mixing of 2010 Eyjafjallajökull eruption

Laeger K.¹, Petrelli M.*¹, Andronico D.², Scarlato P.³, Cimarelli C.⁴, Del Bello E.³, Misiti V.³,
Taddeucci J.³ & Perugini D.¹

1. Dipartimento di Fisica e Geologia, Università di Perugia. 2. INGV, Catania. 3. INGV, Roma.
4. Department of Earth and Environmental Sciences, Ludwig Maximilians Universität, Munich, Germany.

Corresponding email: maurizio.petrelli@unipg.it

Keywords: Magma mixing, melt fractions, high resolution LA-ICP-MS analysis.

The April-May 2010 eruption of the Eyjafjallajökull volcano (Iceland) has become a benchmark for the understanding ash-dominated eruptions. In this work we investigated volcanic ash collected at different locations during the terminal stage of the eruption (18.-23.05.10). The compositional variability of glass compositions, based on 181 data points on 11 samples, claims for syn-eruptive magma mixing. The glasses show continuous evolving trends from trachyandesite to rhyolite (57.13-70.78 wt.% SiO₂). Compositional histograms of MgO, FeO, SiO₂ and CaO and a few trace elements show two populations of concentrations, while Na₂O, Al₂O₃ and K₂O display a single bell-shaped pattern. Numerical simulations of chaotic magma mixing have been performed. Results indicate that the initial stages of magma mixing are dominated by the presence of two compositional populations that, with the passing of time, merge into a single bell-shaped pattern, as for the natural samples. The maximum of the single bell-shaped pattern corresponds to the hybrid composition. In addition, at the same time, while the slow diffusing elements show two compositional populations, the fast diffusing ones display a single peak. Comparing our simulations with natural data we infer that, as Na₂O, Al₂O₃ and K₂O show a single compositional peak, they provide indication about the hybrid composition. Based on the classic two end-member mixing equation we estimated that the initial fractions of end-members were of the order of 0.5 felsic and 0.5 mafic. In conclusion, we show that the combination of high-resolution geochemical mapping of volcanic ash and numerical simulations can provide unprecedented information about end-members fractions. This is essential in order to constrain eruption dynamics and the kinetics of syn-eruptive mixing. Trace element determinations are in progress and will provide stronger constraints about the envisaged processes at Eyjafjallajökull volcano during the 2010 eruptive activity.

Temporal evolution of magma mixing related to the explosivity of volcanic eruptions

Mari N.

Department of Geological and Mining Engineering and Sciences, Michigan Technological University, USA.

Corresponding email: nmari@mtu.edu

Keywords: Magma mixing, volcanic explosivity, disequilibrium textures.

Eruption explosivity dynamics is targeted in volcanic research and observations including magma mixing have illuminated modifications in eruptive style. In this work we investigate whether microscopic evidences for magma mixing can be used to explain variation in explosivity and eruptive style of volcanic eruptions.

Can mixing evidence be related to eruption intensity at a specific volcano? Can this be related to the timing of mixing? In this research two basaltic volcanoes (Pacaya and Fuego, Guatemala) were selected, each with variable eruptive style and intensity in order to see if ejecta and lava flows show mixing effects with similar and correlative variability. We used the Volcanic Explosivity Index (VEI) as an indicator of intensity and selected samples of variable VEI from 0 to 4, both lava flow and tephra.

By textural and chemical analyses a great variability of mixing textures were detected: sieve-plagioclase, boxy-cellular plagioclase, spongy-cellular plagioclase, embayed olivine, sieve-olivine, resorption rims. Plagioclase disequilibrium textures evolve from boxy to sieve and spongy texture as the explosivity increase, while olivine evolve with a linear increasing in the depth and width of the embayments, the width of the resorption rims, and the quantity of broken crystals. Some of these textures are comparable with textures found in other eruptions with the same intensities at other volcanoes.

Through the physicochemical interpretations of these textures, we propose a model about the mixing residence time. Boxy-cellular plagioclase appear to be the texture with the minor residence time prior to the eruption, while sieve and spongy textures in plagioclase are due to heating by recharge events with a primitive melt, spending more time in the magma chamber. Broken crystals are, instead, the product of syn-eruption decompression due to severe events. As a further confirmation of this, the plagioclase CSD analysis show that the residence time of the samples in the shallow magma chamber increase from VEI 0 to VEI 2.

As a result, this study could assert that the relative magma mixing-to-eruption timing is directly proportional to the explosivity of the volcanic event. These considerations could be useful for interpreting deposits of a sequence of deposits, to deduce how conditions changed during a past event.

Timescales of mixing from diffusion chronometry on alkali feldspar phenocrysts from the Agnano-Monte Spina Eruption (4.7 ka), Campi Flegrei (southern Italy)

Mazzeo F.C.^{*1-2}, Fedele L.², Iovine R.³, Aienzo I.⁴, Cavallo A.⁵ & D'Antonio M.²

1. Dipartimento di Fisica "E.R. Caianiello", Università di Salerno. 2. Dipartimento di Scienze della Terra, dell'Ambiente e delle Risorse, Università di Napoli "Federico II". 3. Geowissenschaftliches Zentrum, Georg-August-Universität, Göttingen, Germany. 4. Istituto Nazionale di Geofisica e Vulcanologia, Osservatorio Vesuviano, Napoli. 5. Istituto Nazionale di Geofisica e Vulcanologia, Roma.

Corresponding email: famazzeo@unisa.it

Keywords: Diffusion chronometry, Ba in sanidine diffusion, magma chamber recharge.

Knowledge of the timescales of magma processes, including rising, stagnation and mingling/mixing occurring in the shallow plumbing system, is crucial for the volcanic hazard assessment of an active volcano. A powerful tool to this purpose is the high spatial resolution analysis of major-, minor- and trace elements on zoned phenocrysts, leading to the definition of the diffusion profiles for some key-elements. The Campi Flegrei (southern Italy) is a volcanic district whose active portion is presently inhabited by ~500,000 people and therefore exposed to a very high risk. The application of geochronometric investigations to the Phlegrean volcanism could be thus of notable impact in the mitigation of the volcanic risk related to such a hazardous site. The present study has concentrated on the products of the Agnano-Monte Spina eruption (A-MS, 4.7 ka), the highest magnitude event in the Campi Flegrei recent activity (VEI = 4, 0.85 km³ D.R.E. of emitted magma). The A-MS eruption has been fed by trachytic magmas whose variable ⁸⁷Sr/⁸⁶Sr and trace elements compositions suggest mixing between two different batches. Its volcanological and petrological features make this eruption as a good case-study for the investigation of magma-chamber dynamics, as well as a reliable reference-event for possible future eruptions. The investigated A-MS samples are pumice fragments from which double-polished, 100 μm-thick thin sections have been prepared for the analytical investigations. Back-scattered electrons (BSE) images have been acquired at the scanning electron microscope (SEM) in order to identify alkali feldspar phenocrysts suitable to be analyzed, selected among those in which the zoning pattern is more evident. Alkali feldspar compositions have been determined through combined energy-dispersive and wavelength-dispersive system electron microprobe analyses (EDS-WDS-EMPA) on transects crossing the growth zones of the selected phenocrysts. This allowed to reconstruct the diffusion profiles of Ba and Sr through the growth zones, which combined with BSE observations, were used to construct diffusion models aimed at estimating the timescales of magma processes. The BSE imaging of A-MS alkali feldspars revealed complex zoning and resorption features that might be related to mixing events, thus deserving further investigations. The preliminary time estimates obtained are in the range of 35-183 years. These values can be interpreted as the time required for the magma to collect in the shallow reservoir (2-4 km) prior to the eruption.

Morphochemistry of Structures Produced by Mixing of Rhyolitic and Basaltic Melts: Volcano-Petrological Implications

Morgavi D.*¹, Perugini D.¹, De Campos C.², Ertl-Ingrisch W.² & Dingwell D.B.²

1. Dipartimento di Fisica e Scienze della Terra, Università di Perugia. 2. Department of Earth and Environmental Sciences, Ludwig-Maximilian-University (LMU), München, Germany.

Corresponding email: daniele.morgavi@unipg.it

Keywords: Rhyolite, basalt, mixing.

In this work we present results from a time series experiments performed by mixing two natural melts at high temperature with an high viscosity contrast, using a recently developed apparatus able to trigger dynamics mixing in a magmatic system, as observed on natural outcrops. The morphology of mixing patterns at different times is quantified by measuring their fractal dimension and a linear empirical relationship is derived between mixing time and morphological complexity. Moreover the complexity of mixing patterns is also compared to the degree of homogenization of chemical elements during mixing and experiential relationships are established between the fractal dimension and the variation of concentration variance of chemical elements in time.

Several concepts and potential new tools to study the magma mixing process unfold from the experimental results presented in this work: i) the mixing patterns are fractal and they can be quantified by measuring their fractal dimension; this represents a further step in the quantification of the magma mixing process starting from the analyses of the mixing patterns; ii) the linear relationship between the fractal dimension of the mixing patterns and mixing time may open new fields of research with important volcanological implications: the analyses of the morphology of mixing patterns on volcanic rocks could be complemented by experiments performed with the end-members recognized on outcrops build a new chronometer to estimate the mixing-to-eruption time; iii) the relationships between the fractal dimension of mixing patterns and concentration variance represent the first morphochemical study in igneous petrology: this may allow to make inferences about the compositional variability that should be expected on rock suites and the relative mobility of chemical elements during the time progression of the process by analysing the morphology of mixing structures in the rocks.

The geochemical evolution of the Fogo A eruptive sequence: timing of development of anti-rapakivi textures and implications for dual magma source or zoned magma chamber models

Pensa A.*¹, Jowitt S.M.¹, Giordano G.² & Cas R.A.F.¹

1. School of Earth, Atmosphere and Environment, Monash University, Australia. 2. Dipartimento di Scienze, Università Roma Tre.

Corresponding email: alessandra.pensa@monash.edu

Keywords: Anti-rapakivi texture, magma mixing/mingling, intraplinian ignimbrite.

The 4.6 ka Fogo A eruption, São Miguel, Azores provides insight into the relative timing of magmatic processes; these deposits record inverse compositional zoning from a more trachytic lower member to the trachydacitic compositions of the middle and upper members of the sequence. This variation towards less evolved compositions is reflected by substantial changes in the colour and textural characteristics of juvenile clasts, with pumices varying from white at the base of the deposit to dark grey at the top, with mingled pumice present within transitional members of the sequence. In addition, changing alkali versus silica concentrations and distinctly different trends in incompatible element correlation diagrams indicate that the Fogo A eruption involved at least two separate trachytic and trachydacitic magmas formed at different depths. This is supported by the presence of feldspar phenocrysts with anti-rapakivi textures, where early-formed plagioclase crystals are partially resorbed and overgrown by later-formed sanidine. The appearance of this texture is contemporaneous with the formation of banded pumices at the top of the basal fall-out deposit, providing compelling evidence of mixing and mingling between more evolved anti-rapakivi free trachytic magma (formed before magma mixing) and less evolved anti-rapakivi textured trachydacitic magma that formed after the mixing of the two magmas. The anti-rapakivi texture in the Fogo A deposits formed by a decrease in temperature and pressure of the deeper-sourced trachydacitic magma during ascent towards a shallower magma chamber containing a fractionating- trachytic batch of magma.

The contemporaneous appearance of anti-rapakivi textures and banded pumice suggests that magma mingling occurred after the formation of the sanidine rims, indicating that the trachydacitic magma ponded under the trachyte magma chamber for a time scale of a few months to years. Such evidence of short-lived pre-eruptive mingling-mixing of the two batches of magma provides a possible explanation for the triggering of the Fogo A eruption.

The thermal state of pyroclastic flow deposits of the 4.6 ka Fogo A plinian eruption sequence, São Miguel, Azores, using pTRM analysis and charcoal reflectance data, and implications for eruption and flow processes

Pensa A.*¹, Porreca M.², Corrado S.³, Giordano G.³ & Cas R.A.F.¹

1. Monash University, Victoria, Australia. 2. Dipartimento di Fisica e Geologia, Università di Perugia
3. Dipartimento di Scienze, Università di Roma Tre.

Corresponding email: alessandra.pensa@monash.edu

Keywords: Ignimbrite emplacement temperature, Thermal Remanent Magnetization, charcoal reflectance.

The Fogo A plinian eruptive sequence is characterised by a complex stratigraphy, constituted by an initial Plinian fallout deposit of white trachytic pumices, followed by two intraplinian ignimbrites and one last main ignimbrite, which is dominated by more basic dark pumices, interstratified within the plinian fallout sequence. The aim of this research is to reconstruct the emplacement temperatures of the three ignimbrites and assess the factors that have influenced these. Emplacement temperatures of the three ignimbrites of the Fogo A plinian sequence, have been investigated using thermal remanent magnetization (pTRM) of lithic clasts and a relatively new method of using charcoal reflectance of charcoal fragments embedded within the deposits. A total of 139 oriented lithic clasts from the three ignimbrite deposits, were collected from 15 localities distributed around Fogo volcano. The clast population is dominated by lava trachytic clasts and subordinate syenite clasts. The pTRM analyses show the emplacement temperatures of the two intraplinian ignimbrites were respectively greater than 400 °C and 580 °C; while the temperature reached by the final ignimbrite was 300 to 350 °C. These thermal estimations are supported by the results of the analysis of maceral reflectance within the charcoal fragments entombed in the ignimbrites. The reflectance of 17 samples of charred fragments that the temperature reached by the wood fragments in the first intraplinian ignimbrite correspond to a temperature of 400 to 460 °C, whereas the $Ro\% = 0.85$ of the last ignimbrite indicate temperatures of 300 to 350 °C. The different temperatures for the ignimbrites can be explained by a combination of componentry, especially lithic clast content, collapse level in the eruption column, turbulence level of the pyroclastic flows, degree of incorporation of water vapour from volatilised vegetation, and degree of topography confinement by the pyroclastic flows. The results also show that TRM and charcoal reflectance methods give comparable results, indicating that either method can be used depending on the characteristics of ignimbrites and availability of facilities.

Timescales of Magma Mixing Unraveled by Numerical Simulations

Petrelli M.*¹, El Omari K.², Le Guer Y.² & Perugini D.²

1. Dipartimento di Fisica e Geologia, Università di Perugia. 2. Laboratoire SIAME, CNRS IPRA,
Université de Pau et des Pays de l'Adour, Pau, France.

Corresponding email: maurizio.petrelli@unipg.it

Keywords: Timescales of magma mixing, numerical simulations.

The evolution of an igneous system experiencing the interaction between two different crystal bearing magmas is studied numerically in order to unravel the evolution and the timescales of the mixing process. The non-Newtonian behavior of magmas under the liquidus temperature is addressed in the rheology of the system. Different statistical mixing and energy indicators are used to characterize the efficiency of magma mixing. Timescales of magma mixing are evaluated by comparing two different environments: 1) a buoyancy driven convection, 2) a system experiencing chaotic dynamics.

Results from this study will help in refining the conditions under which magma mixing proceed efficiently and will constrain the timescales of magmatic hybridization as function of the rheology of the interacting magmas and the dynamics occurring within the system. This study has potential implications in both plutonic and volcanic environment. In plutonic environment, it could help in discovering the occurrence of magma mixing and, therefore it could help in constraining the origin and the evolution of the system. In volcanic environment, it could help in constraining the composition of the magmas potentially erupted as function of time and degree of magma mixing.

NIDIS: Non-Isothermal Diffusion Incremental Step model. A new approach to elemental diffusion in volcanic rocks

Petrone C.M.*¹, Bugatti G.¹, Braschi E.² & Tommasini S.³

1. The Natural History Museum, Department of Earth Sciences, London, UK. 2. Istituto di Geoscienze e Georisorse, C.N.R. Firenze.
3. Dipartimento di Scienze della Terra, Università di Firenze.

Corresponding email: C.Petrone@nhm.ac.uk

Keywords: Elemental diffusion, non-isothermal, incremental step.

Volcanic systems are normally considered as isothermal diffusing systems in which the diffusion temperature is treated as “constant” for the duration of the pre-eruptive processes. Diffusion coefficient depends exponentially on temperature and on other intensive thermodynamic variables. However, temperature is the main critical parameter. In cases where the chemical zoning pattern of minerals indicates a substantial difference (~ 50 °C) in the equilibrium temperature of the different zoned portions, we found that this produces a bias in the estimated timescales of a factor of 3 to 5. This is a significant difference and cannot be ignored.

We propose a new approach to take into account a diffusion coefficient for each compositional band in order to match the specific equilibrium temperature of the band. A mineral showing multiple bands of different composition, testifying the arrival of hotter and more mafic magma, will show multiple diffusion profiles which are the results of diffusion at different temperatures for different timescales. It is thus possible to deconstruct the main core-rim diffusion profile into different isothermal steps with its own diffusion coefficient. Each step takes into account the diffusion timescale of the previous step. The final diffusion profile is thus the result of different isothermal steps at different temperatures. We propose to call this approach the non-isothermal diffusion incremental step (NIDIS) model. This novel approach considers the so-far-ignored importance of changes in temperature, and consequently in the diffusion coefficient, also in volcanic systems. This model can also have important implications in reconsidering the meaning of crystal residence time in fast cooling systems.

Magma dynamics during Baia - Fondi di Baia eruption (Campi Flegrei) as inferred by microanalysis of juvenile products

Pompilio M.*¹, Bertagnini A.¹, Pistolesi M.², Di Roberto A.¹, Isaia R.³, Cioni R.², Francalanci L.², Romano C.⁴, Campagnola S.⁴, Di Salvo S.², Voloschina M.⁵ & Mazzone F.⁵

1. Istituto Nazionale di Geofisica e Vulcanologia, Pisa. 2. Dipartimento di Scienze della Terra, Università di Firenze. 3. Istituto Nazionale di Geofisica e Vulcanologia, Osservatorio Vesuviano, Napoli. 4. Dipartimento di Scienze della Terra, Università di Roma Tre. 5. Dipartimento di Scienze della Terra, Università di Pisa.

Corresponding email: massimo.pompilio@ingv.it

Keywords: Campi Flegrei, magmatic environments, magma dynamics.

In the last 15 ka Campi Flegrei (CF) experienced more than 70 eruptions, clustered in three main epochs separated by periods of quiescence of variable duration. Following a 1000 years-long quiescence, the Baia-Fondi di Baia eruption opened the second epoch of activity (9.6 and 9.1 ka ago), during which at least 5 more small scale pyroclastic eruptions occurred. This poorly studied eruption can represent a case study for understanding the magmatic processes leading to the long-term reactivation of the CF plumbing system.

Eruptive activity occurred in the western sector of CF along a N-S trending eruptive fissure and produced fallout alternated with and followed by pyroclastic density current deposits. We analysed the whole succession, in order to characterize magma(s) feeding the eruption and identify possible compositional changes during the eruptive dynamics. Juvenile component comprises glassy (phenocrysts < 5 vol%), highly vesicular pumice sometimes banded, and dense obsidian clasts. Micro-analytical data were collected on glass, minerals, melt inclusions together with a detailed Sr-isotope investigation on different and variably vesicular clasts.

Although glass composition of pumice is mainly trachytic as common for the Phlegrean eruptions, few moderately vesicular clasts show a tephriphonolitic composition, which is poorly represented within the whole CF eruptive history. This compositional variability is recorded at different stratigraphic levels throughout the whole eruptive sequence, and does not seem related to the timing of magma extraction or to the position along the eruptive fissure. Phenocryst assemblage is dominated by feldspars, with minor diopsidic clinopyroxene, biotite and spinel. Most of feldspars are zoned with cores of andesinic plagioclase (about 50% of analysed crystal) and minor sanidine with variable potassium content. Phenocryst rims are mainly sanidine with a variable albite content (40-55%). Most of diopsides shows normal zoning with a Mg-rich core and Fe-rich rims. Mantle shows sometimes oscillatory zoning.

Zoning motifs in feldspars, clinopyroxenes and compositional variation in glass point to a complex interaction between different magmas stored in distinct magmatic environments within the plumbing system of the volcano. We discuss here the role of this complex interaction in determining both the eruptive dynamics (e.g., trigger, evolution in space and time) and the subsequent behaviour of the volcanic system at the scale of the whole epoch.

Somma-Vesuvius's activity over the last 33 ka years: a mineral chemistry prospective

Redi D.*¹, Danyushevsky L.², Lima A.³, Cannatelli C.³, Esposito E.⁴ & De Vivo B.³

1. Dipartimento di Scienze Biologiche, Geologiche ed Ambientali (BiGea), Università di Bologna. 2. CODES – ARC Centre of Excellence in Ore Deposits, University of Tasmania, Australia. 3. Dipartimento di Scienze della Terra, dell' Ambiente e delle Risorse, Università di Napoli "Federico II". 4. Earth, Planetary and Space Sciences, UCLA, Los Angeles, USA.

Corresponding email: daniele.redi@unibo.it

Keywords: Vesuvius, clinopyroxene, antecryst.

The Somma-Vesuvius generated a wide variety of eruptive events during the past 33 ka, ranging from mild effusive eruptions (inter-Plinian) to highly disruptive phenomena (Plinian). Currently, there is no general consensus on whether the primary magma precursors to both eruption styles were of a similar composition. At the same time, the compositions of mineral phases in Somma-Vesuvius volcanic products have received significantly less attention in respect to whole-rock geochemistry. This study characterizes minor and trace elements in both olivine and clinopyroxene crystals from representative lava, scoriae and pumice samples from the main Plinian eruptions and a range of inter-Plinian events over the last 33 ka. New constraints are presented on the factors leading to the different Somma-Vesuvius eruptive styles. In order to achieve this goal, fourteen pumice samples from Plinian pyroclastic deposits as well as three scoriae and eight lava samples from effusive flows were collected, and a representative number of olivine and clinopyroxene crystals (~ 30-50) were selected under an optical microscope from each sample and analysed with an electronic microprobe and by a LA-ICP mass-spectrometer, resulting in a large database containing 2127 EMP and 1259 LA-ICP-MS analyses.

The main findings are: 1) all studied eruptive products contain olivine and clinopyroxene crystals spanning in a wide range of compositions. Olivines show Fo content varying from 91 to 68, while clinopyroxenes display Mg# ranging from 93 to 71; 2) crystals compositions from inter-Plinian eruptive products display a narrower range in respect to Plinian; 3) there is a larger difference in the composition of crystals populations between individual inter-Plinian eruptions than between Plinian eruptions; and 4) in rocks younger than AD 79, the more evolved (Mg#82-72) Plinian and inter-Plinian clinopyroxene crystals show clear Ca enrichment (~ 23.5-24.5 wt.% CaO) in respect to the older rocks (~ 23-21 wt.% CaO).

This study suggests: I) a complex crystallization history depicted by persisting multiple sites of crystallisation where magmas of variable extent of fractionation reside at any given time regardless of the type of eruptive activity; II) chemically similar sources of parental magmas feeding the Somma-Vesuvius system and both Plinian and inter-Plinian eruptions over the last 33 ka; and III) an increasing extent of carbonate assimilation during the last 2 ka.

Therefore, this study suggests that the magma residence times and the magma supply rates are likely the main factors that control Somma-Vesuvius eruptive style. Further investigations and experiments on melt and fluid inclusions within Somma-Vesuvius pristine olivines and clinopyroxenes will provide better constraints on magma residence times and the role of volatiles within this volcanic system.

Inherited and antecrystic zircons as time markers for magma ascent/storage

Rocchi S.*¹, Paoli G.¹, Jacobs J.² & Ksienzyk A.²

1. Dipartimento di Scienze della Terra, Università di Pisa. 2. Department of Earth Science, University of Bergen, Norway.

Corresponding email: sergio.rocchi@unipi.it

Keywords: Zircon, antecryst, pre-eruptive timing.

Magmas released by melting of the continental crust commonly draw minor attention in studies of processes of timing of volcanic processes in magma chambers and eruptive environment. Nevertheless, the complex histories recorded by the growth zones of zircon crystals from Miocene-Pliocene Tuscan anatectic rocks point out the occurrence of time-transgressive crystallization also in crustal igneous processes. In this context, dates from zircon autocrysts (i.e., crystals associated with only the latest pulse of magma) indicate crystallization age, whereas dates on antecrysts (formed from an earlier pulse of magma and re-incorporated in a later pulse) or inherited crystals/cores (that survived sedimentation to anatexis) give informations about processes occurred prior to the final eruption/solidification.

Inherited cores and autocrysts from Tuscan anatectic acidic rocks have been analysed by excimer LA-HR-ICP-MS after previous screening of their internal zoning by SEM-CL. Two main age populations have been recorded: (i) ages much older than crystallization age (Paleozoic to Archean), inferred to represent inherited cores, and (ii) ages that are only slightly older than crystallization age, representing antecrysts. Inherited cores have age distribution including components that have all been found in detrital zircons from the Tuscan Metamorphic Basement, such as near Panafrican (late Neoproterozoic-Cambrian), Ordovician, and Variscan ages. These results point out that the crustal materials involved in Miocene-Pliocene anatexis did include the whole basement section up to the youngest pre-Tethyan sediments, i.e. the Verrucano deposits.

For antecrysts, concordant weighted mean ages are overall older than their respective final solidification/eruption age. The reference example to discuss this issue is represented by the San Vincenzo rhyolite, for its well defined emplacement age. Single-crystal ⁴⁰Ar-³⁹Ar dating (literature data) defines the eruption age based on euhedral, clear sanidine crystals, while subhedral clear and subhedral milky crystals of sanidine give progressively older ages, covering some 300 ka. Even older ages are given by our dating of zircon antecrystic cores, that crystallized over a minimum time interval of 250-300 ka. An overall range of ages of some 650-700 ka is thus covered back from the to eruption age. Similar age distribution for sanidine, biotite hornblende and antecrystic zircon grains from the Fish Canyon Tuff, Colorado has been interpreted as evidence for protracted an extended period of assembly, cooling and rejuvenation of the magma chamber. Recent geochronological data on the time width of possible eruption window for this type of magma raise questions on where did these processes occur: do these data document timescales of magma chamber dynamics or a crystallization history in a column of ascending magma affected by successive pulses of crustal melts?

Glass forming ability of sub-alkaline silicate melts

Vetere F.^{*1-2}, Iezzi G.²⁻⁴, Behrens H.³, Holtz F.³, Ventura G.⁴⁻⁵, Misiti V.⁴, Cavallo A.⁴,
Mollo S.⁴, Dietrich M.³ & Perugini D.¹

1. Dipartimento di Fisica e Geologia, Università di Perugia. 2. Dipartimento di Ingegneria & Geologia, Università di Chieti "G. d'Annunzio". 3. Institute for Mineralogy, Leibniz University of Hannover, Germany. 4. Istituto Nazionale di Geofisica e Vulcanologia, Roma. 5. Istituto per l'Ambiente Marino Costiero, C.N.R. Napoli.

Corresponding email: francesco.vetere@unipg.it

Keywords: Sub-alkaline silicate melts, kinetic, nucleation.

The intrinsic solidification behaviour and glass forming ability (GFA) of natural sub-alkaline silicate melts have been quantified *via* cooling-induced solidification experiments. GFA is measured by the critical cooling rate R_c , the rate at which a melt solidifies ≤ 2 area% of crystals. Cooling rates of 9000, 1800, 180, 60, 7 and 1 °C/h have been run between 1300 °C (superliquidus region) and 800 °C (quenching temperature), at air fO_2 and ambient P for six silicate melts with compositions ranging from basalt (B) to rhyolite (R) (i.e., B₁₀₀, B₈₀R₂₀, B₆₀R₄₀, B₄₀R₆₀, B₂₀R₈₀ and R₁₀₀) and water contents comprised between 53 (B₁₀₀) and 384 (B₂₀R₈₀) ppm. The ranges of cooling rate and chemical compositions from this study are the broadest ever investigated in the earth sciences.

The phase proportions (area%) were determined by image analysis collected over different magnifications. Phases are glass, clinopyroxene (cpx), spinel (sp) and plagioclase (plg). Sp is the most ubiquitous phase with abundance of few area% and nucleates earlier than silicate crystals. Cpx solidifies in all runs except in R₁₀₀ and its abundance follows asymmetric broad Gaussian-like trends as a function of cooling rate. Plg crystallises only at low cooling rates and in SiO₂-poor compositions. In general, the amount of crystals decreases as the cooling rate increases; however, in some cases the amount of crystals does not increase or even decreases for B₈₀R₂₀ with decreasing cooling rate.

R_c values change over 5 orders of magnitude being $< 1, 7, 620, 3020, 8020$ and 9000 °C/h for R₁₀₀, B₂₀R₈₀, B₄₀R₆₀, B₆₀R₄₀ and B₈₀R₂₀ and B₁₀₀, respectively. The variation of R_c can be modelled *via* NBO/T (non bridging oxygen per tetrahedron) parameter by the following equation:

$R_c = a / \{1 + e^{-[(NBO/T - b)/c]}\}$, where a , b and c are fitting parameters equal to 9214, 0.297 and 0.040, respectively. Similar to other glass-forming liquids (network, metallic and molecular systems), the trend of R_c for natural sub-alkaline silicate melts is inversely related to the reduced glass transition parameter Trg ($Trg = Tg/Tm$) and can be quantified with the equation $R_c = a \times Trg^{-b}$, where a and b are 1.19×10^{-4} and 28.7, respectively.

These results may be used to retrieve the solidification conditions of aphyric, degassed and oxidised lavas; in addition, our data provide general constrain of the crystallisation kinetics of natural silicate crystal-bearing melts erupted on Earth (e.g. lavas with phenocrysts). The relationship between crystal content and cooling rate suggest that the solidification paths induced by degassing can be also complex and non-linear. The growth of crystals with size up to 1 mm from a nearly anhydrous superheated silicate melt indicates that variable cooling conditions of lavas have to be accounted for correctly discriminating minerals formed before, during and after eruptions.

Ascent velocity and dynamics of a mud eruption: an analogue for volcanological studies

Vona A.*¹, Giordano G.¹, De Benedetti A.A.¹, Romano C.¹ & Manga M.²

1. Dipartimento di Scienze, Università di Roma Tre. 2. Department of Earth and Planetary Science, University of California, Berkeley, USA.

Corresponding email: alessandro.vona@uniroma3.it

Keywords: Mud, ascent velocity, rheology.

We report and interpret field and laboratory measurements from a mud eruption that began in August 2013, very close to the Fiumicino international airport of Rome, Italy. We monitored the evolution of the eruption and collected samples for laboratory characterization of physical and rheological properties. The complete documentation of this eruption from its beginning to its end (December 2013), together with the detailed stratigraphy and geometry of the conduit, allowed us to reconstruct the evolution of mass transport to the surface. The rheology of mud is typical of pseudoplastic fluids with a yield stress, a behavior similar to what observed for crystal-rich magmas. We computed a minimum ascent velocity of the mud based on the size of large ballistic fragments ejected from the vent along with mud rheology. Results are consistent to those of the gas phase directly measured in situ. The rheology of the suspending fluid also determines bubble mobility relative to the fluid itself, controlling whether the ascending fluid is homogeneous or bubbles can coalesce to form gas slugs and separate. Given the similarity between mud and magma rheology, mud eruptions can be used as “easy-to-study” natural analogues for the understanding of time-scale and dynamics of magmatic eruptions.

SESSION S9

The role of GMPV disciplines in the definition of volcanic hazards

CONVENORS

Mauro Coltelli (INGV-OE, Catania)

Pierfrancesco Dellino (Univ. Bari)

SO₂ degassing during the summer 2014 Etna eruption: a comparison between OMI satellite and ground-based SO₂ flux measurements

Battaglia A.¹, D'Aleo R.¹, Tamburello G.*¹, Bitetto M.¹, Delle Donne D.¹⁻², Coltelli M.³, Patanè D.³,
Cannata A.³ & Aiuppa A.¹⁻⁴

1. Dipartimento di Scienze della Terra e del Mare, Università di Palermo. 2. Dipartimento di Scienze della Terra, Università di Firenze.
3. INGV, Catania. 4. INGV, Palermo.

Corresponding email: giancarlo.tamburello@gmail.com

Keywords: Etna 2014 eruption, SO₂ flux, OMI satellite.

The summer 2014 eruptive phase of Etna Volcano was characterized integrating satellite and ground-based measurements of the sulfur dioxide (SO₂) flux, obtained with the Ozone Monitoring Instrument (OMI) and a network of SO₂ camera run by University of Palermo (In the contest of the ERC-project BRIDGE). We report on data acquired between July and August 2014, during which eruptive activity shifted from an eruptive fracture (EF) at the base of the North-east Crater (NEC) towards the New South-East crater (NSEC). We processed 5 OMI images (7th-9th and 13th-14th August) with the OMIplot software and calculated the total erupted SO₂ mass for each day. The masses ranged from 900-3000 tons of the EF to 4000-5000 tons during the paroxysm from the NSEC on 13th August. Furthermore, we integrated the measured SO₂ column densities along multiple perpendicular transects for each image and multiplied by the plume speed derived by wind speed data in the NOAA READY archived meteorology database. Our calculated OMI SO₂ fluxes allowed to obtain tens of hours long time series before the time of OMI overpass (12:00-13:00 GMT) with a sampling of a few hour and increase the number of observations even during nighttime. During the first stage of the eruptive activity (7th-10th August) both OMI and SO₂ camera network detected an average daily SO₂ flux of ~2000 t·d⁻¹ that rose up to ~5000 t·d⁻¹ during the second stage (11th-15th August). We show that satellite and ground based calculated SO₂ flux time series are consistent and matched well during the entire eruptive period.

Vents Pattern Analysis at Mount Etna volcano (Sicily)

Brancato A.*, Coltelli M., Tusa G., Proietti C. & Branca S.

INGV, Osservatorio Etneo, Catania.

Corresponding email: alfonso.brancato@ingv.it

Keywords: Probabilistic forecasting, spatial analysis, volcanic hazards and risks.

Mt. Etna is the largest, as well as the most active volcano in the Mediterranean Sea. Volcanism started about 500 ky ago and the erupted magmas range from tholeiitic to alkaline affinity. An almost continuous summit activity characterizes the volcano; however, flank eruptions occur at an interval of years, mostly concentrated along the NE, S and W rift zones.

Volcanic hazard, in terms of map of future vent opening, will be explored by means of a spatial point pattern analysis of the known historical positions (154 flank vents) of the last 4.0 ka. The vents indicate that they cluster on a variety of spatial scales. Such clustering suggests that nonhomogeneous Poisson models should be used to forecast future vents distribution. That is spatial intensity (events per unit area) varies across the map region. For this reason, both spatial regularity (first-order feature, with density estimation) and clustering (second-order feature, with minimum distance separation among vents) in the Etna region at different distances are analysed. In particular, a Gaussian kernel technique (Connor & Connor, 2002) and the Ripley K-function (Ripley, 1976) are used to explore both features, respectively.

Some historical vents, which presently result covered, were extracted by the previous geological maps; other vents, mostly related to eruptions occurred before 1600 AD, were located after a reconstruction based on the portions of the lava flow fields still cropping out. The latter invoke an uncertainty, the measurement error zone, which is different from the spatial error, whose possible solution lies in the kernel density estimation, when the bandwidth is applied. Indeed, this bandwidth allows for the sampling error in the location (aleatory uncertainty), that describes what we would see if we could repeat the experiment by observing a different sample of flank vents. Therefore, both uncertainty sources have to be considered in a bandwidth that combines the sampling error and the measurement error (larger for poorly located vents).

Probabilities (retrieved after the density estimation application) have been calculated with the most significant values in line with the SSE sector of the volcano edifice, encompassing S rift as well as the upper slope of Valle del Bove, even though not negligible values were estimated along the NE and W rift areas.

Connor C.B. & Connor L.J. 2009. Estimating spatial density with kernel methods, Volcanic and tectonic hazard assessment for nuclear facilities. Cambridge University Press, Cambridge, UK, 346-368.

Ripley B.D. 1976. The second-order analysis of stationary point process. *J. Appl. Prob.*, 13, 255-266.

Correlation between geochemical and geophysical data on Etna eruption of summer 2014

D'Aleo R.*¹, Battaglia A.¹, Tamburello G.¹, Bitetto M.¹, Delle Donne D.¹⁻³, Coltelli M.², Patanè D.², Cannata A.² & Aiuppa A.¹

1. Dipartimento di Scienze della Terra e del Mare, Università di Palermo. 2. INGV, Catania
3. Dipartimento di Scienze della Terra, Università di Firenze.

Corresponding email: roberto.daleo01@unipa.it

Keywords: Etna 2014 Eruption, SO₂ camera, SO₂ flux.

Mt. Etna volcano contributes time-averaged SO₂ flux emissions of 2 Mt/a corresponding to about 10-15% of global volcanogenic budgets. The studies of SO₂ flux bring important information on how active volcanoes work helping to understand the shallow magma dynamics thanks to the propriety of this gas of exolving at shallow depth, therefore give the possibility to use it as parameter for volcano monitoring. Over the last few years, the technical advances on remote sensing SO₂ flux measurements with UV imaging opened a new window on the continuous monitoring of the degassing activity and offered insights on the transition from quiescence to explosive eruptions and on the integration between geochemical and geophysical dataset. Here, we report on novel SO₂ flux data acquired on Etna during the summer 2014 eruptions using a network of permanent SO₂ cameras run by University of Palermo (in the contest of the ERC-project BRIDGE). The two available SO₂ cameras, installed at Pizzo Deneri and La Montagnola (2 km and 3.5 km from the craters), allowed to separately resolve degassing activity of individual summit craters of Etna (North East Crater, NEC, and New South East Crater, NSEC) with a high temporal (~1Hz) and spatial resolution (a few meters). During the whole eruptive activity, the passive degassing from the NEC has shown values between 1.2 and 4.2 kg/s. A stronger explosive degassing activity was observed from the eruptive fracture (EF) opened at the base of the NEC emitting from 11.5 to 40.5 kg/s. Upon reactivation of NSEC (10th August), a decreased SO₂ flux emissivity from both NEC and the EF was observed. A large SO₂ release (up to 150 kg/s) has been measured during the major (paroxysmal) eruptive phases on 13th August. Our high resolution geochemical dataset was compared with seismic and infrasonic dataset provided by the geophysical network run by the INGV of Catania. The results show that both geophysical signals (tremor and infrasound) and SO₂ degassing shifted toward the NSEC shortly prior/during the eruption, pointing to a clear displacement of the magma/gas mixture within the active craters. The simultaneous variation of SO₂ flux within the summit craters would demonstrate some level of interconnectivity between the craters (which SO₂ flux time-series are inversely correlated) in the shallow conduit system.

A new shape dependent drag correlation formula for non-spherical rough particles

Dioguardi F.*¹⁻² & Mele D.¹

1. Dipartimento di Scienze della Terra e Geoambientali, Università di Bari.
2. Dipartimento di Biologia Ecologia e Scienze della Terra, Università della Calabria.

Corresponding email: fabio.dioguardi@uniba.it

Keywords: Non spherical rough particles, drag coefficient, volcanic ash.

The knowledge of how irregularly shaped particles settle in fluids is fundamental in a wide range of research fields and applications, from industrial to natural processes like explosive eruptions (Chhabra et al., 1999; Bagheri et al., 2015). This process is mainly controlled by the drag force between the particle and the surrounding fluid. From numerous experiments on spherical particles relationships between drag coefficients and particle Reynolds number have been obtained, which are however no longer valid for non-spherical particles, as the drag coefficient is a function of both particle Reynolds number and shape.

In this study the drag of non-spherical rough particles has been investigated in a wide range of Reynolds numbers (0.03 – 10000) (Dioguardi & Mele, 2015). The study is based on experimental measurements of the terminal velocities of irregular particles falling in fluids of different densities and viscosities. The particle shape is described by a shape factor that takes into account both sphericity and circularity, which are measured via image particle analysis techniques (Dellino et al., 2005). This shape factor is particularly suitable for non-spherical highly irregular particles. The drag coefficient has been correlated to the particle Reynolds number and the shape factor and a new correlation law has been found; the correlation has the functional form of a power law. Due to the mutual dependency of the particle terminal velocity on the drag coefficient, which in turn depends on the particle shape and Reynolds number, an iterative procedure needs to be designed for calculating the terminal velocity of particles of a specific size and shape. This procedure has been implemented in a Fortran90 code and in an Excel spreadsheet. The fitting of experimental measurements with our model calculations shows that our new law predicts the drag coefficients and the terminal velocity of irregularly shaped particles, as volcanic ash, more accurately than other shape-dependent drag laws. This will allow more realistic simulations of the multiphase flows typical of explosive volcanic eruptions, e.g. ash clouds and pyroclastic density currents.

- Bagheri G.H., Bonadonna C., Manzella I. & Vonlanthen P. 2015. On the characterization of size and shape of irregular particles. *Powder Technol.*, 270, 141-153, doi:10.1016/j.powtec.2014.10.015.
- Chhabra R.P., Agarwal L. & Sinha N.K. 1999. Drag on non-spherical particles: an evaluation of available methods. *Powder Technol.*, 101, 288-295, doi:10.1016/S0032-5910(98)00178-8.
- Dellino P., Mele D., Bonasia R., Braia G., La Volpe L. & Sulpizio R. 2005. The analysis of the influence of pumice shape on its terminal velocity. *Geophys. Res. Lett.*, 32, L21306, doi:10.1029/2005GL023954.
- Dioguardi F. & Mele D. 2015. A new shape dependent drag correlation formula for non-spherical rough particles. Experiments and results. *Powder Technol.*, 277, 222-230, doi:10.1016/j.powtec.2015.02.062.

Chronology, dynamics and impact of the 2011 Puyehue-Cordón Caulle eruption, Chile

Elissondo M.¹, Baumann V.¹, Bonadonna C.², Pistolesi M.^{*3}, Cioni R.³, Bertagnini A.⁴, Biass S.²,
Herrero J.C.¹ & Gonzalez R.¹

1. Servicio Geológico Minero Argentino (SEGEMAR), Buenos Aires, Argentina. 2. Section des Sciences de la Terre et de l'Environnement, Université de Genève, Suisse. 3. Dipartimento di Scienze della Terra, Università di Firenze
4. Istituto Nazionale di Geofisica e Vulcanologia, Pisa.

Corresponding email: marco.pistolesi@unifi.it

Keywords: Eruptive dynamics, volcanic risk, crisis management.

After about 41 years of repose, the Puyehue-Cordón Caulle volcanic complex (Central Andes) erupted on June 4, 2011, from a system of vents located about 1500 m above sea level on a NW-SE fracture of the Cordón Caulle system. This resulted in the evacuation of ca. 4000 people in Chile and, due to the prevailing winds, widespread disruption to various economic sectors and human activities in Argentina. The eruption developed as a long-lasting rhyolitic activity with plume heights above the vent between ca. 9 and 12 km above the vent during the first 3-4 days, 4 and 9 km during the following week, and < 6 km after 14 June.

We present a detailed chronological reconstruction of the eruption based on information derived from newspapers, scientific reports and satellite images. The main physical parameters driving the different phases of the eruption have been derived from the study of the deposits, and compared with observational data. Chronology of associated volcanic processes and their local and regional effects (i.e. precursory activity, tephra fallout, lahars, pyroclastic density currents, lava flows) are also presented. The eruption had a severe impact on the ecosystem and on various economic sectors, including aviation, tourism, agriculture, and fishing industry. Urban areas and critical infrastructures, such as airports, hospitals and roads, were also severely affected. The concentration of PM10 (Particulate Matter $\leq 10 \mu\text{m}$) was measured during and after the eruption, showing that maximum safety threshold levels of daily and annual exposures were overcome in several occasions. Probabilistic analysis of atmospheric and eruptive conditions showed that the main direction of tephra dispersal is directly towards east of the volcano and that the climactic phase of the eruption, dispersed toward south-east, has a probability of occurrence within 1%. The management of the crisis, including evacuation of people, is discussed, as well as the comparison with the impact associated with other recent eruptions located in similar areas and having similar characteristics (i.e., Quizapu, Hudson, and Chaitén volcanoes). This comparison shows that the regions downwind and very close to the erupting volcanoes, suffered very similar problems, without a clear relation with the intensity of the eruption (e.g. health problems, damage to vegetation, death of animals, roof collapse, air traffic disruptions, road closure, lahars and flooding). This suggests that a detailed collection of impact data can be largely beneficial for the development of plans for the management of an eruptive crisis and the mitigation of associated risk of the Andean region.

Hazard assessment of pyroclastic density currents at Mount Somma-Vesuvius: inference from the 79 AD eruption

Mele D.*¹, Dellino P.¹, Dioguardi F.¹, Doronzo D.M.¹, Isaia R.² & Sulpizio R.¹

1. Dipartimento di Scienze della Terra e Geoambientali, Università di Bari. 2. INGV, Osservatorio Vesuviano, Napoli.

Corresponding email: daniela.mele@uniba.it

Keywords: Pyroclastic density currents, Vesuvius 79 AD eruption, dynamic pressure.

The devastating power of pyroclastic density currents (PDC) is mainly related to flow velocity, particle volumetric concentration and temperature. The main parameter for expressing the impact of PDC is the dynamic pressure, $1/2\rho u^2$ (ρ is flow density and u is velocity along flow direction).

In volcanic history of Vesuvius area, the pyroclastic density currents represented the more frequent event.

The velocity, density and particle volumetric concentration profiles of the stratified current are calculated, together with the profile of dynamic pressure, which is a useful parameter for checking resistance of buildings. We used an improved version of the sedimentological model of Dellino et al. (2008). The model links turbulent boundary layer shear flow theory with particle coupling to gas turbulence. The working procedure starts with the recognition in the field of the fining upward sequence of layers formed during the time integrated depositional history of an individual current. Distinct processes of particle transportation and deposition are associated with the different particle modes composing the bedset. The system of equations for the solution of the fluid-dynamic parameters is implemented in two alternative ways. The first one uses data of particles coming from both the basal coarse layer and the overlying laminated layer of the bedset. The second uses features of two distinct components of the laminated layer. In this version the slope angle, which is difficult to measure or hypothesize, is directly computed via the solution of a new system of equations.

A statistical test is performed for checking model results against experimental data of actual particles. Model calculations give the average solution, as well as solutions corresponding to a range of 68% of probability around the average value. The maximum solution can be considered as a safety value for impact parameters.

To contribute in the development of the hazard assessment at Vesuvius, the methodology is applied to deposits of 79 AD eruption. Values of the maximum expected dynamic pressure were calculated in eight positions placed around the crater. The dynamic pressure ranges from values about 6 kPa in proximal areas to less than 0.8 kPa in more distal areas.

Analysis of high resolution 2D seismic reflection profiles for the determination of the structure of the Solfatara Volcano

Nazzaro I.*¹, Bruno P.P.², Maraio S.³ & Festa G.⁴

1. Amra S.c.a.r.l., Napoli. 2. The Petroleum Institute, Abu Dhabi, United Arab Emirates. 3. Dipartimento di Scienze Biologiche, Geologiche ed Ambientali, Università di Bologna 4. Dipartimento di Scienze Fisiche, Università di Napoli "Federico II".

Corresponding email: imperia.n@libero.it

Keywords: Solfatara Volcano, seismic profiles, Campi Flegrei.

Solfatara volcano is a 0.6 km wide tuff cone situated to the NE of Pozzuoli, within the densely populated Campi Flegrei Caldera (Bruno et al., 2007). The Solfatara is the most active volcano of Campi Flegrei Caldera. Both caldera structure and hydrothermal activity are controlled by a set of NW-SE and NNE-SSW/NE-SW striking faults (Bianco et al., 2004). Most of these faults are sub-vertical and are filled by hydrothermal minerals (Bruno et al., 2007). Solfatara Caldera unrest represents the main hazard for the nearest densely urbanized areas of Pozzuoli and Bagnoli; therefore numerous interdisciplinary studies are aimed at investigating its structure and evolution. Among them, the EU (FP7) funded project MED-SUV RICEN (Repeated Induced Earthquakes and Noise) aims to understand the geophysical processes occurring at the near surface of Solfatara volcanic through repeated observations over time using seismic waves (Serra et al., 2014). The present work, that is part of RICEN, shows the results of two 2D high-resolution (HR) seismic reflection profiles acquired within the Solfatara crater and designed to image the shallow (i.e. 500 m) structure of the crater and to identify faults.

The two 2D HR reflection profiles, striking NE-SW and NW-SE and were acquired in May and November 2014 respectively, using a high resolution vibrating seismic source (IVI-Minivib). The preliminary interpretation shows that Solfatara crater is an asymmetrical structure whose bottom is at -400 ms TWT. In the first 150 ms TWT are clearly visible two horizontal reflectors, probably dissected by sub vertical faults which represent preferential pathways for the CO₂ degassing.

Bianco F., Del Pezzo E., Saccorotti G. & Ventura G. 2004. The role of hydrothermal fluids in triggering the July-August 2000 seismic swarm at Campi Flegrei, Italy: evidence from seismological and mesostructural data. *J. Volcanol. Geotherm. Res.*, 133, 229-246.

Bruno P.P.G., Ricciardi G.P., Petrillo Z., Di Fiore V., Troiano A. & Chiodini G. 2007. Geophysical and hydrogeological experiments from a shallow hydrothermal system at Solfatara Volcano, Campi Flegrei, Italy: Response to caldera unrest. *J. Geophys. Res.*, 112, B06201, doi:10.1029/2006JB004383.

Serra M., Festa G., Bianco F., Bruno P.P., De Landro G., Di Fiore V., Maraio S., Pilz M., Roux P., Vandemeulebroeck J., Woith H. & Zollo A. 2014. RICEN: Repeated Induced Earthquakes and Noise. EGU General Assembly 2014, Vienna, Austria, 16, 9454.

Fractal fragmentation theory on pyroclastic deposits from Vesuvius and Campi Flegrei: Determining explosive eruptions energy

Paredes J.*¹, Morgavi D.¹, Di Vito M.², de Vita S.², Sansivero F.² & Perugini D.¹

1. Dipartimento di Fisica e Geologia, Università di Perugia. 2. INGV, Osservatorio Vesuviano, Napoli.

Corresponding email: joali.paredes@studenti.unipg.it

Keywords: Volcanic fragmentation, explosive energy, grain size distribution.

Despite the growing understanding of the physical processes before and during volcanic eruptions, type of eruptive activity still remains highly unpredictable, and an enhanced knowledge on the topic is required for hazard assessment and risk mitigation. The principles of fractal theory has had a strong influence on the understanding of many geological processes, which is why performing laboratory experiments on deposits of volcanic eruptions along with statistical analysis allow the precise characterization of the generated pyroclasts and open the possibility for substantial advances in the quantification of fragmentation processes.

Recent works have shown that fractal dimension could be utilized as a proxy for estimating the explosivity of volcanic eruptions by analyzing natural grain size distributions. We carried out grain-size analysis on two sets of natural samples from two different localities: (1) Eastern sector of Ischia island, Campi Flegrei (Italy) - Localities of Cretaio and Fiaiano, Cretaio Tephra eruption (1.86 Ka B.P.), (2) NE of Vesuvius Volcano, Napoli (Italy) - Pomice di Avellino Plinian eruption (3.9 Ka B.P.). Two different techniques were applied to determine the grain-size distribution of the samples: manually, by dry sieving for particles larger than 297 μ m, and with the CamSizer-P4 and CamSizer-XT, automated process that allows to get a Cumulative Size Distribution (CSD) based on volume fraction for particles up to 30mm. These size distributions have been studied by fractal fragmentation theory and the fractal dimension of fragmentation (D_f), a value quantifying the intensity of fragmentation, has been measured for each sample. Results show that size distribution of pyroclastic fragments follows a fractal law (i.e. power-law), indicating that the fragmentation process of these samples reflects a scale-invariant mechanism. Matching the results from the two different techniques will allow setting a value of “energy of fragmentation” for the sampled area, and with this we attempt to draw iso- D_f contours to define volcanic zones affected by the fall out of pyroclasts generated by different eruption intensities.

The importance of these results is enable fractal statistics as a tool for addressing volcanic risk based on the analyses of grain size distribution directly on natural samples. A possible future application of this method may be the on-line estimation of explosivity during volcanic eruptions. By placing sets of sieves with different aperture in strategic positions around an erupting volcano it may be possible to collect masses of pyroclasts with specific grain sizes and estimate real-time eruption energy and its time evolution.

Towards a background probability map for vent opening position in a future Plinian-subPlinian eruption of Somma-Vesuvius, with structured uncertainty assessment

Tadini A.^{*1-2}, Bevilacqua A.²⁻³, Neri A.², Cioni R.¹, Aspinall W.P.⁴⁻⁵, Bisson M.², Isaia R.⁶, Valentine G.A.⁷, Vitale S.⁸, Baxter P.J.⁹, Bertagnini A.², Cerminara M.², De Michieli Vitturi M.², Di Roberto A.², Engwell S.², Esposti Ongaro T.², Mazzarini F.², Pistolesi M.¹, Todde A.¹ & Russo A.¹

1. Dipartimento di Scienze della Terra, Università di Firenze. 2. INGV, Pisa. 3. Scuola Normale Superiore, Pisa. 4. Aspinall & Associates, Tisbury, UK. 5. University of Bristol, School of Earth Sciences, Bristol, UK. 6. INGV, Osservatorio Vesuviano, Napoli. 7. Department of Geology, University at Buffalo, NY, USA. 8. Dipartimento di Scienze della Terra, dell'Ambiente e delle Risorse, Università di Napoli "Federico II". 9. University of Cambridge, Institute of Public Health, Cambridge, UK.

Corresponding email: alessandro.tadini@ingv.it

Keywords: Somma-Vesuvius, vent opening probability map, Gaussian kernel.

In this study we combine detailed reconstructions of volcanological datasets and inputs from structured expert judgement (SEJ) to produce a first background (i.e. long-term or base-rate) probability map for vent opening location in the next Plinian or Sub-Plinian eruption of Somma-Vesuvius (SV). The SV volcano has, over its history, exhibited large variability in eruptive styles, and moderate spatial variability in vent locations. In particular, the vent positions associated with large explosive eruptions, i.e. Plinian and Sub-Plinian, have shown shifts within the present SV caldera. Notwithstanding this moderate shift, the location of a new active vent will have a major effect on the run-out and dispersal of pyroclastic density currents mainly due to the presence of the Mt Somma barrier, as also evidenced by past deposit patterns and illustrated by numerical simulations, and therefore will have important implications for hazard mitigation. Thus far, we have focused on three main objectives: i) the collection and critical review of key volcanological features (position of past vents, distribution of faults, etc.) that could influence the spatial distribution of future vent locations; ii) developing spatial probability density maps with Gaussian kernel function modelling to use with our different volcanological and geophysical datasets, and iii) the production of a background probability map for vent opening position, using weighted linear combination of spatial density maps for the identified volcanological and geophysical parameters, with uncertainties explicitly included from structured expert elicitation. Preliminary outcomes obtained by a first elicitation session involving about 17 experts are reported for three expert judgement weighting and pooling models: (a) the Classical Model (CM) of Cooke (1991); (b) the Expected Relative Frequency (ERF) model of Flandoli et al. (2011), and (c) an Equal Weights (EW) combination. The results of combining expert judgements with our spatial modelling illustrate the influence of uncertainties in the various variables on the spatial probability content of the final maps, depicting areas at higher and lower probability of vent opening; second order effects of alternative methods for pooling judgements for quantifying uncertainty sources are discussed.

Cooke R.M. 1991. Experts in uncertainty: opinion and subjective probability in science. New York & Oxford: Oxford University Press.

Flandoli F., Giorgi E., Aspinall W.P. & Neri A. 2011. Comparison of a new expert elicitation model with the Classical Model, equal weights and single experts, using a cross-validation technique. Reliab. Eng. Syst. Safe., 96, 1292-1310.

Effusive dynamics at Stromboli volcano (Aeolian Islands) and implications to volcanic hazard

Valade S.*¹, Pistolesi M.¹, Allocca C.¹, Colò L.¹, Coppola D.², Delle Donne D.³, Genco R.¹, Lacanna G.¹, Laiolo M.², Marchetti E.¹, Ulivieri G.¹ & Ripepe M.¹

1. Dipartimento di Scienze della Terra, Università di Firenze. 2. Dipartimento di Scienze della Terra, Università di Torino.
3. Dipartimento di Scienze della Terra e del Mare, Università di Palermo.

Corresponding email: marco.pistolesi@unifi.it

Keywords: Stromboli, lava flows, volcanic hazard.

Stromboli volcano is well-known for its fascinating mild-explosive activity which attracts thousands of tourists every year. A variable spectrum of phenomena such as crater overflows, fissure-fed lava flows, transient violent explosions, and tsunamogenic landslides however still remain poorly understood; these are unfortunately associated to the highest hazards both for tourists and inhabitants of the island. Yet, these phenomena have all been observed during the last decades. The August-November 2014 effusive crisis is in fact the last of 4 important effusive events occurred in the last 30 years; other eruptive crises, which emplaced along the Sciara del Fuoco >106 m³ of lavas each, occurred in 1985-86, 2002-03 and 2007. A continuous improvement of the geophysical monitoring system of the volcano allowed to precisely describe the 2014 event, with several parameters (seismicity, ground deformation, effusion rate) being recorded during the event. The effusive crisis lasted 107 days and showed remarkable similarities with past lava flows at Stromboli. All the effusive events are in fact preceded by a period of high explosive activity; after the effusive onset, effusion rates show a high peak during the first 3-5 days, during which most of the lava volume is usually emplaced. During this phase, ground deformation systematically shows a rapid deflation. The following phases display variable trends of effusion rates which are related to the geometry of the shallow magmatic system. Quantification of the eruptive parameters and comparison among the considered crises allowed to speculate on the dynamics of lava effusions at Stromboli and on their active role in terms of lateral landslide and large, transient explosion (i.e. paroxysmal eruptions) generation.

SESSION S10

Field studies in modern volcanology

CONVENORS

Marco Pistolesi (Univ. Firenze)

Roberto Sulpizio (Univ. Bari)

Roberto Isaia (INGV Napoli)

Geological reconstruction of the cone building and alternating explosive and effusive activity of Monte dei Porri, Salina Island (Italy)

Baldoni E.*¹, Lucchi F.¹, Sulpizio R.²⁻³, Forni F.⁴, Massaro S.² & Tranne C.A.¹

1. Dipartimento di Scienze Biologiche, Geologiche e Ambientali, Università di Bologna. 2. Dipartimento di Scienze della Terra e Geoambientali, Università di Bari. 3. Istituto per la Dinamica e i Processi Ambientali, CNR, Milano
4. Institute of Geochemistry and Petrology, ETH Zurich, Switzerland.

Corresponding email: leonora.baldoni2@unibo.it

Keywords: Eruptive style transition, cone building, Monte dei Porri.

New geological and stratigraphic data allowed the reconstruction of the alternating explosive and effusive activity leading to the construction of Monte dei Porri stratocone on Salina Island (Aeolian Islands, Italy). The Monte dei Porri stratigraphic succession was split into six eruptive units (EUs) comprising both explosive and effusive activity. The EUs contain pumice and scoria-bearing deposits from variably concentrated PDCs and fallouts, the latter having a main dispersal to the southeast. Thick, blocky lava flows and scoria deposits from strombolian activity interbed the stratigraphic succession. Magma composition ranges from poorly evolved to intermediate/evolved (basaltic andesite, andesite and dacite). Explosive activity is mostly driven by magmatic fragmentation as shown by preliminary SEM image analysis on coarse ash from the different pyroclastic deposits. This is a good example of intense to weak explosive and effusive activity involving magmas of similar composition that alternate in a ky-timescale. After excluding a major role for hydromagmatic fragmentation, the large variations in explosivity deduced from the stratigraphic succession should be explained by the timing of magma rising driven by variations in local tectonic stress combined with variable magma chamber overpressure, which need to be investigated in detail in the next future. The absence of important erosional unconformities and paleosoils interrupting the Monte dei Porri succession indicates that its cone building up to ca. 900 metres occurred without prolonged volcanic quiescences in the time interval between 70-67 and 67-57 ka, as derived from radiometric ages and tephrostratigraphy. This rapid construction of a steep stratocone likely created the conditions for the NW-dipping sector collapse that truncated the northwestern flank and summit of Monte dei Porri and interrupted its activity.

Field evidences of last 5.5 ka ground deformation at Campi Flegrei caldera

Ciarcia S.¹, Iannuzzi E.², Isaia R.*², Prinzi E.P.¹, Tramparulo F.D.A.¹ & Vitale S.¹

1. Dipartimento di Scienze della Terra, dell' Ambiente e delle Risorse (DiSTAR), Università di Napoli "Federico II"
2. Istituto Nazionale di Geofisica e Vulcanologia, Osservatorio Vesuviano, Napoli.

Corresponding email: roberto.isaia@ingv.it

Keywords: Ground deformation, Campi Flegrei caldera, structural survey.

Vitale et al. (2014) and Isaia et al. (2015) highlighted the role of the major faults associated to the volcanism occurred during the last 5.5 ka. Fault activation occurred synchronously to ground deformation uplift episodes that preceded major eruption phases. Presently an unrest phase of the Campi Flegrei caldera is marked by variations of different parameters such as fumarolic, seismic and ground deformation activities. The latter is well recorded by GPS data, topographic leveling and satellite surveys.

The main aim of this study is to define the role of the meso-scale structures during the main episodes of the ground deformation and their relationships with the eruptive activities. This work included a structural survey at Campi Flegrei caldera by means of fracture, dyke and fault analyses. A review of available well log and new field and subsurface data collected in the central sector of the caldera was carried out. We reconstructed in detail the top of several paleo-surfaces of the main volcanic and morphostructural features. Results show as the paleo-morphology was strictly controlled by faults and fractures that formed meso-scale channels and depressions subsequently filled by tephra and volcanoclastic sediments. Several evidences of synsedimentary structures such as faults and sedimentary dykes indicate an extensional deformation accompanying the ground uplift occurred in various stages of the caldera evolution. Stratigraphical relationships between structures and volcanic deposits further constrain the timing of the deformation phases.

Isaia R., Vitale S., Di Giuseppe M.G., Iannuzzi E., Tramparulo F.D.A. & Troiano A. 2015. Stratigraphy, structure and volcano-tectonic evolution of Solfatara maar-diatreme (Campi Flegrei, Italy). *Geol. Soc. Am. Bull.*, in press, doi:10.1130/B31183.1.

Vitale S. & Isaia R. 2014. Fractures and faults in volcanic rocks (Campi Flegrei, southern Italy): insight into volcano-tectonic processes. *Int. J. Earth Sci.*, 103, 801-819.

The importance of fieldwork in volcanology

Dellino P.

Dipartimento di Scienze della Terra e Geoambientali, Università di Bari.

Corresponding email: pierfrancesco.dellino@uniba.it

Keywords: Explosive eruptions.

The field study of volcanic materials, thanks to the use of modern methods of description and interpretation of facies architecture, has in recent years encouraged the proliferation of new conceptual models on the eruptive dynamics. In this way, fieldwork allows a more detailed identification of the stratigraphic units and subunits, and allows a more precise sampling of depositional units. The multiparametric analyses carried out in laboratory are used to define the parameters for solving systems of equations of sediment mechanics, allowing a quantitative assessment of the processes of transport and sedimentation. This approach enables a greater convergence between natural reality and the results of numerical simulation models of the complex processes that regulate the explosive eruptions.

The volcanological evolution of the Island of Vulcano in the last 1000 years

Di Traglia F.*¹, Pistolesi M.¹, Fusillo R.², Rosi M.³ & Gioncada A.³

1. Dipartimento di Scienze della Terra, Università di Firenze. 2. School of Earth Sciences, University of Bristol, UK.
3. Dipartimento di Scienze della Terra, Università di Pisa.

Corresponding email: federico.ditraglia@unifi.it

Keywords: Island of Vulcano, Volcano stratigraphy, caldera volcanism.

The Island of Vulcano (Aeolian Islands, Southern Italy) consists of several volcanic edifices whose formation overlapped in time and space beginning 120 ka ago. The most recent volcanoes are the La Fossa cone and Vulcanello. The former is a 391 m-high active composite cone that began to erupt 5.5 ka ago inside the La Fossa caldera, while the latter is a 123-m-high, composite edifice composed of a lava platform and three partially overlapping scoria cones aligned NE–SW along the northern ring fault of La Fossa caldera. The last 1000 years of eruptive activity and the morphological variations in the La Fossa cone and Vulcanello were investigated through a stratigraphic reconstruction. This was based on 139 natural cuts, 26 machine-excavated and 5 hand-dug trenches in the volcanoclastic succession. It was found that the last 1000-year period can be divided into (in hierarchical order) Eruptive Clusters and Units. Several unconformities of different hierarchical order were also identified (erosional surfaces and/or palaeosols). Stratigraphic relationships between the La Fossa cone, the Vulcanello products and with rhyolitic tephra related to the 13th century eruption of Mt. Pilato in the Island of Lipari (Rocche Rosse tephra) were fundamental in assigning a calendar age to most of the tephra units in the studied sequence. Bulk rock and melt inclusions geochemical data allowed to recognize the compositional variations of the products along the reconstructed stratigraphy. The morphological evolution of the La Fossa cone and Vulcanello was also reconstructed in order to assess the average cone growth rate. This work suggests that several eruptions occurred in two main clusters at both volcanoes in the last 1000 years. We found that the La Fossa cone activity occurred in two clusters of eruptions (11th-13th and 15th - 19th centuries) that led to the formation of westernmost part of the volcano, accompanied by the emplacement of lava flows. The average growth rate of the La Fossa cone was 0.96 km³ ky⁻¹, while the growth rate during the 1888-90 Vulcanian eruption, the last eruption occurred at the La Fossa cone, was ~0.2 m³ s⁻¹. Also the Vulcanello activity occurred in two clusters of eruptions (11th-12th and 17th centuries) that led to the formation of three volcanic cones, each accompanied by the emplacement of lava flows. The erupted volumes of the three pyroclastic cones vary between 2x10⁻³ km³ and 3x10⁻⁶ km³, while the volumes of the three lavas vary between 0.3 (a submarine lava field) and 3x10⁻³ km³, with lava volume/total volume ratio ranging between 0.93 and 0.99, and an average growth rate of the cones in the last 1000 years of 0.28 km³ ky⁻¹.

Stratigraphic reconstruction of the Corbetti caldera (Main Ethiopian Rift)

Fusillo R.*¹, Brooker R.A.¹, Di Traglia F.¹⁻² & Blundy J.D.¹

1. School of Earth Sciences, University of Bristol, UK. 2. Dipartimento di Scienze della Terra, Università di Firenze.

Corresponding email: Raffaella.Fusillo@bristol.ac.uk

Keywords: Volcanology, stratigraphy, unconformity.

The Corbetti Caldera is a poorly-known Quaternary volcano in the central sector of the Main Ethiopian Rift (Mohr, 1966; MacDonald & Gibson, 1969; Di Paola, 1971; Wodegabriel et al., 1991). However Corbetti caldera has recently showed to undergo active deformation in the last twenty years (Biggs et al., 2011).

In the absence of a detailed knowledge of the eruptive history, an assessment of volcanic hazard is primary based on the stratigraphy of the past activity. The stratigraphic reconstruction of Corbetti caldera deposits has been carried out using the Unconformity Bounded Stratigraphic Units method (UBSU, Salvador, 1987) modified for the volcanic terrains (De Rita et al., 1997) in a combination with morphological analysis based on the processing of new LiDAR imagery. The concept of lithosome was also applied (Giordano et al., 2006).

The stratigraphic sequence of Corbetti Caldera has been divided in four lithosomes, the pre- and syn-caldera products (Corbetti lithosome) and post- caldera volcanoes (Urji, Danshe and Chabbi lithosomes), separated by an unconformity surface of the higher rank (S1) corresponding to the caldera collapse faults system. Each boundary between lithosomes marks a change of eruptive centre and it is represented by unconformity surfaces of lower rank (S2). The Corbetti eruptive history was characterized by ten eruptive units and twenty sub-eruptive units.

The stratigraphic reconstruction revealed a complex - multi stage volcanic activity, characterized by the emplacement of pyroclastic deposits followed by obsidian flows, showing a change in volcanic eruption style from explosive to effusive activity, and allowed temporal constraints on the volcanic evolution of Corbetti Caldera and provides a new geological map of the area.

- Biggs J., Bastow I.D., Keir D. & Lewi E. 2011. Pulses of deformation reveal frequently recurring shallow magmatic activity beneath the Main Ethiopian Rift. *Geochem. Geophys. Geosyst.*, 12, 1525-2027.
- De Rita D., Giordano G. & Milli S. 1998. Forestepping - backstepping stacking patterns of volcanoclastic successions: Roccamonfina volcano, Italy. *J. Volcanol. Geotherm. Res.*, 80, 155-178.
- Di Paola G.M. 1970. Geology of the Corbetti Caldera Area (Main Ethiopian Rift Valley). *Bull. Volcanol.*, 35, 497-506.
- Giordano G., De Benedetti A.A., Diana A., Diano G., Gaudioso, F., Marasco F., Miceli M., Mollo S., Cas R.A.F. & Funicello R. 2006. The Colli Albani mafic caldera (Roma, Italy): stratigraphy, structure and petrology. *J. Volcanol. Geotherm. Res.*, 155, 49-80.
- Macdonald R. & Gibson I.L. 1969. Pantelleritic Obsidians from the volcano Chabbi (Ethiopia). *Contrib. Mineral. Petr.*, 24, 239-244.
- Mohr P.A. 1966. Chabbi Volcano (Ethiopia). *Bull. Vulcanol.*, 29, 797-815.
- Salvador A. 1987. Unconformity bounded stratigraphic units. *Geol. Soc. Amer. Bull.*, 98, 232-237.
- Wodegabriel G., Aronson J.L. & Walter C.R. 1990. Geology, geochronology, and rift basin development in the central sector of the Main Ethiopian Rift. *Geol. Soc. Amer. Bull.*, 102, 439-458.

Short-term environmental impact of the Youngest Toba Tuff, ~ 75 ka

Gatti E.*¹, Leszczynska K.², Durant A.³, Jeans C.², Boreham S.², Gibbard P.L.² & Oppenheimer C.⁴

1. NASA Jet Propulsion Laboratory, California Institute Of Technology, Pasadena, CA, USA. 2. Quaternary Palaeoenvironments Group, Department of Geography, Cambridge University, UK. 3. Norwegian Institute for Air Research, Kjeller, Norway. 4. Department of Geography, University of Cambridge, UK.

Corresponding email: emma.gatti@jpl.nasa.gov

Keywords: Youngest Toba Tuff, super-eruptions, tephra fallout.

The ~ 75 ka eruption of Toba, in Sumatra, is considered the largest known eruption of the Quaternary. The exceptional distribution and thickness of the Youngest Toba Tuff (YTT) suggested several hypotheses about the impact of the super-eruption on climate and humans, with consequent reduction of the effective population size of *Homo sapiens*.

Early theories proposed that several millennia of global cooling occurred after the eruption, due to presumed large quantities of sulphur ejected into the atmosphere. Recent theories suggested a more regional and short-term scale - centennial to millennial - environmental impact of the YTT. The eruption clearly had a drastic short-term impact, at least on the areas directly affected by the ash fallout. Nevertheless, the low-resolution of the sediment records in which the YTT is embedded makes assessing the environmental impact of the super-eruption challenging.

The aim of this study is to answer the following questions: 1) How long it took for the ash to be re-deposited and consolidated? And 2) To which extent the ash fallout influenced the receiving environment?

We collected ash, pre-ash and post ash samples from three paleo-lacustrine sequences in Jwalapuram, in South-eastern India. The YTT ash in this locality is preserved in m-thick exposures. We prepared micromorphological thin-sections and x-ray diffraction (XRD) smears of the ash itself and the clay underlying and overlying the tephra. The results were interpreted focusing on proxies indicating ash-induced environmental alteration and combined with pre-existing Optically Stimulated Luminescence (OSL) ages, to assess the environmental impact of the ash on local scale and the time-scale of re-deposition of the ash.

Timing of the shift from leucite-free (Tuscan Magmatic Province) to leucite-bearing (Roman Magmatic Province) magmas in Italy

Laurenzi M.A.*¹, Braschi E.², Casalini M.³⁻⁴ & Conticelli S.²⁻⁴

1. Istituto di Geoscienze e Georisorse, C.N.R. Pisa. 2. Istituto di Geoscienze e Georisorse, C.N.R. Firenze.
3. Dipartimento di Scienze della Terra, Università di Pisa. 4. Dipartimento di Scienze della Terra, Università di Firenze.

Corresponding email: m.laurenzi@igg.cnr.it

Keywords: Geochronology, leucite-free Tuscan Magmatic Province, leucite-bearing Roman Magmatic Province.

Mio-Pleistocene magmatism in Italy roughly drifted diachronously eastward first, from Tuscan archipelago to the Tuscan coastline, and then southeastward along the Tyrrhenian border of the peninsula. The early activity is Miocene to Pliocene in age, with leucite-free ultrapotassic to shoshonitic igneous rocks confined in the Corsica to Southern Tuscany - Northern Latium domains, whilst the leucite-bearing and associated rocks are Pleistocenic in age and do occur from Northern Latium (Vulsini District) till Neapolitan region (Vesuvius volcano). To help deciphering the mechanism that governed the shift from leucite-free (Corsican- and Tuscan-type) to leucite-bearing (Roman-type) ultrapotassic magmas a detailed re-evaluation of the geochronological data is needed. We focus our attention on the area that includes Southern Tuscany and Northern Latium, where a growing number of recent age data on Plio-Pleistocene leucite-free (Tuscan-type) ultrapotassic and associated rocks highlights short periods of intense volcanic activity separated by long periods of quiescence, before hidden in the folds of data often imprecise or inaccurate. Recent data on Cimini Volcanic District evidence a period of activity for the main volcanic edifice from 1.36 to 1.29 Ma (Laurenzi et al., 2014). A new ⁴⁰Ar-³⁹Ar age of 0.85 Ma was obtained on a lava flow of Torre Alfina volcano, while the few data on Radicofani are around 1.3 Ma (Conticelli et al., 2010). ⁴⁰Ar-³⁹Ar dating of rocks from Mt. Amiata evidence that the domes were emplaced in a short interval of time, from 301 to 294 ka, whilst one of the final lava flows is about 60 ka younger. These ages, coupled with previously published data on the Amiata basal formation, limit to few ka the climax of volcanic activity. The oldest Roman-type ultrapotassic rocks of the area under consideration are from the Vulsini District ("Pliniane di Base" Auct.) at 0.59 Ma (Conticelli et al., 2010). The data since now available evidence the presence of two time windows without volcanic activity, one from about 1.29 (Cimini, Radicofani) to 0.85 Ma (Torre Alfina), and the other from about 0.85 to 0.59 Ma (Vulsini). The Monte Amiata volcanic rocks, leucite-free similarly to the older Tuscan-type rocks, display a hybrid nature derived by contamination with newly arrived mafic Roman-type magmas, and coexist in time with Roman-type leucite-bearing rocks.

Conticelli S., Laurenzi M.A., Giordano G., Mattei M., Avanzinelli R., Melluso L., Tommasini S., Boari E., Cifelli F. & Perini G. 2010. Leucite-bearing (kamafugitic/leucititic) and -free (lamproitic) ultrapotassic volcanic rocks and associated shoshonites in the Italian Peninsula: constraints on petrogenesis and geodynamics. *J. Virtual Expl.*, 36, paper 21.

Laurenzi M.A., Mattioli M., Bonomo R., Ricci V. & Vita L. 2014. ⁴⁰Ar-³⁹Ar geochronology and evolution of the Cimini Volcanic District (Central Italy). *Rend. Online Soc. Geol. It.*, 31(1), 444.

Stratigraphic approach to fieldwork and mapping in volcanic areas: examples from Stromboli and the Aeolian Islands

Lucchi F.

Dipartimento di Scienze Biologiche, Geologiche e Ambientali, Università di Bologna.

Corresponding email: federico.lucchi@unibo.it

Keywords: Stratigraphy, volcanic areas, unconformities.

Geological mapping of volcanic areas provides the basic multidisciplinary knowledge for detailed field volcanological studies and for evaluations of volcanic hazard of active or recent volcanoes. Mapping is devoted to the description of volcanic rock bodies and their lithofacies architecture, the morphology of eruptive centres and the bedding attitude of their products, the volcano-tectonic relationships and the recognition of unconformities cross-cutting the volcanic successions. A stratigraphic approach based on current nomenclature rules is suitable to describe the complex geological nature of volcanic areas, thus creating a widely acceptable platform for communication and understanding between stratigraphers and volcanologists working in different areas (and even in other geological environments). This procedure has been established during the geological field study and 1:10.000 scale mapping of Stromboli and the other Aeolian Islands. Fieldwork is based on different rock-stratigraphic units by primarily using unconformity-bounded units (UBUs) in addition to lithosomes and classical lithostratigraphic units (and lithofacies). The latter are the basic mappable units adopted to describe the volcanic deposits and their vertical stratigraphic succession. Informal lithosomes are largely used to identify the main eruptive centres (and non-volcanic source areas) and to define their localization and shifts through time. UBUs display a stratigraphic framework of erosional and volcano-tectonic unconformities valuable for correlations at scale from local (single islands) to regional (Aeolian archipelago). By establishing a direct relationship between UBUs and time-stratigraphic units, the volcanic succession is readable in terms of different and successive eruptive epochs and eruptions (volcanic activity units), separated by periods of volcanic inactivity of varying duration. The different volcanic activity units are characterized by distinctive eruptive vents, eruption types and evolution of the involved magmas. Information on the eruptive behaviour and cyclicity and the transportation and deposition mechanisms is obtained by interpreting the lithostratigraphic units and lithofacies in terms of eruption units, thus providing fundamental insights on the eruptive history of a volcano and the evaluation of volcanic hazard.

Stratigraphic data highlight the conduit erosion behavior during Plinian eruptions: the example of the Pomici di Avellino eruption of Somma-Vesuvius

Massaro S.*¹, Costa A.² & Sulpizio R.¹

1. Dipartimento di Scienze della Terra e Geoambientali, Università di Bari. 2. INGV, Bologna.

Corresponding email: silvia.massaro@uniba.it

Keywords: Conduit erosion, Pomici di Avellino, lithics.

Lithic abundance data provide unique information on conduit evolution during Plinian eruptions and may aid in the reconstruction of eruption dynamics (Varekamp, 1993). Studies of components in explosive volcanic eruptions (Barberi et al., 1989; Sulpizio et al., 2010; Campbell et al., 2013) provided sound geological evidences on the source of lithic production. They highlight how it depends on conditions at fragmentation, mechanical characteristics of country rocks and erosive capacity of pyroclastic mixture on conduit walls. However, key processes of interaction of magma flow with its conduit walls (Macedonio et al., 1994; Costa et al. 2009) are still not well understood. In this scenario we propose a model of conduit erosion using a combination of stratigraphic data of the Pomici di Avellino eruption (Somma-Vesuvius; Sulpizio et al., 2010) and physical modeling, which accounts for the conduit evolution processes through lithic erosion at and above fragmentation level. The amount of lithics in the magmatic Plinian fallout deposits was assessed from field data at different stratigraphic heights, and then used for constraining the physical model. Keeping in mind general approximations, we found that lithic erosion can be responsible for geometry changes between lower and upper conduit during an explosive eruption, causing feedbacks on magma discharge. Therefore, the quantification of lithic component in a volcanic eruption could be essential to understand the evolution of the conduit geometry for assessing the initial mass distribution of the pyroclastic mixture, and also for forecasting the dispersal of tephra.

- Barberi F., Cioni R., Rosi, M., Santacroce R., Sbrana A. & Vecci R. 1989. Magmatic and phreatomagmatic phases in explosive eruptions of Vesuvius as deduced by grain-size and component analysis of the pyroclastic deposits. *J. Volcanol. Geotherm. Res.*, 38, 287-307.
- Campbell M.E., Russell J. & Porritt L.A. 2013. Thermomechanical milling of accessory lithics in volcanic conduits. *Earth Planet. Sci. Lett.*, 377-378, 276-286.
- Costa A., Sparks R.S.J., Macedonio G. & Melnik O. 2009. Effects of wall-rock elasticity on magma flow in dykes during explosive eruptions. *Earth Planet. Sci. Lett.*, 288, 455-462.
- Macedonio G., Dobran F. & Neri A. 1994. Erosion processes in volcanic conduits and application to the AD79 eruption of Vesuvius. *Earth Planet. Sci. Lett.*, 121,137-152.
- Sulpizio R., Cioni R., Di Vito M.A., Mele D., Bonasia R. & Dellino P. 2010. The Pomici di Avellino eruption of Somma-Vesuvius (3.9 ka BP). Part I: stratigraphy, compositional variability and eruptive dynamics. *Bull. Volcanol.*, 72, 539-558.
- Varekamp J.C. 1993. Some remarks on volcanic vent evolution during plinian eruptions. *J. Volcanol. Geoth. Res.*, 54, 309-318.

Volcanic rifts bracketing volcanoes: an analogue answer to an old unsolved problem

Mussetti G.*¹, Corti G.², van Wyk de Vries B.³ & Hagos M.⁴

1. Dipartimento di Scienze della Terra, Università di Firenze. 2. Istituto di Geoscienze e Georisorse, CNR, Firenze. 3. Université Blaise Pascal, Laboratoire Magmas et Volcans, Clermont-Ferrand, France. 4. Mekele Univeristy, Mekele, Ethiopia.

Corresponding email: mussetti giulio@gmail.com

Keywords: Analogue modelling, volcano-tectonics, extensional faults.

It has been observed in Central America that many volcanoes have volcanic alignments and faults at their east and west feet. A quick look at many continental rifts worldwide indicates that this also occurs for this geodynamic setting. While this feature has been noted for at least 30 years, no explanation has ever really been convincingly put forward. In order to analyse this process, we have run different series of analogue models investigating how and how much a volcanic system is deformed during continental rifting. We have implemented the presence of a volcanic edifice with an underlying shallow magma chamber. The models use a rubber sheet that is extended and provides a broad area of extension (in contrast to many moving plate models that have one localised velocity discontinuity). This well suits the situation in many rifts and diffuse strike-slip zones (i.e. Central America and the East African Rift). Model results indicate that the presence of a low-viscosity magma chamber (weaker than the surrounding) strongly localizes strain giving rise to curved faults bracketing the volcano. The resulting fault pattern, although dependent on the position and dimensions of the magma chamber, is very similar to several natural cases. Thus, we think we have found the answer to this long standing puzzle. We propose that diffuse extension of a volcano with underlying magma chamber generates two zones of faulting at the edge of the intrusion that serve to create surface faulting and preferential pathways for dykes. This positioning may also create craters aligned normal to the direction of extension, which is another notable feature of volcanoes in many continental rifts.

The use of AMS in the reconstruction of resurgent blocks kinematics: the Ischia island (Italy) case study

Ort M.H.¹, de Vita S.^{*2}, Marotta E.² & Sansivero F.²

1. School of Earth Sciences and Environmental Sustainability, Northern Arizona University, USA. 2. Istituto Nazionale di Geofisica e Vulcanologia, Osservatorio Vesuviano, Napoli.

Corresponding email: sandro.devita@ingv.it

Keywords: AMS, caldera resurgence, Ischia.

Paleomagnetic techniques are commonly used to recognize tilting of tectonic blocks. Typically, the remanent magnetization (the magnetization the rock acquired parallel to Earth's magnetic field during deposition and/or cooling) is used. This usually requires having a stable reference from which the original remanence can be determined. If the remanence has been altered by chemical or other processes, it may be difficult to identify the original remanence. Anisotropy of magnetic susceptibility (AMS) measures the fabric created by all the magnetic (para- and ferro-magnetic) minerals in a rock. It mimics the rock's structural or depositional fabric and often is little affected by an alteration that affects the remanence. If the rock has a fabric that is related to gravitational processes (e.g. a depositional near-horizontal planar fabric), the rotation of this fabric may be used to determine rotational processes. The island of Ischia is the visible portion of a volcanic complex rising more than 1,000 m above the sea floor in the Bay of Naples. It is an active volcanic field whose evolution is dominated by the caldera-forming eruption of the Mount Epomeo Green Tuff (ME GT; 55 ka). This trachytic ignimbrite partially filled the caldera depression in a submarine environment, and was also emplaced on land outside its margins. The caldera depression was later the site of marine sedimentation, which formed a sequence of tuffites, sandstones and siltstones. Resurgence occurred within the caldera, determining a net uplift of its floor of at least 900 m in the past 30 ky. The resurgent area has a polygonal shape resulting from the reactivation of regional faults and the activation of faults related to volcano-tectonism. The western sector of the resurgent block is bordered by high-angle reverse faults, cut by late normal faults due to gravitational readjustment of the slopes. The northwestern and the southwestern sides are bordered by vertical faults with right transtensive and left transpressive movements, respectively. To the east of the resurgent block, normal faults, generated during resurgence, formed a lowland, which is the site of the most recent volcanic activity. On Ischia, we found that the remanent magnetization was strongly affected by a chemical alteration and thus unreliable for indicating rotations, but AMS has provided another way to assess how much rotation has occurred. The Monte Epomeo Green Tuff has a strong, originally horizontal, planar fabric, likely due to compaction and welding of the deposit, and siltstones and sandstones deposited within the caldera depression before resurgence have a similar fabric. We have used this planar AMS fabric to identify the rotation of various blocks within the resurgent dome. What was previously identified as a simple-shear "trapdoor" resurgent dome appears to be an asymmetric block-resurgence, in which each differentially displaced block shows its own degree and direction of rotation.

The Baia - Fondi di Baia eruptions (Campi Flegrei): from fieldwork to physical volcanology

Pistolesi M.¹, Bertagnini A.², Di Roberto A.*², Isaia R.³, Cioni R.¹, Vona A.⁴, Mazzone F.⁵ & Voloschina M.⁵

1. Dipartimento di Scienze della Terra, Università di Firenze. 2. Istituto Nazionale di Geofisica e Vulcanologia, Pisa. 3. Istituto Nazionale di Geofisica e Vulcanologia, Osservatorio Vesuviano, Napoli. 4. Dipartimento di Scienze della Terra, Università Roma Tre.
5. Dipartimento di Scienze della Terra, Università di Pisa.

Corresponding email: alessio.diroberto@ingv.it

Keywords: Campi Flegrei, Baia-Fondi di Baia eruption, field volcanology.

Campi Flegrei is an active, densely populated caldera, therefore exposed to a very high volcanic risk associated with the possible occurrence of a future explosive eruption. In the last 15 ka this area experienced more than 70 eruptions, clustered in three main epochs separated by periods of quiescence of variable duration. The Baia-Fondi di Baia eruption opened the second epoch of activity which spans between 9.6 and 9.1 ka ago. Nowadays, the main morphological structures left by this eruption are represented by three circular depressions, aligned along a N-S trend, and partially hidden by marine ingression.

We investigated several outcrops in order to reconstruct the sequence of erupted products, the main deposit architecture and emplacement dynamics of tephra deposits. Results indicate that the vent first opened just off the present Baia harbour, possibly in a shallow water (marine/littoral) environment. After the opening phase, marked by the ejection of a coarse lithic-rich breccia, the activity rapidly escalated to the peak of intensity with formation of an eruptive column laid down fallout deposits alternated with minor pyroclastic density currents. The eruption shifted towards a dominant pulsating activity characterized by ballistic launches alternated with phases of pyroclastic density current generation. The analysed deposit sequences suggest that during this phase different vents location were simultaneously active, possibly related to a progressive southward migration of the active vents.

After a short period of rest, the second main explosive event occurred in the Fondi di Baia area, emplacing a second pyroclastic sequence juxtaposed above the deposit of Baia event. The Fondi di Baia eruption was again characterized by an opening phase during which abundant altered material and lithic blocks were ejected. This was immediately followed by the emission of pyroclastic density currents and by ballistic showers of obsidian ballistic bombs.

The results of field study on the tephra sequence are here presented, as well as the main volcanological features and physical parameters (e.g. grain-size, componentry, density and texture of the juvenile material, volumes and column heights) of this important eruptive cluster.

A new debris avalanche deposits on Tenerife (Canary Islands)

Principe C.*¹, Groppelli G.², Gottardi I.³, Faoro S.³, Antonelli A.³, Brogini R.³ & Martí Molist J.⁴

1. Istituto di Geoscienze e Georisorse, C.N.R. Pisa. 2. Istituto per la Dinamica dei Processi Ambientali, C.N.R. Milano. 3. Dipartimento di Scienze della Terra "A. Desio", Università di Milano. 4. Consejo Superior de Investigaciones Científicas (CSIC), Barcelona, España.

Corresponding email: c.principe@igg.cnr.it

Keywords: Debris avalanche deposit, Tenerife, cartography in volcanic areas.

This contribution deals with the new geological map at the 1:15.000 scale of a portion of Tenerife in Canarias and with the characterization of a new *debris avalanche* discovered on the SW sector of the island. Lithostratigraphic units (25) above and under the Platanita *debris avalanche* deposits (PDAD) have been mapped on a surface of about 50 km². In the portion of PDAD deposit still outcropping there are not hummocky morphologies but the deposits lies on faults oriented NNW-SSW, opposite to the debris avalanche dispersion direction in a portion of land still preserving the characteristic horse shaped morphology. The PDAD have been described by means of sedimentological (granulometry and componentry analysis) and petrochemical analyses. PDAD shows a fine matrix and a disequigranular blocks component having a polimodal granulometric distribution as normally happens in DA deposits. Granulometric analyses show about 5-15 % of clays inside the deposit. Blocks refer to 4 different lithologies and vary from subafiric (3) to porphyritic with scarce olivine (1). The porphyritic lava is referable to the Llano de Los Salvajes unit at the base of the PDAD. Clast's chemical analyses highlighted the presence of both alkaline lava (from tefro-basanite to trachi-basalt, basalt and basaltic trachi-andesite) and sub-alkaline lava groups (basaltic trachi-andesite and trachi-andesite). The same chemical typologies form the succession covering the PDAD, inside the Platanita debris avalanche sector collapse. Debris avalanche deposits are loose deposits. At the contrary PDAD is uniformly welded by a fine cement that resulted to be composed by microgranular phillipsite and k-feldspar. They are authigenic minerals (as they are not found inside the rocks forming the debris avalanche deposit nor the nearby lava flows). The origin of welding has been interpreted as due to hydrothermal circulation inside the PDAD. Different temperatures of hydrothermal waters are responsible for the formation of phillipsite (120-150 °C) or k-feldspar (< 300 °C). This secondary alteration can also explain the partial zeolitization of the southernmost portion of the Güimar debris avalanche deposit (SE of Tenerife).

Stratigraphic architecture of the Campania Plain, southern Italy. A key to understand evolution and impact of volcanic activity

Ruberti D.*¹, Vigliotti M.², Ermice A.², Rolandi G.³ & Rolandi R.⁴

1. Dipartimento di Ingegneria Civile, Design, Edilizia, Ambiente, Seconda Università di Napoli. 2. Dipartimento di Scienze e Tecnologie Ambientali, Biologiche e Farmaceutiche, Seconda Università di Napoli. 3. Dipartimento di Scienze della Terra, dell'Ambiente e delle Risorse, Università di Napoli "Federico II". 4. Consultant Geologist.

Corresponding email: daniela.ruberti@unina2.it

Keywords: Campania Plain, volcanic activity, Campania Grey Tuff.

For its important volcanic activity the Campania Plain, a wide flat area extended between Naples and Caserta, and delimited by the Apennine foothills toward north, east and south, and by Tyrrhenian sea, toward west, has been identified as “Campanian Volcanic Zone (CVZ). The CVZ, since the time of its formation, had the structure of a “graben”. The tectonic lines, along which the lowering are well recognizable on the edge of the plain, are faults oriented NE-SW and NW-SE. Considering the CVZ as a regional tectonic depression, many authors believe that many voluminous pyroclastic flow eruptions were vented directly from Apennine sedimentary fault graben, the last being the 39 ky Campania Grey Tuff (CGT), an eruption of 200 km³.

The pyroclastic flow deposits of the CGT blanketed the whole area filling morphological depressions and dipping gently towards the central region of the Plain. Different lithofacies can be recognized within this unit from the base of Apennine foothills to the Plain, mostly derived by the different mineralogic composition in turns related to secondary processes that locally promoted a glass-to-zeolite and analcime/feldspar transformation. On the whole, from top to bottom the succession of CGT lithofacies is characterized by an upper incoherent part, represented by the *cinerazzo* (*cz*) lithofacies, to the coherent *zeolitic yellow tuff* (*tgz*) and *grey tuff* (*tg*), *piperno tuff* (*tp*), and *pipernoide* (*pp*) ones. Close to the bottom of this unit, a soft lithofacies occurs, called *cinerite* (*cn*). The whole thickness of CGT is 50-55 m and it decreases near the piedmont area.

Thin grey, loose ashy deposits (max. 90 cm) related to an intensive volcanic activity dated back 15 ky B.P. (Neapolitan Yellow Tuff - NYT), draped the existing morphology, locally separated from underlying CGT by a paleosol up to 200 cm thick, with brown muddy-ashy matrix and presence of organic matter reworked upward.

A geological characterization of subsoil derived from the study of a dataset including about 1000 lithostratigraphic logs from boreholes reaching the depth of 10-to-150 m b.g.l. coupled with field surveys. The study was based on geological, geomechanical, pedological and hydrogeological data, managed into a GIS environment to reconstruct a 3D geological model.

In particular, specific insights have been delineated on the volcanoclastic lithofacies heteropies of CGT across the entire area of study, also considering the contribution of pedogenesis on the reconstruction of the stratigraphic setting and relative implications on groundwater quality concerns, as paleosols are usually regarded as aquitards. This latter tool can result particularly adequate on land surfaces interested by volcanic activity, due to the intermittent deposition of the involved sediments and possible time span for soil development. Moreover, the detailed recognition of the CGT lithofacies in the subsoil suggested new insights in the processes responsible for the volcanic sequence settling.

The study has also permitted to reconstruct the upper surface of the GCT in the whole Plain and recognize a deep downcutting in correspondence of the modern Volturno river course. The resulting palaeovalley is about 15-20 km wide and up to 30 m deep in the depocentre and was originated as a response to the Last Glacial Maximum sea-level drop. This unit represents the first substrate for the Holocene and recent sedimentation.

Insights on volcanic granular flow dynamics from laboratory experiments and comparison with natural deposits

Sulpizio R.*¹, Sarocchi D.², Dellino P.¹ & Rodriguez-Sedano L.A.³

1. Dipartimento di Scienze della Terra e Geoambientali, Università di Bari. 2. Instituto de Geología, Universidad Autónoma de San Luis Potosí, Mexico. 3. Centro de Geociencias, Universidad Nacional Autónoma de México, México.

Corresponding email: roberto.sulpizio@uniba.it

Keywords: Granular flows, volcanic hazard, laboratory experiments.

The complex transportation and depositional processes of hazardous volcanic coarse-grained dry granular flows are investigated by means of ad hoc designed flume experiments that allowed both documenting the particulate organisation during transportation along a steep slope and visualising aggradational deposition beyond the break-in-slope. The broad grain-size range used in experiments allowed depicting both the behaviour of coarse clasts and that of fine ash. The kinematic of the granular flow shows that the coarse grained flow moves in an inertial regime for slope angles above the internal friction angle of the material, while the main body moves along the slope with a more complex, not inertial behaviour. The granular material show self-organisation of its internal structure since the early stage of the movement along the slope, with formation of a reversely graded flow that suddenly develop Kelvin-Helmholtz like instabilities at the passage between the fine-grained basal part and the coarse grained upper portion. This flow organisation implies that the frictional work is mainly exerted by the basal, fine-grained part, which is pushed along the slope by gravitational force and by the traction effect exerted by the upper portion of the flow. Deposition occurs in the flat area beyond the break in slope due to the increasing frictional forces and to the decreasing contribution of gravitational force to the granular flow motion. Results can help interpreting the mechanisms of natural volcanic flows forming on steep slopes of stratovolcanoes and provide useful insights on behaviour of natural granular flows.

Proximal products of the 16 March, 2013 eruption of Mt. Etna: dynamics and significance of large ejecta

Todde A.*¹, Cioni R.¹, Andronico D.² & Mundula F.³

1. Dipartimento di Scienze della Terra, Università di Firenze. 2. Istituto Nazionale di Geofisica e Vulcanologia, Osservatorio Etneo, Catania. 3. Dipartimento di Scienze Chimiche e Geologiche, Università di Cagliari.

Corresponding email: andrea.todde@stud.unifi.it

Keywords: Ballistic ejecta, bomb shape, Etna.

On March 16, 2013, at the New South-East Crater (NSEC) of Mt. Etna an episode of lava fountain took place, preceded, since the day before by a low-intensity strombolian activity. The analysis of the video-recordings of the monitoring system of the Etnean Observatory (INGV-Catania) suggests that the lava fountain episode lasted for half an hour, and was characterized by at least one violent explosion, occurred in the conclusive phases, during which large magma fragments were radially launched from the vent. Most of these ballistic ejecta landed on the S-SW sector at the base of the NSEC cone.

In order to have insights into the dynamics of the eruption and the large-scale characteristics of the erupting magma, we concentrated our study on a bomb field located in the same sector, up to a distance of 600-750 m from the NSEC, characterized by a large amount of coarse, up to 7 m long, ballistic ejecta.

We collected, described and sampled 34 of these ejecta, measuring dimensions of the three main axes and of their impact craters. Bomb shape can vary from flattened to elongate, from spindle, to ribbon-like to compact, and half of these ejecta have shapes from partially to strongly twisted. Basing on their shape and lithology, four different types of bombs are described: Twisted, Ribbon-Spindle, Blocky and Scoriaceous.

Representative samples from each type were collected, and their density measured using Archimedes' principle. Three density classes can be recognized: <1000 kg m⁻³ (Scoriaceous bombs); 1100-2400 kg m⁻³ (Twisted and Ribbon-Spindle bombs); 2400-2600 kg m⁻³ (Blocky bombs).

Bomb surface is typically smooth, cut by poorly penetrative fractures, that differ in length and orientation. Fractures can either form sets of high-angle cracks, creating polygonal pattern, or develop in groups of constant fracture orientation. Bomb interior ranges from dense to highly vesicular. Vesicle distribution largely varies, from homogeneous, to strongly heterogeneous (in the less vesicular bombs). A distinctive characteristic of Twisted and Ribbon-Spindle bombs is the presence of foliations, marked by vesicle alignments.

Measurements on the different bombs were also used to assess the main physical parameters driving the motion of ballistic ejecta from the vent (ejection angle and velocity) up to their impact on the ground (impact angle and velocity), using the ballistic trajectory calculator *Eject!* (Mastin, 2008) combined with field and density data. Based on the observed differences in texture, we also propose a model for the pre-fragmentation volcanic conduit stratigraphy, linking the four bombs typologies here described to a syn-eruptive vertical and lateral zonation of the conduit.

Mastin L.G. 2008. A simple calculator of ballistic trajectories for blocks ejected during volcanic eruptions, version 1.4, U.S. Geol. Sur. Open File Rep., 01–45.

Structural analysis of fractures, faults and dykes in the Somma-Vesuvio volcano

Tramparulo F.D.A.*¹, Isaia R.² & Vitale S.¹

1. Dipartimento di Scienze della Terra, dell'Ambiente e delle Risorse (DiSTAR), Università di Napoli "Federico II"
2. Istituto Nazionale di Geofisica e Vulcanologia, Osservatorio Vesuviano, Napoli.

Corresponding email: francescodassisi.tramparulo@unina.it

Keywords: Somma-Vesuvio, structural analysis, volcano tectonics.

A geological and structural survey on the Somma-Vesuvio volcanic edifice has been carried out with the main aims to define the contribution of local versus regional stress field in the evolution of the volcano and the relationships between caldera evolution, fractures and faults. Measurements of fractures, faults and dykes were collected, mainly inside the caldera sector, and analyzed to characterize the fracture network affecting volcanic rocks. Structures were recorded both in lavas and pyroclastic rocks. Most of fractures in lavas are cooling joints. Several cooling joint are reactivated as normal faults, following the caldera collapse. Generally fractures both parallel and orthogonal to caldera rim occur. Finally recent fractures are associated to gravity instability of volcano edifice are well evident in the eastern sector of the Mt. Somma. Other normal faults characterized by low angle dips occur along the cliff of Mt. Somma. Dykes appear as planar at places forming an en-echelon pattern or with a ramp-flat geometry. Fractures, dykes and fault show some preferred orientations. A field stress map was carried out from inversion of meso-scale faults and fractures.

SESSION S11

Mineralogy

CONVENORS

Luca Bindi (Univ. Firenze)

Sabrina Nazzareni (Univ. Perugia)

Elastic geobarometry for UHPM rocks: A link between mineralogy and petrology

Alvaro M.*¹, Angel R.J.², Mazzucchelli M.L.¹, Domeneghetti M.C.¹ & Nestola F.²

1. Dipartimento di Scienze della Terra e dell'Ambiente, Università di Pavia. 2. Dipartimento di Geoscienze, Università di Padova.

Corresponding email: matteo.alvaro@gmail.com

Keywords: UHPM rocks, elastic geobarometry, equations of state.

Subduction processes, the key tile of the plate tectonics puzzle controlling the vast majority of the geological processes that affect life on Earth, are still poorly understood. The paradigm that low-density continental crust cannot undergo deep subduction was broken 30 years ago with the milestone discovery of metamorphic rocks of continental affinities containing coesite (Chopin, 1984) and microdiamond (Sobolev & Shatsky, 1990). These discoveries proved that buoyant continental crust can be subducted to depths greater than 100 km and subsequently be returned to the Earth's surface as ultra-high-pressure metamorphic (UHPM) rocks. These UHPM rocks are the key for understanding large-scale geodynamic processes. This information cannot be obtained from real-time geophysical or seismic data, but only by determining the pressure-temperature-time (P-T-t) histories of the UHPM rocks themselves. While the presence of index minerals such as coesite and diamond in UHPM rocks indicates minimum pressures of subduction, they do not provide P or T values.

We therefore provide an independent method of P and T determination that does not rely on the detailed chemistry of the rock, nor on whether chemical equilibrium has been obtained. The elastic behavior of mineral inclusions trapped in host minerals phase contained in UHPM rocks provides such an alternative. The difference in the thermodynamic properties of host and inclusion leads to the inclusion being over-pressured in the recovered rock and this overpressure can be used in combination with the equations of state (EoS) of the minerals to determine the entrapment P and T. We have successfully developed single-crystal diffraction methods to determine inclusion pressures of olivines in diamonds (Nestola et al., 2011), which in combination with new methods of handling the elasticity and EoS problem lead to more precise estimates of entrapment conditions (Angel et al., 2015). These new methods in UHPM rocks allows to pinpoint P,T points in rock history independent of chemistry thus providing critical constraints for understanding the wide range of styles of deep subduction that appear to have occurred in the Earth over its history.

This work was supported by the ERC starting grant n. 307322 to F. Nestola

- Angel R.J., Alvaro M., Nestola F., Mazzucchelli M.L. 2014. Diamond thermoelastic properties and implications for determining the pressure of formation of diamond-inclusion systems. *Russ. Geol. Geophys.*, 56, 211-220.
- Chopin C. 1984. Coesite and pure pyrope in high-grade blueschists of the Western Alps: a first record and some consequences. *Contrib. Mineral. Petrol.*, 86, 107-118.
- Nestola F., Nimis P., Ziberna L., Longo M., Marzoli A., Harris J.W., Manghnani M.H. & Fedortchouk Y. 2011. First crystal-structure determination of olivine in diamond: Composition and implications for provenance in the Earth's mantle. *Earth Planet. Sci. Lett.*, 305, 249-255.
- Sobolev N.V. & Shatsky V.S. 1990. Diamond inclusions in garnets from metamorphic rocks: a new environment for diamond formation. *Nature*, 343, 742-746.

Spontaneous strain variations through the monoclinic-orthorhombic phase transition of ZSM-5 zeolite: effect of adsorbed organic molecules

Ardit M., Martucci A., Rodeghero E. & Cruciani G.*

Dipartimento di Fisica e Scienze della Terra, Università di Ferrara.

Corresponding email: cruciani@unife.it

Keywords: ZSM-5, phase transition, spontaneous strain.

Depending on composition, framework defect density, temperature, or nature and amount of guest molecules in the channels, synthetic ZSM-5 zeolites (MFI framework topology) undergo a polymorphic monoclinic ($P2_1/n$) -to-orthorhombic ($Pnma$, $Pn2_1a$, or $P2_12_12_1$) phase transition. Such a ferroelastic-paraelastic phase transition has been recently characterized through the analysis of the spontaneous strain variation in a highly siliceous ZSM-5. According to the Landau theory, the behavior of the order parameter (Q) revealed that the ZSM-5 zeolite underwent a displacive phase transition at $T_c = 348(1)$ K with a tricritical character (Ardit et al., 2015). Recent investigations have demonstrated that hydrophobic ZSM-5 is extremely promising and efficient as adsorbent for the removal of organic contaminants from waters. This issue engenders particular interest in the scientific community. Therefore, modeling the ferroelastic properties of the $m \leftrightarrow o$ phase transition of ZSM-5 zeolites is very relevant to the understanding of the effects of lattice strain mechanism on adsorption and diffusion properties of these microporous materials. For these reasons, the previously characterized ZSM-5 zeolite (CBV28014, Zeolyst International, $\text{SiO}_2/\text{Al}_2\text{O}_3 \approx 280$) has been loaded with three different organic molecules (i.e. dichloroethane (DCE), methyl tertiary-butyl ether (MTBE) and toluene (TOL), respectively), and its high-temperature behaviour monitored by means of synchrotron X-ray diffraction data (collected *in situ* at ID31, ESRF). Besides causing a strong variation in the $m \leftrightarrow o$ phase transition temperature, i.e. $T_{c(\text{TOL})} = 328(4)$ K $< T_{c(\text{DCE})} = 346(1)$ K $< T_{c(\text{ZSM-5})} = 348(1)$ K $< T_{c(\text{MTBE})} = 360(2)$ K, the presence of organic molecules within the zeolite channels affects the mechanisms of lattice strain. Since the ZSM-5 structure belongs to the "Aizu-type" $mmmF2/m$, the primary order parameter behaves as the symmetry-adapted strain, then a proper spontaneous strain is involved. This means that Q can be coupled with the largest component of the spontaneous strain for each sample, i.e. the shear strain tensor e_{13} . Although the analysis of Q reveals that all the compared samples undergo a displacive phase transition with a tricritical character, our results suggest that the strain effects are dependent not only by the physico-chemical features of ZSM-5 and organics but also by the occurrence of host-guest and guest-guest interactions.

Ardit M., Martucci A. & Cruciani G. 2015. Monoclinic-orthorhombic phase transition in ZSM-5 zeolite: spontaneous strain variation and thermodynamic properties. J. Phys. Chem. C, 119, 7351-7359.

Sodalite-group minerals from Somma-Vesuvius volcano (southern Italy): an EPMA, SIMS and FTIR study

Balassone G.*¹, Bellatreccia F.², Ottolini L.³, Mormone A.⁴, Petti C.⁵, Della Ventura G.² & Ghiara M.R.¹⁻⁵

1. Dipartimento Scienze Terra, dell'Ambiente e delle Risorse, Università di Napoli "Federico II". 2. Dipartimento di Scienze, Università di Roma Tre.
3. Istituto di Geoscienze e Georisorse, CNR, Pavia. 4. INGV, Osservatorio Vesuviano, Napoli. 5. Museo di Mineralogia, Università di Napoli "Federico II".

Corresponding email: balasson@unina.it

Keywords: Sodalite group minerals, Somma-Vesuvius volcano, EPMA.

Sodalite-group minerals (SGM) are Na- and Ca-bearing feldspathoids which can contain chlorine, reduced or oxidized sulfur, and water or hydroxyl groups as extraframework volatile species. The most widespread members are sodalite $\text{Na}_8\text{Al}_6\text{Si}_6\text{O}_{24}\text{Cl}_2$, nosean $\text{Na}_8\text{Al}_6\text{Si}_6\text{O}_{24}\text{SO}_4$, haiüyne $\text{Na}_6\text{Ca}_2\text{Al}_6\text{Si}_6\text{O}_{24}\text{Cl}_2$, and lazurite $\text{Na}_8\text{Al}_6\text{Si}_6\text{O}_{24}\text{S}$. SGM typically occur in undersaturated alkaline igneous rocks, and in some hydrothermal and metamorphic rocks. SGM are of interest for the study of magmatic systems, and their volatile components can be useful because they can provide key information on the genetic environment, like degassing dynamics and fluids behavior during hydrothermal processes. Besides, SGM are very promising in different fields of material science, due to their particular (ultra)microporous structures (Bellatreccia et al., 2009). The present study is focused on crystal-chemical characterization of cationic and anionic components of SSG occurring in various igneous to metamorphic rocks and ejecta from Somma-Vesuvius volcano (southern Italy), deriving from the collection of Mineralogical Museum (Univ. Napoli Federico II). Detailed electron probe microanalysis (EPMA), secondary ion mass spectrometry (SIMS) and Fourier transform infrared micro-spectroscopy (μ -FTIR) investigations have been carried out on thirty-nine samples, ranging from metamorphic and magmatic xenoliths to lavas related to different eruption times. Microbeam techniques, as SIMS and μ -FTIR, are of key importance to probe trace to ultra-trace contents and speciations of volatiles (Bellatreccia et al., 2009; Ottolini et al., 2006). Our investigations show that the studied SGM correspond to sodalite, nosean (here referred as sulfatic sodalite) and haiüyne. SIMS measurements on H, F and C show contents: 0.02 - 5.0 wt.% H_2O , 0.01 - 0.14 wt.% F, and 0.69 - 2.95 wt.% CO_2 . Within the single crystals, F is always very low, whereas concentrations of H_2O and, to a lesser extent, CO_2 can vary from homogeneous to strongly inhomogeneous. μ -FTIR spectra of SGM can be grouped into sodalites and sulphatic sodalites/haiüynes, according to the occurrence of the $^{12}\text{CO}_2$ absorption at 2340 cm^{-1} . The absorption due to H_2O and/or OH groups occurs as a very broad band (3700 cm^{-1} - 3000 cm^{-1}). In all samples FTIR data show the presence of CO_3^{2-} . Homogeneous vs. inhomogeneous distribution of H and C was also revealed by μ -FTIR focal plane array imaging, which shows an antithetical distribution of CO_2 and especially of H_2O , in agreement with the SIMS results. The collected data allow us to fully characterize SGM from Somma-Vesuvius, providing also with some constraints about their genesis.

Bellatreccia F., Della Ventura G., Piccinini M., Cavallo A. & Brilli M. 2009. H_2O and CO_2 in minerals of the haiüyne-sodalite group: an FTIR spectroscopy study. *Mineral. Mag.*, 73, 399-413.

Ottolini L., Cámara F. & Hawthorne F.C. 2006. Strategies for quantification of light elements in minerals by SIMS: H, B and F. *Microchim. Acta*, 155, 229-233.

An insight into the mechanism of Fe (III) acquisition by erionite fibres: a first step toward the comprehension of the mechanisms inducing their carcinogenicity

Ballirano P.*¹, Pacella A.¹, Cremisini C.², Nardi E.², Montereali M.R.², Fantauzzi M.³, Atzei D.³,
Rossi A.³ & Cametti G.⁴

1. Dipartimento di Scienze della Terra, Sapienza Università di Roma. 2. ENEA, S. Maria di Galeria (RM). 3. Dipartimento di Scienze Chimiche e Geologiche, INSTM Research Unit, Centro Grandi Strumenti, Università di Cagliari. 4. Institut für Geologie, Universität Bern, Switzerland.

Corresponding email: paolo.ballirano@uniroma1.it

Keywords: Erionite, zeolite, malignant mesothelioma.

Several experiments for understanding the mechanism of carcinogenicity of erionite fibres from Rome (Oregon, USA) were carried out following the incubation of the fibres in FeCl₃ solutions at different concentrations. Inductively coupled plasma optical emission spectrometry (ICP-OES) was used to monitor the ion release from the fibres into solution, X-ray powder diffraction (XRPD) and scanning electron spectroscopy (SEM) with energy dispersive spectroscopy (EDS) were applied to define both structural and chemical modifications possibly occurring into the fibres, and X-ray photoelectron spectroscopy (XPS) was performed to unveil the chemistry of the fibres surface.

Comparison between released and acquired charges under form of Fe confirms, in agreement with previous studies (Eborn & Aust, 1995), that Fe (III) is almost completely fixed at the fibres surface. This is a completely different behaviour with respect to Fe (II), which is ion-exchanged via a process involving the extra framework (EF) cations, mainly Na (Ballirano et al., 2015). The Fe (III) binding process highlights a direct correlation between the Fe fixed at the fibres surface and the Fe (III) concentration of the solution up to a maximum concentration of 1000 µM FeCl₃. Notably, Fe still resides at the fibre surface after its reduction by fibre incubation in ascorbic acid for 24 h. Chemical (SEM-EDX) and structural (Rietveld refinement) data show that possibly a very small amount of Fe (III) resides at the Ca3 site (ca. 10% of the total Fe (III) bound by fibres). It is worth noticing that ion-exchanged Fe (II) has been located at the same cation site, albeit with a significantly higher population (Ballirano et al., 2015). Besides, in Fe-doped zeolites at rather low Fe content, Fe sites with very low nuclearity (single ions, dimers or oligomers), located in well-defined crystallographic positions, are the most active in the generation of reactive oxygen species (ROS) (Zecchina et al., 2007). On this basis, identification of the segregation of both Fe (II) at Ca3 site and Fe (III) (mainly) on the surface provides very important information for the comprehension of the molecular mechanism/s inducing the strong carcinogenicity of erionite.

Ballirano P., Pacella A., Cremisini C., Nardi E., Fantauzzi M., Atzei D., Rossi A. & Cametti G. 2015. Fe (II) segregation at a specific crystallographic site of fibrous erionite: A first step toward the understanding of the mechanisms inducing its carcinogenicity. *Micropor. Mesopor. Mat.*, 211, 49-63.

Eborn S.K. & Aust A.E. 1995. Effect of iron acquisition on induction of DNA single-strand breaks by erionite, a carcinogenic mineral fiber. *Arch. Biochem. Biophys.*, 316, 507-514.

Zecchina A., Rivallan M., Berlier G., Lamberti C. & Ricchiardi D. 2007. Structure and nuclearity of active sites in Fe-zeolites: comparison with iron sites in enzymes and homogeneous catalysts. *Phys. Chem. Chem. Phys.*, 9, 3483-3499.

Multi-methodological characterization of opals: Defining origin, structure, composition and gemological Properties

Barucca S.¹, Bellatreccia F.*¹⁻², Della Ventura G.¹⁻², Butini F.¹⁻³, Casanova Municchia A.¹, Ricci M.A.¹ & Sodo A.¹

1. Dipartimento di Scienze, Università Roma Tre. 2. Istituto Nazionale di Fisica Nucleare, Laboratori Nazionali di Frascati, Roma.

3. Istituto Gemmologico Nazionale, Roma.

Corresponding email: fabio.bellatreccia@uniroma3.it

Keywords: Opals, synthetics, imitation.

Opals are water-bearing micro- to non-crystalline materials, made-up of micro-spheres of hydrated silica ($\text{SiO}_2 \cdot n \text{H}_2\text{O}$) with a high grade of structural disorder. Owing to their optical features, opals have been largely used in jewelry and as decorative elements in art works. The characteristic optical phenomenon of the opal, called “play of color”, is due to the interaction of light with their pseudo-structure composed mainly of regularly-spaced layers consisting of microscopic (average diameter few hundreds of nm) silica spheres. By the gemological classification, opals are classified upon the presence or absence of this optical phenomenon. Due to their high economic value, rarity and preciousness, various types of imitations and synthetic opals are available on the gems market and could be used to substitute original gems in artworks. Therefore, it is important to distinguish natural opals from synthetic ones and from the various imitations. Based on the mineralogical composition, opals can be classified into three typologies, depending on the leading mineralogical constituent: opal-C (cristobalite- α , less disordered structure), opal-CT (cristobalite- α and tridymite- α , disorder structure), both generally of volcanic genesis, and opal-A (amorphous opal, more disorder structure), commonly of sedimentary genesis. Due to its semi-amorphous, of long-range ordered nature, hydrous silica is a complex material, and its study requires the combination of different analytical methods. Raman spectroscopy is a useful tool to analyze opals (Ostrooumov et al., 1999) and to identify their different geological provenance, precisely for its ability to detect the presence of nano-sized domains of silica polymorphs, as well as the presence of non-crystalline phases. The spectroscopic data can be implemented by XRD (long-range order information), SEM (morphological imaging) and FTIR (presence and distribution of $\text{H}_2\text{O}/\text{OH}$, CO_2 and other molecular arrangements) for a complete characterization of the opal. A set of more than 20 natural opals coming from the main known deposits all around the world (Australia, Madagascar, Slovakia, Mexico, Honduras and Ethiopia) were studied by Raman, FTIR, XRD and SEM, with the aim to defining a method to distinguish their geological occurrence. Comparison with synthetic materials and imitations is also presented. This study shows that by combining the analytical information, it is possible to evidence some features that could be used as fingerprints of the geological origin (volcanic vs sedimentary) and probable provenance. The distinction of synthetic/imitation vs natural opals is also feasible based on the spectroscopic data.

Ostrooumov M., Fritsch E., Lasnier B. & Lefrant S. 1999. Spectres Raman des opales: Aspect diagnostique et aide à la classification. *Eur. J. Mineral.*, 11, 899-908.

FTIR spectroscopy of phosphate minerals with complex H-bonds network

Bellatreccia F.^{*1-2}, Della Ventura G.¹⁻², Cestelli Guidi M.², Ventruti G.³, Schingaro E.³, Capitelli F.⁴ & Grita S.¹

1. Dipartimento di Scienze, Università Roma Tre. 2. Istituto Nazionale di Fisica Nucleare, Laboratori Nazionali di Frascati (RM). 3. Dipartimento di Scienze della Terra e Geoambientali, Università di Bari. 4. Istituto di Cristallografia, C.N.R. Monterotondo (RM).

Corresponding email: fabio.bellatreccia@uniroma3.it

Keywords: Phosphates, FTIR, hydrogen bond.

Phosphates are among the most complex and variegated compounds in the entire mineral kingdom. Currently the total number of distinctive phosphate species is about 300 and most of them contains hydrogen as OH, H₂O or in HPO₄²⁻ group. Hydrogen bond has a central role in stabilizing the hydroxy-hydrated phosphate (HHP) structures because it supplies the additional bond-valence (0.1 - 0.3 vu) contribution to the anions. Hence the (PO₄) groups can link easily to all other interstitial cations (Huminicki & Hawthorne, 2002). For this reason, most HHPs are characterized by the presence of complex tridimensional networks of O-H...O hydrogen bonds, which connect the polyhedral units making up a three dimensional framework. Consequently, the dimensionality of the structural unit is controlled primarily by the amount and role of hydrogen in the structure (Hawthorne, 1998). This could explain the observed correlation between the position in the paragenetic sequence of pegmatitic phosphates, and the amount of H₂O in their formula (Fisher, 1958). FTIR spectroscopy is a powerful tool for the study of hydrogen in minerals, but HHPs are rather challenging to study because of their complex structures. Moreover, due the high OH/H₂O contents, these minerals show extremely intense IR absorptions in the OH region. In this work, we describe the results obtained by IR spectroscopy in different spectral regions of selected phosphates (veszelyite, whiteite, vauxite, paravauxite, metavauxite, augelite, wardite, wavellite, lazulite, arrojadite). O-H and hydrogen bonds orientation were studied by single crystal polarized light m-IR-spectroscopy, and experiments at HT- and LT were performed to study phase transitions and dehydration mechanisms with the aim of defining the thermal stability of these minerals. Finally, some applications done by using the novel FPA-FTIR imaging methods are presented.

Fisher D.J. 1958. Pegmatite phosphates and their problems. *Am. Mineral.*, 43, 181-207.

Hawthorne F.C. 1998. Structure and chemistry of phosphate minerals. *Mineral. Mag.*, 62, 141-164.

Huminicki D.M.C. & Hawthorne F.C. 2002. The Crystal Chemistry of the Phosphate Minerals. In: Kohn M.L., Rakovan J. & Hughes J.M. Eds., *Phosphates Geochemical, Geobiological, and Materials Importance*. *Rev. Mineral. Geochem.*, 48, 123-254.

Applications of Raman spectroscopy to the study of natural manganese oxides

Bernardini S.*¹, Bellatreccia F.¹, Casanova Municchia A.², Della Ventura G.¹ & Sodo A.²

1. Dipartimento di Scienze - Sezione di Geologia, Università di Roma Tre.

2. Dipartimento di Scienze - Sezione di Nanoscienze e Nanotecnologie, Università di Roma Tre.

Corresponding email: SIM.BERNARDINI@stud.uniroma3.it

Keywords: Manganese oxides, Raman spectroscopy, infrared spectroscopy.

This work relates on the use of Raman spectroscopy as a tool for studying manganese compounds. The final aim is to build a Raman spectra database of well-characterized Mn minerals (both synthetic and natural), to be used, in particular, to characterize pigments in pottery, frescos and illuminated manuscripts.

There are many incongruences regarding the Raman spectra of natural and synthetic Mn compounds reported in literature (Buciuman et al., 1999; Julien et al., 2006). This is due to the difficulties in their study, the low Raman activity of manganese oxides, the high sensitivity of manganese compounds under the laser beam and, in the case of the synthetic compounds, in different synthesis methods.

Mn minerals occur typical as fine-grained mixtures of different phases: essentially oxides and hydroxides, but also carbonates and silicates. The poor crystallinity of many Mn oxides/hydroxide makes difficult their study by standard X-ray diffraction methods. Indeed, the XRPD patterns show typically few and broad peaks, so that an accurate identification of the material is rather difficult. The presence of other phases, such as silicates and carbonates, further complicates the identification of the single constituents. Potter & Rossman (1979) showed that FTIR spectroscopy is a very powerful tool, coupled with XRPD, to characterize Mn minerals. In fact, IR spectroscopy yields reliable information on disordered and poor crystalline materials as Mn oxides typically are. It also provides evidence for the presence of H₂O and OH in the sample.

Ten oxides/hydroxide Mn minerals (chalcophanite, cryptomelane, hausmannite, hollandite, lithiophorite, manganite, manganosite, pyrolusite, ramsdellite, rancieite, romanechite) were characterized by using XRPD coupled with FTIR and Raman spectroscopy. The results show that, in the case of samples consisting of intermixed Mn-phases, Raman spectroscopy, because of its high spatial resolution, provides an efficient tool to differentiate them.

Buciuman F., Patcas F., Craciun R. & Zahn D.R.T. 1999. Vibrational spectroscopy of bulk and supported manganese oxides. *Phys. Chem. Chem. Phys.*, 1, 185-190.

Julien C.M. 2006. Local structure of lithiated manganese oxides. *Solid State Ionics*, 177, 11-19.

Potter R.M. & Rossman G.R. 1979. The tetravalent manganese oxides: Identification, hydration, and structural relationships by infrared spectroscopy. *Am. Mineral.*, 64, 1199-1218.

Structural complexity in sulfosalts – “Cu-sterryite” and meerschautite: two new expanded derivative of owyheeite from Italy

Biagioni C.*¹, Bindi L.² & Moëlo Y.³

1. Dipartimento di Scienze della Terra, Università di Pisa. 2. Dipartimento di Scienze della Terra, Università di Firenze
3. Institut des Matériaux Jean Rouxel, CNRS, Université de Nantes, France.

Corresponding email: biagioni@dst.unipi.it

Keywords: “Cu-sterryite”, meerschautite, sulfosalts.

Two new expanded derivatives of owyheeite, a rare Ag-Pb-Sb sulfosalt having a composition close to $\text{Ag}_3\text{Pb}_{10}\text{Sb}_{11}\text{S}_{28}$, have been described from hydrothermal ores in Italy. The new species, “Cu-sterryite” and meerschautite, are closely related to sterryite and parasterryite, whose crystal structures were recently solved by Moëlo et al. (2012) on samples from the Pollone mine, Tuscany, Italy.

“Cu-sterryite” is the Cu-isotype of sterryite, ideally $\text{Cu}(\text{Cu},\text{Ag})_3\text{Pb}_{19}(\text{Sb},\text{As},\text{Bi})_{22}(\text{As}_2)\text{S}_{56}$. It occurs as very rare black tubular crystals, up to 150 μm in size, in quartz veins from the Esperance superiore tunnel, Tavagnasco mine, Torino, Piedmont. Electron-microprobe data gave (in wt%): Cu 2.33, Ag 0.53, Hg 0.98, Tl 0.78, Pb 44.06, Bi 1.75, Sb 23.90, As 4.66, S 20.37, sum 99.38. On the basis of 56 S atoms per formula unit, the chemical formula of “Cu-sterryite” is $(\text{Cu}_{3.23}\text{Ag}_{0.43}\text{Hg}_{0.43})_{\Sigma 4.10}(\text{Pb}_{18.74}\text{Tl}_{0.34})_{\Sigma 19.08}(\text{Sb}_{17.30}\text{As}_{5.48}\text{Bi}_{0.74})_{\Sigma 23.53}\text{S}_{56}$. The crystal structure ($R_1 = 11.72\%$ for 21304 observed reflections) is topologically identical with that of sterryite. Unit-cell parameters are $a = 8.178(2)$, $b = 28.223(6)$, $c = 42.452(5)$ Å, $\beta = 93.55(2)^\circ$, $V = 9779.5(5)$ Å³, space group $P2_1/n$. The crystal structure is based on a building block formed by a complex column with a pseudotrigonal prismatic core and two “arms” of unequal lengths (long and short arms, respectively). The complex columns are interconnected to form a fish-bone column layer along **b**. Localized As–As bonds occur in the short arm.

Meerschautite, ideally $(\text{Ag},\text{Cu})_{5.5}\text{Pb}_{42.4}(\text{Sb},\text{As})_{45.1}\text{S}_{112}\text{O}_{0.8}$, was found as black acicular crystals embedded in granoblastic baryte from the Pollone mine, Apuan Alps, Tuscany. Its crystal structure has been solved and refined in the space group $P2_1$, with unit-cell parameters $a = 8.2393(1)$, $b = 43.6015(13)$, $c = 28.3688(8)$ Å, $\beta = 94.128(2)^\circ$, $V = 10164.93(2)$ Å³. Owing to the bad diffraction quality of the available crystals, the R converged to a relatively high value (12.2% on the basis of 49037 observed reflections). The crystal structure is formed by two different kinds of complex columns, mainly differing in their short arms. Indeed, one short arm is Ag-rich, whereas the other is characterized by localized Sb–O–Sb bonds of the kermesite type.

The crystallization of “Cu-sterryite” and meerschautite, as well as that of the related minerals sterryite and parasterryite, is related to minor chemical changes, essentially acting on the nature of the short arms connecting the fundamental columns. Consequently, it is likely that the genesis of such complex and unpredictable crystal structures is favoured by the geochemical complexity of the natural hydrothermal solutions, characterized by the occurrence of minor elements (Ag, Cu, and O), filling specific atom positions and stabilizing these very rare minerals. Narrow $f(\text{S}_2)$ or $f(\text{O}_2)$ conditions also appear necessary for the incorporation of oxygen or As–As pair.

Moëlo Y., Guillot-Deudon C., Evain M., Orlandi P. & Biagioni C. 2012. Comparative modular analysis of two complex sulfosalt structures: sterryite, $\text{Cu}(\text{Ag},\text{Cu})_3\text{Pb}_{19}(\text{Sb},\text{As})_{22}(\text{As}-\text{As})\text{S}_{56}$, and parasterryite, $\text{Ag}_4\text{Pb}_{20}(\text{Sb},\text{As})_{24}\text{S}_{58}$. Acta Crystallogr., B68, 480-492.

Structural complexity in sulfosalts – Chovanite: two new occurrences from the Apuan Alps and its 8 Å crystal structure

Biagioni C.*¹, Moëlo Y.² & Guillot-Deudon C.²

1. Dipartimento di Scienze della Terra, Università di Pisa. 2. Institut des Matériaux J. Rouxel, CNRS, Université de Nantes, France.

Corresponding email: biagioni@dst.unipi.it

Keywords: Chovanite, oxysulfosalts, crystal structure.

Among lead-antimony sulfosalts, the most complex structures are represented by the so-called boxwork structures (Makovicky et al., 2001). Such a structural complexity is favoured by the occurrence of oxygen atoms, generating “kermesite-like rods”, first identified in lead sulfosalts from Apuan Alps (i.e., scainiite - Orlandi et al., 1999). Chovanite, ideally $Pb_{15-2x}Sb_{14+2x}S_{36}O_x$, first described by Topa et al. (2012) from Slovakia, is the last oxysulfosalt identified in the hydrothermal veins from Apuan Alps. Two new occurrences of chovanite were identified at the Monte Arsiccio (MA) and Pollone (PI) mines.

Chovanite from MA occurs as black acicular crystals, up to 5 mm long, associated with robinsonite, rouxelite, and valentinite in dolostone vugs. Its unit-cell parameters are $a = 48.38(5)$, $b = 4.11(4)$, $c = 34.18(4)$ Å, $\beta = 106.26(2)^\circ$, $V = 6521(64)$ Å³, space group $C2/m$. Very weak reflections indicate the doubling of the b parameter. Owing to the bad quality of the available crystals, the crystal structure was refined down to $R_1 \sim 23\%$ on the basis of 2118 observed reflections. Electron-microprobe data gave (in wt%): Ag 0.28, Tl 1.51, Pb 45.57, Sb 31.00, As 1.09, S 19.73, Se 0.05, Cl 0.02, sum 99.25. On the basis of $\Sigma Me = 58$ apfu, the chemical composition of chovanite from MA is $Ag_{0.30}Tl_{0.86}Pb_{25.56}Sb_{29.59}As_{1.69}S_{71.51}Se_{0.07}Cl_{0.06}$. Adding one oxygen atom, this mean analysis is close to the stoichiometric formula $TlPb_{26}(Sb,As)_{31}S_{72}O$.

Chovanite from PI was found in only two specimens. It occurs as black prismatic crystals, up to 1 cm in length, associated with baryte and quartz. The high quality of the available material allowed the solution and refinement of the 8 Å crystal structure in the space group $P2_1/c$, with unit-cell parameters $a = 34.052(3)$, $b = 8.2027(7)$, $c = 48.078(4)$ Å, $\beta = 106.258(4)^\circ$, $V = 12891.9(19)$ Å³. The refinement converged to $R_1 = 9.15\%$ on the basis of 19853 observed reflections. Electron-microprobe data gave (in wt%): Ag 0.12, Tl 0.54, Pb 48.34, Bi 0.20, Sb 26.71, As 3.37, S 20.23, Cl 0.07, sum 99.57. It corresponds to the formula $Ag_{0.12}Tl_{0.30}Pb_{26.94}Bi_{0.11}Sb_{25.33}As_{5.20}S_{72.86}Cl_{0.21}$. Without Tl, Ag, and Cl (according to $(Tl,Ag) + Sb = 2 Pb$ and $Pb + Cl = Sb + S$), as well as Bi, and neglecting the S excess (not supported by structural data) one obtains the idealized formula $Pb_{28}(Sb,As)_{30}S_{72}O$.

Makovicky E., Balić-Žunić T. & Topa D. 2001. The crystal structure of neyite, $Ag_2Cu_6Pb_{25}Bi_{26}S_{68}$. Can. Mineral., 39, 1365-1376.

Orlandi P., Moëlo Y., Meerschaut A. & Palvadeau P. 1999. Lead-antimony sulfosalts from Tuscany (Italy): I. Scainiite, $Pb_{14}Sb_{30}S_{54}O_5$, the first Pb-Sb oxy-sulphosalt from Buca della Vena mine. Eur. J. Mineral., 11, 949-954.

Topa D., Sejkora J., Makovicky E., Pršek J., Ozdín D., Putz H., Dittrich H. & Karup-Møller S. 2012. Chovanite, $Pb_{15-2x}Sb_{14+2x}S_{36}O_x$ ($x \sim 0.2$), a new sulphosalt species from the Low Tatra Mountains, Western Carpathians, Slovakia. Eur. J. Mineral., 24, 727-740.

Crystal structure refinement of römerite and melanterite, two hydrated iron sulfates with complex hydrogen bond systems

Biagioni C., Mauro D. & Pasero M.*

Dipartimento di Scienze della Terra, Università di Pisa.

Corresponding email: marco.pasero@unipi.it

Keywords: Römerite, melanterite, crystal structure.

Römerite, ideally $\text{Fe}^{2+}\text{Fe}^{3+}_2(\text{SO}_4)_4 \cdot 14\text{H}_2\text{O}$, and melanterite, ideally $\text{Fe}^{2+}(\text{SO}_4) \cdot 7\text{H}_2\text{O}$, are two hydrated iron sulfates. Both minerals were discovered in mid-nineteenth century and, as of today, have been reported from several worldwide occurrences.

We herewith present accurate crystallographic data on two samples of römerite and melanterite collected at the Fornovolasco pyrite–magnetite mine, Apuan Alps, Tuscany, Italy. Here römerite and melanterite occur together with other well-crystallized sulfates, genetically related to the pyrite ores, involving a complex series of oxidation, dehydration, and neutralization reactions.

Even if the crystal structures of römerite and melanterite are already known, this study allowed the accurate determination of the hydrogen atom positions and the assessment of the hydrogen bond system on natural samples. The previous study of römerite (Fanfani et al., 1970) was not completely satisfactory due to the limited software capability – dating back to almost half a century ago – which prevented a full-matrix refinement. The previous refinements of melanterite (Peterson, 2003) did not include the hydrogen atoms. However, results very similar to those here presented were obtained with a deuterated synthetic analogue of melanterite (Anderson et al., 2007).

SCXRD data were collected with a Bruker Smart Breeze diffractometer, equipped with air-cooled CCD detector and graphite-monochromatized $\text{MoK}\alpha$ radiation.

Römerite crystallizes in the space group $P-1$, with unit-cell parameters $a = 6.4512(6)$, $b = 15.3227(15)$, $c = 6.3253(6)$ Å, $\alpha = 89.869(5)$, $\beta = 100.900(4)$, $\gamma = 94.034(4)^\circ$, $V = 612.4(1)$ Å³. The refinement converged to $R1 = 0.024$ on the basis of 4346 observed [$F_o > 4\sigma F_o$] reflections. The crystal structure is composed by isolated $[\text{Fe}^{2+}(\text{H}_2\text{O})_6]^{2+}$ octahedra and by groups formed by Fe^{3+} -centered octahedra and two $[\text{SO}_4]$ tetrahedra through edge-sharing, giving rise to $[\text{Fe}^{3+}(\text{H}_2\text{O})_4(\text{OSO}_3)_2]^-$ groups. These groups and the isolated octahedra are bonded through hydrogen bonds.

Melanterite crystallizes in the space group $P2_1/c$, with unit-cell parameters $a = 14.0751(8)$, $b = 6.5014(4)$, $c = 11.0426(6)$ Å, $\beta = 105.632(3)^\circ$, $V = 973.1(2)$ Å³. The refinement converged to $R1 = 0.026$ on the basis of 3457 observed [$F_o > 4\sigma F_o$] reflections. The crystal structure shows two independent $\text{Fe}(\text{H}_2\text{O})_6$ octahedra and a SO_4 group, bonded through hydrogen bonds.

In both römerite and melanterite, bond-valence balance calculations confirmed the correctness of the hydrogen bond schemes.

Anderson J.L., Peterson R.C. & Swainson I.P. 2007. The atomic structure and hydrogen bonding of deuterated melanterite, $\text{FeSO}_4 \cdot 7\text{D}_2\text{O}$. *Can. Mineral.*, 45, 457-469.

Fanfani L.A., Nunzi A. & Zanazzi P.F. 1970. The crystal structure of roemerite. *Am. Mineral.*, 55, 78-89.

Peterson R.C. 2003. The relationship between Cu content and distortion in the atomic structure of melanterite from the Richmond mine, Iron Mountain, California. *Can. Mineral.*, 41, 937-949.

Expanding the number of arsenic sulphides having a layered structure: duranusite, a new structural type related to arsenolamprite

Bonazzi P.* , Lepore G.O. & Bindi L.

Dipartimento di Scienze della Terra, Università di Firenze.

Corresponding email: paola.bonazzi@unifi.it

Keywords: Duranusite, arsenic sulphide, layered structure.

Most of the natural and synthetic compounds belonging to the binary As-S system exhibit a structure based on the packing of discrete cage-like molecules whereas only a few examples of layered structures are known (Bonazzi & Bindi, 2008). Namely among the minerals, As_4S_n molecules are present in the structure of both α - and β -dimorphites ($n = 3$), realgar, pararealgar and bonazziite ($n = 4$), alacranite ($n = 4$ and $n = 5$) and uzonite ($n = 5$). In contrast, orpiment, As_2S_3 , exhibits a layered structural arrangement. Last, the mineral wakabayashilite, ideally $[As_2S_3]_3[As_4S_5]$, consists of As_4S_5 molecular groups and $[M_6S_9]$ -bundles which, when their cylindrical surface is ideally developed, are very similar to the layer present in the orpiment.

Besides the above sulphides, having As:S ratios ranging between 4:3 and 4:6, another As-sulphide, fitting the atomic ratio 4:1, was found at Duranus (Maritime Alps, France) in association with native As and realgar (Johan et al., 1973). The mineral, named duranusite for the type-locality, has been later reported four more times but the small crystal size and the poor crystallinity have impeded its structural characterization so far.

In a recent paper examining all the theoretically possible types of cage molecules ranging from As_4S_6 to As_4 , Kyono (2013) hypothesized that the structure of duranusite could consist of As_4S molecular groups, although no experimental evidence supported this assumption.

Here we report the crystal structure of duranusite which exhibits a new kind of layered structure related to that observed in one of the natural polymorph of arsenic (arsenolamprite) and shows heretofore unknown feature in the As-S bonding geometry. The structure, $Pmna$ space group, consists of an alternated stacking along the [010] axis of two kinds of corrugated layers which match the As_2 and As_2S composition, respectively. The crystal structure determination of duranusite expands the number of the known layered structures of As sulphides suggesting that in minerals and stable compounds the As_4S_n molecules are limited to those having $n = 3, 4$ and 5 .

Bonazzi P. & Bindi L. 2008. A crystallographic review of arsenic sulphides: Effects of chemical variations and changes induced by light exposure. *Zeit. Kristallogr.*, 223, 132-147.

Johan Z., Laforêt C., Picot P. & Ferard J. 1973. La duranusite, As_4S , un nouveau minéral. *Bull. Soc. Franç. Minéral. Cristallogr.*, 96, 131-134.

Kyono A. 2013. Ab initio quantum chemical investigation of arsenic sulphide molecular diversity from As_4S_6 and As_4 . *Phys. Chem. Min.*, 40, 717-731.

An unusual occurrence of gahnite in lower Cambrian dolostones of southwest Sardinia (Italy): chemical characterization and genetic hypotheses

Boni P., Balassone G.*, Mondillo N. & Boni M.

Dipartimento di Scienze della Terra, dell'Ambiente e delle Risorse, Università di Napoli "Federico II"

Corresponding email: balasson@unina.it

Keywords: Gahnite, southwest Sardinia, Cambrian dolostone host rock.

Gahnite, ideally $ZnAl_2O_4$, is the Zn-Al endmember of the oxide spinels group (AB_2O_3). These compounds show a cubic symmetry (main space group $Fd3m$), and represent one of the archetype structures based on a cubic close packing of anions (Biagioni & Pasero, 2014). The major element chemistry of gahnite is comprised of varying proportions of Zn^{2+} in the tetrahedral A site, with minor contents of Fe^{2+} , Mg^{2+} (Mn^{2+}), and Al^{3+} (Fe^{3+}) in the octahedral B site, producing common solid solutions mainly with hercynite and spinel s.s. Gahnite occurs as an accessory mineral in many geological settings, preeminently metamorphic/magmatic, and its major and trace element chemical composition is an exploration guide to metamorphosed ores (O'Brien et al., 2015). Hence mineralogical, geochemical and genetic studies of the Zn-spinel are of interest for ore mineralogy and geology. This work reports the first recorded occurrence of gahnite approaching to endmember composition in sedimentary rocks, represented by dolostones (Gonnesa Group) belonging to lower Cambrian succession of the Iglesiente area, southwest Sardinia. Gahnite has been found in two localities close to Buggerru village, the Malfidano and Planu Sartu mining areas exploited in the past for nonsulfide Zn(Pb) ores (Boni et al., 2003). This occurrence in dolostones is unusual, because these sedimentary host rocks in SW Sardinia do not seem affected by metamorphism. Metamorphic grade in the Iglesiente area is generally very low, or there is some contact metamorphism only close to granite intrusions, which is not the case of the gahnite-bearing rocks. The Sardinian gahnite is chemically homogenous and show a composition very close to that of endmember gahnite, with up ~ 98.5 mol% of the $ZnAl_2O_4$ component. The remaining composition is mainly dominated by the hercynite component ($FeAl_2O_4$), with very minor spinel component ($MgAl_2O_4$). Mn in trace amounts is locally detected. Gahnite can be euhedral to subeuhedral, locally replaced by illite; fluoroapatite randomly occurs as tiny crystals. Considering the Zn-spinel composition in relation to paragenesis (O'Brien et al., 2015), the Sardinian gahnite compositions mainly fall within the field of diasporites and metabauxites. However, possible genetic inferences, i.e. a magmatic/hydrothermal derivation possibly biased by structural control, and a detritic origin (paleoplacer?), are also considered.

- Biagioni C. & Pasero M. 2014. The systematics of the spinel-type minerals: An overview. *Am. Mineral.*, 99, 1254-1264.
- Boni M., Aversa G., Balassone G. & Gilg H.A. 2003. The calamine of SW Sardinia (Italy): geology, mineralogy and stable isotope geochemistry of a supergene Zn-mineralisation. *Econ. Geol.*, 98, 715-729.
- O'Brien J.J., Spry P.G., Teale G., Jackson S.E. & Rogers D. 2015. Major and trace element chemistry of gahnite as an exploration guide to broken Hill-type Pb-Zn-Ag mineralization in the Broken Hill domain, New South Wales, Australia. *Econ. Geol.*, 110, 1027-1057.

Progressive thermal deprotonation of staurolite during crustal anatexis: NanoSIMS, TEM and experimental constraints

Cesare B.*¹, Viti C.², Mugnaioli E.², Schmidt M.W.³ & Remusat L.⁴

1. Dipartimento di Geoscienze, Università di Padova. 2. Dipartimento di Scienze Fisiche, della Terra e dell'Ambiente, Università di Siena. 3. Geowissenschaften ETH, Zurich, Switzerland. 4. CNRS and MNHN, Paris, France.

Corresponding email: bernardo.cesare@unipd.it

Keywords: Staurolite, TEM, hydrogen.

Staurolite is a common mineral in amphibolite-facies metapelites, but owing to the multiple substitutions allowed by its complex crystal chemistry, it is stable also in mafic systems at high pressure, or in partially melted Al-rich compositions. In the latter, experiments have so far demonstrated the supersolidus stability of staurolite in the range 700-825 °C and 6-12 kbar. Throughout its wide P-T stability field, staurolite also displays huge variations of the H content (from 2.7 to 6.0 atoms per 48 oxygens) that appear to be positively correlated with P and negatively with T. However, direct analysis of H has been performed only in a limited number of studies, and never in staurolite stable at supersolidus conditions.

We have analyzed by NanoSIMS the H content in staurolite coexisting with melt from three experimental run products from the melting of fine-grained powder of a graphitic metapelite at 785°C/5 kbar (sample BC4), 835°C/8 kbar (sample 854) and 893°C/8 kbar (sample 833). The staurolite from the starting material has an X_{Fe} of 0.83, and an H₂O in the range 1.43 - 1.80 wt.%, corresponding to 2.7 - 3.3 OH groups per 48 oxygens.

During the experiment the assemblages melt-Qtz-Grt-Sil-Ilm-Her-St, (sample BC4), melt-Qtz-Grt-Sil-Rt-Bt-Kfs-St (sample 854) and melt-Qtz-Grt-Sil-Ilm-Crn-Her-St (sample 833) are produced, and St is partially to completely rimmed by hercynitic spinel in two of three runs. The staurolite is more magnesian (X_{Fe} respectively 0.81; 0.58-0.66 and 0.67-0.72) and contains respectively 4400, 1500 and 1300 ppm H₂O, with a 1s error of 200 ppm. These values correspond to 0.80, 0.28 and 0.24 OH groups per 48 oxygens, respectively. Along with the dramatic deprotonation demonstrated by NanoSIMS, the experimental staurolite shows higher total contents of Al and (Fe+Mg), in agreement with previously proposed exchange vectors for deprotonation.

In order to verify that the low-OH staurolite is not an amorphous product of the thermal decomposition of precursor crystals from the starting material, three FIB foils were obtained from sample BC4 and examined by TEM. SAED patterns show intense and sharp reflections, and d-spacings consistent with orthorhombic-pseudo orthorhombic symmetry. Both diffraction and HR images confirm high crystallinity and crystal order.

These results suggest that, similarly to other hydroxylated minerals like biotite, staurolite undergoes a progressive T-dependent deprotonation, and that this process may reach completion with the occurrence of H-free terms at (U)HT supersolidus conditions. The thermodynamic model for staurolite should be improved to account also for this T-dependent deprotonation, but more data are needed to understand which exchange vector(s) is responsible for it.

New data on melanophlogite (type I clathrate) from Fortullino (Livorno, Italy)

D'Alessio D.*, Tribaudino M., Gaboardi M., Magnani G., Pontiroli D. & Riccò M.

Dipartimento di Fisica e Scienze della Terra "Macedonio Melloni", Università di Parma.

Corresponding email: daniela.dalessio@fis.unipr.it

Keywords: Melanophlogite, gas storage, clathrate.

Melanophlogite (MEP) is a tectosilicate belonging to silica clathrate compounds, zeolite-like materials with a framework of interconnected [SiO₄] tetrahedra with pentagonododecahedral [5¹²] and tetrakaidecahedral [5¹²6²] isolated cages between them, in which guest gases can be present and act as templates for mineral crystallization (Gunawardane et al., 1987).

MEP is found in few localities all around the world (some of them are in Italy) and each of them has characteristic guest gases. Structural refinements of samples from Varano Marchesi (Parma, Italy) and Mt. Hamilton (Santa Clara County in California, USA) are the only ones available at the moment and have showed cubic *Pm3n* and tetragonal *P4₂/nbc* structures respectively at temperature close to 300 K. Samples from Varano Marchesi, containing simply CH₄ in structural cages, show transition from cubic to tetragonal symmetry at pressure close to 1.2 GPa (Gatta et al., 2014) and those from Mt. Hamilton a transition to cubic symmetry at temperatures slightly higher than 300 K (Nakagawa et al., 2005).

XRPD analyses using conventional and unconventional sources [ID22 at ESRF: $\lambda_{\text{exp}} = 0.354205(6) \text{ \AA}$] have been conducted changing temperature on samples from Fortullino. At temperatures higher than 313 K, Rietveld refinements can be performed with cubic *Pm3n* structure; close to 300 K site occupancies show a filling of about 60% of [5¹²] and [5¹²6²] cages. At 315 K the length of lattice parameter *a* is 13.4097(1) Å. At increasing temperature a partial loss of CO₂ is observed with a maximum decrease to an occupancy of 50% at temperatures higher than 500 K; moreover the thermal expansion coefficient α_V is different from that of cubic samples from Mt. Hamilton, due to kind of guest gases present in structural cages [$\alpha_{V, \text{Fortullino}} = 6.1(8) \cdot 10^{-5} \text{ K}^{-1}$; $\alpha_{V, \text{Mt. Hamilton}} = 4.0(5) \cdot 10^{-5} \text{ K}^{-1}$, calculated below 400 K]. At temperatures lower than 313 K a split in diffraction peaks marks a symmetry decrease from cubic to a phase still to identify, since Rietveld refinements using low temperature tetragonal symmetry peculiar of Mt. Hamilton MEP (Nakagawa et al., 2005) failed to fit experimental data properly.

It appears that the nature of guest gases (CO₂ in samples from Fortullino and CH₄, CO₂ and N₂ in those from Mt. Hamilton) affects the symmetry of low temperature phase and transition from cubic is likely due to ordering of guest gases within a little changed silica framework.

- Gatta G.D., Bersani D., Lottici P.P. & Tribaudino M. 2014. High-pressure Raman study of CH₄ in melanophlogite (type I clathrate). *Mineral. Mag.*, 78, 1661-1669.
- Gunawardane R.P., Gies H. & Liebau F. 1987. The Effect of "Help Gases" on the Formation and Stability of Clathrasils. *Z. Anorg. Allg. Chem.*, 546, 189-198.
- Nakagawa T., Kihara K. & Fujinami S. 2005. X-ray studies of structural changes in melanophlogite with varying temperature. *J. Miner. Petrol. Sci.*, 100, 247-259.

Raman study of $\text{MgAl}_2\text{O}_4\text{--CoAl}_2\text{O}_4$ and $\text{MgAl}_2\text{O}_4\text{--MgCr}_2\text{O}_4$ solid solutions

D'Ippolito V.*¹, Andreozzi G.B.¹, Bersani D.² & Lottici P.P.²

1. Dipartimento di Scienze della Terra, Sapienza Università di Roma. 2. Dipartimento di Fisica e Scienze della Terra, Università di Parma.

Corresponding email: veronica.dippolito@uniroma1.it

Keywords: Raman spectroscopy, spinel, solid solution.

Spinel is a very important mineral in terrestrial and extraterrestrial rocks as well as materials of high relevance from a gemological and technological point of view for their remarkable physical properties. Ten synthetic spinels belonging to the $\text{MgAl}_2\text{O}_4\text{--CoAl}_2\text{O}_4$ and to the $\text{MgAl}_2\text{O}_4\text{--MgCr}_2\text{O}_4$ solid solutions have been studied by Raman spectroscopy to examine how substitution of the divalent and trivalent cation affects the Raman modes. Raman investigation on the Raman spectral change into a solid solution can be used to obtain semi-quantitative chemical information.

The spinels were synthesized by flux growth method and analyzed chemically by electron microprobe and structurally by single-crystal X-ray diffraction. Raman spectra were collected with a Jobin Yvon LabRam micro-spectrometer using two different laser wavelengths. A 632.8 nm He-Ne laser was used for the samples with high Cr content to avoid the fluorescence, while in the samples containing Co the spectra were recorded with a 473.1 nm wavelength from a solid state laser.

When the substitution $\text{Co}^{2+}\rightarrow\text{Mg}$ occurs in the $\text{MgAl}_2\text{O}_4\text{--CoAl}_2\text{O}_4$ series, a continuous and monotonic shift of the five Raman modes is observed for all Raman modes. The E_g , $F_{2g}(2)$ and $F_{2g}(3)$ modes show a shift toward lower wavenumbers with the increase of the cobalt content, in agreement with the change in the divalent cation mass. The $F_{2g}(1)$ and A_{1g} modes exhibit a slight shift toward higher wavenumbers along the series revealing a dependence of these modes on the trivalent cation. In the CoAl_2O_4 end-member the most characteristic peak at 516 cm^{-1} is attributable to the $F_{2g}(2)$ mode. This peak can be followed along the series and a good linear correlation between the wavenumber of the $F_{2g}(2)$ mode and the Co content (Co_{tot}) is obtained. In the $\text{MgAl}_2\text{O}_4\text{--MgCr}_2\text{O}_4$ series, all observed Raman modes exhibit one-mode behavior, with the exception of the E_g mode. The E_g mode of the Cr-poor spinels at $\sim 405\text{ cm}^{-1}$ decreases its intensity with the increase up to $\sim 50\text{--}60\%$ of the chromite content. From this composition another E_g mode starts to grow at $\sim 450\text{ cm}^{-1}$ becoming well defined in the pure chromite end-member. The $F_{2g}(3)$ and A_{1g} modes show large shifts demonstrating a strong influence of the trivalent cation. In addition, a linear correlation can be observed relating the variation of the A_{1g} mode and the local Cr-O bond distances along the series.

Si-P substitution mechanisms in olivines: Rietveld characterization of the $\text{LiMgPO}_4\text{-Mg}_2\text{SiO}_4$ solid solution

De Grisogono F., Giuli G.* & Paris E.

Scuola di Scienze e Tecnologie - Sezione di Geologia, Università di Camerino.

Corresponding email: gabriele.giuli@unicam.it

Keywords: Lithium, olivines, Si-P substitution.

P-bearing olivines have been synthesized and studied by powder X-ray diffraction in the aim of understanding the structural modifications induced by the P/Si substitution within the series $\text{LiMgPO}_4\text{-Mg}_2\text{SiO}_4$ (LMP-Fo). This study is important in order to structurally characterize one among possible P/Si substitution mechanisms and to verify how much P can enter the olivine lattice. The synthetic samples, prepared by solid state reaction at 1300 °C, have been characterised by the Rietveld method and the results compared with structural data from literature on the end-member compositions (e.g. Hanic et al., 1982; Kirfel et al., 2005). Run products display the presence of a single phase near the end-member compositions, whereas display the simultaneous presence of 2 olivine phases, suggesting the presence of a miscibility gap, in the compositional range LMP(70%)-Fo(30%) and LMP(30%)-Fo(70%).

The unit cell volume V_0 increases markedly as a function of the Si content in the tetrahedral site, with the b_0 and the c_0 parameter displaying the largest and the least variations respectively. As expected, the distance undergoes a marked increase from ca. 1.53 to 1.65 Å in going from the P to the Si end-member. Moreover, the distance undergoes a noticeable decrease (from ca. 2.16 to 2.11 Å) as a response to the Li-Mg substitution, whereas the distance display a small but detectable increase (from ca. 2.10 to 2.12 Å).

The size variation of the tetrahedral site affects greatly the geometry of both the M1 and M2 sites because of the edge and corner connectivity among these sites: in particular, T size variations affect greatly the distribution of the different O3-O3 edge lengths thus affecting the distortion of the M2 sites. Moreover, strong increase of the O1-O2-O1 angle along the M1 chain as a function of the Si content in the T site clearly explains elongation the octahedral M1 chain (and, thus, the b_0 parameter increase) despite the contraction of the distance.

Hanic F., Handlovic M., Burdová K. & Majling J. 1982. Crystal structure of lithium magnesium phosphate, LiMgPO_4 : Crystal chemistry of the olivine-type compounds. J. Chem. Crystallogr., 12, 99-127.

Kirfel A., Lippmann T., Blaha P., Schwarz K., Cox D., Rosso K. & Gibbs G. 2005. Electron density distribution and bond critical point properties for forsterite, Mg_2SiO_4 , determined with synchrotron single crystal X-ray diffraction data. Phys. Chem. Min., 32(4), 301-313.

Synthetic potassic-ferro-richterite: HT behavior and deprotonation process by single-crystal FTIR spectroscopy and structure refinement

Della Ventura G.¹, Susta U.*¹, Bellatreccia F.¹, Cavallo A.² & Oberti R.³

1. Dipartimento di Scienze, Università Roma Tre. 2. Istituto Nazionale di Geofisica e Vulcanologia, Roma
3. Istituto di Geoscienze e Georisorse, C.N.R. Pavia.

Corresponding email: umberto.susta@uniroma3.it

Keywords: Fe-richterite, deprotonation, FTIR spectroscopy.

Most natural (geologic/geophysic) and technical/industrial processes do involve dehydration/dehydroxylation/deprotonation processes, chemical transformations and phase-transitions which need to be properly characterized by using combinations of analytical techniques such as TG/DTA, HT-XRD and HT spectroscopies. Dehydroxylation/deprotonation in minerals are associated to oxidation processes of multi-valence elements, such as Fe or Mn, and may affect the physical properties of the rock where they occur. For instance, the increase in electrical conductivity in subduction zones has been related to transformations in OH-bearing phases such as amphiboles or micas (Wang et al., 2012). The thermal stability and HT behavior of amphiboles have been widely studied in the last few years, and crystal-chemical details controlling HT behavior have now been identified (Tribaudino et al., 2008; Zema et al., 2012). Important issues still need to be studied, including the way protons diffuse throughout the mineral matrix, and the role of multiple-valence elements in this process. In this work we describe the HT-FTIR analysis of a sample close to the boundary between potassic-ferro-richterite and potassic-arfvedsonite, synthesized by Redhammer & Roth (2002) and recently re-examined by SC-XRD by Oberti et al. (in prep). Both *in situ* and *ex-situ* (quenched) absorbance data were collected on doubly-polished single-crystal sections using a Linkam HT heating stage, able to work up to 1200 °C. A significant absorbance increase in the OH-stretching region was observed *in situ*, which was explained by a strong increase with T in the absorption coefficient. In contrast, data collected after quenching show that the complete deprotonation occurs in a limited T range (~100°). Combination of FTIR and SC-XRD refinement (Oberti et al., in prep.) shows that H loss is paralleled by Fe oxidation at the M(1) site. Attempts to constrain the kinetics of H loss under isothermal annealing at different T are underway.

- Redhammer G.J. & Roth G. 2002. Crystal structure and Mössbauer spectroscopy of the synthetic amphibole potassic-ferri-ferrichterite at 298 K and low temperatures (80–110 K) Eur. J. Mineral., 14, 105-114.
- Tribaudino M., Bruno M., Iezzi G., Della Ventura G. & Magiolaki I. 2008. The thermal behavior of richterite. Am. Mineral., 93, 1659-1665.
- Wang D., Guo Y. & Yu Y. 2012. Electrical conductivity of amphibole-bearing rocks: influence of dehydration. Contrib. Mineral. Petrol., 164, 17-25.
- Zema M., Welch M.D. & Oberti R. 2012. High-T behaviour of gedrite: thermoelasticity and dehydrogenation. Contrib. Mineral. Petrol., 163, 923-937.

Na₂Ca₃Al₂F₁₄ - A new fluoride phase from fumaroles on Eldfell, Hekla and Vesuvius

Garavelli A.*¹, Balić-Žunić T.², Pinto D.¹, Mitolo D.¹, Jakobsson S.P.³ & Leonardsen E.⁴

1. Dipartimento di Scienze della Terra e Geoambientali, Università di Bari. 2. Natural History Museum of Denmark, University of Copenhagen, Denmark. 3. Icelandic Institute of Natural History, Reykjavik, Iceland. 4. Hundedsted, Denmark.

Corresponding email: anna.garavelli@uniba.it

Keywords: New minerals, fluorides, volcanic sublimates.

A new fluoride phase, with ideal formula Na₂Ca₃Al₂F₁₄, was identified among encrustations collected from fumaroles on Eldfell and Hekla volcanoes, Iceland, after the eruptions in 1973 and 1991, respectively. The same mineralogical phase was identified in a sublimate sample belonging to the Pelloux collection and stored in the Mineralogical section of the Museo di Scienze della Terra at Bari University. The original label of this Museum sample, where the 1925 date is reported, indicated it as "Avogadrite from Vesuvius".

In Icelandic samples, the new phase forms massive aggregates and sometimes crystals up to 20 μm in diameter with rhombic dodecahedral habit, found in yellow to brown crusts, typically in mixture with ralstonite and hematite, sometimes also with jakobssonite, anhydrite, leonardsenite, jarosite and meniaylovite. The temperature in the fumarole where the type specimen was found was 170 °C at the time of sampling. In the museum samples, the new phase is strictly associated to ralstonite and together with it forms a yellowish and soft crust. Additional minerals found in the same Museum sample are hieratite and knasibfite.

The new phase is yellowish and transparent but the minute dimensions of the crystals prevented the determination of physical properties. The calculated density is 2.974 g/cm³ (from the empirical formula). SEM-EDS quantitative chemical analysis shows the following range of concentrations (wt.%): Ca 21.64-24.74 (average 23.195), Al 11.63-12.41 (average 12.01), Na 8.57-10.1 (average 9.45), F 52.64-56.88 (average 54.57). The empirical chemical formula, calculated on the basis of 7 atoms pfu, is Na_{2.01}Ca_{2.82}Al_{2.17}F_{14.02}. X-ray single-crystal study is not possible to perform because of tiny crystals. X-ray powder diffraction pattern closely resembles that of synthetic Na₂Ca₃Al₂F₁₄ (PDF 36-1496), which is cubic, space group *I*2₁3. Calculated unit-cell parameters are *a* = 10.264(1) Å, *V* = 1081.4(3) Å³, *Z* = 4.

On the basis of chemical analyses and X-ray data, the new mineral corresponds to the synthetic compound Na₂Ca₃Al₂F₁₄ (Courbion & Ferey, 1988) which is stable up to 719 °C in the system NaF-CaF₂-AlF₃ and decomposes at higher temperatures to a mixture of the high-temperature NaCaAlF₆ and fluorite (Courbion & Ferey 1988). It forms readily at temperatures lower than 600 °C in the part of the phase system with equal molar amounts of Na, Ca and Al and is crystallized rather than the low-temperature form of NaCaAlF₆ which needs special conditions for crystallization (Hemon & Courbion 1990).

The new species will be submitted soon for approval to the IMA-CNMNC.

Courbion G. & Ferey G. 1988. Na₂Ca₃Al₂F₁₄: A New Example of a Structure with "Independent F⁻" - A New Method of Comparison between Fluorides and Oxides of Different Formula. *J. Solid State Chem.*, 76, 426-431.

Hemon A. & Courbion G. 1990. The NaF-CaF₂-AlF₃ System: Structures of β-NaCaAlF₆ and Na₄Ca₄Al₇F₃₃. *J. Solid State Chem.*, 84, 153-164.

Structural characterization of Cu_{2-x}S ultra thin films obtained by electrodeposition

Giaccherini A.¹, Di Benedetto F.*², Cinotti S.¹, Montegrossi G.³, Guerri A.¹, Carlà F.⁴, Felici R.⁴ & Innocenti M.¹

1. Dipartimento di Chimica, Università di Firenze. 2. Dipartimento di Scienze della Terra, Università di Firenze. 3.- CNR - Istituto di Geoscienze e Georisorse. 4. European Synchrotron Radiation Facility (Grenoble, France).

Corresponding email: francesco.dibenedetto@unifi.it

Keywords: SXRDR, chalcocite, materials science.

Semiconductors of interest in the solar energy conversion field were prepared by electrodeposition. In particular, we are interested in using the E-ALD (Electrochemical Atomic Layer Deposition) method to synthesize a p-n junction in a single step. The electrodeposited films are usually ultra thin, thus requiring specific investigation methods to be fully characterized. In this study, the obtained ultra thin films were studied by means of SXRDR (Surface X-Ray Diffraction), with the aim of performing a structural characterization of the grown films.

In-situ SXRDR measurements were performed at ESRF (Grenoble) and focused to the investigation of the growth mechanism of Cu-S ultra thin films on the 111 crystal plane of a silver single crystal, commonly used as a working electrode. The growth of the film was monitored by following the evolution of the Bragg peaks after each E-ALD step. Results point to the occurrence of a self-standing film with a definite crystal structure after 15 E-ALD cycles. After the Bragg reflections are observed for the first time, only minor changes of the structural arrangement are registered.

Breadth and profile analysis of the Bragg peaks lead to a qualitative interpretation of the growth mechanism, in the normal and in-plane directions, with respect to the Ag surface. Namely, the contribution of crystal strain and crystallite size were identified in the width of the Bragg reflections.

The preliminary interpretation of the experimental reciprocal lattice, coupled to the SEM investigation, suggests that the samples show a pseudo single crystal diffraction pattern. This can be described by a new hexagonal unit cell. The crystal structure of this electro-deposited Cu_{2-x}S could be related to that of chalcocite, in particular considering the layering of triangular Cu sites and octahedral Cu sites.

The influence of the applied electric potential on the stability of the electro-deposited crystal structure has been monitored by means of SXRDR measurements performed during the switch off of the potential. A structural change was, in fact, registered, and correlated to the occurrence of the stable phases under conventional laboratory conditions.

Morphology and chemistry of erionite and offretite: increasing data of carcinogenic fibrous zeolites

Giordani M.* & Mattioli M.

Dipartimento di Scienze della Terra, della Vita e dell'Ambiente, Università di Urbino.

Corresponding email: matteo.giordani@uniurb.it

Keywords: Erionite, offretite, zeolites.

Zeolites belonging to erionite and offretite families were recently discovered to be very dangerous for the human health since demonstrated to be carcinogenic (e.g. Carbone et al., 2007; Dogan et al., 2008). Notwithstanding this, the morphologies of erionite and offretite fibers have not yet been fully understood and many mineralogical and toxicological aspects are still unknown. Moreover, it is unclear whether the mineralogical similarity between erionite and offretite has any health implications. For these reasons, it is of paramount importance to improve the knowledge of their physical and chemical properties because they may be related to the carcinogenic potential of these fibrous zeolites.

Identification of (and distinction between) erionite and offretite can be difficult because of (i) their mineralogical similarities and (ii) the possibility of intergrowth of the two species within each crystal (Passaglia et al., 1998). Here we present morphological and chemical data of erionite and offretite samples, collected from various localities. Four main morphological types of crystals have been observed. (I) Elongated prisms, often grouped in sub-spherical forms, with a strong tendency to develop thin fibers. (II) Very elongated, fibrous prisms, terminated by a wider, massive form with pseudo-hexagonal section. (III) Stocky prismatic forms, with a strong tendency to generate fibers at the ends of the crystals. (IV) Extremely fibrous crystals with "soft" appearance, which can be found both as single-phases and in epitaxial growth with other minerals.

Chemical data indicate the presence of a wide range of compositions, based on extra-framework dominant cation. Types I and III can be referred to both offretite and erionite compositions; this latter has been found as K-, Na- and Ca-erionite. Type II shows a notably chemical variation: the prismatic, fibrous body corresponds to Na-erionite, while the wider, massive termination is offretite. Type IV is always erionite (both K- and Ca-members) and no offretite samples have been found with this extremely fibrous habit. Intermediate chemical compositions could be natural or due to intimate intergrowths of these two minerals. A better understanding of the potential toxicity is needed across the range of erionite and offretite compositions.

- Carbone M., Emri S., Dugan A.U., Steele I., Tuncer M., Pass H.I. & Baris Y.I. 2007. A mesothelioma epidemic in Cappadocia: scientific developments and unexpected social outcomes. *Nat. Rev. Cancer*, 7, 147-154.
- Dogan A.U., Dogan M. & Hoskins J.A. 2008. Erionite series minerals: mineralogical and carcinogenic properties. *Environ. Geochem. Health*, 30, 367-381.
- Passaglia E., Artioli G. & Gualtieri A. 1998. Crystal chemistry of the zeolites erionite and offretite. *Am. Mineral.*, 83, 577-589.

Xenotime-(Y) from LCT and NYF Tertiary pegmatites of the Central Alps

Guastoni A.¹, Pozzi G.¹, Secco L.*¹, Fioretti A.M.² & Pennacchioni G.¹

1. Dipartimento di Geoscienze, Università di Padova. 2. Istituto di Geoscienze e Georisorse, C.N.R. Padova.

Corresponding email: luciano.secco@unipd.it

Keywords: Alpine pegmatite, LCT and NYF pegmatites, xenotime.

Within the Southern Steep Belt (SSB) of the Central Alps, a field of Tertiary, Alpine age pegmatite dikes extends for about 100 km in an E-W direction and 15 km in a N-S direction north of the Periadriatic Fault, from the Bergell pluton to the E, to the Ossola valley to the W. The mineral assemblage and the geochemical characters of the pegmatite dikes allow to classify them among LCT (lithium, cesium, tantalum) family and rare elements and miarolitic classes, NYF (niobium, yttrium, fluorine) and mixed LCT-NYF families, and rare elements class. LCT pegmatites of the Central Alps did not reach a high degree of geochemical evolution, whereas NYF are near end-member.

The most fractionated LCT pegmatites are found in the Codera area and contain Mn-rich elbaite, triplite, pink-beryl, xenotime, Cs-Rb-rich feldspar, spessartine garnet and green feldspar. NYF pegmatites are in the Vigizzo valley and contain aeschynite-(Y), allanite-(Y), yttrian-fluorite, euxenite-(Y), gadolinite-(Y), monazite-(Ce), yttrian-spessartine and xenotime-(Y) (Guastoni et al., 2014).

Electron microprobe analysis was carried out on xenotime-(Y), (Y,REE)PO₄ from four localities of the pegmatite field: (1) Codera valley; (2) Chiavenna valley and (3) Cama valley (all from LCT dikes) and (4) Vigizzo valley (from NYF dike). Xenotime-(Y) occurs as micrometric to millimetric stout dipyrramids intimately intergrown with monazite-(Ce) and zircon. Uraninite and thorite are observed as inclusions in xenotime from LCT pegmatite.

BSE images of polished samples show minor growth zoning on larger crystals. Patchy zoning and spongy texture is typical of altered samples.

In all xenotimes Y dominates in the M site (more than 0.76 atoms per formula unit - apfu), HREE (Gd, Tb, Dy, Ho, Er, Yb) amount is up to 0.18 apfu and LREE (La, Ce, Nd, Sm) amount is up to 0.03 apfu. Except for Vigizzo valley, xenotime is characterised by a significant U content (up to 0.045 apfu) as already observed by Demartin et al. (1991). Altered portions of xenotime show depletion in U⁴⁺ and Si⁴⁺ balanced by enrichment in YREEs³⁺ and P⁵⁺. Xenotime-(Y) of LCT pegmatites (Codera, Cama and Chiavenna valleys) is characterised by mean HREE content of 0.18 apfu and by mean Y content of 0.77 apfu, while xenotime from the NYF pegmatite of Vigizzo valley shows lower HREE content (0.07 apfu) and higher Y content (0.93 apfu).

Single crystal XRD analysis of U-rich xenotime-(Y) from Chiavenna valley yields $a = 6.8994(9) \text{ \AA}$ and $c = 6.0328(15) \text{ \AA}$ unit cell parameters in $I4_1/amd$ space group; $V_{\text{cell}} = 287.18(9) \text{ \AA}^3$ is within the range reported by Demartin et al. (1991).

Demartin F., Pilati T., Diella V., Donzelli S., Gentile P. & Gramaccioli C.M. 1991. The chemical composition of xenotime from fissures and pegmatites in the Alps. *Can. Mineral.*, 29, 69-75.

Guastoni A., Pennacchioni G., Pozzi G., Fioretti A. M. & Walter J.M. 2014. Tertiary pegmatite dikes of the Central Alps. *Can. Mineral.*, 52, 191-219.

Characterization of natural clays for rare earth ions recovery from WEEE

Iannicelli-Zubiani E.M.¹, Cristiani C.¹, Dotelli G.¹, Gallo Stampino P.¹, Pelosato R.¹,
Lacalamita M.*², Mesto E.² & Schingaro E.²

1. Dipartimento di Chimica, Materiali e Ingegneria Chimica “Giulio Natta”, Politecnico di Milano. 2. Dipartimento di Scienze della Terra e Geoambientali, Università di Bari “Aldo Moro”.

Corresponding email: maria.lacalamita@uniba.it

Keywords: Rare Earths, clays, recovery.

Two mineral clays, both montmorillonite clays, were tested as solid sorbents for the recovery of Rare Earths (REs) from Waste Electric and Electronic Equipment (WEEE) leached solutions. Firstly, the clays were contacted with Lanthanum model solutions (chosen as representing element of REs family). Both uptake and release tests were performed on the different samples in order: to verify the solids capability not only to capture but also to recover metal ions; to evaluate the involved mechanisms; to study the operative parameters, such as contact time and pH; and to fully characterize the material after REs adsorption and desorption. The solids were analysed by X-ray diffraction (XRD) and X-ray photoelectron spectroscopy (XPS) while optical emission spectroscopy (ICP-OES) analyses were performed on the liquid phase. Later, the clays were tested on Neodymium model solutions with the aim of testing the reproducibility of the materials, using other REs with outstanding economic importance. Finally, experiments using real leached scraps solutions were carried out. In particular a NdFeB magnet was etched and REs uptake and release were studied and discussed.

The main results showed that: both the clays are able to capture (efficiency around 50%) and release (efficiency around 70%) La and Nd ions, when the uptake and release processes are respectively performed at pH 5 and pH 1; the involved mechanism was proven to be an ions exchange mechanism; a strong effect of the matrix is present when Nd in the magnet solution is considered. The matrix composition affects both uptake and release thus lowering the efficiency of the Nd global process (4% in the complex matrix, to be compared with 35% in a single ion solution).

Crystal-structure determination of chromites from NWA6077 and NWA725 achondrites

Lenaz D.*¹ & Schmitz B.²⁻³

1. Dipartimento di Matematica e Geoscienze, Università di Trieste. 2. Division of Nuclear Physics, Department of Physics, Lund University, Sweden.
3. Hawai'i Institute of Geophysics and Planetary Science, University of Hawai'i at Manoa, Honolulu, U.S.A.

Corresponding email: lenaz@units.it

Keywords: Achondrites, chromites, crystal chemistry.

Chromite is a minor but regular constituent of ordinary chondrites and achondrites, its chemistry being studied since the 60es. Structural studies via X-ray single crystal diffraction have been performed only by Lenaz et al. (2015) on some chromites from the Kernouvé H6 chondrite, from ~ 470 Ma old fossil micrometeorites and from an acapulcoite.

The here studied chromites are from the NWA6077 and the NWA725 achondrites. According to Garvie (2012) the NWA 6077 is classified as an achondrite meteorite (ungrouped, brachinite-like) with an olivine-rich assemblage with protogranular (possibly cumulate) texture exhibiting triple-junction grain boundaries. Additional minerals include orthopyroxene, clinopyroxene, altered kamacite, chromite, chlorapatite, Ni-bearing troilite and/or pyrrhotite. NWA725 meteorite has been classified as acapulcoite with olivine, orthopyroxene and clinopyroxene by Grossman & Zipfel (2001), but Greenwood et al. (2012) on the basis of its oxygen isotope composition ascribed it to winonaites.

Crystal chemistry on six different grains of chromite (3 for each meteorite) have been studied by single crystal X-ray diffraction. The obtained results show that the cell edges are very similar within each meteorite and also among the two meteorites [8.3331-8.3352 for NWA6077 and 8.3362-8.3433 for NWA725]. On the contrary the oxygen positional parameters of the two meteorites are rather different being about 0.2629 for NWA6077 and 0.2622 for NWA725. The H6 chondritic chromites show cell edges ranging from 8.3480 to 8.3501 Å and oxygen positional parameter comprised between 0.2627 and 0.2629 while it is between 0.2625 and 0.2627 in L chondritic chromites (similar to the acapulcoite) (Lenaz et al., 2015).

NWA6077 is a brachinite-like meteorite and brachinites are the result of metamorphosed chondrite or partial melting residue. Their chromites differ from those of the H6 chondrite for having the same oxygen positional parameter but a lower cell edge due to a major amount of Al₂O₃. Their structural parameters recall those of two spinels from the anorthosites-chromitites layering of the Bushveld complex.

As regards the NWA725 chromites, their structures show similarities with the previously analysed acapulcoite. Their structural parameters recall those of komatiitic chromites.

Garvie L.A.J. 2012. The Meteoritical Bulletin, No. 99, April 2012. Meteorit. Planet. Sci., 47, E1–E52, doi: 10.1111/maps.12026.

Greenwood R.C., Franchi I.A., Gibson J.M. & Benedix G.K. 2012. Oxygen isotope variation in primitive achondrites: the influence of primordial, asteroidal and terrestrial processes. Geochim. Cosmochim. Acta, 94, 146-163.

Grossman J.N. & Zipfel J. 2001. The Meteoritical Bulletin, No. 85, 2001 September. Meteorit. Planet. Sci., 36, A293-A322.

Lenaz D., Princivalle F. & Schmitz B. 2015. First crystal-structure determination of chromites from an acapulcoite and ordinary chondrites. Mineral. Mag., in print.

A multimethodic approach to the characterization of a Mn-rich celadonite from Cerchiara mine, Eastern Liguria, Italy

Lepore G.O.*¹, Bindi L.¹, Bonazzi P.¹, Ciriotti M.E.², Di Benedetto F.¹, Mugnaioli E.³, Viti C.³ & Zanetti A.⁴

1. Dipartimento di Scienze della Terra, Università di Firenze. 2. Associazione Micromineralogica Italiana, Cremona. 3. Dipartimento di Scienze Fisiche, della Terra e dell'Ambiente, Università di Siena. 4. Istituto di Geoscienze e Georisorse, CNR, Pavia.

Corresponding email: giovanniorazio.lepore@unifi.it

Keywords: Mn-mica, Cerchiara mine, new mineral.

In the manganeseiferous ores associated to the metacherts of the ophiolitic sequences at the Cerchiara mine, Eastern Liguria (Italy), two new minerals belonging to the mica group have recently been found and characterized. The first one, balestraitite, $\text{KLi}_2\text{VSi}_4\text{O}_{10}\text{O}_2$, is a trioctahedral mica belonging to the 1M polytype, space group C2; the mineral is characterized by unusual geometrical features related to its Li, V-rich chemical composition with V present as V^{5+} (Lepore et al., 2015). The second one (labeled C1176) occurs as orange-brown extremely thin, elongated lamellae associated with calcite, hematite and braunite.

Preliminary qualitative EDS analyses showed a very unusual chemical composition with Si, Mg, K and Mn as major elements. WDS chemical data confirmed unusually high Mn contents, besides F and low concentrations of Fe and Al. After an unsuccessful search for a single crystal suitable for X-ray intensity data collection, a powder diffraction pattern was collected. The refined unit-cell values are: $a = 5.15(1)$, $b = 8.92(1)$, $c = 10.30(1)$ Å, $\beta = 102.0(1)^\circ$, suggesting a dioctahedral character of this mica. A subsequent TEM study showed that the mineral occurs in bended lamellae that can be as thin as 20 nm; furthermore, the analysis of reconstructed three-dimensional electron diffraction volume confirmed that the mineral belongs to the mica group and revealed a strong diffuse scattering of reflections along c^* .

The lack of structural data and the difficulty to determine the H_2O content and the valence state of Mn, together with the likely presence of Li inferred from the paragenesis, required the aid of other techniques to provide a reliable characterization of this phase. In particular, an EPR spectrum indicated the presence of Mn^{3+} and Mn^{4+} only, with a strong dominance of Mn in the trivalent state, while a Raman spectrum clearly evidenced the presence of OH groups in the structure. Finally, LA-ICP-MS measurements assessed the presence of considerable amounts of Li.

Assuming all Mn as Mn^{3+} and that the mica is fully hydrated, the empirical formula, normalized on 22 negative charges, can be written as: $(\text{K}_{0.83}\square_{0.17})(\text{Mn}^{3+}_{1.14}\text{Mg}_{0.80}\text{Li}_{0.20}\text{Fe}^{3+}_{0.02})(\text{Si}_{3.89}\text{Al}_{0.10})\text{O}_{10}(\text{OH}_{1.92}\text{F}_{0.08})$ with the octahedral cations sum indicating a "transitional" character between di- and tri-octahedral, as often reported for Li-rich micas in particular.

This formula ideally corresponds to the Mn^{3+} analogue of celadonite, thus further expanding the range of solid solution in the celadonite family.

Lepore G.O., Bindi L., Zanetti A., Ciriotti M., Medenbach O. & Bonazzi P. 2015. Balestraitite, $\text{KLi}_2\text{VSi}_4\text{O}_{10}\text{O}_2$, the first member of the mica group with octahedral V^{5+} . *Am. Mineral.*, 100, 608-614.

Structural and chemical variations in phlogopites from lamproitic rocks of the Western Mediterranean Region

Lepore G.O.*¹, Bindi L.¹, Bonazzi P.¹, Pedrazzi G.² & Conticelli S.¹

1. Dipartimento di Scienze della Terra, Università di Firenze. 2. Dipartimento di Neuroscienze, Università di Parma.

Corresponding email: giovanniorazio.lepore@unifi.it

Keywords: Mica, phlogopite, lamproite.

Micas from mafic ultrapotassic rocks with lamproitic affinity from various localities of the Western Mediterranean region have been studied through SCXRD, EMPA and SIMS; in order to reduce the number of unknown variables and uncertainties in the interpretation of data, Mössbauer techniques, when feasible, were also applied.

Lamproitic samples from Val D'Albard, (Western Alps), Sisco (Corsica), Montecatini Val di Cecina and Orciatico (Southern Tuscany) and Torre Alfina (Northern Latium) were analysed.

The studied crystals show distinctive chemical and structural features; they all belong to the phlogopite-annite solid solution and crystallize in the $1M$ polytype, except for micas from Torre Alfina, where both $1M$ and $2M_1$ polytypes have been found. They have variable but generally high F and Ti, with Mg/(Mg+Fe) ranging from ~0.5 to ~0.9; $2M_1$ crystals from Torre Alfina radically differ in chemical composition, showing high contents of Ti and Fe as well as of Al in both tetrahedra and octahedra, leading to distinctive structural distortions, especially in tetrahedral sites. SIMS data indicate that these micas are generally dehydrogenated with OH contents ranging from ~0.2 apfu for Orciatico and Torre Alfina to ~1.4 for Val d'Albard crystals; this feature is as well testified by structural considerations regarding the length of c parameter: the shorter the c parameter, the higher the loss of hydrogen and/or F→OH substitution (Cruciani & Zanazzi, 1994). Chemical and structural data suggest that the entry of high charge cations in the structure, especially Ti and Fe³⁺, is mainly balanced via an *oxy* mechanism. However, a component of M^{3,4+}-Tschermak substitution, especially regarding the incorporation of ^{VI}Al has to be taken into account. Our data confirm that Ti preferentially partitions into the M2 site. Ti appears indeed to be well related to the bond-length distortions in M2, as well as to other structural parameters suggesting the presence of high-charge cations in M2 (Cruciani & Zanazzi, 1994). Different Ti, as well as different K/Al and F contents are distinctive features; their variation has been mainly related by Foley (1989; 1990) in his experimental studies to different fluid compositions and, especially, to different f_{H_2O} with a lower control exerted by pressure and temperature.

Cruciani G. & Zanazzi P.F. 1994. Cation partitioning and substitution mechanisms in $1M$ phlogopite; a crystal chemical study. *Am. Mineral.*, 79, 289-301.

Foley S.F. 1989. Experimental constraints on phlogopite chemistry in lamproites: 1. The effect of water activity and oxygen fugacity. *Eur. J. Mineral.*, 1, 411-426.

Foley S.F. 1990. Experimental constraints on phlogopite chemistry in lamproites: 2. Effect of pressure-temperature variations. *Eur. J. Min.*, 2, 327-342.

Large-channels zeolites at high pressure: the case of Na-mordenite and AlPO₄-5

Lotti P.*¹, Gatta G.D.¹, Arletti R.², Merlini M.¹, Pastero L.² & Liermann H.-P.³

1. Dipartimento di Scienze della Terra "A. Desio", Università di Milano. 2. Dipartimento di Scienze della Terra, Università di Torino.
3. Photon Sciences, DESY - PETRA III, Hamburg, Germany.

Corresponding email: paolo.lotti@unimi.it

Keywords: Zeolites, high pressure, large channels.

The interest on the high-pressure (HP) behavior of zeolites significantly increased during the last decades, as reflected by the number of published studies (e.g. Gatta & Lee, 2014; Vezzalini et al., 2014). The chemical composition, the framework topology and the framework-extraframework interactions may significantly affect the response of this class of materials in response to the applied pressure. *P*-induced displacive phase transitions are among the mechanisms adopted by zeolites to accommodate the applied stress, along with the mutual rotation of the TO₄ tetrahedra around the shared oxygen hinges (Gatta & Lee, 2014). A further field of interest concerns the compression of zeolites in potentially pore-penetrating *P*-transmitting fluids (PTF). The *P*-induced penetration of PTF molecules into the zeolite structural cavities may lead to a change of the physical-chemical properties of the studied material, for example inducing the hyperconfinement of supramolecular aggregates with functional properties. We are investigating the HP-behavior of two chemically and topologically different zeolites, synthetic Na-mordenite [MOR] (topological symmetry *Cmcm*) and AlPO₄-5 [AFI] (t.s. *P6/mcc*), which share the presence of large 12-membered rings (12mR) channels in their crystal structures, serving as suitable materials to explore any potential crystal-fluid interaction at the atomic scale under extreme conditions. The compression of Na-mordenite in non penetrating silicone oil (s.o.) showed the occurrence of a phase transition, between 1.68(7) and 2.70(8) GPa, from a *C*-centered (space group *Cmcm* or *Cmc2₁*) to a primitive orthorhombic structure (s.g.: *Pbnm*, *Pbnn* or *Pbn2₁*). The high-*P* primitive polymorph showed a high bulk volume compressibility ($K_{V0} = 25(2)$ GPa, $K_V' = 2.0(3)$) with a remarkable elastic anisotropy ($\beta_b \gg \beta_c > \beta_a$). The bulk compression is strongly accommodated by the increase in ellipticity of the large 12mR-channels. The synthetic AlPO₄-5 zeolite was studied using both non-penetrating s.o. and a potentially penetrating methanol:ethanol:H₂O = 16:3:1 mixture (m.e.w.) as PTF. Interestingly, the diffraction patterns of this zeolite show evidence of superstructure reflections. The preliminary results show a significant compressibility of this zeolite in s.o. ($K_{V0} = 11.4(4)$ GPa and $K_V' = 2.3(3)$), whereas the compression in m.e.w. shows a remarkable decrease in compressibility and a different structure deformation at the atomic scale, ascribable to the *P*-induced penetration of PTF molecules into the large 12mR-channels.

The authors acknowledge the Italian Ministry of Education, MIUR-Project: "Futuro in Ricerca 2012 - ImPACTRBFR12CLQD".

Gatta G.D. & Lee Y. 2014. Zeolites at high pressure: A review. *Mineral. Mag.*, 78, 267-291.

Vezzalini G., Arletti R. & Quartieri S. 2014. High-pressure-induced structural changes, amorphization and molecule penetration in MFI microporous materials: a review. *Acta Cryst.* B70, 444-451.

Structural disorders in narsarsukite structure

Mesto E.*¹, Kaneva E.², Lacalamita M.¹, Schingaro E.¹, Scordari F.¹ & Vladykin N.²

¹ Dipartimento di Scienze della Terra e Geoambientali, Università di Bari.

² The A.E. Favorsky Institute of Geochemistry, Irkutsk, Russia.

Corresponding email: ernesto.mesto@uniba.it

Keywords: Narsarsukite, structural disorder, SCXRD.

Narsarsukite, $[\text{Na}_2(\text{Ti,Fe})\text{Si}_4(\text{O,F})_{11}]$, is a rare titanosilicate mineral usually found in alkali pegmatitic rocks in Narsarsuk, Greenland. Titanosilicate minerals represent excellent materials for selective recovery of valuable ions from waste (Su & Balmer, 2000). They also exhibit exceptional catalytic activities and selective for oxidation reactions (Clerici et al., 1997).

Narsarsukite microporous framework is made up of tubular tetrahedral chains running parallel to the *c* direction linked by corner-sharing Ti-octahedra. The cavities between the tetrahedral and octahedral chains contains Na^+ ions.

A structural study of two single crystals of narsarsukite from Murun is here presented. For both samples, the structure refinements, carried out in the space group *I4/m*, show residual peaks of $\approx 6 \text{ e}/\text{\AA}^3$, which were interpreted as a splitting of Ti site due to a $\text{Ti}^{4+} \rightarrow \text{Fe}^{3+}$ replacement. In addition, in the Fourier difference maps, another less intense peak ($\approx 1.4 \text{ e}/\text{\AA}^3$), was found close to Na site. This was included in the refinement as a positional disorder of Na site. The modeling of both kinds of disorder yielded a final R-index of $\approx 1.4\%$. In the analysed samples the Ti-octahedron is strongly distorted compared to Fe-octahedron, while Na-O bond distances show that the ordered Na-polyhedron is seven-fold coordinated (ord-O $> = 2.52 \text{ \AA}$, for both samples) and the disordered Na-ion is surrounded by 8 oxygen atoms (dis-O $> = 2.72 \text{ \AA}$, for both studied crystals).

In the narsarsukite structure there are five independent oxygens. O1 and O2 oxygens are shared between Ti-octahedra, O4 oxygens are shared between Ti-octahedra and Si-tetrahedra, while O3 and O5 oxygens link Si-tetrahedra. As a consequence of the mentioned structural disorder the following arrangements in the structure are possible: a) octahedral chain consisting of only Ti octahedra; b) octahedral chain consisting of only Fe octahedra; c) Fe octahedra located between adjacent Ti octahedra; d) Fe octahedra adjacent and linked through the O2 oxygen; e) Fe octahedra adjacent and linked through O1 oxygen. Bond valence analyses for each of the listed cases indicate that O1 and O2 sites can be occupied by F^- , $(\text{OH})^-$ or O^{2-} . Taking into account EPMA, SCXRD and Mössbauer results, it can be hypothesized that the disordering of Na promotes $\text{O}^{2-} \rightarrow \text{OH}^-$ substitution, while the splitting of Ti site, related to the amount of Ti^{4+} and Fe^{3+} in the structure, can affect the replacement of F^- for O^{2-} at the bridging O1 and O2 sites.

Clerici M.G., Bellussi G. & Romano U. 1997. Synthesis of propylene oxide from propylene and hydrogen peroxide catalyzed by titanium silicalite. *J. Catal.*, 129, 159-167.

Su Y. & Balmer M.L. 2000. Raman Spectroscopic Studies of Silicotitanates. *J. Phys. Chem. B*, 104, 8160-8169.

Electron diffraction tomography for the characterization of sub-micrometric minerals: application to metamict phases

Mugnaioli E.*¹, Capitani G.C.² & Viti C.¹

1. Dipartimento di Scienze Fisiche, della Terra e dell'Ambiente, Università di Siena. 2. Dipartimento di Scienze dell'Ambiente e del Territorio e di Scienze della Terra, Università di Milano-Bicocca.

Corresponding email: enrico.mugnaioli@unisi.it

Keywords: Metamict minerals, electron diffraction, electron microscopy.

Single-crystal X-ray diffraction can be performed only on crystalline domains of some cubic microns, while most of hitherto unsolved minerals and many new synthetic phases do not grow in crystals of such dimensions. On the other hand, interpretation of X-ray powder diffraction data may be problematic for polyphasic samples and structures characterized by large cell parameters or pseudo-symmetry. Electron diffraction is able to deliver 3D structural data from single crystallites of few nanometers. This ability derives from the high cross section between electrons and matter and the possibility to focus the electron beam into a nanometric probe. In the last years, electron diffraction tomography (EDT) emerged as an efficient method for acquiring complete and quasi-kinematic data sets for ab-initio structure determination of sub-micrometric phases (Kolb et al., 2011).

The mineral charoite was one of the first structures determined on the basis of EDT data, and still one of the trickiest crystallographic cases faced by electron diffraction. Despite the fact that charoite is a well-known and commercially exploited mineral, its symmetry and structure determination was hampered because two commensurate and pseudo-symmetric polytypes grow together inside fibers less than 1 μm thick (Rozhdestvenskaya et al., 2011). In recent years, tomographic electron diffraction has been used for the characterization of several minerals and products of experimental geology occurring as minor, sub-micrometric phases in poly-mineralogical associations. The porous $(\text{S}_2)_{1+x}[\text{Bi}_{9-x}\text{Te}_x(\text{OH})_6\text{O}_8(\text{SO}_4)_2]_2$ was the first natural phase initially recognized, and subsequently structurally determined, by EDT alone (Capitani et al., 2014).

Recently, EDT has been employed for the characterization of metamict phases. Metamict minerals undergo structural changes and amorphization due to the radioactive decay of hosted elements. Phase identification is commonly done on the basis of compositional data alone, or by powder diffraction performed after the sample has been heated in order to produce re-crystallization. Still, different compositional and mineralogical domains may merge in the process. We therefore exploited EDT for the characterization of sub-micrometric crystalline relicts in metamict domains, allowing single-crystal ab-initio determination of natural samples without the need of any physical treatment.

Capitani G.C., Mugnaioli E., Rius J., Gentile P., Catelani T., Lucotti A. & Kolb U. 2014. The Bi sulfates from the Alfenza Mine, Crodo, Italy: An automatic electron diffraction tomography (ADT) study. *Am. Mineral.*, 99, 500-510.
Kolb U., Mugnaioli E. & Gorelik T.E. 2011. Automated electron diffraction tomography – a new tool for nano crystal structure analysis. *Cryst. Res. Technol.*, 46, 542-554.
Rozhdestvenskaya I., Mugnaioli E., Czank M., Depmeier W., Kolb U. & Merlino S. 2011. Essential features of the polytypic charoite-96 structure compared to charoite-90. *Mineral. Mag.*, 75, 2833-2846.

High-pressure single-crystal X-ray synchrotron diffraction of pentahydrate

Nazzareni S.*¹, Comodi P.¹ & Hanfland M.²

1. Dipartimento di Fisica e Geologia, Università di Perugia. 2. ESRF, Grenoble, France.

Corresponding email: sabrina.nazzareni@unipg.it

Keywords: Sulphate, single-crystal X-ray diffraction, synchrotron.

Sulphates are typical minerals in evaporitic environments but they became more and more intriguing when they were found as a very common components on the surface of other planets of our solar system. Moreover the hydrated sulphates having both OH groups and water molecules in their structures can be considered as a proxy to study the behaviour of hydrogen bonds in minerals. In the system $\text{MgSO}_4 - \text{H}_2\text{O}$ many minerals may form at different degrees of hydration (Alpers et al., 2000): $\text{MgSO}_4 \cdot n\text{H}_2\text{O}$ with $n = 1, 1\frac{1}{4}, 2, 2\frac{1}{2}, 3, 4, 5, 6, 7,$ and 11.

Pentahydrate, $\text{Mg}(\text{SO}_4) \cdot 5\text{H}_2\text{O}$, is triclinic (sp. gr. P-1), its structure is characterised by Mg-octahedra and S-tetrahedra to form $[\text{Mg}(\text{H}_2\text{O})_4 \text{SO}_4]$ chains extending parallel to $[110]$. The chains are connected to each other by hydrogen bonds, formed by the water oxygen atoms in the chain and by the fifth water molecule, which is not coordinated to a Mg atom.

We studied the HP behaviour of pentahydrate by single-crystal X-ray synchrotron diffraction. Crystals were loaded in DAC with ruby chips as pressure calibrant, and He as pressure transmitting media. The experiments were performed at ID09 (ESRF, Grenoble) up to 12 GPa.

Pentahydrate shows a structural stability up to 12 GPa but a change in the compressional style at 5 GPa occurs with a discontinuity in the lattice parameters c and b (that strongly decrease) and a angles (that increases). Fitting the P - V data up to 5 GPa with a 2nd-order Birch-Murnaghan EoS the bulk modulus is $K_0 = 32.6(1)$ GPa, $V_0 = 365.3(8)$ Å³. The 0-5 GPa lattice parameters fitted by a BM2 EoS yield to: $K_{0a} = 39(4)$ GPa, $a_0 = 6.275(2)$ Å; $K_{0b} = 21(1)$ GPa, $b_0 = 10.547(3)$ Å, $K_{0c} = 26(2)$ GPa, $c_0 = 6.080(5)$ Å. The axial compressibility is $\beta_a = -8.5 \cdot 10^{-3}$ GPa, $\beta_b = -15.8 \cdot 10^{-3}$ GPa and $\beta_c = -12.8 \cdot 10^{-3}$ GPa. The lattice anisotropy is $\beta_{0a}:\beta_{0b}:\beta_{0c} = 0.54:1:0.81$, with the a parameter that is twice less compressible than b lattice parameters suggesting a strong anisotropy in the compression of the lattice parameters. The bulk modulus of pentahydrate in the 6-12 GPa P -range is 60(5) GPa (with $V = 305(1)$ Å³) obtained fitting P - V data with a BM2 EoS.

The 0-5 GPa range bulk modulus of pentahydrate is of the same order as other Mg-sulphates such as bloedite, $\text{Na}_2\text{Mg}(\text{SO}_4)_2 \cdot 4\text{H}_2\text{O}$, $K_0 = 36(1)$ GPa and $K' = 5.1(4)$ (Comodi et al., 2014), and kainite, $\text{KMg}(\text{SO}_4) \cdot \text{Cl} \cdot 3\text{H}_2\text{O}$, $K_0 = 31.8(3)$ GPa $K' = 4$ (unpub. data). Structural refinements to explain the compressional behaviour are under execution.

Alpers C.N., Jambor J.L. & Nordstrom D.K. (Eds.) 2000. Sulfate minerals: Crystallography, Geochemistry and Environmental Significance. Volume 40. Rev. Mineral. Geochem., 608 pp.

Comodi P., Nazzareni S., Balic-Zunic T., Zucchini A. & Hanfland M. 2014. The high-pressure behavior of bloedite: A synchrotron single-crystal X-ray diffraction study. Am. Mineral., 99, 511-518.

Impossible or unusual solid-solutions in oxo-amphiboles: mangano-mangani-ungarettiite vs. "oxo-mangani-leakeite" and potassic-fluoro-richterite vs. "oxo-potassic-richterite"

Oberti R.*¹, Boiocchi M.² & Hawthorne F.C.³

1. Istituto di Geoscienze e Georisorse, CNR Pavia. 2. Centro Grandi Strumenti, Università di Pavia
3. Department of Geological Sciences, University of Manitoba, Canada.

Corresponding email: oberti@crystal.unipv.it

Keywords: Amphibole, oxo-component, crystal-chemistry.

The oxo-component (${}^{\text{W}}\text{O}^{2-}$) in amphiboles is crucial both for mineralogy (it is the first discriminating parameter in the new and crystal-chemistry-based scheme for amphibole classification, Hawthorne et al., 2012) and petrology (it is a clue for f_{O_2} conditions of crystallization). Also, oxo-amphiboles are far more common than previously thought.

${}^{\text{W}}\text{O}^{2-}$ can be stabilized by two crystal-chemical mechanisms, which both occur mainly at the $M(1)$ site and secondly at the $M(3)$ site: (1) the oxidation of Fe^{2+} , and (2) the presence of Ti^{4+} or Mn^{3+} . Whereas the first mechanism is typical of magmatic systems, and can be simulated and studied *in operando* in the lab, the second mechanism implies peculiar bulk compositions and f_{O_2} conditions of crystallization. This is the case for the two new end-members introduced in this work: "oxo-mangani-leakeite", ${}^{\text{A}}\text{Na}{}^{\text{B}}\text{Na}_2{}^{\text{C}}(\text{Mn}^{3+}_4\text{Li}){}^{\text{T}}\text{Si}_8\text{O}_{22}{}^{\text{W}}\text{O}_2$, and "oxo-potassic-richterite", ${}^{\text{A}}\text{K}{}^{\text{B}}(\text{NaCa}){}^{\text{C}}(\text{Mg}_4\text{Ti}){}^{\text{T}}\text{Si}_8\text{O}_{22}{}^{\text{W}}\text{O}_2$ (inverted commas are due because approval by IMA-CNMNC is still underway).

"Oxo-mangani-leakeite" occurs together with mangano-mangani-ungarettiite, ${}^{\text{A}}\text{Na}{}^{\text{B}}\text{Na}_2{}^{\text{C}}(\text{Mn}^{2+}_2\text{Mn}^{3+}_3){}^{\text{T}}\text{Si}_8\text{O}_{22}{}^{\text{W}}\text{O}_2$, in strongly foliated oxidized assemblages in the Hoskins' Mn mine (Australia). However, these two amphiboles never occur in the same sample, because the first requires both the presence of ${}^{\text{M}(3)}\text{Li}$ and complete oxidation of Mn at $M(1,2)$, whereas the second requires significant Mn^{2+} and has an inverse ordering scheme for C cations: C^{2+} at $M(2)$, C^{3+} at $M(1,3)$. Solid-solution between the two end-member compositions is therefore crystal-chemically not possible. Accordingly, we have characterized "oxo-mangani-leakeite" compositions with $0.65 < {}^{\text{C}}\text{Li} < 0.50$ apfu but could only find nearly stoichiometric mangano-mangani-ungarettiite compositions.

"Oxo-potassic-richterite" was found in a lava dome at Leucite Hill, Wyoming, a locality known for potassic-fluoro-richterite. The rock sample contains acicular amphibole crystals, with a strong zoning in Ti, where lower Ti contents correspond to higher ${}^{\text{W}}\text{F}^-$ and lower ${}^{\text{W}}\text{O}^{2-}$ contents. This unusual solid-solution must be related to variations in the composition of the circulating fluids. It is noteworthy that amphiboles with richteritic compositions rarely contain high-charged cations other than Ti (in lamproites), and this Ti occurs as both a C and a T cation (they usually have low ${}^{\text{W}}\text{O}^{2-}$ contents; Oberti et al. 1992). Even more interesting, synthetic oxo amphiboles with compositions similar to "oxo-potassic-richterite" were obtained many years ago (Tiepolo, unpublished) while trying to model trace-element partitioning in high-Si Ti-enriched lamproites.

Hawthorne F.C., Oberti R., Harlow G.E., Maresch W.V., Martin R.F., Schumacher J.C. & Welch M.D. 2012. Nomenclature of the amphibole supergroup. *Am. Mineral.*, 97, 2031-2048.

Oberti R., Ungaretti L., Cannillo E., Hawthorne F.C. 1992. The behaviour of Ti in amphiboles: I. Four- and six-coordinated Ti in richterites. *Eur. J. Mineral.*, 4, 425-439.

HT-FTIR micro-spectroscopy of CO₂ in cordierite: temperature dependence of the absorption and diffusion kinetics

Radica F.^{*1}, Della Ventura G.^{1,2}, Bellatreccia F.^{1,2}, Cinque G.³, Marcelli A.^{2,4} & Cestelli Guidi M.²

1. Dipartimento di Scienze, Università Roma Tre. 2. INFN-LNF, Frascati.
3. Diamond Light Source, Didcot, UK. 4. Rome International Center for Materials Science (RICMASS), Roma.

Corresponding email: francesco.radica@uniroma3.it

Keywords: FTIR spectroscopy, diffusion, CO₂.

The intensity evolution of the CO₂ FTIR bands of cordierite has been obtained as a function of T , by comparing data obtained from *in situ* vs. quenching measurements. Spectroscopic data have been used also to evaluate the kinetic process of CO₂ desorption deriving the outward diffusion coefficients of cordierite.

The evolution of CO₂ FTIR absorption bands in a natural well-characterized cordierite from Kragero, Norway (Della Ventura et al., 2012) was studied up to 1200 °C using a heating stage fitted on a FTIR microscope. Two different oriented sections (001) and (010), respectively, were used to check the effect of the channel orientation on the CO₂ release from the matrix. Spectra collected *in situ* show that increasing temperatures induces an increase of peak width for all CO₂-related bands. The effects on the integrated absorbance A_i are different for the different bands. Most notably, the integrated intensity A_i of the anti-symmetric stretching mode (ν_3) increases significantly up to 800 °C, then progressively decreases to 1000/1200 °C, depending on the sample orientation. Data obtained on quenched samples reveal that there is no variation in the band intensity for $T < 900$ °C, thus the absorbance increase observed for *in situ* measurements must be related to an increase in the molar absorption coefficient ϵ . Combination of *in situ* with quenched data reveals that the CO₂ loss from the cordierite matrix starts around 800 °C and is strongly dependent on the thickness and shape of the examined sample: it is favored for small and tabular shaped grains, while being significantly reduced for large and prismatic grains. Fracturing along direction normal to [001] multiplies the diffusion interfaces, thus enhancing the CO₂ loss from the matrix.

Following these considerations, we performed several isothermal heating experiments on (001) oriented sections cut out from a CO₂-rich sample. Single-crystal slabs of different thicknesses were heat-treated up to 1000 °C and the intensity of the ν_3 anti-symmetric stretching mode of CO₂ at 2348 cm⁻¹ was monitored as a function of time. The experimental curves were modeled using different approaches. Two different Avrami equations, in particular, were found to be sensitive to the sample thickness. The mono-dimensional plane sheet diffusion approach (Ingrin et al., 1995), on the other side, is not influenced by sample thickness variation and fitted data yield a value of $-\log D_0 = 4.4 \pm 0.7$ m²/sec and $E_a = 204 \pm 15$ kJ/mol.

Della Ventura G., Radica F., Bellatreccia F., Cavallo A., Capitelli F. & Harley S. 2012. Quantitative analysis of H₂O and CO₂ in cordierite using polarized FTIR spectroscopy. *Contrib. Mineral. Petrol.*, 164, 881-894.
Ingrin J., Hercule S. & Charton T. 1995. Diffusion of hydrogen in diopside: results of dehydration experiments. *J. Geophys. Res-Sol. Ea.*, 100, 15489-15499.

The diffusion of CO₂ in cordierite and beryl: an FTIR-FPA spectroscopy study

Radica F.*¹, Della Ventura G.¹⁻², Bellatreccia F.¹⁻², Freda C.³, Marcelli A.²⁻⁴ & Cestelli Guidi M.²

1. Dipartimento di Science, Università di Roma TRE. 2. INFN-LNF, Frascati (Roma). 3. INGV, Roma.
4. Rome International Center for Materials Science (RICMASS), Roma.

Corresponding email: francesco.radica@uniroma3.it

Keywords: FTIR spectroscopy, imaging, CO₂.

In this work, we address the diffusion of CO₂ into cordierite and beryl, two isostructural microporous rock-forming minerals, using FTIR spectroscopy coupled with a FPA (focal-plane-array) detector. Fragments of a natural, almost Mg end-member cordierite (Della Ventura et al., 2012) and CO₂-free synthetic beryl (Bellatreccia et al., 2008) were used as starting materials for the diffusion experiments. Starting materials were treated in a CO₂-saturated atmosphere at different pressure, temperature and time conditions, using a non end-loaded piston-cylinder apparatus. Ag-carbonate was used as a source for carbon dioxide. After the experiments, the recovered crystals were oriented using a spindle stage, cut and doubly polished, and analyzed using FTIR imaging and polarized micro-FTIR spectroscopy to study the distribution of CO₂ across the sample and quantify its concentration. The data obtained show that pressure plays a major role on the incorporation of gaseous CO₂ in both cordierite and beryl, whereas the effect of temperature is limited.

The spectroscopic results show that the diffusion of CO₂ occurs preferentially along the structural channels parallel the *c*-axis direction. Sample cracks formed during the treatment at high pressure and high temperature were found to enhance significantly the gas diffusion within the samples.

Diffusion coefficients (*D*) for beryl were calculated using the formalism for the mono-dimensional diffusion in a semi-infinite medium (Crank, 1975); obtained values are of the order of 10⁻¹⁴ m²/s in the 700-900 °C T range. Fitting of the diffusion coefficients in the Arrhenius plot yielded $-\log D_0 = 7.2 \pm 0.7$ m²/sec and an activation energy $E_a = 122 \pm 15$ kJ/mol. Our data suggest that, compared to similar silicate structures, the structural channels of cordierite and beryl act as fast paths for the mobility of large molecular groups, and for this reason the diffusion coefficients are similar to those typically observed for grain boundary diffusion or to the behavior of CO₂ in non-crystalline materials, like silicate melts (Watson et al., 1982).

- Bellatreccia F., Della Ventura G., Piccinini M. & Grubessi O. 2008. Single-crystal polarized light IR study of an historical synthetic water poor emerald. *Neues Jb. Miner. Abh.*, 185, 11-16.
- Crank J. 1975. *The Mathematics of Diffusion*. Clarendon Press, Oxford.
- Della Ventura G., Radica F., Bellatreccia F., Cavallo A., Capitelli F. & Harley S. 2012. Quantitative analysis of H₂O and CO₂ in cordierite using polarized FTIR spectroscopy. *Contrib. Mineral. Petr.*, 164, 881-894.
- Watson E.B., Sneeringer M.A. & Ross A. 1982. Diffusion of dissolved carbonate in magmas: experimental results and applications. *Earth Planet. Sci. Lett.*, 61, 346-358.

The first 50 years of Electron Probe Micro-Analysis applications to the Geosciences: developments and perspectives

Rinaldi R.*¹ & Llovet X.²

1. ex Dipartimento di Fisica e Geologia, Università di Perugia. 2. Scientific and Technological Centers (CCiTUB), Universitat de Barcelona, España.

Corresponding email: romano.rinaldi@unipg.it

Keywords: Electron probe microanalysis, developments, perspectives.

In connection with the centennial of X-Ray Crystallography, a technique born in 1914-15 with the first structural determination of a simple mineral, this year marks the 50th anniversary of the application of another fundamental technique in the Geosciences; Electron Probe Micro-Analysis (EPMA or EMPA). Some 36 years after the Braggs' discovery, another crystallographer, well known to mineralogists (André Guinier) and a physicist (Raymond Castaing) set up, as part of the PhD thesis of the latter, "*A method of chemical and crystallographic point analysis based on electron probes*", where the X-rays generated by the impact of a focused electron beam on metal alloys, were analysed with a Bragg spectrometer reflecting off a mica crystal. Refinement of the technique yielded the first commercial instruments by the end of the 1950's. The first systematic mineralogical applications date to 15 years later when, in 1964-65 some 60 scientific articles appeared worldwide, reporting applications of the technique to the study of minerals and rocks.

In these first 50 years EPMA techniques and their mineralogical applications have provided a great change of perspective in the study of geo-materials, as well as of materials in general. With the advent of digital electronics and computerized automation, at the beginning of the 1970's, the technique had a first leap forward which coincided with the study of rocks and minerals retrieved by the first Lunar missions and the following extension of the same level of curiosity to the study of terrestrial samples. The impact was comparable to that of the polarizing petrographic microscope some 120 years before.

In the 1980-1990's, the diffusion of EPMA, also thanks to the development of energy dispersive spectrometry (EDS) and the full automation of analytical procedures, turned it into a routine investigation. This sort of "short-cut" for an analytical method still based on a high level of conceptual and physical complexity, contributed to providing the user, in the last 10-15 years with the perception of a "mature technique", where one could expect few and infrequent novelties still to come. A very wrong assumption, as revealed by the latest developments.

The use of field effect electron sources, new devices for wavelength (WDS) and EDS spectrometry, the development of sophisticated simulation techniques based on refined models of electron-matter interactions, in combination with other spectroscopic and diffraction (EBSD) techniques, just to mention the main novelties, are providing a totally new reference frame for EPMA with the extension of quantitative analysis to sub-micrometric volumes, both as isolated or matrix embedded particles, thin films or lamellae and at trace concentration levels (ppm), even for ultra-light elements ($Z > 2$) or heavy actinides. The technique will therefore undoubtedly bring further interesting developments to the study of minerals and rocks, some of which can be easily envisaged as of today.

The role of oxidation on the high-temperature behavior of Almandine

Scandolo L.*¹, Alvaro M.¹, McCammon C.², Milani S.³, Di Prima M.¹, Domeneghetti M.C.¹ & Nestola F.³

1. Dipartimento di Scienze della Terra e dell'Ambiente, Università di Pavia. 2. Bayerisches Geoinstitut, University of Bayreuth, Germany.
3. Dipartimento di Geoscienze, Università di Padova.

Corresponding email: lorenzo89.scandolo@gmail.com

Keywords: Almandine, oxidation, high-temperature.

The study of mineral inclusions still trapped in other mineral phases provides information about the Earth's interior and its active geodynamics. Determination of the pressures at which mineral inclusions were entrapped is hence fundamental for constraining the chemico-physical environment in which they formed. An alternative method to conventional chemical geothermobarometry is based on the residual pressure (P_{inc}) on the inclusion still trapped in the diamond at room temperature and pressure as recently developed by Angel et al. (2014, 2015). This method can be potentially applied to any single mineral inclusion, but requires accurate knowledge of the thermoelastic parameters of both host and inclusion.

Oxygen maintains a degree of reactivity with its environment, despite being primarily locked up within crystal structures. Oxygen fugacity can change with temperature variation; therefore is crucial to control such oxygen reactivity while performing experiments with iron-bearing samples.

In order to evaluate any possible role of oxidation during high-temperature experiments on garnet, we performed *in situ* high-temperature single-crystal X-ray diffraction up to 700 °C on two almandine samples using (i) no buffering system; and (ii) iron-wüstite buffer to control the fO_2 while performing the experiments. The powdered iron-wüstite mixture was placed together with the crystal in the vial as described by Alvaro et al. (2015). The oxidation state of iron in garnet was evaluated using single-crystal Mössbauer spectroscopy on the untreated 'natural' sample and on the two samples recovered after the high-T experiments.

The thermal expansion data seem to be in good agreement with one another (i.e. there is no evident effect of the different fO_2 conditions in the vial) and Mössbauer data indicate that no oxidation occurs for the Fe-rich garnets up to at least 700 °C. The small amount of Fe^{3+} that appears in the untreated crystal ($Fe^{3+}/\Sigma Fe = 0.04 \pm 0.02$) appears to be reduced when heated with either no buffer or at iron-wüstite buffer conditions.

This work was supported by ERC starting grant 307322 to F. Nestola.

Angel R.J., Alvaro M., Nestola F. & Mazzucchelli, M.L. 2015. Diamond thermoelastic properties and implications for determining the pressure of formation of diamond inclusion systems. *Russ. Geol. Geophys.*, 56, 225-234.

Angel R.J., Mazzucchelli M.L., Alvaro M., Nimis P. & Nestola F. 2014. Geobarometry from host-inclusion systems: the role of elastic relaxation. *Am. Mineral.*, 99(10), 2146-2149.

Alvaro M., Angel R.J., Marciano C., Milani S., Scandolo L., Mazzucchelli M.L., Zaffiro G., Rustioni G., Briccola M., Domeneghetti M.C. & Nestola F. 2015. A new micro-furnace for "in situ" high-temperature single crystal X-ray diffraction measurements. *J. App. Cryst.* In press.

Ti-rich garnets: an EPMA, SIMS, MÖSSBAUER, XRPD and SCXRD investigation

Schingaro E.¹, Lacalamita M.*¹, Mesto E.¹, Ventrucci G.¹, Pedrazzi G.², Ottolini L.³ & Scordari F.¹

1. Dipartimento di Scienze della Terra e Geoambientali, Università di Bari "Aldo Moro". 2. Dipartimento di Neuroscienze, Università di Parma. 3. Istituto di Geoscienze e Georisorse, CNR, Pavia.

Corresponding email: maria.lacalamita@uniba.it

Keywords: Ti-bearing garnets, multi-methodic approach, crystal chemistry.

A suite of Ti-bearing garnets from magmatic, metamorphic and carbonatitic rocks was studied by Electron Probe Microanalysis (EPMA), X-ray Powder Diffraction (XRPD), Single Crystal X-ray Diffraction (SCXRD), Mössbauer spectroscopy and Secondary Ion Mass Spectrometry (SIMS) in order to better characterize their crystal chemistry. The studied garnets show TiO₂ varying in the ranges 4.9(1)-17.1(2) wt.% and variable Fe³⁺/ΣFe content. SIMS analyses allowed quantification of light elements yielding H₂O in the range 0.091(7)-0.46(4), F in the range 0.004(1)-0.040(4) and Li₂O in the range 0.0038(2)-0.014(2) wt%. Mössbauer analysis provided spectra with different complexity, which could be fitted to a number of components variable from one (^YFe³⁺) to four (^YFe²⁺, ^ZFe²⁺, ^YFe³⁺, ^ZFe³⁺). A good correlation was found between the Fe³⁺/ΣFe resulting from the Mössbauer analysis and that derived from the Flank method (Höfer & Brey, 2007).

X-ray powder analysis revealed that the studied samples are a mixture of different garnet phases with very close cubic unit cell parameters as recently found by other authors (Antao, 2013). Single crystal X-ray refinements using anisotropic displacement parameters were performed in the *Ia-3d* space group and converged to *R*₁ in the range 1.63-2.06 % and *wR*₂ in the range 1.44-2.21 %. Unit cell parameters vary between 12.0641(1) and 12.1447(1) Å, reflecting different Ti contents and extent of substitutions at tetrahedral site.

The main substitution mechanisms affecting the studied garnets are: ^YR⁴⁺ + ^ZR³⁺ ↔ ^ZSi + ^YR³⁺ (schorlomite substitution); ^YR²⁺ + ^ZR⁴⁺ ↔ 2^YR³⁺ (morimotoite substitution); ^YFe³⁺ ↔ ^YR³⁺ (andradite substitution) with ^ZR⁴⁺ = Ti; ^YR⁴⁺ = Ti, Zr; ^YR³⁺ = Fe³⁺, Al³⁺, Cr³⁺; ^ZR³⁺ = Fe³⁺, Al³⁺ and ^YR²⁺ = Fe²⁺, Mg²⁺, Mn²⁺. The 2^YTi⁴⁺ + ^ZFe²⁺ ↔ 2^YFe³⁺ + ^ZSi⁴⁺, the hydrogarnet substitution [(SiO₄)⁴⁻ ↔ (O₄H₄)⁴⁻], the F⁻ ↔ OH⁻ and the ^YR⁴⁺ + ^XR⁺ ↔ ^YR³⁺ + ^XCa²⁺, with ^YR⁴⁺ = Ti, Zr; ^YR³⁺ = Fe³⁺, Al³⁺, Cr³⁺; ^XR⁺ = Na, Li also occur.

The garnet crystal chemistry and implications in terms of nomenclature and classification (Grew et al., 2013) are discussed.

Antao S.M. 2013. The mystery of birefringent garnet: is the symmetry lower than cubic?. Powder diff., 28(4), 281-287.
Grew E.S., Locock A.J., Mills S.J., Galuskina I.O., Galuskina E.V. & Hålenius U. 2013. Nomenclature of the Garnet Supergroup. Am. Mineral., 98, 785-811.
Höfer H.E. & Brey G.P. 2007. The iron oxidation state of garnet by electron microprobe: Its determination with the flank method combined with major-element analysis. Am. Mineral., 92, 873-885.

Analysis of the mineralogical content of incoherent lava portions containing fibrous minerals from volcanic products found in localities around S. Maria di Licodia town (CT), Italy

Stelluti I.*¹, Ioli P.¹, Mura F.² & Gianfagna A.¹

1. Dipartimento di Scienze della Terra, Sapienza Università di Roma.
2. Laboratorio di Nanotecnologie e Nanoscienze, Sapienza Università di Roma.

Corresponding email: igor.stelluti@uniroma1.it

Keywords: Fibrous orthopyroxene, fibrous inosilicate, Etnean mineralizations.

Santa Maria di Licodia is a locality of Sicily interested by “Ellittico” volcanism of Mount Etna (Romano, 1982). It is characterized by domes and lava flows, from mugearitic to benmoreitic compositions. The domes were developed through autometasomatic processes, which followed the formation of autobrecciated external portions. Micrometric minerals and fibrous orthopyroxenes were found in these materials (Gianfagna et al., 2012; Stelluti et al., 2013; 2014), whose presence was never observed in volcanic environment before. Given the potential environmental impact of inhalable fibrous minerals, this study concerned a detailed investigation of the brecciated portions, in order to define their compositions and verify the presence, diffusion and areal distribution of such fibrous minerals. The sampling was performed in four different volcanic areas around S. Maria di Licodia and the samples were studied by means of Optic Microscopy (OM), Field Emission Scanning Electron Microscopy (FESEM) and Rietveld Refinement of Powder X-Ray Diffraction (XRPD) after fibrous mineral enrichment by gravimetric method. Nevertheless the similarity of mineralogical composition of the rocks studied, orthopyroxenes show a wide variability in presence, abundance and morphological characteristics between the different localities. The presence of fibrous orthopyroxenes in his different morphologies, coupled with chemical analysis of both the minerals and host rocks, can be used as an instrument in order to understand the mechanisms of lava dome cooling rate during the intrusion processes of the study area.

- Gianfagna A., Mazziotti Tagliani S. & Stelluti I. 2012. Acicular and fibrous orthopyroxenes in the volcanics of Santa Maria di Licodia (Sicily, Italy). European Mineralogical Conference, 1, EMC2012-533.
- Romano R. 1982. Succession of the volcanic activity in the Etnean area. Mem. Soc. Geol. It., 23, 27-48.
- Stelluti I., Viti C. & Gianfagna A. 2013. Mineralogical characterization and crystallization kinetics of fibrous and acicular volcanic orthopyroxenes from Mt. Etna, Sicily, Italy. Mineral. Mag., 77, 2261.
- Stelluti I., Mura F. & Gianfagna A. 2014. FESEM-FIB-EDS investigation on fibrous and acicular volcanic orthopyroxenes from Etnean products, Italy. A.1 Rend. Online Soc. Geol. It., Suppl. N.1 Vol. 31, 376.

Crystal chemistry and HT behavior of riebeckite from Malawi: a combined XRD and FTIR study

Susta U.*¹, Della Ventura G.¹, Bellatreccia F.¹, Hawthorne F.C.², Boiocchi M.³ & Oberti R.³

1. Dipartimento di Scienze, Università Roma Tre. 2. Department of Geological Sciences, University of Manitoba, Canada.
3. Istituto di Geoscienze e Georisorse, CNR, Pavia.

Corresponding email: umberto.susta@uniroma3.it

Keywords: FTIR, riebeckite, high temperature.

Fe-amphiboles play a major role in enhancing the electrical conductivity of subducted rocks in convergent margins (Reynard et al., 2011). This issue has been shown to be related to the Fe²⁺ to Fe³⁺ oxidation within the octahedral sites and not directly to the released fluids (e.g. Wang et al., 2012). These particular aspects of the amphibole physical properties have never been studied in detail, thus an accurate description of the deprotonation mechanisms and their relationship with oxidation of multi-valence elements is necessary.

In this work we examine a riebeckite from Malawi, chosen among our collection of Fe-rich samples as a representative of the sodic amphiboles group species, common in high-P geological environments. As a starting point to model any modification induced during high temperature treatments, the sample was characterized in details at room-T by means of single crystal XRD refinement, EPMA, IR and Mössbauer spectroscopy. The crystal-chemical formula turned out to be very close to the ideal end-member composition Na₂Fe²⁺₃Fe³⁺₂Si₈O₂₂(OH)₂. HT-IR data collected *in-situ* on single-crystals showed a significant increase in the absorption coefficient with T, a feature already observed by Della Ventura et al. (2015). Spectra collected on quenched specimens showed an abrupt and complete hydrogen loss in the 550-650 °C T range. The behavior of the OH-stretching absorption of riebeckite is different to that of potassic-ferro-richterite (Della Ventura et al., 2015): a decrease in intensity of all bands is observed, and no components to be assigned to the presence of Fe³⁺ are present in the spectra. This behavior is interpreted in terms of the lack of vibrational coupling (Della Ventura et al., 2007) between facing anionic sites in the structure. The H diffusion mechanism across the structure was addressed by means of isothermal HT-IR experiments, using both doubly-polished single crystals and powders. We observed that the kinetics of deprotonation is strongly influenced by the atmosphere within the heating stage, suggesting a strong control of the oxygen availability during the experiment on the hydrogen diffusion. This issue is presently under detailed investigation.

- Della Ventura G., Oberti R., Hawthorne F.C. & Bellatreccia F. 2007. FTIR spectroscopy of Ti-rich pargasites from Lherz, and the detection of O²⁻ at the anionic O³ site in amphiboles. *Amer. Mineral.*, 92, 1645-1651.
- Della Ventura G., Susta U., Bellatreccia F., Cavallo A. & Oberti R. 2015. Synthetic potassic-ferro-richterite: HT behavior and deprotonation process by single-crystal FTIR spectroscopy and structure refinement. This meeting.
- Reynard B., Mibe K. & Van de Moortèle B. 2011. Electrical conductivity of the serpentinised mantle and fluid flow in subduction zones. *Earth Planet. Sci. Lett.*, 307, 387-394.
- Wang D., Guo Y. & Yu Y. 2012. Electrical conductivity of amphibole-bearing rocks: influence of dehydration. *Contrib. Mineral. Petrol.*, 164, 17-25.

The importance of a multimethodic approach for the characterization of platinum group minerals (PGM) and associated phases: some cases of study

Zaccarini F.*¹, Bindi L.², Garuti G.¹ & Bakker R.J.¹

1. Department of Applied Geoscience and Geophysics, University of Leoben, Austria.

2. Dipartimento di Scienze della Terra, Università di Firenze.

Corresponding email: federica.zaccarini@unileoben.ac.at

Keywords: Platinum group minerals, multidisciplinary, analyses.

Platinum Group Minerals (PGM) are the carriers of the Platinum Group Elements (PGE). PGM are rare and represent only the 2.6% of the phases officially approved by IMA. Nevertheless, based on their composition, more than 500 PGM are potentially new mineral species. However, it is exceedingly hard to structurally characterize them to the degree required for acceptance as new minerals because, generally, they occur as very tiny grains (less than 10 μm) intimately associated with other phases. Under the circumstance, optical and electron microscopy, microprobe analysis and Raman spectroscopy are the most used techniques for the identification of PGM, coupled, when possible, with a X-ray diffraction study. Here we report five cases of study in which the use of complementary methods provided the opportunity for a proper identification of minute PGM grains and associated phases. (1) PGM composed of Ru, Os, Fe and O in ophiolitic chromitites. Based on their composition and optical properties it was supposed that they might have represented true PGE oxides. However, X-ray data proved that this phases actually are ruthenium-magnetite mixtures, in which Ru-O ligands are absent. (2) Three grains with stoichiometry Pt_2Pd , PtPd and PtPd_2 in a Brazilian nugget. Their composition suggests that they may consist of three distinct mineral species. However, structural analyses showed that all these phases are cubic and crystallize in the same space group $Fm-3m$. Data indicate that the PGM are natural intermediates members in the palladium-platinum solid solution series. (3) A potential new mineral with composition Cu_3Au_2 associated with a Pt-Fe nugget collected in the Urals. The X-ray investigation has shown that the alloy actually consists of a Cu-rich tetraauricupride (ideally AuCu). (4) One grain characterized by a rugged surface and chemical zoning in the Nurali chromitite, Urals. Electron microprobe analyses suggest that the grain consists of two compounds with the following stoichiometries: $(\text{Pt,Pd,Fe,Cu,Ni})\text{O}$ and $(\text{Fe,Pt,Ni,Pd,Cu,Rh})_2\text{O}$. Its chemically zoning prevents the study by X-ray diffraction. However, Raman spectroscopy established the presence of a diffuse 500–700 band and a sharp peak at 657 cm^{-1} that strongly resemble the Raman spectra of synthetic PtO and PdO . The Nurali grain probably represents a PGE oxide and does not consist of a mixture of native PGE with Fe oxide or hydroxide. (5) The last example deals with the results obtained on minerals of the bowieite-kashnite solid solution. The grains with stoichiometry $(\text{Rh}_{1.16}\text{Ir}_{0.82}\text{Cu}_{0.02})_2\text{S}_3$ and $(\text{Ir}_{1.06}\text{Rh}_{0.87}\text{Cu}_{0.04})_{1.97}\text{S}_{3.03}$ occur in a dunite of the Urals. In this case, X-ray data confirm that both the minerals are orthorhombic with similar cell dimensions. The Raman spectra show similar characteristic bands at about $287\text{--}308\text{ cm}^{-1}$ and $308\text{--}311\text{ cm}^{-1}$ and at about 374 cm^{-1} and 387 cm^{-1} , respectively. Therefore, in this case, the ultimate methodology to distinguish them was the electron microprobe analyses.

SESSION S12

Mantle mineralogy

CONVENORS

Paola Comodi (Univ. Perugia)

Luca Ziberna (Univ. Bristol)

Majorite stability and melting relations in the mantle transition zone: new constraints from first-principles thermodynamics

Belmonte D.*¹, Ottonello G.¹, De La Pierre M.² & Vetuschi Zuccolini M.¹

1. DISTAV, Università di Genova. 2. Nanochemistry Research Institute, Curtin Institute for Computation, Department of Chemistry, Curtin University, Perth, Australia.

Corresponding email: donato.belmonte@unige.it

Keywords: Majorite, thermodynamics, first-principles.

Although there exists general evidence of the peculiar features of the mantle transition zone (MTZ) with respect to the upper and lower mantle, a deep understanding of their ultimate origin is still elusive. The effects of multiple seismic discontinuities on the convective flow, the increased steepness of the seismic velocity gradients, the geodynamic role of phase transitions and compositional heterogeneities in the MTZ are just few of the controversial aspects related to this part of the Earth's interior. Majorite garnet is a major mineralogical component of the MTZ, ranging in volume from 40% to 70% according to different petrological models. Despite the relative abundance of structural and seismic data, thermodynamic properties are still poorly constrained and their extrapolation at high pressure and temperature conditions is affected by large uncertainties. In this work, we use a quantum mechanical approach based on DFT and computational thermodynamics to provide new constraints on the stability and melting relations of majorite at MTZ conditions. Phase diagrams topology, along with subsolidus, solidus and liquidus phase relations in the simplified binary system MgO-SiO₂, are predicted in a broad range of P-T conditions by first principles theory, with few additional constraints based on the melting behaviour of pure liquid components and the enthalpy of fusion of solid phases. The main implications of our calculations are that i) majorite, undergoing phase transitions at HP-HT, has a more effective impact than olivine components in determining multiple seismic discontinuities between 520 and 720 km depths; ii) structural disorder in majorite may sensibly affect its phase equilibria in the MTZ and iii) melting relations of majorite at HP-HT give useful insights on the crystallization history of a deep magma ocean in the Hadean considering that garnet, together with perovskite and ferropericlaase, was presumably a dominant liquidus phase in the Earth's primordial mantle due to the higher temperature gradients.

The influence of cation substitution on the elastic behaviour of MgSiO₃ bridgmanite in the lower mantle

Boffa Ballaran T. *, Kurnosov A., Frost D.J. & Marquardt H.

Bayerisches Geoinstitut, Universität Bayreuth, Germany.

Corresponding email: tiziana.boffa-ballaran@uni-bayreuth.de

Keywords: Lower mantle, bridgmanite, elasticity.

Seismic velocity anomalies in the lower mantle have been identified in a number of studies. Such anomalies may have a chemical origin likely involving bridgmanite with a composition different from that of the surrounding mantle. If lower and upper mantle have the same composition, then MgSiO₃ bridgmanite should also contain significant concentrations of Fe and Al whose variation could create the lateral heterogeneities observed in seismic models. The composition of the Earth's lower mantle, however, can only be determined by comparing experimental estimates of S and P wave velocities of potential lower mantle assemblages with seismic observations.

Simultaneous high-pressure X-ray single-crystal diffraction and Brillouin spectroscopy experiments have been performed on MgSiO₃, (Mg,Fe)SiO₃ and (Mg,Fe)(Si,Al)O₃ bridgmanite crystals to determine their densities and acoustic phonon velocities at different pressures up to 30 GPa. The crystals were loaded in diamond anvil cells with helium or neon as pressure transmitting medium. At least two crystals of each composition having different non-specific orientations were measured at any pressure in order to obtain all nine independent C_{ij} elastic constants required for the orthorhombic symmetry of bridgmanite and to calculate S and P wave velocities at lower mantle conditions. These results can be used in self consistent thermodynamic mineralogical models to interpret seismic wave velocities in the lower mantle in terms of chemical variations.

Hydrogen diffusion in nominally anhydrous minerals: implications for mass and charge transport

Del Vecchio A.*¹, Poe B.T.¹, Misiti V.² & Cestelli Guidi M.³

1. Dipartimento INGEO Ingegneria e Geologia, Università di Chieti "G. D'Annunzio".
2. INGV, Roma. 3. INFN-LNF, Frascati (Roma).

Corresponding email: alessandro.delvecchio@unich.it

Keywords: NAMs, hydrogen diffusion, hydrous forsterite.

Over the last few decades, knowledge about hydrogen diffusion in nominally anhydrous minerals has become essential towards understanding the dynamics of processes occurring in the Earth's mantle.

Even in small concentrations (ppm wt.%) water, mainly incorporated as hydroxyl ion OH⁻ and to a lesser part as molecular H₂O, can have major effects on the physical and chemical properties of the mantle such as melting temperature, electrical conductivity, diffusivity and rheology, and in particular on the strength of olivine, main mineralogical phase of the upper mantle, with particular implications on viscosity and convection.

In this study, particular attention has been given to the hydrogen self-diffusion in olivine, process of isotope exchange in absence of chemical gradient, through synthesis of polycrystalline natural and synthetic samples hydrated with H₂O and D₂O.

Starting materials are natural samples of San Carlos olivine (Fo₉₂) and a synthetic forsterite obtained by mechano – chemical synthesis, derived from a combination of mechanical activation and heat treatment of starting materials hydrated with liquid H₂O or D₂O by microsyringe.

High pressure and high temperature experiments were carried out at the HP and HT Laboratory of INGV (Rome): starting materials were placed in platinum capsules and synthesized in a piston – cylinder apparatus at 1,5 GPa and 1100 °C for 120 minutes. Portions of each run product were then analyzed by FTIR and RAMAN spectroscopy.

FTIR spectroscopy was carried out at the INFN laboratories of Frascati, for analysis of vibrational bands typical of OH and OD stretching. Analysis of the spectra led to H₂O concentrations in a range between 60-150 ppm wt.%, using the Paterson method for non-polarized spectra. Additionally, features in the spectra were found to be in good agreement with the identification of peaks attributable to both hydroxyl silicate defects and titanoclinohumite defects.

RAMAN spectroscopy was carried out at the Laboratory of Experimental Volcanology of Università degli Studi Roma Tre, over a lower frequency range characteristic of silicate lattice vibrations (ca. 400-1000 cm⁻¹): Raman bands in the OH and OD stretching region were not detected in any of the samples. Analysis of the Raman spectra allow us to study the effect of water on Si-O stretching vibrations of tetrahedral units, but also vibrational modes of tetrahedron / octahedron system in the olivine crystal lattice.

Pairing H₂O and D₂O bearing samples having like concentrations allow for experiments to determine self-diffusion coefficients at temperatures and pressures consistent with depths of the upper mantle. The diffusivities determined by analyzing profiles of OH and OD concentrations by FTIR spectroscopy can then be compared with other physical properties of olivine that are strongly dependent on the presence of hydrogen such as electrical conductivity, elasticity and deformation.

Two new high pressure hydrated phases in the MASH system discovered with fast electron diffraction tomography: bringing water beyond the chlorite breakdown

Gemmi M.^{*1}, Merlini M.², Palatinus L.³, Fumagalli P.², Fischer J.² & Poli S.²

1. Center for Nanotechnology Innovation @NEST, Istituto Italiano di Tecnologia, Pisa.
2. Dipartimento di Scienze della Terra "A. Desio", Università di Milano. 3. Institute of Physics, Czech Academy of Sciences, Prague, Czech Republic.

Corresponding email: mauro.gemmi@iit.it

Keywords: Chlorite, electron diffraction, subduction.

The system MgO-Al₂O₃-SiO₂-H₂O (MASH) is a simplified model for studying hydrated mantle rocks but also for investigating a variable range of lithologies at the slab–mantle interface, where mass transfer in mélangé zones generates hybrid rocks. Chlorite is one of the most important hydrated phases in the system and the knowledge of its stability field and how its structure breaks down releasing water, is a key point for understanding the hydration of the mantle wedge overlying the subducting slab. During a series of experiments aimed to investigate the chlorite stability field we had both chemical and crystallographic evidence of the presence of new high pressure phases beyond the chlorite breakdown ($P > 5$ GPa and $T > 700$ °C) (Fumagalli et al., 2014). However the small amount of recovered material and the presence of several phases made the crystallographic investigation with the standard powder x-ray diffraction difficult. To overcome this problem we developed a fast automatic procedure for collecting electron diffraction tomography data on crystal grains as small as 100 nm. With this procedure single crystal electron diffraction data set can be collected in 2 minutes allowing the screening of several crystalline grains in a single TEM session. We investigated in this way those high pressure-high temperature experiments whose X-ray powder diffraction pattern could not be fully interpreted with the known crystal phases of the MASH system. We discovered two unknown phases: Mg₆Al(OH)₇(SiO₄)₂ (Phase1) which is usually disordered, and Mg₃Al(OH)₃(Si₂O₇) (Phase2). Once the new phases were identified, we selected well crystallized grains and performed on them precession assisted electron diffraction tomography experiments which give a large coverage of the reciprocal space and quasi-kinematical electron diffraction intensities. With these data sets both crystal structures have been solved with direct methods and refined with a procedure which takes into account the dynamical scattering (Palatinus et al., 2015). Both phases show new topologies among silicates and host a large amount of water in their structure in terms of OH groups. Phase1 is an orthosilicate with a layered structure formed by layers of isolated SiO₄ tetrahedra alternated with double layers of face sharing octahedra in which the shared layer of anion is formed only by OH group. Phase2 is a layer sorosilicate with a structural motif similar to inosilicates in which the SiO₄ chains are broken into Si₂O₇ groups.

Fumagalli P., Poli S., Fischer J., Merlini M., Gemmi M. 2014. The high pressure stability of chlorite and other hydrates in subduction mélanges: experiments in the system Cr₂O₃-MgO-Al₂O₃-SiO₂-H₂O. *Contrib. Mineral. Petr.* 167, 979-994.

Palatinus L., Petricek V., Correa C.A. 2015. Structure refinement using precession electron diffraction tomography and dynamical diffraction: theory and implementation. *Acta Crystallogr.*, A71, 235-244.

Oxo-amphiboles in mantle xenoliths: a key to understand the hydrous rich metasomatic melts circulating beneath Harrow Peaks, Victoria Land, Antarctica

Gentili S.*¹, Bonadiman C.², Biagioni C.³, Comodi P.¹, Coltorti M.², Zucchini A.¹ & Ottolini L.⁴

1. Dipartimento di Fisica e Geologia, Università di Perugia. 2. Dipartimento di Fisica e Scienze della Terra, Università di Ferrara.
3. Dipartimento di Scienze della Terra, Università di Pisa. 4. Istituto di Geoscienze e Georisorse, CNR, Pavia.

Corresponding email: silvia.gentili@studenti.unipg.it

Keywords: Oxo-amphiboles, crystal chemistry, mantle metasomatism.

Amphibole was found as the most widespread hydrous metasomatic phase in spinel-bearing lherzolites, harzburgite and wehrlite xenoliths from Harrow Peaks (HP), Northern Victoria Land (Antarctica). It occurs both in veinlets and disseminated in the peridotite matrix. In order to better understand the mechanism of amphibole formation at upper mantle conditions and to broaden the knowledge of the actual role of water circulation during metasomatic processes in the Antarctic region, four amphibole crystals were fully characterized, by means of single-crystal X-ray diffraction, electron microprobe analysis, secondary ion mass spectrometry and micro-Mössbauer spectroscopy.

Compositionally, they present relatively low Mg# values (69.3-84.1) and high TiO₂ contents (2.74-5.30 wt.%). The FeO_{tot} contents range from 3.40 to 6.90 wt.%. The measured Fe³⁺/Fe_{tot} ratios (0.53-0.66), reveal anomalously high Fe₂O₃ contents (2.34-4.52 wt.%). The amount of O²⁻ at the O(3) site (0.984-1.187 apfu), together with the anomalously high Fe₂O₃ contents, testify for the presence of the *oxo* component in the Harrow Peaks amphiboles. The volatile content is mainly represented by H₂O (0.70-1.01 wt.%) with F and Cl, in the range of 0.04-0.24 wt.% and 0.03-0.08 wt.%, respectively. The coexistence of amphibole with the primary peridotitic phases allows to investigate the chemico-physical parameters that control the amphibole formation. The *a*H₂O values were calculated at 1.5 GPa by dehydration equilibrium equations written as H₂O-buffering equilibria among end-member components of amphibole and coexisting peridotitic phases. Three out of four HP amphibole-bearing peridotites show *a*H₂O ranging from 0.122 to 0.335; the fourth sample has *a*H₂O remarkably higher (0.782) and close to an ideal H₂O saturation. These values are not unexpected, due to the predominance of the *oxo* components in the amphiboles.

The HP *f*O₂ values were calculated using both olivine-spinel-orthopyroxene oxygeobarometer and amphibole dehydration/dissociation reaction. Amphibole-derived *f*O₂ values record extremely variable redox conditions (*f*O₂ between QFM-2.60 and QFM +6.8) remarkably different from the *f*O₂ values calculated on the peridotite assemblage (*f*O₂ between QFM -1.77 and QFM +0.01).

In sample HP124, the oxy-amphibole equilibrium is attained at high *a*H₂O and the extremely high *f*O₂ values (up to QFM +6.8) clearly displaced with respect to the redox conditions recorded by the co-existing anhydrous minerals (close to QFM buffer). A possible scenario interprets the amphibole-forming reaction as a relatively recent process, far from having reached a potential equilibrium with the peridotite matrix, and/or amphibole seems to be formed by the precipitation of migrating hydrous rich fluid/melts with a negligible contribution of the peridotite system.

Structural and photoelectric properties of chalcostibite at high pressure

Guidoni F.*¹, Comodi P.¹, Balic-Zunic T.², Nazzareni S.¹, Bini R.³, Fanetti S.³ & Brizi E.¹

1. Dipartimento di Fisica e Geologia, Università di Perugia. 2. Danish Natural History Museum, University of Copenhagen, Denmark. 3. LENS - European Laboratory for Non-Linear Spectroscopy, Università di Firenze.

Corresponding email: paola.comodi@unipg.it

Keywords: Sulfosalts, bandgap, high pressure.

The sulfosalts are a class of minerals belonging to the group of sulfides, their general formula is $A_mB_nS_p$ where A is a metal that can be commonly Ag, Cu, Fe and Pb (Me^+ , Me^{2+}); B is a semi-metal such as Bi, Sb, As and Te; and S is S and rarely Se and Te.

This class presents many examples of modular structures of variable complexity with octahedral and higher-number coordination. They are interesting low pressure analogue for high pressure silicate phases of deep mantle, for example the post-perovskite phase of $MgSiO_3$ belongs to the same homologous series as lillianite ($Pb_3Bi_2S_6$) (Olsen et al., 2008).

Sulfosalts can have interesting semiconducting and ion-conducting properties because of the nature of the metalloid-sulfur bond, a complex atom substitution and presence of the s^2 LEP (Lone Electron Pair) of metalloids and some typical accompanying cations (like Pb and Tl), which could imply potential use of sulfosalts in photovoltaic applications (thin film solar cells).

Some of them showed interesting phase transition at high pressure (e.g. Olsen et al., 2011) which could involve dramatic change in semiconducting gap.

In this paper, we study the behavior under-pressure of chalcostibite, both what concerns the structural evolution as well as the photoelectric properties. Samples have been investigated at room pressure by a multimethodic approach: SEM, SCXRD, RAMAN and UV-Vis-NIR spectroscopy. The results indicate a well ordered crystal structure (single crystal refinements give a $R_1 = 0.013$ and cell parameters very similar to those present in literature), without important chemical substitution as indicated by SEM and Raman data.

The evolution of IR absorption properties of chalcostibite with pressure has been studied employing NIR (Near InfraRed) absorption spectroscopy. A micrometric layer of powder placed on a KBr substrate has been compressed in DAC (Diamond Anvil Cell) at LENS (European Laboratory for Non-linear Spectroscopy, Florence, Italy). Ruby chips were used as pressure calibrant.

The absorbance band dependence with pressure, up to 20 GPa, was found linear with a gradient of about $-300 \text{ cm}^{-1}/\text{GPa}$ which implies a change in the band gap. The behavior was reversible on decreasing pressure. Diffractometric and spectroscopic studies at high pressure are in progress to better constrain this behavior and to relate the photoelectric properties to structural evolution.

Olsen L.A., Balic-Zunic T. & Makovicky E. 2008. High-Pressure Anisotropic Distortion of $Pb_3Bi_2S_6$: a Pressure-Induced, Reversible Phase Transition with Migration of Chemical Bonds. *Inorg. Chem.*, 47, 6756-6762.

Olsen L.A., Friese K., Makovicky E., Balic-Zunic T., Morgenroth W. & Grzechnik A. 2011. Pressure induced phase transition in $Pb_6Bi_2S_9$. *Phys Chem Minerals*, 38, 1-10.

Mantle xenoliths of Cameroon, Morocco and Libya: A structural and chemical (major oxides, trace elements, REE, OH and B) study of their mineral assemblage

Lenaz D.*¹, De Min A.¹, Hålenius U.², Kristiansson P.³, Musco M.E.¹⁻⁴, Nilsson C.³, Perugini D.⁵, Petrelli M.⁵, Princivalle F.¹, Ros L.³, Skogby H.², Caldeira R.⁶⁻⁸, Grillo B.¹, Marzoli A.⁷, Mata J.⁸, Boumehdi M.A.⁹, Idris Ali A.B.⁹ & Youbi N.⁸⁻⁹

1. Dipartimento di Matematica e Geoscienze, Università di Trieste. 2. Swedish Museum of Natural History, Stockholm, Sweden. 3. Department of Physics, University of Lund, Sweden. 4. Istituto Nazionale di Oceanografia e di Geofisica Sperimentale, Trieste. 5. Dipartimento di Fisica e Geologia, Università di Perugia. 6. Geology, Hydrogeology and Coastal Geology Unit, National Laboratory for Energy and Geology, Amadora, Portugal. 7. Dipartimento di Geoscienze, Università di Padova. 8. Instituto Dom Luiz, Faculdade de Ciências, Universidade de Lisboa, Portugal. 9. Department of Geology, Faculty of Sciences-Semlalia, Cadi Ayyad University, Morocco.

Corresponding email: lenaz@units.it

Keywords: Africa, spinels, clinopyroxenes.

The lithospheric architecture of Africa consists of several Archean cratons and smaller cratonic fragments, stitched together and flanked by younger fold belts. The three larger cratons (West Africa, Congo and Kalahari Cratons) are underlain by Sub Continental Lithospheric Mantle (SCLM) extending to ≥ 300 km depth and having a prevailing depleted composition. Three series of spinel peridotite xenoliths from Waw-En-Namus (Libya; LB hereafter), Tafraoute and Bou-Ibalrhatene (Morocco; MOR), Barombi Mbo and Lake Nyos (Cameroon; CA) have been investigated to provide a new knowledge of the mantle beneath North-Western Africa continent. In particular MOR and LB should reflect peri- and meta-cratonic conditions, respectively while CA are from the Cameroon volcanic line whose products outcrop within a polycyclic mobile belt.

According to their chemistry, the spinels from CAM and MOR xenoliths are magmatic cumulates while LB are representatives of ambient lithospheric peridotites. From a structural point of view, the CAM and MOR spinels are rather similar having comparable cell edges and oxygen positional parameters. The cation distribution allows the determination of an intracrystalline temperature in the range 560-750 °C. Spinel from LB can be divided in two groups with very different oxygen positional parameter and cell edges. The intracrystalline temperature is < 640 °C for the first group and > 680 °C for the second. There is a similarity of V_{cell} between the CAM, MOR and LBI cpx ($< 434 \text{ \AA}^3$) while those from LBII show $V_{\text{cell}} > 435 \text{ \AA}^3$. According to their REE contents, CAM cpx can be divided in 2 groups (depleted and enriched in LREE compared to CPX-DMM), in MOR there are two, both enriched, but with different behavior of the LREE suggesting evolutions starting from a DMM like composition. LB cpx show 4 groups, all of them being more or less depleted. The OH contents are lowest for the LB cpx (100-300 ppm H₂O), while the CAM samples are intermediate (200-400 ppm H₂O) and the MOR samples show the highest contents (380-610 ppm H₂O). Boron is nearly absent apart from two samples (one olivine and one cpx) from CAM.

The xenoliths sampled from a probably juvenile lithosphere at the edge of the Cameroon and Morocco lithospheric roots apparently have cumulus-like spinels probably crystallized in situ from percolating melts and thus do not represent a real spinel-peridotites facies; on the contrary peridotite mantle xenoliths from Libya exhibit spinels with features compatible with a slow ascent of a mantle plume.

The juvenile behaviors shown by CAM and MOR spinels seem also to be reflected by the cpx-HREE patterns showing typical DMM features. As opposed, for LB ones, where very depleted HREE patterns appear, recent chemical changes seem to have been superimposed to ancient (and/or deeper?) depletion.

Funding was provided by the FRA 2013 project of the Trieste University.

On the determination of the entrapment pressure for garnet inclusions in diamonds

Milani S.^{*1}, Scandolo L.², Zaffiro G.², Di Prima M.², Mazzucchelli M.L.², Alvaro M.²,
Domeneghetti M.C.² & Nestola F.¹

1. Dipartimento di Geoscienze, Università di Padova. 2. Dipartimento di Scienze della Terra e dell'Ambiente, Università di Pavia.

Corresponding email: sula.milani@studenti.unipd.it

Keywords: Diamond inclusions, 'elastic geobarometer', X-ray diffraction.

Although inclusion-bearing diamonds are so rare (about 1% of the diamond retrieved), they are geologically relevant because they are the only direct and unaltered samples that we have from the Earth's mantle. Investigation of mineral inclusions still trapped in diamond allows retrieving several pieces of information about the Earth's interior and its active geodynamics (e.g. providing the definition of the initiation of subduction processes, capturing the redox state of the mantle etc... - Shirey et al., 2013).

Therefore it is clear that the determination of the entrapment pressure (i.e. depth of formation) of these mineral inclusions is a fundamental tile for the understanding of the Earth's mantle dynamic as it allows constraining the chemico-physical environment in which diamond and their inclusions formed. The recently developed 'elastic geobarometer' method (Angel et al., 2014) allows retrieving the entrapment pressure for diamond-inclusion pairs provided the knowledge of the thermoelastic parameters for both diamonds and trapped inclusions.

Since mineral inclusions in diamonds from the subcratonic lithospheric mantle are mostly represented by garnet (38%) together with olivine (18%), clinopyroxene (16%), orthopyroxene (8%), Mg-chromite (18%) and sulphides (2%) our study has been focused on the determination of reliable elastic properties for endmember garnets (e.g. pyrope, almandine, grossular and uvarovite). Knowledge of the thermoelastic properties for endmember garnets should in principle allow calculating thermoelastic parameters for potentially any garnet composition commonly found in diamonds. In particular, here we present the investigation of endmember garnets thermal expansion by in situ single crystal X-ray diffraction at high-temperature conditions. The measurements have been performed on the same crystals used by (Milani et al., 2015) for their high-P investigation adopting the same methods for the unit-cell parameters determination (e.g. 8-position centring using SINGLE software, (e.g. King & Finger, 1979; Angel & Finger, 2011). Further details on the high temperature apparatus and measurements method here adopted are reported in Alvaro et al. (2015). The thermal expansion so calculated allowed retrieving the entrapment pressure 5.67 GPa at 1500 K for an eclogitic garnet with composition $\text{Py}_{51}\text{Al}_{22}\text{Gr}_{27}$.

Alvaro M., Angel R.J., Claudio Marciano C., Milani S., Scandolo L., Mazzucchelli M.L., Zaffiro G., Rustioni G., Briccola M., Domeneghetti C.M. & Nestola F. 2015. A new micro-furnace for "in situ" high-temperature single crystal X-ray diffraction measurements. *J. Appl. Crystallogr.*, accepted.

Angel R.J. & Finger L.W. 2011. SINGLE: a program to control single-crystal diffractometers. *J. Appl. Crystallogr.*, 44, 247-251.

Angel R.J., Mazzucchelli M.L., Alvaro M., Nimis P. & Nestola F. 2014. Geobarometry from host-inclusion systems: the role of elastic relaxation. *Am. Mineral.*, 99, 2146-2149.

King H.E. & Finger L.W. 1979. Diffracted beam crystal centering and its application to high pressure crystallography. *J. Appl. Crystallogr.*, 12, 374-378.

Milani S., Nestola F., Alvaro M., Pasqual D., Mazzucchelli M.L., Domeneghetti M.C. & Geiger C.A. 2015. Diamond-garnet geobarometry: the role of garnet compressibility and expansivity. *Lithos*, 227, 140-147.

Shirey S.B., Cartigny P., Frost D.J., Keshav S., Nestola F., Nimis P., Pearson D.G., Sobolev N.V. & Walter M.J. 2013. Diamonds and geology of mantle carbon. In: Hazen R.M., Jones A.P. & Baross J.A. Eds., *Carbon in Earth*, Rev. Mineral. Geochem, 75, 355-421.

The effect of spinel-to-garnet peridotite transition on density variations in the upper mantle

Ziberna L.*¹ & Klemme S.²

1. School of Earth Science, University of Bristol, UK. 2. Mineralogisches Institut, Westfälische-Wilhelms-Universität Münster, Germany.

Corresponding email: luca.ziberna@bristol.ac.uk

Keywords: Upper mantle, thermodynamic modelling, density.

It is well known that the mineralogical variations in the upper mantle have a critical influence on both the tectonic evolution of the lithosphere and the generation and evolution of magmas that may or may not reach the Earth's surface. Mantle xenoliths and orogenic peridotite massifs are often used to understand what is the extent of the mineralogical variations in the mantle, but to understand what controls these variations phase equilibria experiments and thermodynamic constraints are needed. Only recently thermodynamic models have been calibrated also for complex systems, which allow now the application to close-to-natural compositions. In this contribution we show how the results of phase equilibria calculations in different mantle compositions can be reconciled with the evidence from natural mantle samples.

We present data on the response of bulk rock density to pressure, temperature and compositional changes in the lithospheric mantle. To do this, we examine the mantle xenolith suite from the Quaternary alkali basalts of Pali-Aike, Patagonia, using phase equilibria calculation in four representative compositions and for two different geothermal gradients. Our results show that the density change related to the spinel-garnet transition is not sharp and strongly depends on the bulk composition. In a depleted mantle composition, the spinel to garnet transition is not reflected in the density profile, while in a fertile mantle this transition leads to a relative increase in density with respect to more depleted compositions. In mantle sections characterized by hot geothermal gradients the spinel-garnet transition may overlap with the lithosphere-asthenosphere boundary.

SESSION S13

Characterization and use of geomaterials for sustainable industry and the environment

CONVENORS

Michele Dondi (CNR-ISTEC Faenza)

Laura Gaggero (Univ. Genova)

V-doped zircon: new diffraction and optical spectroscopy data on industrial pigments

Ardit M.*, Cruciani G. & Dondi M.

Dipartimento di Fisica e Scienze della Terra, Università di Ferrara.

Corresponding email: rdmtt@unife.it

Keywords: Zircon, V⁴⁺, V accommodation.

Vanadium bestows a deep turquoise color to zircon, making it an excellent ceramic pigment. Questions about vanadium valence and location in the zircon structure gave rise to many diffraction and spectroscopy studies. From the literature, an overall convergence emerges about the occurrence of vanadium as V⁴⁺, while controversial are the results about its accommodation at the Si tetrahedral site or at the Zr cubic site. Convincing diffraction (Siggel & Jansen, 1990) and spectroscopic studies (Niesert et al., 2002) point to V⁴⁺ hosted at a peculiar four-fold coordinated interstitial site. However, current knowledge is not able to explain the variation in color shade usually observed in pigment manufacturing. In order to overcome this limit, four industrial pigments were considered (representing high V concentrations) together with zircon literature data (low to intermediate V contents) and isostructural phases (Hf and Th silicates and germanates). Industrial zircon pigments were characterized by XRF, XRPD and DRS to get chemical composition, unit-cell and structural parameters (e.g. metal-oxygen distances, polyhedral volumes, and distortion parameters), energy of the main optical bands and crystal field strength. The V⁴⁺ incorporation into the zircon structure is testified by a progressive increase of the unit-cell volume with the V concentration. XRF analysis indicates a deficiency in Si suggesting a Si–V balanced substitution. Such a substitution might occur through a Si by V⁴⁺ replacement at the tetrahedral site 4*b* (point symmetry $-4m2$) or with V⁴⁺ hosted at the interstitial site 16*g* (point symmetry $..2$) coupled to a Si vacancy. Very different from those of structures containing VO₂²⁺ vanadyl complexes, the optical spectra of V-doped zircon exhibit three main bands in the 4000–22000 cm⁻¹ range which can be attributed to electronic transitions of V⁴⁺ at tetrahedral coordination. Although challenging to calculate because of three-fold splitting of the ²T₂ band, the crystal field strength values obtained from samples containing different amounts of V and isostructural phases give rise to a linear relationship with the mean V–O distances at the interstitial tetrahedron from diffraction data (on average 1.894 Å). Such findings support the occupancy of an interstitial site by tetravalent vanadium when incorporated into the zircon crystal structure. The changes in turquoise color appear to depend in complex way on the amount of vanadium actually incorporated, the local environment at the interstitial site, the Zr/Si ratio in zircon, and particle size distribution.

Niesert A., Hanrath M., Siggel A., Jansen M. & Langer K. 2002. Theoretical study of the polarized electronic absorption spectra of vanadium-doped zircon. *J. Solid State Chem.*, 169, 6-12.

Siggel A. & Jansen M. 1990. Röntgenographische Untersuchungen zur Bestimmung der Einbauposition von Seltenen Erden (Pr, Tb) und Vanadium in Zirkonpigmenten. *Z. Anorg. Allg. Chem.*, 683, 67-77.

Geotechnical and environmental aspects of the use of Mt. Etna volcanic tephra in embankment structures

Barone G.¹, Mazzoleni P.*¹, Di Benedetto F.², Giuffrida A.¹, Capilleri P.³, Massimino M.R.³, Motta E.³,
Genovese C.⁴ & Raccuia S.A.⁴

1. Dipartimento di Scienze Biologiche, Geologiche e Ambientali, Università di Catania.

2. Dipartimento di Scienze della Terra, Università di Firenze.

3. Dipartimento di Ingegneria Civile ed Architettura, Università di Catania.

4 Istituto per i Sistemi Agricoli e Forestali del Mediterraneo, CNR, Catania.

Corresponding email: pmazzol@unict.it

Keywords: Mt. Etna tephra, mineralogy and geochemistry, Geotechnical engineering.

Mt. Etna is one of the most active volcanoes in the world and in recent times it has been characterized by eruptions consisting of recurrent lava fountains. Although these paroxysmal events have shown different characteristics in terms of magnitude, intensity, duration and eruptive styles as a common feature, they all produced an eruption plume associated with a tephra fallout which was recorded at different distances from the feeding center. As evidenced by literature, ash deposits can have a number of adverse economical drawbacks negatively affecting local infrastructures and agricultural production. Furthermore, tephra fallout can affect human health. The strong impacts of volcanic ashes on human lives and livelihoods request after every eruption the collection of enormous quantity of deposited tephra. Until now, this waste materials are mainly accumulated on landfill. In this scenario, the correct use of tephra may be contribute to resolve the disposal problem and represent an economical resource. However, recent medical studies on the health effects of pristine tephra suggest us to avoid their reuse with a direct contact with air. Thus, reuse in embankments, earth retaining walls or other geotechnical structures are particularly indicated. Furthermore, release of water soluble chemical compounds has to be carefully taken into account (Barone et al., 2014) and consequently appropriate engineering remedial for protection of aquifers has to be designed. Finally, most studies have focused on old volcanic deposits (Pallares et al., 2015); while the geotechnical properties of fresh volcanic products, such as Mt. Etna ash, have not been rarely investigated (Orense et al., 2006). In this communication, we present preliminary geotechnical results on fresh fallout pyroclastites of Mt. Etna, regarding its grain size, deformation and strength behavior, with the aim to evaluate the possibility to use these materials for embankments or earth retaining walls. The possible effects on the groundwater are estimated by the dosage of anions and cations released in water during leaching experiments. Finally, bioremediation techniques to prevent environmental damages are considered.

Barone G., Ciliberto E., Costagliola P. & Mazzoleni P. 2014. X-ray photoelectron spectroscopy of Mt. Etna volcanic ashes. *Surf. Interface Anal.*, 10-11, 847-850, doi:10.1002/sia.5395.

Orense R.P., Zapanta A., Hata A. & Towhata I. 2006. Geotechnical characteristics of volcanic soils taken from recent eruptions. *Geotech. Geol. Engin.*, 24, 129-161, doi:10.1007/s10706-004-2499-y.

Pallares C., Fabre D., Thouret J.C., Bacconnet C., Charca-Chura J.A., Martelli K., Talon A. & Yanqui-Murillo C. 2015. Geological and geotechnical characteristics of recent lahar deposits from El Misti volcano in the city area of Arequipa, South Peru. *Geotech. Geol. Engin.*, 33, 641-660, doi:10.1007/s10706-015-9848-x.

Comparison between ultrasonic treatment and hydrothermal method for waste material transformation into useful secondary products

Belviso C.*, Cavalcante F. & Lettino A.

Istituto di Metodologie per l'Analisi Ambientale, CNR, Tito Scalo (PZ)

Corresponding email: claudia.belviso@imaa.cnr.it

Keywords: Fly ash, red mud, zeolite.

Fly ash is the most abundant coal combustion by-product. Although it is partly used in concrete and cement manufacturing, over a half of the production is disposed of in landfills. In the last few years, much research has been focused on the use of fly ash for zeolite formation mainly by hydrothermal process (e.g. Belviso et al., 2012). However, the effects of ultrasounds for the synthesis of zeolites have also been investigated (e.g., Wang et al., 2008). Recent literature data indicate that hydrothermal process preceded by sonication determines the crystallization of zeolite at a lower incubation temperature (Belviso et al., 2013).

Red mud is a waste material formed during the production of alumina when the bauxite ores are subject to caustic leaching. The risk associated with red mud wastes is primarily due to the cumulative contamination of land and the surrounding dwellings. The use of this waste material for zeolite synthesis through hydrothermal method has been reported in previous study (Belviso et al., 2015). In our knowledge, the application of ultrasounds for the crystallization of newly-formed minerals has yet to be reported.

In this study, ultrasonic radiation method is used for synthesising zeolites from both fly ash and red mud. The process was compared with hydrothermal synthesis. Both irradiation and hydrothermal incubation time were set in the 2-4hour range. The results indicate that treatments in water bath with or without the action of ultrasounds determine the synthesis of newly-formed minerals already starting from 2 h. Moreover, the amount of zeolite formed from red mud by sonication is higher when compared to the hydrothermal process. Fly ash, instead, displays higher metastable behaviour vs time by using hydrothermal incubation.

Belviso C., Cavalcante F., Huertas F.J., Lettino A., Ragone P. & Fiore S. 2012. The crystallisation of zeolite (X and A-type) from fly ash at 25 °C in artificial sea water. *Micropor. Mesopor. Mat.*, 162, 115-121.

Belviso C., Cavalcante F. & Fiore S. 2013. Ultrasonic waves induce rapid zeolite synthesis in a seawater solution. *Ultrason. Sonochem.*, 20, 32-36.

Belviso C., Agostinelli E., Belviso S., Cavalcante F., Pascucci S., Peddis D., Varvaro G. & Fiore S. 2015. Synthesis of magnetic zeolite at low temperature using a waste material mixture: fly ash and red mud. *Micropor. Mesopor. Mat.*, 202, 208-216.

Wang B., Wu J., Yuan Z.-Y., Li N. & Xiang S. 2008. Synthesis of MCM-22 zeolite by an ultrasonic-assisted aging procedure. *Ultrason. Sonochem.*, 15, 334-338.

Microstructural features of geopolymer-based mortars: insights from high resolution SEM

Clausi M.¹, Tarantino S.C.¹, Tedeschi C.², Riccardi M.P.¹, Zema M.¹

1. Dipartimento di Scienze della Terra e dell'Ambiente, Università di Pavia.
2. Dipartimento di Ingegneria Civile e Ambientale, Politecnico di Milano.

Corresponding email: marina.clausi01@universitadipavia.it

Keywords: Geopolymer mortars, sewage sludge, microstructure.

The search for alternative construction materials to traditional cements has allowed the development of a new class of materials, called geopolymers, obtained by alkali-activated aluminosilicates. Nature of raw materials, mix design as well as processing conditions play an important role in binder development and properties of the final product (see Provis et al., 2014 and references therein), including the potential CO₂ footprint.

In view of a possible use as building materials, a processing route at room temperature and a geopolymer formulation characterized by high water content is proposed to improve workability. Geopolymers have been synthesized from metakaolin and sodium silicate solution, by varying the water/solid ratio between 0.33 and 0.66 and maintaining SiO₂/Al₂O₃ and Al₂O₃/Na₂O molar ratios constant at 1.85 and 1.04 respectively. Specimens have been cured at 20 °C and 65% relative humidity for 28 days.

Sewage sludge from ornamental stones have been added to the most fluid geopolymer formulation in order to reduce metakaolin content and evaluate the differences in microstructural features and mechanical properties when recycled aluminosilicate waste is used.

Geopolymers have been characterized by XPRD, FT-IR, SEM, mercury porosimetry and mechanical strength test according to UNI EN 196-1. The differences in mechanical properties have been correlated to microstructural features. SEM investigations have clarified how binder texture becomes less homogeneous, less tied and more porous with increasing water content. High mechanical properties have been displayed by all specimens, with compressive and flexural strength of binders reaching values as high as 72 MPa and 6 MPa, respectively and decreasing with increasing water/solid ratio.

Finally, geopolymer-based mortar with binder/sand ratio of 1:2 has been produced by adding standard sand to the geopolymer slurry, in order to evaluate the binding efficiency of a fluid geopolymer mixture. The mechanical behavior and microstructure of mortar has been evaluated to understand the relationships between aggregates and geopolymer binder and identify the differences due to the content of water.

Provis J.L. & Bernal S.A. 2014. Geopolymers and Related Alkali-Activated Materials. *Ann. Revi. Mater. Res.*, 44, 299-327.

Assessment for the use of waste of trachyte in the brick production

Coletti C.*¹⁻², Maritan L.¹, Mazzoli C.¹ & Cultrone G.²

1. Dipartimento di Geoscienze, Università di Padova. 2. Department of Mineralogy and Petrology, University of Granada, España.

Corresponding email: chiara.coletti@studenti.unipd.it

Keywords: Fired clay bricks, recycling wastes, sustainable construction materials.

Recently many studies have been focusing on the production of bricks from waste recycling.

It has already been demonstrated that the use of waste can be a competitive and an alternative way to meet the ahead challenges for a sustainable market uptake, with an important benefit for the environment, without compromising the requisite aesthetic and technological qualities of traditional bricks.

The present study describes how the use of trachyte, waste cutting from Euganean Hills quarries (north-eastern of Italy), influence the quality of the brick production.

Nine types of bricks were created using three different mixtures obtained adding 5%, 10% and 15% of sand-size trachyte to a clay materials normally used in the brick production and firing them in a electric oven at the temperatures of 900, 1000 and 1100 °C, according to the standard consolidated industrial procedure.

The behaviour of adding trachyte in the mixes was evaluated through a combined approach focused on several aspects at different scales of investigation. Mineralogy and texture sintering degree were observed by microscopic methods and X-ray powder diffraction. Porosity, physical-mechanical properties and durability were checked using the traditional methods (uniaxial compressive test, MIP, ...) and standard tests (hydric test, salt crystallization test, freeze-thaw test, ...).

The good response to the stress conditions and the lack of a strong difference among the samples prove that the use of trachyte allows to obtain a brick with proper qualities already at a firing temperature of 900 °C, lower respect to the temperatures adopted for the brick production just using the clay. This is due to the high content of feldspars in the trachyte that play an important role as fluxing agents in the ceramic body improving the melting and the formation of bridges of connexion between the grains and the matrix. Moreover, the addition of trachyte seems to reduce the thermal conductivity, producing refractory bricks suitable in case of presence of the thermal shocks or high temperatures.

These preliminary results confirm that the use of waste of trachyte could be a way to improve the brick production, avoiding the recovery of raw materials, improving the final products and optimizing the firing temperatures, with a overall saving in terms of exploitation of resources, energy and costs.

The influence of quartz and waste glass particle size distribution on the evolution of sanitary-ware vitreous body

Diella V.*¹, Marinoni N.², Pavese A.² & Francescon F.³

1. Istituto per la Dinamica dei Processi Ambientali, C.N.R. Milano. 2. Dipartimento di Scienze della Terra "A. Desio", Università di Milano. 3. Ideal Standard International, C.O.E., Ceramic Process Technology.

Corresponding email: valeria.diella@cnr.it

Keywords: Waste glass, sanitary-ware body, particle size distribution.

Experimental Procedure

The system kaolinite, quartz, Na-feldspar and waste glass (50, 28, 15-22, 0-7 wt.%, respectively), the latter in partial substitution of flux, was explored using three different particle size distribution for waste glass (≤ 100 , ≤ 75 and ≤ 45 μm) and two for quartz (≤ 160 and ≤ 20 μm). Samples have been fired at 1140 and 1170 °C for 20, 40, 60, 80 and 240 minutes and then characterized in terms of phase composition (X-ray diffraction using Rietvel Method), micro-structure occurrence (Scanning Electron Microscopy), water absorption, linear shrinkage and modulus of rupture.

Results

Differences in phase composition are present: in particular, glass substituting Na-feldspar accelerates the mullite growth (Marinoni et al., 2001; 2013) and the same effect is achieved by decreasing the quartz grain size, which leads to a higher reactivity of the starting slip and to a lesser vitrification grade. Cristobalite occurs only in the samples containing waste glass and more complex effects due to the waste glass particle size are observed. The slopes of the mullite phase at given temperature increase in function of time exhibit behaviors in keeping with earlier findings (Bernasconi et al., 2011). Furthermore, secondary mullite seems more abundant and better shaped in samples with small-size quartz. The particle size distribution of the silica-components, soaking time and heating temperature influence the thermal-mechanical properties, as shown by tests on macroscopic ceramic bodies. The presence of smaller quartz together with larger waste glass preserves acceptable technological properties.

- Bernasconi A., Diella V., Pagani A., Pavese A., Francescon F., Young K., Stuart J. & Tunnicliffe L. 2011. The role of firing temperature, firing time and quartz grain size on phase-formation, thermal dilatation and water absorption in sanitary-ware vitreous bodies. *J. Eur. Ceram. Soc.*, 31, 1353-1360.
- Marinoni N., Pagani A., Adamo I., Diella V., Pavese A. & Francescon F. 2011. Kinetic study of mullite growth in sanitary-ware production by in situ HT-XRPD. The influence of the filler/flux ratio. *J. Eur. Ceram. Soc.*, 31, 273-280.
- Marinoni N., D'Alessio D., Diella V., Pavese A. & Francescon F. 2013. Effects of soda-lime-silica waste glass on mullite formation kinetics and micro-structures development in vitreous ceramics. *Journal of Environmental Management* 124, 100-107.

The Cs-cycle in nuclear processes: From Cs-nanosponges to ceramic Cs-bearing materials

Gatta G.D.*¹, Brundu A.², Cappelletti P.³, Cerri G.², de Gennaro B.⁴, Farina M.²,
Fumagalli P.¹, Guaschino L.¹ & Mercurio M.⁵

1. Dipartimento di Scienze della Terra, Università di Milano. 2. Dipartimento di Scienze della Natura e del Territorio, Università di Sassari. 3. Dipartimento di Scienze della Terra, dell'Ambiente e delle Risorse, Università di Napoli "Federico II". 4. Dipartimento di Ingegneria chimica, dei Materiali e della Produzione Industriale, Università di Napoli "Federico II". 5. Dipartimento di Scienze e Tecnologie, Università del Sannio.

Corresponding email: diego.gatta@unimi.it

Keywords: Zeolites, CsAlSi₅O₁₂, nuclear wastes.

Caesium is one of the most common fission product. Clinoptilolite is a zeolite employed for caesium decontamination, acting as "subnano-sponge". Thermal treatments are generally used to prevent Cs⁺ release from spent clinoptilolite. Temperatures up to 1300-1500 K are required to attain an almost complete Cs immobilization in a glassy matrix (Cappelletti et al., 2011). We have recently developed a protocol to obtain crystalline CsAlSi₅O₁₂ (CAS) by thermal treatment of Cs-clinoptilolite, as potential host for radioactive caesium (Brundu & Cerri, 2015), and its thermal and chemical stability is under investigation. In this study, a Sardinian zeolite was used to prepare a clinoptilolite-rich powder by authogenous comminution, dry sieving and wet separations. The material (clinoptilolite ≈ 90 wt.%) was initially Na-, then Cs-exchanged, reaching a caesium content of 22.5 wt.%. Cs-aluminosilicate glass and a crystalline material made by CsAlSi₅O₁₂ (and minor pollucite-like phase CsAlSi₂O₆) were prepared by heating the Cs-clinoptilolite for 2 h at 1323 K and 1473 K, respectively.

Cs-aluminosilicate glass and CsAlSi₅O₁₂ were subjected to release control tests (reverse exchange), in order to evaluate the effective immobilization of Cs. Reverse exchange tests showed that amorphous Cs-aluminosilicate released 1.10 mg/g of Cs, while CsAlSi₅O₁₂ does not release any Cs (below L.O.Q). For a structural characterization of CsAlSi₅O₁₂, synchrotron powder diffraction data were collected and the Rietveld refinement was performed, proving that the material has the CAS-type structure reported by Gatta et al. (2008). *In-situ* high-temperature X-ray powder diffraction data were collected up to 1700 K. The diffraction patterns showed that the crystallinity of this compound decreases at $T > 1400$ K and an irreversible amorphization occurs between 1600 and 1650 K. The role of pressure and temperature on the stability of CsAlSi₅O₁₂ is under investigation with a piston cylinder apparatus.

One of the most important findings of this preliminary characterization is represented by the minor amount of Cs released by the crystalline material if compared to its amorphous counterpart.

GDG acknowledge the Italian Ministry of Education, MIUR-Project: "Futuro in Ricerca 2012 - ImPACTRBFR12CLQD".

Brundu A. & Cerri G. 2015. Thermal transformation of Cs-clinoptilolite to CsAlSi₅O₁₂. *Micropor. Mesopor. Mater.*, 208, 44-49.

Cappelletti P., Rapisardo G., de Gennaro B., Colella A., Langella A., Graziano S.F., Bish D.L. & de Gennaro M. 2011. Immobilization of Cs and Sr in aluminosilicate matrices derived from natural zeolites. *J. Nucl. Mater.*, 414, 451-457.

Gatta G.D., Rotiroti N., Fisch M., Kadiyski M. & Armbruster T. 2008. Stability at high-pressure, elastic behaviour and pressure-induced structural evolution of CsAlSi₅O₁₂, a potential nuclear waste disposal phase. *Phys. Chem. Minerals*, 35, 521-533.

Fly-ash as a filler in environmentally-friendly hot mix asphalt

Ghizzardi V.*¹, Mantovani L.², Romeo E.¹, Tribaudino M.² & Montepara A.¹

1. Dipartimento di Ingegneria Civile, dell'Ambiente, del Territorio e Architettura, Università di Parma. 2. Dipartimento di Fisica e Scienze della Terra "M. Melloni", Università di Parma.

Corresponding email: valeria.ghizzardi@studenti.unipr.it

Keywords: Fly ashes, X-ray diffraction, waste recycling.

In Municipal Solid Waste Incinerators (MSWI), waste products are mainly bottom ash, that is approximately 20 to 30% by weight of the solid waste input. The European Directives encourage the reuse and the recycling of waste by promoting their use as secondary raw material with the aim of reducing waste land-filling. However, fly ash residues are classified as hazardous waste, because of the significant presence of heavy metals, like Zn and Pb. Therefore the reuse of MSWI fly ash as a second-hand raw material is forbidden in many countries and research on new inertization processes is a key environmental issue (Bontempi et al. 2010a, b).

In this study the behavior of the fly ash as a filler in the hot mix asphalt production is investigated. Three different fillers, two types of fly ash (washed WW and unwashed NWW) and a commonly used filler (CaCO₃), were associated to asphalt binders (one unmodified and two polymer modified) to obtain nine hot asphalt mixtures. All the mixtures were produced mixing filler and asphalt binder with the same aggregate type and same gradation in order to compare the filler influence on HMA final performances and the rheological properties of the mastics (filler + asphalt binder).

Preliminary XRD mineralogical investigation showed that fly ash were mainly formed by calcium carbonate, quartz, and calcium sulfide and phosphate. The mineralogical composition was unchanged after the addition of the asphalt binder, showing that no interaction was present between asphalt and the filler. The cracking behavior of the asphalt mixtures was investigated using the standardized Superpave IDT procedure (at 10 °C) using an MTS (Material Test System) closed-loop servo-Hydraulic loading system; the rheological behavior was analyzed using a Bending Beam Rheometer. From a mechanical point of view, the performance of the asphalt mixture containing fly ashes is comparable to that with conventional fillers (mostly based on carbonates) for most conditions; lower performance, but still within the range of acceptable usage for temperate climate, was found in cracking at lower temperature and permanent deformation at the highest temperatures. As a result fly ash can be a good alternative to the traditional mineral filler in the hot mix asphalt production.

Bontempi E., Zacco A., Borgese L., Gianoncelli A., Ardesi R. & Depero L.E. 2010a. A new method for municipal solid waste incinerator (MSWI) fly ash inertization based on colloidal silica. *J Environ. Monit.*, 12, 2093-2099.

Bontempi E., Zacco A., Borgese L., Gianoncelli A., Ardesi R. & Depero L.E. 2010b. A new powder filler, obtained by applying a new technology for fly ash inertization procedure. *Adv. Sci. Technol.*, 62, 27-33.

Synthesis and color performance of $\text{CaCo}_x\text{Mg}_{1-x}\text{Si}_2\text{O}_6$ pyroxenes as ceramic pigments

Gori C.¹, Tribaudino M.*¹, Mantovani L.¹, Skogby H.², Hålenius U.², Delmonte D.¹⁻³,
Mezzadri F.³⁻⁴, Gilioli E.³ & Calestani G.³⁻⁴

1. Dipartimento di Fisica e Scienze della Terra "Macedonio Melloni", Università di Parma. 2. Department of Mineralogy, Swedish Museum of Natural History, Stockholm, Sweden. 3. Istituto dei Materiali per l'Elettronica ed il Magnetismo, CNR, Parma.
4. Dipartimento di Chimica, Università di Parma.

Corresponding email: claudia.gori@studenti.unipr.it

Keywords: Pyroxene, synthesis, pigment.

A new ceramic pink pigment, based on the Co-pyroxene ($\text{CaCoSi}_2\text{O}_6$) structure, has been recently synthesized (Mantovani et al., 2015). Co-pyroxene performs as a dye in most ceramic treatments, where the color turns into blue. Here we present our further investigation on Co-pyroxene with varying substitutions of Mg for Co ($\text{CaCo}_x\text{Mg}_{1-x}\text{Si}_2\text{O}_6$). The aim is to verify whether the same coloring performance can be obtained with lower Co content, and to provide a synthesis route for a material with higher melting point than pure $\text{CaCoSi}_2\text{O}_6$ pyroxene; it is hoped that the Mg-doped CaCo-pyroxene will be more stable in the aggressive environment typical of the ceramic industry. Last, substitution of the less expensive Mg for Co will have a strong output for the economic point of view, and reduce environmental concerns for Co toxicity.

The $\text{CaCo}_x\text{Mg}_{1-x}\text{Si}_2\text{O}_6$ series was synthesized following three different routes and then analysed by XRPD:

1) samples with $x = 0.2, 0.4, 0.5, 0.6$ and 0.8 were synthesized by solid state heating of oxide mixtures. The ground mixtures were calcined at $T = 1500^\circ\text{C}$ for 2 hours in an electric furnace and quickly quenched to room temperature to get glasses which were annealed at 1000°C for 24h to obtain polycrystals. The single crystals were grown by sintering these polycrystalline powders at 1100°C for 250h. The resulting samples show a single phase with pyroxene stoichiometry, single crystals sized up to $100\ \mu\text{m}$ and different shades of pink color;

2) above mentioned compositions were heated in an electric furnace at room pressure and 1500°C for 2h to obtain glasses. Afterwards, the glasses were annealed at $T = 1250^\circ\text{C}$ (at $T = 1100^\circ\text{C}$ for the sample with $x = 0.8$) and then quenched. Here the major phase obtained is pyroxene, with single crystals sized up to $500\ \mu\text{m}$. All the runs produced a pink pigment, with the same intensity independently from the Co content. The pink color, also in the Mg-richer samples, is tentatively described by the larger size of the crystals;

3) samples with $x = 0.25, 0.50$ and 0.75 were synthesized by flux growth method using $\text{Na}_2\text{B}_4\text{O}_7$ as a flux compound. Starting mixtures were prepared by grinding oxide mixtures with some excess silica and the flux. The mixtures were annealed at 1100°C for 24h in a furnace, cooled down to 700°C at the rate of $2-4^\circ\text{C}/\text{h}$, and finally quenched. Powder diffraction showed that the only phase is pyroxene but the color here is pink-brownish probably due to a small amount of Co^{3+} in the structure.

Single crystals obtained from the second route were investigated also by single crystal X-ray diffraction, obtaining an agreement factor between 2.0 and 2.7%; Co is almost completely confined in the M1 site with a little amount (2-3%) in the M2 site. Colorimetric and UV-Vis-NIR/IR analysis were also done, and the results will be discussed.

Mantovani L., Tribaudino M., Dondi M. & Zanelli C. 2015. Synthesis and color performance of $\text{CaCoSi}_2\text{O}_6$ pyroxene, a new ceramic colorant. *Dyes Pigments* (in press).

Manufacturing of high efficiency concretes: potential production of lightweight aggregates (LWA) from glass recycling

Graziano S.F.¹, D'Amore M.¹, Correggia C.¹, Dondi M.², Zanelli C.², Cappelletti P.*¹, Langella A.³ & de Gennaro R.¹

1. Dipartimento di Scienze della Terra, dell'Ambiente e delle Risorse, Università di Napoli "Federico II".

2. Istituto di Scienza e Tecnologia dei Materiali Ceramici, C.N.R. Faenza.

3. Dipartimento di Studi Geologici ed Ambientali, Università del Sannio.

Corresponding email: piergiuilio.cappelletti@unina.it

Keywords: Glass, recycling, concrete.

New interest in Lightweight Aggregates' (LWA) sector is evident from increasing number of academic articles on LWA from waste of different sources. According to Uni EN 13055-1, LWA must possess: i) a particles' mass/volume ratio not higher than 2000 kg/m³; ii) a bulk unit weight not higher than 1200 kg/m³. The market demand for new kind of lightweight concretes and mortars enhanced the production of LWA obtained by expansion of natural materials such as clays, vermiculite and perlite. Recent studies demonstrate that it is possible to produce LWA by using further natural materials such as volcanic tuffs, ignimbrites and zeolitized epiclastites as well as industrial wastes and recycled materials (Kazantseva et al., 1997; de Gennaro et al., 2004; 2008; 2009; Mueller et al., 2008). Good results were obtained with porcelain stoneware and ornamental stone polishing muds which contain small amounts of abrasive (max 3 wt.% SiC), that is the expanding agent necessary for bloating. In many cases the LWA obtained show similar or even better features than those currently marketed and provide a good prospect for the production of lightweight structural concretes. The experimental case, here reported, demonstrates that glass can be used with profit for the production of expanded aggregates with good technical properties in the cement industry (Ducman, 2002; Lebullenger, 2010). Two different kinds of glass were used: 1 – Bottle glass (Na-Ca recycled glass); 2 – PC and TV screen glass, rich in Ba-Sr (Dondi et al., 2009). As regards the second ones, the presence of Ba and Sr may represent a problem for recycling since this kind of glass should be only landfill disposed. By mixing screen glass powders with porcelain stoneware polishing mud heated at high temperatures it was possible to exploit the expanding action of SiC, the abrasive agent occurring in mud to obtain LWA with controlled physical properties to be used in the concretes industry. A laboratory pilot production of LWA was performed in order to manufacture two different kinds of concrete: 1 - A structural lightweight concrete (SLC); 2 - A cellular lightweight concrete (CLC). Test results evidenced that glass-bearing LWA can be used in structural lightweight concretes manufacturing obtaining concrete's density between 1400 and 2000 kg/m³ and compressive strength higher than 20 MPa. The use of the same type of LWA for the realization of CLC, moreover, definitely improve thermal features of these concretes, making the product even more competitive whenever compared to traditional materials used for thermal insulation.

- de Gennaro R., Cappelletti P., Cerri G., de Gennaro M., Dondi M. & Langella A. 2004. Zeolitic tuffs as raw materials for lightweight aggregates. *Appl. Clay Sci.*, 25, 71-81.
- de Gennaro R., Langella A., D'Amore M., Dondi M., Colella A., Cappelletti P. & de Gennaro M. 2008. Use of zeolite-rich rocks and waste materials for the production of structural lightweight concretes. *Appl. Clay Sci.*, 41, 61-72.
- de Gennaro, R., Graziano S., Cappelletti P., Colella A., de Gennaro M., Langella A. & Dondi M. 2009. Structural Concretes with Waste-Based Lightweight Aggregates: From Landfill to Engineered Materials. *Env. Sci. Technol.*, 43, 7123-7129.
- Dondi M., Guarini G., Raimondo M. & Zanelli C. 2009. Recycling PC and TV waste glass in clay bricks and roof tiles. *Waste Manag.*, 29, 1945-1951.
- Ducman V., Mladenovic A. & Suput J.S. 2002. Lightweight aggregate based on waste glass and its alkali-silica reactivity. *Cem. Concr. Res.*, 32, 223-226.
- Kazantseva L.K., Belitsky I.A. & Fursenko B.A. 1997. Zeolite-containing rocks as raw material for Siberfoam production. *Natural Zeolites, Sofia '95*. Pensoft Publications, 33-42.
- Lebullenger R., Chenu S., Rocherullé J., Merdrignac-Conanec O., Cheviré F., Tessier F., Bouzaza A. & Brosillon S. 2010. Glass foams for environmental applications. *J. Non-Cryst. Solids*, 356, 2562-2568.
- Mueller A., Vereshchagin V.I. & Sokolova S.N. 2008. Characteristics of lightweight aggregates from primary and recycled raw materials. *Constr. Build. Mater.*, 22, 703-712.

Secondary raw materials for the production of lightweight aggregates: some case studies

Graziano S.F.¹, D'Amore M.¹, Dondi M.², Zanelli C.², Cappelletti P.*¹, Langella A.³, Mercurio M.³ & de Gennaro R.¹

1. Dipartimento di Scienze della Terra, dell'Ambiente e delle Risorse, Università di Napoli "Federico II". 2. Istituto di Scienza e Tecnologia dei Materiali Ceramici, C.N.R. Faenza. 3. Dipartimento di Studi Geologici ed Ambientali, Università del Sannio.

Corresponding email: piergiulio.cappelletti@unina.it

Keywords: Recycling, waste management, lightweight aggregates.

Some case studies in R&D of LightWeight Aggregates (LWA) are overviewed. Aggregates are natural or artificial cohesionless materials constituted by elements with different grain size. LWA must possess: i) a particles' mass/volume ratio not higher than 2000 kg/m³; ii) a bulk unit weight not higher than 1200 kg/m³ (EN 13055-1). LWA historically used in architecture are natural products such as pumice, diatomites, etc. During the fifties, the growing market demand enhanced the production of new LWA obtained by expansion through heating at high temperatures of some natural materials such as clays, vermiculite and perlite. Reference parameters that influence expansion are: SiO₂:Al₂O₃ ratio and fluxing oxides (Fe₂O₃+MgO+CaO+Na₂O+K₂O); but a key factor is the presence of gas developing substances at raw materials' softening temperature. Other natural materials have been lately used for the production of LWA such as volcanic tuffs, ignimbrites and zeolitized epiclastites (de Gennaro, 2004; 2008; 2009). They are generally mixed with muds deriving from polishing operations on porcelain stoneware and ornamental stone, which contain small amounts of SiC, representing the expanding agent necessary for the bloating. The experimental cases reported also account for environmental positive benefits as these wastes of the ceramic, stone industry (tuffs included), quarry operations or dredging operations have no current applications and need to be landfill disposed. Glass is also a recycled material useful for the production of expanded aggregates with good technical properties in the cement industry (Ducman, 2002; Lebullenger, 2010). Expanding agents are also calcium carbonate or chalk, sodium sulphate, mixture of iron oxide with carbon, silicon carbide and nitride compounds. Other industrial wastes tested in the LWA production are fly ashes and sewage sludge from wastewater treatment plant (Cheeseman & Viridi, 2005; Ramamurthy & Harikrishnan, 2006). A further application sector is the manufacturing of lightweight cement-based insulating panels, to improve the energetic efficiency of buildings.

- Cheeseman, C.R. & Viridi, G.S. 2005. Properties and microstructure of lightweight aggregate produced from sintered sewage sludge ash. *Resour. Conserv. Recycl.*, 45, 18-30.
- de Gennaro R., Cappelletti P., Cerri G., de Gennaro M., Dondi M. & Langella A. 2004. Zeolitic tuffs as raw materials for lightweight aggregates. *Appl. Clay Sci.*, 25, 71-81.
- de Gennaro R., Langella A., D'Amore M., Dondi M., Colella A., Cappelletti P. & de Gennaro M. 2008. Use of zeolite-rich rocks and waste materials for the production of structural lightweight concretes. *Appl. Clay Sci.*, 41, 61-72.
- de Gennaro, R., Graziano S., Cappelletti P., Colella A., de Gennaro M., Langella A. & Dondi M. 2009. Structural Concretes with Waste-Based Lightweight Aggregates: From Landfill to Engineered Materials. *Env. Sci. Technol.*, 43, 7123-7129.
- Ducman V., Mladenovic A. & Suput J.S. 2002. Lightweight aggregate based on waste glass and its alkali-silica reactivity. *Cem. Concr. Res.*, 32, 223-6.
- Lebullenger R., Chenu S., Rocherullé J., Merdrignac-Conanec O., Chevire F., Tessier F., Bouzaza A. & Brosillon S. 2010. Glass foams for environmental applications. *J. Non-Cryst. Solids*, 356, 2562-2568.
- Ramamurthy K. & Harikrishnan K.I. 2006. Influence of binders on properties of sintered fly ash aggregate. *Cem. Concr. Comp.*, 28, 33-38.

The use of pressure to tailor the “sponge-like” behavior of zeolites: the case of SiO₂-ferrierite

Lotti P.*¹, Gatta G.D.¹, Arletti R.², Quartieri S.³, Vezzalini G.⁴ & Merlini M.¹

1. Dipartimento di Scienze della Terra "Ardito Desio", Università di Milano. 2. Dipartimento di Scienze della Terra, Università di Torino.
3. Dipartimento di Fisica e Scienze della Terra, Università di Messina. 4. Dipartimento di Scienze Chimiche e Geologiche, Università di Modena e Reggio Emilia.

Corresponding email: paolo.lotti@unimi.it

Keywords: Zeolites, ferrierite, P-induced molecule penetration.

Zeolites represent a class of materials with open-framework microporous structures, exploited in a large number of technological applications for their selective cation and molecular exchange capacity. Overall, the diverse applications of zeolites are somehow governed by their “sponge-like” behavior. During the last 15 years, the number of studies devoted to the high-pressure (HP) behavior of zeolites significantly increased (Gatta & Lee 2014), leading to a better characterization of their bulk compressibility and structural deformation mechanisms at the atomic scale. In addition, these studies showed that pressure may also be used as a tool to enhance or modify the behavior of zeolites: e.g. forcing the penetration of ions or molecules from the *P*-transmitting fluid (PTF) into the zeolite cavities. It follows that pressure, in combination with a potential “pore-penetrating” PTF, may be exploited to tailor the physical-chemical properties of zeolites (e.g. Santoro et al., 2013). In this light, we have investigated the HP-behavior of a pure synthetic SiO₂-ferrierite (Si-FER) compressed in non-penetrating silicone oil (s.o.) and in potentially pore-penetrating methanol:ethanol:H₂O = 16:3:1 mixture (m.e.w.), ethylene glycol (e.gl.) and 2methyl-2propen-1ol (m.p.o.). The compression of Si-FER in s.o. shows the remarkable flexibility of this framework, which undergoes two displacive phase transitions with change in density and symmetry: from the *Pmmn* to the *P12₁/n1* space group, at ca. 0.7 GPa, and from *P12₁/n1* to *P2₁/n11* (through *P-1*), at ca. 1.24 GPa, respectively. The compression of Si-FER in potentially pore-penetrating PTF showed the occurrence of a lower bulk compressibility, different phase-transition paths and diverse atomic-scale deformation mechanisms with respect to the compression in s.o., suggesting the onset of significant crystal-fluid interactions, likely due to the *P*-induced penetration of PTF molecules. These preliminary results suggest that Si-FER is a suitable framework-type in order to create new tailor-made materials by forcing crystal-fluid interactions under extreme conditions, opening a new scenario for potential applications of this zeolite.

The authors acknowledge the Italian Ministry of Education, MIUR-Project: “Futuro in Ricerca 2012 – ImPACT - RBFR12CLQD”.

Gatta G.D. & Lee Y. 2014. Zeolites at high pressure: A review. *Mineral. Mag.*, 78, 267-291.

Santoro M., Gorelli F.A., Bini R., Haines J. & Van Der Lee A. 2013. High-pressure synthesis of a polyethylene/zeolite nano-composite material. *Nat. Commun.*, 4, 1557-1563.

High silica zeolites used to clean-up water polluted with sulfonamide antibiotics: from multidisciplinary model studies to real applications and regeneration techniques

Martucci A.*¹, Blasioli S.², Marchese L.³, Buscaroli E.², Mzini L.L.² & Braschi I.²

1. Dipartimento di Fisica e Scienze della Terra, Università di Ferrara. 2. Dipartimento di Scienze Agrarie, Università di Bologna.
3. Dipartimento di Scienze e Innovazione Tecnologica, Università del Piemonte Orientale "A. Avogadro".

Corresponding email: mrs@unife.it

Keywords: Sulfonamides, zeolite recyclability, water depollution.

Sulfonamide antibiotics are persistent pollutants present in surface and subsurface waters in both agricultural and urban environments. Their pH-dependent anionic nature makes them highly mobile along soil profile and is responsible for their accumulation into water bodies. Owing to their environmental diffusion and persistence, sulfonamides are responsible to induce high level of resistance in bacteria through by-pass mechanism. Sulfamethoxazole (SMX), a broad spectrum biostatic sulfonamide, has become a point of interest because of its prevalence in contaminated wastewaters at concentrations which induce bacterial resistance and genetic mutations in organisms. To limit the diffusion of resistance determinants, it is of utmost importance to identify sustainable strategies against this antibiotic class to be adopted for water clean up purpose. In this work, high silica zeolites (Y, mordenite, and ZSM-5) has been positively evaluated to clean-up water polluted with sulfonamides through an irreversible adsorption mechanisms in a wide range of pH values. SMX incorporation and localization into the pore of each zeolite was defined along with medium-weak and cooperative host-guest interactions. Rietveld structure refinement revealed that the incorporation of SMX molecules caused changes in the dimension of the zeolite channel systems, when compared to the parent zeolite, and a close vicinity of the heterocycle ring nitrogen to the framework. The coadsorption of dissolved natural organic matter, always present in real waters, and the antibiotics was evaluated on zeolite Y as well: big sized humic material does not clog the zeolite pores whereas small sized humic monomers can compete with SMX for the adsorption sites. Finally, to define possible strategies for the exhausted zeolite regeneration, the efficacy of some chemical and physical treatments on the zeolite loaded with different sulfonamides were evaluated. The evolution of photolysis, Fenton, thermal treatments, and solvent extraction, as well as the occurrence in the zeolite pores of organic residues eventually entrapped, were elucidated by a combined thermogravimetric (TGA-DTA), diffractometric (XRPD), and spectroscopic (FTIR) approach. the recyclability of regenerated zeolite was evaluated over several adsorption/regeneration cycles, due to the treatment efficacy and its stability and ability to regain the structural features of the unloaded material. Finally, among several regeneration techniques applied to exhausted zeolite samples, thermal treatment and solvent extraction showed the best performance.

Hydrothermal synthesis and characterization of kalsilite by using a kaolinitic rock (Sardinia, Italy) and its application in the production of biodiesel

Novembre D.*¹, Pace C.¹, Gimeno D.², d'Alessandro N.¹ & Tonucci L.³

1. Dipartimento di Ingegneria e Geologia, Università di Chieti. 2. Departamento de Geoquímica, Petrología i Prospecció Geològica, Universitat de Barcelona, España. 3. Dipartimento di Scienze Filosofiche, Pedagogiche ed Economico-Quantitative, Università di Chieti.

Corresponding email: dnovembre@unich.it

Keywords: Kaolin, kalsilite, biodiesel.

Kalsilite is a feldspathoid characterized by a framework structure of linked (Si, Al)O₄ tetrahedra. Kalsilite application as cement in restorative dentistry has been explored in the recent past, especially as component in porcelain-fused-to-metal systems (Liou et al., 1994; Zhang et al., 2007). Nano-sized kalsilite has been demonstrated to show an excellent and highly improved oxidation activity of carbon toward diesel soot combustion (Kimura et al., 2008). More recently, kalsilite was used as a heterogeneous catalyst for transesterification of soybean oil with methanol to biodiesel (Wen et al., 2010). A hydrothermal protocol of synthesis of kalsilite by a kaolinitic precursor is here presented. Kaolin coming from Romana (Sassary, Italy) was used as starting material. It deals of a rock originated by the alteration of oligocenic rhyolite-rhyodacites (Ligas et al., 1997). The experimental protocol requires the dissolution of kaolinite in a KOH solution at temperature of 190 °C and room pressure. Crystallization of Kalsilite is attested at 12h in association with kaliophilite H₂, as metastable phase. Chemo-physical, crystallographical, morphological characterization and infrared and nuclear magnetic resonance (²⁹Si) experiments were carried out. Estimation of the amorphous phase in the synthesis powders was performed through the quantitative phase analysis using the combined Rietveld and reference intensity ratio methods, resulting in a final product of 95.2% kalsilite. We tested kalsilite as transesterification catalyst for the production of biodiesel, starting from fried olive oil in presence of methanol at 50 °C. Nuclear magnetic resonance (¹H) experiments confirmed a single peak at 3.5 ppm due to methoxy groups of fatty acid methyl esters, supporting the formation of biodiesel. This result confirmed the interesting activity of kalsilite as transesterification catalyst even at mild temperature and using a non-edible, cheap and largely available oil as fried olive oil.

- Kimura R., Wakabayashi J., Elangovan S.P., Ogura M. & Okubo T. 2008. Nepheline from K₂CO₃ nanosized sodalite as a prospective candidate for diesel soot combustion. *J. Am. Ceram. Soc.*, 130, 12844-12849.
- Ligas P., Uras I., Dondi M. & Marsigli M. 1997. Kaolinitic Materials from Romana (North-West Sardinia, Italy) and their ceramic properties. *Appl. Clay Sci.*, 12, 145-163.
- Liu C. L., Komarneni S. & Roy R. 1994. Seeding Effect on Crystallization of KAlSi₃O₈, RbAlSi₃O₈ and CsAlSi₃O₈ Gels and Glasses. *J. Am. Ceram. Soc.*, 77, 3105-3112.
- Wen G., Yan Z., Sinth M., Zhang P. & Wen B. 2010. Kalsilite based heterogeneous catalyst for biodiesel production. *Fuel*, 89, 2163-2165.
- Zhang Y., Lv M., Chen D. & Wu J. 2007. Leucite crystallization kinetics with kalsilite as a transition phase. *Mater. Lett.*, 61, 2978-2981.

Effects of compositional and textural characteristics of clay based plasters on the control of indoor relative humidity

Randazzo L.* & Montana G.

Dipartimento di Scienze della Terra e del Mare (DiSTeM), Università di Palermo.

Corresponding email: luciana.ranadazzo@unipa.it

Keywords: Geomaterials, clay-based plasters, green building.

Air humidity in contained spaces has a significant impact on health of inhabitants. The control capability of indoor relative humidity (RH) of clay-based plasters was tested on a series of commercially available products specifically designed for wall undercoating and on a natural earth collected in the surrounding area of Palermo. The innovative practice of “green building”, since several years, led the interest of research to recyclable and reusable traditional materials that, in several cases, are a sustainable alternative to concrete and lime mortars. Earthen plasters, in general, have the ability to balance indoor humidity like no other classic building materials. The studied samples have been previously characterized in plastic behaviour, mineralogical and chemical composition, grain-size and pore-size distribution through a multi-analytical approach (Montana et al., 2014). This study was aimed to understand how compositional and textural characteristics of clay-based plasters may influence their end performances. Tests for determining Equilibrium Moisture Content (EMC) were performed in agreement with the norm UNI 11086:2003. Clay-based plasters seem to combine the advantages of internal drywall construction with the properties of the clayey binder which is a healthy and versatile material. Specific performances seem to vary mainly depending on textural characteristics (i.e. aggregate/binder ratio and grain-size distribution, total open porosity, etc.). The results could be also useful in directing the selection of local raw materials for developing regional manufacture of clay-based plasters.

Montana G., Randazzo L. & Sabbadini S. 2014. Geomaterials in green building practices: comparative characterization of commercially available clay-based plasters. *Environ. Earth Sci.*, 71(2), 931-945.

Thermal decomposition of calcite: CaO properties and growth model

Salviulo G.*¹, Strumendo M.², Zorzi F.¹ & Biasin A.²

1. Dipartimento Geoscienze, Università di Padova. 2. Dipartimento di Ingegneria Industriale, Università di Padova.

Corresponding email: gabriella.salviulo@unipd.it

Keywords: Calcination, crystallite size, X-ray diffraction.

The thermal decomposition of calcite plays an important role in several geological processes and has important technological applications (Rodriguez-Navarro et al., 2009). The thermal decomposition of calcite, commonly called calcination, follows the equation $\text{CaCO}_3(\text{s}) \ll \text{CaO}(\text{s}) + \text{CO}_2(\text{g})$. CaO obtained through calcinations of naturally occurring calcite has been identified as a promising candidate for anthropogenic CO₂ capture. The calcination reaction is reversible and hence this technology should be based on cyclic stages of carbonation and of calcinations. Despite the apparent simplicity of the chemistry involved, several aspects of the carbonation reaction and its kinetics are still not clearly understood. The calcination process determines the structural properties of fresh CaO, which is an active sorbent for CO₂ (Zhu et al., 2011). The changes in the CaO microstructure significantly influence the CO₂ sorption reactivity and durability. Several contributions have focused the attention on the impact of porosity and specific surface area, or pore distribution on the carbonation reaction and its kinetics (Valverde et al., 2015). While it is known that the specific surface area and pore volume distribution are most relevant parameters in determining the kinetics of a non catalytic gas-solid reaction such as the CaO carbonation, the impact of the CaO crystallite size (CS) on the sorbent performances are not completely clear. Since it was previously observed (Biasin et al., 2015) that the average size of CaO crystalline domains at the beginning of the carbonation reaction affects the carbonation kinetics, in the present work the effect of the calcination conditions in determining the size of CaO crystallites was analyzed. The evolution of the CaO sorbent CS during the calcination was monitored using *in-situ* X ray diffraction (XRD), at different experimental conditions. The experiments were performed monitoring the evolution of the CaO-CS as function of the calcination temperature, heating rate, gas atmosphere maintained during the thermal decomposition of CaCO₃ particles by means of *in situ* high temperature powder diffraction (HTXRPD). Results highlighted that: the residence time at a fixed temperature causes an increase in CaO-CS because, the nascent CaO crystallites begin to recrystallize; CaO-CS increasing is favoured by the presence of CO₂. The calcination conditions (atmosphere, temperature, heating rate) are crucial for both the values of CS at the beginning of the process and the crystal growth rate. A mathematical model capable to describe the observed crystal growth process was elaborated.

- Biasin A., Segre C.U., Salviulo G., Zorzi F. & Strumendo M. 2015. Investigation of CaO-CO₂ reaction kinetics by *in situ* XRD using synchrotron radiation Chem. Eng. Sci., doi:10.1016/j.ces.2014.12.058.
- Rodriguez-Navarro C., Ruiz-Agudo E., Luque A., Rodriguez-Navarro A.B. & Ortega-Huertas. 2009. Thermal decomposition of calcite: mechanisms of formation and textural evolution of CaO nanocrystals. Am. Mineral., 94, 578-593.
- Valverde J.M., Sanchez-Jimenez P.E. & Perz-Maqueda L.A. 2015 Limestone calcination nearby equilibrium: kinetics, CaO crystal structure, sintering and reactivity. J. Phys. Chem., 119, 1623-1641.
- Zhu Y., Wu S. & Wang X. 2011. Nano CaO grain characteristics and growth model under calcination. Chem. Eng. J., 175, 512-51.

Multiscale approach to rock porosity and its distribution

Scrivano S.*¹, Gaggero L.¹, Cnudde V.², De Kock T.², Derluyn H.² & Gisbert Aguilar J.³

1. Dipartimento di Scienze della Terra dell'Ambiente e della Vita, Università di Genova. 2. UGCT – PProGRess, Department of Geology & Soil Science, Ghent University, Germany. 3. Departamento de Ciencias de la Tierra, Universidad de Zaragoza, Spain.

Corresponding email: simona-scrivano@libero.it

Keywords: X-ray micro-CT, porosity, weathering.

The pore space in rocks is an important feature of interest for ornamental lithotypes and for rock-reservoirs. Different pore-sizes can lead to different modes of water absorption and in wider terms to different flow dynamics. Therefore the study of the pore-size distribution can be useful in predicting rock performances (Molina et al., 2011). Several techniques can be used to evaluate this parameter with the aim of predicting decay processes or trapping capacity. As each technique can investigate only part of the entire range of pore sizes, therefore it is useful to interpolate datasets of different origins to build the full porosimetric histogram.

One of the techniques to study pore sizes in 3D is micro-CT (Cnudde et al., 2011). This study is centred on the results obtained from the high-resolution X-ray micro-CT analysis of four ornamental rocks. The analysis were performed at the UGCT laboratory of the Ghent University, using HECTOR (Masschaele et al., 2013) in combination with Octopus Reconstruction software.

Vlassenbroeck et al. (2007) for the reconstruction of the scans. The voxel-resolution of the reconstructed datasets varies between about 5 and 7 μm , depending on the sample-size.

Both fresh and salt-weathered samples were analysed to investigate the modification triggered in the porous network by crystallization.

The samples chosen are four different sedimentary lithotypes: Arenaria Macigno, a greywacke made up of thickened clasts of quartz, plagioclase and K-feldspar cemented by micritic calcite and phyllosilicates; Breccia Aurora, a calcareous breccia where nodules of compact limestone and micritic cement joints alternate with clastic texture; Rosso Verona, a biomicrite where the compact micritic matrix with microfossils is cut by veins of clay minerals; and Vicenza Stone, an organogenic limestone rich in micro and macro foraminifera, algae, bryozoans and remains of echinoderms, with trace aluminium- and iron oxides. The technique allowed studying the range of capillary pores greater than about 15 μm up to 600 μm .

An appropriate description of the porous network variation and recognition of the origin of secondary porosity was attained. These results were linked with capillary rise analysis, and compared with other techniques for pore size measurements, such as image analysis, mercury porosimetry and hygroscopic behaviour, defining the whole pore-size distribution to model the mechanisms of water transport and decay susceptibility of these lithotypes.

Cnudde V., Boone M., Dewanckele J., Vlassenbroeck J., Van Hoorebeke L. & Jacobs P. 2011. 3D characterization of sandstone by means of X-ray computed tomography. *Geosphere*, 7, 54-6.

Masschaele B., Dierick M., Van Loo D., Boone M.N., Brabant L., Pauwels E., Cnudde V. & Hoorebeke L.V. 2013. HECTOR: A 240kV micro-CT setup optimized for research. In: Xu H, Wu Z. & Tai R. Eds., 11th International Conference on X-ray Microscopy (XRM). *Jo. Phys. Confer. Series*, 463, 1-4.

Molina E., Cultrone G., Sebastián E., Alonso F.J., Carrizo L., Gisbert J. & Buj O. 2011. The pore system of sedimentary rocks as a key factor in the durability of building stones. *Engin. Geol.*, 118, 110-121.

Vlassenbroeck J., Dierick M., Masschaele B., Cnudde V., Van Hoorebeke L. & Jacobs P. 2007. Software tools for quantification of X-ray microtomography. *Nucl. Instrum. Meth. A*, 580, 442-445.

Sulfate-bearing kaolins: an unexploited resource. Implications for their use as alkali activated materials precursors

Tarantino S.C.*, Occhipinti R., Gasparini E., Riccardi M.P. & Zema M.

Dipartimento di Scienze della Terra e dell'Ambiente, Università di Pavia.

Corresponding email: serenachiara.tarantino@unipv.it

Keywords: Alkali activated materials, kaolin, alunite.

Alunite, $\text{KAl}_3(\text{SO}_4)_2(\text{OH})_6$, is present in kaolin deposits deriving from trachyte, rhyolite, and similar potassium-rich volcanic rocks, and normally hinders the use of these clays in the ceramic industry due to the release at high temperature of SO_x , which damages furnaces refractories. The feasibility of using low-grade kaolins containing sulfates to synthesize alkali activated materials (AAMs) has been assessed. Metakaolinite obtained by annealing alunite-containing kaolins at $T = 550$ °C, i.e. below desulfation temperature, has been used for alkali activation.

First, the effects of temperature (in the range 40-90 °C) and time (in the range 1-29 h) of curing, on compressive strength and linear shrinkage of geopolymers have been studied by experimental design technique using a high-quality kaolin as starting material. Geopolymers characterized by high strength (> 60 MPa) and low shrinkage (< 1%) have been obtained when long curing times are applied at $T < 65$ °C. Then, geopolymers have been synthesized at the curing conditions suggested by the statistical model and using the alunite-bearing kaolin from Piloni di Torriella mine as starting material. The results are promising as the synthesized samples revealed to be composed mainly by an amorphous gel and characterized by high thermal stability and strength, with compressive strength higher than 80 MPa. All samples have been characterized by thermal analysis, X-ray powder diffraction and infrared spectroscopy. A petrographic approach has been used to analyze the textural features of geopolymers at different lengths of scale by using optical and scanning electron microscopies.

Finally, samples have been prepared by mixing 10 wt.% alunite to high-quality kaolinite to better identify sulfate by-products in the AAMs. More studies are needed in order to improve the sulfate retention as well as to identify all the silico-sulfate phases and understand the possible interactions between precipitated nanocrystalline sulfate phases and geopolymer binder.

Nanomaterials addition to raw mixtures for portland clinker production. A way to decrease clinkerization temperature

Zucchini A.*¹, Comodi P.¹, Di Michele A.¹, Blasi P.², Gentili S.¹, Santinelli F.³ & Neri A.³

1. Dipartimento di Fisica e Geologia, Università di Perugia. 2. Scuola di Scienze del Farmaco e dei Prodotti della Salute, Università di Camerino. 3. Colacem S.p.A., Gubbio (PG).

Corresponding email: azzurra.zucchini@unipg.it

Keywords: Portland clinker, nanomaterials, clinkerization temperature.

Decreasing the CO₂ emission from industrial processes is one of the most attractive topics of the last decades. Cement industry, in particular, produces more than 8% of the total antropogenic emitted CO₂. Such emission derives from the energy consumption of the kilns as well as from the decarbonation of carbonates, during firing. The present work is devoted to decrease the CO₂ emitted by clinker production cycle by using nano-CaO and nano-SiO₂ in the raw mixture.

Nano-CaO was prepared by sonochemical synthesis using CaCl₂ as source and NaOH as precipitator and spray dried. Nano-SiO₂ was obtained by hydrolysis of TEOS (tetraethyl orthosilicate) under high powered ultrasound. The synthesized nano-materials were characterized by means of field emission scanning electron microscopy, dynamic light scattering, X-ray powder diffraction (XRPD) and BET analysis. Results confirmed the nanometric dimension of the synthesized additives.

The raw mixtures were obtained by mixing carbonates, silicates and nano-sized additives in appropriate proportions. In particular, three raw mixtures were prepared maintaining the same chemical bulk composition: (i) the standard portland clinker raw mixture (PC); (ii) a portland clinker added with a 5 wt.% of nano-CaO (PCCA), (iii) a portland clinker added with a 2 wt.% of nano-SiO₂ (PCSI). The burning temperature (*T*) was set at 1250 °C to analyse the evolution of clinker mineral phases, in particular alite (C3S) and belite (C2S), and free lime (CaO).

Clinkers after cooling were analysed by XRPD. Collected data were treated by means of the Rietveld method as implemented in TOPAS Academic software.

Results showed that PC and PCSI clinkers have approximately the same mineral composition (C2S ~ 45 wt.% and C3S ~ 10 wt.%); whereas, PCCA have a significantly different composition being C2S ~ 30 wt.% and C3S ~ 20 wt.%. Thus, the nano-CaO addition to the raw mixture seems to promote the alite formation at the expenses of belite even at 1250 °C, remarkably lower than the commonly known *T* needed to form this mineral phase (1450 °C). On the contrary, the nano-SiO₂ effect on the mineral composition of the clinkers is negligible.

The preliminary results indicate that the nano-CaO addition to the raw mixture decreases the burning temperature for the portland clinker production and increases its cooking efficiency. As a consequence of the clinker burning *T* decrease, the CO₂ emission is expected to decrease as well as the increase of the cooking efficiency is directly related to an improvement of the plant productivity.

Further experiments to establish the PCCA optimum burning temperatures are in progress.

This study should allow to better understand the clinker production processes using nano-materials.

SESSIONE S14

**Environmental mineralogy and geochemistry: natural environment
versus human activities**

CONVENORS

Rosa Cidu (Univ. Cagliari)

Francesco Di Benedetto (Univ. Firenze)

Heavy metal analyses on core of polluted submarine sediments from Taranto: preliminary results

Agrosi G.*¹, Tempesta G.¹, Lisco S.¹, Moretti M.¹, Scardino G.¹, Cotecchia F.², Sollecito F.², Vitone C.²,
Lacalamita M.¹, Mesto E.¹, Schingaro E.¹ & Mastronuzzi G.¹

1. Dipartimento di Scienze della Terra e Geoambientali, Università di Bari. 2. Dipartimento di Ingegneria Civile, Ambientale, del Territorio, Edile e di Chimica, Politecnico di Bari.

Corresponding email: giovanna.agrosi@uniba.it

Keywords: Heavy metals, submarine sediments, geochemical and mineralogical analyses.

Taranto (southern Italy) is one of the areas recently declared as “at high risk of environmental crisis” by the national government because it represents one of the most complex industrial sites in Europe located nearby urban areas of high population density (Italian law n. 349/86). The characterisation of the contaminants occurring within the submarine sediments from this area, is currently being studied in order to address the identification of the most suitable mitigation strategies to apply to the sediments. This study reports some of the preliminary results about the heavy metal concentrations on the most polluted area of Mar Piccolo, located in the first bosom, and known as “the 170 ha area”. The research has required site investigations and laboratory testing, that has been most complex given the difficulties of off-shore sampling, the very low sediment consistency, and the nature of contaminants which affect also the laboratory tests. To the best of our knowledge, this study is the first in the Mar Piccolo that covers depths larger than 5 m below the seafloor. Specifically, the investigation has involved samples of sediments taken up to depths of about 20 m from the seafloor. The vertical sedimentary succession shows monotonous alternations of fine-grained deposits with slight differences in grain-size and with a general homogenized texture. On these sediments, even if wet, in continuous measure of magnetic susceptibility (MS) and X-Ray Fluorescence (XRF) have been performed directly onto opened cores with portable instruments. The analyses performed by means of MS showed high sensitivity to low amount of heavy metals. The Portable X-Ray Fluorescence spectrometer (PXRF) represents a highly productive geochemical tool with its technological development and its non-destructive approach. Actually, PXRF allows to detect trace element below the limit permitted by European law for environmental protection. To correct and reduce the matrix effect, the effects due to the water content and grain size variability, in XRF analyses, some samples have been prepared and analysed with laboratory high-resolution X-ray Fluorescence Spectrometer (HRXRF) for a quantitative analysis. The preliminary results show a good correlation between the peaks of magnetic susceptibility and the concentration variations of six pollutants (As, Cr, Cu, Ni, Pb and Zn), as trace elements, that have been reported at different depths. To determine the availability and distribution of these pollutants, analyses of the mineral phases by XRPD as well as, at the nanoscale, by TEM are under way. The results show that the sediments polluted by heavy metals are located not only in the upper portion of the sedimentary column and have an anomalous vertical distribution. The whole set of data shows that large portions of the original sedimentary succession have been remobilized and re-deposited inducing an anomalous and hardly-predictable vertical distribution of the pollutants.

Removal of divalent metals by inducing precipitation of Layered Double Hydroxides from mine-waste drainages (Iglesias, Italy)

Atzori R.*¹, Ardau C.¹, Podda F.¹, Agrosi G.² & Frau F.¹

1. Dipartimento di Scienze Chimiche e Geologiche, Università di Cagliari. 2. Dipartimento di Scienze della Terra e Geoambientali, Università di Bari.

Corresponding email: roberta.atzori@unica.it

Keywords: Mine drainages, metal contamination, waste-water treatment.

The removal of toxic metals from waste waters is an important issue in mining environments and several technologies to reduce the release of toxic metals to the environment have been developed. Layered double hydroxides (LDH) are a series of lamellar compounds with general formula $[M^{2+}_{1-x}M^{3+}_x(OH)_2](A^n)_{x/n} \cdot mH_2O$, widely studied for the removal of anionic pollutants from water (Ardau et al., 2012;2013). Starting point of our study was the finding of LDH spontaneously formed in mining environments and their efficacy in the attenuation of As content in drainage water (Ardau et al., 2011). Our idea was to use M^{3+} -poor drainages from the impoundment of “Red Muds” (metallurgical wastes from an electrolytic plant used in processing oxidized Zn-ores) in the Monteponi mine area (Iglesias, Sardinia) as a reagent for the precipitation of LDH and the consequent removal of metals. These drainages are characterised by neutral pH and high levels of SO_4 (~ 4000 mg/L), Mg (~ 600 mg/L), Zn (~ 200 mg/L) and other metals (Pb, Mn, Cd), but very low concentrations of trivalent metals (Fe^{3+} and Al^{3+}). The experiment was carried out by adding to water an adequate amount of a salt of Al [$Al_2(SO_4)_3 \cdot 18H_2O$] and NaOH to maintain a neutral pH, in order to induce the LDH precipitation through different batch tests. The main parameter controlling the removal of metals and the type of precipitate seemed to be the pH. As a function of pH variations during the batch experiments, XRD analysis of precipitate and chemical analysis of water (before and after the experiment) and precipitate showed either the formation of poor crystalline LDH combined with complete removal of dissolved Zn (98%), as well as removal of significant amounts of Mn, Cd, Pb and Ni, or the formation of well crystalline LDH combined with significantly lower removal of Zn (63%), Mn, Cd, Pb and Ni. In all experiments, Al added was not detected in solution, indicating a complete precipitation. The precipitates have been also characterized by HRTEM-EDS-SAED. These results encourage further investigations on the removal of divalent metals from M^{3+} -poor waste waters by inducing LDH precipitation at different pH conditions.

This study was financially supported by the Consorzio AUSI (Consorzio per la Promozione delle Attività Universitarie del Sulcis-Iglesiente).

Ardau C., Cannas C., Fantauzzi M., Rossi A. & Fanfani L. 2011. Arsenic removal from surface waters by hydrotalcite-like sulphate minerals: field evidences from an old mine in Sardinia, Italy. *Neues Jb Miner. Abh.*, 188, 49–63.

Ardau C., Frau F., Dore E. & Lattanzi P. 2012. Molybdate sorption by Zn-Al sulphate layered double hydroxides. *Appl. Clay Sci.*, 65-66, 128-133.

Ardau C., Frau F. & Lattanzi P. 2013. New data on arsenic sorption properties of Zn-Al sulphate layered double hydroxides: Influence of competition with other anions. *Appl. Clay Sci.*, 80-81, 1-9.

The End of the Anthropocene and Beyond

Bardi U.

Dipartimento di Scienze della Terra, Università di Firenze.

Corresponding email: ugo.bardi@unifi.it

Keywords: Anthropocene, Complex Systems, resource depletion.

The history of the Earth system is characterized by discontinuities in the stratigraphic record defining the geological time subdivisions. These transitions are often related to increases in the energy transduction capabilities of the system as a result of the existing energy potentials dissipated by the ecosystem, mainly solar and geothermal energy. The latest manifestation of this trend is the start of the “Anthropocene” epoch; mainly the result of the increased energy processing capability of the human industrial system. This increasing capability is mainly attributable to the combustion of fossil carbon and, in a smaller measure, to the controlled fission of the uranium 235 isotope. As a geological time subdivision, the Anthropocene is destined to be short lived since the energy potentials that created it are being rapidly dissipated with the fossil carbon accumulated over the past hundreds of millions of years being combined with atmospheric oxygen. Because of this factor, it is argued here that the Anthropocene, in its present form, cannot last for more than a few centuries, at most. The possibility of further stages of evolution of the Earth system after the Anthropocene are also discussed.

Particulate matter exposure influencing the global DNA methylation in women: a cross-sectional study in Catania, Italy

Barone G.¹, Mazzoleni P.*¹, Acquafredda P.², Costagliola P.³, Barchitta M.⁴⁻⁵, Quattrocchi A.⁴,
Maugeri A.⁴ & Agodi A.⁴⁻⁵

1. Dipartimento di Scienze Biologiche, Geologiche e Ambientali, Università di Catania. 2. Dipartimento di Scienze della Terra e Geoambientali, Università di Bari "Aldo Moro". 3. Dipartimento di Scienze della Terra, Università di Firenze. 4. Dipartimento Dipartimento di Anatomia, Patologia Diagnostica, Medicina Legale, Igiene e Sanità Pubblica "G.F. Ingrassia", Università di Catania. 5. LaPoSS, Università di Catania.

Corresponding email: pmazzol@unict.it

Keywords: Particulate matter, mineralogy, DNA methylation.

Increasing evidence shows that environmental and lifestyle factors can be potentially modified epigenetic changes, including DNA methylation. The aim of this study was to explore if the exposure to particulate matter (PM) may influence global DNA methylation level, using LINE-1 methylation in leukocytes as biomarker.

PM₁₀ and PM_{2.5} samples were monitored and collected in various areas urban centre of Catania during 2015 using a DustTrak Aerosol 8530 sampler. Additional PM₁₀ mass data were obtained by the monitoring network of the Environmental Department of the Municipality of Catania in the period 2010-2014.

The mineralogical composition of these samples was studied by X-ray diffraction, Micro Raman spectroscopy and SEM.

A cross-sectional study, including 378 healthy women living in the metropolitan area of Catania, was performed including: a) information on socio-demographic and lifestyle data, including education level, smoking habits, obstetric history and physical activity were obtained from a questionnaire; b) georeferentiation of women by Geographical Information System (GIS) methodology using their home address was performed; c) adherence to the Mediterranean dietary pattern was measured by a validated food frequency questionnaire. The DNA methylation level of these woman was measured by pyrosequencing methylation analysis that were conducted on a LINE-1 promoter.

The present study revealed a significant association between global methylation level and home address. In this scenario the mineralogical characterization of PM is essential to determine the role of environmental exposure and to assess the risk of hypomethylation in healthy women.

Enrichment of toxic elements in a Mn deposits associated with the Santa Severa (Latium, Italy) travertine quarry

Bernardini S.*¹, Armiento G.³, Bellatreccia F.¹, Cavallo A.⁴, Della Ventura G.¹, Proposito M.³ & Sodo A.²

1. Dipartimento di Scienze, Sezione di Geologia, Università di Roma Tre. 2. Dipartimento di Scienze, Sezione di Nanoscienze e Nanotecnologie, Università di Roma Tre. 3. ENEA - UTPRA, Roma. 4. Istituto Nazionale di Geofisica e Vulcanologia, Roma.

Corresponding email: SIM.BERNARDINI@stud.uniroma3.it

Keywords: Cryptomelane, hollandite, heavy metal.

This work relates on the occurrence of As, Tl, V, Be, Co, Th, U and REE in Mn-rich levels within the travertine quarry of Santa Severa (north of Rome, Latium). The deposit consists of brownish and relatively loose nodules, which, under the binocular microscope, are clearly characterized by layers, from millimetric to sub-millimetric, of Mn-oxides.

Preliminary XRD analyses confirmed that the layers are composed of cryptomelane [$K(Mn^{4+}, Mn^{3+})_{10}O_{16}$], hollandite [$Ba(Mn^{4+}, Mn^{3+})_8O_{16}$] and calcite. The structure of these Mn minerals consists of double chains of MnO_6 octahedra forming tunnel with square cross sections, measuring two octahedra on a side (Post, 1999), containing K^+ (cryptomelane), or Ba^{2+} (hollandite), in addition to other cations and water molecules. The high specific surface area, ~ 300 m^2/g (Oscarson et al., 1983) and the point of zero charge, PZC, generally < 3 (McKenzie, 1981; Oscarson et al., 1983) make them particularly reactive, and with an high adsorption capacity. For this reason, these are important minerals in controlling the distribution of heavy metals and other potentially toxic elements between solid phases and aqueous systems.

The Mn minerals have been characterized by a combination of XRPD, XRF, IR and Raman spectroscopy. XRF maps show that Ba is almost ubiquitous, with cryptomelane having higher K contents with respect to hollandite. EMP-WDS analyses show that in hollandite MnO₂ ranges from 39.33% to 67.99%, while in cryptomelane it ranges from 68.12 to 70.45%; K ranges from 0.40% to 1.51% in hollandite, and from 2.48% to 5.52% in cryptomelane. XRF maps also show significant As which is concentrated essentially within the Mn minerals, reaching levels (as As₂O₅) up to 1.39 wt.% in hollandite and 0.82 wt.% in cryptomelane, suggesting that the arsenic distribution is controlled by the crystallization of Mn-minerals. ICP-MS analyses show that the Mn-oxides contain also very high amounts of REE, particularly Ce (69.6 ppm) and Eu (6.73 ppm), Tl (55.0 ppm), Be (27.1 ppm), Co (572.0 ppm), V (823.0 ppm), Th (7.75 ppm), and low U (0.78 ppm). Considering that, due to the excavation of travertine in the quarry, the Mn deposit is exposed to the weathering and considering its high geochemical mobility, under changing redox conditions, it follows that the Mn-ores may act as a source for the diffusion of these toxic elements in the environment, with a potential risk for the human health. Further studies are in progress at present.

McKenzie R.M. 1981. The surface charge of manganese dioxides. *Aust. J. Soil Res.*, 19, 41-50.

Oscarson D.W., Huang P.M., Liaw W.K. & Hammer U.T. 1983. Kinetics of oxidation of arsenite by various manganese dioxides. *Soil Sci. Soc. Am. J.*, 47, 644-648.

Post J.E. 1999. Manganese oxide minerals: Crystal structures and economic and environmental significance. *P. Natl. Acad. Sci. USA*, 96, 3447-3454.

Lead and arsenic concentrations in groundwater from Sardinia (Italy). Natural background and influence of mining activities

Biddau R.*¹, Cidu R.¹, Lorrai M.² & Mulas G.²

1. Dipartimento di Scienze Chimiche e Geologiche, Università di Cagliari. 2. Regione Autonoma della Sardegna - Servizio tutela e gestione delle risorse idriche, vigilanza sui servizi idrici e gestione delle siccità. Direzione generale del distretto idrografico della Sardegna.

Corresponding email: r.biddau@gmail.com

Keywords: Arsenic, Lead, groundwater background.

The chemistry of groundwater varies widely as a function of complex hydrogeochemical factors which control its chemical evolution. In order to understand potential anthropogenic impacts on the aquatic systems, it is essential to know the natural background values of potential contaminants; moreover, assessing the groundwater quality is essential to achieve the purposes of the European Community Water Framework Directive (WFD), which defines background level as: “the concentration of a chemical substance present in solution corresponding to undisturbed conditions or only very minor anthropogenic alterations”.

The background concentrations of several elements in groundwater of Sardinia are currently under evaluation in a scientific collaboration between the Sardinian Regional Government and the University of Cagliari. Sardinia was one of the most important mining regions in Italy and the elements Pb and As have been selected to distinguish natural factors from mining impacts.

According to the requirements of WFD, 38 main hydrogeologic complexes were recognized in Sardinia; they are constituted of one or more hydrogeologic units with homogenous lithology and degree of permeability, and are divided in 114 groundwater bodies. Chemical data on 1789 groundwater samples from springs and wells were obtained from the Sardinian groundwater-monitoring program (2011-13 period) and several surveys carried out at the University of Cagliari (2000-13 period). The median value and 95th percentile have been taken respectively as first approximation of background value and its upper limit (Edmunds et al., 2003).

The widespread presence of mineralization in Sardinia has a strong effect on the chemical quality of groundwater. As compared to background values estimated at regional scale, higher median and upper limit concentrations of Pb and As have been found respectively in 5/114 and 13/114 groundwater bodies, with the 95th percentile exceeding the Italian standards for drinking water. Excess of Pb and As is related to natural sources, i.e., derived from water-rock interaction processes in areas of known mineral occurrences. Three water bodies are affected by anthropogenic contamination of Pb and As related to past mining.

Acknowledgements. Research funded by Regione Autonoma della Sardegna, Servizio tutela e gestione delle risorse idriche.

Edmunds W.M., Shand P., Hart P. & Ward R.S. 2003. The natural (baseline) quality of groundwater: a UK pilot study. *Sci. Total Environ.*, 310, 25-35.

Geochemical and mineralogical tracers of geothermal power plants input into the atmosphere: the case study of the Mt. Amiata geothermal field

Capecchiacci F.¹, Zoppi M.¹⁻², Cabassi J.¹, Marchionni S.¹, Tassi F.¹, Vaselli O.¹, Pratesi G.², Giannini L.¹, Venturi S.¹, Ulivi M.¹, Forni F.⁴, Scodellini R.⁴ & Tommasini S.*¹

1. Dipartimento di Scienze della Terra, Università di Firenze. 2. Museo di Storia Naturale, Università di Firenze. 3. Istituto di Geoscienze e Georisorse, C.N.R. Firenze. 4. Settore energia, tutela della qualità dell'aria e dall'inquinamento elettromagnetico e acustico, Regione Toscana.

Corresponding email: simone.tommasini@unifi.it

Keywords: Geothermal power plant, PM10, atmospheric pollutants.

Tuscany provides an outstanding example of a thermal perturbation caused by magma emplacement at shallow levels in the crust during Late Miocene-Quaternary times. This magmatism is responsible for extensive mesothermal fluid circulation and mineralisation and feeds a large-scale positive thermal anomaly that has resulted in the active geothermal areas of Larderello-Travale and Mt. Amiata. These geothermal fields are among the most important geothermal reservoirs in the world because of both their long-term industrial exploitation, dating back the first half of the 19th century, and their productivity. In Tuscany, the production of geothermal energy covers some 25-30% of the entire regional demand (ca. $20 \cdot 10^9$ kWh, yearly consumption) and certainly contributes to reduce the emission of greenhouse gases into the atmosphere owing to fossil fuel combustion.

Despite being considered a renewable source of energy, geothermal power plants do not produce completely green energy. For example, considerable amounts of H₂S, NH₃, and CO₂ are yearly delivered into the atmosphere, although modern technological advancements of geothermal power plant design (e.g. AMIS device) have greatly reduced their emissions.

PATOS (Particolato Atmosferico in TOscana) is a joint research project with the Air Quality bureau of the Tuscan Region aiming at identifying robust geochemical and mineralogical tracers to assess the contributions of geothermal power plant emissions into the atmosphere. Accordingly, we have carried out a twelve months sampling of PM10 and air in the locality of Piancastagnaio, Siena, nearby one of the geothermal power plants of the Mt. Amiata area, along with a urban background locality as a reference site. Samples have been analysed for a wide range of geochemical parameters including inorganic major and trace elements, volatile organic compounds, radiogenic (Sr, Nd, Pb) and stable (S) isotopes along with mineralogical analyses to detect the phases occurring in the PM10.

This study has revealed that the emissions into the atmosphere of the geothermal power plant of Piancastagnaio have a number of geochemical and mineralogical tracers, significantly distinct to other anthropogenic sources, that are liable to be used as specific markers, namely: Zn/Cu and the occurrence of mascagnite [(NH₄)₂SO₄] and letovicite [(NH₄)₃H(SO₄)₂] in the PM10, along with C₇H₈/C₆H₆, in air samples. The outcome of this research project, if extended to the other geothermal power plants of Tuscany, is a potential powerful tool to be used in meteorological models to assess the contributions of geothermal power plants to the total budget of anthropogenic emissions into the atmosphere, thus monitoring the fluxes of geothermal air masses in Tuscany.

Airborne inorganic fibers in Turin: identification and quantification by SEM-EDS

Capella S.^{*1-3}, Fioretti E.¹ & Belluso E.¹⁻²⁻³

1. Dipartimento di Scienze della Terra, Università di Torino. 2. Istituto di Geoscienze e Georisorse, CNR, Torino. 3. Centro Interdipartimentale per lo studio degli amianti e di altri particolati nocivi, "G. Scansetti", Università di Torino.

Corresponding email: silvana.capella@unito.it

Keywords: Asbestos, airborne fibers, SEM-EDS.

The air quality control is an important issue in the field of human health and environmental protection. The air pollution can occur owing to many substances including inorganic fibers. Therefore, the study of dimensional, morphological and chemical characteristics of airborne inorganic fibers and particles, and the assessment of their amounts, can provide an important contribution to the definition of environmental background. This knowledge is necessary to evaluate the situations of environmental pollution.

The aim of this research was to study the background of airborne inorganic fibers in general, and asbestos in particular, collected in 24 districts of Turin (Piedmont - Italy). The airborne fibers were captured on the filters, and then they were characterized and quantify by Scanning Electron Microscopy (SEM) with annexed Energy Dispersive Spectroscopy (EDS). We considered fibers classified as "breathable" by the WHO (World Health Organization) and the Italian law (D.Leg. 257/92) i.e. with a length > 5 µm, diameter 3. Different mineral species, but also synthetic inorganic compounds have been identified. Because the SEM-EDS technique does not allow a sufficient characterization to discriminate some species chemically very similar, some mineral species were grouped (e.g. tremolite/actinolite asbestos and chrysotile/antigorite). The only kind of asbestos fibers detected belongs to the group tremolite/actinolite asbestos, the presence of which is due only to natural sources, since in Italy they have not been industrially used. Their maximum concentration detected, in one of the 24 districts, is 0.17 ff/l. Crocidolite, grunerite asbestos and anthophyllite asbestos, present in many asbestos-containing materials, were not detected in any district. Chrysotile/antigorite fiber group was the most abundant and present in all districts. The group of *tremolite/horneblenda/edenit* efibers was found to be the second most abundant. The third group for abundance is that of phyllosilicates clay. The greatest amount of total fibers by district is 2.22 ff/l, while the lowest is 0.34 ff/l. In no-one district was highlighted a situation of asbestos pollution, if we consider the maximum limit of 2 ff/l established for environments reclaimed by D.M. 06/09/1994.

WHO 1986. Asbestos and other natural mineral fibres. International Programme for Chemical Safety. In: Environmental Health Criteria, Geneva, Switzerland.

D.Leg. 257/92. Norme relative alla cessazione dell'impiego dell'amianto. In: Supplemento ordinario della Gazzetta Ufficiale n. 87.

D.M. 06/09/1994 (allegato 2B). Normative e metodologie tecniche per campionamento e analisi mediante microscopia elettronica in scansione. In: Supplemento ordinario della Gazzetta Ufficiale n. 220.

Forensic mineralogy and pathology: a case-control study

Capella S.^{*1-4}, Bellis D.²⁻⁴ & Belluso E.¹⁻³⁻⁴

1. Dipartimento di Scienze della Terra, Università di Torino. 2. Dipartimento di Servizi, Anatomia Patologica, ASL TO1, Ospedale Martini, Torino.
3. Istituto di Geoscienze e Georisorse, CNR, Torino. 4. Centro Interdipartimentale per lo studio degli amianti e di altri particolati nocivi "G. Scansetti", Università di Torino.

Corresponding email: silvana.capella@unito.it

Keywords: Asbestos, mesothelioma, SEM-EDS.

Because asbestos diseases represent a complex pattern of legal, social and political issue, a multidisciplinary approach of their diagnosis helps to investigate the relationship between the occurrence of mesothelioma (or other pathologies related to respiratory apparatus) and occupational or environmental asbestos exposure at the individual level, to resolving critical medico-legal aspects.

When an asbestos disease is identified, it is important to find all information about job history (occupational exposure) and other possible asbestos exposure (para-occupational, or anthropogenic/natural environmental) of the subject. The presence of some morphological asbestos markers of exposure (i.e. mesothelioma, pleural plaques, asbestosis, and asbestos bodies) helps in the study of a causal relationship between their presence and health impairment or death. But there is nothing more persuasive than visual evidence that asbestos is in the lung tissue in elevated concentrations. So, one of the best ways to demonstrate that a subject has developed an asbestos-related disease is to highlight the presence of asbestos fibers in its lung tissue.

The aim of the present study was to correlate mineralogical data with pathological information of a subject died of mesothelioma perhaps because of occupational exposure in the petrochemical industrial area where he worked. Our purpose was to assess the possible presence of asbestos fibres or other inorganic fibrous species, identify and determine their burden by SEM-EDS investigation in the tissue of both lungs according to a published protocol (Belluso et al, 2006). Different kinds of inorganic fibres were detected, and among them some asbestos (crocidolite, tremolite asbestos and anthophyllite asbestos) with prevalence of anthophyllite asbestos. This last was the asbestos indicated in many work plans for the reclamation of asbestos containing materials of the involved petrochemical industrial area presented over the years to the Local Health Authority competent. The amount of total asbestos fibres per gram of dry tissue in the right lung was greater than the threshold indicative of significant occupational exposure to asbestos, lower in the left. Therefore we can conclude that the subject has been professionally exposed.

We confirm that the mineralogical analysis (identification and quantification of inorganic fibres in general, and asbestos in particular) of the fibres detected in the lung tissues is necessary to complete the pathological diagnosis of asbestos-related malignancies.

Belluso E., Bellis D., Fornero E., Capella S., Ferraris G. & Coverlizza S. 2006. Assessment of inorganic fibres burden in biological samples by SEM-EDS. *Microchim. Acta*, 155, 95-100.

PTE (Potential ecotoxic Element) mobility in stream and marine sediments: the case of Gromolo Torrent (eastern Liguria, Italy)

Carbone C.*¹, Consani S.¹, Dinelli E.², Cutroneo L.¹, Capello M.¹, Salviulo G.³, Zorzi F.³ & Lucchetti G.¹

1. DISTAV, Università di Genova. 2. Dipartimento di Scienze Biologiche, Geologiche e Ambientali, Università di Bologna.
3. Dipartimento di Geoscienze, Università di Padova.

Corresponding email: carbone@dipteris.unige.it

Keywords: AMD, Gromolo Torrent, PTE.

The Gromolo Torrent is a metal-polluted Apennine stream flow located near Sestri Levante (Liguria, Italy). It springs from the Monte Rocca Grande (850 m a.s.l.), and flows for 11.5 km through the Gromolo Valley before flowing into the Ligurian Sea. Inside Gromolo basin is located the abandoned Fe-Cu mine of Libiola, which was the most important sulfide deposit of the Ligurian Apennines. In this mining site, extensive Acid Mine Drainage (AMD) processes are active, both inside the mine tunnels and in the sulfide rich waste-rock dumps: the solutions generated are characterised by low pH values and high amounts ($EC > 6000 \mu S$) of dissolved SO_4^{2-} , Fe, and other PTE elements such as Cu, Zn, Pb, Al, Co, and Ni. Moreover, extensively precipitation of Fe and Cu-rich secondary minerals occur both as soft crusts inside the mine adits and as loose suspensions associated with overland flow of mine drainage. AMD waters flowed into the uncontaminated ($pH = 8,33$ $EC = 344 \mu S$) Gromolo Torrent where abundant precipitation of amorphous Fe(III)-oxy-hydroxides occurred.

The aims of this work are: 1) to evaluate the PTE mobility of colloidal stream precipitates for about 7 km up to its mouth in the Ligurian Sea; 2) to verify the presence of colloidal precipitates into the marine sediments and 3) to determine colloidal capacity to retain in the solid fraction some PTE (Fe, Al, Cu, Zn, Mn, Ni, Pb, Co, Cd, and Cr) using bulk leaching test experiments. Eleven stream and twelve marine bottom sediments were sampled and analysed using XRPD and ICP-MS. Moreover, in order to verify the possible interaction with rain and sea waters, bulk leaching experiments were performed.

The results showed that colloidal nanoparticles are characterized by amorphous Fe(III)-oxy-hydroxides with a strong environmental impact, as they act as sinks for chemical elements scavenging almost the entire amounts of dissolved metals from the solutions. These Fe amorphous phases evidenced a major enrichment of all chemical elements, with the exception of Fe and SO_4^{2-} , compared to AMD precipitates such as ferrihydrite and schwertmannite.

The bulk leaching test results, performed with deionized water, showed that the colloidal nanoparticles are an efficient sink for metals, with the exception of Pb which reaches high concentrations in the leachates (up to the 86% of the amounts of the solid fraction). Alongside Pb, sea water remobilized high amounts of Mn and Cd (up to 42% and 30% of the amounts of the solid fraction, respectively) and remarkable amounts of Co and Ni (up to 16% and 6% of the amounts of the solid fraction, respectively).

Effect of the atmospheric fallout on the Rare Earths distribution in leaves

Cibella F.¹, Falcone E.E.*², Latteo V.¹, Saiano F.³, Marcenò C.⁴ & Censi P.²

1. Istituto di Biomedicina e di Immunologia Molecolare, CNR, Palermo. 2. Dipartimento di Scienze della Terra e del Mare, Università di Palermo. 3. Dipartimento di Scienze Agrarie e Forestali, Università di Palermo. 4. Istituto di Bioscienze e Biorisorse, CNR, Palermo.

Corresponding email: paolo.censi@unipa.it

Keywords: REE, atmospheric dust, plant leaves.

This study was carried out for recognising if atmospheric particulates can influence the plant composition with respect to the soil contribution and the extent of this process. We investigated Rare Earths (REE) content in several plant specimens selected for their spreading in natural and contaminated ecosystems.

Although REE studies on plants increased during the last 20 years with the progressive growth of REE exploitation in Hi-Tech industry, they were mainly confined to the investigation of the element migration from soil to plants. Only recently, some studies were focused on the geochemical behaviour of REE during the metabolic processes occurring in the plants (Censi et al., 2014). In the present study we would like to recognise if another interface between plant and surrounding environment occurs in leaves where atmospheric dust is usually depositing. We suggest that the effects of the chemical changes in the environment quality related to the atmospheric pollution could be faster recorded at the leaf-atmospheric dust interface rather than through the plant rhizosphere. In order to corroborate this hypothesis we exploit the well-known REE capability to describe the mechanism of geochemical process at the interface scale.

According to this scenario, the studied plants were collected in six areas of Sicily, in the south Mediterranean area, different for lithology, extent, and type of anthropogenic pressure in industrial areas, coastal marine, mountain, and urban ecosystems. Both plant leaves and their particulate coating were analysed and obtained results compared to the REE concentration and distribution in soils of studied areas.

Our findings indicate that the leaf composition is strongly influenced by that of atmospheric particulate showing a different REE signature than the environmental soils. Shale-normalised REE patterns always show positive Eu and La anomaly values. The former were previously recognised in other plants worldwide and explained with the larger organic Eu-complexes in xylem fluids during metabolic processes in plants. On the contrary, the latter represent the effect of industrial oil refinery occurring in one of the studied sites on the composition of atmospheric particulate (Kulkarni et al., 2007). Unlike the differences relative to REE behaviour in soils, the large similarity between REE distribution in plant and particulates demonstrates that the composition of atmospheric particulates can influence the elemental distribution in leaves suggesting their possible exploitation as environmental indicators of outdoor air quality.

Censi P., Saiano F., Pisciotta A., Tuzzolino N. 2014. Geochemical behaviour of rare earths in *Vitis vinifera* grafted onto different rootstocks and growing on several soils. *Sci. Total Environ.* 473-474, 597-608.

Kulkarni P., Chellam S. & Fraser M. 2007. Tracking petroleum refinery emission events using lanthanum and lanthanides as elemental markers for PM_{2.5}. *Environ. Sci & Technol.* 41, 6748-6754.

Toxic metal dispersion in mining areas: from point source to diffusion pollution. The case of Mt. Amiata Hg mining district (southern Tuscany - Italy): first results

Colica A.*¹, Chiarantini L.², Rimondi V.², Benvenuti M.¹, Costagliola P.¹, Lattanzi P.³, Paolieri M.¹ & Rinaldi M.¹

1. Dipartimento di Scienze della Terra, Università di Pisa. 2. Istituto di Geoscienze e Georisorse, CNR, Firenze
3. Dipartimento di Scienze Chimiche e Geologiche, Università di Cagliari.

Corresponding email: antonella.colica@gmail.com

Keywords: Hg, point source vs. diffusion pollution, Mt. Amiata.

Mining areas are considered point sources of pollution, but draining river systems may give rise to diffusion pollution as contaminants are dispersed and accumulated downstream into different morphological units. The target area of our study includes the upstream section of the Paglia River's catchment (southern Tuscany). The Paglia River drains the SE portion of the Mt. Amiata mercury (Hg) district, the fourth most important worldwide (exploited from 1880 to 1980 with total production of 100,000 tonnes Hg) before becoming a tributary of the Tiber River, which directly flows into the Mediterranean Sea. Mercury is mainly transported as particulate in river systems, especially during flood events, and may accumulate in large amounts downstream. The goals of this study are: (1) to recognize and distinguish the different morphological units along the Paglia River watercourse, (2) to determine the spatial/temporal distribution and concentration of Hg (and other toxic elements, particularly As) in different units, and (3) to assess vulnerability of individual units. We present here the first results obtained by mapping the evolution over time of the morphological units along the upstream part of the Paglia River by accurate analysis of recent orthophotographs (2000 and 2012), as well as historic aerial photos (1945) and topographic maps (1880). The analysis of morphological units was made along a total of eleven transects, selected across the Paglia watercourse (10 transects) and one of its tributaries, the Siele River (1 transect), which upstream drains various Hg mines. Five unit types have been distinguished: stream, bar, floodplain and two post-Pleistocene terraces, approximately dated, respectively, to the mid of past century ("recent") and the beginning of mining/metallurgical activity (end of XIX cent.: "early"). A total of 96 samples have been taken from various units in the selected transects, geo-referenced and then analyzed for their Hg and As contents (on the ≤ 250 mm fraction) by ICP-OES. Moreover, four samples were taken from a soil profile trench excavated in a Pleistocene terrace (surely predating any mining activity). Arsenic contents in the transects almost never exceed 10 mg/kg (stream sediments: $4.1 \div 8.2$ mg/kg; bars: $4.1 \div 6.6$ mg/kg; floodplains: $4.7 \div 6.6$ mg/kg; recent terrace: $5 \div 7.1$ mg/kg; early terrace: $3.1 \div 10.13$ mg/kg). Overall Hg contents in present-day stream sediments and bars in the Paglia River are extremely variable ($0.17 \div 25.1$ mg/kg and $0.36 \div 22.4$ mg/kg respectively), and show a sharp increase only downstream of confluence with the Siele River. The floodplain sediments (discharged by a major 2012 flooding event) may reach up to 97 mg/kg. Both recent and early terraces show variable Hg contents ($0.45 \div 53.6$ mg/kg and $0.12 \div 66.9$ mg/kg, respectively). The Pleistocene terrace, on the contrary, shows very low Hg concentrations ($0.33 \div 0.60$ mg/kg) well below the natural geochemical background level in the Mt. Amiata region ($2 \div 6$ mg/kg).

Temperature-induced phase transition and remobilization of potential ecotoxic elements (PTE) in AMD colloidal precipitates

Consani S.*¹, Carbone C.¹, Salviulo G.², Zorzi F.², Dinelli E.³ & Lucchetti G.¹

1. DISTAV, Università di Genova. 2. Dipartimento di Geoscienze, Università di Padova.
3. Dipartimento di Scienze Biologiche, Geologiche e Ambientali, Università di Bologna.

Corresponding email: sirio.consani@edu.unige.it

Keywords: Colloidal particles, AMD, PTE.

Colloidal particles, as a direct consequence of their small size, have enormous sorption capacities due to their very high surface area to volume ratio, and can play a major role in the control of the dispersion and mobility of metal ions or organic pollutants (Schemel et al., 2000). Acid Mine Drainage (AMD), a weathering process of sulphides in mining areas, leads to the generation of very acidic waters with high amounts of dissolved SO_4^{2-} , Fe, and other ecotoxic elements such as Cu, Zn, Pb, As, Co, Ni, Cd, and Hg. In AMD settings, the formation of amorphous to semi-crystalline, usually metastable, colloidal nanoparticles occurs as loose suspension acting as sinks for chemical elements and as a secondary source of pollution through destabilization (dehydration-dehydroxylation) or desorption reactions. The stability of these phases depends on several factors including pH, Eh, water chemistry, T, isomorphous substitutions, chemical impurities, and adsorbed ions. Thus, the stability of colloidal phases and their behaviour during phase transitions is a critical point to determine the fate of ecotoxic elements in AMD environment (Acero et al., 2006). In this work, two Fe-rich colloidal precipitates with different mineralogical assemblages (schwertmannite and goethite + jarosite, respectively) and one Al-Cu-rich colloidal precipitate (allophane + woodwardite) from Libiola mine site, are considered. The aim of this work was to test the capacity of these colloidal precipitates to retain in the solid fraction ecotoxic elements before and after temperature-induced dehydration-dehydroxylation. A partial dissolution of all samples during leaching tests is to be excluded, as Fe, Al, and Cu were almost absent in the leachates.

The results obtained showed that unheated and high temperature (800-900 °C) heated sample precipitates release low amounts of metals in the leachates (generally < 5% of the amounts of the solid fraction), with little exceptions for Cd, Mn, and Co. On the contrary, low temperature (300-500 °C) heated precipitates show a dramatic increase for metals release in solution, specially for goethite + jarosite precipitates, were an average of the 40% of metals amount of the solid fraction was released.

The results highlighted that natural colloidal precipitates occurring at the Libiola mine site are an efficient sink for ecotoxic metals. However, the destabilization of these phases through dehydration-dehydroxylation reaction can remobilize important amounts of ecotoxic elements.

Acero P., Ayora C., Torrentò C. & Nieto J.M. 2006. The behaviour of trace elements during schwertmannite precipitation and subsequent transformation into goethite and jarosite. *Geochim. Cosmochim. Acta*, 70, 4130-4139.
Schemel L.E., Kimball B.A. & Bencala K.E. 2000. Colloid formation and metal transport through two mixing zones affected by acid mine drainage near Silverton, Colorado. *Appl. Geochem.*, 15, 1003-1018.

Inside the mine: interactions between hydrosphere, atmosphere, biosphere and the thallium-rich pyrite ores from southern Apuan Alps

D'Orazio M.*¹, Biagioni C.¹, Vezzoni S.¹ & Dini A.²

1. Dipartimento di Scienze della Terra, Università di Pisa. 2. Istituto di Geoscienze e Georisorse, CNR, Pisa.

Corresponding email: massimo.dorazio@unipi.it

Keywords: Thallium, pyrite, Apuan Alps.

Pyrite is the most common sulfide mineral of the Earth's crust and the main responsible for the production of acid rock drainage (ARD) and acid mine drainage (AMD). Where the geologic, climatic and biologic conditions are those most favourable to the oxidation of pyrite (i.e. circulation of oxygenated water through fine-grained pyrite ores in presence of iron-oxidizers bacteria), the production of acidic waters can pose severe environmental issues. This is the case of the southern Apuan Alps (one of the rainiest area of Italy), where several types of polymetallic sulfide/oxide ore deposits, hosted within highly to moderately permeable metamorphic rocks, have been mined since ancient times and up to the end of the last century. One of the most important of these ore deposits is represented by a series of baryte-pyrite-iron oxide orebodies aligned along a ~10 km SW-NE discontinuous mineralized belt located between Valdicastello Carducci (Pietrasanta, LU) and Forno Volasco (Fabbriche di Vergemoli, LU). Pyrite ores mainly occur as microcrystalline lensoidal masses, often in association with baryte, within the quartz-muscovite-chlorite phyllites of the Paleozoic basement or at the contact between the phyllites and the overlying Triassic dolostones. Only recently it was recognized that the pyrite ores still occurring in large amounts in this mining area, and widely exposed in the abandoned tunnels, is strongly enriched in thallium (typically 200-300 mg/kg and up to 1100 mg/kg). In some specific localities (i.e. Monte Arsiccio mine, Sant'Anna di Stazzema, LU) Tl also occurs as macroscopic Tl-Pb-Sb-As-Hg sulphosalts, emphasizing the exceptional nature of these mineralizations. Thallium is a relatively rare but highly toxic element that is readily transferred, along with other toxic or potentially toxic elements (particularly As, Sb, Pb, Hg, Cd, Zn, etc.), from pyrite ores to the aqueous phase. Indeed the internal waters of these mines may reach extreme concentrations of Tl (typically 500-1000 µg/l and up to 9000 µg/l). The stability of the main Tl species – the Tl⁺ ion – dissolved in the AMD-contaminated waters over extended intervals of pH and Eh conditions, enhances the dispersion of this element into the environment; indeed it is neither easily precipitated as an insoluble solid phase nor easily adsorbed onto jarosite/ferrihydrite/schwertmannite/goethite precipitating from Fe- and sulphate-rich waters.

Origin of manganese, sulphates and trichloromethane in groundwater at Portoscuso (Sardinia-Italy)

Da Pelo S.*¹, Mulas G.², Ghiglieri G.¹, Ardau C.¹, Cidu R.¹, Frau F.¹ & Porcheddu A.¹

1. Dipartimento di Scienze Chimiche e Geologiche, Università di Cagliari. 2. Comune di Portoscuso (CI).

Corresponding email: sdapelo@unica.it

Keywords: Volcanic aquifer, groundwater contamination, stable isotope.

The municipality of Portoscuso extends over an area of about 39 km² on the west coast of Sulcis-Iglesiente region (South-Western Sardinia, Italy). It comprises the industrial area of Portovesme, which developed in the late 1960s. The large industrial development had a considerable environmental impact such that the whole territory has been designed as contaminated site of national interest by the Italian Government (D.M., March 12, 2003). Groundwater contamination in the wide area is a serious environmental issue. In the Portoscuso area outcrops a volcanic ignimbrite succession up to 500 m thick, belonging to the Tertiary volcanism of the Sulcis region. Most of the volcanic rhyolites and comendites succession hosts an extended manganese mineralization, which shows a frequent manjiroite-cryptomelane association and a less frequent psilomelane (Marcello et al., 2004). An aquifer with variable permeability from low to medium, depending on vertical and lateral extension of the deposits and on the structural framework, occurs. On the coastal area the volcanic basement is overlaid by a quaternary succession, mainly sands, which hosts a shallow aquifer up to 50 m thick near the shoreline in the industrial area. A strong alkalization of the shallow groundwater in the industrial area and the presence of heavy metals and organic pollutants of clear anthropogenic origin were recognized (Barbieri & Ghiglieri, 1998) and environmental remediation is still ongoing. The whole municipal territory outside the industrial area has been investigated between July 2009 and March 2010 (Vecchio et al., 2010; 2012). Besides the diffuse presence in soil of elements such as Zn, Pb and Cd, due to fall-out from the industrial area, groundwater up-gradient the industrial district showed screening levels exceeding only for Mn, SO₄ and trichloromethane. In order to verify the origin of such elements, studies on stable S and B isotope ratios (δ³⁴S; δ¹¹B) in soils and groundwater and further insights on mineralogy of Mn mineralizations and on the sources of trichloromethane are now ongoing.

Barbieri G. & Ghiglieri G. 1998. Inquinamento degli acquiferi sabbiosi nell'area industriale di Portovesme (Sardegna sud-occidentale). Atti della Facoltà di Ingegneria, Vol. 42, XXVII, 27-35.

Marcello A., Pretti S., Valera P. & Fiori M. 2004. Tertiary manganese occurrences in Sardinia (Italy). IAGOD Conference: Vladivostok, Russia, 487-490.

Vecchio A., Guerra M., Mulas G., Andrisani M.G., Da Pelo S., Mura R. & Pilia M. 2010. Piano della caratterizzazione delle aree esterne al polo industriale di Porovesme - Risultati della caratterizzazione e Analisi di Rischio - Relazione finale (ISPRA).

Vecchio A., Guerra M., Mulas G. 2012. Manganese and sulphate background in groundwater at Portoscuso (Sardinia): a tool for water management in a large contaminated area. In: Quercia F.F. & Vidojevic D. Eds., Clean Soil and Safe Water, NATO Sci. Peace Secur., 77-90.

Physico-chemical properties of quartz from industrial manufacturing and its cytotoxic effects on alveolar macrophages: the case of green sand mould casting for iron production

Di Benedetto F.^{*1}, Gazzano E.², Tomatis M.³, Turci F.³, Pardi L.A.⁴, Bronco S.⁴, Fornaciai G.⁵, Innocenti M.⁵, Montegrossi G.⁶, Muniz Miranda M.⁵, Zoleo A.⁷, Capacci F.⁸, Fubini B.³, Ghigo D.² & Romanelli M.¹

1. Dipartimento di Scienze della Terra, Università di Firenze. 2. Dipartimento di Oncologia, Università degli studi di Torino. 3. Centro Interdipartimentale "Giovanni Scansetti" per lo Studio degli Amianti e di Altri Particolati Nocivi, Università di Torino. 4. Dipartimento di Chimica, Università di Torino. 5. Istituto per i Processi Chimico-Fisici, C.N.R. 6. Dipartimento di Chimica, Università di Firenze. 7. Istituto di Geoscienze e Georisorse, C.N.R. 8. Dipartimento di Scienze Chimiche, Università di Padova. 9. Agenzia Sanitaria di Firenze.

Corresponding email: francesco.dibenedetto@unifi.it

Keywords: Crystalline silica, health effects, spectroscopic characterization.

Understanding the relationships between quartz surface reactivity and the context experienced by the materials undergoing industrial processing is a key information to describe specific features of the production process. These, in turn, can be used in comparison with biochemical and epidemiological evidences to clarify the mechanisms modulating the rise of the crystalline silica related diseases. In this study, industrial samples coming from the production of the cast iron are considered. Quartz rich sands before their use to form the mould and the materials recovered after the dismantling of the mould were sampled. Samples were investigated by XRD and SEM/EDS microanalysis, to check the mineralogical speciation and the sand morphology, by ATR and microRaman spectroscopies, to gain details about the nature of the phase associated to the sands during the processing, and by cw- and pulsed EPR spectroscopies, to investigate the presence and the speciation of the radicals associated to quartz microcrystals. EPR, associated to the spin trapping technique, was also used to evaluate the potential of samples to generate particle-derived free radicals in cell-free tests. Finally, cytotoxic effects of the dust recovered after mould demolition were evaluated on murine alveolar macrophages (MH-S).

Sands before their use in the casting process reveal the unique presence of h_{Al} radicals, conventionally found in many quartz-bearing raw materials. Conversely, powder materials recovered from the dismantled mould exhibit a single paramagnetic species, attributed to a carbonaceous radical, interacting with neighbouring protons and related to the presence of a carbon coating. Remarkably, under the adopted experimental conditions, the intensity of the original signal attributed to the h_{Al} radicals appears as depleted below the detection limit in the processed powders. Sand recovered after mould dismantling contains a slightly larger amount of respirable particles than the raw sand, is able to catalyze carboxyl radical generation, but show lower surface reactivity in hydroxyl radical generation with respect to the raw materials and does not elicit cytotoxic response in alveolar macrophages.

Physico-chemical modifications, occurring during cast iron production, lead to a quartz-rich dust largely contaminated by a poor reactive amorphous carbon, which probably hide some of the reactive surface sites responsible for free radical generation and cell-particle interaction. The change in radical speciation also occurs involving a complete annihilation of the inorganic radicals present in the original sands.

Antimony removal from polluted mining water using Layered Double Hydroxides

Dore E.*, Cidu R. & Frau F.

Dipartimento di Scienze Chimiche e Geologiche, Università di Cagliari.

Corresponding email: elisabettadore@yahoo.it

Keywords: Antimony, Layered Double Hydroxides, remediation.

Antimony (Sb) is considered a pollutant of priority interest and is widely present in the environment through both natural and anthropogenic sources. Typical Sb concentrations in natural unpolluted waters are less than $1 \mu\text{g L}^{-1}$, but can increase up to 10^3 - $10^4 \mu\text{g L}^{-1}$ in areas near mining sites and smelter activities (Cidu et al., 2014). Under oxidizing condition the Sb(V) prevails over the more toxic but less mobile Sb(III), and is stable in solution as anionic complex $[\text{Sb}(\text{OH})_6]^-$ in a wide range of pH values (Accornero et al., 2008). A suitable solution for the Sb(V) removal from aqueous solutions is represented by the Layered Double Hydroxides (LDHs), a class of natural and synthetic compounds widely used in remediation studies. LDHs have general formula $[\text{M}^{2+}_{(1-x)}\text{M}^{3+}_x(\text{OH})_2]^{x+} [(\text{A}^{n-})_{x/n}]^{x-} \cdot m\text{H}_2\text{O}$, with large compositional variability (e.g. $\text{M}^{2+} = \text{Mg}, \text{Zn}$; $\text{M}^{3+} = \text{Al}, \text{Fe}$; $\text{A}^{n-} = \text{NO}_3^-, \text{CO}_3^{2-}, \text{SO}_4^{2-}$). The LDH structure consists of brucite-like sheets positively charged and stacked along the *c* axis, with anionic species and water molecules in the interlayer. Thank to their anion exchange capacity LDHs are able to remove pollutants stable in neutral and slightly alkaline waters as (oxy)anions. Also the $\text{M}^{2+}\text{M}^{3+}$ oxides derived from calcined LDH can be used to remove toxic (oxy)anions from water, because are able to reconstruct the layered structure trough rehydration and sorption of (oxy)anions (Goh et al., 2008). Preliminary studies performed with synthetic solutions showed the potential use of calcined and uncalcined LDHs for Sb removal from aqueous solutions. Successively, selected calcined LDHs were tested with the Sb polluted waters draining the abandoned Sb mine of Su Suergiu (SE Sardinia, Italy). Waters flowing at Su Suergiu are characterized by circumneutral-slightly alkaline pH values and oxidizing condition, show high Sb concentration (up to $10^4 \mu\text{g L}^{-1}$) and flow untreated in the main river of south Sardinia, the Flumendosa River that supplies water for agricultural and domestic uses. Results show that Sb prevails in solution as $\text{Sb}(\text{OH})_6^-$, while $\text{Sb}(\text{III}) \leq 6\%$ of $\text{Sb}(\text{tot})$. Sorption tests were performed on water collected in the slag drainage of Su Suergiu, characterized by high concentration of $\text{Sb}(\text{tot})$ ($9900 \mu\text{g L}^{-1}$) and also SO_4^{2-} , HCO_3^- and As, that can compete for the entry in the interlayer of LDH. Results show the substantial capacity of Sb and As removal from solution by LDH and encourage further investigation.

Thanks to: PRIN 2009 (R. Cidu); PRIN 2011-2012 (P. Lattanzi).

Accornero M., Marini L. & Lelli M. 2008. The dissociation constant of antimonite acid at 10-40 °C. *J. Solution Chem.*, 37, 785-800.

Cidu R., Biddau R., Dore E., Vacca A. & Marini L. 2014. Antimony in the soil-water-plant system at the Su Suergiu abandoned mine (Sardinia, Italy): strategies to mitigate contamination. *Sci. Total Environ.*, 497-498, 319-331.

Goh K-H., Lim T-T. & Dong Z. 2008. Application of layered double hydroxides for removal of oxyanions: a review. *Water Res.*, 42, 1343-1368.

Severe contamination of waters and stream sediments in an abandoned mine land from Alta Versilia (Southern Apuan Alps, Italy)

Franceschini F. *, D'Orazio M., Biagioni C., Vezzoni S., Petrini R. & Giannecchini R.

Dipartimento Scienze della Terra, Università di Pisa.

Corresponding email: f.franceschini@arpat.toscana.it

Keywords: Acid mine drainages, heavy metals, water pollution.

Natural weathering and human activities may both be sources of toxic and potentially toxic elements that are released and transported through contaminated plumes by surface and subsurface waters. Remediation strategies, to be effective, require knowledge of the source zone of contamination and of the processes that control the migration of the different contaminants, including the role of physical and chemical processes such as advection, dispersion and diffusion, besides the redox, chemical speciation adsorption/desorption and dissolution/precipitation reactions. In this context, the acid mine drainages that may develop as effluents from abandoned mine sites likely represent one of the largest environmental problems facing the mining industry.

In the present study, preliminary results concerning the fate of toxic and potentially toxic elements released from acid mine drainages into the surface waters and stream sediments of the Baccatoio river, crossing abandoned mine sites in southern Apuan Alps (Tuscany region) and the Valdicastello Carducci village, are reported. The mining activity, that exploited ore bodies of pyrite + baryte and iron oxides + baryte hosted at the contact between the phyllites, related to the Paleozoic basement of Apuan Alps, and Triassic dolostones, ended in 1989.

The data on mine effluents indicate that sulfide oxidation was the primary source of contaminants, releasing acid waters with high Fe (up to 14 g/L), Mn (19 mg/L), Al (270 mg/L), Cd (2 mg/L), Sb (19 mg/L), Pb (3 mg/L), Zn (270 mg/L), Ni (5 mg/L), Tl (9 mg/L) and As (30 mg/L) concentration. After the outflowing in the superficial waters of the Baccatoio stream, most metals and metalloids are scavenged by the formation of large amounts of iron precipitates when Fe(II) is oxidized to Fe(III), whose composition is controlled by sulfate ion concentration, water pH and aging, ranging from jarosite to schwertmannite, ferrihydrite and goethite. In addition, the rate of Fe(II) oxidation is highly pH dependent, and, at the pH values measured in the Baccatoio waters, Fe(II) might increase its residence time, allowing further precipitation downgradient.

Iron-rich stream sediments are characterized by high concentrations of Sb, As, Ni, Pb, Zn and Hg (up to about 540, 3600, 9200, 2100 and 80 mg/kg, respectively), acting as effective scavengers for these contaminants. However, the data indicate that Tl behaves almost conservatively in the surface waters of the Baccatoio, and it is readily transported by the aqueous phase. Indeed this very highly toxic element is missing or present in very low concentrations in the Baccatoio stream sediments while it persists in relatively high concentrations in the aqueous matrix, becoming a cause for concern for the environment and human health.

Environmental impact of a near-neutral mine drainage on surface waters and dissolved metal load to the Mediterranean Sea

Frau F.*, Da Pelo S., Atzori R. & Cidu R.

Dipartimento di Scienze Chimiche e Geologiche, Università di Cagliari.

Corresponding email: frauf@unica.it

Keywords: Mine drainage outflow, Green rust precipitation, Metal discharge to the Mediterranean Sea.

Lead-zinc sulfide veins hosted in Palaeozoic silicate-dominant rocks of the Arburese mining district (SW Sardinia, Italy) have been exploited in a system of interconnected galleries at depths of up to 600 m below ground level. To keep the galleries dry, a total flow in the range of 55 to 70 L/s of water was pumped out of the mines. In 1973 (under active mining), the water pumped from the Casargiu mine (Montevecchio) was circumneutral (pH 7.5), with relatively high concentrations of sulfate (1400 mg/L) and metals (e.g. 70 mg/L Zn, 4.6 mg/L Fe, 0.5 mg/L Mn). After mine closure in the 1980s and subsequent shutdown of the dewatering system, groundwater rebound led to drainage outflow from the Casargiu gallery since 1997. At first, the mine water outflow had a pH of 6.0 and dissolved concentrations of sulfate (5000 mg/L) and metals (e.g. 1000 mg/L Zn, 230 mg/L Fe, 150 mg/L Mn) much higher than those previously measured under dewatering conditions. This increase in dissolved concentrations can be explained taking into account that the underground workings were kept dry during exploitation; groundwater rebound flooded the mine galleries and allowed the contact of water with sulfide minerals (especially sphalerite), promoting their oxidation, and the dissolution of secondary minerals and soluble efflorescent salts. The acidity produced by the oxidation of sulfide minerals (e.g. pyrite, Fe-bearing sphalerite) has been buffered by the occurrence of ankerite-siderite gangue in the Casargiu ore. As compared with the first stages of rebound at Casargiu, a very high contamination level still persists after more than 15 years of flushing.

Mine drainage from Casargiu (20-70 L/s; pH 6.0±0.2; Zn-Mg-Ca-SO₄ composition) flows into the Rio Irvi. Sampling along this stream for about 6 km almost to its mouth in the Mediterranean Sea showed a pH decrease from 6.0 to 4.0. Precipitation of amorphous Fe(III)-(oxy)hydroxides occurs at the Casargiu outflow and along the Rio Irvi. Moreover, sulfate-bearing green rust is observed to flocculate in the reach of the Rio Irvi where pH is still circumneutral. As a consequence of precipitation, about 46% of dissolved Fe is lost between the Casargiu outflow and the last sampling point 6 km downstream. Concentrations of sulfate and most metals, such as Zn, Mn, Co, Ni and Cd, show small variations downstream, but Pb initially exhibits a strong decrease of 68% by adsorption onto Fe(III)-(oxy)hydroxide, then a significant increase due to desorption as pH drops below 5. Dissolved As shows a decrease of 96% because of its stable adsorption onto Fe(III)-(oxy)hydroxide at acidic pH.

The estimated amount of dissolved metals discharged into the Mediterranean Sea is significant (e.g. 900 kg/day Zn, 1.4 kg/day Cd, 5 kg/day Ni). In particular, a conservative estimation of the amount of Zn discharged to the sea is about 330 ton/year, which would correspond to 1.4% of the global annual flux of dissolved Zn from uncontaminated rivers to the oceans.

Chromium and nickel distribution in ultrabasic soils of the Voltri Massif (Ligurian Alps)

Marescotti P.*¹, Crispini L.¹, Fornasaro S.¹, Beccaris G.², Scotti E.², Poggi E.³ & Lucchetti G.¹

1. DISTAV, Università di Genova. 2. Agenzia Regionale per la Protezione dell'Ambiente Ligure (ARPA-Liguria)
3. Geospectra S.r.l. (Spin Off Università di Genova).

Corresponding email: marescot@dipteris.unige.it

Keywords: Serpentinites, peridotites, ecotoxic metals.

With this work we investigated the mineralogy, the mineral chemistry, and the bulk chemistry of undisturbed soil profiles chosen in an area with tectonic contacts between high pressure metamorphic serpentinites and peridotites of the Voltri Unit "(Bric del Dente Serpentinite" and "Monte Tobbio Peridotite" Formations, Ligurian Alps).

Trace element concentrations were assessed *in situ* and in laboratory by means of field-portable X-ray fluorescence spectrometer and ICP-OES. The mineralogy and the mineral chemistry were determined by optical microscopy, scanning electron microscopy (SEM-EDS), and electron microprobe analyses (WDS). Eh, pH, soil colour, and granulometry were also assessed.

All the studied soil profiles are restricted in depth (10-50 cm from the surface to the coherent parent rocks) and show a low degree of maturity, varying from lithosols, with weakly developed horizons, to rankers. The bedrock shows a decimetric oxidation halo mostly developed around open fractures and joints.

Measured concentrations of chromium and nickel (874-3020 ppm and 1900-3900 ppm, respectively) do not evidenced significant and systematic variation between the unaltered and the weathered bedrock, thus suggesting that the recognized Cr- and Ni-bearing minerals are resistant to weathering in the early steps of supergenic alteration.

The mineral distribution along soil profiles evidenced a significant increase of weathering from the parent rock toward the superficial horizons in all sites. The most weatherable minerals resulted, in order of decreasing alteration degree, olivine, pyroxene, magnetite and serpentine minerals. Conversely, chlorite, plagioclase, and chromites were weakly altered or unaltered. Authigenic secondary minerals were mainly represented by microcrystalline Fe-oxyhydroxides occurring either as replacement of primary minerals or within the clay fraction. Clay minerals are subordinate components and occur mainly toward the upper horizons and in the more evolved profiles.

The bulk chemistry of the soil profiles evidenced a conservative behaviour of Cr which is strongly correlated with the Cr concentration of the parent rocks. Chromium concentration ranged from 1200 to 2500 ppm without significant variations along the soil profiles. Conversely, the Ni elemental distribution evidenced a high variability and a general increase in the upper horizon (up to 4500 ppm) due to the weathering of the primary Ni-bearing minerals (mainly olivine and serpentine minerals) and to the uptake by the authigenic secondary minerals (mainly Fe-oxyhydroxides and clay minerals).

These results evidenced that all the studied soil profiles have a baseline values of Cr and Ni well above the concentration limits of the Italian laws. Nevertheless, most of these ecotoxic metals are presumably not available for plant uptake because they are present in weathering resistant phases, such as Cr-spinels, or sequestered in stable authigenic minerals (Fe-oxyhydroxides and clay minerals).

Mineralogical and geochemical spatial analyses of waste-rock dumps: a case study from the abandoned Rio Bansigo sulphide mine (eastern Liguria, Italy)

Marescotti P.*¹, Solimano M.¹, Marin V.², Salmona P.², Vassallo P.¹, Brancucci M.³ & Lucchetti G.¹

1. DISTAV, Università di Genova. 2. Dipartimento di Scienze per l'Architettura, Università di Genova.
3. Geospectra S.r.l. (Spin Off Università di Genova).

Corresponding email: marescot@dipteris.unige.it

Keywords: Field portable EDXRF, waste-rock dumps, ecotoxic metals.

The waste-rock dumps are heterogeneous deposits piled up during mining exploitation which are often sites of environmental concern because they commonly contain high concentrations of metals and metalloids, which may be released to the circulating waters during weathering. One of the major problems in characterizing the chemistry and the metals distribution of the waste-rock dumps is represented by the significant vertical and lateral heterogeneities in grain size, lithology and mineralogy. In fact, these deposits are commonly piled up during the different phases of mining exploitation over tens of years and contain either low-grade mineralizations or several types of host rocks. Moreover, the erosion processes continuously transform the deposit redistributing sediments downslope. For these reasons, the design of a sampling and analysis plan by means of traditional techniques may have unsustainable costs due to the large number of samples required. With this work we investigated the chemical composition and the metals distribution within a sulphide-bearing waste-rock dump using a field portable energy dispersive X-ray fluorescence spectrometer (FP-EDXRF, XMET7500, Oxford Instruments). The FP-EDXRF analyzer is designed to provide rapid, real-time analysis of metal concentrations in soil and mining samples. With this instrument, elements of atomic number ≥ 12 (Mg) can be detected and quantitated from trace level (ppm) to 100% in few minutes. The site chosen for this study is a small-sized dump (about 3500 m²) from an abandoned Cu-sulphide mine (Rio Bansigo mine, eastern Liguria, Italy).

The use of FP-EDXRF allowed to perform a sampling plan using a sampling grid of 5 x 5 m within the waste rock dump perimeter and to apply a radial grid centered on selected metals hot spots resulted from the preliminary in situ analyses. The average throughput was 10 to 15 analyses per hour using a live count of 120 seconds. Analyses were performed on sample cups filled with sieved samples (< 2 mm).

Grain size, color, mineralogy, mineral chemistry and acid mine drainage potential were also determined on selected samples. The analytical data were processed using one-way analysis of variance (ANOVA) and the multidimensional scaling (MDS). Very detailed contour maps were then drawn for each metals, which allowed to evaluate the metal distribution in the entire mine dump area. Our results evidenced the feasibility of a detailed evaluation of metal hazard within waste-rock dumps using field-portable XRF device. The results obtained with the geostatistical elaboration promise to be a powerful tool to discern the composition of mine dumps and support the exploitation and remediation phases.

Rare earth elements fractionation processes during mine waste weathering and secondary phases precipitation under near-neutral conditions

Medas D.*, Cidu R., De Giudici G. & Podda F.

Dipartimento di Scienze Chimiche e Geologiche, Università di Cagliari.

Corresponding email: dmedas@unica.it

Keywords: Rare earth elements, mining wastes, secondary phases.

Rare earth elements (REE) can be useful for identifying different sources of contaminants in order to develop efficient remediation strategies of contaminated sites such as abandoned mining areas. This study investigates the behaviour REE in near-neutral waters of the Naracauli stream, draining the abandoned mining area of Ingurtosu (SW Sardinia, Italy), to identify the main factors that control the REE geochemistry.

Different types of samples were investigated: waters, mine tailings and secondary precipitates. The mine tailings are the main REE source reaching 300 mg/kg Σ REE, and show a light REE enrichment respect to heavy REE when normalized to Post-Archean average Australian Shale (PAAS) and Upper Continental Crust.

Drainages from mine wastes show near-neutral pH values (6.2 to 7.0 pH), a Zn-sulphate dominant composition, and a mean concentration of 53 μ g/l Σ REE. Mine waste drainages flow into the Naracauli stream waters that show the highest REE concentrations in samples collected under high flow conditions. Moreover, concentration of REE along the Naracauli stream decreases dramatically about 400 m downstream of source, matching Fe and Zn decrease because of Fe-hydroxides and bio-hydrozincite precipitation. These observations suggest that aqueous transport of the REE might occur via fine particles (i.e. 0.4 μ m), and that variation in REE concentration depends on the precipitation of secondary phases. Moreover, although the waters show small pH variations, the decrease of dissolved REE matches pH increase suggesting a pH dependence of aqueous REE even in non-acidic environments.

The REE show the highest affinity for Fe-hydroxides precipitating at Naracauli, which are characterized by a marked positive Ce anomaly consistent with the observed Ce affinity for Mn- and Fe-(hydr)oxide phases (Bau & Koschinsky, 2009). On the other hand, Ce shows a poor affinity for the bio-hydrozincite, suggesting a biological mediation of the oxidative scavenging of Ce⁺⁴ (Moffett, 1994), and/or the complexation of Ce⁺⁴ with organic ligands that might maintain Ce in solution (Tanaka et al., 2010).

The PAAS-normalized REE patterns in the waters generally reflect the PAAS-normalized REE patterns in mine wastes or secondary phases with which the water interacts, suggesting that the REE might be useful for identifying the sources of contaminants.

Bau M. & Koschinsky A. 2009. Oxidative scavenging of cerium on hydrous Fe oxide: Evidence from the distribution of rare earth elements and yttrium between Fe oxides and Mn oxides in hydrogenetic ferromanganese crusts. *Geochem. J.*, 43, 37-47.

Moffett J.W. 1994. The relationship between cerium and manganese oxidation in the marine environment. *Limnol. Oceanogr.*, 39, 1309-1318.

Tanaka K., Tani Y., Akahashi Y., Tanimizu M., Suzuki Y., Kozai M. & Ohnuki T. 2010. A specific Ce oxidation process during sorption of rare earth elements on biogenic Mn oxide produced by *Acremonium* sp. strain KR21-2. *Geochim. Cosmochim. Acta*, 74, 5463-5477.

Apparent solubility constant of hydrozincite: effect of crystal size and surface energy

Medas D.*¹, De Giudici G.¹, Podda F.¹, Meneghini C.² & Lattanzi P.¹

1. Dipartimento di Scienze Chimiche e Geologiche, Università di Cagliari.

2. Dipartimento di Fisica, Università di Roma Tre.

Corresponding email: dmedas@unica.it

Keywords: Hydrozincite, apparent solubility product, biomineral.

Hydrozincite, $Zn_5(CO_3)_2(OH)_6$, biomineralization controls the mobility of Zn, Pb, Cd, Cu and Ni in the Naracauli stream waters (SW Sardinia, Italy). Naracauli bio-hydrozincite precipitates around bacterial filaments (*Scytonema* sp.) forming globules, typically in late spring and early summer. It is a composite material made up of an organic matrix, mainly composed by extracellular polymeric substances, and nano-scale crystalline mineral.

Biominerals, such as bio-hydrozincite, play a key role in the harmful element cycle (Hazen & Ferry, 2010), and thus also in remediation strategies such as bioremediation. Biominerals reactivity and solubility are still poorly understood, and often differ significantly from their abiotic analogues (Giuffrè et al., 2013). In this context, the apparent solubility product (K_s^{app}) was estimated for hydrozincite samples of different nature: natural abiotic ("geologic"), synthetic abiotic, and natural biominerals. A systematic increase in K_s^{app} was recorded from the geologic sample ($\log K_s^{app} = 6.2 \pm 0.1$), to synthetic analogues ($\log K_s^{app}$ between 7.0 ± 0.2 and 7.5 ± 0.2), and bio-hydrozincite ($\log K_s^{app}$ between 8.8 ± 0.2 and 9.1 ± 0.2).

In order to detect parameters affecting K_s^{app} values, hydrozincite structural properties were investigated by Scanning and Transmission Electron Microscopy, Synchrotron Radiation X-rays Powder Diffraction (SR-XRPD), and Zn K-edge X-rays Absorption Spectroscopy (EXAFS). Bio-hydrozincite shows systematic structural differences with respect to the abiotic analogue phase. In detail, refining SR-XRPD data, it was found that cell volume is largest for bio-hydrozincite, intermediate for synthetic samples, and smallest for the geologic sample. Moreover, XRPD and EXAFS data suggest an increasing disorder from geologic to synthetic to biomineral samples. The same systematic variation was recorded for crystal size, decreasing from geologic sample to synthetic samples to biominerals.

The effects of particle size and cell volume increase on K_s^{app} were calculated by classical thermodynamic equations. The surface energy (γ) of hydrated hydrozincite increases by at least one order of magnitude from geologic to biologic sample. The increase in K_s^{app} is mainly due to a decrease in the crystal size and an increase in γ , whereas the effect of cell volume variation is considered small, being of the same order of magnitude of the error in solubility measurements. The measured K_s^{app} values were used to build predominance diagrams; specifically for biominerals, only the use of K_s^{app} derived in this study predicts fairly well the seasonal precipitation of bio-hydrozincite along the Naracauli stream.

Giuffrè A.J., Hamm L.M., Han N., De Yoreo J.J. & Dove P.M. 2013. Polysaccharide chemistry regulates kinetics of calcite nucleation through competition of interfacial energies. Proc. Natl Acad. Sci. U.S.A., 110, 9261-9266.

Hazen R.M. & Ferry J.M. 2010. Mineral evolution: Mineralogy in the fourth dimension. Elements, 6, 9-12.

Mobility of potentially toxic elements in urban soils: a comparison between Rome and Novi Sad

Montereali M.R.*¹, Angelone M.¹, Manojlovic M.², Armiento G.¹, Čabilovski R.², Crovato C.¹, De Cassan M.¹, Massanisso P.¹ & Vidojević D.³

1. ENEA, CR Casaccia, Roma. 2. Faculty of Agriculture, University of Novi Sad, Republic of Serbia
3. Ministry of Agriculture and Environmental Protection, Republic of Serbia.

Corresponding email: mariarita.montereaali@enea.it

Keywords: Heavy metals, urban soils, metal mobility.

Urban environments are areas of great interest for the study of the cumulative effects of pollution related to intense anthropogenic activities. As a consequence, population can be exposed to serious health hazards. In the framework of a scientific collaborative project between Serbia and Italy, supported by MAECI (Italian Ministry of Foreign Affairs), a study on soils, plants and road dust has been carried out in urban parks and nearby areas in Rome and Novi Sad in order to identify the anthropogenic influence in two settings different in traffic intensity, industrial activities, number of inhabitants and geomorphology.

The determination of the total content of potentially toxic elements evidenced a great difference between the two cities. For example, Pb in Rome is eight times higher than in Novi Sad and the levels remain still very high even after 25 years since the catalytic converter introduction. In Novi Sad, owing to the recent catalyst introduction, PGE (Platinum Group Elements) levels are very low (<1,6 ng/g) also compared to those found in Rome: Pt 3-15 and Pd 4-16 ng/g, confirming the correlation between catalytic converters and PGE presence in the urban environment (Spaziani et al., 2008). Although most of the national environmental directives set strict limits concerning total concentrations of toxic elements, more suitable information on the associated risk and bioavailability could be obtained by mobility studies. This can be achieved applying the procedure developed by the Measurement and Testing Programme of the European Commission (BCR) (Rauret, 1999).

Preliminary data show that the metal content is higher for samples collected near main roads and that they are also characterized by a significant metal mobility. Samples from Novi Sad, despite their lower total metal concentrations, exhibit higher mobility than that measured in Rome urban soils. This result can be explained by the presence of different mineral phases in soil parent materials of the two towns and by a different anthropogenic influence. Rome urban soils mainly originate from volcanic rocks characterized by high natural metals concentrations. In Novi Sad soils mainly derive from river and eolic sediments (loess) characterized by a lower metal content but they probably are affected by an additional metal input related to previous industrial activities that are absent in Rome, where anthropogenic pollution is mainly due to vehicular traffic.

Rauret G., Lopez-Sanchez J.F., Sahuquillo A., Rubio R., Davidson C., Ure A. & Quevauviller P. 1999. Improvement of the BCR three step sequential extraction procedure prior to the certification of new sediment and soil reference materials. *J. Environ. Monit.*, 1, 57-61.

Spaziani F., Angelone M., Coletta A., Salluzzo A., & Cremisini C. 2008. Determination of Platinum Group Elements and Evaluation of Their Traffic-Related Distribution in Italian Urban Environments. *Anal. Lett.*, 41, 2658-2683.

Heavy element contamination in soil and accumulation in earthworms in the urban area of Siena (Italy)

Nannoni F.*, Protano G. & Rossi S.

Dipartimento di Scienze Fisiche, della Terra e dell'Ambiente, Università di Siena.

Corresponding email: giuseppe.protano@unisi.it

Keywords: Heavy elements, soil, earthworms.

A biogeochemical study was carried out to assess the influence of vehicular traffic on heavy element contamination in soil and accumulation in earthworms in the urban area of Siena (Italy). Total contents of Cd, Co, Cr, Cu, Ni, Pb, Sb, U e Zn and their distribution in extractable, reducible, oxidable and residual fractions were determined in soil samples collected in urban, peri-urban, green-urban and non-urban sites of Siena municipality. Heavy element concentrations were also measured in *Nicodrilus caliginosus* (Savigny) earthworm specimens collected in the soil sampling sites. The aim of study was: i) to assess the influence of vehicular traffic on heavy element distribution in soil; ii) to define the heavy element mobility in soil and potential bioavailability in relation to contamination level; iii) to establish the relationship between the heavy element content and fractionation in soil and their uptake by earthworms. Analytical data indicated that vehicular traffic affected the distribution of Cd, Cu, Pb, Sb and Zn in soil, with the highest total contents in urban and peri-urban soils. Based on the enrichment factor, Pb and Sb were the main soil contaminants. The heavy element fractionation in soil highlighted that Cd was the most mobile element being largely in the extractable (bioavailable) fraction. Pb was mainly associated with the reducible and residual fractions, and Co, Cr, Cu, Ni, Sb, U e Zn with the residual fraction. Contamination due to vehicular circulation caused variation in the distribution of the traffic-related heavy elements in soil fractions. Anthropogenic Cd, Cu, Pb, Sb and Zn were accumulated in the extractable, reducible and oxidable soil fractions with difference in partitioning related to the affinity of the element for organic complexation and non-specific and specific adsorption. Concentrations of Cd, Cu, Pb, Sb and Zn in earthworms showed a distribution pattern similar to that in soil, suggesting that soil contamination affected the accumulation of the traffic-related heavy elements in earthworms. The fractionation of these heavy elements in soil ruled their uptake by earthworms. The absorption of Cd, Pb, Sb and Zn by earthworms mostly depended on the extractable fraction, whereas the oxidable soil fraction influenced Cu uptake.

Rare earth elements and Heavy metals in soils of an open landfill

Nigro A.*¹, Barbieri M.¹ & Sappa G.²

1. Dipartimento di Scienze della Terra, Sapienza Università di Roma.

2. Dipartimento di Ingegneria civile, edile ed ambientale, Sapienza Università di Roma.

Corresponding email: angela.nigro@uniroma1.it

Keywords: Heavy metal, rare earth elements, landfill.

Five soils samples and four clay samples have been collected during December 2014 in a landfill of Central Italy to evaluate the environmental status in the area. The main objective of this study is the characterization of soil samples in relation to heavy metals values and to critically assess the measured values with respect to anthropogenic input vs lithogenic background. Heavy metals in soils can be associated with several reactive materials and may exist in various forms that reflect their solubility and availability. To evaluate the various chemical forms present in the soils, steps I (exchangeable) and V (residual) of the sequential extraction procedures established by Tessier et al. (1979) and optimised by Frankowski et al. (2010) have been used. Elements investigated are V, Cr, Fe, Ni, Cu, Zn, As, Rb, Cd, Sb, Tl and Pb. The results of analyses have been used for statistical analyses and to determine enrichment factor (EF) and geoaccumulation index (I_{geo}). These index have been calculated using average crustal values, lithosphere values and clay values of the study area, for determining differences between values. Furthermore, have been determined the rare earth elements in samples. The Rare earths elements abundance in soils usually exhibit the typical distribution pattern reported in geological samples, although fractionation is possible, controlled by pedogenic factors such as pH, redox condition and organic matter content. Have been determined the REE in clay samples representative of geologic pattern of the area sampled in different deep.

Tessier A., Campbell P.G.C. & Bisson M. 1979. Sequential extraction procedure for the speciation of particulate trace metals. *Anal. Chem.*, 51(7), 844-851.

Frankowski M., Ziola-Frankowska A. & Siepak J. 2010. Speciation of aluminum fluoride complexes and Al₃ in soils from the vicinity of an aluminum smelter plant by hyphenated high performance ion chromatography flame atomic absorption spectrometry technique. *Microchem. J.*, 95, 366-372.

Rare earths elements and $^{87}\text{Sr}/^{86}\text{Sr}$ in groundwater landfill

Nigro A.*¹, Barbieri M.¹ & Sappa G.²

1. Dipartimento di Scienze della Terra, Sapienza Università di Roma.

2. Dipartimento di Ingegneria Civile, Edile ed Ambientale, Sapienza Università di Roma.

Corresponding email: angela.nigro@uniroma1.it

Keywords: Rare earths elements, strontium isotope, municipal solid waste landfill.

A study was carried out to assess the water quality situation of groundwater in a municipal solid waste landfill of Central Italy. Landfill leachate is a serious problem for the groundwater contamination, because it contains a large amount of contaminants which are likely to pollute groundwater. In this study, beyond to determination of major ions and trace elements we have determined the concentrations of rare earths elements and Sr isotopes. This study was conducted also to investigate the use of different geochemical methods for evaluating the landfill impact in the area. The determination of major ions and trace element has show that there is a contamination of groundwater situated downgradient of the site. The principal contaminants are Cl, NH_4^+ , Fe, As, B, Hg and Cr. Furthermore, we have determined the concentrations of rare earths elements and the Sr isotopes in some piezometers around the landfill for studying the geochemical characteristics of the waters and to test the use of these elements as tracers of contamination. In recent years rare earths elements were used for many high technology products and processes resulted in an increase of interest for these elements. Some studies show an enrichment of these in river water of the big city, furthermore there is an evidence of their presence in municipal solid waste. We have analysed the REE concentrations in groundwater and one piezometer show a positive Gadolinium anomaly that could be due at landfill leachate. This is an important data because confirm the enrichment of REE in natural matrix in relation of human activity. $^{87}\text{Sr}/^{86}\text{Sr}$ isotopic ratio can be used as a tracer for understanding the lithological composition in which the groundwaters circulated and for the reconstruction of the potential areas of recharge for the aquifer levels. Sr isotope have been analysed for five water points. The results show that the values of $^{87}\text{Sr}/^{86}\text{Sr}$ range from 0.70895 to 0.70905, with a clear marine signature (0.70905-0.70910). Uncontaminated groundwater presents a value of 0.70905 while in contaminated piezometers the values lower (0.70895 in piezometer more contaminated).

Thallium ecosystem diseases in dismissed mine sites as a threat for public health: the Valdicastello-Pietrasanta (Italy) case history

Petrini R.*¹, D'Orazio M.¹, Giannecchini R.¹ & Bramanti E.²

1. Dipartimento di Scienze della Terra, Università di Pisa. 2. ICCOM, CNR, Pisa.

Corresponding email: riccardo.petrini@unipi.it

Keywords: Acid Mine Drainage, thallium contamination, thallium human exposure.

The legacy of mining activity may be the production of metal-rich acidic drainage and the release of toxic compounds to the receiving ecosystem. The mitigation of the environmental impact from metals and metalloids in mine drainages mostly produced by sulfide mineral oxidation is of great environmental concern, and, even if the acidity of drainages often receives most of the attention, the primary sources of toxicity for the biota and humans are the dissolved toxic and potentially toxic metals. Furthermore, the possible increase of pH and alkalinity that occur in superficial- and ground-waters by the interactions of acid waters with carbonate minerals and/or by the admixing of calcium-bicarbonate waters do not necessarily prevent metal transport through waters from causing negative environmental impacts. In fact, even if some metals, such as iron and arsenic, are readily scavenged from the aqueous phase by precipitation and adsorption processes as the pH increases, other ionic species of elements such as thallium may stay in solution in some cases reaching concentrations of concern. Previous studies demonstrated that in the dismissed mine areas of Valdicastello Carducci-Pollone and Mt Arsiccio in the Versilia area (Tuscany Region, Italy) thallium is hosted in base metal sulfides such as pyrite up to wt.% amounts. From these sources thallium is readily mobilized to waters during weathering oxidation of the sulfide minerals, reaching up to 9000 µg/L in drainages, and is dispersed into the ecosystem via water transport pathways with low attenuation when dissolved Fe(II) starts oxidizing and precipitating as insoluble oxyhydroxides. In the study area thallium-contaminated groundwater was used as supply in the potable water distribution network of Valdicastello Carducci and part of Pietrasanta town, and thallium was retained in scale encrustation within the pipeline walls at wt% concentration and then released to drinking waters. A non-invasive study on inhabitants of Valdicastello and Pietrasanta was performed in order to quantify the thallium concentration in urine and hair samples, in addition to saliva samples. The preliminary data show that about 50% of the urine samples are characterized by a thallium concentration above 0.5 µg/L and about 70% of hair samples has a thallium concentration exceeding 10 ng/g. These results highlight the links between changes in the state of the environment and human exposures.

Chrysotile, crocidolite, asbestiform erionite: mineralogical characterization and citotoxic effects

Pugnali A.*¹, Tiano L.², Capella S.³, Vigliaturo R.³ & Belluso E.^{3,4}

1. Dipartimento di Scienze Cliniche e Molecolari, Università Politecnica delle Marche. 2. Dipartimento di Scienze Cliniche Specialistiche ed Odontostomatologiche, Sezione di Biochimica, Biologia e Fisica, Università Politecnica delle Marche. 3. Dipartimento di Scienze della Terra, Università di Torino. 4. Istituto di Geoscienze e Georisorse, C.N.R. Torino.

Corresponding email: armanda.pugnali@univpm.it

Keywords: TEM-EDS, mineralogical characterization, cytotoxic effects.

UICC chrysotile, chrysotile from Val Malenco, erionite from Nevada and UICC crocidolite fibers were characterized through Transmission Electron Microscopy (TEM) with annexed Energy Dispersive Spectroscopy (EDS). The TEM study was performed forward on three levels for each single sample.

The first observed aspect was the morphological and dimensional study: typical fibrous morphology was observed for all the analyzed samples. For each sample 100 fibers were investigated: were registered their dimension (length and diameter) and the L/d ratio were calculated in order to understand if the fibers population can entry in particular dimensional categories (e.g. WHO criteria, Stanton's Hypothesis criteria or EPA dimensional limits). The second observed aspect was the chemical composition of the fibers. Also the chemistry match well with the expected for this minerals. In particular, both the chrysotile samples show the presence of aluminum and iron as substitute of tetrahedral and octahedral typical cations; the crocidolite bears an adding of calcium and the erionite has magnesium and iron cations normally unexpected in the general formula. At the latter investigation level, all the fibers showed a high degree of crystallinity in the diffraction patterns study, without evidence of natural amorphization (e.g. weathering).

These characterized mineral fibres were administrated for 6, 12, 24 and 48h in human bronchial and mesothelial cells, at the concentration of 50 µg/ml, to evaluate their cytotoxic effects; some biofunctional parameters at time points were evaluated: % number of alive, death and apoptotic cells; % number of cells with low, medium, high ROS content. These data confirm higher cytotoxic effects exerted by UICC crocidolite and UICC chrysotile, particularly evident since short times of contact (6, 12h). Our next purpose will be to characterize the same fibers extracted from cells after culture treatments.

Hydrological and Biogeochemical processes in the critical hyporheic zone along a mine-polluted-river (Rio San Giorgio – SW Sardinia-Italy)

Pusceddu C.*¹, Medas D.¹, Podda F.¹, Cidu R.¹, Lattanzi P.¹, Wanty R.², Kimball B.³ & De Giudici G.¹

1. Dipartimento Scienze Chimiche e Geologiche, Università di Cagliari. 2. US Geological Survey, Denver, USA
3. US Geological Survey, Salt Lake City, USA.

Corresponding email: claudia.pusceddu@unica.it

Keywords: Biosphere-geosphere interaction, mine pollution, bioremediation.

In this study, a mine polluted stream belonging to the past Pb-Zn mine district of Sulcis Iglesiente (Sardinia SW, Italy), Rio San Giorgio, was investigated. San Giorgio riverbed is characterized by widespread occurrence of vegetation. Plant species predominating at Rio San Giorgio, are *Phragmites australis* (PA) and *Juncus acutus* (JA). They are known to accumulate high concentrations of Zn (Caldelas et al., 2011; Mateos-Naranjo et al. 2014). Moreover, during periodic surveys, it can be observed that vegetation affects the riverbed section morphology, water velocity and, thus, erosional processes.

In mine environments, dispersion and attenuation of heavy metals can be mediated by processes occurring at the critical zone where water, sediments and biosphere meet. As the interface between surface and groundwater, the hyporheic zone of riverbed sediments is recognized as a critically important ecotone where biogeochemical reaction takes place (Byrne et al., 2010). Recently, some hydrological tracer studies probed water exchange between riverbed and hyporheic zone can be very intense (Bencala et al., 2011; De Giudici et al., 2014), this affecting the oxygen access to hyporheic zone, the biogeochemical processes, the redox interface and, overall, heavy metal dispersion.

In this study, an hydrological tracer approach (Kimball et al., 2002) was chosen to investigate the water discharge and the evolution of the metal load through the river section. The water discharge increases from 17.4 L/s to 36.7 L/s along the river. The load of Zn shows an abrupt peak of 6 kg/day after receiving tributaries from mine wastes. Then, it decreases by 10%. We notice that a particularly high tracer loss was found.

Mineralogical analysis of cores sampled along the river indicate that some relevant biogeochemical processes take place. Particularly, SEM imaging with EDS microanalysis allowed us to recognize the occurrence of micrometric framboids of pyrite. These micrometric framboids were interpreted as the process of microbial sulphate reduction and consequent formation of secondary pyrite. It is worth noting that pyrite framboids were commonly found on the surface of both PA and JA roots, at a depth from 60 to 200 cm.

Overall, the data presented in this work, indicate that processes of interaction between riverbed and PA and JA roots, are likely to play a substantial role at the hyporheic critical zone. Specifically the observed tracer loss, is higher with compared to non vegetated systems. In addition, biogeochemical processes seems to influence heavy metal mobility in the hyporheic critical zone. Ongoing research is aimed to better understand the biosphere -geosphere interaction processes and their effect.

- Bencala K.E., Gooseff M.N. & Kimball B.A. 2011. Rethinking hyporheic flow and transient storage to advance understanding of stream-catchment connections. *Water Resour. Res.*, 47, W00H03, doi:10.1029/2010WR010066.
- Byrne P., Reid I. & Wood P.J. 2010. Sediment geochemistry of streams draining abandoned lead/zinc mines in central Wales: the Afon Twymyn. *J. Soils Sediments*, 10, 683-697.
- Caldelas C., Dong S., Araus J.L. & Weiss D.J. 2011. Zinc isotopic fractionation in *Phragmites australis* in response to toxic levels of zinc. *J. Exp. Bot.*, 62, 2169-2178.
- De Giudici G., Wanty R.B., Podda F., Kimball B.A., Verplanck P.L., Lattanzi P., Cidu R. & Medas D. 2014. Quantifying biomineralization of zinc in the Rio Naracauli (Sardinia, Italy), using a tracer injection and synoptic sampling. *Chem. Geol.*, 384, 110-119.
- Kimball B.A., Runkel R.L., Walton-Day K. & Bencala K.E. 2002. Assessment of metal loads in watersheds affected by acid mine drainage by using tracer injection and synoptic sampling: Cement Creek, Colorado, USA. *Appl. Geochem.*, 17, 1183-1207.
- Mateos-Naranjo E., Castellanos E.M. & Perez-Martin A. 2014. Zinc tolerance and accumulation in the halophytic species *Juncus acutus*. *Env. Exp. Bot.*, 100, 114-121.

Fibrous minerals from Somma-Vesuvio volcanic complex

Rossi M.^{*1-2}, Nestola F.³, Ghiara M.R.¹⁻² & Capitelli F.⁴

1. Real Museo Mineralogico di Napoli, Università di Napoli "Federico II".

2. Dipartimento di Scienze della Terra, dell'Ambiente e delle Risorse, Università di Napoli "Federico II".

3. Dipartimento di Geoscienze, Università di Padova. 4. Istituto di Cristallografia, CNR, Monterotondo (Roma).

Corresponding email: manuela.rossi@unina.it

Keywords: Fibrous minerals, Somma-Vesuvio volcanic complex, morphological analyses.

A survey on fibrous minerals coming from the Somma-Vesuvio volcanic complex (Italy) was performed by means of a multi-methodological approach, based on morphological analyses, EMPA/WDS and SEM/EDS applications.

105 rock samples, belonging to the Somma-Vesuvius collection of Real Museo Mineralogico (Università degli Studi "Federico II", Naples) were investigated. The whole sample set consist in rocks of Mount Somma and Vesuvius products, *i.e.* lavas and conglomeratic and metamorphosed ejectas (1631, 1851, 1872 and 1906). Textural analyses revealing that 41% of samples are characterized by the presence of minerals with fibrous habit, found in vesicles or covering the rocks. The fibrous habit often coexists with the acicular one. The fibers are isolated, grouped or found in bundles, and in some cases simulating the acicular habit and/or showing fibrils. The average diameter of fibers observed is 2µm, while lengths are variable, with elongation ratio of 5:1 generally. In mount Somma rocks there are only fibrous crystals of kaliophilite, whereas in 1631 Vesuvius eruption we have wollastonite and vonsenite, both fibrous. In the rocks of 1851, 1872 and 1906 eruption there are only fibrous amphibole, except one sample characterized by fibrous wollastonite. The chemical amphibole composition (according to Hawthorne et al., 2012) range from potassium-rich fluoropargasite and potassium-rich fluoro-magnesium-hastingsite, covering entire spectrum between the end members. The amphiboles show Fe³⁺ ranging from 0.10 apfu up to 0.64 apfu, and these values are very similar to those observed in amphibole officially recognized as "asbestiform minerals" (0.32-0.52 apfu). Generally, the investigated amphiboles present Fe²⁺/Fe³⁺ >1 ratio, and for A-site Na/K ~1 ratio, while fluorine ranges from 1.19 apfu up to 1.79 apfu (F>Cl,OH).

This work, which for the first time describes the morphological features and crystal chemistry of Somma-Vesuvius amphiboles, updates the systematic and regional mineralogy of Somma-Vesuvius area, and also provides new data for geochemical-petrogenetic implications and materials and human sciences, reporting for the first time the fluoro-pargasite, and the fluoro-magnesium-hastingsite as fibrous minerals; moreover, it emphasizes the presence of mineral with fibrous habit in volcanic environments.

Hawthorne F.C., Oberti R., Harlow G.E., Mareach W.V., Martin R.F., Schumacher J.C. & Welch M.D. 2012. IMA Report: Nomenclature of the amphibole supergroup. *Am. Mineral.*, 97, 2031-2048.

Removal of Cr(VI) in contaminated water of Stoppani S.p.a. site (Liguria, Italy) by surface active maghemite nanoparticles

Salviulo G.*¹, Magro M.²⁻³, Baratella D.², Bonaiuto E.², Carbone C.⁴, Dinelli E.⁵ & Vianello F.²⁻³

1. Dipartimento Geoscienze, Università di Padova. 2. Dipartimento di Biomedicina Comparata e Alimentazione, Università di Padova. 3. Regional Centre of Advanced Technologies and Materials, Department of Physical Chemistry, Palacky University in Olomouc, Czech Republic. 4. DISTAV, Università di Genova. 5. Dipartimento di Scienze Biologiche, Geologiche e Ambientali, Università di Bologna.

Corresponding email: gabriella.salviulo@unipd.it

Keywords: SAMNs, Cr(VI) removal, superparamagnetic nanoparticles.

The importance of the interface between geosphere and biosphere represents one of the most fascinating frontiers of mineral science. Heavy metal release, transport and dispersion into the biosphere have a direct impact on the environment and on human health. New technologies for water and soils remediation represent a main task, and magnetic nanoparticles emerge as one of the most promising mean in this field. Environmental applications and risk assessment of manufactured nanoparticles greatly depend on the understanding of their interactions with water and soils. Novel superparamagnetic nanoparticles (Surface Active Maghemite Nanoparticles, SAMNs) constituted of stoichiometric maghemite, characterized by specific surface chemical behavior without any coating or superficial modification, stable in water for months as colloidal suspensions, were used as adsorbent of chromium(VI) in water. SAMNs can be superficially modified by simple incubation in presence of $K_2Cr_2O_7$, forming a hybrid nanomaterial, SAMN@Cr(VI), stable without any release of Cr(VI) in solution. The aim of this work is to test the efficiency of SAMNs for Cr(VI) removal from Stoppani Spa site, an extreme environmental polluted Cr(VI) site. Stoppani industry located in the Cogoleto and Arenzano Area (Genova, Italy), transformed Cr(III) from chromite mineral ($FeCr_2O_4$) (Piccardo et al., 1989) to Cr(VI). It ceased the activity at the beginning of 2003, and since 2001, the Stoppani S.p.A. has been included, with DM n.468, into the national program of environmental remediation and restoration. In the 1918-1982 period, it discharged up to 1 million tons of post-treatment mud on the neighbouring beaches, groundwater resulted heavily polluted by Cr(VI). The water samples object of this work are representative of 3 pumping wells distinguished on the basis on the Cr(VI)-content in: sample W1 ($527 < Cr(VI) < 11700$ g/l); W6 ($83800 < Cr(VI) < 146000$ g/l); W9 ($10500 < Cr(VI) < 232000$ g/l). Water temperature, electrical conductivity, alkalinity by acidimetric titration, pH, and Eh were determined during sampling. In the laboratory, waters have been analyzed for: Mg, and Ca by AAS, Na and K by AES Cl, SO_4^{2-} , and NO_3^- by ion-chromatography, Si, Fe, minor and trace elements by ICP-OES. The application of SAMNs (100 mg mL^{-1}) of three water samples removed 75-80% of Cr(VI), while, if the same treatment was accomplished at pH 3.0, Cr(VI) removal was about 95% with respect the initial concentration. Temperature, in the 4-25 °C range, did not influence Cr(VI) removal by SAMNs. A second SAMN treatment on the same water samples increased Cr(VI) removal efficiency up to 98 %, leading to a final Cr(VI) concentration below the limits stated by Italian law. SAMNs represent efficient candidates for Cr(VI) removal from aqueous polluted environments.

Piccardo G.B., Rampone E. & Scambelluri M. 1989. The alpine evolution of the Erro-Tobbio peridotites (Voltri Massif, Ligurian Alps): some field and petrographic constraints. *Ofioliti*, 13, 169-174.

Coverage intervals for trace elements in human scalp hair are site and also gender-specific

Tamburo E.*, Varrica D. & Dongarrà G.

Dipartimento di Scienze della Terra e del Mare (DiSTeM), Università di Palermo.

Corresponding email: elisa.tamburo@unipa.it

Keywords: Coverage intervals, biomonitoring, risk assessment.

Hair analysis is a powerful tool for assessing human exposure to metals and metalloids (MM). The basis for interpreting laboratory results lie on the use of coverage intervals (CI), computed between the 0.025 and 0.975 fractiles, from a well-defined group of reference individuals reflecting normal and healthy people.

A critical point in efficient use of CI, when used for comparative decision-making processes, forensic and clinic considerations, is constituted by confounding factors as the specific living site of study population and gender of participants. Our study aims to demonstrate that hair levels of trace elements are site specific and also gender specific.

We have taken into account the levels of 20 trace elements in hair samples from children of the same age (11-14 years old) residing in Sicilian sites characterized by different environmental conditions. The dataset consisted of hair samples collected within the urban area of Palermo, in several small towns located around the volcanic area of Mt. Etna and close to the industrial area of Gela.

The study was organized as follow: (a) the first part was addressed to establish whether coverage intervals for MM in human scalp hair are to be considered site specific reflecting local environmental conditions; (b) the second part was intended to provide more information about the gender effect on MM distribution in human scalp hair.

The obtained main results can be summarized as follows:

a) for many elements, the computed CIs are clearly not equivalent for the different sites, but rather the interval of an element for a site extends far beyond that one calculated for another site, suggesting that what is normal for one site may not be normal for another site. Therefore CIs are valid only for a well defined area and can hardly be extended to other areas with different characteristics.

b) CIs of several elements computed for hair samples from female subjects are statistically different from those computed for male subjects. For example, Cd, Li and Rb male coverage intervals extend far beyond those calculated for females, instead, those of Cu, Mn, Ni, Sr, V and Zn are wider for females than males. The Mann-Whitney test ($p < 0.01$) showed statistically significant differences, between males and females, for Al, Ba, Cd, Co, Cr, Cu, Mn, Ni, Pb, Rb, Sb, Se, Sr, V and Zn. Linear Discriminant Analysis indicated a clear-cut separation in terms of Sr, Ni, Zn, V, Cd, Cu, Mn, Mo and Pb levels for females and Se, Cr, As, Li, Rb and Sb levels for males. We have concluded that CI computed for human hair are to be considered gender specific and they reflect the different basal metabolism between boys and girls.

Therefore, the levels of trace elements in hair cannot strictly comparable between different areas and between subjects of different sex. This issue is particularly relevant when identification of anomalous (peculiar) environmental exposures are requested or even in detecting physiological disorders.

Historical reconstruction of heavy metal pollution in the Taranto area with dendrochemistry

Tiepolo M.*¹, Langone A.², Sacchi E.²⁻³, Nola P.³, Ficocelli S.⁴ & Giua R.⁴

1. Dipartimento di Scienze della Terra "A. Desio", Università di Milano. 2. Istituto di Geoscienze e Georisorse, C.N.R. Pavia. 3. Dipartimento di Scienze della Terra e dell'Ambiente, Università di Pavia. 4. Centro Regionale Aria, ARPA Puglia.

Corresponding email: massimo.tiepolo@unimi.it

Keywords: Heavy metals, dendrochemistry, laser ablation.

Heavy metals pollution is among the most relevant ecotoxicologic subjects of the last decades. Introduction of heavy metals in the environment, as a consequence of both natural and anthropic actions, may impact soils, waters and air with direct consequences on human health.

In order to better relate human health and environmental pollution is necessary to have precise historical archives on heavy metals distribution and variations. The most used natural archives to study atmospheric pollution and environmental quality are ice cores and lacustrine sediments. However, because of the limited diffusion, their practical use is limited. Dendrochemistry, the study of the chemical composition of tree ring, is a potential powerful natural archive for heavy metals pollution. Several studies pointed out the complexity of using tree rings as environmental markers (e.g., Garbe-Schonberg et al., 1996) for the multiple factors affecting element incorporation in wood. However, Watmough (1999) concluded that although not all the tree species are suitable to be used for dendrochemistry, useful information on the level of heavy metals in the environment can be obtained from tree ring analysis.

Here, we investigated the potential of dendrochemistry to track historical variations in heavy metal concentrations in one of the most industrialized areas of Southern Italy, the Taranto area, which is affected by severe contamination by heavy metals. *Pinus pinaster Aiton* cores were sampled at increasing distances from the industrial area and then characterized for relative chronology. The most preserved and well-developed cores were analyzed for heavy metal concentrations with laser ablation (LA)-ICP-MS.

Investigation of heavy metal variations with time reveals the presence of well identified concentration peaks, suggesting a direct relation with an emission event. For many elements these peaks correspond in time to the different phases of upgrade of the steel plant, thus suggesting a direct relation between the industrial history, environmental contamination and tree response. Notwithstanding, for some elements the correspondence between tree recording and historical reconstruction is weak, possibly in relation to elemental translocation.

Preliminary data, suggest that dendrochemistry may give a valid support in the historical reconstruction of heavy metal pollution. However, in order to precisely constrain the timing of the pollution events and in turn allow a more rigorous application of the methodology, eventually with forensic applications, more detailed studies on elemental mobility are required.

Garbe-Schönberg C.D., Reimann C. & Pavlov V.A. 1997. Laser ablation ICP-MS analyses of tree-ring profiles in pine and birch from N Norway and NW Russia – A reliable record of the pollution history of the area? *Environ. Geol.*, 32(1), 9-16.

Watmough S.A. 1999. Monitoring historical changes in soil and atmospheric trace metal levels by dendrochemical analysis. *Environ. Pollut.*, 106, 391-403.

Influence of industrial activity on metal and metalloid contents in scalp hair of adolescents

Varrica D. *, Tamburo E. & Dongarrà G.

Dipartimento di Scienze della Terra e del Mare (DiSTeM), Università di Palermo.

Corresponding email: daniela.varrica@unipa.it

Keywords: Metals in human hair, human biomonitoring, environmental geochemistry.

Petrochemical industries represent a controversial although important economical resource. They offer a great deal of *job* opportunities producing also a development of several areas. However, such kind of industrial plants are responsible for the change of the environmental background through the emission of toxic pollutants such as metals-metalloids and organic compounds. People living in cities close to such industrial plants are particularly exposed to a severe environmental decline, which implies the deterioration of the quality of air, soil, water and food with the consequent human health concerns.

The municipalities of Gela (GL) and Pace del Mela (PM), located respectively along the Mediterranean southern coast and Tyrrhenian northern coast of Sicily, hosting large petroleum refineries, have been declared “areas at high risk of environmental crisis”, since 1986. The purpose of this study was to assess whether the degree of human exposure to trace elements in young subjects living in these towns may be revealed by hair analysis. Nineteen elements (Al, As, Ba, Cd, Co, Cr, Cu, Fe, Li, Mn, Mo, Ni, Pb, Rb, Sb, Se, Sr, U, V and Zn) were analysed by inductively coupled mass spectrometry (ICP-MS) in 245 samples of human scalp hair collected from adolescents (11-14 years old) of both genders. The obtained results were compared with those from other less polluted areas.

The distributions of Al, As, Ba, Cd, Cu, Mo, Ni, Sr, U, V and Zn pointed to a common origin of these elements, likely related to the petrochemical plants and to collateral anthropogenic activities, confirming findings of other authors carried out at Gela on samples of pine needles and road dust showing high concentrations of V, Ni, As near the industrial plants and Zn, Pb, Sb and Cu in the vicinity of the urban area. Other studies performed on lichen samples, soils and fruit products at Pace del Mela showed anomalies for As, Cr, Pb, Zn, Ni and V, as well as human biomonitoring studies conducted on blood and urine samples, at GL and PM, showed accumulation of As, Ni, Cr and Cd.

Our data were compared to those from the urban center of Palermo (Sicily), where a similar study was conducted on young students of the same age. The results suggested that Al, Ba, Li, Mo, Rb, Sb, Se and Zn are comparable, whereas As, Cr, Mn, Sr, U and V are higher in the industrial areas than in Palermo city. Linear discriminant analysis (LDA) indicated an industrial factor made up As, Sr, U and V, and a second factor, concerning the urban site, characterized by Cd, Cu, Ni, and Mo.

The results obtained in this study evidence the dispersal of heavy metals close to petrochemical plants and also confirm that hair analysis can be used as a screening procedure where environmental exposure are of concern.

Active real-time analyzers vs. passive/diffusive samplers for hydrogen sulfide (H₂S) in air: a critical comparison

Venturi S.*¹⁻², Cabassi J.¹⁻², Tassi F.¹⁻², Capecchiacci F.¹⁻², Vaselli O.¹⁻², Bellomo S.³ & Calabrese S.⁴

1. Dipartimento di Scienze della Terra, Università di Firenze. 2. Istituto di Geoscienze e Georisorse, CNR, Firenze
3. INGV, Palermo. 4. Dipartimento di Scienze della Terra e del Mare, Università di Palermo.

Corresponding email: stefania.venturi@unifi.it

Keywords: Air quality, passive monitoring, hydrogen sulfide analyzer.

Hydrogen sulfide (H₂S) is a gas pollutant discharged in air from a large number of natural and anthropogenic sources. Its peculiar rotten-egg smell, causing odor nuisance to neighboring communities, is detectable at concentrations between 0.7 and 42 µg/m³ (Schiffman & Williams, 2005). High H₂S concentrations could cause eye irritation, damage to the upper respiratory apparatus and loss of smell. The effects of long-term low level (< 2,800 µg/m³) exposures to H₂S are still matter of debate (Bates et al., 2013). Hence, the development of techniques for accurate measurements of H₂S in air at a wide range of concentrations is a primary issue in environmental monitoring. Two different approaches are currently used: 1) passive samplers and 2) real-time measurements. The latter are generally expensive and require a power supply. On the contrary, passive samplers are low cost and can be deployed in the field with minimal maintenance. Therefore, passive samplers offer an appealing alternative to real-time measurements, especially for regional-scale monitoring. However, the reliability of passive samplers in outdoor applications strongly depends on several environmental factors, such as temperature, humidity and wind speed (Delgado-Saborit & Esteve-Cano, 2006). In this study a comparison between H₂S measurements using diffusive radial-type passive samplers (Radiello) and a real-time gas analyzer (Thermo Scientific Model 450i) based on pulsed fluorescence, is presented. The measurements were carried out in areas affected by both anthropogenic and natural sources using both techniques. The results show substantial differences. The passive samplers systematically produce higher H₂S concentrations than those of the active analyzer. The relative error was up to > 1,000% for concentrations < 7 µg/m³ and exposure duration ≥ 2 hours. H₂S measurements by Radiello were affected by meteo parameters (wind, rain, humidity, temperature). The efficiency of this method was demonstrated to be also strongly dependent on H₂S concentrations. In addition, passive samplers give an average concentration value for the exposure period, but are not able to detect short-term H₂S increments. These results show that the use of passive samplers for environmental monitoring should thus be limited to preliminary large-scale semi-quantitative assessment. A reliable study on the dispersion dynamics of contaminants in air cannot exclude the acquisition of high-frequency data through active analyzers.

- Bates M.N., Garrett N., Crane J. & Balmes J.R. 2013. Associations of ambient hydrogen sulfide exposure with self-reported asthma and asthma symptoms. *Environ. Res.*, 122, 81-87.
- Delgado-Saborit J.M. & Esteve-Cano V. 2006. Field study of diffusion collection rate coefficients of a NO₂ passive sampler in a Mediterranean coastal area. *Environ. Monit. Assess.*, 120, 327-345.
- Schiffman S.S. & Williams C.M. 2005. Science of odor as a potential health issue. *J. Environ. Qual.*, 34, 129-138.

Tremolite asbestos: characterization by analytical electron microscopy, Raman spectroscopy and PCA data elaboration

Vigliaturo R.*¹, Giorelli M.², Tagliaferro A.² & Belluso E.¹⁻³

1. Dipartimento di Scienze della Terra, Università di Torino. 2. DISAT, Politecnico di Torino.

3. Istituto di Geoscienze e Georisorse, CNR, Torino.

Corresponding email: ruggero.vigliaturo@unito.it

Keywords: Transmission electron microscopy, tremolite, principal component analysis.

Tremolite $\text{Ca}_2\text{Mg}_5\text{Si}_8\text{O}_{22}(\text{OH})_2$ is a member of the calcic amphibole group of silicate minerals and it is classified asbestos when grown as fiber with length $> 5 \mu\text{m}$, width $< 3 \mu\text{m}$ and ratio length/width > 3 . In this work asbestos fibers were characterized by Raman Spectroscopy, field emission scanning electron microscope (FeSEM) and transmission electron microscope (TEM), both microscopes equipped with an energy dispersion microanalysis system (EDX). Given its importance from the health point of view, foreseeing subsequent study on its transformations inside the biological environment, it is important to characterize the starting natural material using multiple and complementary analytical techniques. Appropriate knowledge of the base material obtained by a multiple technique approach overcome weakness of a single technique approach and allows to better follow the evolution in biological environments. As a matter of fact our approach reveals unexpected presence of different phases, both as defects and/or contaminants in the sample. Raman spectroscopy and FeSEM-EDX provided useful information (e.g. presence of hydroxyl anions, morphological and chemical semi-quantitative data). TEM-EDS investigations were performed on two levels to allow collection of morphological, dimensional (diameter, length and their ratio), and chemical semi-quantitative data on 100 single fibers. Representing an high number of data, we used principal component analysis (PCA) as a tool that allows to better interpret data containing a lot of variables (8 for each single fiber) with the possibility to highlight for example the typical amphiboles Mg/Fe substitution in the octahedral site. The second level of analyses was performed with a punctual approach through the collection of selected area electron diffraction patterns (SAED) and high resolution imaging (HRTEM). It showed high crystallinity of the fibers, and highlighted crystal structures details such as structural defects.

PM₁₀ emission near the Mt. Amiata geothermal field

Zoppi M.^{*1-2}, Pratesi G.¹, Capecchiacci F.¹, Cabassi J.¹, Marchionni S.¹, Tassi F.³, Vaselli O.¹,
Giannini L.³, Venturi S.¹, Ulivi M.¹, Forni F.⁴, Scodellini R.⁴ & Tommasini S.¹

1. Museo di Storia Naturale, Università di Firenze. 2. Dipartimento di Scienze della Terra, Università di Firenze
3. Istituto di Geoscienze e Georisorse, C.N.R. Firenze. 4. Regione Toscana, Settore energia, tutela della qualità dell'aria e dall'inquinamento
elettromagnetico e acustico.

Corresponding email: matteo.zoppi@unifi.it

Keywords: Aerosol, geothermal, micro-Raman.

Ambient air PM₁₀ collected in the geothermal area of Piancastagnaio town, Siena province, Italy, was studied employing extensively Raman micro-spectroscopy with the help of scanning electron microscopy (SEM). Particulate matter was collected between the fall 2013 and the fall of 2014 according to the project Patos II of the Regione Toscana. In the area under investigation two geothermoelectric industrial plants of ENEL S.p.A are present along with natural wells and a pipeline system. This work represents a first effort aiming to understand the nature of ambient aerosol related to geothermal emissions and their deployment, and provides a useful starting point for taking into account the potential impact of such aerosol on human health. The nature of the solid fraction related to the geothermal emissions was studied collecting Raman spectra of more than a thousand particles, randomly selected, and identifying their mineralogical composition. On the total by number, the majority of particles belong to the group of sulphates (56.1%), followed by soot (21.8%), nitrates (5.0%), silicates (3.6%), oxides (3.6%), carbonates (3.0%) and others (6.9%). Among sulphates the 38.7%, by particles number, is due to mascagnite [(NH₄)₂SO₄], 13.8% to a not well characterized phase "matteuccite-like" (NaHSO₄·H₂O), 13.8% to gypsum, 10.1% to Na₂SO₄(III), 8.9% to letovicite [(NH₄)₃H(SO₄)₂], and 3.9% to barite (BaSO₄), being the ammonium and sodium cations largely abundant. Particles of sulphates exhibit dimensions typical of the secondary aerosol and, even if their presence is highly variable during the days of sampling, there is a rough inverse correlation between the pairs mascagnite plus letovicite and matteuccite-like plus Na₂SO₄(III). Even though the presence of mascagnite and letovicite has been detected in polluted urban areas the high amount of ammonium and sodium sulphates found in Piancastagnaio town, along with their peculiar proportions, represents a particular kind of aerosol strictly related to the geothermal emission.

SESSION S15

The geosciences for Cultural Heritage and Archeometry: consolidated and innovative approaches

CONVENORS

Isabella Memmi Turbanti (Univ. di Siena)

Celestino Grifa (Univ. Sannio)

Mauro La Russa (Univ. della Calabria)

Geosciences and the Cultural Heritage: the time line of human activities

Artioli G.

Dipartimento di Geoscienze, Università di Padova.

Corresponding email: gilberto.artioli@unipd.it

Keywords: Cultural Heritage, archaeometry, conservation.

The scientific investigation of cultural heritage materials and problems is broadly focused on diagnostics (i.e. knowledge acquisition) and/or conservation purposes. Both archaeometry and conservation science share not only common conceptual and experimental tools, but also the general scope of projecting the investigated human activities and their product into a time line, so that the measured data and the derived understanding of the analysed material evidence (from objects to landscapes) needs to be extrapolated into the past (i.e. archaeometry) or the future (i.e. conservation). Since tangible (and intangible) cultural heritage contemplates the whole spectrum of human experience, studies of cultural heritage materials are at the same time extremely fascinating but also very demanding and intrinsically complicated.

Many disciplines within the geosciences, having a basic perception of natural materials and processes at different space scales and a reasonable understanding of the evolution of physico-chemical systems (i.e. kinetics) at different time scales, are bound to have a significant and increasing role in cultural heritage studies. Specific examples of multi-scale analysis of artworks and archaeological sites will be discussed. It is argued that the specific needs of cultural heritage investigations require very high standards of competence, ingenuity, and a great deal of cross-disciplinary activity. Academia may well supply competence and ingenuity, although clearly a entirely different degree of cultural awareness is needed by economical and political managements.

Preliminary archaeometric investigations on ancient mortars from archaeological site of Velia (Salerno, Southern Italy)

Balassone G.¹, Cicala L.², D'Orazio L.³, De Bonis A.¹, De Rosa F.², Guarino V.*¹, Morra V.¹ & Tardugno M.L.²

1. Dipartimento di Scienze della Terra, dell'Ambiente e delle Risorse, Università di Napoli "Federico II". 2. Dipartimento di Studi Umanistici, Università di Napoli "Federico II". 3. Istituto per i Polimeri, Compositi e Biomateriali, CNR, Pozzuoli.

Corresponding email: vincenza.guarino@unina.it

Keywords: Elea-Velia, Campania, mortars.

Elea-Velia is an important Greek colony of *Magna Graecia*, founded by the inhabitants of *Phocaea* (Turkey), in the last quarter of the sixth century BC. The town, known for the Philosophical School of Parmenides and Zeno, develops considerably between the Classical and Hellenistic age, preserving, in Roman period, an important role in the medium and lower Tyrrhenian sea. The *Masseria Cobellis* building, recently investigated by this research team, is one of the most interesting examples of public architecture during the Roman period of the town. This complex is built on the site of a natural spring. It presents in its last phase of construction, dating to the end of the first century AD, a large rectangular open area, bordered by porticoes, with a *nymphaeum* and an aula in axial and highlighted position. The building seems to rework some models also popular in Campania during the early Imperial age, pointing features of the local architectural repertoires and the new élites' needs. The building, whose interpretation is still debated, could have a religious character, due to the presence of natural spring, but it is not ruled out a link with the cult of the Imperial Family. The complex shows construction techniques in different phases of its building, that may indicate the activity of different workers. As a matter of fact, for other buildings of Velia (*Insula II*) it has been suggested the presence of workers from Campania. Then the sampling of the mortar was initiated on masonry structures of the various construction phases to analyze the building site organization and verify the use of different binders. It is worth noting that mortars may supply with important information on the constructive history of ancient stony buildings, as well as on local raw materials used to make them. Mortar samples were investigated by means of XRD, SEM-EDS, OM, XRF and TGA techniques. Macroscopically, mortars vary in color from light gray, to creamy white and to light yellow; they can be friable to very hard. Preliminary mineralogical and petrographic characterization show that the Velia mortars can be subdivided into two groups, i.e. the calcite-bearing and the calcite-free samples. Mortars of the first group are composed by a mixture of variable amounts of quartz, K-feldspar, micas, illite and likely analcime. In the calcite-bearing samples, calcium carbonate occurs together with quartz, K-feldspar, Na-feldspar, illite, micas, and locally trace of gypsum, kaolinite, clinopyroxene, and likely phillipsite. Observation under polarized optical microscopy provided information about the various types of components forming the aggregates and the porosity of the investigated samples. Clues for provenance studies, also extended to probable limestone caves used for the preparation of mortars components, will also be discussed.

Heavy metals in black crusts on limestones as markers of environmental conditions influencing human health

Barca D.*¹, Perez-Monserrat E.M.², Török A.³, Aly N.⁴, Gomez-Heras M.², Fort R.², Varas-Muriel M.J.², Alvarez de Buergo M.², Valeria C.⁵ & Ruffolo S.¹

1. Dipartimento di Biologia, Ecologia e Scienze della Terra (DiBEST), Università della Calabria. 2. Departamento de Geomateriales, Instituto de Geociencias IGEO (CSIC, UCM), Madrid, España. 3. Department of Construction Materials and Engineering Geology, Budapest Technical University, Hungary. 4. Department of Science and Mathematics, Faculty of Petroleum and Mining Engineering, University of Suez, Egypt. 5. Dipartimento di Scienze Biologiche, Geologiche e Ambientali, Università di Catania.

Corresponding email: empmon@geo.ucm.es

Keywords: Air pollution, stone decay, LA-ICP-MS technique.

Black crusts develop on cultural heritage materials as a consequence of air pollution. This paper presents data from samples covering a wide range of locations in terms of climate and pollution levels. Consequently, the morphological, mineralogical and chemical characterization of black crusts on limestone from historic buildings of Cairo, Milano, Budapest and Madrid has been carried out in addition to suspended and settling particulate matter analysis. By means of traditional techniques, such as POM, XRD, SEM-EDS and FT-IR, combined with innovative application of laser ablation inductively coupled plasma mass spectrometry (LA-ICP-MS), a complete characterization in terms of trace elements distribution (including heavy metals) from the black crusts and host limestone has been achieved. Some of the studied areas display high levels of pollutants and important concentration of heavy metals (Cd, Cu, Pb, Ni, Zn) in suspended dust (El-Bady, 2014). High concentration of gypsum within laminar and dendritic black crusts was recorded, with increased amount of different elements and metals (Si, Al, Ti, Fe) derived from atmospheric inputs and, in particular, by anthropogenic pollution; siliceous fly-ash particles are more common than carbonaceous ones in dust samples and mineral fragments representing windblown particles were also detected (Perez-Monserrat et al., 2011; Török et al., 2011). Heavy metals content (Pb, Zn) are higher in black crusts than in substrates, confirming the influence of polluted atmospheres on their formation. Moreover, some specific heavy metals tend to migrate from the crust to the unaltered stone, becoming catalysts for new crust (Barca et al., 2014; La Russa et al., 2014). Black crusts composition is proposed as a marker of major combustion sources responsible for stone decay and of the changes on the fuels used over time. The study of black crusts is presented as a marker of air quality with implications for human health, as trace element concentration is directly related with environmental conditions.

- Barca D., Comite V., Belfiore C.M., Bonazza A., La Russa M.F., Ruffolo S.A., Crisci G.M., Pezzino A. & Sabbioni C. 2014. Impact of air pollution in deterioration of carbonate building materials in Italian urban environments. *Appl. Geoch.*, 48, 122-131.
- El-Bady M.S. 2014. Road Dust Pollution by Heavy Metals along the Sides of Expressway between Benha and Cairo, Southern of Nile Delta, Egypt. *J. Appl. Environ. Biol. Sci.*, 4, 177-191.
- La Russa M.F., Belfiore C.M., Comite V., Barca D., Bonazza A., Ruffolo S.A., Crisci G.M., Pezzino A. 2013. Geochemical study of black crusts as a diagnostic tool in cultural heritage. *Appl. Phys. A*, 113, 1151-1162.
- Perez-Monserrat E.M., Varas M.J., Fort R. & de Buergo Alvarez M. 2011. Assessment of different methods for cleaning the limestone facades of the former workers Hospital of Madrid, Spain. *Stud. Conserv.*, 56, 298-313.
- Török Á., Licha T., Simon K. & Siegesmund S. 2011. Urban and rural limestone weathering: the contribution of dust to black crust formation. *Environ. Earth Sci.*, 63, 675-693.

Element distribution within the cementitious matrix of pozzolanic roman mortars: a new approach using image processing via x-ray map analyser

Belfiore C.M.*¹, Fichera G.V.², Ortolano G.¹, Pezzino A.¹ & Visalli R.¹

1. Dipartimento di Scienze Biologiche, Geologiche e Ambientali, Università di Catania. 2. Laboratorio Arvedi di analisi diagnostiche non invasive dell'Università di Pavia, Museo del Violino, Cremona.

Corresponding email: cbelfio@unict.it

Keywords: Pozzolanic mortars, hydraulic phases, X-Ray-Map-Analyser.

A new semi-automated image processing procedure has been here used to compute the element distribution between and within specific phases, recognised inside a hydraulic Roman mortar sample. This new tool package, based on the semi-automated combined use of the Principal Component Analysis (PCA) and of the supervised Maximum Likelihood Classification (MLC) of X-ray maps, is largely centred on functions implemented in ArcGis® (Ortolano et al., 2014). These functions are able to highlight, for instance, the local reaction phenomena responsible for the compositional variability within the same phase, and also allow to combine different primary outputs useful to extrapolate complex reaction indexes (e.g. Hydraulicity Index - HI, Boynton, 1980).

Three different micro-domains were selected within the investigated archaeological mortar, whose hydraulic properties were reached by mixing an aerial lime with a pozzolanic aggregate from the Alban Hills. Attention has been here focused on the cementitious matrix in order to assess the distribution of hydraulic phases within the investigated domains. To this aim, three different X-Ray map arrays have been acquired with a SEM-EDS device at 1024*800 pixel resolution with a magnification closely ranging from 120 to 230X.

Starting from these EDS X-ray maps, the procedure included two different cycles of analysis: the first processed the entire selected domain in order to classify all the recognisable components (cementitious matrix, aggregate and pores); the second allowed to investigate in more detail the element distribution within the cementitious matrix to put into evidence the effect of the differential hydraulic reactions that develop between pozzolanic aggregate and hydrated lime. In addition, the application of the kernel density function permitted us to obtain the density distribution of Ca, Al, Si, Mg, K and Fe within the cementitious matrix. The use of raster calculator functions allowed then to obtain further derived maps showing, for instance, the variability of the HI within the three selected domains.

Obtained results highlight as the used tool package proved to be powerful in the study of pozzolanic mortars since it provides a simple visualization of the newly formed phases and their distribution within a restricted but compositionally complex system.

Boynton R. 1980. Chemistry and technology of lime and limestone, 2nd Edition. John Wiley & Sons, New York.

Ortolano G., Zappalà L. & Mazzoleni P. 2014. X-Ray Map Analyzer: a new ArcGIS® based tool for the quantitative statistical data handling of X-ray maps (Geo- and material-science applications). *Comput. Geosci.*, 72, 49-64.

The carbonate building stone of the Ortygia Island (Syracuse, Italy): characterization and decay processes

Belfiore C.M.*¹, Fichera G.V.², Pezzino A.¹, Ruffolo S.³, Calabrò C.¹, Maniscalco R.¹ & Malagodi M.²

1. Dipartimento di Scienze Biologiche, Geologiche e Ambientali, Università di Catania. 2. Laboratorio Arvedi di analisi diagnostiche non invasive dell'Università di Pavia, Museo del Violino, Cremona. 3. Dipartimento di Biologia, Ecologia e Scienze della Terra, Università della Calabria.

Corresponding email: cbelfio@unict.it

Keywords: Carbonate stones, decay, textural features.

During the XVIII century, the historic centre of Syracuse (*Ortygia*) was interested by intense building activity, which took place after the severe earthquake of 1693. Ortygia and the other cities of the Hyblean area (south-eastern Sicily) were characterized by a close relationship between building stone and geological context, since the wide use of local calcarenites characterized and defined their urban planning and architecture.

This contribution, dealing with the study of limestones used in the historic buildings of Ortygia, is part of a wider research project aimed at the characterization of different types of carbonate rocks, employed in the Baroque architecture of the Hyblean area, and their decay processes. Different shades of colour and textural features characterize the Ortygia façades, due to the use over time of several types of limestone taken out from diverse extraction sites or different layers of quarrying. Specifically, six local calcarenites, belonging to four geological formations (Monti Climiti Formation: *Pietra di Siracusa* and *Pietra Bianca di Melilli*; Carrubba Formation: *Calcare a lumachelle* and *Calcare oolitico*; Palazzolo Formation: *Pietra di Noto*; Panchina pleistocenica: *Pietra giuggiulena*), were used both as structural component and decorative element in the historic buildings. These carbonate rocks have different chemical, physical and mechanical characteristics which lead, over time, at different and more or less intense alteration and degradation processes of the façades.

Here, we focus on the study of *Pietra di Siracusa*, *Pietra Bianca di Melilli*, *Calcare oolitico* and *Pietra giuggiulena*, through the analysis of rock samples collected from historical quarries. These four lithotypes underwent mineralogical-petrographic and physical-mechanical investigations with two aims: 1) to frame the different types of limestone used in the historic centre of Syracuse; b) to individuate the causes responsible for long or short term durability of each limestone when placed in the same outdoor environment at identical climatic conditions. The obtained results were also compared with literature data concerning the other two limestones (*Noto stone* and *Calcare a lumachelle*) used in the façades of historic buildings in Ortygia, whose behaviour with respect to weathering is markedly different. Results obtained are consistent with deterioration types observed in the monuments, and highlight the close relationship between textural characteristics of the stone and its damage. In addition, such information are extremely useful for both the safeguard of monuments and their restoration.

Preliminary chemical and mineralogical characterization by non-invasive analytical techniques of the *fibula di Montieri* from the archaeological site of the Canonica di S.Niccolò (Montieri, GR)

Bianchi G.¹, Mitchell J.², Agresti J.³, Osticioli I.³, Siano S.³, Memmi Turbanti I.*⁴ & Pacini A.⁵

1. Dipartimento di Scienze Storiche e dei Beni Culturali, Università di Siena. 2. School of Art History and World Art Studies, University of East Anglia, UK. 3. Istituto di Fisica Applicata "Nello Carrara", C.N.R. Firenze. 4. Dipartimento di Scienze Fisiche, della Terra e dell'Ambiente, Università di Siena. 5. Libero professionista.

Corresponding email: isabella.turbanti@unisi.it

Keywords: Fibula from Montieri, Portable Raman and XRF, medieval jewels.

The archaeological excavations begun in 2009 on one of the terraces of the hill at Montieri (GR) brought to light the remnants of a religious complex, built between the XI and XII century AD, probably to be identified as the Canonica di S.Niccolò, a foundation of the bishop of Volterra. Inside the church, a splendid *fibula* in gold and precious stones was recovered from its original place of deposit. It was placed in a hollow beneath the pavement at the centre of the building, probably during a ritual related to the foundation of the church. The church, a structure of unusual design, characterized by six circling apses, was built in the first decades of the XI century. The subsequent development of the site closely parallels the development of Montieri, founded to control and extract ore minerals abundant in the Colline Metallifere region.

The brooch is a domical gold disc, with a setting of translucent colored enamel embellished with a central red stone (most likely garnet), amethysts, and opaque glass beads. The surrounding surfaces are filled with dense configurations of branching gold filigree.

Comparisons with iconographic parallels and with some of the rare surviving brooches of similar type, indicate a date for the Montieri fibula at the first half of the XI century. This is supported by archaeological evidence. A particular feature of the Montieri brooch are patterns which appear to have their origins in Islamic art.

The brooch has been subjected to preliminary analyses using portable and non-invasive Raman and XRF. The Raman spectrum of the central stone shows vibrational bands characteristic of the mineral almandine, whereas analysis of the pinkish-violet lateral stones points to the amethyst variety of quartz. The Raman spectra of the white stones and the enamel show very wide vibrational bands typical of glass compounds.

XRF measurements indicate that the brooch's gold alloy is a ternary one consisting of gold, silver, and copper, in concentrations (Au 93 wt.%, Ag 4 wt.%, Cu 3 wt.%) which were measured using the fundamental parameters of XRF analysis, taking into account the excitation spectrum of X ray tube. A analysis of the *cloisonné* enamel led to the identification of the characterizing elements of the pigments and the opacifying agents. The green glaze is characterized by a high concentration of Cu e Sb with traces of Sn, whereas the blue glaze contains a high concentration of Co e Pb. The elements Fe, Mn, Ca, K, Sr and Ti are present in similar concentrations.

Analysis of the pinkish-violet stones revealed only traces of Fe. This substantiates the Raman analysis, indicating quartz, in which Fe impurities contribute to the color of amethyst variety.

Analysis of the white stones revealed the characteristic peaks of Ca, K, Sr and Pb and an elevated concentration of Sb. This suggests that it is a glass opacified with calcium antimoniate. The presence of intense peaks of Fe on the central red stone's XRF analysis confirm the Raman results.

Innovative conservative strategies applied in Herculaneum archaeological site (Naples, Italy): the case of *Villa dei Papiri*

Comite V.¹, La Russa M.F.¹, Ricca M.¹, Rovella N.*¹, Ruffolo S.A.¹, Urzì C.², Arcudi A.³ & Silvestri C.³

1. Dipartimento di Biologia, Ecologia e Scienze della Terra, Università della Calabria. 2. Dipartimento di Scienze Biologiche ed Ambientali, Università di Messina. 3. Conservazione Beni Culturali (C.B.C.), Roma.

Corresponding email: natalia.rovella@unical.it

Keywords: Nanoparticles, plasters, degradation.

Herculaneum ruins and their associated villas, represent one of the most important and best preserved memorials of ancient Roman life. This important town was covered by a series of pyroclastic surges and flows from the famous eruption of Vesuvius in 79 A.D. that destroyed also Pompeii.

Nowadays many buildings of the area are affected commonly by alteration and decay phenomena threatening their stability and conservation. In this regard, the Villa dei Papiri is one of the most impressive examples of architecture in Herculaneum and existing before the volcanic eruption of 79 A.D. It was discovered almost by accident in April 1750 during the digging of a well. The stone materials constituting the building show decay phenomena.

This research was focused on the plasters from walls located outside the villa, which suffer strong biodeterioration phenomena and salt efflorescence. The characterization of the plasters and their degradation phases allowed us to determine the state of conservation of such materials and identify the biological species. It has been monitored the microclimatic parameters of the area in order to correlate them to the degradation patterns. Plaster specimens, having similar composition of the original ones, have been prepared in laboratory and coated with photoactive nanoparticles with bio-protective features, and placed next to the original plasters in a sample holder. The biological activities of the sample surfaces have been monitored over time in order to assess the bio-inhibition of treatments in a specific microclimatic condition. Results allowed to identify the most suitable material to be applied on the original plaster, in a second stage experimentation.

This research is funded by POR Calabria FESR project "NANOPROTECH" (NANO PROtection TEchnology for Cultural Heritage).

Multidisciplinary approach to characterize degradation products and archaeological materials from Roman *Thermae* of Reggio Calabria (Calabria, South Italy)

Comite V.¹, Ricca M.*¹, Rovella N.¹, Ruffolo S.A.¹, Bonazza A.², Sardella A.², Urzi C.³, Arcudi A.⁴ & Silvestri C.⁴

1. Dipartimento di Biologia, Ecologia e Scienze della Terra, Università della Calabria. 2. Istituto di Scienze dell'Atmosfera e del Clima, CNR, Bologna. 3. Dipartimento di Scienze Biologiche e Ambientali, Università di Messina. 4. C.B.C. Conservazione Beni Culturali.

Corresponding email: michela.ricca@unical.it

Keywords: Reggio Calabria, Roman *Thermae*, archaeological materials.

In this multidisciplinary contribution, several diagnostic tests were carried out in order to characterize the archaeological materials, as well as the alteration and degradation products present in the Roman *Thermae* of Reggio Calabria (Calabria, South Italy). Founded between the I and II century B.C., this archaeological area represents one of the greatest evidence of Roman architecture and it includes ancient imperial ruins of thermal sources. The imperial bath complex was built around three principal rooms: the *calidarium* (hot bath), the *tepidarium* (warm bath) and the *frigidarium* (cold bath), which were connected through different entrances to a central room. The latter is decorated by a suggestive Roman floor mosaic in geometric design, with black and white *tesserae*, dating between the II and III century A.D. Fragments of several archaeological materials, such as brick, limestone and marble, have been studied with different and complementary techniques. In particular polarized optical microscopy, scanning electron microscopy with energy-dispersive spectroscopy and laboratory biological culture analysis were performed in order to characterize the materials employed to construct the site, evaluate their state of preservation and identify the microorganisms composing the biological patinas. Results allowed us to define suitable restoration procedures, in terms of cleaning method, biocide and consolidating products, applied to the stone materials.

Multi-technique spectroscopic investigation in Cultural Heritage

Crupi V.*¹, Majolino D.¹, Pezzino A.², Ruffolo S.³ & Venuti V.¹

1. Dipartimento di Fisica e di Scienze della Terra, Università di Messina. 2. Dipartimento di Scienze Biologiche, Geologiche e Ambientali, Sezione di Scienze della Terra, Università di Catania. 3. Dipartimento di Biologia, Ecologia e Scienze della Terra (DiBEST), Università della Calabria.

Corresponding email: vcrupi@unime.it

Keywords: TOF-ND, SR-XAS, decorated pottery.

As is well established, the archaeometric research in cultural heritage is a multidisciplinary work. Therefore, a complete and correct investigation needs to join different points of view and several qualified expertise, ranging from chemistry to physics, from geology to biology. The archaeological considerations are important to classify the aesthetic style of an artwork and hypothesize the possible historical and geographical context in which it has to be framed. This approach helps to understand the meaning and the sense of the object in the artist's mind, in order to point out the problem we are requested to solve. Nevertheless, the scientific investigation allows to unambiguously characterize the materials and provide information about the manufacture techniques, the production site, the historical age of the artifact.

Here, we present a twofold innovative investigation with the main goal to characterize, from one hand, the ceramic body of ancient Sicilian pottery fragments and on the other hand the decorated surface of the pottery. In particular we report on a non-destructive study performed by Time of Flight Neutron Diffraction (TOF-ND) technique on "proto-majolica" pottery fragments dated back to the 12th to 13th centuries AD, coming from South Italy (Milazzo and Messina, Sicily), with the aim of quantitatively investigate the mineral phase contents of the ceramic bulk. The adopted procedure was absolutely non-destructive, so that measurements were performed on the entire fragments without any sampling. The information derived, by applying the Rietveld analysis method, allowed us to formulate hypotheses concerning the fabrication processes of the artefacts.

Furthermore, we also present a non-destructive analysis of ancient potteries performed by SR X-ray absorbance spectroscopy in order to characterize the pigmented surface of pottery shards excavated from the archeological site of Caltagirone (Sicily), a well-known ceramic production center. Aesthetical criteria and morphological observations allowed us to attribute the samples to quite different historical periods, starting from the 18th century B.C. up to the 16th century A.D. An extensive time interval led us to suppose that different materials and techniques were used for the production of the ceramic paste and also for the preparation of pigments. XAS measurements were performed at the Cu and Fe K-edges.

Radiocarbon dating of heavily altered bone apatite from the Al Khiday archaeological site (Central Sudan): is pristine apatite carbonate preserved?

Dal Sasso G.*¹, Maritan L.¹, Angelini I.¹, Usai D.², Salvatori S.², Zerboni A.³ & Artioli G.¹

1. Dipartimento di Geoscienze, Università di Padova. 2. Centro Studi Sudanese e Sub-Sahariani (CSSeS), Treviso.
3. Dipartimento di Scienze della Terra "A. Desio", Università di Milano.

Corresponding email: gregorio.dalsasso@studenti.unipd.it

Keywords: Bioapatite, radiocarbon dating, Sudan.

Human bones, frequently recovered from archaeological contexts, represent a valuable source of information on the past life of ancient populations. However, the reliability of such information depends on the preservation state of bone material. Bone is constituted by the association of an organic matrix and bioapatite nanocrystals, the composition of which resembles that of hydroxyapatite, but it considerably departs from stoichiometry, as several types of ionic substitutions occur in the crystal structure. When buried, bones undergo taphonomic and diagenetic processes, causing the alteration of their organic and mineral constituents.

This research is addressing the radiocarbon dating, and the assessment of results reliability, of heavily altered human bones coming from the archaeological site 16D4 - Al Khiday 2 (Central Sudan), where a multi-stratified cemetery was excavated and several burial phases were recovered: the site was used as a burial ground at different periods along the Holocene. Collagen deterioration, bioapatite recrystallization, microbially mediated alteration and secondary mineral phases precipitation were detected among samples.

Radiocarbon dating of altered bones, in particular when collagen completely lacks, may represent a challenging task. An alternative source of ¹⁴C for bone dating can be found in the carbonate ions incorporated in the bioapatite crystals, but diagenetic alterations can significantly affect the ¹⁴C determination. The well-defined archaeological context provided a set of samples suitable to investigate the reliability of the radiocarbon dating of bioapatite as well as the influence on bone diagenesis of environmental/climatic changes, occurring in Central Sudan along the Holocene. Therefore, a multi-disciplinary study on bones and associated soil sediments has been carried out, in order to provide a model for bone diagenesis, taking into account pedogenic processes and changes in environmental, climatic and local burial conditions. Then, AMS-¹⁴C dating of selected bioapatite samples was performed. Results from this case study prove that the radiocarbon dating of bioapatite of heavily altered bone samples may not be reliable. Characterization of bones (SEM, m-CT, XRPD, FTIR and m-Raman spectroscopy) and associated soils and sediments (XRPD, optical and CL microscopy, SEM and ¹⁴C-AMS dating) provided valuable information on the diagenetic history of bones and on the influence that changes in environmental and local burial conditions had on bone preservation. Finally, results highlight the relevance of a multi-disciplinary approach to the study of the archaeological and palaeoenvironmental contexts.

Technology and Provenance of the Unglazed Pottery from the masjed-i jom'e of Isfahan (Iran)

De Bonis A.*¹, D'Angelo M.², Guarino V.¹, Massa S.³, Saiedi Anaraki F.⁴, Genito B.² & Morra V.¹

1. Dipartimento di Scienze della Terra, dell'Ambiente e delle Risorse (DiSTAR), Università di Napoli "Federico II". 2. Dipartimento Asia Africa e Mediterraneo, Università di Napoli "L'Orientale". 3. Università Cattolica, Milano. 4. Iranian Centre for Archaeological Research, Isfahan, Iran

Corresponding email: alberto.debonis@unina.it

Keywords: Unglazed pottery, production indicators, masjed-i Jom'e.

The masjed-i jom'e (Friday Mosque) of Isfahan represents one of the earliest mosque of Iran. Since 1970s the Italian activities of ISMEO, the Istituto Universitario Orientale di Napoli, now Università degli Studi di Napoli "L'Orientale", and the Università degli Studi di Roma "La Sapienza", in collaboration of the Ministero Italiano degli Affari Esteri contributed at identifying the earliest building and architectural phases of the monument, starting a conservation and archaeological project. An extensive investigation was then carried out in order to complete the historical, archaeological and artistic knowledge of the monument. Since 2003 a new project (ADAMJI) started in order to resume a digital catalogue of the archaeological data and materials.

Aim of this study has been also the archaeometric investigation of the unglazed pottery uncovered during the excavation activities. Pottery samples were selected among a huge amount of fragments (416,000) analysed on a macroscopic basis.

Minero-petrographic analyses (PLM, XRPD, XRF, and SEM-EDS) were performed on 23 pottery samples selected among the most representative ceramic fabrics of storage, table and cooking wares; 7 production indicators (spacers, kiln elements, slags), 2 bricks and a local clay sample, used in a workshop near the mosque, were also analysed for comparison.

Most samples (mainly storage and tableware) are characterised by a high CaO concentration (11.2-22.5 wt.%), while 4 samples show significant lower values (1.4-4.9 wt.%). A group of high-CaO samples is represented by large-walled fragments with a coarse and heterogeneous texture, containing arenites, mudstone and occasional metamorphic debris. Other samples, characterised by thinner walls, show a similar petrographic composition, but contain fine/well-sorted grains. A sample differs for its peculiar calcitic temper composition.

SEM-EDS and XRPD performed on high-CaO samples showed pyrometamorphic transformation pointing to firing temperatures from about 850 to 1100 °C. A range consistent with the temperatures used to produce high-quality storage and table wares. Some coarse-grained samples are characterised by lower firing temperature (700-800 °C).

Low-CaO samples are characterised by fine quartzose inclusions with sporadic coarser grains, represented in one sample by igneous rock fragments. Temperatures ranging from 800 to 950 °C were estimated and the low-CaO composition could be related to their specific function devoted to cooking foods.

Provenance of most samples was constrained by the petrographic composition of the inclusions compatible with the main lithologies outcropping in the Isfahan area and in the drainage basin of the Zayandeh river. High-CaO pottery showed a mineralogical assemblage and chemical composition similar to that of production indicators and bricks collected in the mosque, as well as to the clay sample. These evidences could suggest the presence of workshops active in the immediate vicinity of the mosque.

UV fluorescence as tool to evaluate the biotic encrustation pervasiveness on underwater medieval amphorae near Crotona (Calabria - Italy)

De Francesco A.M.¹, Scarpelli R.*¹, Mastandrea A.¹, Guido A.¹ & Marino D.A.M.²

1. Dipartimento di Biologia, Ecologia e Scienze della Terra, Università della Calabria.

2. Soprintendenza Archeologia del Friuli Venezia Giulia, MIBACT.

Corresponding email: roberta.scarpelli@unical.it

Keywords: Underwater ceramics, UV Fluorescence, encrustation.

Underwater ceramic sherds, found in the harbor of Crotona (Calabria, Italy), were analyzed with different analytical methods. The pottery fragments, mostly *amphorae*, are characterized by a great layer of deterioration on the surface. Archaeological information are very poor, no assumption about provenance and technology, these ceramics are only doubtfully dated to Medieval times. The first part of this work consisted in assessing the technological variations among the samples and possibly identifying their provenances by petrographic (Optical Microscopy) and chemical (X-Ray Fluorescence) characterization. Petrographic observations show considerable heterogeneity in particular for aplastic inclusions, which allowed the distinction into two groups, the first one with a prevalence of quartz and volcanic grains and the second one with limestone and fossils. XRF analysis confirmed the difference in the chemical composition of the ceramics. The comparison with literature data showed that the largest group of ceramics has high affinity with the ceramics produced in the Strait of Messina, while the other ones are similar to ceramics from the Aegean area.

The pottery fragments are diffusely covered by biotic crusts made of bryozoans, red algae, serpulids, sponges and other organisms. UV fluorescence observations allowed to recognize the intensity of pervasiveness of the biotic colonization and its relationship with the degree of preservation of the ceramics fragments. No fluorescence has been observed below the pottery surface meaning the absence of organic matter in the ceramic matrix. The observations revealed a bright fluorescence limited to the biotic encrustation and a sharp boundary with the ceramic surface. Fluorescence was induced by an Hg vapor lamp linked to an Axioplan II imaging microscope (Zeiss) equipped with high-performance, wide band pass filters (BP 436/10 nm/LP 470 nm for green light; BP 450-490 nm/LP 520 nm for yellow light).

This approach allows to characterize the underwater ceramics from a multidisciplinary point of view. The petrographic and chemical features of the archeological fragments, together with the characterization of skeletal organisms and their organic matter distribution, permit to evaluate the role of biotic encrustation as preservation/alteration factor in submarine environments.

Characterization and provenance of plasters from residential buildings of 18th century in Lamezia Terme (Calabria, Southern Italy)

De Luca R. *, Gigliotti V., Panarello M., Bloise A., Crisci G.M. & Miriello D.

Dipartimento di Biologia, Ecologia e Scienze della Terra, Università della Calabria

Corresponding email: raffaella.deluca@unical.it

Keywords: Archaeometry, plasters, pigments.

The present work concerns the study of six plasters coming from three important residential buildings of the 18th century, located in Lamezia Terme (Calabria, Southern Italy). The buildings analyzed are: Palazzo Statti, Palazzo Nicotera and Palazzo Cerra. In the 18th century, the upper class of the city commissioned, at important plasterers, elaborated decorations for their buildings, to declare their social prestige (Fagiolo, 2010). For this reason, the buildings of this period are characterized by particular decorations with sophisticated symbolic meanings and they represent a particular expression of the baroque and rococo styles.

The plaster samples, coming from these buildings, were analyzed by polarized optical microscopy (OM), X-ray powder diffraction (XRPD), scanning electron microscopy (SEM) with energy dispersive X-ray spectroscopy (EDS) and Raman Spectroscopy.

In addition to the historical plasters, geological samples of sand and limestone, coming from the quarries near Lamezia, were also studied to determine the provenance of the raw materials used for the production of the plasters.

The study allowed to determine the petrographical, mineralogical and chemical features of the plasters, highlighting differences and similarities among them and identifying the pigments used for the coloration of the superficial layer of the some plasters.

The comparison with the geological samples of sand and limestone, allowed also to make hypothesis on the provenance of the raw materials used to make the plasters.

The data produced by this work have provided important information on the constructive history of the buildings and on the production technology of the plasters in the 18th century in Lamezia Terme. At the same time, the information obtained will be useful to make repair mortars for future restoration by using a mixing approach and optimization methods (Miriello & Crisci, 2007; Miriello et al., 2013; Miriello et al., in press).

Fagiolo M. 2010. Atlante tematico del barocco in Italia. Residenze nobiliari. Italia meridionale. De Luca editori d'arte, Roma.

Miriello D. & Crisci G.M. 2007. The Mixing and provenance of raw materials in the bricks from the Svevian castle of Rocca Imperiale (North Calabria - Italy). *Eur. J. Mineral.*, 19, 137-144.

Miriello D., Lezzerini M., Chiaravallotti F., Bloise A., Apollaro C. & Crisci G.M. 2013. Replicating the chemical composition of the binder for restoration of historic mortars as an optimization problem. *Comput. Concr.*, 12, 553-563.

Miriello D., Bloise A., De Luca R., Apollaro C., Crisci G.M., Medaglia S. & Taliano Grasso A. In press. First compositional evidences on the local production of Dressel 2-4 amphorae in Calabria (Southern Italy): characterization and mixing simulations. *Appl. Phys. A: Mater. Sci. Process.*, doi:10.1007/s00339-015-9143-y.

Building stratification in tower area of Montecorvino (Foggia, 11th -15th century): evidences of norman masonry techniques

Eramo G.*¹ & Giuliani R.²

1. Dipartimento di Scienze della Terra e Geoambientali, Università di Bari. 2. Dipartimento di Studi Umanistici, Università di Foggia.

Corresponding email: giacomo.eramo@uniba.it

Keywords: Montecorvino, lime mortars, Norman masonry.

The medieval village of Montecorvino was founded by Byzantines in the 11th century, and evolved until the 15th century through an articulated building stratification. Since 2006 the University of Foggia launched a systematic investigation of the village's remains using a multidisciplinary approach, which involved aerial photography, geophysical prospection, archaeological surveys and excavation and material characterisation. In this contribution we drew our attention to the main tower and the annexe structures. In the building stratigraphy of this area we observed distinctive morphological and constructive features and we suppose that Norman specialised workers were used.

In order to prove this hypothesis, 57 samples of lime mortar from the main tower, the wall belt, the base of the pentagonal tower and other minor structures were investigated by optical microscopy (OM), scanning electron microscope (SEM), X-ray powder diffraction (XRPD) and X-ray fluorescence (XRF).

A comparison of the petrofacies expressed by the aggregates and calcination relics of mortars and the petrofacies of the alluvial deposits at the feet of Montecorvino hill points to these sediments as source for mortar preparation and building stones.

The petrographical and chemical groupings substantially confirmed the building stratification identified by the archeologists and gave new insights into the building phases of each structure.

The microstructures observed in thin section suggest the use of hot lime mortar techniques for most of the investigated samples from the main tower. Although the petrofacies of the aggregate is in common among all the analysed mortars and bulk chemistry and mineralogy are very similar, the lime microstructures seem to be distinctive of a Norman knowhow. The use of this preparation technique is supposed to be particularly useful for the building of the main tower, because of their early strength, low expansion and high durability.

Early Greek Colonization in Southern Italy: archaeometric analyses of ceramic local production and Greek imports in the Siris area (Basilicata)

Eramo G.*¹, Muntoni I.M.², Gallo S.³ & De Siena A.⁴

1. Dipartimento di Scienze della Terra e Geoambientali, Università di Bari. 2. Soprintendenza Archeologia della Puglia, Centro Operativo per l'Archeologia della Daunia, Foggia. 3. Dipartimento di Scienze dell'Antichità e del Tardoantico, Università di Bari. 4. già Soprintendente Archeologia della Basilicata.

Corresponding email: giacomo.eramo@uniba.it

Keywords: Policoro, Greek imports, Early Archaic.

This article focuses on the issue of early Greek colonization in Southern Italy, especially in the coastal area of the Taranto Gulf along the Ionian coast of Southern Italy, through archaeometric analyses (OM, SEM/EDS, XRPD and XRF) of Greek imports, Greek-style pottery and local reference materials.

The 34 potsherds of Early Archaic Pottery, from five recently excavated deposits dated to the middle of the 7th century BC in the modern city of Policoro (the ancient *Siris/Polleion*), are mineralogically non-homogeneous and ten different fabrics can be distinguished on the basis of their composition and grain-size distribution, suggesting both local and non-local (imports from Greece) provenances.

Fabrics IC, ICC, ICA, ICF, ICP and ICX (n = 27) can be ascribed to the use of a Ca-rich clay, and fabrics Q, QCG, GC and IG (n = 7) to the use of a Ca-poor clay.

Pottery made of calcareous clay (IC) can be associated with the local marine Plio-Pleistocene silty clay (Argille subappennine clay) that outcrops in the area, while the presence of different NPIs (pyroxenes, chert, non-calcareous argillite and ferruginous aggregate) in fabrics ICP, ICC, ICA and ICF likely suggest the use of alluvial deposits as a raw material with a significant elutriation as inferred from its very fine texture. Fabric ICX presents very fine primary calcite in the matrix.

Pottery made of non-calcareous clays presents very different NPIs (quarzarenitic and chert clasts, quartz and/or calcareous clasts and non-calcareous grog, and calcareous grog) indicating a non-local production.

The Ca-poor samples generally present low to medium sintering ($500 < T_{max} < 800$ °C), while Ca-rich ones present high sintering ($900 < T_{max} < 1050$ °C) with neo-formed gehlenite, diopside and anorthite.

The statistical treatment of the XRF data (major and trace elements) confirms the local production of most of the samples analysed, alongside the presence of different types of imports such as Type-A Corinthian amphorae, sub-Geometric pottery (Proto-Corinthian *aryballoi*) and surprisingly also firing pots (*chytrai*). The analyses confirm the local production of two pots (a *deinos* and a crater) stylistically attributed to the *Analatos* Painter, the most important pottery painter of the Early Proto-Attic period who was therefore probably also active in the Siris area. In conclusion, the existing relationships between the various ceramic classes, their form and/or use and provenance are discussed.

Spectroscopy and electron microscopy for the characterization of CdS_xSe_{1-x} Quantum Dots in a Glass Matrix

Fornacelli C.^{*1-2}, Mugnaioli E.², Colomban P.³ & Memmi I.²

1. Dipartimento di Scienze della Terra, Università di Pisa. 2. Dipartimento di Scienze Fisiche, della Terra e dell'Ambiente, Università di Siena. 3. MONARIS UMR 8233, CNRS, Sorbonne Universités, Paris, France.

Corresponding email: fornacelli@unisi.it

Keywords: Nanoparticles, glass, TEM.

Besides their use as optical cut-off filters and some recent applications as non-linear optical devices and photonic dots (micro-sized glass spheres), the CdS_xSe_{1-x} quantum dots started to be widely used in the production of stained glass windows from about the 1920 thanks to their bright colors.

When semiconductor particles are reduced in scale to nanometer dimension, their optical and electro-optical properties strongly differ from those of bulk crystals of the same composition. Since sampling is often not allowed concerning Cultural Heritage artefacts, the potentialities of two non-invasive techniques, such as Raman and Fiber Optic Reflectance Spectroscopy (FORS), have been investigated. The results of the analysis on some original glasses of different colours (from yellow to orange and deep red) and periods (from the second decade of the 20th century to present days) are reported in the present study.

The evaluation of the wavenumbers and the broadening/asymmetry of the LO phonons bands in the Raman spectra have been used for the evaluation of the NCs composition. However, when considering the optical-phonons wavenumbers, the important role of the compressive strain arising from the glass matrix and the possible diffusion of zinc from the matrix to the nanocrystals should be also taken into account.

The optical band gap varies from 2.42 eV (pure CdS) to 1.70 eV (CdSe). For the compositional range between $0.5 \leq x \leq 0.2$, the presence of two absorption edges has been related to the contribution of both CdS_xSe_{1-x} mixed and pure CdS NCs; the latter probably consists of crystals of unaltered cubic zinc blende-structured CdS that is not taking part to the formation of the solid solution occurring only between hexagonal CdS and CdSe.

The band edge tailing originating from the disorder of the system has been assumed, together with the FWHM of the Raman signal, as a good parameter to evaluate the degree of topological disorder and a good discrimination between modern and Art Nouveau glasses have been obtained.

The composition of the glass matrix was also investigated by scanning electron microscopy (SEM) and energy-disperse spectroscopy (EDS) mapping. SEM-EDS mapping showed a peculiar distribution of the major constituents of the glass matrix (fluxes and stabilizers), especially concerning those samples where a layered structure has been assumed thanks to the spectroscopic study.

Finally, transmission electron microscopy (TEM), TEM-EDS and electron diffraction tomography (EDT) were used to get high-resolution information about nanocrystals (NCs) and heterogeneous glass layers. Results have been compared with the information extrapolated by the spectroscopic techniques. The presence of ZnO NCs (< 4 nm) dispersed in the matrix has been verified for most of the samples, while, for those samples where a disorder due to a more complex distribution of the size and/or composition of the NCs has been assumed, the TEM clearly verified/confirmed all the assumption made by the spectroscopic techniques.

Decay in heritage granite ashlars. Its dependence with exfoliation microcracks

Freire-Lista D.M.^{*1-2} & Fort R.¹⁻²

1. Instituto de Geociencias IGEO (CSIC, UCM), Madrid, España. 2. CEI Campus Moncloa, UCM-UPM y CSIC, Madrid, España.

Corresponding email: dafreire@geo.ucm.es

Keywords: Degradation, cultural heritage, granite.

Decay of granite heritage ashlars is determined by the type of quarry from which they are extracted. In general, the oldest ashlars were extracted from shallow quarries and subaerial granite boulders, characterized by pseudo concentric exfoliation microcracks and by being more altered. While the quarries deepen over the centuries, extracted granite is less altered and has better petrophysical properties, with exfoliation microcracks planes that are flat and parallel to the surface of paleo-relief. The exfoliation microcracks are anisotropy planes in heritage granite ashlars. The carve styling and weathering among others factors, contribute to the decay of granite ashlar. Scaling, as defined by ICOMOS, is detachment of stone as a scale or a stack of scales, not following any stone structure and detaching like fish scales or parallel to the stone surface. Microscopic techniques and petrophysical analysis has shown that exfoliation microcracks play an important role in the granite anisotropy, which traditional quarrymen use to cut the building stone (rift plane). Granite ashlars from bowling have a scaling according to the curved planes of exfoliation microcracks, producing a rounding at its vertices. In granite ashlars extracted since the nineteenth century, the scaling occurs frequently parallel to the face side of the ashlar. Therefore, the granite ashlars scaling are closely related to the stone structure (exfoliation microcracks) and therefore the quarrying type. Thus it is common to find ashlars of the first rows of a heritage building with distinct decay patterns to the upper rows that have been extracted from a deeper quarry level.

The sanctuary of Sant'Angelo in Criptis at Santeramo in Colle, Apulian region, Italy: a multi-disciplinary approach for the conservation

Garavelli A.¹, Marsico A.*¹, Pinto D.¹, Monno A.¹, Andriani G.¹, Germinario G.², Laganara C.³, Albrizio P.³,
Piepoli L.³, Depalo M.R.⁴, Longobardi F.⁴ & Simonetti A.⁴

1. Dipartimento di Scienze della Terra e Geoambientali, Università di Bari. 2. Dipartimento di Chimica, Università di Bari. 3. Dipartimento di Scienze dell'Antichità e del Tardo Antico, Università di Bari. 4. MIBACT, Ministero dei Beni e delle Attività Culturali e del Turismo.

Corresponding email: antonella.marsico@uniba.it

Keywords: Cave survey, archaeometry, terrestrial laser scanner.

Since time immemorial, numerous caves in Puglia were used as places of worship, then became churches or small sanctuaries. Several of them was dedicated to Saint Michael Archangel, commonly known as Sant'Angelo, protector of the Lombard stock, imported from the near East and spread through center and southern Italy. Sant'Angelo in Criptis at Santeramo in Colle (Bari) is a great medieval complex better known as "Iazzo-Sant'Angelo", consisting of several buildings in local hard stone, and a natural cave behind featuring a beautiful natural architecture in which stalactites and stalagmites serve as capitals and columns delimiting unique niches carved into the rock. Some fine, stratified frescos enrich the cave, but actually they are in very precarious conditions and needs urgent restoration. All the cave walls collect engravings and graffiti art from various time periods indicating the sacredness of the place, which was an important religious pilgrimage destination since early Christian periods. This important Cultural Heritage is subject to a severe deterioration due to chemical, physical, mechanical and biological causes often interrelated.

The degradation processes have been different also in the small space of the same site. They are conditioned by petrographic, physical and mechanical characters of the calcareous stone: rock cementation degree and its fabric. An important role is played by the micro-climate conditions existing in the grotto and by the falls of water along the walls covered by the frescos. They are responsible of the important alteration phenomena involving the superficial part of the rock of the caves, as well as of the disfiguring effect connected to physico-chemical rock degradation processes by means of water infiltration from the rock. To the degradation effects contribute also the small but detrimental activity of rock joints. Special attention has to be given to frescoes affected by processes of decalcification and gypsification. The movement from the surface of water rich in carbonates and other salts (such as sulphates and nitrates) arouses patinas and plaques more or less thick enclosing carbon particles and biofilms formed by pervasive algae, musk, lichen and fungi colonies that damage the paintings and the speleothems of the cave.

In this aim, a multidisciplinary approach for a better knowledge, conservation and enjoying the heritage is necessary. It consists of geological, mineralogical and archeometric investigation on materials from the cave and from the buildings. A Terrestrial Laser Scanner (TLS) survey is also useful to create a 3D virtual model of the building complex and of the grotto behind it, in order to gather, for example, cave dimensions, joints measures and speleothems characterisations. Furthermore, TLS virtual images of the sanctuary could be used as an important tool to promote and to enjoy the site, as well as to increase interest in the Earth sciences in society at large.

Combining μ -XRF and SEM-EDS mapping in low and high resolution for determining the provenance quarry of volcanic porphyritic stones

Germinario L.*¹, Cossio R.², Mazzoli C.¹, Maritan L.¹ & Borghi A.²

1. Dipartimento di Geoscienze, Università di Padova. 2. Dipartimento di Scienze della Terra, Università di Torino.

Corresponding email: luigi.germinario@gmail.com

Keywords: X-ray maps, image analysis, Euganean trachyte.

The traditional studies on provenance of stone used in cultural heritage are based on the comparison of bulk-chemical or microchemical composition with existing databases, built from data acquired on materials of known origin (normally from quarries). For stones with very similar composition, in many cases from the same extraction basin, this approach is not always effective, and requires the contribution of petrography. How can a complete petrographic and geochemical characterization be achieved, in a cheap, rapid and non-invasive way, but still yielding quantitative information?

Here, image analysis of X-ray maps acquired by μ -XRF and SEM-EDS is proposed. While the latter is a well-known technique, μ -XRF has been only recently becoming popular thanks to the realization of dedicated compact spectrometers; the resolution attainable with bench-top μ -XRF is poorer, but the detection limits are lower and the analyses cost effective and faster, so that cm-sized surfaces can be quickly mapped, even on large objects without previous sampling.

In this study, microchemical mapping was performed on trachytes from the main historical quarries on the Euganean Hills (Veneto): Monselice, Monte Merlo and Monte Oliveto. Euganean trachyte is a volcanic porphyritic rock widely used in cultural heritage of northern and central Italy, especially from the Roman times, in numerous artifacts, monuments and infrastructures. It has been exploited since the 7th century BC in tens of quarries, in which outcropping rocks are visually and compositionally very similar. The aim of this work is to get mineralogical and textural quantitative information about both phenocrysts and groundmass, the analysis of which requires different resolutions. Therefore, μ -XRF was applied over $\sim 5 \times 4$ cm areas with a resolution of 100 μm , whereas with SEM-EDS $\sim 800 \times 650$ μm areas were analyzed with a resolution of 1.5 μm , focusing on phenocrysts and matrix, respectively. The X-ray maps were processed by digital image analysis, and the relative abundance of each mineral phase, its size and shape properties (Feret diameter, area, perimeter, circularity and aspect ratio) were statistically treated, as well as porphyritic index and crystal size distribution.

The information provided by the map processing indicates that the various trachyte quarries can be distinguished on the basis of mineralogy and texture, as an instance: presence, abundance, size and distribution of feldspar phenocrysts; phenocrysts-groundmass ratio; composition, size and shape of feldspar microlites in the matrix; presence and abundance of intercrystalline glass and cristobalite. A principal component analysis of these parameters further supports the possibility to effectively differentiate the quarries. Based on these results, the multianalytical approach will also be applied to all the other historical trachyte quarries on the Euganean Hills, in order to define quantitative petrographic criteria for archaeometric provenance studies.

Neolithic polished greenstone implements from Castello di Annone (Italy): mineralogical and archaeometric aspects

Giustetto R.*¹⁻², Perrone U.¹ & Compagnoni R.¹

1. Dipartimento di Scienze della Terra, Università di Torino. 2. NIS - Nanostructured Interfaces and Surfaces, Torino.

Corresponding email: roberto.giustetto@unito.it

Keywords: Prehistoric greenstone implement, eclogite, Na-pyroxenite.

High-pressure (HP) meta-ophiolites, so-called greenstones, were used in Neolithic to produce polished stone implements all over the Western Europe. Their accurate petrographic description may help in inferring the provenance of the raw materials, thus reconstructing the migratory routes of our ancestors. The lithic industry of Castello di Annone (Northwestern Italy) was investigated with a multi-disciplinary approach including density measurements, XRPD, optical microscopy, SEM-EDS and geothermometry. More than half of the studied tools (52%) are made of fine-grained eclogites, gathered in three different groups each with a peculiar metamorphic history. Na-pyroxene rocks represent a residual 26%, with mixed Na-pyroxenites being more abundant than jadeitites, while serpentinites and minor lithologies form the remaining fraction. In most greenstone implements, both pyroxenes and garnets show a complex compositional zoning. Such a heterogeneity is typical of these tools but almost unknown in geologic samples, due to the lack of petrologic data from the few known outcrops. Though these HP meta-ophiolites belong to the Piemonte Zone, their sharper provenance may only be inferred through a systematic field survey and comparative study on geologic samples. A recent prospection in the upper Carbonieri Valley brought to uncover small boudins of fine-grained eclogites and omphacitites, similar to those found in the Neolithic tools. The Castello di Annone eclogites, poorly manufactured and probably collected from fluvial pebbles, have to be considered low quality materials. This confirms the marginal role of this site in the production and distribution network of greenstone implements in Northern Italy during Neolithic.

Traditional ceramic production in central and southern Madagascar: first insights from mineralogy and petrology of bricks

Grifa C.¹, Germinario C.*¹, Mercurio M.¹, Langella A.¹, Cucciniello C.², Cappelletti P.², Zollo D.¹, Izzo F.¹,
De Bonis A.², Monetti V.² & Morra V.²

1. Dipartimento di Scienze e Tecnologie, Università del Sannio. 2. Dipartimento Scienze della Terra, dell'Ambiente e delle Risorse, Università di Napoli "Federico II".

Corresponding email: chiara.germinario@unisannio.it

Keywords: Bricks, Madagascar, traditional ceramic production.

The traditional buildings of Madagascar are mainly built by using bricks. The huge brick production is mainly organized in local workshops close to the clayey deposit outcrops where the sediments are extracted, moulded in bricks, dried and then fired in open-air furnaces.

Samples of bricks from four workshops located in central and southwestern Madagascar were collected to establish the firing technology of the Malagasy traditional brick "industry". For each site, the samples consist of one unfired brick and two or three fired bricks collected at different distance from the fuel source. Mineralogical and petrographic analyses have been performed to achieve a technological characterization.

The unfired bricks from central Madagascar are made up of lateritic soils formed from *in situ* alteration of intrusive or metamorphic basement rocks. These deposits experienced low transportation rate, as showed by the unsorted granulometric distribution of subangular quartz, altered feldspar, opaque oxides, detrital rocks fragments, with rare amphibole, hematite and olivine grains. Siderite is found in central Madagascar samples. The clayey sediments from south-western Madagascar have well sorted grain size distribution, with quartz as prevailing constituent. Calcite and fossils also occur, attesting a marine depositional environment.

After moulding the clayey deposits are fired in open-air furnaces and the type of fuel mostly depends on wood availability in the area. In fact, the inner areas of central Madagascar suffer a strong deforestation, thus the bricks are fired by using peat fuel. The time of firing is quite longer for peat (up to 15 days) with respect to for wood furnaces (1-2 days).

The samples from central Madagascar are fired at ca. 550 °C, as confirmed by the lack of the dehydroxylation peak (TG analysis) of kaolinite (detected in unfired samples) between 450 and 550 °C.

The absence of siderite in fired samples from central Madagascar with respect to unfired ones, allowed confirming a firing temperature of 500 - 550 °C given that decomposition of siderite to Fe-oxides takes place within this temperature range. Little differences have been recorded in phyllosilicates content among the samples thus inferring a variable diffusion of heat.

Samples from south-western Madagascar are fired at slight lower temperatures because since kaolinite in fired samples still persist (weak endothermic peak at 470-500 °C in TG curves). Anomalous heat diffusion within this kind of furnace is here supposed due to significant variations of kaolinite content among the investigated samples.

The Archaic cooking ware and *instrumenta* in Cuma: Italic and Greek traditions

Guarino V.*¹, De Bonis A.¹, Grifa C.², Langella A.², Munzi P.³ & Morra V.¹

1. Dipartimento di Scienze della Terra, dell'Ambiente e delle Risorse, Università di Napoli "Federico II". 2. Dipartimento di Scienze e Tecnologie, Università del Sannio. 3. Centre Jean Bérard, USR 3133 CNRS-École Française de Rome, Napoli.

Corresponding email: vincenza.guarino@unina.it

Keywords: Archaic cooking ware, Greek *instrumenta*, Cuma.

Cuma is the oldest Greek colony of the Occident founded in the second half of the VIII century B.C. at the border with the indigenous world (Etruscan and Italic). Cuma has been the centre of an important research and promotion project (Kyme project) sponsored by the Soprintendenza Archeologica di Napoli, which involved other major scientific institutions as the Università degli Studi di Napoli Federico II, Università degli Studi di Napoli L'Orientale and Centre Jean Bérard.

In this study, thirteen ceramic fragments of common cooking ware and *instrumenta* from the second half of the VI to the first half of the V century B.C. were examined via mineralogical and chemical analyses. The most common cooking ware used in Cuma are *ollae* and cup-lid both of Italic tradition, with minor forms belonging to the Greek tradition (*chytrai*, *caccabai*, and *lopades*). Other forms founded in Cuma are the *instrumenta* such as trays, tripod cooking plates, cooking plates and bell-shaped portable ovens that are comparable to kitchen tools used again in the Greek tradition.

Samples are represented by five *ollae*, two *chytrai*, one *lopas*, one *caccabè*, one cover-cup, one tripod cooking plate, one cooking plate and one bell-shaped portable oven. Four *ollae* and the cover-cup are made with low-CaO clay (2.4-3.9 wt.%) and temper characterised by local volcanic inclusions (e.g., crystals of feldspars and clinopyroxene, pumice and leucite-bearing volcanic fragments). Similar petrographic features are observable for the cooking plate and bell-shaped portable oven, but characterised by a moderate CaO amount of 5.8 and 8.9 wt.%, respectively.

Marked petrographic differences were noticed for the other studied samples due to the presence of exotic inclusions. One *olla* and the *caccabè*, show again low-CaO clay (2.6 and 4.5 wt.% respectively), but volcanic inclusions are mainly rhyolitic pumice and orthopyroxene. The tripod cooking plate is characterised by a moderate CaO amount (6.8 wt.%) and inclusions represented by amphibolite and serpentine fragments. The two *chytrai* and the *lopas* show a very low CaO concentration (1.3-1.6 wt.%) and predominant quartzose grains with minor feldspars, mica and amphibole.

The four *ollae* together with samples of cover-cup, cooking plate and bell-shaped portable oven, containing volcanic inclusions related to Somma-Vesuvius and Phlegraean volcanic district, have strong affinity with other studied products and can be assigned to the Bay of Naples production.

The remaining fragments with volcanic (one *olla* and the *caccabè*) or metamorphic (tripod cooking plate) or sedimentary (*chytrai* and *lopas*) inclusions are different from the ceramic productions so far studied in the same area and represent imported products.

Archaeometric study of ceramic materials from archaeological excavations at the roman iron-working site of San Giovanni (Portoferraio, Elba island)

Manca R.P.*¹, Pagliantini L.², Pecchioni E.¹, Benvenuti M.¹, Chiarantini L.⁴, Cambi F.², Corretti A.³, Costagliola P.¹, Orlando A.⁴ & Santo A.P.¹

1. Dipartimento di Scienze della Terra, Università di Firenze. 2. Dipartimento di Scienze Storiche e dei Beni Culturali, Università di Siena. 3. Laboratorio di Scienze dell'Antichità, Scuola Normale Superiore di Pisa. 4. Istituto di Geoscienze e Georisorse, C.N.R. Firenze.

Corresponding email: rosa-rosa@hotmail.it

Keywords: Elba Island, opus doliare, provenance.

Dolia are large pottery containers used in Roman times for the storage and fermentation of wine. Together with bricks and other building materials they constituted the so-called *opus doliare* and were probably produced in the same specialized ceramic workshops (*figlinae*). *Opus doliare* was typically marked with specific epigraphical stamps, which represent a major tool to unravel their provenance and trade.

In this work we present the results of a study - conducted in the framework of the AITHALE project - related to the origin of two *dolia defossa* recently found at S. Giovanni (Portoferraio, Elba Island) during 2012-2014 archaeological excavations, which brought to light a Roman farm (1st cent. BC-1st cent. AD), devoted to wine production and constituting the *pars rustica* of the adjacent "Villa delle Grotte". Based on archaeological evidences, four different provenance hypotheses have been put forward: 1) Elba Island, where the *dolia* have been found, although there is no clear evidence of the presence of *figlinae* specialized in *opus doliare* on the island; 2) the municipal *figlinae* of the territory of Pisa, where some tiles found at S. Giovanni may have been produced; 3) the middle catchment of the Tiber river (central Latium) where "urban" *figlinae* occurred; 4) the *figlinae* of Minturno (southern Latium), a locality known both for wine production and exportation and for the presence of ancient *figlinae*.

Minero-petrographic and chemical compositions of the *dolia* have been compared with those of raw materials available in the four areas cited above. The study focused on the ceramic framework, particularly on lithic fragment in the *dolia* and their clinopyroxene (Cpx) composition. Lithic fragments show trachytic - latitic composition, which is compatible only with source regions (3)- *urban figlinae* along the Tiber valley, Roman Magmatic Province - and (4) - Minturno, in the Ernici-Roccamonfina Magmatic Province. Cpx major element composition (cores in the range Wo 43.7-52.8, En 30-47.5, Fs 6.4-22.5 and rim Wo 45.6-51.8, En 29-47.9, Fs 16.6-22.5) is also compatible with a provenance from these two areas. However, optical observation and mineral-chemistry indicate the coexistence of colourless (high-Mg and Si) and pale green (high-Fe and Al) Cpx. These particular features have been commonly found in rocks belonging to the Roccamonfina trachytic series (Ghiara & Lirer, 1976; Giannetti & Luhr, 1983), thus suggesting that Minturno was the most likely production area of the two *dolia* unearthed in S. Giovanni.

Giannetti B. & Luhr J.F. 1983. The white trachytic tuff of Roccamonfina volcano (Roman region, Italy). *Contrib. Mineral. Petrol.*, 84, 235-252.

Ghiara M.R. & Lirer L. 1976. Mineralogy and geochemistry of the «Low potassium» series of the Roccamonfina volcanic suite (Campania, South Italy). *Bull. Volcanol.*, 40, 39-56.

A mineralogical approach to the authentication of an archaeological artifact: real ancient bronze from Roman Age or fake?

Mantovani L.*¹, Tribaudino M.¹ & Facchinetti M.²

1. Dipartimento di Fisica e Scienze della Terra "M. Melloni", Università di Parma.
2. MiBAC - Soprintendenza per i Beni archeologici della Lombardia, Milano.

Corresponding email: luciana.mantovani@unipr.it

Keywords: Bronze statue, Roman Age, XRD.

The results of a mineralogical investigation, aimed to determine whether a bronze statue coming from judicial seizure is authentic or fake are here reported.

Two main questions had to be addressed: 1) the provenience of the artefact and, 2) the historical period of production. The iconological aspects and compatibility with ancient bronze production in Imperial Roman age seem to be clear at the archaeologist, but a doubt on the authenticity was cast by the presence of nineteenth-century copies of original Herculaneum statues produced by Chiurazzi smelter.

The bronze statue represents a sylvan deity holding in his left hand a snake. The artefact was in good state of conservation, with some signs of corrosion, covered with a light green patina; the right arm was missing and there were signs of fractures on the legs. Small pieces of soil between the draperies, clays-core (the soil used before the casting), fibres inside the missing arm and little chips of bronze were taken and analysed at optical and electron microscope (SEM-EDS) and by powder X-ray diffraction. The small pieces of soil attached to the external bronze showed the presence of sanidine, phlogopite, analcime, and sometimes phillipsite: such mineralogical association, together with the observation of pumice, could support a provenance from the Vesuvius area (Cioni & Sulpizio, 1998). The green patina of alteration of the bronze was mainly formed by copper chlorides, in particular paratacamite and botallackite, which suggested a burial of the bronze statue close to the seashore. To note, a well-developed and stratified alteration patina was found, a point which could support that the patina is a natural one formed over long periods.

However further analysis showed that the artefact is actually a forgery. The residuals of the clays-core highlighted the presence of quartz and gypsum, and the absence of clay minerals, which are instead found in imperial clays-cores; in addition, the fibres used for the casting were tissues, differently from the straws or plant residues used in the Roman period (Formigli, 2012).

The alloy formed by copper, zinc and tin was heterogeneous, with some areas very rich in zinc. The high Zn content is unusual for statues from the Roman age, and instead was found from Renaissance onwards (Formigli, 2012). Eventually the C14 dating, done on a small piece of fibres, showed that the artefact was done after the seventieth century.

The above evidences indicate that, given the appropriate conditions, a well-developed alteration patina can be formed also over relatively short periods, and that cannot be taken as unique criterion of authenticity.

Cioni R. & Sulpizio R. 1998. Le sottopopolazioni granulometriche nei depositi vulcanici di caduta. *Atti Soc. Tosc. Sci. Nat.*, 105, 81-97.

Formigli E. 2012. La datazione tecnologica dei grandi bronzi antichi: il caso della Lupa Capitolina. *INHA*.

Multi-disciplinary approach to the characterization of *an ornamental stone*: the case study of “Busca Onyx”

Marengo A.*, Borghi A. & Costa E.

Dipartimento di Scienze della Terra, Università di Torino.

Corresponding email: alessandra.marengo@unito.it

Keywords: Busca Onyx, calcite-alabaster, characterization.

Multi-technique and multi-disciplinary approach for the characterization of a lithological material is presented through the *Busca Onyx* case study.

Busca Onyx, or *Busca Alabaster*, is an ornamental stone quarried in Piedmont. It was one of the most appreciated stones by Savoy's architects, especially by Filippo Juvarra. It was mainly used for baroque panels and objects. One example is St. Filippo Neri Church where it was employed for columns, altars and balustrades. Its distinctive aesthetic appearance and the low quantity of available material made it to be considered as a precious rarity. Its quarry has been operating from the XVII to the XX century. First evidences of activity date back to 1640-1650; after a thriving period in the XVIII century, its economic decline began and the exploitation gradually decreased until it stopped in the very first years of the XX century. The quarry officially closed in 1963.

The “onyx” deposits are located a few kilometers from the town of Busca (Cuneo province). The quarry is formed by four parallel canyons deriving from the gradual extraction of the material. The deposits are hosted in dolomitic marble, which represents the Triassic-Liassic metamorphic cover of southern sector of Dora-Maira Massif (Penninic domain of Western Alps). The area is a karst region, in fact the deposits originated in an ancient cave system.

The common denominations of the rock are both misleading since, in petrographic terms, it is neither an alabaster nor an onyx. Actually, *Busca Onyx* is an orthochemical sedimentary rock that originates from the precipitation of calcium carbonate crystals in cave environment, it is thus to be correctly indicated as a speleothem.

The host rock is a dolomitic marble characterized by crystals of muscovite and hematite. The interface is constituted by a layer of clay minerals, typical of karst environments. *Busca Onyx* shows, as most speleothems do, a layered concretion structure with brownish and white laminae. The morphology and the size of calcite crystals in the layers is irregular, with predominant columnar fabric, conferring its heterogeneous aspect. This feature is linked to the environmental variations which affected its depositional dynamics through time. In some cases, between two calcite layers there are strata of fine grained detrital material deriving from the surrounding rocks. Their presence is due to the mechanical transport (e.g. episodic flooding of cave passages) of mineral fragments of quartz, hematite, muscovite, paragonite, fluorapatite, rutile, epidote, zircon, wollastonite, fluorophlogopite and amphiboles.

The mineralogical characterization is done by micro-Raman spectroscopy; chemical analyses of mineral phases are performed with SEM-EDS, while geochemical analyses have been carried out by trace elements identification using micro-XRF and ICP-OES. Furthermore, U/Th dating and ^{18}O and ^{13}C isotopic analyses were done to reconstruct the paleo-environment at the time of deposition.

A multidisciplinary geo-archaeological approach to reconstruct the evolution of the Corfinio site (AQ)

Marinangeli L.*¹, Agostini S.², Antonelli S.¹, Baliva A.¹⁻³, Cardinale M.¹, Colantuono L.³, La Salvia V.¹, Menozzi O.¹, Moderato M.¹, Pompilio L.¹, Santoro S.¹ & Somma M.C.¹

1. DiSPUTer, Università di Chieti "G. d'Annunzio". 2. Soprintendenza per i Beni Archeologici dell'Abruzzo, Chieti
3. GEO-Logica snc, Roma.

Corresponding email: lucia.marinangeli@unich.it

Keywords: Geo-archaeology, remote sensing, geophysical survey.

Remote and proximal sensing techniques are able to strongly support the archaeological research in terms of regional to local scale studies. The development of the so-called landscape archaeology has to include remote sensing analyses to better understand the context where ancient settlements developed. Contextual studies of the landscape can be accomplished via both morphometric analyses using Digital Elevation Models (DEMs) and estimates of the ancient land cover distribution using multispectral sensors. Alongside the regional investigation, the archaeological research requires information about the underground - where possible ancient structures can occur - to be acquired. Underground studies are accomplished using geophysical investigation techniques, like GPR (Ground Penetrating Radar) and a tridimensional ERT (Electrical Resistivity Tomography), which are generally carried out for geological investigations and, being non-invasive, are suitable for the investigation of possible buried features.

We used such a multidisciplinary approach to study the landscape archaeology in the central part of the Abruzzo region (Italy) with detailed underground investigations of the Corfinium settlement in the proximity of the "Valvense Abbey" (XI-XII sec.). The aim of the research is to: a) provide a regional context to archaeological studies in the Corfinium site, and b) unravel the complicate asset of the Corfinium site which has been populated several time in ancient periods.

In order to accomplish these main objectives we used: a) remote sensing techniques for the extraction of morphometric features and land use estimates; b) geophysical techniques to identify buried structures. This work was also supported by the archaeological digging.

The remote sensing analyses was carried out with aerial multispectral data available from Regione Abruzzo and a dedicated flight performed by Guardia Costiera - Nucleo di Pescara. A 3D model was also obtained by a drone image coverage. Some interesting features were identified using a stretched NDVI processing tool, though this area is strongly modified by agriculture activities which alter the potential response of buried remnants.

We found interesting response from the GPR survey which was carried out in the plain area near the Valvense Abbey with the identification of a large structure at about 4 m depth.

The 3D ERT survey was carried out only in selected areas of the Corfinium settlement chosen following the available bibliographical data and/or the response of the GPR data. We also have found some interesting response between 4-6 m of depth, which is in agreement with the GPR result. Based on these findings, we are investigating the possibility of the presence of a buried water reservoir of roman age which was not identified before.

Mineralogical and petrographic analysis of early-Hellenistic mortars from a Punic-Roman residential area discovered at Palermo (Sicily)

Montana G., Randazzo L.* & Cerniglia M.R.

Dipartimento di Scienze della Terra e del Mare (DiSTeM), Università di Palermo.

Corresponding email: luciana.ranadazzo@unipa.it

Keywords: Early-Hellenistic mortars, Palermo (Sicily), mineralogical and petrographic analysis.

Lime based mortars dated back to 4th-3rd century BC were sampled in a Punic-Roman residential area recently brought to light in the historical centre of Palermo. The collected mortars have been analyzed by optical microscopy (PLM), X-ray powder diffraction analysis (XRPD) and scanning electron microscopy coupled with energy dispersive spectrometry (SEM-EDS). The study was aimed to characterize these materials from the textural and compositional point of view in order to define the recipes. The mineralogical and petrographic investigations allowed to establish 4 different recipes used for the formulation of the studied floor and wall mortars in terms of both compositional and textural features. The aggregate resulted to be composed by different proportions of alluvial calcareous and siliceous sand or else by “cocciopesto”. Aerial lime based mortars (for the most part magnesium-bearing) have been used for wall coatings and decorations, while the use of hydraulic lime based mortars was mainly documented for floor covering. Furthermore, it is interesting to report an unusual mosaic floor covering manufactured with “tesserae” obtained from overfired limestone scraps (locally produced) and aerial lime-based binder. These results contribute to improve the knowledge concerning raw materials and recipes (relative to the end-use) employed for mortar manufacturing at Palermo in antiquity. A diachronic correlation with previously studied mortars manufactured in Baroque and Neoclassic periods was also made. It allowed to demonstrate a surprising continuity both in the selection criteria of the raw materials and in the formulation of the specific recipes. Moreover, through the study of the ancient recipes it will be possible to formulate restoration mortars with full awareness.

Chromatism and the chromatic alteration of the florentine sandstone pietra serena

Pecchioni E.*¹, Fratini F.², Cantisani E.², Vettori S.² & Ricci M.³

1. Dipartimento di Scienze della Terra, Università di Firenze. 2. Istituto per la Conservazione e la Valorizzazione dei Beni Culturali, CNR, Sesto Fiorentino (FI). 3. Dipartimento di Chimica "Ugo Schiff", Università di Firenze.

Corresponding email: elena.pecchioni@unifi.it

Keywords: Pietra Serena, chromatism, chromatic alteration.

Pietra Serena is one of the materials more used in Florentine architecture. It is a sandstone that crops out in the hills north of the city in the municipality of Fiesole and it has been employed mainly for ornamental purposes. This litotype belongs to the Macigno/Monte Modino Formation (Oligocene Upper- Miocene Lower) which consists of beds of turbiditic sandstones separated by pelitic levels which are the finest components of each single turbidity layer. Petrographically, Pietra Serena can be defined as a medium-coarse-grained lithic arkose made of quartz, feldspars, micas, fragments of metamorphic and magmatic rocks. The clayey matrix is quite abundant while the carbonatic cement is present in a lower amount.

Generally the decay process of sandstones is related to the type of matrix, the amount of cement, the kind of clay minerals and to the pore size distribution: the water infiltration causes swelling of the clay minerals, loss of the clayey matrix, with resulting exfoliation, peeling of the stone artefacts and change of colour. Pietra Serena usually has a bluish-grey colour in fresh cut but with time it can lose its original colour acquiring a brown and/or reddish colour on the surface of buildings.

In this research the correlation between the composition and physical characteristics of Pietra Serena employed in architectural decorations in the centre of Florence and its chromatism and chromatic alteration has been investigated.

The results point out that, given the almost constant iron content, the kind of exposition to atmospheric agents and the petrographical and physical characteristics (eg. amount of calcitic cement, porosity) play a main role on the chromatic alteration of the stone.

In the case of the formation of a red chromaticity, it is possible to assume that the source of iron is mainly related to biotite $K(Mg,Fe^{2+})_3[AlSi_3O_{10}(OH,F)_2]$ and chlorite $(Mg,Fe^{2+})_5Al(AlSi_3O_{10})(OH)_8$: the chemical alteration of these minerals due to hydrolysis gives rise to release of Fe^{2+} , easily oxidized to Fe^{3+} in an oxidative environment.

In case of an high amount of calcite cement which occludes the porosity, the chemical alteration of biotite and chlorite is inhibited due to a lower action of the percolating water thus hindering the diffusion of iron, preserving the original grey colour of the rock.

The case of the variety of Pietra Serena called Pietra Bigia is different; this sandstone has a typical yellow-brown colour, not only superficially but in the whole rock outcrop; the colour was formed in geological times in areas close to fractures from which a front of oxidation propagated, developing this particular chromatic variation different from the typical grey colour.

Archaeometrical investigations of painted wall plasters from an Hellenistic *domus* at Arpi (Foggia, III sec. a.C.)

Pinto D.*¹, Garavelli A.¹, Muntoni I.M.², Bellizzi F.¹ & Lamacchia A.¹

1. Dipartimento di Scienze della Terra e Geoambientali, Università di Bari.

2. Soprintendenza Archeologia della Puglia, Centro Operativo per l'Archeologia della Daunia, Foggia.

Corresponding email: daniela.pinto@uniba.it

Keywords: Painted plasters, pigments, Arpi.

This work deals with the archaeometric study of painted plaster fragments coming from the mural paintings of the so-called Hellenistic peristyle *domus* "dei leoni e delle pantere" in the archaeological site of Arpi (Foggia), one of the main Daunian centre, excavated in the ninety of the last century in the ONC28 locality by the Soprintendenza Archeologia della Puglia (Mazzei, 2002). The fragments were sampled from pieces of faux-marble-painted rectangular blocks decorating inner walls of two rooms of the *domus* attributed to a wealthy Daunian family. Thirty five samples, showing different colours (red, yellow, black, blue, green, white), were taken from several blocks of painted "marbles" attributed to the two rooms identified, from their large floor mosaics, as "sala del mosaico dei delfini" and "sala dei leoni e delle pantere". The aim of the study was the characterization of the mortars, the identification of the pigments and the correlation of plaster fragments coming from different sampling areas and stratigrafic units, also with the aim to contribute to the ongoing restoration work. Mortars and painted layers were investigated by optical microscopy (OM), scanning electron microscopy equipped with Energy Dispersive System (SEM-EDS) and X-ray diffraction techniques (XRD). OM observations in thin sections showed that samples from the "sala del mosaico dei delfini" are characterized by a inner layer of plaster with a calcitic binder and an aggregate mainly composed by carbonate rock fragments and flint, with minor amounts of micas, pyroxenes, fossils and cocchiopesto. On the surface of the plaster a single, or often double layer, of a refined mortar (marmorino) obtained by the use of spatic calcite as aggregate, is present. In samples with a double layer of finishing plaster, the calcite crystals show very different grain size in the two layers (about 0.8 mm in the inner layer and about 0.2 mm in the external one). Painted plaster fragments from the "sala dei leoni e delle pantere" showed an inner layer of plaster with the aggregate only composed by large and rounded carbonate rock fragments and flint grains, under a single layer of finishing plaster with spatic calcite crystals. The pigments identified in samples from both the rooms are: red and yellow ochres, carbon black, Egyptian blue. Green colours were found to be made by a mixing of yellow ochre, carbon black, Egyptian blue and green earths.

Mazzei M. 2002. La Daunia e la Grecia settentrionale: riflessioni sulle esperienze pittoriche del primo ellenismo. In: Pontrandolfo A. (a cura di), La pittura parietale in Macedonia e Magna Grecia, Paestum, Pandemos, 67-80.

***In-situ* LA-ICP-MS analysis of white marble for provenance purpose: application on Carrara quarry district and Musei Capitolini artifacts**

Poretti G.*¹, De Vito C.¹, Conte A.M.², Borghi A.³, Brilli M.⁴, Gunter D.⁵ & Zanetti A.⁶

1. Dipartimento di Scienze della Terra, Sapienza Università di Roma. 2. Istituto di Geoscienze e Georisorse, CNR, Roma. 3. Dipartimento di Scienze della Terra, Università di Torino. 4. Istituto di Geologia Ambientale e Geoingegneria, CNR, Roma. 5. Department of Chemistry and Applied Biosciences, ETH Zürich, Switzerland. 6. Istituto di Geoscienze e Georisorse, CNR, Pavia.

Corresponding email: poretti.giulia@gmail.com

Keywords: White marble (Carrara), study of provenance, LA-ICP-MS.

Numerous methodologies have been trying in the past to discriminate among different ancient white marbles from Mediterranean basin. These techniques involve petrographic analyses (including MGS parameter), carbon and oxygen isotope mass-spectrometry, cathodoluminescence, manganese electron paramagnetic/spin resonance (EPR/ESR). However, provenance determinations using multianalytical approaches are still insufficient because overlapping results, due to the growing sets of databases. Trace elements have been used to great advantage for petrogenetic interpretations of different metamorphic rock-forming minerals, but similar studies on white marble have been fewer. In this work we investigate the behavior of trace elements in white marble from four quarrying area of the Carrara district (i.e., Fossacava, Gioia, Colonnata and Torano) by LA-ICP-MS (Laser Ablation Inductively Coupled Plasma Mass Spectrometry). In order to assess the feasibility of this technique to provenance studies, we have applied it also to the archaeological artifacts from the Musei Capitolini collection of certain provenance. The use of LA-ICP-MS, an appropriate technique in the analysis of trace elements (due to its extremely low detection limits), can provide new geochemical markers useful to discriminate white marble of different geological contexts. In the Carrara and Musei Capitolini study case the concentration of the REE (ppm) has allowed identifying different compositional results, based both on absolute concentrations of these trace elements and their distribution patterns. Samples of Carrara marble, despite showing similar trends to almost all quarries, differ in the absolute concentrations of the REE elements. Moreover, statistical treatment of data by means of principal component analysis (PCA) discriminates clearly Torano samples from those of the other three quarries examined (Gioia, Fossacava and Colonnata). Furthermore, the comparison with the absolute concentrations and patterns of distribution between archaeological and geological samples showed the goodness of the analytical method, suggesting that marble samples of Musei Capitolini were probably mined in Colonnata valley.

The comparisons of LA-ICP-MS results of white “Carrara marble” samples extensively used both as architectural stones and for statuary, with archaeological artifacts seem to offer an opportunity to explore raw material acquisition, trade route and exchange.

Provenance study of marbles used as covering slabs in the archaeological submerged site of Baia (Naples, Italy): the case of the “Villa con ingresso a protiro”

Ricca M.*¹, La Russa M.F.¹, Belfiore C.M.², Ruffolo S.A.¹, Barca D.¹ & Crisci G.M.¹

1. Dipartimento di Biologia, Ecologia e Scienze della Terra (DiBEST), Università della Calabria.

2. Dipartimento di Scienze Biologiche, Geologiche e Ambientali, Università di Catania.

Corresponding email: michela.ricca@unical.it

Keywords: White marbles, submerged site, provenance.

This study, belonging to the framework of the national research project “COMAS” (Planned CONservation, “in situ”, of underwater archaeological artifacts), funded by the Italian Ministry of Education, Universities and Research (MIUR), focuses on archaeometric investigations of white marbles collected from the submerged archaeological site of Baia (Naples). The marine area includes the ruins of the ancient Roman city, whose structures range from luxurious maritime villas and imperial buildings with private *thermae* and *tabernae*, to more modest houses. Analyses were performed on fifty marble fragments of covering slabs, belonging to several pavements of the monumental villa, called *Villa con ingresso a protiro*, in order to ascertain their provenance. For such a purpose, minero-petrographic and geochemical techniques were used, including polarized optical microscopy, scanning electron microscopy coupled with energy dispersive spectrometry (SEM-EDS), carbon and oxygen stable isotope ratio determinations, inductively coupled plasma mass spectrometry and X-ray diffraction. In addition, in order to identify the marble sources, results were compared with existing databases of white marbles commonly used in antiquity, especially in the Mediterranean basin. Analytical data showed that a variety of precious marbles was used in the ancient roman city of Baia, confirming the importance of the archaeological submerged site and also allowing to broaden the existing literature data.

***Piscina Mirabilis*: preliminary characterization of geomaterials**

Rispoli C.*¹, Esposito R.², Cappelletti P.¹, Morra V.¹ & Talamo P.³

1. DiSTAR, Università di Napoli "Federico II". 2. Dipartimento di Scienze Umanistiche, Università di Napoli "Federico II". 3. Soprintendenza Speciale per i Beni Archeologici della Campania

Corresponding email: concetta.rispoli@unina.it

Keywords: *Piscina Mirabilis*, tobermorite, hydraulic mortars.

This work is the result of the interaction between archeological and geological investigations on the *Piscina Mirabilis*, one of the most important archeological sites in Campania region, situated in an area of great geological and archeological interest: the Campi Flegrei.

Objectives of this work are to improve the knowledge of Roman construction techniques by means of detailed microstructural and compositional examinations of the cementitious binding matrix, and aggregates, to point out the provenance of raw materials, mix-designs proportioning, mineralogical secondary processes.

Thanks to the permission allowed by Special Superintendence of Archeological Heritage of Campania has been possible to take out small non-invasive, but representative, samples of geomaterials in order to reach our characterization scopes and to provide useful information on probable future restoration activities.

Mineralogical-petrographic characterization of samples taken by pillars and walls have been performed mainly by X-ray powder diffraction (XRPD) scanning electron microscopy analysis (SEM) and Energy Dispersive X-ray Spectroscopy (EDS).

Results confirmed that the Roman engineers extensively used tuff aggregate, lime hydrated, and cocchiopesto.

The typical mineralogical association of phillipsite > chabazite > analcime, in particular points out the provenance for the tuff aggregate from the Yellow Neapolitan Tuff (NYT) formation, which is connected to the Campi Flegrei volcanic activity, dated back to 15.000 years ago.

Extremely interesting is the composition of the cementitious binding matrix, with the contemporary presence of gel-like C-S-A-H, derived from the reaction between the lime and cocchiopesto, calcite and, finally tobermorite.

The presence of calcite is likely connected to the not-well reacted clast of underburned lime, although it is not possible to exclude that some carbonation subsequently happened, from the residual portlandite, since mortars cured in a subaerial environment.

As far as the tobermorite, there is not a reliable interpretation to explain its formation, at the current state of knowledge. This phase is concentrated within relict of lime clasts, but also inside mortar porosities.

Its formation was previously related to those of natural rock-forming cement systems in pyroclastic deposits immersed in the ocean and in saline lake brines. Literature attests that tobermorite forms at higher temperatures, 150-200 °C, than those of lime-based materials; moreover it is wellknown that the heat of hydration in pozzolanic cements is lower than normal cements (Collepari et al., 2009). The long curing time in water is probably the key-factor in understanding the formation of tobermorite from gel-like C-S-A-H at ordinary temperatures. This topic will be the object of forthcoming researches.

Collepari M., Collepari S. & Troli R. 2009 . Il nuovo calcestruzzo, Enco S.r.l., Ponzano Veneto, Grafiche Tintoretto, 5th Ed., Villorba, Treviso, 533 p.

The use of nano particles in Cultural Heritage: examples of application on stone materials

Ruffolo S.A.* & Crisci G.M.

Dipartimento di Biologia, Ecologia e Scienze della Terra, Università della Calabria.

Corresponding email: silvestro.ruffolo@unical.it

Keywords: Restoration, nanolime, nanosilica.

Deterioration of stone materials used in artistic/architectural field (lime-based wall paintings, calcareous stones) is one of the most serious problems facing conservation today. Air pollution, soluble salts and biodeterioration are the main causes of decay, and the existing literature includes many papers concerning the investigation of their mechanisms of action. In the last years, various nanoparticles have been widely used in the treatment of construction materials of historical monuments for consolidation and conservation of such structures.

Nanoparticles based on titanium dioxide are used to provide self-cleaning and antimicrobial properties to stone surface, located both in aerial and in underwater environment.

Nanostructured consolidants are recently used to boost a more compatible and sustainable restoration taking into account the material itself, the restorer's health and the environment. Nano sized lime has the advantage to be fully compatible with limestone, mortars and plaster, as well as the nanosilica has a great affinity with silica rich stones.

This contribution deals with several application of those nanoparticles to stone materials, carried out both in laboratory and *in situ*.

Multi-analytical characterisation of Egyptian Flint as a means for understanding seasonality in the Nile valley and Western Desert (Egypt)

Santello L.*¹, Maritan L.¹, Mazzoli C.¹, Germinario L.¹, Nestola F.¹, Hanchar J.M.² & Usai D.³

1. Dipartimento di Geoscienze, Università di Padova. 2. Department of Earth Sciences, Memorial University of Newfoundland, Canada.
3. Centro Studi Sudanesi e Sub-Sahariani, Treviso.

Corresponding email: lisa.santello@unipd.it

Keywords: Egyptian flint, chert, Nile Valley.

Seasonal mobility of ancient populations occurred during Early Holocene in the area of the II Cataract of the Nile River (Northern Sudan) and the Western Desert region (Southern Egypt), as attested by different archaeological indicators, among them pottery and lithics. A distinct feature in the lithic assemblages is the presence of a flint type that has been called "Egyptian flint". The main macroscopic characteristic of the Egyptian flint is its dark and pale grey colour. Limestones rich in cherts crop out mainly in the Western Desert in the Eocene formations and are not present in the geological substrate around the II Cataract area. However, along the Nile valley, it is possible to find chert-cobbles in the fluvial secondary deposits, probably deriving from other chert-rich deposits of Jurassic age, cropping out in the area of Jebel Abyad (West of Dongola, Sudan, at the latitude of the III Cataract). This study aims at ascertaining if a common chert-source for both lithic assemblages found at the II Cataract and in the Western Desert sites was used. Therefore, in order to determine whether the dark grey/grey Egyptian flint from the II Cataract and Western Desert derive from the same source, a microstructural, compositional and mineralogical analysis was performed on the samples.

For this purpose we analysed a set of 22 flint tools from 11 sites of the Western Desert region (Egypt) and near the II Cataract (Sudan), sampled from two lithic collections (Wendorf and Colorado) stored at the British Museum (London, UK). SEM, μ XRD, LA-ICP-MS and μ PIXE analyses were performed to characterize the considered tools. The microstructure of the flints, observed at the SEM, resulted to be in most of the cases not homogeneous, composed mainly by microcrystalline quartz, associated to numerous microfossil traces, dolomite and calcite crystals, apatite fragments and minor oxides, sulphides and sulphates, in few cases with crystal dissolution traces and pores.

Mineralogical analysis indicates that in addition to the quartz, these samples contains also small amount of moganite, mainly crystallised inside microfossils, as attested by μ Raman mapping.

The moganite is accompanied by higher Fe content than the surrounding microcrystalline quartz, as observed from μ PIXE mapping and LA-ICP-MS analysis: this element seems to favour the moganite crystallization.

The “*Vie Cave*” archaeological and geologica

Santo A.P.¹, Pecchioni E.P.*¹, Piccini L.¹, Di Fazio L.², Garzonio C.A.¹ & Fratini F.³

1. Dipartimento di Scienze della Terra, Università di Firenze. 2. Orto Botanico, Museo di Storia Naturale di Firenze. 3. ICVBC, CNR, Firenze.

Corresponding email: elena.pecchioni@unifi.it

Keywords: "Vie Cave", archaeological and geological site, conservation.

The territory of Southern Tuscany, on the Lazio border, is characterized by the presence of extensive pyroclastic deposits emplaced by the Latera Volcano (part of the Monti Vulsini volcanic district). The area displays a peculiar tabular morphology, which was incised by deep gorges; these latter are characterized by a particular microclimate able to preserve patches of beech thermophilic forest of glacial-relict origin. In the areas of Fiora river confluence, the erosion formed tuff spurs bordered by steep slopes, upon which many settlements have sprung up since the Etruscan period, among which the present villages of Pitigliano, Sovana and Sorano, in Tuscany, had a particular development during the Etrusco-Roman Age and later during the Middle Age. In this unique landscape, the Etruscan civilization had built up a dense road network connecting towns, workplaces, places of worship and necropolises located throughout the territory; in order to overcome the difference in height between the bottom of the gorges and the plateaus above them, long cuts into the tuff were dug, the so called *Vie Cave*, taking into account the morphology and the mechanical characteristics of pyroclastic deposits. Over the centuries, many of these pathways have lost their function of connection between the gorges and the agricultural lands of the plateaus and their regular maintenance was no longer carried out. As a consequence, the situation of abandonment has led to the complete degradation and naturalization of the sites, particularly in the areas where the major rock falls have occurred, but at the same time contributed to preserve the landscape generated by these pathways. This represents the greatest threat to the conservation of these sites but also the natural evolution suffered by the rock cliffs. The World Monument Found promoted in 2004 the “*Vie Cave*” as assets of global interest; this represents an important recognition and an incentive to take actions to protect this unique heritage. Currently the *Vie Cave* walls and several archaeological structures carved into them show a precarious stability, the constituent materials display high grade of decay intensified by the dense vegetation that has developed over the rocky scarps. The interventions of recovery should be carried out trying to prevent further degradation processes responsible of the roads and walls surface erosion and of the detachment of large block tuffs from the walls. The preservation of this important site and of its millenarian historical remains can be achieved only through a “holistic” approach, which has to take into account all the environmental components, either natural or anthropic, according to a long-term project of territorial management.

Trace element analysis of archaeological glasses: comparison between LA-ICPMS and Electron Microprobe analysis

Silvestri A.¹⁻², Fioretti A.M.*² & Zanetti A.³

1. Dipartimento di Geoscienze, Università di Padova. 2. Istituto di Geoscienze e Georisorse, C.N.R. Padova.

3. Istituto di Geoscienze e Georisorse, C.N.R. Pavia.

Corresponding email: anna.fioretti@igg.cnr.it

Keywords: LA_ICPMS, Electron Microprobe Analysis, glass.

Chemical characterization of archaeological glass is a powerful tool to gain information on the raw material and its provenance and on the production techniques. Trace elements are fundamental in distinguishing compositional classes with different archaeological meaning, reconstructing the original recipes and in identifying possible re-use. Both electron microprobe and LA-ICPMS data are often reported in literature and direct comparison is sometime questionable.

We present here the results and a comparison of chemical analyses carried out by both EMPA and LA-ICP-MS on a batch of archaeological glass and on the international reference material Corning glass B as an unknown sample.

The CAMECA SX50 electron microprobe of CNR-IGG-Padova, equipped with four wavelength-dispersive spectrometers (WDS) was used to measure both major and trace elements.

Trace elements were analysed by LA-ICP-MS at CNR-IGG-Pavia.

Precision and accuracy were also calculated for both sets of measures. The precision of EMPA data was generally between 0.5% and 10% for major and minor elements. Accuracy was lower than 1% for SiO₂, Na₂O, and FeO, lower than 5% for CaO, K₂O, P₂O₅, and Sb₂O₃, and higher than 12% for other major and minor elements, except TiO₂. In the case of Al₂O₃, CuO and ZnO, the accuracy levels improved considerably when the theoretical composition of Corning B was considered (Brill, 1999). LA-ICP-MS results showed that, for most trace elements, precision was about 2% and accuracy highly variable, but usually within 5-20% (except for B, Cr, Ba, Sn and Pb). The same accuracy range was also reported for LA-ICP-MS measurements, carried out on the same standard by Vicenzi et al. (2002). In the case of LA-ICP-MS data, accuracy levels for Sn and Pb also improved considerably when the theoretical composition of Corning B was considered (Brill, 1999).

Note that some minor or trace elements, such as Ti, Mn, Fe, Co, Cu, Zn, Sr, Ba, Sn, Sb and Pb, were determined by both EMPA and LA-ICP-MS in order to compare the precision and accuracy of both methods. When the above elements were present in concentrations above the detection limits of EMPA, chemical data obtained by LA-ICP-MS typically provided higher precision than EMPA but more or less comparable accuracy.

Brill R.H. 1999. Chemical analyses of early glasses. Catalogue and Tables of Analyses. The Corning Museum of Glass, Corning, New York.

Vicenzi E.P., Eggins S., Logan A. & Wyszczanski R. 2002. Microbeam Characterization of Corning Archeological Reference Glasses: New Additions to the Smithsonian Microbeam Standard Collection. J. Res. Natl. Inst. Stan. Technol., 107, 719-727.

SESSION S16

Fluid geochemistry in volcanic, geothermal and seismic areas

CONVENORS

F. Frondini (Univ. Perugia)

B. Capaccioni (Univ. Bologna)

Geochemistry of groundwater from Parrano and Fonti di Tiberio (TR), a tool for evaluating the geothermal potential of southern-western Umbria

Beddini G.* & Frondini F.

Dipartimento di Fisica e Geologia, Università di Perugia.

Corresponding email: giuliobeddini@gmail.com

Keywords: Geothermal energy, geochemistry of waters, Umbria.

Umbria shows some zones where it is possible to find middle-low enthalpy geothermal systems, most of these areas are located in the Southern-Western part of the region. These geothermal zones are probably connected with the Vulsini Volcanic District and the sporadic and monogenetic centres of the Intra Appenninic Province, like Volcanic Centre of S.Venanzo, close to Peglia Mount.

This study has been focused on two systems: Parrano (Tr), near to Volcanic area of S.Venanzo, and Fonti di Tiberio (Tr), located at the eastern border of the Vulsini Mts volcanic district. Both the systems are close to the Torre Alfina Geothermal System, which is a middle enthalpy system widely studied in last years.

The surveys and the sampling have been focused both on normal and thermal springs (or wells) present into the selected areas, in order to obtain information about the circulation in the regional aquifer, on the reactions among groundwater and the host rocks (dolostones, evaporites and limestone) and on the mixing with deep CO₂-rich fluids of mantle origin.

For each sampling point the major ions content, Si content, trace elements concentration and O, H and C isotopes have been determined. Subsequently, aqueous speciation calculation performed with the PHREEQC code (Parkhurst, 1995; Appelo & Postma, 1993) permitted to determine the PCO₂ value and the saturation indexes with respect to relevant mineral phases; the application of specific geoindicators for carbonate-evaporite systems and classical geothermometers based on silica solubility allowed the estimation of reservoir temperatures and PCO₂; isotope geochemistry and mass balance calculations have been used to track the origin of the fluids.

The composition of sampled waters range from Ca-HCO₃ type to a Na-Cl(HCO₃) type, and clearly shows that thermal fluids composition derives from mixing processes of a deep thermal component with a shallow, cold component.

Results show that both systems are mainly fed by meteoric water but in both cases a deep component, characterised by an high CO₂ content, can be recognised. This component, characterising most of deep fluids on the Tyrrhenian side of Central Italy is probably related to a mantle source. Geothermometry and geobarometry calculations indicate (i) temperatures between 80 and 100 °C, and PCO₂ of 60-80 bar at Fonti di Tiberio and (ii) temperatures of 100-120 °C and PCO₂ higher than 60 bar for the deep system feeding Parrano springs.

Appelo C.A.J. & Postma D. 1993. Geochemistry, groundwater and pollution: Rotterdam, A.A. Balkema.

Parkhurst D.L. 1995. User guide to PHREEQC: A computer program for speciation, reaction-path, advective-transport, and inverse geochemical calculations. U.S. Geol. Surv. Water Resour. Invest. Rep., 95-4227, 151 pp.

Surface phenomena witnessed during and after the 2012 Emilia earthquakes: Fact or Fiction? A response from water and gas geochemistry

Bonzi L.¹, Capaccioni B.^{*2}, Castaldini D.³, Coltorti M.⁴, Cremonini S.², Di Giuseppe D.⁴, Ferrari V.¹, Severi P.¹, Sciarra A.^{4,6}, Vaccaro C.⁴ & Todesco M.⁵

1. Servizio Geologico, Sismico e dei Suoli, Regione Emilia-Romagna, Bologna. 2. Dipartimento di Biologia, Geologia e Ambiente, Università di Bologna. 3. Dipartimento di Scienze Chimiche e Geologiche, Università di Modena. 4. Dipartimento di Fisica e Scienze della Terra, Università di Ferrara. 5. INGV, Bologna. 6. INGV, Roma.

Corresponding email: bruno.capaccioni@unibo.it

Keywords: Gas geochemistry, water geochemistry, 2012 Emilia earthquakes.

The occurrence of anomalous surface phenomena accompanying seismic events of particular intensity is well known for a long time. During the recent 2012 Emilia earthquakes a number of anomalous events were experienced by local population: uprising of salty waters with bubbling gas (11 cases); heating of soil, groundwater and lake water often followed by fish death (13 cases); fracturing and subsidence (6 cases) and appearance of sand boils (about 20 cases) (<http://ambiente.regione.emilia-romagna.it/geologia/temi/geologia/fenomeni-geologici-particolari>). During and after the seismic crisis, both satellite IR thermal sensors and direct in situ measurements have revealed the existence of surface thermal anomaly, whose origin is still matter of debate. With the exception of small areas where the structural highs of the carbonate rocks are closed to the surface, the measured geothermal gradient in the area is normally quite low (1°C/100 m), with temperature not exceeding 50 °C at 2000 m depth. Moreover, no evidence of uprising of thermal fluid has been documented. With the aim of shedding light on the real characteristics of this thermal phenomena and on its origin a particular area directly affected by the 2012 seismic crisis known as “Warm Earths of Medolla” (TCM; literally, “Terre Calde di Medolla”) has been investigated in detail. TCM is a farming area, located in the Po Plain about 30 km far from the town of Modena (Emilia-Romagna region, northern Italy), which has already been known by local population for the relatively high temperatures of the soil. A measurements campaign, carried out after the devastating 2012 Emilia earthquake, showed soil temperatures up to 50 °C, i.e. 25-30 °C above the background value, coupled with diffuse fluxes of CH₄ (0-2432 g×m⁻²×d⁻¹) and CO₂ (0-1184 g×m⁻²×d⁻¹). According to the lateral and vertical distributions of the measured temperatures and chemical and isotopic compositions of the soil gases, the most reliable explanation consists in an exothermic oxidation of diffuse biogenic methane seeping at very shallow depth (< 1 m). Such a process occurs in the presence of free oxygen and methanotrophic bacteria and can thus explain (i) the observed ground heating up, (ii) the diffuse emission from the soil of CO₂ characterized by an extremely negative isotopic (¹³C/¹²C) signature, and (iii) the lack of diffuse and low CH₄ fluxes. Numerical modelling of heat generation and gas propagation toward the surface confirmed that this mechanism can sustain the observed anomaly. This mechanism of heat generation due to a strain-induced variability of CH₄ fluxes and possible oxidation at shallow depths could explain most of the observed surface anomalies apparently associated with the 2012 Emilia earthquake, such as ground and groundwater heating, increasing turbidity of superficial waters and fish death, uprising of deep salty waters, other than, of course, the sudden appearance of sand boils.

Geochemistry of water and gas discharges from the Tenorio volcanic system (Costa Rica)

Capecchiacci F.^{*1-2}, Tassi F.¹⁻², Liegler A.³, Fentrees S.³, Deering C.³, Vaselli O.¹⁻², Martinez M.⁴ & Taylor Castillo W.⁵

1. Dipartimento di Scienze della Terra, Università di Firenze. 2. Istituto di Geoscienze e Georisorse, CNR, Firenze. 3. Department of Geological and Mining Engineering and Sciences, Michigan Technological University, Houghton, USA. 4. OVSICORI-UNA-Observatorio Vulcanológico y Sismológico de Costa Rica, Universidad Nacional, Heredia, Costa Rica. 5. ICE - Instituto Costarricense de Electricidad, San José, Costa Rica.

Corresponding email: francesco.capecchiacci@unifi.it

Keywords: Tenorio volcanic system, fluid geochemistry, Costa Rica.

Tenorio (10.673°N, 85.015°W) is a complex basaltic-andesitic volcano constituting the south-east end of the Guanacaste Volcanic Chain (NW Costa Rica) that also includes Rincon de la Vieja and Miravalles volcanoes. The Tenorio complex consists of a series of NNW-aligned structures and two twin-craters. No historical eruptions are recorded, although a legend tells about an eruption (never documented) in 1816 (Alvarado, 2000). Tenorio lies on a Pre-Pleistocene regional basement composed by andesite and basaltic lavas and continental sedimentary rocks. The eruptive sequence consists of alternate deposits of lavas and pyroclastic rocks. In this area, geothermal investigations have been carried out by ICE since the late 80's. Exploratory wells (down to -2,200 m) were drilled in the SW flank of the volcano. To the best of our knowledge, no detailed geochemical and isotopic data have been published for the fluids discharged from the Tenorio volcanic system, with the exception of few geochemical data, which date back more than 20 years ago (Giggenbach and Corrales, 1992). In the framework of a long lasting scientific cooperation, started in 1998, between Costa Rica Institutions (i.e. OVSICORI-UNA and ICE) and the Department of Earth Sciences of the University of Florence (Italy), and the recent collaboration with the Michigan Technological University, several sampling campaigns were carried out in the Tenorio area. The current database consists of 28 thermal and cold waters and 9 gas samples. Springs have temperatures between 18 and 94 °C, pH values from 2 to 7.2. Most waters show Ca-SO₄ and Ca-Cl-SO₄ chemical compositions, whereas Ca-HCO₃, Na-Cl-HCO₃ and Na-Ca-HCO₃ chemical facies are less abundant. The chemical composition of gases is typical of hydrothermal emissions, being dominated by CO₂, H₂S, N₂ and CH₄, with minor concentrations of O₂, Ar, H₂, He, CO and Ne, but there are significant differences between different areas of gas discharges. The $\delta^{13}\text{C-CO}_2$ values range from -5.44 to -2.06‰ V-PDB, i.e. similar to those characterizing gases from both Rincon de la Vieja and Miravalles, suggesting that in the whole Guanacaste region the magmatic CO₂ source is significantly contaminated by limestone. Most fluids are discharged along the main fault systems and the thermal waters are affected by mixing with surficial aquifers at different degrees. The peculiar sky blue color of the Celeste River is probably due to light-scattering effects caused by colloidal material suspended in the water. The deep reservoir temperature calculated by aqueous and gas geothermometer is likely between 200 and 300 °C.

Alvarado G.E. 2000. Los Volcanes de Costa Rica: geología, historia y riqueza natural, EUNED San José, Costa Rica, 269 pp.

Giggenbach W.F. & Corrales R.F. 1992. Isotopic and chemical composition of water and steam discharges from volcanic-magmatic- hydrothermal systems of the Guanacaste Geothermal Province, Costa Rica, Appl. Geochem., 7, 309-332.

Carbon isotope fractionation of light hydrocarbons in hydrothermal fluids from Copahue volcano, Argentina

Caponi C.*¹, Tassi F.¹⁻², Vaselli O.¹⁻², Fiebig J.³, Agosto M.⁴, Caselli A.⁵ & Liccioli C.⁵

1. Dipartimento di Scienze della Terra, Università di Firenze. 2. Istituto di Geoscienze e Georisorse, CNR, Firenze. 3. Institut für Geowissenschaften, Goethe-Universität, Frankfurt am Main, Germany. 4. GESVA-IDEAN, Departamento Ciencias Geológicas, FCEN, Universidad de Buenos Aires, Argentina. 5. GESVA, IIPG, Universidad Nacional de Río Negro, Roca, Argentina.

Corresponding email: franco.tassi@unifi.it

Keywords: Copahue, hydrocarbons, C-isotope.

Copahue volcano is part of the Copahue-Caviahue Volcanic Complex (CCVC), located in the Southern Volcanic Zone (SVZ: 33.3°-46° S) along the border between Chile and Argentina, ~30 km east of the present volcanic arc-front. In the last century, this system experienced several eruptive cycles, the latter being started in December 2012 and still ongoing. A well-developed hydrothermal reservoir at temperatures up to > 300 °C fed a number of hydrothermal discharges located at the foot of the volcanic structure. This area is considered of interest for geothermal exploitation.

In the framework of a scientific collaboration developed between the University of Rio Negro (Argentina) and the university of Florence (Italy) and Frankfurt (Germany), in March 2014 gas samples from the main fumarolic gas discharges (Las Maquinas, Las Maquinitas, Piedra Copahue, Anfiteatro and Chanco-co) of Copahue volcano were collected for chemical and isotopic analyses. The aim of this study was to investigate the origin of light hydrocarbons and the chemical-physical conditions controlling their behavior. Although unambiguous geochemical criteria for discriminating genetic processes of these organic species in a natural environment are not strictly defined, lab experiments have shown that the carbon isotopic signature of the alkane series may provide useful information. However, carbon isotope data on n-alkanes from volcanic-hydrothermal fluids have rarely been determined due to their low concentrations. For the Copahue gases, this problem was solved by using a new pre-concentration technique, developed at the Stable Isotope Laboratory of Frankfurt, allowing the analysis of ¹³C/¹²C ratios of C₁-C₄ alkanes at concentrations as low as few nanomoles. The analytical results showed that the 5 analyzed gases were characterized by positive C₁-C₄ isotopic trends, which are considered the typical evidence for a thermogenic genesis, although Anfiteatro and Chanco-co evidenced the presence of possible biogenic contribution. This would exclude the attainment of chemical and isotopic equilibrium between CH₄ and CO₂, in contrast with the indication retrieved from the application of gas geothermometry in the H₂O-CO₂-CO-CH₄-H₂ system. Such an apparent contradiction poses some concerns regarding the commonly accepted interpretation of the isotopic data of the light alkanes, suggesting that in a volcanic-hydrothermal environment the fate of CH₄ is controlled by interaction with CO₂, whereas that of light hydrocarbons only depends on organic matter degradation.

Soil CO₂ flux degassing at Solfatara of Pozzuoli (Campi Flegrei, Italy): 1998-2015, sixteen years of measurement

Cardellini C.*¹, Chiodini G.², Rosiello A.¹, Bagnato E.¹, Avino R.³, Frondini F.¹, Donnini M.⁴ & Caliro S.³

1. Dipartimento di Fisica e Geologia, Università di Perugia. 2. Istituto Nazionale di Geofisica e Vulcanologia, Bologna
3. Istituto Nazionale di Geofisica e Vulcanologia, Osservatorio Vesuviano, Napoli. 4. Istituto di Ricerca per la Protezione Idrogeologica, C.N.R. Perugia.

Corresponding email: carlo.cardellini@unipg.it

Keywords: CO₂ flux, volcano monitoring, Solfatara of Pozzuoli.

Solfatara of Pozzuoli is one of the largest studied volcanic-hydrothermal system of the world realising a flux of deeply derived fluids of about 5000 t/d to which is associated an energy release of about 100 MW. Since 1998, extensive soil CO₂ flux surveys were performed using the accumulation chamber method over a large area (1.45 km²), including the crater area and its surroundings. Soil CO₂ degassing at Solfatara is fed by both biological activity in the soil and by the degassing of the hydrothermal system. The statistical analysis of CO₂ flux, coupled with the investigation of the CO₂ efflux isotopic composition, allowed to characterize the different CO₂ sources and to investigate their temporal variability. The geostatistical elaboration of CO₂ fluxes based on sequential Gaussian simulations, allowed to define the spatial structure of the degassing area, pointing out the presence of a well defined diffuse degassing structure interested by the release of deeply derived CO₂ (Solfatara DDS). Solfatara DDS results well correlated to volcanic and tectonic structures interesting the crater area and the eastern area of Pisciarelli. The extension of the DDS experienced relevant variations varying between 4.5x10⁵ m² to 12.3 x10⁵ m², with two major enlargements, the first consisted in its doubling in 2003-2004 and the second in further enlargement of about 30% in 2011-2012, the latter occurring after period of decreasing trend which interrupted 4-5 years of relative stability. These variations mainly occurred external to the crater area in correspondence of a NE-SW fault system where fluxes increased from background to values typical of the endogenous source. The first event was previously correlated with the occurrence in 2000 of a relatively deep seismic swarm, which was interpreted as the indicator of the opening of an easy-ascent pathway for the transfer of magmatic fluids towards the shallower portion of the hydrothermal system; the second event of DDS enlargement well correlates with the recent unrest phase of the system, characterised by an acceleration of the ground uplift. With the same geostatistical approach the total amount of released CO₂ has been estimated, and ranged between about 700 t/d and about 1500 t/d (with an error in the estimate varying between 9 and 15% until the January 2015 when there was an increase up to 2800 t/d. The CO₂ variations in the last two years seems to follow the trend depicted by ground deformations, with increases of fluxes during the uplift accelerations and decreases of fluxes during the phases of "no-uplift". The comparison of the CO₂ flux data with the chemical composition of the main fumaroles suggests that the variation of in the DDS extension are controlled by processes of condensation of the gas plume feeding the Solfatara manifestation, which is accompanied by an overall increase of the temperatures.

Episodes of magmatic fluid injections into the Hydrothermal system of Campi Flegrei: geochemical evidences and physical simulations

Chiodini G.*¹, Avino R.², Caliro S.², Cardellini C.³, Mangiacapra A.² & Minopoli L.⁴

1. INGV, Bologna. 2. INGV, Napoli. 3. Dipartimento di Fisica e Geologia, Università di Perugia. 4. ENEA, Centro Ricerche Portici (NA).

Corresponding email: giovanni.chiodini@ingv.it

Keywords: Hydrothermal fluids, physical simulations, Campi Flegrei.

An accelerating process of ground deformation is currently affecting the Campi Flegrei caldera. The deformation pattern was recently explained with the overlapping of two processes: short time pulses that are caused by injection of magmatic fluids into the hydrothermal system; and a longer time process of heating of the rock. The short pulses were highlighted by comparing fumarolic compositions and ground deformations. The two independent data sets show the same sequence of anomalous peaks with a delay of ~ 200 days of the geochemical signal with respect to the geodetic signal. The heating of the hydrothermal system, which parallels the long-period accelerating curve, is inferred by temperature-pressure gas geoindicators. Referring to a recent interpretation that relates variations in the fumarolic inert gas species to open system magma degassing, we infer that the heating is caused by enrichment in water of the magmatic fluids and by an increment in their flux. Physical simulations of the process show that total injected magmatic fluid masses are the same order of magnitude as those emitted during small-medium size volcanic eruptions, and their cumulative curve highlights a current period of increasing activity. The simulations, constrained by the $\text{CO}_2/\text{H}_2\text{O}$ and CO_2/CH_4 fumarolic ratios, surprisingly well reproduce the thermal evolution of Campi Flegrei system as independently suggested by the CO based gas geo-indicators.

***In situ* determination of the carbon isotopologues of the CO₂ emitted by soils**

Di Martino R.M.R. *, Camarda M. & Capasso G.

INGV, Palermo.

Corresponding email: robertomr.dimartino@gmail.com

Keywords: Carbon isotopologues of CO₂, ground gases, laser-based isotope analyzer.

The stable carbon isotopes of CO₂ provide constraints about the sources and the fluxes between different carbon reservoirs and sinks such as the atmosphere, the biosphere, the carbon dioxide of deep origin, and the oceans. From a volcanological standpoint, the amount of CO₂ emitted by soils during unrests equals or exceeds the carbon dioxide released from the craters of the volcanoes. Among the techniques of volcano surveillance, the stable isotope composition of carbon of the CO₂ emitted from the ground is a proxy for magmatic activity. Since decades, the carbon isotope composition has been analyzed in the laboratory by mass spectrometer on the gas samples collected in field. Since a few years ago, the development of new optical class of isotope analyzer based on the infrared laser allowed to determine in situ the isotope composition of the atmospheric CO₂.

This study focuses on the measurement in situ of $\delta^{13}\text{C}$ of the CO₂ emitted by soils and shows the results of the tests carried out in the laboratory and in field. A special gas sampling method has been fine tuned to collect the gas at a constant flux rate from a depth of 50 cm in the soils, and to identify the isotopologues of the CO₂. The method has been tested in the laboratory and in field with a Delta Ray™ Isotope Ratio Infrared Spectrometer of the ThermoFisher Scientific, field-able to analyze the $\delta^{13}\text{C}$ and $\delta^{18}\text{O}$ of CO₂. The gases were collected by a pumping system, and addressed online to the analyzer through a precision valve. This tailor-made device was added to the standard equipment of the instrument in order to adjust the gas flow in input to the analyzer. In this way, the CO₂ concentration in the cell fulfills the concentration range of the analyzer (200 - 3500 ppm vol) in spite of the CO₂ concentration in the ground gases.

The spatial survey of carbon isotopologues of CO₂ emitted by soils were performed at Vulcano (Aeolian Islands) on a sampling grid that consists of 20 measurement points on a 2.2 km² area at the base of the La Fossa cone. The measurement of the soil CO₂ flux was also performed in the same sampling grid according to the dynamic concentration method.

The results indicate that the sampling system allows the measurement of $\delta^{13}\text{C}$ in the ground gases with CO₂ concentration in the range from < 1000 ppm vol to 100% vol. During the spatial survey we measured $\delta^{13}\text{C}$ of CO₂ values in the range -22‰ (organic source) to 0‰, that represents the signature of deep source of CO₂ at Vulcano. Furthermore, the measurement of the $\delta^{13}\text{C}$ allowed to differentiate the sources (volcanic, biogenic, atmospheric) involved in the CO₂ emissions from the soils, and identify two areas of degassing with isotopic signature of deep origin at Faraglione and Grotta dei Palizzi. Furthermore, the results of the extensive investigation of both the spatial distribution of the carbon isotopologues and the CO₂ flux from soils allowed to assess the budget of CO₂ of deep origin emitted from the degassing areas.

The concentration transients of CO₂, H₂, and He in the volcanic gases: theoretical model and experimental results

Di Martino R.M.R.*¹, Camarda M.¹, Gurrieri S.¹ & Valenza M.²

1. INGV, Palermo. 2. Dipartimento DiSTeM, Università di Palermo.

Corresponding email: robertomr.dimartino@gmail.com

Keywords: Concentration transients, ground gases, retention times.

The thorough understanding of the gas transport through the porous media is of considerable interest in several environmental issues. Potential applications of this knowledge include the topics of contaminant transport through the soils, and the gas leakages from carbon sequestration and storage plants. In volcanology, the gas transport process through the porous media affects the compositions of the ground gases, that are the proxy of the magmatic activity.

Herein we targeted the transients of the chemical composition of the ground gases through the formulation of a theoretical model, and the gas flux simulations carried out in the laboratory. The model accounts for the gas released by soils in volcanic areas, and takes into account the process of the mass transfer triggered by disequilibrium conditions in the system. The theoretical results describe the time-dependent evolution of the composition of the ground gases as the result of the pristine gas mixture, the thickness of the medium, the gas velocity, and the diffusivity of the chemical, that is a substance-dependent quantity. Moreover, the results indicate that the difference in the diffusivities of the different mixture components produce asynchronous transients of the concentrations in the ground gases.

Carbon dioxide (CO₂), hydrogen (H₂), and helium (He) were used in a laboratory-scaled flux simulator with the purpose of investigating the time-dependent evolution of the gas composition profile through a porous medium. The structure of the porous medium (porosity and tortuosity) in the flux simulator, the composition of the pristine mixture, the gas flux velocity, and the thickness of the medium were fully constrained.

The results of this study indicate that the theoretical computations fulfill the experimental data for the compositional range of the gases typically emitted by soils of volcanic and geothermal areas. Furthermore, the measurement of the delays between the concentration transients of two or more components with large difference in diffusivity (e.g. H₂ and CO₂) provide constraints between the chemistry of the ground gases and the depth of the gas reservoir.

Carbon isotopic signature of light hydrocarbons (C₁–C₄) in fluids emitted from fumarolic discharges at São Miguel Island (Azores Archipelago, Portugal)

Ricci A.*¹, Tassi F.¹⁻², Vaselli O.¹⁻², Fiebig J.³ & Viveiros F.M.⁴

1. Dipartimento di Scienze della Terra, Università di Firenze. 2. Istituto di Geoscienze e Georisorse, C.N.R. Firenze. 3. Institut für Geowissenschaften, Goethe-Universität, Germany. 4. Centro de Vulcanologia e Avaliação de Riscos Geológicos, Universidade dos Açores, Portugal.

Corresponding email: ricciandrea89@gmail.com

Keywords: Hydrocarbons, stable Isotopes, hydrothermal.

Magma degassing, crustal carbonates and decomposition of organic matter are the main potential sources of CO₂. The relative contribution of these three sources can be assessed by coupling chemical and isotopic parameters (e.g. $\delta^{13}\text{C-CO}_2$ and $\text{CO}_2/{}^3\text{He}$). However, there are no equally clear indicators to identify the origin of methane and higher hydrocarbons, mainly due to the poor understanding of biogeochemical processes involving organic compounds, especially in volcanic-hydrothermal environments. The goal of this investigation is to evaluate the chemical-physical conditions of hydrothermal fluid reservoir(s) feeding the fumarolic discharges of São Miguel Island (Azores Islands) on the basis of conventional inorganic geochemistry and isotopic and chemical composition of light hydrocarbons. Gases have the typical hydrothermal compositions, with H₂O and CO₂ as major components, followed by H₂, H₂S, N₂, CH₄ and CO. Inorganic and organic gas geothermometers in the H₂O-H₂-CO₂-CO-CH₄, CO-CO₂, H₂-H₂O and C₂-C₃ alkenes-alkanes systems indicated equilibrium temperatures between 250 and 400 °C, at redox conditions more oxidizing than those typical of hydrothermal systems. The CO₂-CH₄ pair systematically occurs in strong chemical and isotopic disequilibrium, suggesting that secondary processes, probably mediated by microbial activity, affect both the CO₂/CH₄ molar ratio and the $\delta^{13}\text{C-CH}_4$ values. Similarly, the fractionation patterns of the ¹³C/¹²C ratios of the C₁–C₄ alkane series seem to depend on biogenic processes. Metabolic processes carried out by microorganisms simulate the carbon isotopic trend commonly ascribed to thermogenesis (direct trend: $\delta^{13}\text{C}_{\text{C}_1} < \delta^{13}\text{C}_{\text{C}_2}$) or abiogenesis (reverse trend: $\delta^{13}\text{C}_{\text{C}_1} > \delta^{13}\text{C}_{\text{C}_2}$). However, it cannot be excluded that abiogenic CH₄ oxidation to CO₂, e.g. through thermochemical sulfate reduction (TSR), also occur. According to the low concentrations of C₂₊ hydrocarbons, the flat patterns of the C₂-C₄ isotopic trends consistently indicate a highly mature organic source, where primary cracking proceeds under open system conditions. These findings challenge the suitability of conventional criteria for the classification of hydrocarbons emitted from hydrothermal environments and suggest that the chemical and isotopic deep signature of light hydrocarbons can be easily masked by biogenic and abiogenic secondary processes.

Chromatography Monitoring Station. Potential and applications

Sortino F.*¹, Barberi F.², Carapezza M.L.³, Gattuso A.³, Ranaldi M.², Tarchini L.², Zanolin F.¹, Cosenza P.¹, Foresta Martin L.¹, Francofonte V.¹, Mastrolia A.¹ & Melián G.⁴

1. Istituto Nazionale di Geofisica e Vulcanologia, Palermo. 2. Dipartimento di Scienze, Università Roma Tre
3. Istituto Nazionale di Geofisica e Vulcanologia, Roma 1. 4. Instituto Tecnológico de Energías Renovables, Tenerife, España.

Corresponding email: francesco.sortino@ingv.it

Keywords: Volcanology, monitoring, geochemistry.

The rise up of volcanic fluids to the surface produces anomalies that are function of the volcano structure and of the volcano-tectonics of the upper crust. According to the volcanic activity, sampling and analysis methods are provided for the geochemical surveillance. The micro gas-chromatograph (m-GC) offers a valid alternative to the monitoring of the main released gases, especially allowing a much higher frequency of analysis. Furthermore m-GC monitoring can be applied in seismic areas as well.

A chromatography monitoring station (CMS) equipped with a m-GC, implemented with a sampling system, a computer and a router, has been developed to allow complete remote control of the instruments and the automatic transmission of data. Some specific parts have been manufactured in order to adapt the characteristics of the m-GC to the automatic collection of gas samples from both fumaroles and soil, but also dissolved in water.

The CMS was tested on different sites. We show a soil gas data series acquired at Zafferana Etnea during lava fountaining episodes from the southeastern crater of Etna in 2011. Data series shows a pre-paroxysm steady state marked by CO₂ degassing without significant variations; a pulsing degassing which lasted for some days during paroxysm, followed by a marked and clear decrease (CO₂ from 12% to 2% in few hours); a final slower recover to pre-paroxysm degassing levels.

We interpret the steady signal of equilibrium in gas emission as being disrupted by the arrival of small batches of magma that disturb the signal and likely mark the beginning of the strombolian activity. Such magma dynamics are extremely fast and the vesiculation during ascent does not allow the gas to reach peripheral sites. Possibly a degassing associated to such eruption, may occur and be detected at sites closer to the active crater.

Seventeen years (1998-2014) of geochemical observations at the Poás volcano (Costa Rica) fumarolic system

Vaselli O.^{*1-2}, Tassi F.¹⁻², Fernandez E.³, Duarte E.³, Fischer T.⁴, De Moor M.³, Tardani D.⁵ & Martinez M.³

1. Dipartimento di Scienze della Terra, Università di Firenze. 2. Istituto di Geoscienze e Georisorse, C.N.R. Firenze. 3. OVSICORI-UNA, Heredia, Costa Rica. 4. Department of Earth and Planetary Sciences, University of New Mexico, USA. 5. Departamento de Geología, Santiago, Chile

Corresponding email: orlando.vaselli@unifi.it

Keywords: Costa Rica, gas geochemistry, Poas volcano.

From 1998 to 2014 the chemical and isotopic composition of fumarolic gas discharges from Poás volcano (Costa Rica) was investigated in the framework of a joint collaboration between the local observatory (OVSICORI) and the Department of Earth Sciences of Florence (Italy) and increased by the recently data published by Fisher et al. (2015). In this span of time, strong visual and chemical modifications occurred at the fumarolic fields characterizing the Active Crater, presently hosting a hyperacid lake and where the last magmatic eruption took place in 1953-54 when a pyroclastic dome was emplaced.

In 1998 the fumarolic activity was principally concentrated at the interface between the pyroclastic dome and the lake, whereas sporadic gas discharges were distributed throughout the inner crater with temperature never exceeding that of boiling water. From 1999 to 2000 the fumarole close to the lake (dome fumarole) was persisting, whereas new fumarolic vents formed in the inner NE and E sector of the crater with temperature up to 120 °C (Vaselli et al., 2003). Despite the relatively low outlet fumarolic temperatures, concentrations of magmatic gases, such as SO₂, HCl and HF, were abundant. No significant modifications of the fumarolic fields were recorded up to 2006, although in 2005 the lake level started to decline. In 2001 the lake depth was indeed of 41 m and dropped down to 10 m in 2014 (Fisher et al., 2015), approaching the 1989-1994 period when the lake completely dried out.

In March 2006 a new phase of phreatic activity commenced and after the January 2009 earthquake at Chinchona (8 km E of Poás) the temperature of the dome fumarole started to increase up to 800 °C in 2011. Presently, the high degassing level of the dome fumarole does not allow to approach the discharging vent.

The chemical composition of the fumarolic gases and the changes observed from 1998 to 2014 are likely resulting by combined effects at different degrees between the magmatic and hydrothermal system and the acidic lake. According to Vaselli et al. (2003) and Fisher et al. (2015), injection of new and undegassed magma in late 2000-early 2001, heating of the hydrothermal system and gas pressure build-up, and hydrofracturing through 2006 are the main processes that have affected the magmatic-hydrothermal system of Poás.

Fischer T.P., Ramírez C., Mora-Amador R.A., Hilton D.R., Barnes J.D., Sharp Z.D., Le Brun M., de Moor J.M., Barry P.H., Füre E., Shaw A.M. 2015. Temporal variations in fumarole gas chemistry at Poás volcano, Costa Rica. *J. Volcanol. Geotherm. Res.*, 294, 56-70.

Vaselli O., Tassi F., Minissale A., Montegrossi G., Duarte E., Fernandez E., Bergamaschi F. 2003. Fumarole migration and fluid geochemistry at Poás Volcano (Costa Rica) from 1998 to February 2001. *Mem. Geol. Soc. London, Sp. Issue on: "Volcanic degassing"*, Oppenheimer C., Pyle D.M. & Barclay J. Eds., 213, 247-262.

Experimental studies of mineral-catalyzed dehydrogenation of C₆ cyclic hydrocarbons under hydrothermal conditions

Venturi S.^{*1-2}, Tassi F.¹⁻², Gould I.R.³, Shock E.L.³⁻⁴, Lorange E.D.⁵, Bockisch C.³ & Fecteau K.³

1. Dipartimento di Scienze della Terra, Università di Firenze. 2. Istituto di Geoscienze e Georisorse, CNR, Firenze. 3. Department of Chemistry and Biochemistry, Arizona State University, Tempe, USA. 4. School of Earth and Space Exploration, Arizona State University, Tempe, USA. 5. Department of Chemistry, Vanguard University, Costa Mesa, USA.

Corresponding email: stefania.venturi@unifi.it

Keywords: Mineral-catalyzed organic reactions, hydrothermal fluids, catalytic reforming.

Hydrothermal gases are characterized by a complex mixture of organic volatiles. Patterns in the relative abundances of the main classes of organics are found in gases from natural systems (e.g. volcanoes, geothermal sites) characterized by similar T and redox, which suggests that the compositions of the gas mixtures are sensitive to physical and chemical conditions. The attainment of metastable equilibrium between organic compounds has been demonstrated experimentally (Seewald, 1994). Studies on fumarolic gases (Taran & Giggenbach, 2004) have shown that alkane/alkene interconversion can approach equilibrium in natural environments. Reversible catalytic reforming may be responsible for the high abundance of benzene observed in hydrothermal gases relative to saturated hydrocarbons (Capaccioni et al., 1993). Cyclic hydrocarbons are enriched in gases originating at T 6 cyclic hydrocarbons as intermediates. We are investigating the mechanisms for formation of benzene from cyclic hydrocarbons under laboratory conditions. The reactions of cyclohexane, cyclohexene and cyclohexadiene have been studied at 300 °C and 85 bar. Benzene production is observed, together with various oxidation, hydration and isomerization products, depending upon the conditions. Dehydrogenation of cyclohexadiene to form benzene is very efficient in water alone, but the corresponding reaction of cyclohexane gave negligible benzene even after reaction for 10 days. However, formation of both benzene and cyclohexene from cyclohexane was enhanced in the presence of minerals, in particular, sphalerite. Experiments with varying ratios of cyclohexane and sphalerite showed that dehydrogenation is a surface catalyzed reaction. Experiments in D₂O showed that sphalerite very efficiently catalyzes breaking C-H bonds, even when conversion to benzene is low. For cyclohexene, benzene formation is negligible compared to oxygenation products in the absence of minerals, but sphalerite catalyzes formation of both benzene and cyclohexane. Finally, solution phase oxidation using Cu(II) forms primarily oxygenation products, suggesting that formation of benzene requires surface catalysis by minerals.

Capaccioni B., Martini M., Mangani F., Giannini L., Nappi G. & Prati F. 1993. Light hydrocarbons in gas-emissions from volcanic areas and geothermal fields. *Geochem. J.*, 27, 7-17.

Seewald J.S. 1994. Evidence for metastable equilibrium between hydrocarbons under hydrothermal conditions. *Nature*, 370, 285-287.

Taran Y. & Giggenbach W.F. 2004. Evidence for metastable equilibrium between hydrocarbons in volcanic gases. In: Wany R.B. & Seal R.R. Eds., *Water-Rock Interaction*. 193-195. A.A. Balkema, Leiden.

SESSION S17

From Rocks to Stars

(The Nuclear History of the Galaxy as Written in Solar System Solids)

CONVENORS

M. Busso (Univ. Perugia)

G. Pratesi (Univ. Firenze)

A.M. Fioretti (IGG-CNR)

Nano-mineralogical study of mesostases in enstatite chondrite

Agrosi G.*¹, Manzari P.², Melone N.¹ & Tempesta G.¹

1. Dipartimento di Scienze della Terra e Geoambientali, Università di Bari. 2. Istituto di Astrofisica e Planetologia Spaziali, I.N.A.F. Roma.

Corresponding email: giovanna.agrosi@uniba.it

Keywords: Enstatite chondrite, mesostasis, TEM.

Enstatite chondrites (EC) are the rarest and most reduced chondrite clan. EC are subdivided into two groups, Low Metal EC (EL) and High Metal (EH), based on modal iron-metal abundances. ECs are characterized by the presence of nearly pure enstatite and silicon-bearing metal, with ferroan-alabandite (MnS) in EL and niningerite (MgS) in EH (Keil, 1968). Although the increasing of studies in these last years on EC, their origin remains unclear. Investigation on nanomineralogy of mesostasis could bring to light new elements that could help to solve the issue on the reciprocal relationship between chondrules and matrix. With this aim a fragment of mesostasis extracted from one chondrule of Sahara 97072 labelled S2AC5, was studied by TEM. High-resolution images and electron diffractions showed that really the mesostasis consists of several nanocrystal phases in the amorphous matrix. Preliminary EDS analyses of these nanocrystals revealed the occurrence of Fe particles, Fe-Cr sulfides, Cr-sulfide and Ti-sulfide (Manzari, 2010). About the Cr-sulphide two minerals are known: brezinaite (Cr₃S₄) found in an iron meteorites Tucson (Bunch & Fuchs, 1969) and Gibeon (Petaev, 1997), and murchisite (Cr₅S₆) found in one chondrule olivine of Murchison carbonaceous chondrite (Ma et al., 2011). It is worth noting that in our study it is the first time that the Cr-sulfides are found into an EC and, furthermore, into a chondrule mesostasis. Moreover, the nanocharacterization of this sulphide furnish new elements about the EC origin.

- Bunch T.E. & Fuchs L.H. 1969. A new mineral: brezinaite, Cr₃S₄, and the Tucson meteorite. *Amer. Mineral.*, 54, 1509-1518.
- Keil K. 1968. Mineralogical and chemical relationships among Enstatite Chondrites. *J. Geophys. Res.*, 73(22), 6945-6976.
- Ma C., Beckett J.R. & Rossman G.R. 2011. Murchisite, Cr₅S₆, a new mineral from the Murchison meteorite. *Amer. Mineral.* 96, 1905-1908.
- Manzari P. 2010. Investigation of Enstatite Chondrites: Mineralogical and chemical features Of Eh3 and El3 Chondrules, PhD Thesis.
- Petaev M.I. 1997. Cr-bearing minerals in the Gibeon IVA iron: indicators of sulfur and oxygen fugacities in the parent body. *Lunar and Planetary Science*, XXVIII, 1649.

Plagioclase composition by Raman spectroscopy: a new tool in the analysis of extraterrestrial samples

Aliatis I.¹, Tribaudino M.*¹, Lambruschi E.¹, Mantovani L.¹, Bersani D.¹, Lottici P.P.¹ & Gatta G.D.²

1. Dipartimento di Fisica e Scienze della Terra, Università di Parma. 2. Dipartimento di Scienze della Terra "A. Desio", Università di Milano.

Corresponding email: mario.tribaudino@unipr.it

Keywords: Raman spectroscopy, plagioclase, planetary bodies.

In situ analysis of the extraterrestrial samples has reached overwhelming interest in recent time. Exploration using robot probed spectroscopy and X-ray diffraction is currently done in spacecraft exploration of Mars (Downs et al., 2015). Raman spectroscopy is a technique especially suitable, since it provides definite spectra in mineral mixtures, with a resolution down to 1 μm , so to analyze at the same resolution separate phases. A Raman spectrometer (MMRS) is actually planned for the NASA Mars 2020 mission, and research on Raman sample spectroscopy and instrumental engineering is underway. Raman spectra of the most important minerals and their solid solutions are therefore actively investigated, in order to provide models for the interpretation of the spectra from planetary exploration. A key mineral phase in planetary bodies is plagioclase: it makes most of the moon surface, is a major phase in Martian crust, and in asteroids like Vesta. Also, plagioclase composition is crucial to determine the petrologic evolution of the investigated rocks. However, preliminary investigation (Freeman et al., 2008) did not show clear trends relating the position of given Raman peaks with the composition of the plagioclase. A major problem in handling the plagioclase behaviour is that careful analysis of the degree of order, microstructures, phase transitions and composition has to be undertaken. We have therefore investigated by Raman spectroscopy a series of well characterized plagioclases, previously investigated by XRD, TEM and in some cases by IR spectroscopy (Carpenter et al., 1985; Tribaudino et al., 2010). Where not available, the degree of order was obtained by new single-crystal X-ray diffraction experiments. We found linear trends of the Raman shifts vs composition, with different slopes, corresponding to the C-1, I-1 and P-1 feldspar structures. The plagioclase composition therefore may be measured, by the wavenumber difference between the two major peaks. By this method, the anorthite content of plagioclase in Juvinas eucrite and into a CAI inclusion within the Renazzo carbonaceous chondrite were determined to be $85\pm 5\%$ and $97\pm 2\%$, respectively, in good agreement with experimental determinations.

Carpenter M.A., McConnell J.D.C. & Navrotsky A. 1985. Enthalpies of ordering in the plagioclase feldspar solid solution. *Geochim. Cosmochim. Acta*, 49, 947-966.

Downs R.T. & MSL Science Team. 2015. Determining mineralogy on Mars with the CheMin X-ray diffractometer. *Elements*, 11, 45-50.

Freeman J.J., Wang A., Kuebler K.E., Jolliff B.L. & Haskin L.A. 2008. Characterization of natural feldspars by Raman spectroscopy for future planetary exploration. *Can. Mineral.*, 46, 1477-1500.

Tribaudino M., Angel R.J., Cámara F., Nestola F., Pasqual D. & Margiolaki I. 2010. Thermal expansion of plagioclase feldspars. *Contr. Mineral. Petrol.*, 160, 899-908.

The comet 67P/Churyumov-Gerasimenko, a primitive Kuiper Belt body: results from the Rosetta mission

Capaccioni F.*¹ & the VIRTIS Team

1. Istituto di Astrofisica e Planetologia Spaziali, INAF Roma.

Corresponding email: fabrizio.capaccioni@iaps.inaf.it

Keywords: Comets, solar system, organics.

The Visible InfraRed Thermal Imaging Spectrometer (VIRTIS) onboard the ESA's mission Rosetta, has, among other tasks, the goal to characterise the surface composition of the comet 67P/Churyumov-Gerasimenko and to study its thermal properties. VIRTIS is a Mapping Spectrometer and a High Resolution Spectrometer covering the spectral range 0.25-5.0 μm (Coradini et al., 2007). The nucleus observations were performed at a spatial resolution varying from the initial 500 m (in July 2014) down to 2.5 m and have generated compositional maps of the illuminated areas (Filacchione et al., 2014). The surface temperature has been measured since the first distant observations of the nucleus in the thermal emission region, above 3.5 μm . The highest surface temperature measured until September 2014 is 220 K, which is an indication of a surface structure largely covered by a porous crust, mainly devoid of water ice (Tosi et al., 2015). The nucleus is very dark with an integrated normal albedo of 0.062 ± 0.003 at 0.55 μm and reflectance spectrum which displays gradients in the VIS and IR regions (slopes of 5-25 and 1.5-5 % $\text{k}\text{\AA}^{-1}$ respectively). Such low reflectance and spectral slopes suggest a surface made of an association of carbon bearing species and opaque minerals, such as iron sulfides. A broad absorption feature in the 2.9-3.6 μm spectral region has been observed; this band is present across the entire illuminated surface and is remarkably uniform (Capaccioni et al., 2015). The shape and width of this band are compatible with absorptions due to non-volatile organic macromolecular materials, complex mixture of various types of C-H and/or O-H chemical groups (Quirico et al., 2015). Ice rich regions of very limited extent have also been observed (De Sanctis et al., 2015). The VIRTIS observations of the widespread abundance of organics on the surface of 67P indicate an origin of the cometary nucleus in a low temperature environment at large distances from the Sun, such as the Kuiper Belt region.

Capaccioni F., Coradini A. & other 76 authors. 2015. The organic-rich surface of comet 67P/Churyumov-Gerasimenko as seen by VIRTIS/Rosetta. *Science*, 347.

Coradini A., Capaccioni F. & other 43 authors. 2007. VIRTIS an imaging spectrometer for the Rosetta mission. *Space Sci. Rev.*, 128, 529-559.

De Sanctis M.C., Capaccioni F. & other 19 authors. 2015. Detection of Transient Water Ice on Comet 67P/Churyumov-Gerasimenko. 46th Lunar Planetary Science Conference, 1832, 2021.

Filacchione G., Capaccioni F. & other 26 authors. 2015. Compositional Maps of 67P/CG Nucleus by Rosetta/VIRTIS-M. 46th Lunar Planetary Science Conference, 1832, 1756.

Quirico E. & other 19 authors. 2015. Composition of Comet 67P/Churyumov-Gerasimenko Refractory Crust as Inferred from VIRTIS-M/Rosetta Spectro-Imager. 46th Lunar Planetary Science Conference, 1832, 2092.

Tosi F. & other 18 authors. 2015. Thermal Maps and Properties of Comet 67P as derived from Rosetta/VIRTIS Data. 46th Lunar Planetary Science Conference, 1832, 2156.

New data about the early stages of asteroidal accretion by neutron diffraction studies of iron meteorites

Caporali S.*¹, Grazzi F.², Scherillo A.³ & Pratesi G.⁴

1. Consorzio INSTM, Firenze. 2. Istituto dei Sistemi Complessi, C.N.R. Sesto Fiorentino. 3. STFC ISIS Neutron source, Oxford, UK. 4. Museo di Storia Naturale, Università di Firenze.

Corresponding email: stefano.caporali@unifi.it

Keywords: Iron meteorites, neutron diffraction, texture.

Iron meteorites consist overwhelmingly of nickel-iron alloys (taenite and kamacite) and are assumed to be from the cores of asteroids that have undergone extensive melting and fractional crystallization. Compared to the stony meteorites they are fairly rare, comprising about 5-7% of witnessed falls, but are easy to find them after a fall, even as large pieces. Therefore, finds of iron meteorites are relatively common (Buchwald, 2005) accounting for almost 90% of the mass of all known meteorites, about 500 tons. Age-dating now show that the most part of iron meteorites were formed during the early stages of Solar System's formation (Markowski et al. 2006). Therefore, an in depth knowledge of these meteorites results of particular importance to understand the formation of asteroids and rocky planets. Some of the physico-chemical conditions experienced during the formation of an iron meteorite; mainly temperature, pressure, cooling rate, post forming annealing etc.. are traditionally acquired by means of metallographic investigations. However, information such as: mosaicity, morphology, preferred orientation (texture) and extended spatial mapping of the grains of the two main different phases (kamacite and taenite) are not achievable unless a significative part, if not all the whole sample, is cut in pieces. Vice versa, by means of neutron diffraction analysis it is possible to obtain an accurate set of physico-chemical data in a non-destructive and qualitative way (Peetermans et al., 2013). In this study seven iron meteorites representative of different groups (Grady et al., 2014) (Campo del cielo, Nantan, ont Dieu, Castiglione del Lago, Chinga, Sikote Alin and Slaghek's iron), available in the collection of the Museo Scienze Planetarie della Provincia di Prato, have been analyzed to determine the texture degree, preferential orientation of the grains and mosaicity of the large crystallites presents. The differences and peculiarities highlighted by neutron diffraction were related to the different formation pattern and provided useful information about the early stages of asteroidal evolution.

Buchwald V.F. 2005. Iron and Steel in Ancient Times, *Historisk-filosofiske Skrifter* 29. The Royal Danish Academy of Sciences and Letters.

Grady M., Pratesi G. & Moggi-Cecchi V. 2014. Atlas of Meteorites, Cap 15 Iron Meteorites. Cambridge Univ. Press, 322-330.

Markowski A., Quitté G., Halliday A.N. & Kleine T. 2006. Tungsten isotopic compositions of iron meteorites: chronological constraints vs. cosmogenic effects. *Earth Planet. Sci. Lett.*, 242, 1-15.

Peetermans S., Grazzi F., Salvemini F., Lehmann E.H., Caporali S. & Pratesi, G. 2013. Energy-selective neutron imaging for morphological and phase analysis of iron-nickel meteorites. *Analyst*, 138, 5303-5308, doi:10.1039/C3AN00985H.

Effects of shock loading on ordinary chondrites: an X-ray microtomography study

Caporali S.*¹, Loglio F.², Pratesi G.³ & Folco L.⁴

1. Consorzio INSTM, Firenze. 2. Centro Cristallografia Strutturale, Sesto Fiorentino (FI). 3. Museo di Storia Naturale, Università di Firenze.
4. Dipartimento Scienze della Terra, Università di Pisa.

Corresponding email: stefano.caporali@unifi.it

Keywords: Microtomography, ordinary chondrites, impact shock.

Ordinary chondrites account for the vast majority of known meteorites and are distinguished from each other through differences in bulk chemical and isotopic composition, chondrule size and oxidation state (Grady et al., 2014). Each of these attributes was primarily established prior to accretion within the solar nebula and/or by incorporation of nebular components. However, thermal processes experienced by these meteorites; mainly due to hypervelocity impacts, account of post accretion metamorphism that further contributes to the differentiation of these meteorites. In order to investigate the effects of impact-related phenomena, a serie of 9 meteorites of H 4 group found in Antartica and available in the collection of the Museo Nazionale dell'Antartide, identical as concern chemical and isotopical composition but different regarding the shock degree were analyzed by means of X-ray micro-tomography (m-XRCT). In this relatively new technique the reconstruction of threedimensional semi-transparent images of the meteorites (Friedrich et al., 2008) and other geologic materials (Pratesi et al., 2014) is possible on the ground of X-ray selective absorption. In such a way a complete set of 3D data of the low melting components of the meteorites; i.e. taenite/kamacite (metallic) and troilite (sulphide) phases were reconstructed. In particular, for every meteorite, the size, shape, density (number cm⁻³) and preferred orientation of the opaque mineral structures were determined. Finally, we have tried to connect the so determined opaque phases forms and distribution with the shock degree responsible of the meteorite metamorphism and vice versa finding that hypervelocity impacts play an active role on the distribution and shape of the low-temperature melting phases.

Friedrich J.M., Wignarajah D.P., Chaudhary S., Rivers M.L., Nehru C.E., Ebel D.S. 2008. Three-dimensional petrography of metal phases in equilibrated L chondrites - Effects of shock loading and dynamic compaction. *Earth Planet. Sci. Lett.*, 275, 172-180.

Grady M., Pratesi G., Moggi-Cecchi V. (Eds.) 2014. *Atlas of Meteorites*, Cap 3 Ordinary chondrites, 71-81.

Pratesi G., Caporali S., Loglio F., Giuli G., Dziková L. & Skála R. 2014. Quantitative Study of Porosity and Pore Features in Moldavites by Means of X-ray Micro-CT. *Materials*, 7, 3319-3336.

Reflectance spectra of hed, analogues of 4Vesta

Carli C.*¹, Pratesi G.²⁻³, Capaccioni F.¹, Santoro S.⁴ & Moggi Cecchi V.³

1. Istituto di Astrofisica e Planetologia Spaziali, I.A.P.S. Roma. 2. Museo di Storia Naturale, Università di Firenze
3. Dipartimento di Scienze della Terra, Università di Firenze. 4. Saitec Srl, Firenze.

Corresponding email: cristian.carli@iaps.inaf.it

Keywords: Reflectance spectroscopy, HED, 4Vesta.

4Vesta asteroid is supposed to be the parental body of Howardite, Eucrite and Diogenite (HED) meteorites. These achondrites show igneous-like characteristics (e.g. composition, texture) and they have visible and near-infrared (VNIR) spectra analogue to those of Vesta's asteroid family (e.g. Feierberg and Drake, 1980). Recently, Dawn Mission (NASA) have investigated 4Vesta from the orbit, producing a first detailed global mapping. This mission has confirmed that all the body is characterized by spectra compatible with HEDs (De Sanctis et al., 2012), revealing the two dominating pyroxenes absorptions, around 1 and 2 μm (Burns, 1983). In particular, spectral characteristics are within the Howardites field, and, partially, within those of Eucrites and Diogenites (Ammannito et al., 2013a). Moreover, bright and dark materials are visible, which are, probably, fresher excavated regions (Zambon et al., 2014) and CC-like materials-rich regions (Palomba et al., 2014), respectively. Ammannito et al. (2013b) identified areas where the olivine could be present in significant amounts in two craters of the north hemisphere, and Ruesch et al. (2014) indicated that olivine could be present also in other regions. Unexpectedly, no evidence for olivine was detected in RheaSilvia Basin, where diogenites are clearly present (Ammannito et al., 2013a) and the mantle could be exposed.

Here we present spectral characteristics of several HED slabs belonging to the Museo di Storia Naturale dell'Università degli Studi di Firenze. We considered the variability in reflectance and absorption parameters of eucrites and diogenites, and comparing these with pyroxene, plagioclase and olivine compositions. In particular, we measured the spectral variations within an olivine diogenite (NWA6232) and how the absorptions change between the matrix and an olivine grain. Moreover we discuss how to extrapolate the olivine relative abundance respect to the surrounding materials.

Ammannito E., De Sanctis M.C., Capaccioni F., Teresa Capria M., Carraro F., Combe J.-P., Fonte S., Frigeri A., Joy S.P., Longobardo A., Magni G., Marchi S., McCord T.B., McFadden L.A., McSween H.Y., Palomba E., Pieters C.M., Polanskey C.A., Raymond C.A., Sunshine J.M., Tosi F., Zambon F. & Russell C.T. 2013a. Vestan lithologies mapped by the visual and infrared spectrometer on Dawn. *Meteor. Planet. Sci.*, 48, 2185–2198. doi: 10.1111/maps.12192.

Ammannito E., De Sanctis M.C. Palomba E., Longobardo A., Mittlefehldt D. W., McSween H. Y., Marchi S., Capria M.T., Capaccioni F., Frigeri A., Pieters C. M., Ruesch O., Tosi F., Zambon F., Carraro F., Fonte S., Hiesinger H., Magni G., McFadden L.A., Raymond C.A., Russell C.T. & Sunshine J.M. 2013b. Olivine from vesta's mantle exposed on the surface. *Nature*, 504, 122-125.

Burns R. 1993. *Mineralogical Applications of Crystal Field Theory*. Second Edition. Cambridge University Press.

De Sanctis M.C., Ammannito E., Capria M.T., Tosi F., Capaccioni F., Zambon F., Carraro F., Fonte S., Frigeri A., Jaumann R., Magni G., Marchi S., McCord T.B., McFadden L.A., McSween H.Y., Mittlefehldt D.W., Nathues A., Palomba E., Pieters C.M., Raymond C.A., Russell C.T., Toplis M.J. & Turrini D. 2012. Spectroscopic Characterization of Mineralogy and Its Diversity Across Vesta. *Science*, 336, 697-700.

Feierberg M.A. & Drake M.J. 1980. The meteorite-asteroid connection - The infrared spectra of eucrites, shergottites, and Vesta. *Science*, 209, 805-807.

Palomba E., Longobardo A., De Sanctis M.C., Zambon F., Tosi F., Ammannito E., Capaccioni F., Frigeri A., Capria M.T., Cloutis E.A., Jaumann R., Combe J.-P., Raymond C.A. & Russell C.T. 2014. Composition and mineralogy of dark material deposits on Vesta. *Icarus*, 240, 58-72.

Ruesch O. Hiesinger H., De Sanctis M.C., Ammannito E., Palomba E., Longobardo A., Zambon F., Tosi F., Capria M.T., Capaccioni F., Frigeri A., Fonte S., Magni G., Raymond C.A. & Russell C.T. 2014. Detections and geologic context of local enrichments in olivine on Vesta with VIR/Dawn data. *J. Geophys. Res.*, 119, 2078-2108, doi: 10.1002/2014JE004625.

Zambon F., De Sanctis M.C., Schröder S., Tosi F., Longobardo A., Ammannito E., Blewett D.T., Mittlefehldt D.W., Li J.-Y., Palomba E., Capaccioni F., Frigeri A., Capria M.T., Fonte S., Nathues A., Pieters C.M., Russell C.T., Raymond C.A. 2014. Spectral Analysis of the Bright Materials on the Asteroid Vesta. *Icarus*, 240, 73-85.

The diversity of the lunar crust as told by the new polymict regolith breccia Mount DeWitt 12007 (Antarctica)

Collareta A.*¹⁻², D'Orazio M.¹, Gemelli M.¹, Pack A.³ & Folco L.¹

1. Dipartimento di Scienze della Terra, Università di Pisa. 2. Dottorato Regionale in Scienze della Terra "Pegaso", Università di Pisa. 3. Georg-August-Universität Göttingen, Geowissenschaftliches Zentrum, Abteilung Isotopengeologie, Germany.

Corresponding email: massimo.dorazio@unipi.it

Keywords: Lunar regolith, Moon, Antarctica.

The lunar crust is a unique window into early planetary differentiation processes in the solar system, bridging the gap between incipient igneous activity in asteroids and the more evolved geodynamics of terrestrial planets like the Earth. Decades after the epic *Apollo* and *Luna* missions, the crustal diversity of the Moon remains an outstanding issue which the lunar meteorites - random samples of the lunar surface materials - can contribute to resolve. The new meteorite Mount DeWitt (DEW) 12007 was collected in Victoria Land during the XXVIII PNRA Antarctic Campaign. DEW 12007 is a polymict regolith breccia mainly consisting of glassy impact-melt breccia particles, gabbroic clasts, feldspathic clasts, impact and volcanic glass beads, crystalline basaltic clasts and mingled breccia clasts embedded in a matrix dominated by fine-grained crystals; vesicular glassy veins and rare agglutinates are also present. Main minerals are plagioclase (generally An_{>85}) and clinopyroxene (pigeonites and augites, sometimes interspersed). The presence of tranquillityite, coupled with the petrophysical data, the O-isotope data ($\Delta^{17}\text{O}=-0.075$) and the FeO_{tot}/MnO ratios in olivine (91), pyroxene (65) and bulk rock (77) indicate a lunar origin for DEW 12007. Impactites consist of Al-rich impact melt splashes and plagioclase-rich meta-melt clasts whose parent rocks could be associated to the so-called Mg-suite or to the ferroan anorthosite (FAN) suite of early lunar intrusives. The volcanic products belong to the Very Low Titanium (VLT) or Low Titanium (LT) suites; an unusual subophitic particle could be cryptomare-related. Gabbroic clasts could represent part of a shallow intrusion within a mare volcanic complex with prevailing VLT affinity. DEW 12007 is classified as a mingled regolith breccia which developed on a VLT volcanic complex near a magnesian feldspathic terrane. DEW 12007 is a good compendium of lunar materials which samples a high crustal diversity, comprising clasts from the major Moon terranes (the Feldspathic Highland Terrane, the Procellarum KREEP Terrane and the basaltic maria) and some rare lunar lithologies (i.e., a putative pre-mare basalt and some VLT-like gabbros). DEW 12007 is by now unpaired. A preliminary petrographic and geochemical comparison suggests that a possible launch-pairing relationship between DEW 12007 and other lunar meteorites (Y 793274/981031, QUE 94281 and EET 87521/96008) should be properly investigated. Based on the *Clementine* remote sensing compositional data, and in light of a comparison with the *Apollo* and *Luna* samples, we suggest that a region near the margin of Mare Serenitatis could represent a reliable context for the formation and the ejection of DEW 12007; however, similar locations within Mare Fecunditatis or Mare Crisium could provide an analogous scenario.

Acknowledgements - This work is supported by the Italian *Programma Nazionale delle Ricerche in Antartide* (PNRA) through the PEA2013 AZ2.04 "Meteoriti Antartiche".

Thermal Expansion of *C2/c* Pyroxenes: Implications for the Thermal Infrared Spectroscopy of Solar System Bodies

Ferrari S.¹, Alvaro M.³, Nestola F.², Maturilli A.¹, Helbert J.¹, Domeneghetti M.C.^{*3}, Massironi M.² & Zorzi F.²

1. Institute for Planetary Research, Berlin-Adlershof, Germany. 2. Dipartimento di Geoscienze, Università di Padova.
3. Dipartimento di Scienza della Terra e dell'Ambiente, Università di Pavia.

Corresponding email: chiara.domeneghetti@unipv.it

Keywords: TIR spectroscopy, thermal expansion, pyroxenes.

Spectroscopy in the thermal infrared (TIR) region is extensively used in the exploration of the solar system, mainly because of its capability to reveal the mineralogical composition of emitting surfaces of planets and asteroids. Specifically, TIR spectral features arise from the combination of the vibrational modes of the shallow materials, suiting markers for the structural properties of several silicates. The interpretation of these spectra is extremely challenging because of the space-weathering degradation and impact-induced structural modifications of solar system shells. In addition, the thermal expansion driven by the wide range of daily temperatures range of many bodies significantly affects the crystal structure of the surface minerals and as a consequence, their TIR spectral signature.

In this study, we have measured the lattice parameters and the TIR emissivity spectra in vacuum at high temperature (Alvaro et al. 2015; Helbert et al., 2013) of two Ca-rich clinopyroxenes (sp. group *C2/c*) with different Mg# and similar Ca amount. Monoclinic pyroxenes were chosen as they can be considered representative for the surface silicates of the solar system. In this specific case, diffraction and spectroscopy under vacuum up to 775 K reveal the relationship between thermal expansion and spectral signature changes occurring at the most likely environment of the surface of Mercury (Ferrari et al., 2014).

Single-crystal X-ray diffraction was performed at the Department of Earth Sciences and Environment of the University of Pavia (Italy): samples were sealed in vacuum and data were collected at 298 K and increasing temperature of 50 K steps up to 723 K, then during the cooling at 698 K, 498 K and 323 K. Spectral measurements were performed at the Planetary Emissivity Laboratory (DLR, Berlin): samples were heated once and emissivity were collected under a pressure of 1 mbar at 343 K and 723 K with increasing temperature.

We show that spectra of clinopyroxenes with similar calcium content display a deepening of the main absorption bands, and a shift of the band minima toward higher wavelengths with increasing temperatures. Interestingly, each band shifts by a different amount, representing a marker for the real chemistry of the sample. Similar shifts can also be observed at constant temperature with increasing Fe content in the M2 site. Therefore, the thermal expansion induced by the increasing temperature simulates the presence of a larger cation (i.e. Fe vs. Mg) within the mineral structure. Concerning remote spectral data, eluding the surface temperature information could induce to misinterpret the solid solution.

As clearly demonstrated by our study, a detailed and systematic investigation of silicates behavior is crucial to localize those spectral bands sensitive to the greatest daily temperature ranges typical of the solar system surfaces. This will allow constraining the mineralogical interpretation of any remote TIR spectral data.

Alvaro M., Angel R.J., Marciano C., Milani S., Zaffiro G., Scandolo L., Mazzucchelli M.L., Rustioni G., Briccola M., Domeneghetti M.C. & Nestola F. 2015. Development of a new micro-furnace for "in situ" high-temperature single crystal X-ray diffraction measurements. *J. Appl. Crystal.*, accepted.

Ferrari S., Nestola F., Massironi M., Maturilli A., Helbert J., Alvaro M., Domeneghetti M.C. & Zorzi F. 2014. In-situ high-temperature emissivity spectra and thermal expansion of *C2/c* pyroxenes: Implications for the surface of Mercury. *Am. Mineral.*, 99, 786-792.

Helbert J., Nestola F., Ferrari S., Maturilli A., Massironi M., Redhammer G.J., Capria M.T., Carli C., Capaccioni F. & Bruno M. 2013. Olivine thermal emissivity under extreme temperature ranges: Implication for Mercury surface. *Earth Planet Sci. Lett.*, 371-372, 252-257.

A new Enstatite chondrite found in Italy

Fioretti A.M.*¹, Mattiuz A.² & Goodrich C.A.³

1. Istituto di Geoscienze e Georisorse, C.N.R. Padova. 2. Dipartimento di Geoscienze, Università di Padova
3. Planetary Science Institute, Tucson (AZ), USA.

Corresponding email: anna.fioretti@igg.cnr.it

Keywords: Enstatite chondrite, San Leo, Italian meteorites.

On May, 2nd, 2007, during an excursion organized by the Padua section of the Italian Alpine Club (CAI) in the zone of Montefeltro (Rimini) and that had as final destination the fortress of S. Leo (where the famous count Cagliostro died, in prison), Mr. Alberto Parri spotted a small piece of rock that, according with his own words, had nothing to do with the surrounding rocks he had already collected during the walk: a limestone, a sandstone and a conglomerate. He picked up the rock, numbered it, and stored it. It was only six years later that, after attending a conference on the Antarctic meteorites given by the senior author, he contacted her and asked for an expertise on his “presumed” meteorite.

The sample, of 39.7 g, shows brown-reddish mass colour, with 'bread-crust' cracking pattern and is not attracted by a magnet. Possible relics of fusion crust (or “desert varnish”) are observed on a very small area. The presence of quartz grains inside superficial cracks were seen as suspicious of a provenance from desert areas. Mr Parri however confirmed he never bought or exchanged meteorites and that his collection of rocks is only local. The presence of sandstone levels in the San Leo area is compatible with the presence of quartz grains.

The rock is well recrystallized, with homogeneous grain size, and showing only one poorly defined chondule. Silicate and opaque phases were analysed by electron microprobe. Pyroxene ($\text{En}_{98.3}\text{Fs}_{0.3}\text{Wo}_{1.4}$) is euhedral; plagioclase, in small patches, is albitic ($\text{Ab}_{79.9}\text{An}_{15.6}\text{Or}_{4.5}$), with no zoning. Alteration has almost completely obliterated the opaque, non silicate phases. Relics of daubréelite, troilite and schreibersite are occasional. Euhedral graphite laths have also been observed. Alteration of opaque phases is almost complete. The meteorite shows severe shock effects.

Enstatite can occur in meteorites either in monocline state (clinoenstatite) typical of lower petrologic types or orthorhombic state (ortoenstatite), characteristic of higher petrologic types. Single-crystal X-ray diffraction on San Leo pyroxene yielded cell parameters ($a = 18.260(4) \text{ \AA}$; $b = 8.818(2) \text{ \AA}$; $c = 5.182(1) \text{ \AA}$) and volume $V = 834.4(3) \text{ \AA}^3$ typical of orthorhombic state.

Based on these data, the new found meteorite can be classified as an Enstatite Chondrite of high (6-7) petrologic type. It is the first Enstatite chondrite found in Italy. The official classification as “San Leo, Enstatite chondrite” is now being submitted to the nomenclature committee of the Meteoritical Bulletin. Until its approval, the proposed name and the classification are to be considered as preliminary.

Oxygen isotopes in cosmic spherules and the composition of the near Earth interplanetary dust complex

Folco L.*¹ & Cordier C.²

1. Dipartimento di Scienze della Terra, Università di Pisa. 2. Université Grenoble Alpes/CNRS/IRD, ISTERre, France.

Corresponding email: luigi.folco@unipi.it

Keywords: Micrometeorites, cosmic dust complex, oxygen isotopes.

A long-standing controversy in the micrometeorite community regards the relative contribution of primitive asteroids or comets and of evolved asteroids to the interplanetary dust cloud (e.g., Grün. et al., 2001). Three-oxygen isotopic composition is a powerful tool for the classification of planetary materials and their attribution to parent bodies in the solar system (Clayton, 2008). We compiled and studied a large set of oxygen isotopic data from the literature on cosmic spherules from different collections covering different influx periods within the last ≈ 1 Myr. Cosmic spherules (micrometeorites melted during atmospheric entry) are the most abundant micrometeorites in worldwide collections. According to several models, they are representative of the composition and origin of micrometeorites $> 50 \mu\text{m}$ in size. Spherule statistics (136 spherules, 50–2280 μm in size) indicate that at least 20% of the micrometeoroid complex is fed by asteroids observed in the inner asteroid belt: the ordinary chondrite and secondarily the HED parent asteroids likely belonging to the S-type and V-type spectral classes, respectively. Another $\approx 60\%$ (or more) is related to primitive objects of the Solar System with carbonaceous chondrite compositions: either primitive asteroids belonging to the C-, D- or P-type spectral classes in the outer asteroid belt or comets. Contribution from terrestrial planets has not been identified yet. Oxygen isotopes also document that the composition of the micrometeoroid complex is different from that of macroscopic meteoroids, since the latter is dominated by materials from evolved and differentiated asteroids rather than primitive asteroids or comets. Cosmic spherule statistics show that the contribution of ordinary chondrite material to the composition of the micrometeoroid complex increases with micrometeorite size, thereby documenting a continuum between meteorites and micrometeorites. The transition in terms of relative abundance of the two cosmic spherule populations occurs around $\approx 500 \mu\text{m}$ in size. This work has been recently published in *Geochimica et Cosmochimica Acta* (Cordier & Folco, 2014).

Acknowledgements - This work is supported by the Italian *Programma Nazionale delle Ricerche in Antartide* (PNRA) through the PEA2013 AZ2.04 "Meteoriti Antartiche". LF research is also supported by Pisa University's *Fondi di Ateneo*. ISTERre is part of Labex OSUG@2020 (ANR10 LABX56).

Clayton R.N. 2008. Oxygen isotopes in the early Solar System – A historical perspective. In *Reviews in Mineralogy: Oxygen in the Solar System* (ed. G. J. MacPherson). Min. Soc. Am., Washington, 5-14.

Cordier C. & Folco L. 2014. Oxygen isotopes in cosmic spherules and the composition of the near Earth interplanetary dust complex. *Geochim. Cosmochim. Acta*, 146, 18-26.

Grün E., Gustafson B.A.S., Dermott S.F. & Fechtig H. (Eds.) 2001. *Interplanetary Dust*. Springer, Berlin, pp. 803.

High precision $d^{17}\text{O}$ isotope analyses for micro-volumes: development of a new strategic resource for the Italian Planetary Sciences community

Gemelli M.*¹, Mugnaioli E.², Di Rocco T.³ & Boschi C.⁴

1. Dipartimento di Scienze della Terra, Università di Pisa. 2. Dipartimento di Scienze Fisiche, della Terra e dell'Ambiente, Università di Siena. 3. Geowissenschaftliches Zentrum, Abteilung Isotopengeologie, Georg-August-Universität, Göttingen, Germany. 4. Istituto di Geoscienze e Georisorse, CNR, Pisa.

Corresponding email: maurizio.gemelli@unipi.it

Keywords: Oxygen isotopes, meteorites, planetary sciences.

Oxygen is the third most abundant element in the Solar System and the most abundant element of the terrestrial planets. It consists of three stable isotopes, ^{16}O , ^{17}O and ^{18}O . For terrestrial rocks isotopic fractionation results in changes of the $^{17}\text{O}/^{16}\text{O}$ ratio being approximately half the magnitude of the change in the $^{18}\text{O}/^{16}\text{O}$ ratio. Therefore, on a triple oxygen isotope diagram, terrestrial rocks fall along a line of slope ~ 0.5 called terrestrial fractionation line (TFL). As a consequence, $d^{17}\text{O}$ is rarely measured on terrestrial materials. Since the pioneering work of Clayton et al. (1973) it has been demonstrated that chondritic components are isotopically anomalous, falling off the TFL line, making triple O isotope data an invaluable tool in interpreting meteoritic data. Currently, there are no laboratories in Italy to measure triple oxygen isotopes of silicates and Italian researchers have no option but to send their samples to laboratories abroad for high precision $d^{17}\text{O}$ analysis, thereby transferring human and financial resources to foreign institutions. This contribution is part of the "Exploring the nanoworld" MIUR - Futuro in Ricerca 2013 project that is devoted to the installation of the first electron diffraction tomography (EDT) system and the first three-oxygen isotope line in Italy. The combination of oxygen isotopic analysis and EDT on extraterrestrial materials can significantly enlarge our understanding about crucial issues of Planetary Sciences: i) early protoplanetary disk conditions; ii) compositions of chondrite components (refractory inclusions, chondrules, and matrix); iii) heterogeneity and transport of materials in the early solar nebula. The Italian community involved in Planetary and Space Sciences is growing rapidly, as testified by the increasing involvement of Italian research teams in projects supported by ESA, NASA and JAXA over the last two decades. This project intends to consolidate the growing role of Italy in Planetary and Space Sciences. In this regard, such facility will be strategic in the view of the current ESA involvement in sample-return space missions. We believe that the introduction of three-oxygen isotope analyses in Italy will significantly enhance the research capacity and competitiveness of Italy in the field of planetary materials.

Acknowledgements - This work is supported by the Italian Ministero dell'Istruzione, dell'Università e della Ricerca, MIUR 'Futuro in Ricerca Programme 2013'(projectID#:RBF13FIVO).

Clayton R.N, Grossman L. & Mayeda T.K. 1973. A component of primitive nuclear composition in carbonaceous meteorites. *Science*, 182, 485-488.

Mapping the sedimentary rocks on Mars and implications for planet evolution

Marinangeli L.*¹, Pompilio L.¹, Tangari A.C.¹, Cardinale M.¹, Piluso E.² & Baliva A.¹

1. Laboratorio di Telerilevamento e Planetologia, DiSPUTer, Università di Chieti "G. d'Annunzio".
2. Dipartimento di Biologia, Ecologia e Scienze della Terra, Università della Calabria.

Corresponding email: lucia.marinangeli@unich.it

Keywords: Mars, hyperspectral, planetary geology.

Mars is certainly the most studied planet of the Solar System, due to its particular exobiological interest related to the widespread morphological and sedimentological evidences of water bodies, suggesting past, or even present, habitability. These findings were carried out based on the considerable availability of high resolution dataset, provided by the numerous missions.

At the present, the liquid water is absent on the Martian surface, except for ice sheets at the poles, and a considerable quantity is believed to exist below the surface as an extensive global cryosphere.

However, morphological and sedimentary evidences of water, as valleys network, outflow channels and paleolakes are widely imprinted in the ancient Martian geology. Gullies and near-surface polar ice observed by recent missions, indicate that the liquid water may continue to produce chemical alteration and physical erosion, although its presence is probably rare and sporadic, due to the influence of the orbit and inclination of axes rotation. We present the result of the CRISM hyperspectral mapping for the identification of sedimentary deposits in the equatorial region of Mars.

We found the typical spectral adsorption bands of Al-rich clays, such as illite and montmorillonite belonging to the smectite group, in several sites nearby Valles Marineris region. The spectral signature of allophane (poorly crystalline clay), vermiculite, chlorite and other phyllosilicates belonging to the Fe/Mg smectite group, such as saponite and nontronite has been also found in Margaritifer Chaos. Large surrounding areas are dominated by basaltic composition with no evidence of clays diagnostic bands. We have tried to distinguish between hydrothermal and sedimentary alteration of the basaltic bedrock to produce the identified spectral signatures.

Another very interesting spectral response has been identified in the Elorza crater where a volcano-like morphology is associated to carbonates. We discuss the implication of having a carbonatitic deposition here rather than sedimentary carbonates. This hypothesis seems to be supported by the absence of any feature associated to the presence of water as well as the lack of clays.

These two sites confirm the variability of composition on the surface of Mars which is not always corresponding to the petrography of meteoritic samples.

Strata and the inner structure of 67P Churyomov-Gerasimenko comet

Massironi M.^{*1-2}, Simioni E.³, Marzari F.⁴, Cremonese G.³, Giacomini L.¹, Pajola M.², Jorda L.⁵, Naletto G.⁶⁻²,
Lowry S.⁷, Ramy El-Maarry M.⁸, Preusker F.⁹, Scholten F.⁹ & the OSIRIS team

1. Dipartimento di Geoscienze, Università di Padova. 2. Centro di Ateneo di Studi ed Attività Spaziali “Giuseppe Colombo” (CISAS), Università di Padova. 3. Istituto Nazionale di Astrofisica, Osservatorio Astronomico, Padova. 4. Dipartimento di Fisica e Astronomia, Università di Padova. 5. Laboratoire d'Astrophysique de Marseille, CNRS, Aix Marseille Université, France. 6. Dipartimento di Ingegneria dell'Informazione, Università di Padova. 7. School of Physical Sciences, The University of Kent, Canterbury, UK. 8. Physikalisches Institut, Universität Bern, Switzerland. 9. Deutsches Zentrum für Luft- und Raumfahrt (DLR), Institut für Planetenforschung, Berlin, Germany.

Corresponding email: matteo.massironi@unipd.it

Keywords: 67P/CG, Rosetta, strata.

The peculiar bi-lobe shape of 67P Churyomov-Gerasimenko (67P/CG) has soon raised the question if it is the expression of two distinct objects or the result of a well-localized excavation on the nowadays-active region in-between the two lobes. The widespread stratification involving most of 67P/CG surface seems to give an unambiguous answer to this topic.

We used both the OSIRIS NAC and WAC images acquired from 6 August 2014 up to 17 March 2015 with a spatial scale ranging between 0.5 m/px to 4.5 m/px depending on cometocentric distances and the derived shape models to infer presence, distribution and attitudes of strata throughout the entire comet surface. Strata were interpreted in ARC-GIS environment and their orientations derived from best fit planes reconstructed on the bases of shape models nodes of morphological terraces and cuestas-like features. 3D reconstructions were realized using Mesh-lab and Mat-lab softwares. These data allowed us to realize geological sections across the comet in order to infer the subsurface structure of the two lobes. In addition gravity vector fields were calculated for the entire bi-lobe shape body as well as for the two isolated (and reconstructed) lobes. Stereographic projections are then used to describe statistics of the orientation of planes in the relative reference system of the gravity fields. This enabled us to evaluate the angular relationship between the gravity vectors and the strata planes at different regions of the comet both considering the entire nucleus or two distinct objects.

Our results show that 67P/CG stratification forms a nearly continuous (up to 150 m thick) envelope of the major lobe (the main body), which is independent for an analogues envelope of the minor lobe (the head). Thus the geo-structural analysis revealed that strata are neither continuous nor compatible between the two lobes. Gravity vectors are nearly perpendicular to the strata considering the two separated lobes and diverge from perpendicularity considering the entire comet nucleus.

All the above-mentioned evidences are in favor of 67P/CG being an accreted body of two distinct objects with onion-like layered envelopes formed before their aggregation.

Our findings imply to revisit the concept of strata by including particles aggregation from protosolar nebula among the sedimentary processes and to find new models of growth and evolution of comets in the early Solar System.

Are magmatic processes at volcanoes from motionless plates analogues to those of the giant shield volcanoes on Mars?

Meyzen C.M.*¹, Massironi M.¹⁻² & Pozzobon R.¹⁻³

1. Dipartimento di Geoscienze, Università di Padova. 2. Istituto Nazionale di Astrofisica, Osservatorio Astronomico di Padova.
3. IRSPS-DISPUTer, Università di Chieti "G. d'Annunzio".

Corresponding email: christine.meyzen@unipd.it

Keywords: Volcanism, Mars, Antarctic.

The near “one-plate” planet evolution of Mars has led to the edification of long-lasting giant shield volcanoes. Unlike the Earth, Mars would have been a transient convecting planet, where plate tectonic would have possibly acted only during the first hundreds of million years of its history. On Earth, where plate tectonic is active, most plates are regenerated and recycled through convection. However, the Nubian and Antarctic plates could be considered as poorly mobile surfaces of various thicknesses that are acting as conductive lids on top of Earth’s deeper convective system. In these environments, volcanoes do not show any linear age progression at least for the last 30 Ma, but constitute the sites of persistent, spatially focused long-lived magmatic activity. Here, the near stationary absolute plate motion probably exerts a primary control on volcanic processes, and more specifically, on the melting ones. Depleted mantle residues left behind by the melting processes are difficultly dragged away from the melting locus. The thickening of the near-stationary depleted layer progressively forces the termination of melting to higher depths, reducing melt production rate, extraction and increasing mantle lithospheric-melt interactions. With time, it might cause long-term fluctuations of the volcanic activity, in generating long periods of quiescence. The pronounced topographic swells/bulges observed in these environments are thus probably both supported by large scale mantle upwelling and residual mantle roots. Most of these processes are likely similar to those observed on Martian giant shield volcanoes. The goal of this presentation will be to describe the essential characteristics of intra-oceanic magmatic processes on slow moving plates on Earth and to point out their similarities with those of the large shield volcanoes from the Tharsis region (Meyzen et al., 2015).

Meyzen C.M., Massironi M., Pozzobon R. & Dal Zilio L. 2015. Are plumes on motionless plates analogues to Martian plume feeding the giant shield volcanoes? Volume 401. Volcanism and tectonism across the inner solar system, Geol. Soc. Sp. Publ., 107-126.

Acapulcoites, winonaites and lodranites: new evidences on petrologic and minerochemical trends from X-ray maps and EMP analyses

Moggi Cecchi V.*¹, Caporali S.² & Pratesi G.¹⁻³

1. Dipartimento di Scienze della Terra, Università di Firenze. 2. Dipartimento di Chimica, Università di Firenze.
3. Museo di Storia Naturale dell'Università di Firenze.

Corresponding email: yanni.moggicecchi@unifi.it

Keywords: Primitive achondrites, acapulcoite, lodranites.

A comprehensive classification of primitive achondrites is difficult due to the high compositional and textural variability and the low number of samples available. Besides the oxygen isotopic analysis, other minerochemical and textural parameters may provide an useful tool to solve taxonomic and genetic problems related to these achondrites (Grady et al., 2014; Rubin, 2007). In order to determine these parameters a detailed modal, textural and minerochemical analysis on both the matrix and the chondrules of a set of 18 meteorites belonging to primitive achondrites has been performed and the results have been compared with literature data. The results of modal, textural and minerochemical analyses of a set of primitive achondrites are presented, and compared with literature data (Patzner et al., 2004; Mittlefehldt et al., 1996; Greenwood et al., 2012; Moggi Cecchi & Caporali, 2015). All the samples show an extremely variable modal composition among either silicate and opaque phases. A general trend of troilite depletion vs silicate fraction enrichment has been observed, with differences among coarse-grained and fine-grained meteorites. As concerns the mineral chemistry, olivine shows marked differences between the acapulcoites-lodranite and winonaite groups, while a compositional equilibrium between matrix and chondrules for both groups was observed. The analysis of Cr and Mn in clinopyroxene evidenced two separate clusters for acapulcoite/lodranite and winonaite groups, while the analysis of the reduction state evidenced three separate clusters. An estimate of equilibrium temperatures for acapulcoite-lodranite and winonaites groups is provided. Finally, hypotheses on the genetic processes of these groups are discussed.

- Grady M., Pratesi G. & Moggi Cecchi V. 2014. Atlas of Meteorites, 1st ed., Cambridge University Press, Cambridge, United Kingdom.
- Greenwood R.C., Franchi I.A., Gibson J.M. & Benedix G.K. 2012. Oxygen isotope variation in primitive achondrites: the influence of primordial, asteroidal and terrestrial processes. *Geoch. Cosmoch. Acta*, 94, 146-163.
- Mittlefehldt D.W., Lindström M.M., Bogard D.D., Garisson D.H. & Field S.W. 1996. Acapulco- and Lodran-like achondrites: petrology, geochemistry, chronology and origin. *Geoch. Cosmoch. Acta*, 60, 867-882.
- Moggi Cecchi V. & Caporali S. 2015. Petrologic and minerochemical trends of acapulcoites, winonaites and lodranites: new evidences from image analysis and EMPA investigations. *Geosciences*, 5, in press, doi:10.3390/geosciences50x000x.
- Patzner A., Hill D.H. & Boynton W.V. 2004. Evolution and classification of acapulcoites and lodranites from a chemical point of view. *Meteorit. Planet. Sci.*, 39, 61-85.
- Rubin A.E. 2007. Petrogenesis of acapulcoites and lodranites: A shock-melting model. *Geoch. Cosmoch. Acta*, 71, 2383-2401.

Clinopyroxene Fe-Mg exchange reaction applied to Martian nakhlites

Murri M.*¹, Scandolo L.¹, Alvaro M.¹, Domeneghetti M.C.¹ & Fioretti A.M.²

1. Dipartimento di Scienze della Terra e dell'Ambiente, Università di Pavia. 2. Istituto di Geoscienze e Georisorse, CNR, Padova.

Corresponding email: mara.murri01@universitadipavia.it

Keywords: Martian nakhlites, clinopyroxenes, geothermometer.

The broadest application of intracrystalline Fe²⁺-Mg partitioning between the *M1* and *M2* crystallographic sites in the pyroxene structure is the determination of the closure temperature (T_c) of Fe²⁺-Mg exchange reaction that provides important constraint on the cooling rate of the pyroxene-bearing host rocks (eg. Ghose & Ganguly, 1982). Although this approach has been successfully developed and applied for orthopyroxene and pigeonite-bearing rocks, relatively few data are available for clinopyroxenes (cpxs). The most recent calibration for cpxs has been obtained by Brizi et al. (2000). Calculations performed for cpxs in some Earth and planetary contexts, provided (i) T_c consistent among different samples and coherent with their respective geological setting; (ii) cooling rates for different samples from the same context in significant disagreement one to another. Domeneghetti et al. (2013) showed that the relative low T_c calculated for augite from Miller Range nakhlite (MIL03346) using the available geothermometers would correspond to a slow cooling rate inconsistent with the petrologic evidence for an origin from a fast-cooled lava flow.

In order to account for these discrepancies Alvaro et al. (2015) performed a new *ex situ* equilibrium annealing study on augite crystals from Miller Range nakhlite (MIL03346). This calibration has been therefore applied to the augite from Theo's Flow (always regarded as the terrestrial analogue for MIL03346). With the new calibration is clear that the nakhlites T_c (c.a. 600 °C) is lower than that of TS7 (720 °C) sample, which was supposed to be cooled at a burial depth of 85 m. However, despite the similar geological setting, the difference in T_c could be just ascribed to the differences in Fe content that may affect the Mg-Fe equilibrium behaviour.

Therefore, we have carried out a new equilibrium annealing experiments at 700, 800 and 900 °C in order to obtain a new geothermometric calibration on a Fe-poor augite. This new calibration will enable us to evaluate the compositional effects (mainly Fe content) by comparison with the data previously obtained on cpxs with different composition.

This work has been supported by the Italian PdR PNRA 2013/AZ2.04 (Meteoriti Antartiche) to L. Folco.

- Alvaro M., Domeneghetti M.C., Fioretti A.M., Cámara F. & Marinangeli L. 2015. A new calibration to determine the closure temperatures of Fe-Mg ordering in augite from nakhlites. *Meteorit. Planet. Sci.*, 50(3), 499-507.
- Brizi E., Molin G. & Zanazzi P.F. 2000. Experimental study of intracrystalline Fe²⁺-Mg exchange in three augite crystals: Effect of composition on geothermometric calibration. *Amer. Mineral.*, 85, 1375-1382.
- Domeneghetti M.C., Fioretti A.M., Cámara F., McCammon C. & Alvaro M. 2013. Thermal history of nakhlites: a comparison between MIL03346 and its terrestrial analogue Theo's flow. *Geochim. Cosmochim. Acta*, 121, 571-581.
- Ghose S. & Ganguly J. 1982. Mg-Fe Order-Disorder in Ferromagnesian Silicates. In: Saxena S.K. Ed., *Advances in Physical Geochemistry*. Springer-Verlag New York Inc., 2, 3-99.

Meteorite grains of red giant origins: when rocks help in modelling stars

Palmerini S.

Laboratori Nazionali del Sud, Istituto Nazionale di Fisica Nucleare, Catania.

Corresponding email: palmerini@lns.infn.it

Keywords: Meteorite grains, stars, stellar nucleosynthesis.

Since the small is the mass the large is the number of objects in a galaxy, low mass stars contribute to the chemical evolution of the interstellar medium as well as more massive, but less frequent supernovae. During the late stages of their evolution stars with mass smaller than $6-8M_{\odot}$ become Red Giants and are characterized by an extended, dusty and cold convective envelope, where products of stellar nucleosynthesis might condensate in grains. Part of these solids, which came to us as inclusions in meteorites felt on the Earth, provide very precise hints of the nucleosynthesis of stars where they formed. Indeed, geochemical analysis can determine the isotopic composition of these solids with an extremely high precision, which is not allowed to stellar spectroscopy.

According with the C/O ratio in the stellar envelopes SiC grains (if $C/O \geq 1$) or oxide grains (Al_2O_3 , if $C/O < 1$) might form. The majority of oxide grains belongs to the so-called group 1 and 2, which show an excess of ^{17}O and a large depletion of ^{18}O with respect to the solar values. Standard stellar models failed in reproducing these oxide grain compositions and 3 decades of studies were needed to prove that group 1 and 2 grains form in red giant stars (less massive than $2M_{\odot}$) where nuclear reactions of H burning are coupled with mixing phenomena.

We show that while $^{17}O/^{16}O$ and $^{18}O/^{16}O$ ratio can be reproduced by our state-of-the-art code for stellar nucleosynthesis including mixing, the Al isotopic ratios measured in the same grains (namely group 2 grains) offer a so strong constrain to the mixing mechanism, occurring in progenitor stars, that they might be used as selection rule for the physical phenomenon triggering the mass transport.

Finally, we show the challenging case of the Mainstreams SiC grains, which show values of C/N and $^{12}C/^{13}C$ ratio in agreement with the predictions of stellar models for C-rich red giant stars, but a large spread of values for the $^{14}N/^{15}N$ isotopic ratio, which is instead unexplained.

Cracks associated to mud-volcanic fields on Mars: clues for recent methane degassing?

Pozzobon R.*¹, De Toffoli B.², Cremonese G.¹ & Massironi M.²

1. Istituto Nazionale di Astrofisica, Osservatorio Astronomico di Padova. 2. Dipartimento di Geoscienze, Università di Padova.

Corresponding email: riccardo.pozzobon@oapd.inaf.it

Keywords: Mars, methane, mud volcanism.

The presence of methane hydrates in Martian atmosphere have been recently observed by several authors (Geminale et al., 2008; Mumma et al., 2009) as well as a spatial variation of its concentration. However, its origin and release mechanism is still debated. Martian gas hydrates would possibly be a binary system of methane and carbon dioxide occupying subsurface cavities. Several methane hydrate sources were located on the surface involve the north polar cap, Terra Sirenum and Claritas Fossae/Thaumasia highlands, Tharsis and Elysium volcanic provinces and Arabia Terra (Fonti & Marzo, 2010). The origin of methane is still unclear but could be likely linked to several release mechanisms such as volcanic degassing, permafrost seasonal variation at low/mid latitudes or indirect release in subsurface traps (impact cratering, landslides etc.). The coexistence of methane, carbon dioxide and sulfur (King & McLennan, 2010) has also been observed on Mars. More importantly, on Earth carbon and sulfur cycles are intrinsically linked through both inorganic and biological processes. On Earth methane hydrates release is mostly associated to mud volcanoes and several mud volcanic fields have been recognized on Mars for example in Acidalia Planitia (Oehler et al., 2010) and Arabia Terra (Pondrelli et al., 2015). In particular Arabia Terra mud-volcanoes are often associated to impact craters and likely the impact process itself provided a preferential fractures network that allowed fluid to reach the surface. The short permanence time of methane in Martian atmosphere suggests that active release of gas would be active also nowadays. Whether geochemical or biochemical in nature, the observed methane indicates a chemically active subsurface exchanging with the atmosphere on Mars today. We recently recognized on Firsoff and Crommelin craters interior on HiRISE (0.25 m/px) some small fractures and cracks (hundreds of meters long and only a few meters wide) that cut the inner sedimentary formation and mud-volcanic edifices being thus the most recent feature, and that could likely be related to recent methane degassing observed in this area. This observation along with the strong presence of sulphates and pervasive water-related activity and clay alteration minerals (Pondrelli et al., 2015) could be a proxy of active degassing possibly associated with deep gas and hydrocarbon traps in the subsurface of Arabia. Moreover these particular geologic settings could be a preferential location of astrobiological interest for future missions like ExoMars TGO (Trace Gas Orbiter). The primary science goals of the TGO mission are to seek evidence for extant subsurface zones of habitability and habitancy.

Fonti S. & Marzo G.A. 2010. Mapping the methane on Mars. *Astron. Astrophys.*, 512, A51.

Geminale A., Formisano V. & Giuranna M. 2008. Methane in Martian atmosphere: average spatial, diurnal, and seasonal behaviour. *Planet. Space Sci.*, 56, 1194.

King P.L. & McLennan S.M. 2010. Sulfur on Mars. *Elements*, 6, 107-112.

Mumma M.J., Villanueva G.L., Novak R.E., Hewagama T., Bonev B.P., DiSanti M.A., Mandell A.M. & Smith M.D. 2009. Strong release of methane on Mars in Northern summer 2003. *Science*, 323, 1041-1045.

Pondrelli M., Rossi A. P., Le Deit L., Fueten F., van Gasselt S., Glamoclija M., Cavalazzi B., Hauber E., Franchi F. & Pozzobon R. Equatorial layered deposits in Arabia Terra, Mars: Facies and process variability. *Geol. Soc. Am. Bull.*, doi:10.1130/b31225.1.

How to study Mercury's surface in remote sensing: experimentally acquired and *ab initio* calculated HT-IR vibrational frequencies

Stangarone C.*¹, Tribaudino M.¹, Prencipe M.² & Helbert J.³

1. Dipartimento di Fisica e Scienze della Terra, Università di Parma. 2. Dipartimento di Scienze della Terra, Università di Torino. 3. Institut für Planetenforschung Leitung und Infrastruktur, Deutsches Zentrum für Luft und Raumfahrt (DLR), Berlin, Germany.

Corresponding email: claudia.stangarone@studenti.unipr.it

Keywords: Mercury, remote sensing, *ab initio* methods.

Planetary surfaces are made of solid matter and, by analogies to planet Earth, they underwent to all those physical and mechanical processes that influenced their actual morphology and composition.

We study spectral signatures of minerals, since they are intimately related to the crystal structure and they represent a remote sensing method to determine a surface composition by analysing their spectral reflectance.

The aim of this work is to interpret the thermal emissivity spectra that will be carried out at the Institute of Planetary Research (DLR, Berlin-Adlershof) of the main mineral families that compose the surface of Mercury. To do so, focusing on pyroxenes and feldspars (Sprague et al., 2007; 2009), we will perform quantum mechanical simulations of the IR spectra of the above minerals, both at room and high temperature, exploiting the accuracy of the CRYSTAL14 code (Dovesi et al., 2014).

Results will be useful to create a theoretical background to interpret HT-IR reflectance spectra that will be collected by MERTIS, a spectrometer developed by DLR, that will be on board of the next ESA spacecraft, BepiColombo, whose launch is scheduled at the beginning of 2017 (Hiesinger & Helbert, 2010).

The goal is to point out the most interesting spectral features for a geological mapping of Mercury and other rocky bodies, simulating the environmental conditions of the inner planets of Solar System.

Dovesi R., Saunders V.R., Roetti C., Orlando R., Zicovich-Wilson C.M., Pascale F., Civalleri B., Doll K., Harrison N.M., Bush I.J., D'Arco P., Llunell M., Causà M. & Noël Y. 2014. CRYSTAL14 User's Manual, University of Torino.

Hiesinger, H. & Helbert, J. 2010. The Mercury Radiometer and Thermal Infrared Spectrometer (MERTIS) for the BepiColombo mission. Comprehensive Science Investigations of Mercury: The scientific goals of the joint ESA/JAXA mission BepiColombo. Planet Space Sci., 58, 144-165.

Sprague A.L., Warell J., Cremonese G., Langevin Y., Helbert J., Wurz P., Veselovsky I., Orsini S. & Milillo A. 2007. Mercury's surface composition and character as measured by ground-based observations. Space Sci. Rev., 132, 399-431.

Sprague A.L., Donaldson Hanna K.L., Kozłowski R.W.H., Helbert J., Maturilli A., Warell J.B. & Hora J.L. 2009. Spectral emissivity measurements of Mercury's surface indicate Mg- and Ca-rich mineralogy, K-spar, Na-rich plagioclase, rutile, with possible perovskite, and garnet. Planet Space Sci., 57, 364-383.

Slow neutron captures contribution for isotope anomalies in the Fe-group elements of meteorites

Trippella O.*¹, Palmerini S.², Busso M.M.¹⁻³ & Wasserburg G.J.⁴

1. Istituto Nazionale di Fisica Nucleare, Perugia. 2. Istituto Nazionale di Fisica Nucleare, Laboratori Nazionali del Sud, Catania. 3. Dipartimento di Fisica e Geologia, Università di Perugia. 4. Lunatic Asylum, Geological & Planetary Sciences, California Institute of Technology, Pasadena, USA.

Corresponding email: oscartrippella@gmail.com

Keywords: AGB stars, s-process, Fe-group.

The elements of the "iron-group" show anomalies in macroscopic samples of meteorites. In particular, these isotopic effects are common in calcium-aluminum-rich inclusions (CAIs) in meteorites, but are also wide spread at lower levels in "bulk" samples of different groups of meteorites. In the different classes of data that are available we must consider both presolar grains, each of which come from a particular stellar source, and macroscopic samples of solar system material, that come from blends from different stellar sources.

We focus our attention on Ti, Cr, Fe, Ni, and Zn that are considered to be members of the "Fe-group". The production of these nuclei is commonly attributed to supernovae (SNe), both core collapse and SNeIa. However, as large fractions of the interstellar medium (ISM) were reprocessed in AGB stars, these elements were reprocessed by slow neutron captures, too. A special emphasis was dedicated to chromium, iron, and nickel showing anomalies in ⁵⁴Cr, ⁵⁸Fe, and ⁶⁴Ni. We expect that the effect of s-processing on Cr, Fe, and Ni (originally synthesized in SNe) is to produce the heavier isotopes of these elements, the same mentioned above, in over-abundance. We calculate the effects of such reprocessing on Cr, Fe, and Ni through 1.5 M_o and 3 M_o AGB models, adopting solar and 1/3 solar metallicities. All cases produce excesses of these isotopes, hence, the observations may be explained by AGB processing. The enrichment factors E_{ik} of isotope "i" relative to an index isotope "k" for an initial solar isotopic pattern (E_{i,k} = (N_i/N_k)/(N_i/N_k)_o - 1) were calculated following the post-process nucleosynthesis code NEWTON.

Consequences for other "Fe group" elements are then explored. The connection of s-processing to Si, Ca and Ti is more complex as has been widely noted in the literature, particularly considering data on those circumstellar condensates (CIRCONS) which are associated with AGB stars. They include ⁵⁰Ti excesses, and some production of ^{46,47,48}Ti excesses. In many circumstellar condensates, Ti quantitatively reflects these effects of AGB neutron captures. Scatter in the data results from small variations in the isotopic composition of the local ISM. For Si, the main effects are instead due to variations in the local ISM from different SNe sources. The problem of Ca is also discussed, particularly with regard to ⁴⁸Ca. The effects we calculate for ⁴⁶Ca are very large and no observations support this. Again the Ca shifts in s-processing are relatively weak as compared to Ti, Cr, Fe and Ni. The measured data are usually represented assuming terrestrial values for ⁴²Ca/⁴⁴Ca. Materials processed in AGB stars or sources with variable initial ⁴²Ca/⁴⁴Ca ratios can give apparent ⁴⁸Ca excesses/deficiencies, attributed to SNe. The broader issue of Galactic Chemical Evolution is also discussed in view of the isotopic granularity in the ISM. It is hoped that the above simple considerations on AGB processing may aid in clarifying some of the isotopic shifts found in some Fe group nuclei.

SESSION S18

Geological, geophysical and geochemical prospection for economic geology and geothermal resources

CONVENORS

Maria Boni (DSTAR - UNINA)

Domenico Montanari (CNR-IGG)

Secondary enrichment of the Capricornio (Chile) epithermal Au-Ag-Cu mineralization and implications for the exploration

Arfé G.*¹, Boni M.¹, Mondillo N.¹, Aiello R.¹ & Arseneau V.²

1. Dipartimento Scienze della Terra, dell' Ambiente e delle Risorse, Università di Napoli "Federico II". 2. Arena Minerals Inc., Cile.

Corresponding email: giuseppe.arfe@unina.it

Keywords: Au-Ag epithermal mineralization, supergene enrichment, Chile

The Capricornio epithermal Au-Ag-Cu deposit in Chile consists of multiple epithermal quartz-adularia-carbonate veins, ranging from 150-200 m a.s.l. to ~ 400 m in depth. The epithermal system has been exposed at surface by trenching and shallow reverse circulation drilling, defining over 8 km of Au bearing quartz veins. A better mineralized Au-Ag zone, with average grades of >12 g/t Au and >340 g/t Ag, is located at the uppermost 50 m to 100 m of the vein system. Below 150-200 m in depth a net decrease in the Au and Ag values is observed. The primary ore association is represented by base metals sulfides (galena, pyrite, chalcopyrite, sfalerite, bornite), as well as by electrum, sulfoarsenides, sulfoselenides, sulfoantimonides and Ag-sulfosalts. The veins are hosted in Paleocene and early Eocene mafic to felsic volcanic rocks, which are hydrothermally altered similarly to those, which caused the deposition of the far greater El Peñón deposit at 100 km to the south. At El Peñón the individual mineralized shoots range from less than 1 km to 4 km in strike length, and measure up to 350 m in down-dip direction.

In both El Peñón and Capricornio deposits, the economic mineralization is mainly concentrated in the supergene alteration zone. At Capricornio, the supergene processes have defined a cementation zone, represented by a mineral association consisting of covellite, chalcocite, cerussite, electrum (secondary) and acanthite, and an oxidation zone containing electrum, native Au and other minerals (chlorides, chlorocarbonates and halides), which have been traced from the surface to 50 m in depth.

At El Peñón (1300 to 2000 m a.s.l.) the secondarily enriched interval is developed for 350 m, while at Capricornio (980 m a.s.l.) the supergene alteration cannot be traced deeper than 150-200 m from the surface, and Au is enriched mainly in the first 50 m. Measured ages of supergene alunite from El Peñón and from other deposits in the region (Warren et al., 2008), indicate that the weathering of the primary ores occurred from 23 to 17 Ma, under a semiarid to arid climate, prior to the onset of the hyperarid period (Clarke, 2006).

Thereby, Au, Ag and Cu exploration for most deposits in the Capricornio area should be focused to the supergene alteration zone, whose thickness would represent an important control on the ore potential. The variable thickness of the supergene alteration zone between El Peñón and Capricornio, which is probably associated with the variable uplift and erosion stages from Eocene onwards, represents one of the causes affecting the different economic potentials of the two mineralized areas.

Clarke J.D.A. 2006. Antiquity of aridity in the Chilean Atacama Desert. *Geomorphology*, 73, 101-114.

Warren I., Archibald D.A. & Simmons S.F. 2008. Geochronology of epithermal Au-Ag mineralization, magmatic-hydrothermal alteration, and supergene weathering in the El Peñón district, northern Chile. *Econ. Geol.*, 103, 851-864.

A pilot study to test the reliability of the ERT method in the identification of mixed sulphides bearing dykes: the example of Skoura mine (Morocco)

Bernardinetti S.*¹, Colonna T.¹, Pieruccioni D.¹⁻⁴, Abbigliati M.¹, Trotta M.¹, Algeri G.¹, Tufarolo E.¹, Minucci S.¹, Mugnaioli E.²⁻³, Talarico F.M.²⁻³, Viti C.², Harroud A.⁵, Guernouche M.⁵ & Cinà A.⁵

1. Centro di Geotecnologie, Università di Siena. 2. Dipartimento di Scienze Fisiche, della Terra e dell' Ambiente, Università di Siena. 3. PetroLogicSynergy (SPL) srl spin-off Università di Siena. 4. Dipartimento di Scienze Chimiche e Geologiche, Università di Cagliari. 5. Société Marocaine de Géo-Technologies (SMG) srl spin-off Università di Siena.

Corresponding email: diegopieruccioni@hotmail.it

Keywords: Geophysical survey, petrographical analyses, mixed sulphides.

A multidisciplinary study, including an integrated application of geological, petrographical and geophysical methods and techniques, is under progress with the aim of identifying and assess the geometry and volume of the main mineralized bodies (mixed sulfides, Zn-Pb and Fe-Cu, and potential Ag) in an area of the Anti-Atlas chain located SE of the town of Skoura (Ouarzazate, Morocco). The initial phase of exploration - just completed - included extensive field work (structural investigations and sampling) and a detailed geoelectrical survey (electrical resistivity) to verify the effectiveness and reliability of this geophysical method with respect to a number of key aspects such as: sensitivity, resolution level according to the pitch electrode, control of the geometry of mineralized bodies in depth, contrast of resistivity between the mineralized dykes and country rocks, possible correlations between the type and amount of sulphides and mean values of resistivity. The geophysical survey was accompanied by a geological survey to reconstruct the structural setting of the mineralization(s) and their relationships with the deformational history of country rocks, specifically two main fault systems and possible more than one generations of dyke swarms, mainly of acid composition. A representative set of samples was sampled from both sulphide-bearing cataclasites (with either quartz or carbonate gangues), and from altered and unaltered country rocks (mainly very low/low grade metapelites and metabasalts). Preliminary mineralogical analyses suggest a distinction of sulphide-bearing assemblages in two distinct paragenesis, one with galena and wurtzite (respectively included in gangues of quartz and carbonate minerals) and another with chalcocite and chalcopyrite. The composition of the mineralized veins will provide essential data to compare with similar occurrences in other areas of the Anti-Atlas, and constrain the regional metallogenic model. The geometry of the underground was investigated in situ through 15 two-dimensional geoelectric prospections, each with 96 electrodes and inter-electrode step with a variable value (between 2 to 3 meters) over an area of approximately 5 hectares. The used arrays of acquisition were the dipole-dipole and mutual Schlumberger. The acquisition lines were arranged orthogonally to the trend of the dykes keeping a configuration of acquisition completely consistent with the one of direct theoretical models. The results arising from this approach made it possible to answer specific questions asked during the design phase of the test. The results shown by the geoelectric tomography suggest the presence of bodies with low resistivity, well distinct from the resistive context of the country rocks, and with a sub-vertical geometry which is consistent with the structural trend of the mineralized bodies as obtained by photo-interpretation and field observations.

Supergene nonsulfide zinc ores: from exploration to processing

Boni M.

Dipartimento di Scienze della Terra, dell'Ambiente e delle Risorse, Università di Napoli "Federico II".

Corresponding email: boni@unina.it

Keywords: Nonsulfide Zinc, exploration, processing.

Supergene nonsulfide zinc deposits (NSZ) have recently enjoyed a revival in exploration throughout the world, and a renewed commercial interest due to new processing technologies. Nevertheless, at several mines both capital and operating costs and metal recoveries have not completely met the feasibility study expectation, while other NSZ resources are still battling with technical and/or political issues. Many technical problems can be mitigated by a better identification of the mineralogical association of the metallic minerals and gangue. This should be a fundamental step in the exploration of this kind of mineral deposits, because the extraction process is highly sensitive to mineralogy (Boni & Mondillo, 2015). Supergene zinc deposits contain hydrated zinc silicates and carbonates, such as hemimorphite ($Zn_4Si_2O_7(OH)_2 \cdot H_2O$) and hydrozincite ($Zn_5(CO_3)_2(OH)_6$), or the most common smithsonite ($ZnCO_3$).

Supergene nonsulfides are derived from the weathering of primary sulfides: a combination of conditions is needed for the development of economically significant deposits of this type. Key conditions include: (1) pre-existing zinc ores, (2) efficient oxidation promoted by tectonic uplift and/or prolonged weathering; (3) permeable wall rock to allow for ground-water movement; (4) effective trap sites and hydrogeological environments that do not promote dispersion and loss of Zn-bearing fluids.

As a first prerequisite, exploration programs for NSZ must establish the presence of geologic situations favorable for the existence of primary zinc deposits, preferably in carbonate host rocks. Exploration must then recognize the geomorphologic characteristics that engender favorable paleosurfaces, beneath which oxide-dominated zinc deposits may have evolved. Discovery of outcropping supergene deposits will depend on recognition of the zinc minerals. Ground search for supergene zinc can be augmented by the use of "zinc zap", a chemical compound that, upon contact with nonsulfide zinc minerals, turns a scarlet color.

Litho geochemistry should focus on defining negative anomalies in and around former zinc-bearing gossans, and should seek to define the direction of ground-water flow by targeting subtle metallic anomalies.

Direct geophysical detection of NSZ ores is difficult, owing to the absence of minerals that provide electrical or magnetic response. However, geophysics can contribute useful information on weathering profiles and detection of karstic zones that may host the supergene deposits. These zones are characterized by low density and low resistivity compared with denser and more highly resistive unweathered carbonate rocks. Detailed resistivity surveys, and possibly shallow seismic surveys, may be able to define weathered zones leading away from the original sulfide body down the ground-water flow gradient.

Boni M. & Mondillo N. 2015. The "Calamines" and the "Others": The great family of supergene nonsulfide zinc ores. *Ore Geol. Rev.*, 67, 208-233.

Persistent Scatterer Interferometry (PSI) to detect surface deformation in the Larderello-Travale geothermal area (Tuscany, Italy)

Botteghi S.*¹⁻², Montanari D.¹, Del Ventisette C.² & Moretti S.²

1. Istituto di Geoscienze e Georisorse, CNR, Firenze. 2. Dipartimento di Scienze della Terra, Università di Firenze.

Corresponding email: s.botteghi@igg.cnr.it

Keywords: PSInSAR data, ground deformation, monitoring.

The present study aims to verify applied PSInSAR techniques over Larderello and Travale/Radicondoli geothermal areas, where surface deformation has been already monitored using precise topographic levelling methods. In these area, located in southern Tuscany (Italy) about 15 km apart, two main interconnected reservoirs have been identified: a shallow reservoir hosted in sedimentary units (limestone and anhydrite) and a deeper reservoir hosted within metamorphic and intrusive rocks.

We have analysed PS information, from radar satellites ERS (European Remote Sensing Satellite) for the period 1993-2000, and ENVISAT (Environmental Satellite) satellite acquired between 2003 and 2010. For ERS satellites, only descending geometry data set was available. Analysis of the data showed that, in the period 1993-2010, the Larderello and Travale/Radicondoli geothermal fields were subject to subsidence phenomena with maximum rates of deflection of about 15 mm/yr and 29 mm/yr, respectively. The zones of greater subsidence are localized in the central part of the geothermal fields, and show a good correlation with the areas of greatest exploitation.

Unfortunately there are no satellite data covering periods prior than 1993; however, previous monitoring of ground vertical movements performed with precise topographic levelling (from 1973 to 2003), allow us to reconstruct the subsidence trends of the area and to make a comparison between the two different methodologies for the 1993-2003 time span.

This study confirmed that mapping and monitoring land surface deformation can provide useful information on time evolution of geothermal system from exploration to exploitation. The analysis of spatial and temporal changes of these phenomena can be used to prevent and minimize environmental and infrastructure impact.

Geochemistry of Volatile Organic Compounds (VOCs) in fluids from the Krafla and Reykjanes geothermal systems, Iceland

Capecchiacci F.^{*1-2}, Eyjólfsson E.I.³, Tassi F.¹⁻², Vaselli O.¹⁻² & Ruggieri G.²

1. Dipartimento di Scienze della Terra, Università di Firenze. 2. Istituto di Geoscienze e Georisorse, CNR, Firenze
3. ISOR, Iceland Geosurvey.

Corresponding email: francesco.capecchiacci@unifi.it

Keywords: VOCs, geothermal systems, Iceland.

In the framework of the IMAGE (Integrated Methods for Advanced Geothermal Exploration) European project, a sampling campaign for fluids from boreholes and fumaroles was carried at two different geothermal fields: Krafla and Reykjanes in North-East and South-West Iceland, respectively. The Krafla high-temperature geothermal system lies in the northern part of the neo-volcanic zone, within the caldera of the Krafla central volcano formed about 105 years ago. The Reykjanes geothermal field, located at the southwest tip of the Reykjanes peninsula, 55 km southwest of Reykjavík, is characterized by extensive Postglacial lava fields. Sampling was carried out by researchers from IGG (Institute of Geosciences and Earth Resources) of CNR and ISOR (Iceland Geosurvey) between 19 and 23 May 2014. Three boreholes (depth from 800 to 2248 m) and three fumaroles were sampled from each system in order to constrain the relationship between the composition of the Volatile Organic Compounds (VOC's) and the chemical physical conditions at their source.

The inorganic main gas composition of the two areas is typical of hydrothermal emissions, being dominated by steam ($H_2O > 96\%$) and showing a dry gas phase mainly consisting of CO_2 , H_2S , H_2 , N_2 , with minor concentrations of CH_4 , Ar, O_2 , and He. The $\delta^{13}C-CO_2$ values ranged from -4.15 to -0.57permil vs. V-PDB. Up to 16 different VOCs, pertaining to the alkane (7 compounds), alkene (2 compounds), aromatic (4 compounds), sulfonated (3 compounds) groups, were identified and quantified. The composition of aromatics was largely dominated by Benzene (up to 1,800 ppb), whereas Thiophene (up to 1,600 ppb) was the most abundant among S-bearing compounds. These two gases typically become enriched at hydrothermal conditions, whereas they tend to be degraded in presence of hot, highly oxidizing fluids, such as those released from a magma source. On the contrary, furans (O-substituted) are typical products of gases deeply influenced by magmatic fluid contributions (Tassi et al., 2010). Thus, their absence in the analyzed samples, coupled with that of acidic gases (i.e. SO_2 , HCl and HF), suggests that the possible inflow of magmatic fluids is efficiently buffered by the two hydrothermal reservoirs.

Tassi F., Montegrossi G., Capecchiacci F. & Vaselli O. 2010. Origin and Distribution of Thiophenes and Furans in Gas Discharges from Active Volcanoes and Geothermal Systems. *Int. J. Mol. Sci.*, 11, 1434-1457.

Geological and numerical modeling to support electric production in geothermal fields: a case test in Central Italy

Colucci F.*, Moia F., Guandalini R. & Agate G.

Ricerca sul Sistema Energetico - RSE S.p.A., Milano.

Corresponding email: francesca.colucci@rse-web.it

Keywords: Geothermal reservoir, electric production, numerical modeling.

This study describes the geological and numerical modeling strategies that can be adopted to support electric production in a medium-enthalpy geothermal field located in Castel Giorgio-Torre Alfina area, close to Bolsena Lake in Central Italy. The simulations have been carried out in order to verify the sustainability for geothermal electric production by a 5 MWe nominal power pilot plant that foresees a total fluid re-injection in the same original reservoir, and which process is based on the binary ORC (Organic Rankine Cycle) because it allows the geothermal field exploitation at temperatures lower than those of an high enthalpy field.

The considered geothermal reservoir is located in permeable and fractured carbonate formations belonging to the Complex of Tuscan facies while the caprock has been identified in the overlying Complexes of Ligurian and internal Austro-alpine facies. The top reservoir depth ranges from about -800 m to -1700 m a.s.l. while reservoir temperature ranges from 125 °C to 150 °C.

An accurate 3D numerical model including geological and spatial discretisation has been realized in order to perform simulations devoted both to reproduce the natural state of the geothermal system and to perform predictive analyses in order to support the electricity production by the ORC industrial process. The accuracy of numerical simulation related to the natural state of the field has been verified by comparing simulated and measured temperatures in correspondence to a number of exploration wells drilled in the interesting area.

The correctness of the natural state simulation allowed to analyze a number of different operating scenarios, all considering a production period of 50 years being the geothermal fluid extracted from five wells and totally re-injected into four different wells, with the aim of optimizing the production flow rate. Also the time necessary to recovery the natural state conditions after the end of production/reinjection activity has been estimated by numerical simulation. As the result, a constant flow rate of 1050 t/h has been considered as reference value, since in this case a very efficient convective circulation inside the geothermal system has been observed to be kept, and production sustainability is guaranteed for all the period. Furthermore, the over pressure field around the re-injection wells is limited to 2% of pre-existing one and no interference effect has been highlighted between the production and re-injection wells, which locations are such to ensure that the re-injected fluids are heated before reaching the production wells. Finally, the original natural pressure state is recovered in less than a century, while temperature seems to reach more slowly its natural equilibrium.

Geothermal heating and cooling in the FVG Region: the realization of the Grado District Heating Pilot Plant and the Pontebba Ice Rink

Della Vedova B.* & Cimolino A.

Dipartimento di Ingegneria e Architettura, Università di Trieste.

Corresponding email: dellavedova@units.it

Keywords: Low temperature geothermal resources, geothermal heating and cooling, carbonate platform.

We present two new running applications of direct uses of low temperature geothermal resources for heating and cooling of public buildings, realized with public fundings in the Friuli Venezia Giulia Region - RFVG (Northeastern Italy) in the last three years.

The *Grado Geothermal Pilot Project* is an ambitious project, initiated in 2002 and completed in early 2015, supported by EU funding. The main challenge of the project was to demonstrate the feasibility of a district heating system, sustained by a geothermal doublet (one production and one re-injection wells), drilled into the buried Mesozoic carbonate platform of the cold Adriatic foreland. The specific goals were to: characterize the geothermal carbonate reservoir of the Grado area, assess its geothermal potential by drilling the first exploration borehole, evaluate the production capacity by drilling the second borehole, carry out hydraulic pumping and interference tests, complete the technical design the district heating network and plant, simulate its functioning and operation to evaluate impacts and sustainability management.

The project had a total cost of 5 Millions Euro and included two phases. The 1st phase, completed in 2008, verified the feasibility of the district heating plant in Grado, confirmed the existence of a low temperature geothermal reservoir within the buried carbonate platform. Several geophysical surveys were completed to assist the location of the wells. The first exploration borehole Grado-1 was drilled down to 1110 m, into a terrigenous cover and a Paleogene-Mesozoic carbonate basement high. The 2nd phase (2012 - 2015) included further geophysical prospecting to extend reservoir investigations and to locate the 2nd borehole. Grado-2 was drilled in 2014, at about one km distance to the East of Grado-1, down to 1200 m. By December 2014, two km of the district heating distribution network were deployed and the first two public buildings were connected to the network for the first tests.

We focus here mainly on the geophysical exploration, well data and on the pumping tests that were acquired before, during and after the drilling of the two wells. The data set allowed the characterization of the reservoir and the assessment of its geothermal potential. The main results are: the identification of production areas, the comprehension of the hydraulic circulation systems, the assessment of the geochemical facies of waters and the design for their sustainable utilization. The Grado reservoir is a confined fractured aquifer hosting anoxic fossil seawaters (salinity exceeding 30‰), temperatures up to 49 °C in Grado-2 (about 7 °C higher than Grado-1), pressures of 250 kPa at wellhead and spontaneous artesian outflows of about 100 tons/h from both wells. Pumping test results indicate a sustainable water production up to 140 tons/h. The circulating system is a complex network of permeable vugs and highly transmissive karst-fractured discontinuities, interested by several fault systems driven by Alpine and Dinaric deformation phases. Interference pumping tests proved the hydraulic connectivity between wells, but, due to the poor system recharge, the hydraulic sustainability of the geothermal plant requires total re-injection. 3-D thermo-fluid dynamic numerical modeling results, calibrated by experimental data, will allow to optimize the geothermal reservoir production and manage the sustainability of the geothermal plant. The initial functioning of the district heating plant, envisaging a geothermal heating of several connected buildings during cold seasons (up to about 3 MW_{th} heating load), will allow a significant economical saving of the order of 100,000 €/year. Nevertheless, the geothermal production capacity of the doublet would afford to foster other relevant integrated uses, besides the district heating, to increase substantially the capacity factor, presently amounting to 0.2 only.

The groundwater heating and cooling system of the *ice rink of Pontebba* town (UD), located close to the Austrian border, was realized in late summer 2012; it consists of an open loop heat pump system using groundwater thermal energy that provides both ice production and maintenance, and heating and hot water needs of the ice stadium. Two new ammonia heat pumps were installed, supported by two production water wells (32 m deep) and one re-injection water well (30 m deep), drilled in the gravel deposits of the Fella river. A total production rate of up to 200 tons/h could be derived from the shallow unconfined aquifer, with an average temperature of about 8.5-9.0 °C. Numerical modelling of groundwater flow supported the assessment of the production and re-injection rates, as well as the assessment and minimization of the impacts on the groundwater resource and environment, during the plant management in various hydraulic regimes. Over the first two years of operation, cost reductions of the order of 45% have been achieved.

Redox state of magmas and granite-related Mo mineralization: evidences from Late Variscan F-bearing granites from Southern Sardinia (Italy)

Fadda S.¹, Fiori M.¹, Matzuzzi C.¹, Naitza S.*² & Secchi F.³

1. Istituto di Geologia Ambientale e Geoingegneria, C.N.R. Cagliari. 2. Dipartimento di Ingegneria Civile, Ambientale e Architettura, Università di Cagliari. 3. Dipartimento di Scienze della Natura e del Territorio, Università di Sassari.

Corresponding email: snaitza@unica.it

Keywords: Oxygen fugacity, F-bearing granite, greisens.

Redox state of magmas has been invoked to explain the metallogenic behaviour of intrusive magmatism (Ishihara, 1981). Thus, Sn deposits are linked to low- fO_2 , ilmenite series, while Mo deposits are better bracketed into high- fO_2 , magnetite series. In Variscan Europe Mo deposits are represented in a few districts, including Eastern Erzgebirge, France and Sardinia. In Sardinia, small Mo deposits are related to a post-collisional F-bearing granite suite dated close to 290 Ma by Re/Os on molybdenite (Boni et al., 2003) and $^{40}Ar/^{39}Ar$ on biotite (Dini et al., 2005). This late Variscan suite is dominated by metaluminous biotite leucogranites grading to hololeucocratic microgranitic to granophyric varieties; amphibole biotite monzogranites are locally observed (Monte Sette Fratelli). They emplaced at shallow crustal levels and locally (Ogliastra) grade to felsic volcanics. Thermal effects of the intrusions are limited to narrow contact aureolas (andalusite zone) around the plutons. In SW Sardinia (Sulcis and Monte Linas intrusions), both Mo and Sn deposits occur. Magmatic bodies show a distinctive magmatic zonation, with medium-grained granites dimembered upward by thick, flat-lying fine-grained to porphyritic varieties, including fayalite-bearing pegmatite layers. Fine-grained to porphyritic rocks suffered various degrees of greisenization, and host Mo ores, related to numerous small endo- and exo- quartz-muscovite greisens (e.g. Perda Lada), grading to quartz vein and stockwork systems (Perd'e Pibera, Su Seinargiu, Flumini Binu). Ores are commonly dominated by molybdenite, with subordinate pyrite, chalcopyrite and wolframite. The studied deposits are related to ilmenite rock series, as evidenced by petrography (opaque contents of granites <1%; ilmenite>>magnetite), and confirmed by geochemical ratios (Rb/Sr, FeO/Fe₂O₃, K/Rb). This behavior seems to contrast with the Mo/magnetite series association, and is more coherent with the presence of Sn vein deposits in the same areas (Naitza et al. 2015). A possible explanation involves changes of physicochemical parameters (in particular, fO_2 and HF activity) from magmatic processes during magma emplacement to greisenization; variation of redox conditions are confirmed by discontinuous reverse zoning of plagioclase laths in fine-grained facies, indicating a progressive P_{H_2O} increase with magmatic evolution. Mineralization prevalently occurred in close system conditions, although in some areas (Oridda, Su Seinargiu, Flumini Binu) Mo ores are centered on bodies of porphyritic rocks, showing features close to porphyry-style mineralization (Fiori et al., 1986).

Boni M., Stein H.J., Zimmerman A. & Villa I.M. 2003. Re-Os age for molybdenite from SW Sardinia (Italy): a comparison with $^{40}Ar/^{39}Ar$ dating of Variscan granitoids. In: Eliopoulos K. et al., Eds., Mineral exploration and sustainable development. Millpress, Rotterdam, 247-250.

Dini A., Di Vincenzo G., Ruggieri G., Rayner J. & Lattanzi P. 2005. Monte Ollasteddu, a new gold discovery in the Variscan basement of Sardinia (Italy): first isotopic ($^{40}Ar/^{39}Ar$, Pb) and fluid inclusion data. *Miner. Deposita*, 40, 337-346.

Fiori M., Garbarino C., Padalino G. & Masi U. 1986. Chemical features of wallrocks from Mo-showings of Sardinia (Italy). *Rend. Soc. It. Mineral. Petrol.*, 41, 25-39.

Ishihara S. 1981. Granitoid series and mineralization. *Economic Geology*, 75th anniversary volume, 458-484.

Naitza S., Secchi F., Oggiano G. & Cuccuru S. 2015. A Late Variscan Sn province: the Arburese region (SW Sardinia, Italy). *Geophys. Res. Abs.*, 17, EGU2015-12248-1.

The complex task of inverting gravity data for the estimation of the depth to the carbonate basement

Fedi M. & La Manna M.*

Dipartimento di Scienze della Terra, dell'Ambiente e delle Risorse, Università di Napoli "Federico II".

Corresponding email: lamanna@unina.it

Keywords: Gravity method, carbonate basement, geothermal research.

The reconstruction of the top of the carbonate basement is very useful for the geothermal exploration. It is however an intricate task, reflecting all the complexity of the geological environment where the carbonate rocks are included. Geophysical methods can be applied to this aim, well integrating in large areas the geological and drilling information, which is instead typically of local nature. The gravity method is particularly suited to this end, since we may assume that carbonate rocks are typically denser than sediments. So, if we can make the simplified hypothesis that the gravity field is related to an interface of constant density contrast, we could reconstruct the top of the carbonate basement quite well.

Since, however, the measured field is the sum of different depth effects, the above condition may not occur; furthermore the density contrast may vary, even horizontally, so that a single interface is not the most appropriate hypothesis in complex cases.

To deal with this problem, we tested the splitting of the investigated region in subareas in each of which the "single interface" hypothesis can be considered reasonably valid. Then, we interpreted the vertical derivative of the field instead than the gravity field itself, in order to reduce the effects of the deep sources and to increase those of the shallow ones, so enhancing the contributes related to the top of the surface of the carbonate. As regards the estimate of the depth to the top in each area, the most traditional method is that assuming the density contrast and then solving for the depth to the interface (Peters, 1949). One more efficient method is using instead the information related to the available constraints in the area (e.g., log data). This method (Fedi, 1997) provides the reconstruction of the carbonate surface choosing at least two constraints linked to the depth (top and bottom of this surface) and does not require any a priori estimate of the density contrast.

One more problem is the type of gravity data to use, choosing between free-air or Bouguer anomalies. This choice depends strongly on the geological setting of the area. In practice, where the carbonate is very shallow and outcropping, free air gravimetric anomalies are preferred, giving a good and continuous surface estimation; nevertheless, the inversion must be split in two parts: the first is related to the outcropping basement, which has a very high density contrast, and the second to the underground deepening basement, which corresponds to a sensibly lesser density contrast. Where the carbonate are buried from dense rocks (i.e. marls and marly-clays, volcanic or others), as in the Campanian Plain, near Naples, Italy it is necessary to work with a Bouguer anomaly dataset, in which the effect of the reliefs, other than carbonates, is minimized.

Fedi M. 1997. Estimation of density, magnetization, and depth to source: A nonlinear and noniterative 3-D potential-field method, *Geophysics*, 62, 814-830.

Peters L.J. 1949. The direct approach to magnetic interpretation and its practical application. *Geophysics*, 14, 290-320.

Seismic, structural and geochemical prospections for characterization of a medium-enthalpy geothermal system within the Laga Basin (Central Italy): the Acquasanta Terme case study

Fusari A. *, Invernizzi C. & Carroll M.

Scuola di Scienze e Tecnologie - Sezione di Geologia, Università di Camerino

Corresponding email: alessandro.fusari@unicam.it

Keywords: Geothermal system, medium enthalpy, sedimentary basin.

The energetic supply is one of the most relevant problems the present world has to deal with. The increasing global population implies a high request of energy to answer the needs of the new economic system. Furthermore, decreasing in oil reserves requires all the efforts to find out new renewable resources and different innovative techniques for sustainable exploitation. Geothermal energy is one of the most promising renewable sources for the forthcoming future, due to its low environmental impact and its excellent sustainability, economically too.

The Tyrrhenian side of Italy is characterized by many high-enthalpy geothermal fields. The eastern side of the country has relatively normal thick deformed foredeep sequences and low heat flow. The thickness of the lithosphere ranges between 70 and 90 km. Acquasanta Terme is one of several thermal areas located on the Adriatic side in the central part of Italy. Within the Laga Basin, the hot springs discharge from folded calcareous rocks along the Tronto River valley. They have a maximum temperature of about 44 °C.

The aim of this study is to explain the mechanism responsible for the formation of this geothermal system. Our work included seismic, structural, chemical and isotopic investigations. Seismic data documented a complex tectonic framework. The Laga Basin is dominated by asymmetrical anticlines, like the Acquasanta structure, whose axis plunges northward. Thrust and back-thrust surfaces work as lateral boundaries for deep fluid circulation from South to North, and the WNW – ESE normal fault that cuts orthogonally across the central part of the structure may provide a pathway for the thermal fluids. Fractures related to compressive and extensional events are recognized. Then, a DFN model of the Calcare Massiccio reservoir was built and connectivity properties computed. Chemical data from thermal and cold waters collected every three months indicate the waters are sodium-chloride-sulphate in composition, with some differences and affected by seasonal variations. Changes in temperature, pH, conductivity and concentrations over time reveal three diverse types of water and circuits, as well as complex mixing relationships to the surface. Stable isotopes indicate a meteoric origin with the waters originating from elevations referable to the Laga Mountains. Tritium concentrations are low, indicating the thermal waters are more than 60 years old. Moreover, Sr isotope constrains at least one of the water paths to the Burano Anhydrites Fm, more than 3-km-deep. Geothermometers suggest maximum temperature of approximately 90 °C.

The Jibal Qutman deposit: first notes on a new gold discovery in the Arabian Shield (Kingdom of Saudi Arabia)

Granitzio F.¹, Naitza S.*², Oggiano G.³ & Secchi F.³

1. Kefi Minerals PLC, Jeddah, Saudi Arabia. 2. Dipartimento di Ingegneria Civile, Ambientale e Architettura, Università di Cagliari.
3. Dipartimento di Scienze della Natura e del Territorio, Università di Sassari.

Corresponding email: snaitza@unica.it

Keywords: Arabian shield, shear zone, orogenic gold deposit.

The Jibal Qutman gold deposit (Saudi Arabia) is located in the Asir Terrane (Arabian Shield), a composite Neoproterozoic terrane that includes volcanic, sedimentary and intrusive rocks. This terrane amalgamated between 780-640 Ma during the convergence of an oceanic domain interposed between the incoming east and west Gondwana (Johnson et al., 2011; Flowerdew et al., 2013). The Nabitah-Tathlith fault zone (NTFZ) separates island arc sequences metamorphosed under greenschist facies, in the west, from paragneiss and amphibolites of the Hajizah Gneiss Belt in the east. Along the NTFZ, a belt containing over 40 gold deposit occurs (Worl, 1979). Among them, Jibal Qutman (24°16'N and 45° 04'E), is hosted by lower greenschist metavolcanics and metasediments (Halaban group: 785 Ma). The first study of the area was performed by the USGS on behalf of the then Directorate General of Mineral Resources (Hackett, 1983). Recent exploration performed by Kefi Minerals PLC discovered seven Au mineralised zones in a 5 km long (N-S) and 1 km wide (E-W) area, with estimated 0.733 Moz of gold in indicated and inferred resources. Mineralisation zones are controlled by low-order structures subparallel to the NTFZ. Orebodies include veins, stockworks and disseminations, related to step dipping to low angle brittle to ductile shear zones marked by different stages of hydrothermal alteration and metasomatism. All mineralised zones show definite Au-Ag, Au-Te and (more locally) Au-Pb geochemical correlations; Au-Ag ratios range from 4:1 to 1:4 on average. The Main Zone orebody is a 900 m-long, N-S quartz vein system, with a single high-angle vein up to 4 m thick that, along strike, splits into multiple veins. The ore consists of pyrite and minor tetrahedrite, galena and sphalerite with coarse gold. Ore microscopy and SEM-EDS studies identified a close association between native gold (Au > 85%, Ag 10-15%, traces of Hg), tetrahedrite (Zn- and Ag-bearing), and Pb and Au tellurides (possible altaite and Hg-bearing calaverite). Pb tellurides are mostly present as thin rims around tetrahedrite and major gold grains, while Au tellurides occur with gold as small droplets within tetrahedrite. Milky to sugary quartz is the only gangue mineral. Jibal Qutman shows the features of a shear zone-hosted, mesothermal gold deposit. Different ore styles in the area derived from polyphasic mineralisation related to the ductile-brittle structural evolution of the NTFZ. From the marked Au-Te geochemical correlations, the Ag abundance, and the occurrence of tellurides with Sb- and Hg-bearing minerals, a mesozonal- to epizonal orogenic style of mineralisation (Groves et al., 1998) may be inferred.

- Flowerdew M.J., Whitehouse M.J. & Stoesser D.B. 2013 The Nabitah fault zone, Saudi Arabia: A Pan-African suture separating juvenile oceanic arcs. *Precam. Res.*, 239, 95-105, doi:10.1016/j.precamres.2013.08.004.
- Groves D.I., Goldfarb R.J., Gebre-Mariam M., Hagemann S.G. & Robert F. 1998. Orogenic gold deposits - a proposed classification in the context of their crustal distribution and relationship to other gold deposit types. *Ore Geol. Rev.*, 13, 7-27.
- Hackett D. 1983. The Aflaj oolitic hematite-goethite deposit: Saudi Arabian Directorate General of Mineral Resources, Jeddah. DGMR Open File Report 04-16.
- Johnson P.R., Andresen A., Collins A.S., Fowler A.R., Fritz H., Ghebreab W., Kusky T. & Stern R.J. 2011. Late Cryogenian-Ediacaran history of the Arabian-Nubian Shield: A review of depositional, plutonic, structural, and tectonic events in the closing stages of the northern East African Orogen. *J. African Earth Sci.*, 61, 167-232.
- Worl R.J. 1979. The Jabal Ishmas-Wadi Tathlith gold belt, Kingdom of Saudi Arabia. U.S. Geol. Surv. Open-File Rep. 79-1519, 108 p.

The mercury deposits of the Monte Amiata district: a review of existing data

Lattanzi P.*¹, Ruggieri G.², Benvenuti M.³, Costagliola P.³, Chiarantini L.³ & Rimondi L.²

1. Dipartimento di Scienze Chimiche e Geologiche, Università di Cagliari. 2. Istituto di Geoscienze e Georisorse, CNR, Firenze. 3. Dipartimento di Scienze della Terra, Università di Firenze.

Corresponding email: lattanzp@unica.it

Keywords: Monte Amiata, mercury, metallogeny.

The Mt. Amiata mining district (Southern Tuscany, Italy) is a world class Hg district, with a cumulate production of more than 100,000 tonnes of Hg, mostly occurring between 1870 and 1980. In spite of its importance, description of the most important deposits goes back to the 1970s, or earlier, and is mostly in Italian. Rimondi et al. (2015) recently reported a review of the existing data.

The Hg mineralization at Mt. Amiata is associated with late-Apenninic tectonic structures, and is hosted by a variety of rocks ranging in age from Triassic to Quaternary, belonging both to the Tuscan and Ligurian formations, as well as to the post-orogenic Neogene sediments, and young (0.3 Ma) volcanic rocks of the Mt. Amiata volcano. A typical locus of mineralization is the contact between a comparatively permeable formation (sandstone, limestone) and an impervious cover. Mineralogy is rather simple; cinnabar is the only economic mineral, and calcite the main gangue mineral. The limited fluid inclusion and isotopic data suggest that the mineralizing hydrothermal fluids were of low temperature (70 to 130 °C), low salinity (1-5 wt.% NaCl equivalent), and of essentially meteoric origin. Mineralization is believed to result from shallow hydrothermal systems similar to present-day geothermal fields of the region. There is likely a continuum of Hg deposition to present day, since Hg emission from geothermal power plants is on-going.

The Mt. Amiata deposits present some analogies with “hot-spring type” deposits of western USA, although an ore deposit model for the district is not established. Specifically, the source of Hg (mantle? underlying Palaeozoic schists?) remains highly speculative.

Rimondi V., Chiarantini L., Lattanzi P., Benvenuti M., Beutel M., Colica A., Costagliola P., Di Benedetto F., Gabbani G., Gray J.E., Pandeli E., Pattelli G., Paolieri M. & Ruggieri G. 2015. Metallogeny, exploitation and environmental impact of the Mt. Amiata mercury ore district (Southern Tuscany, Italy). *Ital. J. Geosci.*, 134, 323-336, doi:10.3301/IJG.2015.02.

Geological, hydrogeochemical and isotopic features of the thermal system between Montalcino and Monte Amiata-Scalo (South-eastern Tuscany)

Magi F.*¹, Pandeli E.¹⁻² & Vaselli O.¹⁻²

1. Dipartimento di Scienze della Terra, Università di Firenze. 2. Istituto di Geoscienze e Georisorse, C.N.R. Firenze.

Corresponding email: francesco.magi26@gmail.com

Keywords: Central Italy, Mt. Amiata geothermal area, water and stable isotope geochemistry.

The aim of this work was that to assess the presence of a hydrothermal system at depth inside the boundaries of the Geothermal Exploration Permit named “Ripa d’Orcia” (Mt. Amiata, central Italy).

The study area is located along the Montalcino-Seggiano Ridge and is characterized by large outcrops belonging to the Tuscan, Ligurian and Sub-Ligurian Units, Miocene lacustrine sediments (Velona Basin), Plio-Pleistocene marine and continental sediments and Pleistocene travertines (“Cave Porzia” quarries near Castelnuovo dell’Abate).

A detailed geological mapping (1:10,000) was carried out during which previous geological studies were revised. Particular attention was paid to the travertine deposits and the main stratigraphic and structural features. A geochemical (main and trace solutes) and isotopic (oxygen and hydrogen) survey on well and spring waters and dissolved gases was conducted. These samples were analyzed for chemical, isotopic and geothermometric analyses (silica and HCO₃-F-SO₄²⁻ geothermometers) to understand the origin of the fluids, the hydrogeological circulation and the temperatures of the geothermal *reservoir*.

All studied waters showed a relatively homogeneous chemical composition since most of them had a Ca-HCO₃ to Na-HCO₃ geochemical facies. Three water samples were characterized by temperatures of 35 and 37 °C and a relatively high concentrations of SO₄²⁻ (397 mg/L) and F⁻ (3.44 mg/L). Isotopic data ($\delta^{18}\text{O}$ and δD) suggested that the thermal system is recharged by meteoric water (mean values: $\delta^{18}\text{O} = -7\text{‰}$, $\delta\text{D} = -45\text{‰}$). Nevertheless, the carbon isotopes in CO₂ suggested the presence of a deep source ($\delta^{13}\text{C-CO}_2 = -6\text{‰}$). The geochemical features of the studied waters can mainly be related to water-interaction processes with CaCO₃ and Ca-SO₄-bearing sedimentary rocks at which a CO₂(H₂S)-rich gas phase is added. Mixing processes with shallow aquifers had likely masked the deep component as also suggested by the SiO₂ and HCO₃-F-SO₄²⁻ geothermometers, the latter likely providing the minimum equilibrium temperature of the thermal reservoir (80-85 °C).

Geological and geochemical-geothermometric data are apparently supporting the presence of a deep (> 1,000 m) geothermal *reservoir* located inside the Triassic-Mesozoic carbonate-evaporite successions of the Tuscan Sequence. The relatively high depth of the geothermal *reservoir* allowed us to hypothesize the existence of a *duplex* structure inside the Tuscan Nappe, at the level of the evaporitic Formation of Burano. Notwithstanding the minimum temperature of the thermal *reservoir*, a low-to-medium enthalpy system is likely hosted between Montalcino and Monte Amiata-Scalo and further investigations may provide useful information related to the aquifer volume and the use of the resource whenever the exploitation will take place.

Geochemical behavior of Rare earth elements in magmas

Maimaiti M.* & Carroll M.R.

Scuola di Scienze e Tecnologie - Sezione di Geologia, Università di Camerino.

Corresponding email: marziya.mamat@gmail.com

Keywords: Rare Earth Elements, monazite, solubility.

The rare earth elements (REE) are viewed as 'Green Metals' and used in every car, computer, smartphone, energy-efficient fluorescent lamp as well as in lasers, high-strength magnets, and more, but their global supply (~ 95%) is effectively restricted to several mining districts in China. Therefore, potential resources of REEs become more and more important, and demand is predicted to increase greatly in the next decade. The long-term growth of numerous industries will depend on the ability to secure stable and diverse sources of rare earths. In the frame of larger work aimed at studying geochemical behaviour of REE in different granitic magmas, the purpose of this project is to study the REE enriched minerals (Monazite) saturation and solubility in a series of synthetic silicate glasses of granitic compositions ranging from peralkaline to peraluminous. Initial experiments using a metaluminous granitic composition (HPG8; e.g., Holtz et al., 1992) under water saturated conditions at 780-850 °C, 200 MPa, yield results for La-Monazite and Ce-monazite largely consistent with those found by Montel (1993). Experiments currently in progress are aimed at investigating monazite saturation in peralkaline and peraluminous haplogranitic melts, as well as the potential influence of Fluorine on monazite saturation.

Holtz F., Behrens H., Dingwell D.B. & Taylor R.P. 1992. Water solubility in aluminosilicate melts of haplogranite composition at 2 kbar. *Chem. Geol.*, 96, 289-302.

Montel J.-M. 1993. A model for monazite/melt equilibrium and application to the generation of granitic magmas. *Chem. Geol.*, 110, 127-146.

Significant Zn isotope fractionation in the supergene environment from Yanque, Peru: implications for exploration

Mondillo N.*¹, Mathur R.² & Boni M.¹

1. Dipartimento di Scienze della Terra, dell'Ambiente e delle Risorse, Università di Napoli "Federico II".

2. Department of Geology, Juniata College, Huntingdon, USA.

Corresponding email: nicola.mondillo@unina.it

Keywords: Supergene Zn nonsulfide deposits, Zn stable isotopes, fractionation.

Low temperature water rock interaction has clearly shown potential for measurable Zn isotope fractionation. Currently, the majority of Zn isotope studies have focused on higher temperature (>80 °C) ores and how these isotopes can trace contamination (Zhou et al., 2014, and references therein), with little attention how Zn isotopes behave in supergene economically significant deposits. This study presents Zn isotope compositions of Zn ores from Yanque (Peru); a deposit that resulted from weathering, transport and enrichment of zinc during supergene alteration (Mondillo et al., 2014). The Yanque primary sulfides, considered a magmatic-related polymetallic concentration, have been totally oxidized, and the economic concentrations in the deposit consist of supergene Zn(Pb) nonsulfide minerals (sauconite, hemimorphite, smithsonite and cerussite), mostly contained in siliciclastic conglomerates. Isotope ratios are reported in the delta notation:

$$\delta^{66}\text{Zn} \text{‰} = \left\{ \left[\frac{(^{66}\text{Zn}/^{64}\text{Zn})_{\text{sample}}}{(^{66}\text{Zn}/^{64}\text{Zn})_{\text{IRMM 3702}}} \right] - 1 \right\} * 1000.$$

The $\delta^{66}\text{Zn}$ of the Zn rich ores varies from 1.16 to 3.81‰. No direct relationship exists with the isotope ratios and grades of Zn and Pb. In plan view, the contour plot of the data forms a bull-eye pattern of higher $\delta^{66}\text{Zn}$ values centered on the deposit and lower $\delta^{66}\text{Zn}$ values emanating around towards the periphery of the deposit. In the cross sectional views, higher $\delta^{66}\text{Zn}$ values occur closer to the surface with lower $\delta^{66}\text{Zn}$ occurring at depth.

The $\delta^{66}\text{Zn}$ of the ores measured in the Yanque deposit are distinctly different from all other $\delta^{66}\text{Zn}$ measurements carried out on sphalerite and taken from the literature (Zhou et al., 2014). Specifically, from a comparison of $\delta^{66}\text{Zn}$ between higher temperature and supergene ores, it appears that the isotope compositions of the supergene minerals are higher than in the high temperature ones. The shift to higher Zn isotope values in ores related to oxidation and transport of Zn could be due to the oxidation of sphalerite, which would lead to solutions that have higher isotopic compositions than sphalerite. This pattern mimics the behavior of the copper isotope compositions in supergene ores (Mathur et al., 2012).

Our analyses point out also that this is the largest measured Zn fractionation in natural materials to date.

Mathur R., Ruiz J., Casselman M.J., Megaw P. & van Egmond R. 2012. Use of Cu isotopes to distinguish primary and secondary Cu mineralization in the Canariaco Norte porphyry copper deposit, northern Peru. *Miner Deposita*, 47, 755-762.

Mondillo N., Boni M., Balassone G. & Villa I.M. 2014. The Yanque prospect (Peru): from polymetallic Zn-Pb mineralization to a Nonsulfide deposit. *Econom. Geol.*, 109, 1735-1762.

Zhou J.-X., Huang Z.-L., Zhou M.-F., Zhu X.-K. & Muecher P. 2014. Zinc, sulfur and lead isotopic variations in carbonate-hosted Pb-Zn sulfide deposits, southwest China. *Ore Geol. Rev.*, 58, 41-54.

A multidisciplinary approach to unravel the geothermal fluid circulation within a – regional scale- carbonate reservoir

Montanari D.*, Minissale A., Doveri M., Trumpy E., Gola G. & Manzella A.

Istituto di Geoscienze e Georisorse, C.N.R. Pisa.

Corresponding email: domenico.montanari@igg.cnr.it

Keywords: Geothermal energy, carbonate reservoir, temperature distribution.

With the exception of volcanic areas where geothermal reservoirs are generally developed within permeable volcanic horizons, deep carbonate aquifers host probably the most important world geothermal resources. Although some cases of exploitation of this carbonate reservoirs are already effective both for electric power generation and district heating, it is not yet clear how, on a regional scale, geothermal fluids circulate, determining the temperature distribution at depth. In our vision, Western Sicily could represent a key area to better define how fluids circulate within this kind of reservoirs. We present a review of geochemical, geological and geophysical data, mainly acquired from wells drilled during the oil exploration since the 50s, specifically reread for geothermal purposes, has allowed to understand the western Sicily geothermal system (Fancelli et al. 1991; Montanari et al. 2015; Trumpy et al. 2015) and to reconstruct the modalities and peculiarities of deep fluids circulation within the regional carbonate reservoir. Being the carbonate reservoir as thick as several km, it is affected by the upward of rising CO₂-rich convective deep thermal waters, at several places even with marked ³He/⁴He anomalies, such as in the area of Sciacca, where high-enthalpy systems at relatively shallow depth are possibly located off shore in the Sicily channel. In the remaining areas several structural highs of the carbonates, buried by impermeable flysch units and Neogene clay-rich sediments, likely host fluids with temperatures up to 100 °C at relatively shallow depths, locally affected by convective fluid circulation. The proposed reconstruction of geothermal fluids circulation on a regional scale could be taken as exemplificative of the general behavior of low-to-medium enthalpy geothermal systems hosted in carbonate units that, due to the recent technological developments of binary plants, have become more profitable, not only for direct uses but even for power production.

Fancelli R., Monteleone S., Nuti S., Pipitone G., Rini S. & Taffi L. 1991. Nuove conoscenze idrogeologiche e geotermiche nella Sicilia occidentale. *Geol. appl. idrogeol.*, 24.

Montanari D., Albanese C., Catalano R., Contino A., Fedi M., Gola G., Iorio M., La Manna M., Monteleone S., Trumpy E., Valenti V. & Manzella A. 2015. Contour map of the top of the regional geothermal reservoir of Sicily (Italy). *J. Maps*, 11, 13-24.

Trumpy E., Donato A., Gianelli G., Gola G., Minissale A., Montanari D., Santilano A. & Manzella A. 2015. Data Integration and favourability maps for exploring geothermal systems in Sicily, southern Italy. *Geothermics*, 56, 1-16.

Does subduction polarity control metallogeny?

Nimis P.* & Omenetto P.

Dipartimento di Geoscienze, Università di Padova.

Corresponding email: paolo.nimis@unipd.it

Keywords: Metallogeny, subduction, polarity.

The distribution of economically relevant ore deposits in different sectors of the circum-Mediterranean realm that have been affected by subduction processes since the Cretaceous shows systematic variations in space and time (Nimis & Omenetto 2015). Sectors involved in W-directed subduction (Sardinia, Apennines-Maghrebides, Internal Betics, Tyrrhenian, Western-Eastern Carpathians) show a predominance of epithermal (\pm VMS) deposits, mostly characterized by relatively low sulfidation (LS) state. Orogens formed by NE-directed subduction (Dinarides-Hellenides-Pontides-Anatolides-Taurides; DHPAT) were initially dominated by Andean-type pluton-related porphyry-skarn-high-sulfidation (HS) epithermal associations. These distinct metallogenic styles show similarities with those observed in circum-Pacific belts (Mitchell & Garson, 1981) and can be related to the systematic tectono-magmatic asymmetry of E-NE- and W-directed subduction systems (cf. Doglioni, 1990; Doglioni et al. 1999). We suggest that, on a global scale, subduction polarity may exert a significant first-order control on ore potential by creating the most favorable milieu for specific deposit types. Widespread extension, low relief and the occurrence of reduced magmas, which are typical of W-directed, eastward-retreating subduction zones, are all positive factors for the emplacement and preservation of LS epithermal and VMS deposits. Compressional regimes and crustal thickening, which are typical of E-NE-directed subduction zones, are the most suitable pre-conditions for the emplacement of large, shallow-level, oxidized plutons and of related intrusion-centered porphyry-HS-skarn systems. Exceptions to this simple pattern do occur, however, and are interpreted to be due to second-order geological factors such as superimposition of contrasting subduction trends and inheritance from earlier metallogenic stages (e.g. Apuseni) or interference of subduction processes with subduction-unrelated extension (e.g. Cenozoic Hellenides-West Anatolia).

Doglioni C. 1990. The global tectonic pattern. *J. Geodyn.*, 12, 21-38.

Doglioni C., Harabaglia P., Merlini S., Mongelli F., Peccerillo A. & Piromallo C. 1999. Orogens and slabs vs their direction of subduction. *Earth-Sci. Rev.*, 45, 167-208.

Mitchell A.H.G. & Garson M.S. 1981. *Mineral Deposits and Global Tectonic Settings*. Academic Press, London.

Nimis P. & Omenetto P. 2015. Does subduction polarity control metallogeny? *Terra Nova*, 27, 139-146.

The magnetic method applied to the exploration of porphyry-cu deposits: the case of the Dolores Prospect (Peru)

Pastore Z., Mondillo N.*, Boni M. & Fedi M.

Dipartimento di Scienze della Terra, dell' Ambiente e delle Risorse, Università di Napoli "Federico II".

Corresponding email: nicola.mondillo@unina.it

Keywords: Porphyry-Cu deposits, magnetic method, demagnetization.

The Dolores Cu prospect is located in southern Peru, about 90 km south of the city of Cuzco (Mondillo et al., 2014). We have defined the Dolores porphyry-Cu mineralization by processing magnetometric data, and assessing the results on the basis of the geologic characteristics of the area, as well as on the data from a previous geophysical and soil geochemistry survey.

The geomagnetic total field map shows anomalies that have the typical shape for anomalies at geomagnetic equatorial areas. To get a better location of the source, we calculated the total gradient intensity map, which has the maxima in correspondence of the anomaly sources. These data were compared with the spectrometric data (K, and K/Th), and with the soil geochemistry results. In order to obtain a quantitative estimation of the depth of the magnetic sources, we used the DEXP method (Fedi, 2007).

Comparing the total gradient intensity map with the spectrometric K, and K/Th maps, with soil geochemistry data and with the geology of the area, we noticed a good correspondence between the maxima of the total gradient intensity and the position of the magmatic rocks observed in the field (which represent the main magnetic sources in the area). We were also able to recognize: i) a maximum of the total gradient in correspondence of the sedimentary rocks adjacent to the porphyry; and ii) a minimum of the total gradient in correspondence of the igneous rocks hosting the Cu mineralization. The first situation is probably related to intrusive bodies below the sedimentary rocks. The other characteristic is very important, because it clearly evidences a demagnetization of the Dolores igneous rocks, associated with the hydrothermal alteration related to the Cu sulfide emplacement.

By using the DEXP method, we determined the depths of the subcropping igneous rocks below the sedimentary cover, which resulted to be relatively shallow (15 to 30 m) in some areas, and deeper in others (ca. 300 m).

In conclusion, this study indicates that the Dolores porphyry-Cu deposit is associated with demagnetized igneous rocks, as observed also for other porphyry Cu deposits (Anderson et al., 2013). Thus, when conducting a geophysical exploration for porphyry-Cu ores, it could be useful to keep in mind the potential occurrence of this type of imprint.

Anderson E.D., Hitzman M.W., Monecke T., Bedrosian P.A., Shah A.K. & Kelley K.D. 2013. Geological analysis of aeromagnetic data from southwestern Alaska: implications for exploration in the area of the Pebble porphyry Cu-Au-Mo deposit. *Econ. Geol.*, 108, 421-436.

Fedi M. 2007. DEXP: A fast method to determine the depth and the structural index of potential fields sources. *Geophysics*, 72, I1-I11.

Mondillo N., Boni M., Balassone G. & Villa I.M. 2014. The Yanque Prospect (Peru): from polymetallic Zn-Pb mineralization to a Nonsulfide deposit. *Econ. Geol.*, 109, 1735-1762.

Investigating fossil geothermal systems: the case of Elba Island (Tuscany, Italy)

Rimondi V.*¹, Fregola R.A.², Ruggieri G.¹, Zucchi M.², Chiarantini L.¹, Orlando A.¹, Brogi A.² & Liotta D.²

1. Istituto di Geoscienze e Georisorse, CNR Firenze.

2. Dipartimento di Scienze della Terra e Geoambientali, Università di Bari.

Corresponding email: valentina.rimondi@unifi.it

Keywords: Elba Island, geothermal systems, fluid inclusions study.

In Eastern Elba Island, the Porto Azzurro granitoid (5.9 Ma) intruded in the mid-crust gave rise to a widespread boron-rich contact metamorphic aureole, intense hydrothermal circulation, and Fe-deposits. At Cala Stagnone (Calamita Peninsula), tourmaline-bearing metasomatic bodies, and a complex quartz-tourmaline hydrothermal system, are now exposed at surface, and evaluated as a possible exposed analogue of the deepest part of the present-day Larderello-Travale geothermal fields. The hydrothermal Fe-deposits of the Rio Marina and Porto Azzurro areas (Valle Giove, Bacino, Topinetti, Terra Nera) can be indeed considered the expression of a paleo-geothermal reservoir developed at the depth of the present-day main reservoir at Larderello-Travale geothermal fields.

As part of the EU FP7-funded Integrated Methods for Advanced Geothermal Exploration (IMAGE) project, fluid inclusions (FIs) were studied in quartz-tourmaline veins at Cala Stagnone and in hydrothermal quartz, adularia and calcite from Fe-deposits of Rio Marina and Porto Azzurro areas to derive: i) the characteristics of fluids circulating in a paleo-geothermal system similar to the Larderello-Travale ones, ii) the P-T conditions of the system, and iii) the reactions occurred between the host rocks and fluids.

FIs were studied by optical microscopy and microthermometry. SEM-EDS and Raman spectroscopy were employed as complementary techniques.

FIs were distinguished on the base of phase assemblage at room temperature, and on the homogenization mode: 1) S-type, or polyfasic with 1-4 daughter minerals; 2) L-type, homogenizing in the liquid phase; 3) V-type, homogenizing in the vapor phase.

Specifically, at Stagnone we found: a) hypersaline S-type FIs (37-48 wt.% NaCl eq.) with high total Th (400-600 °C); and b) saline L- and V-type FIs (15-30 wt.% NaCl eq.) with moderate to high Th (up to 600 °C).

At Rio Marina and Porto Azzurro areas, FIs are mainly of L-type and sporadically of S-type, and registered fluid with both variable Th and salinity values (up to ca. 400 °C; <34 wt.% NaCl eq.).

At Stagnone, the hypersaline FIs record the circulation of magmatic derived fluids; the rather high Th and salinity of the saline FIs also suggest that this fluid is, at least in part, of magmatic derivation. The few L inclusions showing lower Th and salinity can record the presence of a partly meteoric-derived fluid in the geothermal system.

On the other hand, FIs in hydrothermal Fe-deposits of Rio Marina and Porto Azzurro areas record the contemporaneous circulation and mixing of a low-salinity fluid of probable meteoric origin and saline fluid, sometimes halite-saturated at room temperature. The saline fluid can be a magmatic derived fluid (similar to that recorded by S-type at Stagnone) that undergone cooling and dilution before entering in the hydrothermal systems of Fe-mineralization or a fluid that interacted with evaporitic levels of the Tuscan Nappe.

3D geological, thermo-physical and rheological modelling for geothermal exploration: the case study of Ischia Island, Southern Italy

Santilano A.*¹, Gola G.¹, Castaldo R.², De Novellis V.², Pepe S.², Tizzani P.², Donato A.¹,
Trumpy E.¹, Botteghi S.¹ & Manzella A.¹

1. Istituto di Geoscienze e Georisorse, C.N.R. Pisa. 2. Istituto per il Rilevamento Elettromagnetico dell'Ambiente, C.N.R. Napoli.

Corresponding email: alessandro.santilano@igg.cnr.it

Keywords: 3D numerical modelling, rheology, geothermal energy.

In the frame of the “Geothermal Atlas for Southern Italy” Project, a detailed 3D geological, thermal and rheological model of Ischia Island was built by integrating geological, geophysical and geochemical data.

A critical review of publicly available data allowed us to organize a complete dataset in Petrel (Schlumberger) environment for the 3D geological modelling. The geological maps, well data and several geophysical data were used to constrain the shallow region of the model from the youngest deposits to the tuff rocks of the St. Nicola Synthem and the deposits of Ancient Ischia (for detail on stratigraphy see, Ispra web site 2015). Seismic data were used to constrain the deeper level of the Ischia Island up to the Meso-Cenozoic Carbonate rocks (Finetti & Morelli, 1974). Moreover, in order to implement the thermal and rheological analysis, we modeled the deeper surfaces of crystalline basement and Mohorovičić discontinuity based on previous studies in literature.

In the second step, we performed a 3D numerical modelling of thermal field by using the a priori geological and geophysical information and by consideration of thermo-hydraulic properties including internal heat production and mechanical heterogeneities of the crust beneath the volcanic island. We solved, in a numerical context, the heat and fluid transport equation in a conductive/convective steady-state regime. We simulated the effects on the thermal field of a laccolith intrusion at shallow level in the crust (Paoletti et al., 2009). Subsequently, a parameters optimization procedure was applied to minimize the difference between the computed and measured temperature data.

Finally, the thermal model was used as a priori information to image the 3D rheological stratification of the shallow crust beneath the volcanic Island of Ischia in order to understand the mechanical behavior of the crust in this area.

As result of our study, we proposed the 3D geometry of the Brittle/Ductile transition, calculated numerically, for the active volcano of Ischia Island. The thermal field in the geothermal reservoir has also been figured out.

Finetti I. & Morelli C. 1974. Esplorazione sismica a riflessione dei golfi di Napoli e Pozzuoli. Boll. Geof. Teor. Appl, XVI, 62-63, 175-222.

Ispra web site, Geological map of Italy at scale 1:50.000, sheet 464, Isola d'Ischia. Last accessed April 2015. http://www.isprambiente.gov.it/Media/carg/464_ISOLA_DISCHIA/Foglio.html

Paoletti V., Di Maio R., Cella F., Florio G., Motschka K., Roberti N., Secomandi M., Supper R., Fedi M. & Rapolla A. 2009. The Ischia volcanic island (Southern Italy): Inferences from potential field data interpretation. J. Volcanol. Geotherm. Res., 179, 69-86.

The use of QEMSCAN® automated mineralogy in exploration for supergene Zn(Pb) nonsulfides characterization: a few examples

Santoro L.*¹ & Boni M.²

1. Natural History Museum, London, UK. 2. Dipartimento Scienze della Terra, dell'Ambiente e delle Risorse, Università di Napoli "Federico II".

Corresponding email: L.Santoro@nhm.ac.uk

Keywords: Zn(Pb)-nonsulfide, QEMSCAN, Automated-Mineralogy.

Supergene Zn(Pb) nonsulfide deposits consist of Zn/Pb-carbonates, Zn-(hydro)silicates, Fe-hydroxides, Zn-clays, minor Fe/Pb-sulfates and Zn/Pb-phosphates, commonly associated with remnants of sulfides. Their mineralogy is complex to characterize. However, since most nonsulfide ores are amenable to be treated by hydrometallurgy, an incorrect evaluation of the modal distribution, or of the relations between ore and gangue minerals could lead to an increase in the production costs, or drive the exploration and the choice of processing route in erroneous directions. In order to improve the accuracy of nonsulfide ores characterization, QEMSCAN® analyses have been carried out on three deposits with different grades of mineralogical complexity: Hakkari (Turkey), Jabali (Yemen), Reef Ridge (Alaska). The results have been compared to those obtained using traditional methods (i.e. OM, CL, SEM-EDS, WDS), to define the advantages and limitations of automated mineralogy techniques on nonsulfide ores.

The analyses have been performed in the field scan analytical mode, which can provide: statistical information on the particles, grain sizes, mineral association and quantitative evaluation for each sample. The building of a mineral list (SIP file) was necessary to classify the mineral compounds on the basis of the chemistry. The results have been compared with previous mineralogical studies of the same deposits.

QEMSCAN® was able to accurately characterize and quantify the economic (smithsonite and hemimorphite), as well as the gangue minerals (calcite, dolomite, Fe-[hydr]oxides), and other phases (sphalerite, galena, cerussite/anglesite) occurring in the deposits. QEMSCAN® was also a powerful tool for the detection and quantification of mixed and amorphous phases (Zn-dolomite, Mg-smithsonite, Zn-Fe-[hydr]oxides), and trace minerals (chlorargyrite, acanthite etc.), which were not quantified by previous studies. Several mineral maps added important information on the minerals distribution throughout the samples, and have been very useful to understand the mineral distribution in the three deposits, to be used for exploration.

However, SEM-EDS analyses were necessary to resolve several issues, as the difficulty to discriminate between minerals with similar spectra, as in the case of smithsonite/ hydrozincite/zincite and hemimorphite/willemite, due to the 1000 counts per spectra used in QEMSCAN® analyses. Other issues were: the distinction between cerussite and anglesite, owing to the X-ray interference of S-K α and Pb M α , which causes an overlap of the Pb and S peaks; the possible misidentification of minerals characterized by large chemical variability and/or smaller than the beam size excitation volume (i.e. clays), or smaller than the resolution (10 μ m) used for routine analyses.

A geochemical conceptual model for the hydrothermal system of the Domuyo volcanic complex (Argentina)

Tempesti L.*¹, Tassi F.¹⁻², Caselli A.³, Liccioli C.³, Vaselli O.¹⁻², Chiodini G.⁴, Augusto M.⁵ & Caliro S.⁶

1. Dipartimento di Scienze della Terra, Università di Firenze. 2. Istituto di Geoscienze e Georisorse, C.N.R. Firenze
3. Instituto de Paleobiología y Geología, Universidad Nacional Rio Negro, Argentina. 4. Istituto Nazionale di Geofisica e Vulcanologia, Bologna.
5. IDEAN-GESVA, Departamento de Ciencias Geológicas, FCEN, Universidad de Buenos Aires, Argentina.
6. Istituto Nazionale di Geofisica e Vulcanologia, Osservatorio Vesuviano, Napoli.

Corresponding email: tempestilorenzo@gmail.com

Keywords: Geothermal fluid, geochemical conceptual model, Domuyo volcano.

In March 2014, an international team involving researchers from Argentina and Italy carried out geochemical survey in the western portion of Domuyo, a volcanic complex of the southern volcanic zone (SVZ) in the province of Neuquen (Argentina). The aim was to collect gas and water samples from the natural discharges for chemical and isotopic analysis to construct a geochemical conceptual model of this hydrothermal system. Last volcanic activity dates back to late Pleistocene and consisted of dacitic and rhyolitic dome extrusions. In February 2003, two phreatic explosions occurred at El Humazo (Mas et al., 2009), one of the main thermal emissions in the western part of the volcanic complex that consist of hot springs and steam jet-like emissions. Most waters show the typical feature of mature fluids, indicating the occurrence of a geothermal brine able to reach the surface at several sites whose location is controlled by local and regional tectonic lineaments. Temperature estimations carried out using geothermometers based on water chemistry (quartz and Na-K-Mg) suggest that the deep reservoir is at up 250 °C, confirming the preliminary indications provided by compositional data on samples collected during a previous survey (Chiodini et al., 2014). Gas geothermometry in the H₂O-CO₂-CH₄-H₂-CO and C₃H₈-C₃H₆ systems highlighted the occurrence of a significant thermal and redox stratification within the hydrothermal reservoir, likely caused by addition from depth of hot, oxidizing fluids having a magmatic origin. The relatively high helium isotopic ratio shown by the fumarole located near the top of the volcanic apparatus (R/Ra = 6.8) confirms this hypothesis. At lower altitudes, where geothermal waters are discharges, a significant contribution of crustal helium masks the mantle isotopic signature. Deep gases feeding these peripheral discharges interacts with a shallow aquifer whose boiling cause a strong air contamination. These geochemical results highlight the huge geothermal resource hosted in this volcanic complex, and claim for an improved definition of the system through geophysical and geostructural investigations.

Chiodini G., Liccioli C., Vaselli O., Calabrese S., Tassi F., Caliro S., Caselli A.T., Augusto M. & D'Alessandro W. 2013. The Domuyo volcanic system: An enormous geothermal resource in Argentine Patagonia. *J. Volc. Geoth. Res.*, 274, 71-77.

Mas G.R., Bengochea L., Mas L.C. & López N. 2009. Hydrothermal explosion due to seal effect in El Humazo geothermal manifestation, Domuyo Vn., Neuquén, Argentina. *Proceedings 32nd Workshop on Geothermal Reservoir Engineering*, Stanford, CA, 5 pp.

Geothermal data integration and favourability maps: a tool for discovering geothermal systems in Sicily, southern Italy

Trumpy E.*, Botteghi S., Caiozzi F., Donato A., Gianelli G., Gola G., Minissale A., Montanari D., Santilano A. & Manzella A.

Istituto di Geoscienze e Georisorse, C.N.R. Pisa.

Corresponding email: e.trumpy@igg.cnr.it

Keywords: Sicily, geothermal energy, GIS Model.

A key requirement for a further production of geothermal energy, by increasing the number of projects as well as the variety of uses, is to clearly identify and rank resources and opportunities.

In this work we provide a practical analytical framework for the systematic capture of information relevant to the assessment of the geothermal resources of Sicily (mainland).

Any geothermal assessment necessitates an extensive search of the existing data. In Italy the most relevant existing information regarding the geothermal resources includes temperature data measured in oil and gas exploration boreholes and physical and chemical data from wells and natural thermal springs.

The data analysed in this study are those gathered in the 1980s by an inventory of the geothermal resources of Italy, which was organized in the National Geothermal Database (Barbier et al., 2000) and is available online (IGG-CNR 2012).

In the frame of the GEOTHERMAL ATLAS OF SOUTHERN ITALY Project, we organized and integrated a subsurface data set, and we provided a methodology to establish a hierarchy of the geothermal areas based on their potential for conventional power production. In particular, we deal with exploitation of moderate to high-enthalpy geothermal resources.

Our fully integrated analysis classified the hydrothermal resources hosted by regional reservoirs suitable for power production and was applied to Sicily (Montanari et al., 2014). Besides the geological and thermal data, the parameters used are: i) the unconventional new parameter “effective reservoir” (based on temperature constrain), ii) the permeability indication and iii) the geochemical favourability.

These parameters have been integrated by Geographic Information System (GIS) models. The result is a geothermal favourability map of Sicily where locations are ranked in five classes from “very low” to “very high”. Our tool is highly flexible: with a simple reclassification it can show future scenarios taking into account new technologies and possibly lower costs.

Besides contributing to reduced exploration risk, we have made the first step towards a more detailed and systematic resource reporting system in Italy. A reporting method is the basis for the portfolio management of geothermal resources and the selection of specific locations for geothermal power production projects.

Barbier E., Bellani, S. & Musmeci F. 2000. The Italian geothermal database. Proceedings of the World Geothermal Congress, 28 May-10 June, Kyushu-Tohoku, Japan.

IGG-CNR. 2012. The Geothopica Web application based on the Italian National Geothermal Database. Accessed May 2015. URL: <http://geothopica.igg.cnr.it>.

Montanari D., Albanese C., Catalano R., Contino A., Fedi M., Gola G., Iorio M., La Manna M., Monteleone S., Trumpy E., Valenti V. & Manzella A. 2015. Contour map of the top of the regional geothermal reservoir of Sicily (Italy). *J. Maps*, 11, 13-24.

Campiglia Marittima skarn deposit: shifting paradigm from exoskarn to reverse telescoping

Vezzoni S.*¹, Dini A.² & Rocchi S.¹

1. Dipartimento di Scienze della Terra, Università di Pisa. 2. Istituto di Geoscienze e Georisorse, CNR, Pisa.

Corresponding email: vezzoni@dst.unipi.it

Keywords: Reverse telescoping, Campiglia Marittima, skarn.

The Campiglia Marittima Fe-Cu-Zn-Pb(-Ag) skarn deposit has long been regarded as a reference example of exoskarn, whose formation started with the emplacement of the causative igneous rock (a mafic porphyry) that triggered the progressive replacement of marbles by skarn and the following deposition of sulfides. The skarn was described as having an outward symmetric mineralogical zoning with respect to the axial mafic porphyry dyke, for both skarn silicates and ore minerals.

Detailed field and underground mapping, integrated with petrographic, mineralogical and geochemical-isotopic data at Campiglia Marittima argue for significant departure from this “normal” evolution of a skarn deposit. In detail, at Campiglia the mafic magma did emplace after skarn formation and triggered the overprinting of a proximal-type high-temperature Fe-Cu sulfide ore onto a previously formed distal-type lower-temperature Zn-Pb skarn deposit. The addition of Fe-Cu, as well as the local remobilization of earlier Zn-Pb ores, led to the formation of a mixed Cu-Zn-Pb(-Ag) ore, as documented by field observations, skarn-ore textural observations, drill core chemical data and bulk-ore grade. Lead isotope data for minerals from the three main ore types lend support to this scenario and shed light on the origin of fluids.

In summary, Campiglia Marittima skarn deposit cannot be anymore considered as a reference example for proximal exoskarn deposits. It is rather a prominent example of distal Zn-Pb(-Ag) skarns that experienced a telescoping process, yet in a reverse way. Such a reverse telescoping process could have been at work wherever late Cu-bearing paragenesis are observed to overprint previously formed Zn-Pb ores, e.g., Madan ore deposit (Bulgaria), Kamioka ore deposit (Japan), Nikolaevsky mining area (Russia).

SESSION S19

Global pollutants: from mercury to POPs

CONVENORS

Stefano Covelli (Univ. Trieste)

Franco Tassi (Univ. Firenze)

Total gaseous mercury concentrations and lichens bioaccumulation in the Northern Adriatic coastal area (Gulf of Trieste, Italy)

Acquavita A.*, Pasquon M., Skert N., Tamberlich F. & Mattassi G.

ARPA FVG, Palmanova.

Corresponding email: alessandro.acquavita@arpa.fvg.it

Keywords: Gaseous elemental mercury, bioaccumulation, Marano and Grado Lagoon.

The Marano and Grado Lagoon (NE Italy) was affected by mercury (Hg) contamination from both historical mining in Idrija (Slovenia) and recent chlor-alkali plant activities in Torviscosa (Acquavita et al., 2012; Covelli, 2012). As a consequence, both sediments and soils of the area display a high degree of contamination. In spite of the previous studies conducted in the area, there is still a lack of knowledge for gaseous elemental mercury (GEM) form, which is primarily involved in inhalation risk for the local inhabitants. In this study a GEM survey and the degree of THg bioaccumulation in epiphytic lichen (*Xanthoria parietina*) were investigated at 13 selected sites. After lichens collection THg was determined following US-EPA method 7473 (DMA Milestone Mercury Analyzer). For GEM monitoring the LUMEX RA-915+ portable analyzer, which has been used in a large number of surveys worldwide, was employed. *X. parietina* showed a restricted range of THg levels (0.05 to 0.15 mg kg⁻¹ d.w.) comparable to those reported for typical uncontaminated areas: these could represent the background levels for the area (Cuny et al., 2004). On the other hand, hot spots were found in the nearby of the chlor-alkali plant and at the Grado seaside (0.40 mg kg⁻¹). GEM field surveys were carried out monthly with different integrating time intervals. The levels recorded were mostly below 10 ng m⁻³ (median = 3.10 ± 0.12 ng m⁻³) with several values below the detection limit (2.00 ng m⁻³). Taking into consideration the seasonal variability the highest values were recorded in summer (5.15 ± 5.71 ng m⁻³), although these were not statistically significant. During summer sand temperatures raise up to 70 °C, but no significant relationship was found between GEM and temperature, thus suggesting that Hg soil species are strongly bound to matrix (mostly in cinnabar form). Moreover, a pivotal role in prompt GEM dispersion is probably due to the action of winds. On the overall, the values found are comparable to some pristine areas investigated worldwide. The data obtained in our surveys are more than one order of magnitude lower than the suggested WHO thresholds, thus a risk for the local inhabitants is not expected.

- Acquavita A., Covelli S., Emili A., Berto D., Faganeli J., Giani M., Horvat M., Koron N. & Rampazzo F. 2012. Mercury in the sediments of the Marano and Grado Lagoon (Northern Adriatic Sea): sources, distribution and speciation. *Estuar. Coast Shelf. Sci.*, 13, 20-31.
- Covelli S. 2012. The MIRACLE Project: An integrated approach to understanding biogeochemical cycling of mercury and its relationship with lagoon clam farming. *Estuar. Coast Shelf Sci.*, 113, 1-6.
- Cuny D., Davranche L., Thomas P., Kempa M. & Van Haluwyn C. 2004. Spatial and temporal variations of trace element contents in *Xanthoria parietina* Thalli collected in a highly industrialized area in Northern France as an element for a future epidemiological study. *J. Atmos. Chem.*, 49, 391-401.

The role of Earth degassing in the global atmospheric mercury budget

Bagnato E.*¹, Sprovieri M.¹, Barra M.², Cardellini C.³ & Tamburello G.⁴

1. Istituto per l'Ambiente Marino Costiero, CNR, Capo Granitola (TP). 2. Istituto per l'Ambiente Marino Costiero, CNR, Napoli. 3. Dipartimento di Fisica e Geologia, Università di Perugia. 4. Dipartimento di Scienze della Terra e del Mare (DiSTeM), Università di Palermo.

Corresponding email: emu.bagnato@gmail.com

Keywords: Volcanogenic mercury, Earth degassing, global pollutant.

In the last decades, particular emphasis has been addressed to the study of mercury (Hg) from Earth degassing, in light of its high toxicity, long-range atmospheric transport and its tendency to bio-accumulate in aquatic ecosystems through methylation processes. All of these features have motivated intensive research on Hg within the framework of a pollutant of global concern. In order to better understand the role of Earth degassing in the global Hg budget, a number of field campaigns were carried out to evaluate the Hg/SO₂ and Hg/CO₂ ratios in volcanic/hydrothermal gases needed in estimating Hg fluxes in the atmosphere. Real-time measurements of SO₂, H₂S, H₂O and CO₂ were carried out in parallel with Hg collection within the emissions from open-conduit vents, fumaroles and soil diffuse degassing, supporting the role of early CO₂ escape from magmas as a carrier gas for Hg. Concentrations of gaseous Hg elevated above background levels were observed on most occasions. Based on our dataset, we propose that an average Hg/SO₂ plume mass ratio of about 7.8×10^{-6} ($\pm 1.5 \times 10^{-6}$; $n_{\text{volcanoes}} = 13$) is best representative of open-conduit quiescent degassing. Taking into account the uncertainty in global SO₂ emissions, we infer a global volcanic Hg flux from persistent degassing of about 76 ± 30 t yr⁻¹. These data suggest that open-conduit volcanoes in a state of passive degassing represent an important contribution to the global volcanic Hg emissions into the atmosphere. It is therefore likely that volcanic contributions to the global atmospheric Hg budget will be even more important during large eruptive events. Conversely, based on our dataset and previous works, we propose that an average GEM/CO₂ molar ratio of $\sim 2 \times 10^{-8}$ is best representative of hydrothermal degassing. Taking into account the uncertainty in global hydrothermal CO₂ emissions from sub-aerial environments ($\sim 10^{12}$ Mol yr⁻¹; Seward & Kerrick, 1996), we infer a global volcanic Hg flux from hydrothermal environments of \sim about 8.5 t yr⁻¹. Our calculations here suggest that hydrothermal contribution to the global volcanic non-eruptive Hg is small if compared to persistently degassing open-vent volcanoes, which dominate the global volcanic Hg budget. This minor contribution mainly reflects both different CO₂ degassing rates and the wall-rock-gas interactions which may support Hg deposition in the hydrothermal envelope, thus limiting its release into the atmosphere. Finally, while Hg contribution from sub-aerial volcanism is now more or less constrained, recent evidences have indicated the influence of submarine geothermal activity in controlling the dispersion of Hg as well. This makes the study on submarine hydrothermal activity among the most challenging and significant scientific advances of the 21st century, in terms of Hg research as a global pollutant.

Seward T.M. & Kerrick D.M. 1996. Hydrothermal CO₂ emission from the Taupo Volcanic Zone. New Zealand. Earth Planet. Sci. Lett., 139, 105-113.

Real-time measurements of Hg⁰ in volcanic, geothermal and anthropogenic systems: a multi-methodological approach using Lumex[®] instrumentation

Cabassi J.*¹⁻², Tassi F.¹⁻², Vaselli O.¹⁻², Capeccchiacci F.¹⁻², Venturi S.¹⁻², Calabrese S.³, Nisi B.⁴ & Rappuoli D.⁵

1. Dipartimento di Scienze della Terra, Università di Firenze. 2. Istituto di Geoscienze e Georisorse, CNR, Firenze. 3. Dipartimento di Scienze della Terra e del Mare, Università di Palermo. 4. Istituto di Geoscienze e Georisorse, CNR, Pisa. 5. Unione dei Comuni Amiata-Val D'Orcia, Siena.

Corresponding email: jacopo.cabassi@unifi.it

Keywords: Gaseous mercury, Lumex, real-time measurements.

Mercury represents a pollutant of global concern and strong environmental impact since is highly toxic. Hg is present in air in the oxidation states of 0 and +2, the former being the dominant species with a residence time of 1-2 years due to its high volatility, relatively low solubility and chemical inertness. Both volcanic/geothermal and anthropogenic systems are crucial contributor to the release of Hg⁰ in the atmosphere. In this work, a Lumex[®] (RA-915M) was used to evaluate the environmental impact in air of Hg⁰ from: i) the abandoned Hg mining site and geothermal areas from Mt. Amiata (Siena, Central Italy) and ii) selected Mediterranean volcanic and geothermal systems.

The Lumex[®] instrumentation, based on atomic absorption spectrometric technique with Zeeman effect, allows to measure Hg⁰ at high frequency, in real-time and at a wide range of concentrations (from 2 to 50,000 ng/m³). Hg⁰ measurements were coupled with those of other pollutants, such as CO₂, H₂S, and SO₂. Carbon dioxide was measured using a Multi-GAS instrument manufactured by INGV-Palermo, whereas H₂S and SO₂ using Thermo Scientific[®] Model 450i analyzer. GPS and meteorological parameters were continuously recorded, too. The data acquisition was carried out along transects at an approximately constant speed or at selected fixed points. Wherever possible, the analytical data were then converted into a spatial interpolation providing a qualitative model for the areal dispersion of the contaminants.

The Lumex[®] device was also applied to measure Hg⁰ concentrations in interstitial soil gases collected from a probe inserted into the soil at 70 cm depth, in order to produce Hg⁰ maximum concentration maps in Hg-polluted areas (e.g. Abbadia San Salvatore Hg mining area, Mt. Amiata). Diffuse Hg⁰ soil fluxes were measured using a chamber positioned above the soil from which, at periodic time intervals, gases were extracted and injected into the Lumex[®] device. This instrument was also applied to measure Hg⁰ concentrations along vertical profiles in thermal wells at Santorini (Greece) and Vulcano (Italy) by using a Rilsan[®] tube lowered into the wells at pre-defined depths. With this approach, a significant stratification of the air masses in terms of Hg⁰, strictly dependent on water temperature, air pressure and well depth, was observed. The efficiency of Lumex[®] for these different approaches demonstrated the reliability of this instrument to produce Hg⁰ data that can be used to identify gaseous Hg-emitters in natural and anthropogenic environments, especially when coupled with other physical and chemical parameters.

A new geochemical approach to estimate the distribution of air pollutants from natural and anthropogenic sources: examples from Solfatara Crater (Campi Flegrei, Southern Italy) and Mt. Amiata Volcano (Siena, Central Italy)

Cabassi J.^{*1-2}, Venturi S.¹⁻², Tassi F.¹⁻², Calabrese S.³, Capecchiacci F.¹⁻², D'Alessandro W.⁴ & Vaselli O.¹⁻²

1. Dipartimento di Scienze della Terra, Università di Firenze. 2. Istituto di Geoscienze e Georisorse, CNR Firenze
3. Dipartimento di Scienze della Terra e del Mare, Università di Palermo. 4. INGV, Palermo.

Corresponding email: jacopo.cabassi@unifi.it

Keywords: New geochemical approach, distribution of air pollutants, Solfatara Crater and Mt. Amiata Volcano.

Volcanic and geothermal systems significantly contribute to the input of volatile contaminants, such as mercury and hydrogen sulfide, into the atmosphere. Mercury has a strong environmental impact. In the atmosphere the prevalent elemental form is Hg^0 (~98 %), whose main physical-chemical features are: high volatility, low solubility and chemical inertness. Hydrogen sulfide (H_2S), one of the most abundant gas compounds in volcanic fluids, is highly poisoning and corrosive and unpleasantly smells of rotten eggs. Measurements of Hg^0 and H_2S concentrations in air are commonly performed by means of passive samplers. However, real-time measurements, coupled with monitoring of local atmospheric conditions, are strongly recommended for a reliable reconstruction of the dispersion dynamics once such contaminants are discharged in air. In this paper, a new real-time measurement method for Hg^0 and H_2S is presented. A portable Zeeman atomic absorption spectrometer with high frequency modulation of light polarization (Lumex RA-915M) and a pulsed fluorescence gas analyzer (Thermo Scientific Model 450i) were used for Hg^0 and H_2S measurements, respectively. These instruments were synchronized and set to high-frequency acquisition. Measurements were carried out along transects at an average speed <10 km/h. GPS data and meteorological parameters (wind direction and intensity) were also recorded. The proposed method was applied in two different sites, characterized by natural (Solfatara Crater, Campi Flegrei, Southern Italy) and anthropogenic (Mt. Amiata Volcano, Siena, Central Italy) emissions.

With this highly efficient and effective approach, a reliable and reproducible Hg^0 and H_2S distribution in air was provided, allowing to identify and characterize the gas sources from such different environments. At Solfatara, the distribution of Hg^0 and H_2S concentrations, the highest values being measured close to the fumarolized areas (>60 ng/m³ and >2,100 µg/m³, respectively), suggests that these gases were discharged from both fumaroles and diffuse degassing from the crater bottom. At Mt. Amiata, the maximum Hg^0 and H_2S concentrations (>100 ng/m³ and >35 µg/m³, respectively) were recorded close to the geothermal power plants of Piancastagnaio. According to detailed dot-maps constructed on the basis of the measured values, as expected, wind was the main environmental parameter able to control the behavior and the dispersion halo of the Hg^0 - and H_2S -rich plumes emitted from the contaminant sources.

Active Moss biomonitoring of mercury in the mine-polluted area of Mt. Amiata (Central Italy)

Calabrese S.*¹, Cabassi J.²⁻³, Tassi F.²⁻³, Vaselli O.²⁻³, Capecchiacci F.²⁻³, Brusca L.⁴, Bellomo S.⁴, Daskalopoulou K.¹, D'Alessandro W.⁴, Parello F.¹, Niccolini M.⁵ & Rappuoli D.⁶

1. Dipartimento di Scienze della Terra e del Mare, Università di Palermo. 2. Dipartimento di Scienze della Terra, Università di Firenze. 3. Istituto di Geoscienze e Georisorse, CNR, Firenze. 4. INGV, Palermo. 5. Unità di Progetto Bonifica, Abbazia San Salvatore (SI). 6. Unione dei Comuni Amiata, Val D'Orcia (SI).

Corresponding email: sergio.calabrese@gmail.com

Keywords: Moss bags, trace metals, mercury.

In the winter 2013, mercury concentrations in air from the mine-polluted area of Mt. Amiata (1738 m a.s.l.), in southern Tuscany (Central Italy), were measured by active moss biomonitoring.

This area is part of the geologic anomaly of Hg in the Mediterranean basin, which contains about 65% of the world's cinnabar (HgS). Mt. Amiata covers some 400 km² and is drained by several rivers. Exploitation activity at Abbazia S. Salvatore, in the SE sector of the mountain, sprang up during the 19th century as one of the largest mercury mining and smelting plants in Europe, after those of Almaden Spain. In this area, Sphagnum moss bags were exposed for about two months, from October to December 2013. At each site (10 sites), one covered and one uncovered moss bag were deployed. Concentrations of mercury in air were also investigated in the same sites with a portable spectrophotometer (Lumex RA-915M). After exposure, mosses were oven-dried, grinded and each sample was divided in two aliquots: one was analyzed for mercury by using a Hydra C cold vapor atomic absorption analyzer (INGV-Palermo), following 7473 US EPA method; the second was microwave digested in acid solution (HNO₃ + H₂O₂). Extraction solutions were analyzed by ICP-MS for total concentrations of a large suite of trace elements, including potentially toxic elements e.g. As, Cd, Cr, Cu, Mo, Sb, Se, V.

Mercury air concentrations measured with the Lumex showed extremely high values in the mine district of Abbazia, with median values ranging from 2,000 to 4,000 ng/m³ and maximum values up to 20,000 ng/m³, in contrast with the lower values (median values from 20 to 200 ng/m³) measured in the distal sites few kilometres from the mine-district area. In agreement with these results, in the vicinity of the district uncovered bags were in the range of 10,000 – 100,000 ng/g of Hg, whereas in the distal sites they were in the range of 1,000 – 10,000 ng/g. The moss-blank (unexposed moss) was ~100 ng/g. Covered moss bags were not significantly enriched in Hg with respect to the concentrations recovered from the moss-blank, suggesting that the mercury trapped in the mosses was mainly in particulate form. The particles carried from the winds were probably associated with soils re-mobilization, as also confirmed by the associated enrichments of some lithophile elements (Li and lanthanides) and anthropogenic element (As, Cr, Cd, Fe, Se, V). These preliminary results confirm the intense contamination of the study area not only for mercury but also for other potentially toxic elements.

Are tree barks a suitable tool for Hg air pollution biomonitoring? Preliminary investigation from the Mt. Amiata region

Chiarantini L.¹, Rimondi V.¹, Benvenuti M.², Beutel M.W.³, Costagliola P.² & Lattanzi P.*⁴

1. Istituto di Geoscienze e Georisorse, CNR, Firenze. 2. Dipartimento di Scienze della Terra, Università di Firenze.
3. Department of Civil and Environmental Engineering, Washington State University, U.S.A.
4. Dipartimento di Scienze Chimiche e Geologiche, Università di Cagliari.

Corresponding email: lattanzp@unica.it

Keywords: Mercury, tree barks, air quality monitoring.

Lichens and mosses have been long used for biomonitoring airborne pollutants, especially mercury (Hg), since they tend to take up these pollutant mainly from the atmosphere, rather than from soils. However, there are some disadvantages in the use of lichens and mosses: they may not be intensively sampled; they show a slow regeneration rate; their sampling requires specialists to differentiate between close-looking varieties. As an alternative, the use of tree bark offers some potential advantages, such as a year-round and almost ubiquitous availability, and easier identification and sampling. Tree barks are capable to efficiently remove Hg from polluted waters, proving an affinity between this metal and barks. Moreover, Hg reaches tree wood and bark through leaves, but not through roots, i.e. the systemic uptake from soils can be considered marginal.

To investigate Hg distribution in tree barks as a potential tool for biomonitoring studies, we sampled *Pinus nigra* barks from the Mt. Amiata region, which was until 1980 the third largest Hg producing region of the world. *Pinus nigra* was selected because of its wide diffusion in the investigated area, and because of its multilayered barks, that may allow to investigate the distribution of Hg across its thickness.

Barks and related soils were collected in different sites, including: the Abbadia San Salvatore mining area; two sites close to geothermal power plants (presently exploited for electricity production), and two sites (Bagni S. Filippo and Vivo D'Orcia) which should provide a local background value. In addition, we choose another area which should be unaffected by Hg contamination (Monte Morello near Florence).

Bark samples were sliced at least in three portions (external, middle and internal), and analyzed separately by means of Direct Mercury Analyzer (Milestone DMA-80). Mercury concentrations were then corrected for water loss.

The maximum Hg contents (in order of mg/kg) were displayed in barks collected in close proximity of the Abbadia mining/retorting facilities, representing the highest Hg concentrations ever recorded in barks. All barks display a general decrease of Hg concentration from the surface inwards, suggesting Hg deposition (and in-depth penetration) from the atmosphere, with no significant systemic intake of Hg from soil. Lower, but still high Hg (hundreds of mg/kg) contents were recorded also in the background areas at Bagni San Filippo, where recently a positive anomaly of Hg in air was reported. Mercury in tree barks around the two geothermal plants is the lowest recorded in the Mt. Amiata region, including the "background" sites.

Mercury concentration in lichens grown on Hg-polluted soils in the area is of same order of magnitude as the analyzed barks, suggesting that barks possibly are as reliable as lichens in recording regional differences of Hg pollution.

Origin and distribution of methane and C₂-C₆ hydrocarbons in hydrothermal and cold gaseous emissions in Greece

Daskalopoulou K.*¹, Cabassi J.²⁻³, Calabrese S.¹, D'Alessandro W.⁴, Grassa F.⁴, Parello F.¹ & Tassi F.²⁻³

1. Dipartimento di Scienze della Terra e del Mare, Università di Palermo. 2. Dipartimento di Scienze della Terra, Università di Firenze.
3. Istituto di Geoscienze e Georisorse, CNR, Firenze. 4. INGV, Palermo.

Corresponding email: kdaskalopoulou@hotmail.com

Keywords: Methane, hydrocarbons, Greece.

The Hellenic territory has a very complex geodynamic setting from a long and composite geological history, giving rise to an intense seismic activity deriving and favoring the occurrence of many cold and thermal gas manifestations. Geogenic sources release huge amounts of gases, which have a significant impact on the global balance of the subaerial Carbon Cycle.

The study of the geochemistry of the natural gas emissions of the Greek territory is actually underway. In the present work, we focus on methane and light hydrocarbons (C₂-C₆) to define their origin. Concentrations of methane range from < 2 to 915,200 mmol/mol and its isotopic ratios cover a wide range (d¹³C from -79.8‰ to +16.9‰; dD from -298‰ to +264‰) indicating different origins or secondary post-genetic processes. Samples from gas discharged located in the Ionian coast and northern Aegean Sea have a prevailing microbial origin, as also shown by the lack of C₄₊ hydrocarbons and the high C₁/(C₂+C₃) ratios. On the contrary, cold and thermal gas manifestations of central and northern Greece display a prevalent thermogenic origin. Methane in gases released along the active volcanic arc seems to be abiogenic in origin, since they show low C₁/(C₂+C₃) ratios, as well as relatively high C₆H₆ concentrations. However in these gases, significant thermogenic contribution cannot be excluded. Gases collected in the geothermal areas of central Greece (Sperchios basin and northern Euboea) are likely affected by strong secondary oxidation processes, as suggested by their highly positive C and H isotopic values (up to +16.9‰ and +264‰ respectively) and low C₁/(C₂+C₃) ratios. Incubation experiments on water and sediments of some of these springs reveal that the oxidation of methane is microbially driven.

Heavy metal speciation and risk assessment in freshwater sediments of an artificial reservoir in the Almadén mining district, Spain

Garcia-Ordiales E.¹, Loredo J.*¹, Covelli S.², Higuera P.³, Esbrí J.M.³ & Lopez-Berdonces M.A.³

1. Mining, Energy and Materials Engineering School, University of Oviedo, España. 2. Dipartimento di Matematica e Geoscienze, Università di Trieste. 3. IGEA, University of Castilla La Mancha, Almadén, Ciudad Real, España.

Corresponding email: jlredo@uniovi.es

Keywords: Mining, heavy metals, contamination.

The Castilseras artificial water reservoir (Almadén, South Central Spain) is receiving runoff water from the most important Hg mines of the Almadén mining district and from other small Pb-Zn mines. This reservoir constitutes the only lentic medium located within the mining district and their sediments can be considered as a sink and/or source of contaminants in the aquatic ecosystem. Then, the ecological risk assessment of these sediments can be considered as priority target in order to assess the environmental quality of the fluvial compartment and the potential uptake of heavy metals for the biota. For this objective, sediments collected in 12 sampling stations have been studied using the Sequential Extraction Procedure (SEP). Results were evaluated using Principal Component Analysis (PCA) and different risk criteria such as Pollution Degree, Mean Probable Effect Concentration Quotient, and Risk Index. In general, the high contents in Hg and other elements such as As and Pb, can be attributed to environmental liabilities of decommissioned mines. The study of the different fraction steps and their statistical multivariate treatment by PCA, showed two differentiate groups of elements in the easily leachable fraction F1. This fact is indicative of the presence of sulfate salts and secondary precipitates of carbonates as the main sink for easily accessible metallic elements. In the reducible fraction F2, chemical analysis revealed a significant relationship between the majority of the analyzed elements and the Fe oxy-hydroxides, with exception of Co, Hg and Ni, which are preferentially associated with Mn oxy-hydroxides. In the oxidisable fraction (F3), a significant relationship between Cu, Fe, Hg and Zn (most representative metals of the ore deposits in the district) and sulfides/organic matter was observed. Finally, the residual fraction F4 showed a first group constituted by As, Ca, Co, Mg, Mn and Ni, elements which are related to the presence of silicates, and a second group related to sulfides or secondary sulfates. The environmental assessment based on the aforementioned criteria provides risk levels varying from moderate to high. The risk appears to be higher at the head of the reservoir, where the highest concentrations of heavy metals and metalloids in the sediment are due to a selective accumulation of fine-grained particles.

Partitioning of geochemical populations on cumulative probability plots: critical comparison of different graphical-numerical methods

Gozzi C.*¹, Menichetti S.² & Buccianti A.¹

1. Dipartimento di Scienze della Terra, Università di Firenze. 2. ARPAT-SIRA, Firenze.

Corresponding email: caterina.gozzi@stud.unifi.it

Keywords: Background, cumulative density plot, perchloroethylene.

Geogenic or natural background of substances in the environment is related to unpolluted or pristine preindustrial conditions. However since a widespread global contamination by several trace constituents often occurs, the term background is frequently not useful and it is replaced by the baseline concentration.

Different graphical-numerical methods are applied in geochemistry to identify baseline concentrations or to estimate threshold values dividing baseline data from anomalies (Reimann et al., 2005). The procedures are somewhat arbitrary, but able to provide fundamental grouping of data values (Sinclair, 1974) or are based on well-defined statistical criteria (R package “classInt”, 2015) as for example quantile breaks (intervals are calculated so that each class contains more or less the same amount of values), partitions by using hierarchical clustering (searching for clusters with low variance and similar size or clusters with cases having short distance from the cluster barycentre) or by using the Fisher-Jenks’ natural breaks classification method (it reduces the variance within classes and maximize the variance between classes). Fractal models have also been used to determine thresholds of geochemical anomalies by investigating the cumulative number of concentrations N greater than or equal to the concentration value c (Agterberg, 2015).

This work deals with the critical comparison of different methods of partitioning of geochemical populations on cumulative probability plots. An application example is presented for perchloroethylene (PCE) concentration in the groundwater of Firenze-Prato (Tuscany Region) alluvial plain. PCE is a common groundwater contaminant due to its wide use in many industrial and commercial operations such as metal degreasing (e.g., trichloroethene or TCE) and dry cleaning (e.g., PCE). These compounds often entered the ground in the solvent phase a few or more decades ago and are known as dense non-aqueous phase liquids (DNAPLs) due to their limited solubility and high density compared to water. They are carcinogenic compounds and their health-based water quality standards and analytical detection limits are several orders of magnitude below their respective aqueous solubility (Puigserver et al., 2014).

Agterber F. 2014. Geomathematics: Theoretical Foundations, Applications and Future Developments. Springer.

Puigserver D., Cortes A., Viladevall M., Nogueras X., Parker B.L. & Carmona J.M. 2014. Processes controlling the fate of chloroethenes emanating from DNAPL aged sources in river-aquifer contexts. *J. Contam. Hydrol.*, 168, 25-40.

Reimann C., Filzmoser P. & Garret R.G. 2005. Background and threshold: critical comparison of methods of determination. *Sci. Total Environ.*, 346, 1-16.

Rpackage ‘classInt’, 2015. <http://cran.r-project.org/web/packages/classInt/classInt.pdf>

Sinclair A.J. 1974. Selection of threshold values in geochemical data using probability plots. *J. Geochem. Explor.*, 3, 129-149.

Geochemical characterization of drainage waters after closure of sulphides extraction activity (Salafossa, Northeastern Italian Alps)

Pavoni E.¹, Covelli S.*¹, Emili A.¹, Lenaz D.¹, Petranich E.¹, Crosera M.², Adami G.², Cattelan R.³ & Higuera P.⁴

1. Dipartimento di Matematica e Geoscienze, Università di Trieste. 2. Dipartimento di Scienze Chimiche e Farmaceutiche, Università di Trieste. 3. Veritas, Laboratori Chimici Venezia Fusina. 4. IGeA, Università di Castilla, La Mancha, España.

Corresponding email: covelli@units.it

Keywords: Heavy metals, mineral deposits, mining.

After decommissioning, the potential impact of mining areas on the quality of water resources is a major concern for local communities. Acid mine drainage resulting from oxidation of metal sulphides associated with mineral veins or mining wastes is often responsible for leaching large amounts of metals in solution, which can be dispersed into the surrounding environment and affect the quality of receiving water bodies. The body ore in Salafossa (NE Italy) was one of the largest lead/zinc deposits in Europe. Mining activity started around 1550 but it was only around 1960 that the richest veins of sulphides were discovered. When the activity definitely stopped in 1985, a little more than 11 million tons of tout-venant (raw material), with an average content of 0.9% for Pb and 4.7% for Zn, were obtained from the mineral deposits. The aims of the present study were to investigate the geochemical properties of the mine drainage waters and to monitor the concentration of trace metals outflowing from the mine galleries into the Piave River, the major tributary downstream the mine. In spite of the sulphides body ore, there is no evidence of acid drainage waters in Salafossa, probably because of the buffering effect produced by carbonate host rocks. However, Zn and Tl, due to their high mobility, are present in solution mostly in ionic form. Conversely, the less mobile Pb (highest concentration: 4 $\mu\text{g L}^{-1}$), is preferably partitioned in the solid phase. Additionally, the oxidizing conditions found in the drainage waters also allow the precipitation of some trace metals (As, Cd, Pb, Tl, Zn) in the form of Fe-Mn oxy/hydroxides and carbonates, which accumulate in the mine galleries sediments. Drainage waters inside the mine were found to be highly enriched in Zn (up to 16 mg L^{-1}), Fe (up to 5 mg L^{-1}) and Tl (up to 260 $\mu\text{g L}^{-1}$), but their concentrations are diluted in the mine before being discharged into the Piave River. Although drainage waters are still characterised by high concentrations of Tl (up to 30 $\mu\text{g L}^{-1}$) at their outflow, dilution in the Piave River seems to be a natural process mitigating the impact of trace metals within the drainage basin.

Bioaccumulation of Thallium and other heavy metals in *Biscutella laevigata* nearby a decommissioned Zn-Pb mine (Salafossa, Northeastern Italian Alps)

Pavoni E.¹, Petranich E.*¹, Crosera M.², Adami G.², Baracchini E.², Lenaz D.¹, Emili A.¹, Higuera P.³ & Covelli S.¹

1. Dipartimento di Matematica e Geoscienze, Università di Trieste. 2. Dipartimento di Scienze Chimiche e Farmaceutiche, Università di Trieste.
3. IGeA, Università di Castiglia, La Mancia, España.

Corresponding email: epetranich@units.it

Keywords: Heavy metals, Thallium, bioaccumulation.

The mineral body cultivated in Salafossa (Eastern Dolomites) was one of the largest lead/zinc-containing mineral deposits in Europe. Both metals were mainly present as sulphides (sphalerite, ZnS and galena, PbS). Mining activity started around 1550 but it was only around 1960 that the richest veins of the minerals were discovered. The mine closed in 1985. The content of several heavy metals (Tl, Fe, Mn, Pb, Zn) was determined in soils and in plants (*Biscutella laevigata*) from twelve sites selected outside the mine. *Biscutella laevigata* is a “pseudometallophyta” species, and it often grows near mining areas, where soil metal contents are significantly higher than natural geochemical background levels. Total metal contents in biological (roots and leaves of *B. laevigata*) and inorganic (soil) samples were determined by Inductively Coupled Plasma Atomic Emission Spectroscopy (ICP-AES). In addition, metal bioavailability in the soil - including the *B. laevigata* root system (rhizo-soil) - was estimated by using an extracting solution (i.e. DTPA - Diethylene Triamine Penta-acetic Acid). Results showed that metals were present in a chemical form available for absorption by the plants roots. In fact, high concentrations of the metals were also found in the roots and leaves of *B. laevigata*, and these concentrations were higher than those in the corresponding rhizo-soil. Thus, *B. laevigata* has shown a marked ability to bioaccumulate heavy metals, especially Tl and, to a lesser extent, Zn, Pb, Fe, Mn, and it can influence metal mobility in the rhizo-soil. In particular, Tl has been recognized as one of the most toxic trace elements for the human health. When present in the aqueous solution, Tl may further be subject to adsorption on the surface of soil and sediment particles, for example in the presence of oxides and hydroxides of Fe and Mn. To assess absorption and translocation processes of heavy metals, resulting in their bioaccumulation, two different indices were calculated: the Enrichment Factor in roots (E_{Fr}), as the ratio between metal concentration in belowground biomass and in the respective rhizo-soil, and the Translocation Factor (TF), as the ratio between metal concentration in leaves and in the corresponding roots. For both indices, values higher than 1 denote an enrichment of the metal in the roots or its translocation to the upper tissues. The results showed that E_{Fr} and TF were considerably high only for Tl, reaching a maximum value of 60 for E_{Fr} and 11.6 for TF. Conversely, the other investigated metals did not show significant bioaccumulation (E_{Fr} < 1) and they showed TF > 1 only at a few sites. These evidences confirmed the ability of *B. laevigata* to absorb metals from the contaminated soil and to accumulate them in the roots and/or translocate them to the aboveground biomass, especially Tl, thus representing a good indicator of Tl bioavailability in the rhizo-soil of the study area.

Critical factors affecting mercury biogeochemical cycle in fish farm contaminated sediments (Grado Lagoon, Adriatic Sea)

Petranich E.*¹, Covelli S.¹, Contin M.², Faganelli J.³, Acquavita A.⁴ & De Vittor C.⁵

1. Dipartimento di Matematica e Geoscienze, Università di Trieste. 2. Dipartimento di Scienze Agrarie ed Ambientali, Università di Udine. 3. Stazione di Biologia Marina, NIB, Piran, Slovenia. 4. ARPA FVG. 5. Sezione Oceanografia, Istituto Nazionale di Oceanografia e Geofisica Sperimentale (OGS).

Corresponding email: epetranich@units.it

Keywords: Mercury, Grado Lagoon, fish farm.

The Marano and Grado Lagoon has been subjected to mercury (Hg) input from two anthropogenic sources. The first long-term source was the Isonzo River, which has been the largest contributor of this metal into the northern Adriatic Sea since the 16th century due to Hg mining in Idrija, western Slovenia. The second was a chlor-alkali plant located in the Aussa-Corno River system flowing into the Lagoon. As a consequence, Hg content in sediments was recognized to be up to three orders of magnitude higher than the natural background level. Since local fish farming is extensively practiced, there is a great concern about the risk posed by potential Hg harmful effects on the trophic chain and consumers. Previous investigations showed Hg bioaccumulation in commercial fish species (e.g. *Sparus aurata*, *Dicentrarchus labrax*). Due to this, a three-years research project has been recently planned in order to understand critical factors affecting Hg cycling in a fish farm and, possibly, to provide useful advices to mitigate Hg bioaccumulation. In this work, a preliminary evaluation of the concentration of Hg in different matrices (sediments, suspended particulate matter and waters) was performed. Moreover, the input/output of Hg associated with tidal flows in a tidal cycle through the sluice gates, which is the only way of water exchange between the Lagoon and the fish farm, was calculated. High Hg concentrations in short core profiles of bottom sediments of shallow ponds (up to 22.3 ± 2.29 mg kg⁻¹), in suspended particulate matter (8.21 mg kg⁻¹) and in the dissolved phase of the water column (201 ± 12.1 ng L⁻¹) characterized the fish farm. From these first evidences, it seems that Hg enters into the fish farm through the sluice gates during the two daily loading phases (259 and 154 ng L⁻¹, at flood tide) showing concentrations higher than those observed when waters flow out from the fish farm at ebb tide (14.1 and 31.8 ng L⁻¹). Conversely, higher concentrations in ebb tide (76 ng L⁻¹) than in flood tide conditions (7 ng L⁻¹) were observed during the whole tidal cycle. Further investigations are to be planned in the next future in order to elucidate how the water circulation, sedimentary inputs and trophic state influence the Hg biogeochemical processes at the water-sediment interface in this complex and heavily modified ecosystem.

Measurements of gaseous elemental mercury (GEM) in diffuse soil emission using the static closed-chamber method

Tassi F.^{*1-2}, Cabassi J.¹⁻², Calabrese S.³, Nisi B.⁴, Venturi S.¹⁻², Capecchiacci F.¹, Vaselli O.¹⁻² & Giannini L.¹

1. Dipartimento di Scienze della Terra, Università di Firenze. 2. Istituto di Geoscienze e Georisorse, C.N.R. Firenze. 3. Dipartimento di Scienze della Terra e del Mare, Università di Palermo. 4. Istituto di Geoscienze e Georisorse, C.N.R. Pisa.

Corresponding email: franco.tassi@unifi.it

Keywords: GEM flux, diffuse degassing, closed static chamber.

Measurements aimed to evaluate the contribution of natural and anthropogenic gaseous elemental mercury (GEM) to the atmosphere are critical for monitoring and mitigating the impact of this highly toxic air contaminant. Notwithstanding, the amounts of GEM originating from different sources are difficult to be estimated, since specific protocols dictating the most appropriate sampling and analytical techniques are lacking. This study was aimed to test a methodological approach enables to measure GEM released through diffuse degassing from the soil, a mechanism that in volcanic and geothermal areas significantly contributes to the discharge of geogenic fluids to the atmosphere. A static closed-chamber (SCC), consisting of a plastic cylinder with a basal area of 201 cm² and an inner volume of 1,810 cm³, was used in combination with a Lumex[®] (RA-915M). This instrument, i.e. a portable atomic absorption spectrometer with Zeeman effect, is able to measure Hg⁰ at high frequency, in real-time and at a wide range of concentrations (from 2 to 50,000 ng/m³). From an operative point of view, four aliquots of the soil gas accumulated in the SCC, were collected at fixed time intervals (when the SCC was positioned on the ground, and after 1, 2 and 3 min), through a pierceable rubber positioned on its top using a 60 cc syringe. The syringe was then connected to the Lumex inlet port through a three-way Teflon valve to allow the free entrance of air during the syringe injection. This external device was necessary to maintain stable the operative flux of the Lumex at 10 L/min during the injection operation, in order to prevent possible noise signals related to flux changes. Moreover, a carbon trap was set at the free air entrance to stabilize the baseline, which otherwise would be unstable, being dependent on the variable GEM concentrations in air. The amount (in ng) of GEM of each injection (K_{SYR}) was calculated on the basis of a calibration curve previously constructed measuring known amounts of GEM saturated gas that were injected in the Lumex port set with the three-way valve device using a micro-syringe. By multiplying the K_{SYR} values for the ratio between the volumes of (i) the syringe and (ii) the SCC, the amount of GEM present in the SCC (K_{SCC}) during each sampling time-series was obtained. GEM fluxes are proportional to the variation in time of GEM amounts in the SCC, as follow: $f(X) = (dK_{SCC}/dt)/A$, where A is the basal area of the SCC.

This method was applied at Solfatara crater (Campi Flegrei, southern Italy), a hydrothermally altered tuff cone characterized by an anomalous diffuse emission of geogenic gases from the soil. The 214 measured fluxes, varying in a wide range of values (4 orders of magnitude), showed that the method was highly sensitive (detection limit: 5,000 ng m⁻² day⁻¹) and reproducible (±5 %).

Effects of microbial activity on C-bearing volatile compounds in interstitial soil gases from the Vicano-Cimino volcanic system (central Italy)

Tassi F.^{*1-2}, Venturi S.¹⁻², Cabassi J.¹⁻², Vaselli O.¹⁻², Gelli I.¹, Cinti D.³ & Capecchiacci F.¹⁻²

1. Dipartimento di Scienze della Terra, Università di Firenze.
2. Istituto di Geoscienze e Georisorse, CNR, Firenze. 3. INGV, Roma.

Corresponding email: franco.tassi@unifi.it

Keywords: Soil gas, VOCs, microbial activity.

Carbon-bearing volatiles emitted from both anthropogenic and natural sources have a strong environmental impact on air quality, global climate and human health. Notwithstanding, a reliable evaluation of the input rates to the atmosphere of these gases is still a challenge. Secondary processes occurring in soils play a fundamental role for the release of gases produced under reducing conditions, such as those released from volcanic and geothermal fluid reservoirs. In this study the effects of microbial activity on the behavior of CO₂, CH₄ and volatile organic compounds (VOCs) originating from the Vicano-Cimino hydrothermal system (Central Italy) were investigated. The database consisted of the chemical composition and d¹³C-CO₂ and d¹³C-CH₄ values of interstitial soil gases from a 150×100 m wide area, located in the surroundings of Viterbo and characterized by intense degassing of deep-originated fluids. Gas samples were collected from 5 vertical profiles (from 10 cm down to 50 cm depth) at regular depth intervals (5 cm), and from 20 sites at 40 cm depth. The vertical trends of the d¹³C-CH₄ values, as well as the vertical gradients of CH₄, H₂S, and O₂ concentrations, consistently indicated that CH₄ strongly depends on microbial activity occurring at < 50 cm depth, where free O₂ is available. On the contrary, according to the d¹³C-CO₂ values, CO₂ was not significantly affected by biodegradation, except for those gases sampled from sites affected by significant air contamination. Microbial activity efficiently degraded hydrothermal alkanes, alkenes, cyclics, and hydrogenated halocarbons, whereas benzene behaved as recalcitrant species. Oxygenated compounds from hydrocarbon degradation consisted of alcohols, with minor aldehydes, ketones and carboxylic acids. A predominance of alcohols at a high rate of degassing flux, corresponding to a short residence time of hydrothermal gases within the soil, indicated incomplete oxidation. N-bearing compounds were also detected and likely produced by humic substances in the soil and/or related to contamination of pesticides. Thus, these species were not related to biodegradation processes of geogenic gases. Similarly, α-pinene was found to trace air entering the soil. These results showed that the microbial communities in the soil of the study area were able to strongly mitigate the impact on air quality of hydrothermal C-bearing gases, especially CH₄, released through diffuse degassing, a mechanism that in Central Italy significantly contributes to the discharge of CO₂-rich gases from deep sources.

Mercury pollution in the former mining area of Abbadia San Salvatore (Siena, Tuscany Region, central Italy): actions, criticalities and perspectives for the remediation process

Vaselli O.^{*1-2}, Rappuoli D.³, Bianchi F.⁴, Nisi B.⁵, Higuera P.L.⁶, Cabassi J.² & Tassi F.¹⁻²

1. Dipartimento di Scienze della Terra, Firenze. 2. Istituto di Geoscienze e Georisorse, C.N.R. Firenze.

3. Unione dei Comuni Amiata-Val D'Orcia, Siena. 4. S.B.C. Geologi Associati, Firenze.

5. Istituto di Geoscienze e Georisorse, C.N.R. Pisa. 6. Institute of Applied Geology, UCLM, Ciudad Real, España.

Corresponding email: orlando.vaselli@unifi.it

Keywords: Central Italy, Mt. Amiata, Hg-mining areas.

Since 2012 a reclamation project in the abandoned Hg mining district of Abbadia San Salvatore (Tuscany, central Italy), whose exploitation ceased in 1976, has started, carrying out a geochemical survey on surface and ground waters, soil and air, as well as in the mining structures and hydraulic, cleaning and engineering activities. The responsible of the reclamation process is the Municipality of Abbadia San Salvatore since 2008, when the former owner (ENI Ltd. - AGIP Division) transferred properties and mining concessions to the public agency. The mining activities ended up without any clean-up strategy. The metallurgical plants and tailings, with huge piles of calcines and roasting products rich in metallic mercury, were abandoned. Mine adits and shafts were closed, leaving flowing drainage tunnels and two unsealed chimneys to disperse to the atmosphere a significant amount of CO₂-rich, deep-originated gases. This occurred without strict environmental regulations that became State laws in 1999. Recently, the mining areas were divided in 6 sub-areas (lots) in accordance with the local Environmental Protection Agency, on the basis of the type of operations to be performed for reclaiming the mining area. Lot 6 represents the most critical one, being the site where cinnabar was managed and roasted to produce liquid mercury after condensation processes. The other lots are less affected by Hg contamination, being mainly characterized by workers and managers buildings.

The Tuscany Region issued a regulation for recovering abandoned mining areas. Suited criteria and threshold concentration limits for Hg were established where a high "natural background" is present. Accordingly, soils were considered contaminated when leaching tests with MilliQ water saturated in CO₂ have Hg concentrations above 1 mg/L and the outdoor concentration of gaseous mercury above ground within the contaminated site is >300 ng/m³, while indoor concentrations in the mining structures and buildings cannot exceed 500 ng/m³. For surface and ground waters, the reference thresholds for Hg and Sb and As, the latter two having a geochemical affinity with Hg, are those dictated for drinkable water, i.e. 1, 5 and 10 mg/L, respectively. Most geological compartments in the mining area are affected by Hg concentrations above the previously reported reference concentrations. In this paper, we present the results of the geochemical investigations carried out since 2012 to highlight actions, criticalities and perspectives for the remediation process, which is focused on environmental restoration and has as ultimate goal the site recovery for historic museum and mining park purposes.

SESSION S20

Multidisciplinary contributes to the understanding of active geodynamic processes

CONVENORS

Marco Bonini (Univ. Firenze)

Riccardo Caputo (Univ. Ferrara)

Giacomo Corti (IGG Pisa)

Ground deformation of the Po-Plain detected through satellite radar interferometry (PSInSAR)

Antonielli B.*¹⁻², Monserrat O.³, Bonini M.⁴, Sani F.¹ & Righini G.⁵

1. Dipartimento di Scienze della Terra, Università di Firenze. 2. Dipartimento di Scienze della Terra, Università di Pisa. 3. Centre Tecnològic de Telecomunicacions de Catalunya (CTTC), Barcelona, España. 4. Istituto di Geoscienze e Georisorse, CNR, Firenze. 5. ENEA, Bologna.

Corresponding email: benedetta.antonielli@unifi.it

Keywords: Po-plain subsidence, thrust-anticlines, tectonic uplift.

This work aims to explore the recent tectonic activity of structures in the outermost sector of the Northern Apennines comprising the structures buried below the Po Plain up to the Pede-Apennine thrust front.

This area represents the active leading-edge of the thrust belt and is dominated by compressive deformation, as shown by the fault plane solutions of earthquakes, in agreement with geological data (Boccaletti et al., 2004; Basili et al., 2008; Fantoni & Franciosi, 2010). In addition to the scattered distribution of seismicity, other factors make the understanding of the seismo-tectonic setting very complex, such as the large thickness of sediments in the Po Plain, and the strong impact of human activity on this area, which may cause significant vertical ground motion.

We have applied the PSInSAR method to obtain new insights into the present-day deformation pattern of the frontal area of the Northern Apennines. Persistent Scatterers Interferometry (PSInSAR) is suitable for high-resolution assessment of surface deformations (submillimeter precision) over a long period of observation using numerous radar images. We used 54 ENVISAT images collected between 2004 and 2010. Thanks to the analysis of the mean velocity maps and of the time series, the ground deformation over a vast sector of the Po Plain (between Piacenza and Sassuolo) has been observed. The time series of six GPS stations validated the results of the PSInSAR technique, showing a good correlation with the PS time series. The PS analysis reveals an important subsidence area (encompassing Reggio Emilia, Correggio and Rubiera), which approximately coincides with a large synform where the sedimentary package is thicker. Anthropogenic causes, as the exploitation of water resources, provide a major contribution to this subsidence. Interestingly, the PS velocity pattern locally shows some ground uplift likely associated to active thrust-related anticlines. PSInSAR has confirmed to be effective in detecting surface deformation of wide regions involved in low tectonic movements.

Basili R., Valensise G., Vannoli P., Burrato P., Fracassi U., Mariano S., Tiberti M.M. & Boschi E. 2008. The Database of Individual Seismogenic Sources (DISS), version 3: summarizing 20 years of research on Italy's earthquake geology. *Tectonophysics*, 453, 20-43, doi:10.1016/j.tecto.2007.04.014.

Boccaletti M., Bonini M., Corti G., Gasperini P., Martelli L., Piccardi L., Severi P. & Vannucci G. 2004. Seismotectonic map of the Emilia-Romagna Region. Emilia-Romagna Region-SGSS and IGG-CNR, Selca, Firenze.

Fantoni R. & Franciosi R. 2010. Tectono-sedimentary setting of the Po Plain and Adriatic foreland. *Rend. Lincei*, 21, S197-S209, doi:org/10.1007/s12210-010-0102-4.

High-resolution seismic exploration in the Mt. Etna offshore: preliminary results and implications with regional tectonics

Barreca G.¹, Monaco C.*¹ & Pepe F.²

1. Dipartimento di Scienze Biologiche, Geologiche e Ambientali - Sezione di Scienze della Terra, Università di Catania

2. Dipartimento di Scienze della Terra e del Mare, Università di Palermo.

Corresponding email: emonaco@unict.it

Keywords: Mt. Etna, seismic profiles, active tectonics.

Mt. Etna in eastern Sicily is an active volcano formed since 500 ky ago by the accumulation of lava flows and pyroclastic products. Presently the volcano exhibits a complicate deformation pattern as a result of different geologic processes, namely volcano-tectonics, flank dynamics and regional tectonics. A grid of ca. 400 km of high-resolution, seismic reflection profiles have been acquired in August 2014 offshore of Mt. Etna using a Sparker source with the aim of investigating active tectonic structures. Preliminary seismo-stratigraphic analysis allows us to identify five seismic units limited by marker reflections. The lowermost appears as reflection-free limited upwards by an erosive truncation and should correspond to the Lower-middle Pleistocene clayey Etnean substratum. It was well recognized along a NE-SW trending seismic line acquired between Catania and Capo Mulini, passing very close to the Ciclopi rocky islets (Aci Trezza). Here, the erosive truncation lies at a depth ranging between 80 and 125 ms (t.w.t.) and above it a number of seismic units occur. A second seismic unit is represented by a zone of disturbed reflections with a shield geometry, limited upward by high-amplitude. It was found in the central portion of the line, corresponding to the submerged portion of the Acitrezza rocky islets formed by Basal Tholeiithics (~500-200 kyr) and was attributed to this unit. A third seismic unit, characterized by high to medium-amplitude reflectors, forms a plateau northwards, just east of the Acireale cliff where the Timpe volcanic unit (200-100 kyr) outcrop. The seismic units associated with volcanic products are both covered by deposits seismically characterized by laterally continuous reflectors that can be correlated to an Upper Pleistocene sedimentary sequence. This latter is limited upwards by an erosive surface that separates it from a thin and chaotic seismic unit, probably corresponding to the post-LGM deposits. Tilted and folded Upper Pleistocene deposits suggest that shortening occurred in the Aci Trezza offshore. Reflectors with divergent geometry suggest syn-tectonic deposition into a piggy-back basin setting (growth folding). Asymmetric folding, which appear also to involve the younger erosive truncation, is observed and it has been related to thrust propagation, being some reflectors displaced in reverse mode. North-eastwards, a belt of normal faults (the seaward extension of the transtensional Timpe fault system) dislocate the 200-100 ky volcanic plateau producing also ruptures in the seafloor. These preliminary data confirm that active contractional and extensional tectonic processes coexist in the south-eastern sector of Mt. Etna. Thrust and folding can be related to the late migration of the Sicilian chain front, whereas oblique faulting to the east is probably part of the major kinematic boundary located in eastern Sicily.

Tephrochronology and biostratigraphy of two exceptional fossil localities in the Pisco Formation (Peru)

Bosio G.*¹, Gariboldi K.³, Di Celma C.⁴, Gioncada A.², Malinverno E.¹, Tinelli C.², Villa I.M.¹⁻⁵, Cantalamessa G.⁴,
Collareta A.³, Lambert O.⁶, Landini W.², Urbina M.⁷ & Bianucci G.²

1. Dipartimento di Scienze dell'Ambiente e del Territorio e di Scienze della Terra, Università di Milano Bicocca. 2. Dipartimento di Scienze della Terra, Università di Pisa. 3. Dottorato Regionale Toscano di Scienze della Terra, Università di Pisa. 4. Scuola di Scienze e Tecnologie - Sezione di Geologia, Università di Camerino. 5. Institut für Geologie, Universität Bern, Switzerland. 6. Institut Royal des Sciences Naturelles de Belgique, D.O. Terre et Histoire de la Vie, Bruxelles, Belgique. 7. Departamento de Paleontología de Vertebrados, Museo de Historia Natural, Lima, Peru.

Corresponding email: anna.gioncada@unipi.it

Keywords: Tephrochronology, biostratigraphy, palaeontology.

An exceptional fossil record of marine vertebrates is hosted in the Pisco Formation, Peru (Bianucci et al., 2015 and references therein), which is attributed to middle Miocene to Pliocene (Brand et al., 2011). Fossil vertebrate remains are numerous, found in many different levels of the Pisco Formation (spanning more than 10 Ma), and often extremely well preserved. Although crucial to reconstruct evolutionary trends, the chronostratigraphic setting is still poorly constrained. High sedimentation rates favoured by the high productivity of this upwelling region could have played a role in the formation of this exceptional fossil record, but they have not been quantified so far. The Pisco Formation is a mainly diatomaceous sedimentary succession with interbedded volcanic ash layers from the Central Andean volcanoes; therefore tephro- and diatom biostratigraphy are suitable chronostratigraphic tools.

Based on a detailed stratigraphic reconstruction (Di Celma et al., 2015), over 70 volcanic ash beds were identified in two non-overlapping sections of about 200 and 300 m respectively. Most ashes have a dacitic to rhyolitic glass composition and a minor crystal fraction of juvenile feldspars and biotite. Crystal-bearing ashes with field characteristics suggestive of distal deposits of single eruptive events were selected for granulometric, SEM-EDS and EPMA analyses, avoiding obvious alteration. Biotite-feldspar pairs from five tuff levels were selected for ⁴⁰Ar/³⁹Ar dating by step-heating. Feldspars were mostly subtly altered, as shown by very high Cl/K ratios. Some but not all biotites were substoichiometric, i.e. also partly altered. Data mining returns age ranges concordant with stratigraphy: 9.0±0.1 (lower allomember) - 7.4±0.2 (upper allomember) Ma for the older Cerro Colorado section and less well constrained ages around 7 Ma in the Cerros Los Quesos section. Those results agree with biostratigraphic evidence of late Miocene ages for both sections.

Bianucci G., Di Celma C., Landini W., Post K., Tinelli C., de Muizon C., Gariboldi K., Malinverno E., Cantalamessa G., Gioncada A., Collareta A., Salas-Gismondi R., Varas R., Stucchi M., Urbina M. & Lambert O. 2015. Distribution of fossil marine vertebrates in Cerro Colorado, the type locality of the giant raptorial sperm whale *Livyatan melvillei* (Miocene, Pisco Formation, Peru). J. Maps, in press, doi:10.1080/17445647.2015.1048315.

Brand L., Urbina M., Chadwick A., DeVries T.J. & Esperante R. 2011. A high resolution stratigraphic framework for the remarkable fossil cetacean assemblage of the Miocene/Pliocene Pisco Formation, Peru. J. South Am. Earth Sci., 31, 414-425.

Di Celma C., Malinverno E., Gariboldi K., Gioncada A., Rustichelli A., Pierantoni P.P., Landini W., Bosio G., Tinelli C. & Bianucci G. 2015. Stratigraphic framework of the late Miocene to Pliocene Pisco Formation at Cerro Colorado (Ica Desert, Peru). J. Maps, in press, doi:10.1080/17445647.2015.1047906.

Salt diapirism in the Persian Gulf

Chiariotti L.¹, Bresciani I.² & Perotti C.*²

1. Edison S.p.A., Milano. 2. Dipartimento di Scienze della Terra e dell'Ambiente, Università di Pavia.

Corresponding email: cesare.perotti@unipv.it

Keywords: Diapirism, Persian Gulf, structural evolution.

The Iranian sector of the Central Persian Gulf Basin is characterized by numerous salt diapirs that warp and pierce the very thick Arabian Platform sedimentary succession, deposited from the Late Proterozoic to Holocene. At least 30 main salt structures have been detected in the study area that has an extension of more than 40,000 km²; they seem all connected to the Neo-Proterozoic evaporitic Hormuz Formation and are distributed into two salt sub-basins (North and South) that are divided by a major regional structural high (the Qatar-South Fars Arch).

Two main types of salt structures have been detected: salt pillows (with concordant deep salt core) that are located in both the north and south sub-basins and salt piercing diapirs (structures where the salt perforates the sedimentary succession and can reach the surface) placed only in the south sub-basin.

The structural evolution of 19 not-piercing diapirs has been reconstructed by the interpretation of over 850 seismic lines, depth conversion and analysis of salt activity. The uplift rates of each diapir and the average sedimentation rate in the entire studied area has been estimated by the sequential restoration of 13 key horizons from Early Permian to Holocene (including seabed), using a method that combines 3D unfolding and decompaction techniques.

Salt uplift started already during the Early Paleozoic and persisted until today with pulses of different intensity and average rates of diapir uplift ranging from 0 to 25 m/Ma. The main phases of salt deformation occurred during the Paleozoic (when a continuous, syn-sedimentary growth took place), Middle Triassic, Cenomanian, Late Oligocene and post-Middle Miocene.

Also the sedimentation and the differential sedimentation rates, from Triassic to present time, show strong variations; the mean values of the sedimentation rate range from about 9 (Early Cretaceous) to 65 m/Ma (Late Oligocene), and in the same periods the differential sedimentation reaches its maximum (Late Oligocene - 23 m/Ma) and its minimum rate (Early Cretaceous - 1 m/Ma).

The diapirs apparently do not uplift under the action of tectonic structures; in fact no relevant faults or folds have been identified in the area and the small deformations (essentially faults) visible in the seismic sections seem induced by the diapiric uplift rather than cause salt deformation. Moreover, no clear link between the uplift of the study diapirs and the regional tectonic events potentially acting at the boundary of the Arabian plate has been found.

The major factor that controls the salt uplift is the differential rate of sedimentation that affect the whole study basin (coefficient of correlation between the salt uplift rate and the differential rate of sedimentation = 0.95). The influence of the differential sedimentation apparently induced this downbuilding mechanism of the diapiric growth over long distances (several tens of kilometers) and not only around the single diapirs (rim anticlines).

Geodynamics of northern Victoria Land (Antarctica): the role of the paleozoic lithospheric discontinuities and their reactivation

Crispini L.*¹, Cianfarra P.², Salvini F.², Federico L.¹ & Capponi G.²

1. DISTAV, Università di Genova. 2. Dipartimento di Scienze Geologiche, Università di Roma Tre.

Corresponding email: crispini@dipteris.unige.it

Keywords: Northern Victoria Land, Antarctica, geodynamics.

In the geodynamic evolution of northern Victoria Land, first rank lithospheric discontinuities played a relevant role. The activity of such regional faults during the Ross Orogeny was established by several papers (e.g. Gibson & Wright, 1985; Capponi et al., 1999) and their Cenozoic reactivation was reported by Salvini et al. (1997). On the other hand a late/post-Ross orogeny activity is less understood and has been reported only in the recent literature as well as the Mesozoic reworking, that is responsible for the separation of Antarctica from Australia, Tasmania, New Zealand and the other fragments of the Gondwana puzzle. Along some lineaments the activity continues until present, as proved by GPS determinations in northern Victoria Land (Dubbini et al., 2010).

The aim of this study is to improve the knowledge of the geodynamic evolution of northern Victoria Land, studying the phases of reactivation of the major paleozoic lithospheric discontinuities and trying to disentangle the several reworking of the existing tectonic lineaments; emphasis will be on the fragmentation stage and separation from the other elements of Godwana, and particularly on the Rennick fault damage area.

Methods of study include a multi-scale analysis of the damage zones of the fracture systems along major tectonic discontinuities, analysis of the kinematic indicators, identification of reactivation and fluid circulation. We compare our data with the GPS evidence (Dubbini et al., 2010) and with the present day tectonics as described in the past literature.

Such analysis results in the preparation of a more constrained structural model for the fault pattern of northern Victoria Land, with emphasis on the Rennick Faulting and a reconstruction of the tectonic evolution of the major lithospheric discontinuities, active during the Ross Orogeny, re-activated in a late/post-Ross phase, in the Mesozoic and finally in the Cenozoic; along some lineaments the activity continues until present, in agreement with GPS data.

Capponi G., Crispini L. & Meccheri M. 1999. Structural history and tectonic evolution of the boundary between the Wilson and Bowers terranes, Lanterman Range, northern Victoria Land, Antarctica. *Tectonophysics*, 312, 249-266.

Dubbini M., Cianfarra P., Casula G., Capra A. & Salvini F. 2010. Active tectonics in northern Victoria Land (Antarctica) inferred from the integration of GPS data and geologic setting. *J. Geophys. Res.*, 115, B12421, doi:10.1029/2009JB007123.

Gibson G.M. & Wright T.O. 1985. Importance of thrust faulting in the tectonic development of northern Victoria Land, Antarctica. *Nature*, 315 (6019), 480-483.

Salvini F., Brancolini G., Busetti M., Storti F., Mazzarini F. & Coren F. 1997. Cenozoic geodynamics of the Ross Sea region, Antarctica: crustal extension, intraplate strike-slip faulting, and tectonic inheritance. *J. Geophys. Res.*, 102 (B11), 24669-24696.

Thermal modelling of an oceanic transform domain: implications on rheology and friction along the fault

Cuffaro M.*¹ & Ligi M.²

1. Istituto di Geologia Ambientale e Geoingegneria, C.N.R. Roma Sapienza. 2. Istituto di Scienze Marine, C.N.R. Bologna.

Corresponding email: marco.cuffaro@igag.cnr.it

Keywords: Computational geodynamics, mathematical modeling, thermal modeling.

We use 3-D finite element simulations to investigate the temperature distribution beneath oceanic transform faults. The developed thermal model includes the effects of mantle flow beneath a ridge-transform-ridge geometry and the lateral heat conduction across the transform fault and the shear heating along the fault. Numerical solutions are presented for a 3-D domain, discretized with a non-uniform tetrahedral mesh, where relative plate kinematics is used as boundary condition, providing passive mantle upwelling. The mantle is modelled as a temperature-dependent viscous fluid, and its dynamics can be described using the Stokes equations and thermal effects. The results show that shear heating along the transform significantly raises the temperature along the fault. In order to test model results, we calculated the thermal structure simulating the mantle dynamics beneath an accretionary plate boundary geometry that duplicates the Vema transform (central Atlantic), assuming the present-day spreading rate and direction of the Mid Atlantic Ridge at 11°N. Thus, the modelled heat flow at the surface has been compared with 23 heat flow measurements in the floor of the Vema Fracture Zone. Laboratory studies on the frictional stability of olivine aggregates show that the depth extent of oceanic faulting is thermally controlled and limited by the 600 °C isotherm. The depth of isotherms of the thermal model were compared to the depths of earthquakes along transform faults. Slip on oceanic transform faults is primarily aseismic, only 15% of the tectonic offset is accommodated by earthquakes. Despite extensive fault areas, few large earthquakes occur on the fault and few aftershocks follow large events. Rheology constrained by the thermal model combined with geology and seismicity of the Vema Transform fault allows to better understand friction and the spatial distribution of strength along the fault and provides insight into slip accommodation on oceanic transforms.

Active faulting in the Gulf of Patti (south-eastern Tyrrhenian Sea, Italy): evidences from high resolution seismic profiles and swath bathymetry data

Cultrera F.¹, Burrato P.², Ferranti L.³, Monaco C.*¹, Morelli D.⁴, Passaro S.⁵ & Pepe F.⁶

1. Dipartimento di Scienze Biologiche, Geologiche e Ambientali - Sezione di Scienze della Terra, Università di Catania. 2. Istituto Nazionale di Geofisica e Vulcanologia, Roma 1. 3. Dipartimento di Scienze della Terra, delle Risorse e dell'Ambiente, Università di Napoli "Federico II". 4. Dipartimento di Matematica e Geoscienze, Università di Trieste. 5. Istituto per l'Ambiente Marino Costiero, C.N.R. Napoli. 6. Dipartimento di Scienze della Terra e del Mare, Università di Palermo.

Corresponding email: emonaco@unict.it

Keywords: South-eastern Tyrrhenian Sea, seismic profiles, active tectonics.

The Gulf of Patti (south-eastern Tyrrhenian Sea, Italy), a marine area separating the central Aeolian volcanic islands from the north-eastern Sicily, is one of most seismically active sector of the southern Tyrrhenian back-arc basin. Over the period 1999-2013, about 600 earthquakes with small-to-moderate magnitude ($1.0 \leq ML \leq 4.8$) and a maximum hypocentral depth of 30 km were registered in this sector. Furthermore, historical dataset revealed that the same area was shaken by a $M = 5.6$ event in April 1978 which caused several damages in the surrounding localities. Available focal solutions indicate that faulting mostly occurs by strike-slip, subordinately normal and reverse kinematics. The main tectonic feature affecting the investigated area is represented by a NNW-SSE trending right-lateral strike-slip fault system called "Aeolian-Tindari-Letojanni" (ATLFS) which has been interpreted as a lithospheric transfer zone extending from the Aeolian Islands to the Ionian coast of Sicily and separating two different tectonic compartments: a contractional one to the west and an extensional one to the north-east. This lithospheric boundary represents an important tectonic element playing a key role in the geodynamics, seismicity and volcanism of southern Tyrrhenian Sea. However, although its large-scale role is widely accepted, several issues about its structural architecture (i.e., distribution, attitude, and slip of fault segments) are poorly constrained and no correlation between faults and seismicity have been satisfactorily produced particularly in the offshore.

In order to better understand the structural and morpho-structural setting of the ATLFS along this sector of the southern Tyrrhenian Sea, we performed high-resolution multi-channel seismic reflection and multibeam survey. This study allowed us to detected several fault segments distributed into two major NW-SE and NE-SW trending systems which also involve Holocene deposits. As suggested by displaced reflectors, detected faults show a prevailing extensional motion even though clues of strike-slip movement along some segments can be inferred. Several faults dislocate the seafloor forming steep scarps and are characterized by an intense seismicity clustered along the same direction. Activity along these faults is also corroborated by the relative focal solutions which indicate a comparable attitude and kinematics. The coexistence of normal and reverse faulting mechanisms within a larger strike-slip fault system can be explained as the result of fault overlapping which may give rise restraining step-over and releasing bend structures.

In conclusion, our analysis suggests the occurrence of active faults that can be interpreted as seismogenic sources useful for the reevaluation of the seismic hazard of this sector of southern Tyrrhenian Sea.

Subsoil geological model of the Leghorn area (Ligurian sea coast, Italy): a stratigraphic approach

Da Prato S.*, Catanzariti R., Ellero A. & Masetti G.

Istituto di Geoscienze e Georisorse, C.N.R. Pisa.

Corresponding email: simone.daprato@igg.cnr.it

Keywords: Stratigraphy, geological model, micropaleontology.

The Leghorn area is located in the North West of Italy, on the Ligurian Sea coast. This is a highly urbanized area with all its consequent environmental issues, including soil pollution, saltwater intrusion, groundwater contamination and soil sealing which led to an increasing attention of the public administration and to the development of scientific research in environmental field.

While the morphological alteration of the territory connected with the rapid urbanization has caused the obliteration of most of the outcrops, on the other side the development of building activities provided new elements for the subsoil stratigraphic knowledge as boreholes and ephemeral outcrops.

Through a multidisciplinary study of these data, involving stratigraphical, lithological-sedimentological and micropaleontological information, a subsoil geological model was realized, aimed at the study of the groundwater resource. This model, taking into account literature data as well (Barsotti et al., 1974; Dall'Antonia et al., 2004; Bossio et al., 2009; Ciampalini et al., 2013), provides 12 stratigraphic-depositional units, which constitute the neogenic-Quaternary sedimentary sequence in the subsoil of the Leghorn area, corresponding to the polycyclic "Leghorn Terrace" (Barsotti et al., 1974; Boschian et al., 2006).

Biostratigraphic data, focused mainly on ostracods, foraminifers and calcareous nannofossils, and facies analysis of identified stratigraphic units, were used for defining the palaeoenvironmental evolution, that represents an important element in providing a detailed reconstruction of the subsoil geology.

Such a model is an essential tool to constrain aquifer dynamics, supporting the management of the natural resources.

Barsotti G., Federici P.R., Giannelli L., Mazzanti R. & Salvatorini G. 1974. Studio del Quaternario livornese, con particolare riferimento alla stratigrafia ed alle faune delle formazioni del Bacino di carenaggio della Torre del Fanale. *Mem. Soc. Geol. It.*, 13, 425-495.

Boschian G., Bossio A., Dall'Antonia B. & Mazzanti R. 2006. Il Quaternario della Toscana costiera. *Studi costieri*, 12, 208.

Bossio A., Ciampalini A., Colonese A.C., Da Prato S., Rafanelli A. & Zanchetta G. 2008. Nuovi dati sulle successioni del sottosuolo di Livorno. *Atti Soc. Tosc. Sci. Nat. Mem. Serie A*, 113, 13-24.

Ciampalini A., Da Prato S., Catanzariti R., Colonese A.C., Michelucci L. & Zanchetta G. 2013. Subsurface stratigraphy of middle Pleistocene continental deposits from Livorno area and biostratigraphic characterization of the Pleistocene substrate (Tuscany, Italy). *Atti Soc. Tosc. Sci. Nat. Mem. Serie A*, 120.

Dall'Antonia B., Ciampalini A., Michelucci L., Zanchetta G., Bossio A. & Bonadonna F.P. 2004. New insights on the Quaternary stratigraphy of the Livorno area as deduced by borehole investigations. *Boll. Soc. Pal. It.*, 43, 141-157.

Modelling of volcanoes: the Mt. Vesuvius

De Matteo A.*⁴, Castaldo R.¹, D'Auria L.¹⁻², James M.R.³, Lane S.³, Massa B.²⁻⁴, Pepe S.¹ & Tizzani P.¹⁻²

1. Istituto per il Rilevamento Elettromagnetico Ambiente, C.N.R. Napoli.
2. Istituto Nazionale di Geofisica e Vulcanologia, Osservatorio Vesuviano, Napoli.
3. Lancaster Environment Centre, Lancaster University, Lancaster, UK.
4. Dipartimento di Studi Geologici ed Ambientali, Università del Sannio.

Corresponding email: massa@unisannio.it

Keywords: Modelling, volcanoes, Vesuvius.

Analogue modelling of volcanic edifices represents a useful tool to investigate deformation styles. We built analogue models using a multilayer of brittle and ductile media mimicking the actual structure of studied volcanoes. Models were monitored by multiple digital time-lapse cameras which enabled sub-millimetric deformations to be measured.

Somma-Vesuvius is a quiescent strato-volcano, lying on a substratum consisting of a Mesozoic carbonatic basement, overlapped by Holocene clastic sediments and volcanic rocks. The volcanic edifice comprises a volcanic cone (The Gran Cono) lying within an asymmetric caldera (Mt. Somma). The Somma caldera is the result of at least 7 Plinian eruptions, the last of which was the 79 CE. Pompeii eruption.

Geophysical and geological evidences (e.g. geodetic measurements, geological and structural data, seismic profiles and surface deformation analysis with DInSAR) indicate for the Somma-Vesuvius an ongoing spreading deformation.

We investigated the spreading processes and associated surface deformation pattern by performing analogue experiments. Our models reproduced the complex shape of the Somma-Vesuvius (at a scale 1:100,000), by using a small cone placed on a large truncated cone. The volcanic edifice was emplaced on a sand layer (mimicking rocks with a brittle behaviour) laid on a silicone layer (mimicking rock layers with an overall ductile behaviour).

Models are based on the Fluid-dynamics Dimensionless Analysis (FDA), according to the Buckingham- Π theorem. During a testing procedure the thickness of the basal sand layer and of the silicone one were varied to find the best configuration. Image sequences from three digital SLR cameras were processed to derive 3-D models and retrieve sub-millimetric vertical and horizontal displacements. Results were compared with the 1992-2010 DInSAR measurements of ground deformations obtained using ERS-ENVISAT satellite data.

The preliminary results confirm that analogue models are able to reproduce the actual Somma –Vesuvius observed ground deformation pattern both in the direction and in the intensity field.

Further studies will be devoted at find the best combination of parameters (media rheology and thicknesses) to best fit the observations. These studies will be integrated with new meso-structural and surface deformation (DinSAR) data, and with numerical modelling.

Graviquakes

Doglioni C. *¹⁻², Carminati E. ¹⁻², Petricca P. ¹⁻³ & Riguzzi F. ⁴

1. Dipartimento di Scienze della Terra, Sapienza Università di Roma. 2. Istituto di Geologia Ambientale e Geoingegneria, CNR, Roma.
3. now at GFZ-German Research Centre for Geosciences, Potsdam, Germany. 4. INGV, Roma.

Corresponding email: carlo.doglioni@uniroma1.it

Keywords: Earthquakes, normal faults, graviquakes.

Earthquakes are dissipation of energy throughout elastic waves. Canonically is the elastic energy accumulated during the interseismic period. However, in crustal extensional settings, gravity is the main energy source for hangingwall fault collapsing. Gravitational potential is about 100 times larger than the observed magnitude, far more than enough to explain the earthquake. Therefore, normal faults have a different mechanism of energy accumulation and dissipation (graviquakes) with respect to other tectonic settings (strike-slip and contractional), where elastic energy allows motion even against gravity. The bigger the involved volume, the larger is their magnitude. The steeper the normal fault, the larger is the vertical displacement and the larger is the seismic energy released. Normal faults activate preferentially at about 60° but they can be shallower in low friction rocks. In low static friction rocks, the fault may partly creep dissipating gravitational energy without releasing great amount of seismic energy. The maximum volume involved by graviquakes is smaller than the other tectonic settings, being the activated fault at most about three times the hypocentre depth, explaining their higher b-value and the lower magnitude of the largest recorded events. Having different phenomenology, graviquakes may show peculiar precursors such as foreshocks along the conjugate antithetic dilated wedge, initial hangingwall subsidence and increase of the fluids flux. Application to the Italian extensional areas will be shown.

Stable isotope stratigraphy and chronology of Langhian marine records from St. Peter's Pool section (central Mediterranean, Malta Island)

Lirer F.¹, Foresi L.M.², Vallefucio M.¹, Baldassini N.^{*3}, Correggia C.¹, Di Stefano A.³, Ferraro L.¹,
Pelosi N.¹, Russo B.⁴ & Sagnotti L.⁵

1. Istituto per l'Ambiente Marino Costiero, C.N.R. Calata Porta di Massa (NA). 2. Dipartimento di Scienze Fisiche, della Terra e dell'Ambiente, Università di Siena. 3. Dipartimento Scienze Biologiche, Geologiche e Ambientali, Università di Catania. 4. Dipartimento di Scienze della Terra, dell'Ambiente e delle Risorse, Università di Napoli "Federico II". 5. Istituto Nazionale di Geofisica e Vulcanologia, Sez. Roma2.

Corresponding email: nbaldas@unict.it

Keywords: Stable isotope stratigraphy, Langhian Stage, central Mediterranean.

The St. Peter's Pool section, which outcrops in the Delimara Peninsula (south-eastern coast of the Malta Island) and belongs to the Upper Globigerina Limestone Member, presents a continuous and well preserved deep marine record for the Langhian time interval (Foresi et al., 2011). The 31 meter thick sedimentary record is characterized by cyclic alternations of calcareous marl, marly limestone and jutting bioturbated hardened limestone and lies on the well-known C2 (Pedley, 1975) phosphate-rich bed.

Biostratigraphic data (Foresi et al., 2011) suggest that the St. Peter's Pool sedimentary record spans a time interval of about 1.2 My (from 15.3 to 16.5 Ma). Oxygen and carbon stable isotope analyses performed on planktonic foraminifera *Globigerinoides quadrilobatus* (surface water proxy) and on benthic foraminifera *Cibicides dutemplei* (deep water proxy), show a good correlation with amplitude oscillation of the astronomical parameter of eccentricity. In particular, $\delta^{18}\text{O}$ *G. quadrilobatus* light values are in phase with eccentricity maxima and $\delta^{13}\text{C}$ *G. quadrilobatus* maxima are in phase with 400 kyr eccentricity minima. Major increases in $\delta^{13}\text{C}$ *C. dutemplei* record document the onset of the carbon isotope events CM3a, CM3b and CM4. In addition, the strong shift in $\delta^{13}\text{C}$ benthic data from open ocean ODP-site 1146, dated about 15.6 Ma, is also documented in the St. Peter's Pool sedimentary record.

Foresi L.M., Verducci M., Baldassini N., Lirer F., Mazzei R., Salvatorini G., Ferraro G. & Da Prato S. 2011. Integrated stratigraphy of St. Peter's Pool section (Malta): new age for the Upper Globigerina Limestone Member and progress towards the Langhian GSSP. *Stratigraphy*, 8, 125-143.

Pedley H.M. 1975. Oligocene-Miocene stratigraphy of the Maltese islands. Unpubl. Ph.D. Thesis, University of Hull.

Quaternary slip rates along the frontal thrust system of the Pede-Apennine margin, between the Enza and Panaro valleys, Emilia Romagna, Italy

Maestrelli D.*¹, Bonini M.² & Sani F.¹

1. Dipartimento di Scienze della Terra, Università di Firenze. 2. Istituto di Geoscienze e Georisorse, CNR, Firenze.

Corresponding email: daniele.maestrelli@for.unipi.it

Keywords: Pede-Apennine Thrust Front, slip rates, trishear.

The study area is located on the Emilia Pede-Apennine Margin, between the Reno and the Enza valleys. This area is marked by the Pede-Apennine Thrust Front (PTF) (Boccaletti et al., 1985), which separates the internal sectors of the Northern Apennines from the external thrust fronts (ETF), buried underneath the Quaternary deposits of the Po Plain. Growth strata layouts, related to PTF activity, can be observed in discontinuous outcrops along the Pede-Apennine Margin. In this study, the reconstruction of Quaternary deformation rates was addressed by means of the analysis of growth strata and structural field data. Therefore, we carried out a structural and geological survey of the stratigraphic units that present a growth strata layout. We collected a dataset made up of mesoscopic joints and faults to which the application of a stress inversion procedure yielded a sub-horizontal N-NE-oriented s_1 . Two sets of numerical models (for a total of 104) were built considering two transects across the PTF, referred herein to as Quattro Castella and Scandiano, where the SSW-dipping Pede-Apennine thrust (PAT, which is the main PTF structure), is nearly surfacing along the margin. The Trishear Fault-propagation Folding mechanism (Erslev, 1991) was applied to the considered transects by using the software Fault Fold (Allmendinger, 1998). For both transects a best fit model was chosen, by comparing the geological data with the obtained outputs. With the data provided by the best fit models, we then obtained the PAT deformation rates in the study area. At Quattro Castella, averaged minimum values over the last 1,07 Myr, are: slip rate 0,79 mm/yr, propagation rate 1,96 mm/yr, shortening rate 0,50 mm/yr, and uplift rate 0,62 mm/yr. At Scandiano averaged minimum values over the last 800 kyr are: slip rate 0,70 mm/yr, propagation rate 2,10 mm/yr, shortening rate 0,44 mm/yr, and uplift rate 0,59 mm/yr. The obtained values are compatible with others determined in adjoining areas, and thus can be considered representative of the PAT in the analysed sector. Finally, our models suggest that, along the considered transects, the PAT is best depicted as a high-angle thrust fault ($> 50^\circ$).

Allmendinger R.W. 1998. Inverse and forward numerical modelling of trishear fault propagation-folds. *Tectonics*, 17, 640-656.

Boccaletti M., Coli M., Eva C., Ferrari G., Giglia G., Lazzarotto A., Merlanti F., Nicolich R., Papani G. & Postpichl D. 1985. Consideration on the seismotectonics of the Northern Apennines. *Tectonophysics*, 117, 7-38.

Erslev E.A. 1991. Trishear fault-propagation folding. *Geology*, 19, 617-620.

Multidisciplinary geophysical approach for investigating the recent activity of blind tectonic structures in the eastern sector of the Po Plain (North Italy)

Mantovani A.*¹, Abu-Zeid N.¹, Bignardi S.¹, Caputo R.¹, Palmieri F.² & Santarato G.¹

1. Dipartimento di Fisica e Scienze della Terra, Università di Ferrara. 2. Istituto Nazionale di Oceanografia e di Geofisica Sperimentale, Centro di Ricerche Sismologiche, Trieste.

Corresponding email: ambra.mantovani@unife.it

Keywords: Po Plain, geophysical surveys, recent tectonic activity.

The bending of the topographic surface and the consequent uplift of the broader epicentral area are among the major coseismic effects due to the reactivation of reverse blind faults as, for example, in the case of the Northern Apennines underlying the Po Plain (Okada, 1985; Bignami et al., 2012). Determining the uplift spatial distribution is crucial for reconstructing the recent tectonic evolution of the region as well as for understanding where active faults are located, and which is their probable seismogenic potential. With this premise, we carried out a set of geophysical surveys across some major tectonic structures of the eastern Po Plain. The investigations included several passive seismic measurements carried out along two profiles, ca. 27 km-long and oriented SSW-NNE, *i.e.* almost perpendicular to the regional trend of the buried structures of the Ferrara Arc. The western one runs between Cento and Bondeno, while the eastern one between Traghetti (near Molinella) and Formignana. We used the ESAC (Aki, 1957; 1964) and Re.Mi. (Louie, 2001) strategies to reconstruct pseudo-2D shear wave velocity sections, providing information about the shallow subsurface (100-150 m depth), and the HVSr technique (Nakamura, 1989) to infer the depth of the major impedance contrasts. In addition, in order to deduce the subsurface density distribution along the eastern profile and to increase the investigation depth of the former seismic methods (down to some km), we carried out a gravimetric survey. Assuming that the overall Vs pattern is determined by lithological variations, the pseudo-2D sections allow to emphasize the occurrence of buried anticlinal structures in correspondence with the higher velocity gradients due to a 'condensed' stratigraphy. Conversely, where gradients are lower, the thickness of the coeval sedimentary units is greater (*i.e.* synclinal structures). The reconstructed shear wave velocity profiles document the possibility to detect the recent tectonic activity of buried structures underlying the Po Plain by means of low-cost geophysical surveys. The comparison with the location of the major tectonic structures at greater depths as inferred using the support of the gravimetric survey and some available seismic reflection profiles suggests that the shallow stratigraphic variations highlighted in this research may be directly associated with a recent activity of the buried folds.

- Aki K. 1957. Space and time spectra of stationary stochastic waves with special reference to microtremors, Bull. Earthq. Res. Inst., 35, 415-456.
- Aki K. 1964. A note on the use of microseisms in determining the shallow structures of the earth's crust. Geophysics, 29, 665-666.
- Bignami C., Burrato P., Cannelli V., Chini M., Falcucci E., Ferretti A., Gori S., Kyriakopoulos C., Melini D., Moro M., Novali F., Saroli M., Stramondo S., Valensise G. & Vannoli P. 2012. Coseismic deformation pattern of the Emilia 2012 seismic sequence imaged by Radarsat-1 interferometry. Ann Geophys., 55, 788-795, doi:10.4401/ag-6157.
- Louie J.N. 2001. Faster, Better: Shear-Wave Velocity to 100 Meters Depth from Refraction Microtremor Arrays. Bull. Seism. Soc. Am., 91, 347-364.
- Nakamura Y. 1989. A method for dynamic characteristics estimation of subsurface using microtremor on the ground surface. Quarterly Report of the Railway Technical Res. Inst., 30, 25-30.
- Okada Y. 1985. Surface deformation due to shear and tensile faults in a half-space. Bull. Seism. Soc. Am., 75, 1135-1154.

Sandstone provenance and biostratigraphy of Modino Unit stratigraphic succession (Lutetian-Aquitanian): a key stage of the Northern Apennine foreland basin

Marchi A.*¹, Pandolfi L.¹⁻² & Catanzariti R.²

1. Dipartimento di Scienze della Terra, Università di Pisa. 2. Istituto di Geoscienze e Georisorse, CNR Pisa.

Corresponding email: alessandra.marchi@dst.unipi.it

Keywords: Northern Apennine, biostratigraphy, sandstone provenance.

The Northern Apennine foredeep is one of the most classic examples of deep-water turbidite basin associated to the development of an orogenic wedge. The sediment fill of this basin mainly consists of deep-water sandstone that were progressively incorporated into the frontal part of the orogen during its eastward thrust propagation and depocentre migration.

The Eocene-Oligocene succession of the Modino tectonic Unit (Tuscan Domain of the Northern Apennine) is a turbiditic sequence deposited during the early collisional and post-collisional stages of the orogen. The meaning of this unit in the Northern Apennine foredeep-belt system of the is not yet clear.

In this work a multidisciplinary approach, consisting of biostratigraphy, high-resolution stratigraphy and provenance analysis, was applied on Modino Unit turbiditic succession in order to understand the main characteristics of its basin and try to give a paleotectonic reconstruction.

The nannoplankton analyses indicate that Modino Unit succession ages is comprised between MNP15 (Lutetian) and MNN1d (Aquitanian) biozones.

The petrographical analysis on arenites show a change in sandstones compositions from the basal to the upper part of the Modino Unit succession, underlined by the decreasing of ophiolitic rock fragments, radiolaritic rock fragments and extrabasinal carbonates (from Lutetian to Aquitanian sandstones).

The data coming from the detailed stratigraphical analysis suggests that the lower part of Modino Unit is influenced by sediment failures and submarine landslides from a proximal and intermittent source, that is represented by the Apenninic Prism.

We think that the lower part of Modino Unit succession (Lutetian-Rupelian) probably represents a stage of dominant Apenninic sedimentation influenced by an high tectonic activity. Although the presence of ponding structures in the basal part of this unit suggests the confinement of the flows, and these evidences can be interpreted like a stage of piggy-back or wedge-top basin sedimentation for the older part of the succession.

While the upper part of the unit, Rupelian-Aquitanian in ages, seems to be less influenced by the “Apenninic source”, and confinement structures are not recognized. A comparison with the literature data suggest that only the upper part of Modino Unit succession can be compared with the Macigno Fm. of Tuscan Nappe. This new data suggests that the turbiditic sedimentation with “Alpine provenance” for the Modino Unit occurs not late than Rupelian (biozone MNP21).

Active deformation in the NW sector of the Sicily Channel based on multiscale seismic profile analysis

Meccariello M.*¹, Ferranti L.¹ & Pepe F.²

1. Dipartimento di Scienze della Terra, dell'Ambiente e delle Risorse (DiSTAR), Università di Napoli "Federico II"

2. Dipartimento di Scienze della Terra e del Mare, Università di Palermo

Corresponding email: melania.meccariello@unina.it

Keywords: NW Sicily Channel, seismic profiles, active shortening.

The NW sector of the Sicily Channel spans the frontal part of the Sicilian-Maghrebian chain. Despite this Channel sector was investigated since the 1960's (Argnani et al., 1986; Antonelli et al., 1988; Catalano et al., 1993), and more recent work has shed light on the geodynamic framework (Corti et al., 2006; Civile et al., 2014), the recent tectonic evolution is not defined in detail. In this perspective, our analysis deals with the recognition and characterization of the main Neogene-Quaternary structures in the area between the Egadi Islands and the Sciacca High. The analysed data consist of multichannel seismic reflection profiles (both from VIDEPI database and from industry) integrated with well log data, and of unpublished high-resolution Sparker profiles.

The seismo-stratigraphic analysis reveals a positive inversion of pre-existing structures separating the Trapanese and Saccense domains, and confirms the already proposed space-time migration of contractional fronts towards the SE. In particular, two foredeep basin are recognized: the older is related to the Middle-Upper Miocene emplacement of the western front (the Maghrebian Thrust Front, MTF) of the chain; the younger is associated to the eastern front (the Adventure Thrust Front, ATF) formed during the Pliocene-Pleistocene (Argnani et al., 1986; Antonelli et al., 1988).

The ATF is the offshore prolongation of the Campobello di Mazara-Castelvetrano alignment, that recent works has shown to be still active and related to the Belice seismogenic area (Barreca et al., 2014).

The joint interpretation of multiscale seismic data points out that NW-SE trending shortening is active in the offshore as well, and is characterized by folding of the recent most depositional sequences. Active shortening is accommodated along high angle NNW-dipping thrust ramps akin to the structure proposed as a possible source for the 1968 Belice earthquake sequence (Monaco et al., 1996).

- Antonelli M., Franciosi R., Pezzi G., Querci A., Ronco G.P. & Vezzani F. 1991. Paleogeographic evolution and structural setting of the northern side of the Sicily Channel. *Mem. Soc. Geol. It.*, 41, 141-157.
- Argnani A., Cornini S., Torelli L. & Zitellini N. 1986. Neogene-Quaternary foredeep system in the Strait of Sicily. *Mem. Soc. Geol. It.*, 36, 123-130.
- Barreca G., Bruno V., Cocorullo C., Cultrera F., Ferranti L., Guglielmino F., Guzzetta L., Mattia M., Monaco C. & Pepe F. 2014. Geodetic and geological evidence of active tectonics in south-western Sicily (Italy). *J. Geodin.*, 82, 138-149.
- Catalano R., Di Stefano P., Nigro F. & Vitale F.P. 1993. Sicily mainland and its offshore: a structural comparison. In: Max M.D. & Colantoni P. Eds., *Geological development of the Sicilian-Tunisian Platform*. UNESCO Rep. Mar. Sci., 58, 19-24.
- Civile D., Lodolo E., Alp H., Ben-Avraham Z., Cova A., Baradello L., Accettella D., Burca M. & Centonze J. 2014. Seismic stratigraphy and structural setting of the Adventure Plateau (Sicily Channel). *Mar. Geophys. Res.*, 35, 37-53.
- Corti G., Cuffaro M., Doglioni C., Innocenti F. & Manetti P. 2006. Coexisting geodynamic processes in the Sicily Channel. *Geol. Soc. Am., Sp. Paper*, 409, 83-96.
- Monaco C., Mazzoli S. & Tortorici L. 1996. Active thrust tectonics in western Sicily (southern Italy): the 1968 Belice earthquakes sequence. *Terra Nova* 8, 372-381.

Neogene re-activation of the Pernambuco Lineament (NE-Brazil): onshore and offshore evidence

Nestola Y.*¹, Balsamo F.¹, Storti F.¹, Ligi M.², Bezzerra F.H.R.³ & Nogueira F.C.⁴

1. Dipartimento di Fisica e Scienze della Terra, Università di Parma. 2. Istituto di Scienze Marine, Geologia Marina, C.N.R. Bologna.

3. Department of Geology, Federal University of Rio Grande do Norte, Brazil.

4. Department of Mechanical Engineering, Federal University of Campina Grande, Brazil.

Corresponding email: yago.nestola@unipr.it

Keywords: Barreiras Formation, NE-Brazil, Pernambuco Fracture Zone.

We performed a structural field survey on the coastal region of the Pernambuco State (NE-Brazil), where the marine Miocene Barreiras sandstones and the overlying post-Barreiras continental sediments are affected by faults with cm- to several m-offsets. The top of the Barreiras sandstones is provided by a Tortonian lateritic paleosoil. We collected structural data that indicate mainly extensional deformations and strike-slip faulting along N-S, WNW-ESE, and NE-SW trends. Faults in the Barreiras sandstones strike mainly WNW-ESE, with also N-S and NE-SW directions, whereas in the post Barreiras sediments only the last two fault orientations occur.

To investigate the possible geodynamic reasons driving such post-rift deformation pattern, we analyzed the distribution of the spreading rates in the Atlantic Ocean sector between the Chain and the Ascension fracture zones. This sector includes the Pernambuco Fracture Zone (PeFZ). Seismic surveys show positive topography when cross-cutting the PeFZ, with different ages and distinct cooling and subsidence evolution at the juxtaposed sides. The activity of the Ascension hotspot may have enhanced the oceanic crust accretion on PeFZ southern side, thus imprint a major right-lateral excess transform shear during the deposition of the Barreiras Formation. A main rotation of the eulerian pole at about 10 Ma (e.g. Bonatti et al., 2005) cause switch to left-lateral shear excess along PeFZ. This evidence provides a kinematic framework for interpreting our structural data as resulting from the onshore accommodation of the oceanic shear transferred along the Pernambuco Fracture Zone. In particular, the fault pattern in the Barreiras Formation fits into a right-lateral strike-slip kinematics, whereas brittle deformation in the post-Barreiras can be explained as resulting from left-lateral shearing along the onshore Pernambuco Lineament. Our data indicate that in the South America plate some post-rift excess transform shear has being transferring from the ocean into the continent.

Bonatti E., Brunelli D., Buck W.R., Cipriani A., Fabretti P., Ferrante V., Gasperini L. & Ligi M. 2005. Flexural uplift of a lithospheric slab near the Vema transform (Central Atlantic): Timing and mechanisms. *Earth Planet. Sci. Lett.*, 240, 642-655.

Diverse pattern of strain at the Afar Triple Junction

Pagli C.*¹, Ebinger C.², Keir D.³ & Wang H.⁴

1. Dipartimento di Scienze della Terra, Università di Pisa.
2. Department of Earth & Environmental Sciences, University of Rochester, USA.
3. National Oceanography Centre Southampton, University of Southampton, UK.
4. Department of Surveying Engineering, Guangdong University of Technology, P.R. China.

Corresponding email: carolina.pagli@unipi.it

Keywords: Afar, rifting, InSAR.

Strain and seismicity show us the mode by which deformation is accommodated in rifting continents. Here we present a combined analysis of InSAR derived strain maps and seismicity of the Afar triple junction from 2006 to 2010. Our analysis shows that the plate spreading motion is accommodated in different modes. A dogbone-shaped seismicity and strain distribution dominates the northern branch of the triple junction, likely as a result of repeated dike intrusions during 2005-2010. In the eastern branch strain is distributed across the central part of several overlapping rifts while seismicity appears decoupled from strain and it focuses at the rifts tips. A third branch shows a narrow and elongated zone of both high strain and seismicity. The pattern suggest that the history of magmatic intrusions and rifting events creates a diverse triple junction accommodation zone.

Paleomagnetism of the Hyblean Plateau, Sicily: A review of the existing data set and new evidence from the Scicli-Ragusa Fault System

Pellegrino A.*¹, Maniscalco R.¹, Speranza F.², Hernandez-Moreno C.² & Sturiale G.¹

1. Dipartimento di Scienze Biologiche, Geologiche e Ambientali, Università di Catania.

2. Istituto Nazionale di Geofisica e Vulcanologia, Roma

Corresponding email: alessandra.g.pellegrino@gmail.com

Keywords: Paleomagnetism, Sicily, block rotation.

Several paleomagnetic data from the Hyblean Plateau of SE Sicily pointed out that the plateau did not undergo any significant rotation with respect to Africa (Schult, 1973; Barberi et al., 1974; Gregor et al., 1975; Grasso et al., 1983). However, Besse et al. (1984) suggested a counterclockwise rotation of about 15° of the Hyblean Plateau with respect to Africa acquired during the Pliocene-Pleistocene rifting of the Pelagian Block in the Strait of Sicily. Additionally, the Hyblean Plateau is dissected by an important tectonically active dextral strike-slip zone, the Scicli-Ragusa Fault System (SRFS), but the possibility that strike-slip tectonics yielded block rotations was never taken into account.

We re-evaluated the existing paleomagnetic data set from the Hyblean Plateau using updated paleo-poles from Africa (Torsvik et al., 2008) and, to explore block rotation pattern along the SRFS, we paleomagnetically sampled 13 sites (133 samples). Measurements were carried out in the shielded room of the paleomagnetic laboratory of the INGV (Roma), using a 2G Enterprises DC-superconducting quantum interference device cryogenic magnetometer. The entire data set confirmed that the Hyblean Plateau did not rotate with respect to Africa and that no significant rotation was induced by the rifting in the Strait of Sicily. The data from the northern sector of the SRFS, showed that blocks within 10 km from the fault are not significantly rotated. Therefore, the SRFS did not induce significant rotations around vertical-axis, and the horizontal displacement along this tectonic feature has to be considered less than 3 Km.

Barberi F., Civetta L., Gasparini P., Innocenti F., Scandone R. & Villari L. 1974. Evolution of a section of the Africa-Europe plate boundary: paleomagnetic and volcanologic evidence from Sicily. *Earth Planet. Evol. Sci.*, 3, 207-221.

Besse J., Pozzi J.P., Mascle G. & Feinberg H. 1984. Paleomagnetic study of Sicily: consequences for the deformation of Italian and African margins over the last 100 million years. *Earth Planet. Sci. Lett.*, 67, 377-390.

Grasso M., Lentini F., Nairn A.E.M. & Vigliotti L. 1983. A geological and paleomagnetic study of the Hyblean volcanic rocks. *Tectonophysics*, 98, 271-295.

Gregor C.B., Nairn A.E.M. & Negendank J.F.W. 1975. Paleomagnetic investigations of the Tertiary and Quaternary rocks: the Pliocene of Southeast Sicily and some Cretaceous rocks from Capo Passero. *Geol. Rundsch.*, 64, 3, 948-958.

Schult A. 1973. Paleomagnetism of Upper Cretaceous volcanic rocks in Sicily. *Earth Planet. Sci. Lett.*, 19, 97-103.

Torsvik T., Müller R., Van Der Voo R., Steinberger B. & Gaina C. 2008. Global plate motion frames: toward a unified model. *Rev. Geophys.*, 46, 3, RG3004, doi:10.1029/2007RG000227.

Towards a seismotectonic map of Bulgaria

Piccardi L.*¹, Dobrev N.², Moratti G.¹, Corti G.¹, Vannucci G.³ & Matova M.²

1. Istituto di Geoscienze e Georisorse, C.N.R. Firenze. 2. Geological Institute, Bulgarian Academy of Science, Sofia, Bulgaria.
3. Istituto Nazionale di Geofisica e Vulcanologia, Bologna.

Corresponding email: piccardi@geo.unifi.it

Keywords: Active tectonics, seismotectonics, Bulgaria.

Several large earthquakes reaching up to $M > 7$ have affected Bulgaria, and testify a significant active tectonics whose associated seismicity threatens large portions of the territory. A detailed knowledge of the main active faults and the understanding of the current tectonic activity and seismicity is therefore fundamental to get a comprehensive picture of the seismotectonics of the region. We have undertaken a study based on field survey, seismicity and paleostress analysis, remote sensing and digital topography interpretation, and integrated this information in a comprehensive map of active faults. This exhaustive dataset provides fundamental information on the state of stress and the seismic proneness of different areas, and represents a first valuable step toward the elaboration of a complete and actualized seismotectonic map of Bulgaria. This has obvious implication for the study of seismic hazard, urban planning and civil protection and gives basic information to the knowledge of the active deformation and geodynamics of the region. Few examples highlight the information that can be derived from such a seismotectonic map.

Southern Bulgaria, south of the Balkan mountains, is mainly affected by normal active faults, which accommodate a roughly N-S to NNE-SSW extension, which is likely related to the northern extent of the Aegean extensional system. Activity of these extension-related structures is responsible for some of the destructive earthquakes which affected Bulgaria in historical times, notably the 1904 Krupnik earthquake ($7.2 < M < 7.8$) due to slip on a major E-W-trending normal fault system.

In the **Balkan mountains** area the active tectonics is more complex, with different kinematics affecting the eastern, central and western sectors of the chain. In the **eastern sector**, focal mechanisms range from purely compressional to strike slip, with P-axis oriented about ESE-WNW. Nonetheless, major normal faults characterize the southern front of the Balkan mountains. Faults are roughly E-W oriented and arranged in an en echelon pattern, to form a right lateral shear zone, compatible with the P-axis indicated by focal mechanisms. In the **western sector**, the southern front of the Balkan mountains results as well composed of a series of almost E-W directed normal faults arranged in an en echelon pattern, whose architecture reveals a component of left lateral shear zone, coherent with a roughly E-W directed horizontal compression. In the **central sector**, the southern border of the Balkan mountain is instead marked by a single frontal thrust. This apparent inconsistency of the tectonic style along the front may be explained only by a partial lateral extrusion of this sector, implying bending of the chain in response to a stress parallel to its axis. Our study shows therefore that the complex coexistence of different tectonic styles and stress regimes in the active deformation of the region may be explained in a simple coherent geodynamic framework.

Active tectonics of Northern Apennines from digital and high resolution topography

Piccardi L.

Istituto di Geoscienze e Georisorse, C.N.R. Firenze.

Corresponding email: piccardi@geo.unifi.it

Keywords: Active tectonics, digital topography, Northern Apennines.

Locating active/capable fault traces and mapping fault topography is basic both to understand on-going geodynamics and for seismic hazard assessment. Moreover, capable faults are expected to rupture/deform the ground surface in the near future, so that surface faulting represents a serious hazard for infrastructures and buildings and is therefore a relevant geohazard to be considered in the seismic microzonation studies. Fault capability is not restricted to strong magnitude events, being observed also aseismically (creep) or in shallow small magnitude events.

In this talk, we shall examine a few key areas in Northern Apennines, with particular focus on the north-western area, and illustrate some evidence of active tectonic structures, whose analysis allows insight into the present tectonic deformation of this sector of the Apennines chain. Our analysis permits to include all active tectonic structures into a single homogeneous deformation framework corresponding to a simple kinematic tectonic model of active deformation and provide insight into the appropriate geodynamic context. In general, the geodynamics of the Apennines reflects the classical scheme of subduction and back arc regime, involving an internal extensional domain and an external compressional domain, orthogonal to the chain axis. However, our study confirms the relevance of components of horizontal shear in the present-day deformation of Northern Apennines. Our results are in agreement with GPS data on the present day motion of the different sectors of the Apennines, which show that both external and internal sectors are moving to the north, but at different rates and direction: the external one with rates of 3-5 mm/yr in an overall NE direction, while the internal one moves with much lower rates in a N-NW direction, implying horizontal components of motion.

Active structures were investigated with the classical techniques of remote sensing and topography study, and structural geology field mapping. Tectonic geomorphology and high resolution topography resulted to be excellent tools to recognize, map and study active/capable faults, allowing identification of such structures over large areas as well as in detail, where high resolution data were available. The study of the geomorphological signal derived from digital terrain models emerged therefore as fundamental to improve knowledge on active tectonic deformation, from detailed mapping and characterization of single active faults to the understanding of the regional geodynamic processes driving present day deformation.

Here we highlight in particular the use of detailed elevation model with resolution up to 5 m as well as Lidar dataset. The widely available digital topography (90 to 30 m) are too coarse to provide representation of small geomorphic features, while the precision allowed by Lidar data make this one of the most useful tools for studying tectonic geomorphology.

Active tectonics at the front of the Eastern Southern Alps in the Carnic Prealps (NE Italy, Friuli)

Poli M.E.*¹, Monegato G.², Zanferrari A.¹ & Falcucci E.³

1. Dipartimento di Chimica, Fisica e Ambiente, Università di Udine. 2. Istituto di Geoscienze e Georisorse, C.N.R. Torino.
3. Istituto Nazionale di Geofisica e Vulcanologia, Roma - L'Aquila.

Corresponding email: eliana.poli@uniud.it

Keywords: Eastern Southalpine Chain, seismotectonics, seismic hazard.

Detailed structural and morphotectonic surveys along the front of the Eastern Southalpine Chain (ESC) in the western Carnic Prealps and surrounding piedmont Friuli plain, show evidence of Late Pleistocene-Holocene tectonic activity. At present the ESC accommodates about 2-3 mm/y shortening (Bechtold et al., 2009) and crustal thickening and propagates towards the Friuli piedmont Plain. According the DBMI11 (Locati et al., 2011) the Carnic Prealps was affected by some $M > 5.5$ historical earthquakes: Bellunese (1873, I_{max} 9-10), Bosco del Cansiglio (1936, I_{max} 9), Sequals (1812, I_{max} 7-8), Tramonti (1784, I_{max} 9). In order to improve the seismotectonic of the area we studied the Maniago-M. Jouf, Arba-Ragogna and Polcenigo-Montereale thrust systems by mean of morphotectonic, structural, paleosismological and stratigraphic surveys. Geophysical investigations in selected sites and the analysis of the seismic profiles (ENI-AGIP) allow us to parametrize the tectonic structures. Along the Maniago-M. Jouf system, at the Cellina valley outlet, the middle Pleistocene succession of Maniago Libero is thrust over the upper Pleistocene fan (Zanferrari et al., 2008). At the Meduna valley outlet, the study of the terrace staircase (Monegato & Poli, 2015) illustrates a long lasting deformation in four phases since the Pliocene. In particular, the deformation of the alluvial unit related to the last aggradation of the Meduna fan (30 to 11 cal ky BP) points to a cumulative slip rate of 0.6 mm/y for the Maniago thrust. The Arba-Ragogna thrust system shows morphotectonic evidence along the piedmont plain such as anomalies of the fluvial drainage and an about 3 m high tectonic scarp between Valeriano and Lestans localities. Moreover the LGM surface of the Tagliamento outwash fan is displaced of about 4 m on the tip line of the Arba-Ragogna thrust, showing a late Pleistocene to Present slip rate of about 0.2 mm/y. The Polcenigo-Montereale thrust system cuts the slope deposits interfingering with the Cellina major alluvial fan along the piedmont area of the Cansiglio-Cavallo massif: locally the deposits related to the LGM Cellina fan are displaced of about 10 m, suggesting also for this sector a recent slip rate of about 0.6 mm/y. The uplift produced a series of telescopic fans; those related to the LGM aggradation show deformation along to the faults of the thrust system.

- Bechtold M., Battaglia M., Tanner D.C. & Zuliani D. 2009. Constraints on the active tectonics of the Friuli/NW Slovenia area from CGPS measurements and three-dimensional kinematic modelling. *J. Geoph. Res.* 114.
- Locati M., Camassi R. & Stucchi M. 2011. <http://emidius.mi.ingv.it/DBMI11>.
- Monegato G. & Poli M.E. 2015. Tectonic and climatic inferences from the terrace staircase in the Meduna valley, eastern Southern Alps, NE Italy. *Quaternary Res.*, 83, 229-242.
- Zanferrari A., Avigliano R., Grandesso P., Monegato G., Paiero G., Poli M.E. & Stefani C. 2008. <http://www.isprambiente.gov.it/Media/carg/friuli.html>.

History of Miocene temperate-type carbonate shelf in a compressive setting (northern Apennines), constrained by a chemostratigraphical, microfacies and compositional study

Salocchi A.*¹, Nereo P.², Fontana D.¹, Conti S.¹, Grillenzoni C.¹ & Argentino C.¹

1. Dipartimento di Scienze Chimiche e Geologiche, Università di Modena e Reggio Emilia.
2. Dipartimento di Geoscienze, Università di Padova.

Corresponding email: auracecilia.salocchi@unimore.it

Keywords: Temperate carbonate shelf, drowning, wedge-top basin.

A detailed chemostratigraphic study associated with microfacies and compositional analysis has been performed on a early middle Miocene shallow-water shelf deposited on a wedge-top basin in the northern Apennines.

More than 140 samples were collected in the representative outcrop of Torriana (Val Marecchia valley, Romagna Apennines) in order to identify factors controlling the inception and crisis of the shelf. The succession is constituted by 100 m thick mixed siliciclastic-carbonate rocks, unconformably overlying the allochthonous Ligurian units.

The evolution of the carbonate shelf passed true four main phases, as shown by the detailed microfacies and compositional study, that evidence the progressive decrease of the carbonate productivity, gradually replaced by detrital sedimentation.

The basal portion consists of rhodalgal rudstones and grainstones dominated by echinoids, bryozoans, coralline algae and benthic foraminifera. The progressive increase of terrigenous components and planktonic and benthic taxa marks the gradual transition to a mixed carbonate-siliciclastic shallow water-facies. The top of the succession is characterized by fine-grained sediments rich in glaucony. The main factors controlling the evolution of the shelf are increased subsidence of the basin, related to the thrust migration, and terrigenous contributions from the erosion of the rising Apennines areas.

The stable isotope study show that the carbonate production has been influenced not only by regional factors, but also by a global fertility event, as the Monterey Event, recorded in the Mediterranean during the late Burdigalian - Serravallian.

Cause of East-West Earth Asymmetry

Scalera G.

INGV, Roma (retired).

Corresponding email: giancarlo.scalera@ingv.it

Keywords: Asymmetric Earth, East-West asymmetry, expanding Earth.

An asymmetric characteristic of our globe is the different slopes of the East and West oriented Wadati-Benioff zones. Using plate tectonic geodynamics, it follows a negligible role of Coriolis effect. Instead, the East-West asymmetry can be explained in the expanding Earth framework in which sudden surfaceward displacements of mantle materials occur by phase change toward more unpacked lattice, producing a rise of the Coriolis force of several magnitude orders. The velocity of rising is not constant but irregular and mainly impulsive, the rising episodes coinciding with changing of phase, and its range can be reasonably assumed as equal to the sliding velocity of the two sides of a fault during an earthquake, namely $V = 1 \text{ m/s} - 10 \text{ m/s}$.

With $\omega = 7.27 \cdot 10^{-5} \text{ rad/s}$, in the case of $V = 1.0 - 10.0 \text{ cm/y} = 3.17 \cdot 10^{-9} - 3.17 \cdot 10^{-10} \text{ m/s}$ (plate tectonics slow velocities), the value of the Coriolis force is (Ricard, 2007) $F_{Cor} = 2\rho\omega V \text{ Nw/m}^3 = 0.15 \cdot 10^{-9} - 1.5 \cdot 10^{-9} \text{ Nw/m}^3$. But I can compute that in the case of impulsive velocities of $V = 1 \text{ m/s} - 10 \text{ m/s}$

$$F_{Cor} = 2\rho\omega V \text{ Nw/m}^3 = 0.48 - 4.8 \text{ Nw/m}^3,$$

about 10 orders of magnitude greater than for the convective slow laminar flow. Then, a deflection of the sudden vertical flows cannot be excluded, producing the East-West asymmetry.

Evidence supporting this interpretation are the coseismic phenomena of great earthquakes (e.g the 2004 Sumatra event, $M=9.4$), in particular the displacement of the instantaneous rotation pole of the Earth (Bianco, 2005). The rotation axis moved along the meridian of the epicenter, going nearly 3 milliarcsec ($\approx 10.0 \text{ cm}$) farther from the epicenter, making clear that mass has been emplaced in the earthquake zone (Scalera, 2012) following a mechanism of extrusion. The data of the GRACE satellites (Han et al., 2006) fit a fault dislocation with a substantial lateral and vertical expansion of the oceanic crust. The great earthquake of Honshu Tohoku (11 March 2011; $M_w=9.1$) has produced similar effects.

A hasty assessment of the magnitude of the involved forces greatly underestimates the role of the Coriolis effect in producing the observed slope differences of the Wadati-Benioff regions. However, astrogeodetic evidence exist not in agreement with plate tectonics, but in accord with an expanding and *emitting* Earth view.

- Bianco G. 2005. Gli effetti del terremoto del sud-est asiatico sulla geodinamica globale. PowerPoint file http://www.fis.uniroma3.it/plastino/seminars/terr_mar.html
- Han S.-C., Shum C.K., Bevis M., Ji C. & Kuo C. 2006. Crustal dilatation observed by GRACE after the 2004 Sumatra-Andaman earthquake. *Science*, 313, 658-662.
- Ricard Y. 2007. Physics of mantle convection. In: Schubert G. Ed., *Treatise on Geophysics*. Elsevier, 7, 31-87.
- Scalera G. 2012. Distensional Mediterranean and World Orogens – Their Possible Bearing to Mega-Dykes Active Rising. In: Scalera G., Boschi E. & Cwojdzinski S. Eds., *The Earth Expansion Evidence – A Challenge for Geology, Geophysics and Astronomy*. Aracne Editrice, 115-160.

The Tethyan roots of the Hyblean-Pelagian foreland domain (Sicily): geodynamic implications and possible modern analogues

Scribano V.¹, Manuella F.C.*¹, Carbone S.¹ & Brancato A.²

1. Dipartimento di Scienze Biologiche, Geologiche e Ambientali, Sezione di Scienze della Terra, Università di Catania.

2. INGV, Osservatorio Etneo, Catania.

Corresponding email: fmanuella@alice.it

Keywords: Sicily, xenoliths, diatremes.

Hyblean diatremic tuff-breccia deposits, Late Tortonian in age, host an assorted variety of wall-rock xenoliths providing the unique opportunity to directly investigate the unexposed lithosphere of south-eastern Sicily. Petrologic and geochemical studies on ultramafic and gabbroic xenoliths, along with a reappraisal of existing geological and geophysical data, confirmed that the volcano-sedimentary sequence of this region lies upon the rest of the Ionian-Tethys Ocean basement, Permian in age, and hence suggested that the entire Sicily mainland and large part of its Pelagian offshore areas are set upon a largely serpentinitized ultramafic basement (Manuella et al., 2013; 2015). In particular, Hyblean xenoliths point to the occurrence of buried Oceanic Core Complex (OCC) structures. These are fault-bounded abyssal highs of serpentinitized mantle peridotites and gabbroic rocks exhumed to the ocean floor along detachment systems in the crest zone of modern (ultra)slow-spreading mid-ocean ridges. Some structural, morphologic and seismic features of the present Ionian-Pelagian-Hyblean foreland domain suggest that Core Complex systems likewise the St. Peter and St. Paul Megamullion (Equatorial MAR), the Atlantis Massif (MAR 30° N) and Rio Grande Rise (South Western Atlantic), can be considered as modern analogues of the buried Tethyan OCC structures. Furthermore, the occurrence of Tethyan serpentinites in the Sicily basement may imply that abundant marine salts formed in these rocks as the result of seawater-driven serpentinitization. These deep-seated salts may have been remobilized by supercritical fluids, which generated saline brines that emplaced at the sea bottom as hypersaline ponds, originating the Triassic and Messinian "Evaporites" in Sicily, as currently observed in the Red Sea floor (Hovland et al., 2015).

Hovland M., Rueslåtten H. & Johnsen H.K. 2015. Red Sea salt formations-a result of hydrothermal processes. In: Rasul N.M.A. & Stewart I.C.F. Eds. *The Red Sea*. Springer-Verlag, Berlin Heidelberg, 187–203.

Manuella F.C., Brancato A., Carbone S. & Gresta S. 2013. A crustal upper mantle model for southeastern Sicily (Italy) from the integration of petrologic and geophysical data. *J. Geodyn.*, 66, 92–102.

Manuella F.C., Scribano V., Carbone S. & Brancato A. 2015. The Hyblean xenolith suite (Sicily): an unexpected legacy of the Ionian–Tethys realm. *Int. J. Earth Sci.*, doi: 10.1007/s00531-015-1151-9.

SESSION S21

Open Poster Session

CONVENORS

Marco Pistolesi (Univ. Firenze)

Geophysical signature of the 11 February 2010 dome collapse at Soufrière Hills Volcano, Montserrat, West Indies

Barfucci G.*, Ripepe M., Delle Donne D. & Lacanna G.

Dipartimento di Scienze della Terra, Università di Firenze.

Corresponding email: giulia.barfucci@gmail.com

Keywords: Montserrat, dome collapse, Infrasound.

The 11 February 2010 collapse of the growing andesitic lava dome at Soufriere Hills Volcano, Montserrat is closing the fifth extrusive phase of the 1995-to-present eruption. The initial dome collapse produced large pyroclastic flows and high-energy surges followed by two violent Vulcanian explosions, injecting 15 Km-high ash plumes in the atmosphere. This large variety of phenomena related to lava dome instability, occurred in only two hours, is studied using seismic and infrasonic records integrated with images of thermal cameras. We show how the intense pyroclastic density currents (PDCs) generated clear seismic and infrasonic signals which unveil the behavior of the initial phase of the dome collapse and can have important implications in the timely assessment of volcanic hazard. The dome collapse starts with a progressively increase of the PDCs activity both in the north and north-east direction reaching the climax during the Vulcanian explosions. Infrasound evidence how the PDCs activity is related to ultra-low frequency oscillation of the atmosphere with periods of several minutes. This is the first time that large pressure waves in the acoustic-gravity range are recorded during PDCs activity. We suggest that the origin of these oscillations can be related to the large-scale displacement of atmosphere above the volcano induced by the large mass movement and the intense heat flow related to almost two kilometers thick co-ignimbrite ash cloud. This activity is the evidence of a flank instability most probably induced by the final upward movement of andesitic plug feeding the dome. The large mass released during this PDCs phase is responsible for the decompression of the magmatic system triggering the two final Vulcanian explosions.

Volatile metals and municipal waste incineration: a comparison with volcanic melting

Bello M.*, Carroll M.R. & Scipioni M.

Scuola di Scienze e Tecnologie - Sezione di Geologia, Università di Camerino.

Corresponding email: marco.bello@unicam.it

Keywords: Municipal solid waste incinerator, volcanic, ashes.

In many countries, waste recycling has led to a reduction in the volume of municipal wastes but difficulties related to their storage still exist.

Such waste materials need to be processed in Municipal Solid Waste Incinerators (MSWI), whose mechanisms and products can be related to the ones occurring in volcanic systems.

In fact, MSWI work in much the same way as volcanic systems, where erupted materials can be associated to the solid wastes burned from municipal wastes (bottom ashes), while the gas phases emitted during volcanic eruptions can be related to the fly ashes produced in the incinerators.

Both bottom and fly ashes are rich in heavy metals: some of them occur as native material (Al, Fe, Cu, brass) of millimeter size and can be separated from the silicate matrix by mechanical or flotation processes. However, more volatile metals like for example Zn and Pb are incorporated in salts and silicates or even silicate glasses, usually forming particles of less than 100 μm . The speciation of these volatile metals in melts, crystals, and vapor-phase condensates in MSWI products are widely unknown and therefore must be determined in order to calculate thermodynamic equilibria in MSWI processes. In addition the kinetics and physico-chemical parameters (pH, Eh, temperature) for their formation must be determined experimentally.

To investigate the decomposition, separation and recovery of resources-relevant metals some innovative methods need to be employed. This represents the main object of the present study, which is mainly focused on the research of the essential processes occurring in the MSWI, in order to infer the same in natural volcanic systems and improve their comprehension.

Minerals, rocks and meteorites on display: the new exhibition at the Pisa University's Natural History Museum

Bonaccorsi E.*, Biagioni C. & D'Orazio M.

Dipartimento di Scienze della Terra & Museo di Storia Naturale, Università di Pisa.

Corresponding email: elena.bonaccorsi@unipi.it

Keywords: Museum, minerals, meteorites.

The mineral gallery of the Museum of Natural History of the University of Pisa has been recently renewed and reopened, after more than three years of inactivity due to serious damage of the roof structure. In this occasion it has been renamed “Antonio D’Achiardi Gallery”, in honour of the ‘father’ of the mineralogical school at the University of Pisa, and first Director of the Museum itself.

Within the new gallery, the visitors will follow a storytelling, by exploring the origin of the Solar System and the information given by the meteorite samples, by looking at the ‘Tuscan rocks’ exhibit and by admiring more than 500 mineral specimens exposed in 25 showcases. The meteorite collection on display includes the 48 kg Bagnone siderite, the historical specimens collected nearly 150 years ago by Antonio D’Achiardi, and the meteorites sampled by the researchers of the University of Pisa, both in Antarctica and at the Kamil Crater (Egyptian Sahara). As regards the minerals, the exposition gives an almost complete sight of the main mineralogical localities and mining districts in Tuscany. Many items are of particular aesthetic and/or scientific relevance. Among them, there are the extraordinary jordanite crystals, originally classified as ‘geocronite’, from the Valdicastello mine (Pietrasanta, Lucca): the larger crystal weighs 1.9 kg, while the smaller one, weighing 470 grams, displays an uncommon morphological perfection. Another interesting specimen is the cinnabar of Ripa (Seravezza, Lucca). This wonderful specimen, considered “unique for its beauty” by important mineralogists during the 19th century, was shattered by the bombings that hit Pisa during the Second World War and just the remaining fragments are on display in a showcase. Other outstanding specimens of the museum mineral collection are the stunning geodic crystallizations from the Bottino mine (Stazzema, Lucca) of the A. CerPELLI collection, and the fine specimens from pegmatite and iron-ore sites of the Elba Island. It is worth to note that most of the specimens from the Colline Metallifere localities that are on display in the Gallery, belongs to a private collection, following a fruitful tradition of collaboration and synergy between the museum and mineral collectors and amateurs.

Besides the meteorite and mineral showcases, the visitors may personally explore some interesting optical and physical properties of minerals. It is possible to discover the mineral habitus of micromounts by using the stereomicroscope, to appreciate the different density of various minerals, or to give an insight into complex phenomena such as pleochroism, birefringence or fluorescence. To complete the visitor experience, two showcases have been devoted to the instruments and devices used by mineralogists in the past two centuries.

The new exhibition seems to be appreciated by specialists, children and tourists, in agreement with the goals of a modern museum.

Geoscience education: teaching and learning Earth Sciences using the virtual worlds (Muves)

Boniello A. & Paris E.*

Scuola di Scienze e Tecnologie - Sezione di Geologia, Università di Camerino.

Corresponding email: leonora.paris@unicam.it

Keywords: Geoscience education, virtual worlds, school.

“When I watch children playing video games at home or in the arcades, I am impressed with the energy and enthusiasm they devote to the task. Why can’t we get the same devotion to school lessons as people naturally apply to the things that interest them?” (Prensky, 2001).

In the last years, two problems became fundamental for science teachers: a) try to increase motivation in students for science, by keeping students motivated enough to stick with the learning process, and b) to provide ways of authentic learning and assessment in science education. To these well known problems, the lack of interest on geosciences studies among students needs to be taken also into consideration, calling for new ways to interact with them and to help teachers in finding engaging methods to teach Earth sciences topics.

This research describes the design, evaluation and experimentation of a three-dimensional immersive virtual environment dedicated to the teaching of the Earth Sciences at school. Multi user virtual environments (Muves) were built with Open Sim technology, addressed to students aged 13 to 18 years old. The aim of the research is to investigate the educational effectiveness of using the immersive virtual worlds to foster knowledge acquisition, develop scientific skills and increase interest in learning geosciences.

To experienced this approach a virtual island has been created on the server of University of Camerino and called UNICAMearth Island, which hosts immersive 3-dimensional paths addressing geosciences topics. In the island students of the secondary school first level, can communicate and learn in a social virtual environment. The immersive environment allows to create simulations of natural environments (volcanoes characteristics, earthquakes, eruptions, rocks and minerals) with animations and interactive objects to obtain a virtual world with scientific contents to develop scientific knowledge and competences. In the all the virtual paths there are pre-tests and post-tests for evaluating the perception and the level of involvement users (learners) in the geosciences. An aspect of this technology is the degree of presence that is simulated through the use of an avatar, a virtual representation of the user. The virtual worlds have a high degree of immersion and presence, therefore, their use in education is spreading as a socio-constructivist environment, where students can use the learning by doing and situated learning.

The paths described here show the potential of virtual worlds for the development of scientific skills in geosciences education and engage students in science education. The results obtained by experimenting the paths both on students and teachers, in a large number of classes and groups of teachers all over Italy, show that the virtual worlds improve the involvement and motivation of the students to geoscience topics and, in general, to scientific studies, especially in the 13-16 years age range, with also an increase of collaborative work and interaction with the teachers.

I- and S-type granites in the late Variscan Serre Batholith (Central Calabria, Italy) and applicability of the Restite and Peritectic Assemblage Entrainment models

Fiannacca P.*, Militello G.M., Lombardo R. & Cirrincione R.

Dipartimento di Scienze Biologiche, Geologiche e Ambientali, Università di Catania.

Corresponding email: pfianna@unict.it

Keywords: Granite petrogenesis, geochemical variations, Serre Massif.

Weakly to strongly peraluminous granodiorites and granites represent the most felsic rocks of the Serre Batholith, which makes up the intermediate portion (c. 13 km thick) of a nearly complete cross section of continental crust exposed in central Calabria. These rocks are Bt±Am granodiorites (BAG), two-mica granodiorites and granites (BMG) and two-mica porphyritic granodiorites and granites (BMPG). In addition to Am, BAG are characterized by accessory phases such as Aln, Ep s.s. and Ttn, all suggesting an I-type affinity, although interstitial Mnz may also occur in the most evolved compositions. BMG show S-type features such as common primary Ms, as well as Zrn and Mnz typically enclosed in biotite and Ap mostly occurring as interstitial phase. S-type features are particularly well developed in the BMPG, characterized by diffuse Sil and greater amounts of Ms and early Mnz. BAG have ASI values mostly below 1.1, while the other rock types show values dominantly close to or greater than 1.1. In the Na₂O vs. K₂O diagram BAG and BMG show transitional features, while BMPG have a clear S-type signature. In the CaO vs. FeO_{tot} diagram, more recently considered as better suited to discriminating I- and S-type granites, BMPG and BMG result mostly having low CaO/FeO ratios; the BAG, although showing the highest CaO contents, are also characterized by low CaO/FeO ratios. According to the I-S scheme, a derivation from a metasedimentary source appears therefore well recorded in BMG and BMPG, while BAG features result ambiguous and may be compatible with derivation from both a contaminated metabasic source or a metasedimentary source containing significant amounts of juvenile components. Harker diagrams show linear trends between some BAG and BMG, manifesting a possible genetic link between them, while trends for BMPG indicate a clear petrogenetic independence of these rocks. The Restite and Peritectic Assemblage Entrainment (PAE) models, considered as the main processes governing chemical variations in wholly crustally-derived granites, have been here tested. A possible role for restite unmixing emerges by using the compositions of metasedimentary and metabasic rocks from the Serre lower crust as potential source rocks; BAG result as possibly derived from metabasite sources, while BMG and BMPG compositions lie along lines connecting them to metagreywackes and metapelites. Results appear also compatible with PAE processes. BMPG and most BMG would represent melts derived from metasedimentary sources, with entrained Grt and Ilm produced by Bt breakdown; BAG are more akin to melts, with entrained peritectic Grt, Cpx and Ilm, deriving from partial melting of source rocks containing Bt and Hbl in a 3:2 ratio. The two models therefore agree in individuating the same magma source for each granitoid type; though, further study is needed to assess their relative importance in contributing to the geochemical diversity of granitoid rocks.

Emission of gas and atmospheric dispersion of SO₂ during the December 2013 eruption at San Miguel volcano (El Salvador)

Granieri D.^{*1}, Salerno G.², Liuzzo M.³, La Spina A.², Giuffrida G.³, Caltabiano T.², Giudice G.³, Gutierrez G.⁴, Montalvo F.⁴ & Papale P.¹

1. Istituto Nazionale di Geofisica e Vulcanologia, Pisa. 2. Istituto Nazionale di Geofisica e Vulcanologia, Osservatorio Etno, Catania. 3. Istituto Nazionale di Geofisica e Vulcanologia, Palermo. 4. Ministerio de Medio Ambiente y Recursos Naturales Area de Vulcanología, Observatorio Ambiental, San Salvador, El Salvador.

Corresponding email: domenico.granieri@ingv.it

Keywords: San Miguel or Chaparrastique volcano, SO₂ chlorine and fluorine discharges, simulation.

San Miguel volcano, also known as Chaparrastique, is a basaltic volcano along the Central American Volcanic Arc (CAVA). Volcanism is induced by the convergence of the Cocos Plate underneath the Caribbean Plate, along a 1200-km arc, extending from Guatemala to Costa Rica and parallel to the Central American Trench. The volcano is located in the eastern part of El Salvador, in proximity to the large communities of San Miguel, San Rafael Oriente, and San Jorge. Approximately 70,000 residents, mostly farmers, live around the crater and the city of San Miguel, the second largest city of El Salvador, ten km from the summit, has a population of ~180,000 inhabitants. The Pan-American and Coastal highways cross the north and south flanks of the volcano.

San Miguel volcano has produced modest eruptions, with at least 28 VEI 1-2 events between 1699 and 1967 (data from Smithsonian Institution <http://www.volcano.si.edu/volcano.cfm?vn=343100>). It is characterized by visible mild degassing from a summit vent and fumarole field, and by intermittent lava flows and Strombolian activity. Since the last vigorous fire fountaining of 1976, San Miguel has only experienced small steam explosions and gas emissions, minor ash fall and rock avalanches. On 29 December 2013 the volcano erupted producing an eruption that has been classified as VEI 2.

While eruptions tend to be low-VEI, the presence of major routes and the dense population in the surrounding of the volcano increases the risk that weak explosions with gas and/or ash emission may pose.

In this study, we present the first inventory of SO₂, CO₂, HCl, and HF emission rates on San Miguel volcano, and an analysis of the hazard from volcanogenic SO₂ discharged before, during, and after the December 2013 eruption. SO₂ was chosen as it is amongst the most critical volcanogenic pollutants, which may cause acute and chronic disease to humans.

Data were gathered by the geochemical monitoring network managed by the Ministerio de Medio Ambiente y Recursos Naturales (MARN) of El Salvador and by a network of geophysical and geochemical stations established on the volcano by the Italian Istituto Nazionale di Geofisica e Vulcanologia (INGV), immediately after the December 2013 eruption, on the request of MARN.

During the eruption, SO₂ emissions increased from a background level of ~330 t d⁻¹ to 2200 t d⁻¹, dropping after the eruption to an average level of 680 t d⁻¹. Wind measurements and SO₂ fluxes during the pre-, syn- and post-eruptive stages were used to model SO₂ dispersion around the volcano. Air SO₂ concentration exceeds the dangerous threshold of 5 ppm in the crater region, and in some middle sectors of the highly visited volcanic cone.

Comparison between catchment geomorphology and alluvial fan seismic stratigraphy in defining the geomorphic process domains in the Val Venosta (Eastern Alps, Italy)

Maraio S.*¹, Pazzaglia F.J.², Bruno P.P.G.³, Picotti V.⁴ & Brardinoni F.⁵

1. Dipartimento di Scienze Biologiche Geologiche e Ambientali, Università di Bologna. 2. Department of Earth and Environmental Science, Lehigh University, Bethlehem, USA. 3. The Petroleum Institute, Abu Dhabi, United Arab Emirates. 4. Department of Earth Sciences, ETH Zurich, Switzerland. 5. Dipartimento di Scienze Geologiche ed Ambientali, Università di Milano-Bicocca.

Corresponding email: stefanomaraio@gmail.com

Keywords: Val Venosta, alluvial fan, geomorphic processes.

The relationship between alluvial fan morphology, catchment hydrology, and sediment dynamics remains an important field of inquiry in mountain settings, in part because of the well known hazards and associated societal impacts. Quantifying geomorphic processes in these settings can be used to understand landscape evolution and represents an essential tool in policy decision regarding natural hazards, given that construction of residential buildings and transport infrastructures on alluvial fans has increased the vulnerability to catastrophic events (i.e., debris flows and debris floods) (Comiti et al., 2014). Here we look for causal linkages between dominant geomorphic processes in the source basin (Montgomery & Foufoula-Georgiou, 1993; Montgomery, 1999), sediment production and delivery to the alluvial fan, and the resulting fan allostratigraphy as revealed by high-resolution reflection seismology. In so doing, we are able to better identify the main geomorphic processes in Val Venosta (Eastern Alps, Italy) and test the original hypothesis that a cluster of anomalously large alluvial fans are the result of immediate post-glacial mega-landslides (Fisher, 1965). To this purpose, we present the results of a stream power law-based slope-area analysis, to delineate process domains in six representative catchments characterized by different basin area-fan area ratio. We also compare the source basin geomorphology with fan stratigraphy of the Gatria fan, one of the biggest fans in the valley. The relationship between the main depositional processes and the internal architecture of the fan has important implications for understanding the alluvial fan origin and growth in Val Venosta. Preliminary results show that slope-area plots and the fan seismic stratigraphy are all consistent with debris flow processes, rather than with mega-landslides.

Comiti F., Marchi L., Macconi P., Arattano M., Bertoldi G., Borga M., Brardinoni F., Cavalli M., D'Agostino V., Penna D. & Theule J. 2014. A new monitoring station for debris flows in the European Alps: first observations in the Gatria basin. *Nat. Hazards*, 73, 1175-1198.

Fischer K. 1965. Murkegel, Schwemmkegel und Kegelimse in den Alpen. *Mitteilungen der Geographischen Gesellschaft München*, 56, 127-159.

Montgomery D.R. 1999. Process domains and the river continuum. *J. Am. Water Res. Ass.*, 35, 397-410.

Montgomery D.R. & Foufoula-Georgiou E. 1993. Channel network source representation using digital elevation models. *Water Resour. Res.*, 29, 3925-3934.

Principal component analysis as a tool in the study of a mineral population. Muscovite case study

Marengo A.* & Vigliaturo R.

Dipartimento di Scienze della Terra, Università di Torino

Corresponding email: alessandra.marengo@unito.it

Keywords: Principal component analysis, muscovite, data elaboration.

The study of a mica species (muscovite) was carried out, collecting dimensional and chemical data through SEM (EDS semi-quantitative analysis), on a population of dozens of crystals. Micas can show a wide-ranging incorporation of elements in their crystal structures. In muscovite $\text{KAl}_2\text{[AlSi}_3\text{O}_{10}\text{](OH)}_2$, a *true K* mica according to Tischendorf et al. (2007), the presence of other elements is infrequent, with some exceptions. In fact, the analyzed mineral population can be classified as a Mg-rich variety of muscovite (Mg for Al substitution in the octahedral sheet). Other elements can substitute K in the interlayer as Ca or Na even if they don't occur in significant concentrations. Furthermore the presence of Fe^{3+} is sometimes detected (this can be due either to a tetrahedral or an octahedral sheet substitution). Concentrations of F as anion are found in several samples. Observing trends and extrapolating conclusions in front of this wide variety of data, can result difficult, easily inducing error and even resulting impossible. Principal component analysis (PCA) is a tool that allows to treat problems described by many aleatory variables, allowing to study all the relationships between every involved variable. This procedure (PCA) was tested on muscovite crystal population, in this case, 33 muscovite crystals are examined considering for each one 9 aleatory variables (length, thickness and chemical composition as: K, Ca, Al, Si, Mg, Fe and F). To conduct PCA Microsoft Excel in combination with Maple software were used in order to have a full control of the inserted commands, unlike an automatic PCA program, and to better explain the meaning of the passages step by step. PCA was performed passing through both the covariance and the correlation matrix, the first approach showed a really good performance, with an error due to the choice of just two principal component inferior to the 3%. The final result of the analysis is an a-dimensional chart showing principal component axis and latent variables distribution. Angles among principal component arrows consent to understand simultaneously all the relations between the considered variables. The most interesting evidenced aspect is that when Ca substitutes in the interlayer, the tetrahedral sheet has an higher concentration of Al and low Si, resulting more negatively charged. When the interlayer space filling better corresponds with the one expected for the muscovite theoretical formula, with K, the tetrahedral layer has a better charge balance with a major presence of Si and lower concentration of Al. Moreover, Mg and Al concentrations are proportional in the octahedral layer with an uniform substitution. The treatment of analytical data by a mathematical approach (PCA), which is not commonly used as one should expect, enhances to SEM semi-quantitative analyses significant information on how concentration patterns are related, providing a strong added value to data interpretation.

Tischendorf G., Förster H.-J., Gottesmann B. & Rieder M. 2007. True and brittle micas: composition and solid-solution series. *Mineral. Mag.*, 71, 285-320.

The research of active and inquiry based learning in Earth sciences in the school

Pieraccioni F.

Dipartimento di Scienze della Terra, Università di Pisa.

Corresponding email: fabio.pieraccioni@for.unipi.it

Keywords: Learning, education, teacher.

The geoscience education is not a matter of pure scientific research and it does not regard only the human sciences. It is the Earth sciences researcher, with didactic and pedagogic skills, who has got a qualification to explore new ways to educate the young generations to the issues connected to the environment and the exploitation of the resources in a sustainable way. It is always him that can indicate to teachers - hardly ever with a geological culture - how to transmit knowledges and skills without turning them into heavy misconceptions (Libarkin & Kurdziel, 2001). Such misconceptions can negatively influence the conscience of future citizens, which will be often called to answer about compelling choices.

The academic geoscience community in Italy has often delegate the teachers' training courses to the school, at difference of what happens to mathematics, chemistry and physics. On this matter it is worth to note that in other countries (Libarkin et al., 2003) the geoscience researchers have been engaged since a long time in the education field, from primary to secondary school.

The research in this field has to advance upon two fronts: on the one hand there is the continue exploration of active and manipulative educational paths, so to motivate students (Renshaw, 2014) without being trivial or unsuitable. This process has to provide significant skills not only for future professionals in the Earth Science, but also for all future citizens. On the other hand it is necessary to carry out a survey to keep monitoring the students' geological knowledge, in particular Earth Sciences freshmen, in order to define possible corrections or improvements as regards the learning strategies (Libarkin et al., 2005).

For example the Berlinguer Commission of 2007 suggests that universities promote the educational research of scientific matters engaging teachers in didactic and scientific research.

It is necessary to give dignity to the didactic research in the geological field in order to contribute to the building of an environmental education both for future citizens and for the ruling classes. This is the starting point of a virtuous cycle school-scientific research where both institutions interplay with a common target.

Libarkin J.C. & Kurdziel J.P. 2001. Research Methodologies in Science Education: Assessing Students' Alternative Conceptions. *J. Geosci. Educ.*, 49, 378-383.

Libarkin J.C., Beilfuss M. & Kurdziel J.P. 2003. Research Methodologies in Science Education: Mental Models and Cognition in Education. *J. Geosci. Educ.*, 51, 121-126.

Libarkin J.C., Anderson S.W., Scince J.D., Beilfuss M. & Boone W. 2005. Qualitative Analysis of College Students Ideas about the Earth: Interviews and Open-Ended Questionnaires. *J. Geosci. Educ.*, 53, 17-26.

Renshaw C.E. 2014. Design and Assessment of Skill-Based Curriculum. *J. Geosci. Educ.*, 62, 434-438.

Geochemical and mineralogical characterization of marine sediments in the mud diapir province of the Paola basin (Southern Tyrrhenian Sea)

Rashed H.*¹, Rovere M.², Pecchioni E.¹, Gamberi F.² & Vaselli O.¹⁻³

1. Dipartimento di Scienze della Terra, Università di Firenze. 2. Istituto di Scienze Marine (ISMAR), CNR, Bologna.
3. Istituto di Geoscienze e Georisorse, CNR, Firenze.

Corresponding email: hibarashed86@hotmail.com

Keywords: Geochemistry, mineralogy, Paola Basin.

The study area is located along the Paola Ridge, a NNW-SSE 60-km-long anticline that confines the Paola Basin westward (north-western Calabrian margin), in the south-eastern Tyrrhenian Sea. The Paola Ridge has recently been interpreted as due to a mobile mud belt (comprised of D1, D2, D3 diapirs and MMV, RMV mud volcanoes) connected with a set of extensional NW-SE to NNW-SSE trending faults (Gamberi & Rovere, 2010). In August-September 2011 the MVP11 oceanographic cruise was carried on board the R/V CNR Urania. During the cruise, multi-beam bathymetric data, Chirp profiles, gravity coring and box cores, were acquired to define the sedimentological, petrographical, mineralogical and geochemical features of the marine sediments. In this work a detailed mineralogical and geochemical investigation of sediments collected from cores and box cores along the specific structures of the Paola Ridge is reported. The studied samples include: limestone crusts, carbonates of tubular form, iron oxy-hydroxide crusts, pyrite and sulfur crusts and cohesive muds. Each sample was characterized and analyzed by means of optical petrography, XRD, SEM-EDS, XRF, ICP-AES and ICP-MS. Selected samples were chosen for carbon, oxygen and sulfur isotopic analyses. The petrographical, mineralogical, chemical and isotopic data, obtained from the cored sediments and the rock samples, allowed to define the depths of the biogeochemical zones and the geochemical processes affecting the depositional environment into which the marine sediments were deposited (Rovere et al., 2015). Organogenic carbonate crusts consist of calcite, aragonite and dolomite, few phyllosilicates, feldspars and pyroxenes, and associated with macro fauna bivalves that are symbionts of sulfur oxidizing bacteria and usually live in extreme environments, as cold seeps (Rovere et al., 2015). Stable isotopes (C and O) on the organogenic carbonates are depleted in $\delta^{13}\text{C}$ and slightly enriched in $\delta^{18}\text{O}$. Tubular authigenic carbonates contain siderite, quartz and few phyllosilicates. Stable isotopes (C and O) on the siderite are enriched in both heavy carbon and oxygen isotopes. Iron oxy-hydroxide crusts are comprised of goethite. Pyrite and sulfur crusts have pyrite and/or sphalerite, quartz and few feldspars. Cohesive muds showed a quartz, halite, feldspars, muscovite and clay minerals (illite, vermiculite, chlorite, kaolinite) and in some sample calcite or dolomite, siderite, hematite and pyrite.

Gamberi F. & Rovere M. 2010. Mud diapirs, mud volcanose and fluid flow in the rear of the Calabria Arc orogenic wedge (southeaster Tyrrhenian Sea). *Basin Res.*, 22, 452-464.

Rovere M., Rashed H., Pecchioni E., Mercorella A., Ceregato A., Leidi E., Gamberi F. & Vaselli O. 2015. Habitat mapping of cold seeps associated with authigenic mineralization (Paola Ridge, southern Tyrrhenian): combining seafloor backscatter with biogeochemistry signals. *Ital. J. Geosci.*, 134, 23-31.

Variable radius cartography - Birth and perspectives of a new experimental discipline

Scalera G.

Istituto Nazionale di Geofisica e Vulcanologia, Roma (retired).

Corresponding email: giancarlo.scalera@ingv.it

Keywords: Variable radius cartography, history of cartography, expanding Earth.

The present paper aims to show that in the last century cartography was used in a more or less complex way, to various extents intertwined with other disciplines and databases, not as a pure representation or in the spirit of simple 'fits' that supported continental displacements, but in experiments of greater complexity and with a weight of proof in favor of planet expansion, and raising numerous issues for Physics, Astrogeodesy, Astronomy, and Cosmology.

The expanding Earth hypothesis today is considered the major alternative to plate tectonics, and is destined to supercede the rival theory on the basis of a larger number of interconnected explanations of phenomena, not only in the field of Geology and Geophysics, but also in more general fields (Scalera et al., 2012). Its principal merit is that it has freed the Earth sciences from subordination to Physics and Cosmology. An expanding Earth strongly infers that our knowledge of the physical world must start from the only celestial body of which we have direct experience, using as a test-body what lies beneath our feet.

This concept created the need for new types of experimentation – typically cartographical in nature. It might be said that the expanding Earth hypothesis has transformed cartography into an experimental science. The success of the paleogeographical reconstructions on smaller radius globes is not only a good geological experiment but takes on a new and more general significance: the fields involved were not only geology, geodynamics, and tectonics, but inevitably new issues were posed for physics, astronomy, and cosmology, inducing all these disciplines towards a perspective of a more dynamic, "mobilistic" view, revealing the inadequacy of many current conceptions. The experiments in cartography are certainly very *low cost* but the results can be considered *weighty*, like those arriving from the *great physics* of the giant particle accelerators (Scalera et al., 2012).

The possibility of performing cartographical tests with the help of precise computer assisted variable radius mapping tools would avoid the flimsiness both of certain studies and of the critical comments addressed to them. Assigning the Earth's correct radius $r = R(t)$ to each geodetic datum could lead to a more correct procedure in geodesy, as is already the case in paleogeodesy.

Old and more recent classical experiments are recalled, besides the ones performed at INGV and their link with other disciplines (Scalera, 2013).

Scalera G. 2013. The variable radius cartography - history and perspectives of a new discipline. In: Pisano R., Capecchi D. & Lukeova A. Eds., Proceedings of the 32th International Congress of the Italian Society of Historians of Physics and Astronomy (SISFA), Rome 27-29 September 2012. The Scientia Socialis Press, 367-374.

Scalera G., Boschi E. & Cwojdzinski S. Eds. 2012. The Earth Expansion Evidence - A Challenge for Geology, Geophysics and Astronomy. Rome, Aracne Ed., xiv + 493 pp.

Volcanic sands and benthic Foraminifers in a forensic soil related to a murder case: Can these particles support intelligence for establishing soil provenance?

Somma R.*¹, Maniscalco R.², Sabatino G.³ & Schiavone S.⁴

1. Dipartimento di Scienze dell'Ambiente, della Sicurezza, del Territorio, degli Alimenti e della Salute (S.A.S.T.A.S.), Università di Messina. 2. Dipartimento di Scienze Biologiche, Geologiche e Ambientali - Sezione Scienze della Terra, Università di Catania. 3. Dipartimento di Fisica e Scienze della Terra, Università di Messina. 4. Reparto Investigazioni Scientifiche (RIS) Carabinieri di Messina.

Corresponding email: rsomma@unime.it

Keywords: Forensic geology, foraminifers, volcanic glass.

In the case of serious crimes, the contact of objects (such as shoes, boots, and clothes) with soil can determine the transfer of materials that may represent an important physical evidence to be analysed in forensic soil science. In this study, we better analysed composition of one forensic sample, related to a murder case (Romeo et al., 2013). The sample was mostly formed by inorganic particles with a lower content in organic component (little stems, roots, seeds, and leaves). Most of the inorganic component was formed by marly-clayey aggregates. Inorganic component was represented by mono- and polymineral silicate clasts and black amorphous grains showing a sandy to silty texture. The main minerals were quartz, muscovite, feldspar, and biotite. XRPD analyses evidenced also the occurrence of minor calcite, clinocllore, montmorillonite, and augite; XRPD indicated that the feldspar was anorthite. The main polymineral clasts were represented by sericite phyllites and gneiss. The EDX and XRPD analyses on the black amorphous grains indicated that the glass derived from hawaiitic-type magma. Several mm-size fossils of marine environment, such as foraminifera (less than 30), or bioclasts of mollusks and gastropods were also found. Particularly foraminifera, smaller than 2 mm in size, were mainly benthic. *Amphistegina lessonii* d'Orbigny was the most common species, followed in abundance by *Elphidium crispum* (Linnaeus). We found only one specimen, which can be assigned to *Planulina ariminensis* d'Orbigny. Small globigerinids were also found. Compositional data suggested that the forensic sample was formed by a wide range of inorganic particles (in order of abundance: sedimentary, metamorphic, and volcanic) and fossils. The here presented data would suggest that the forensic soil presumably originated from a geological area where the three groups of rocks coexist. An important constraint was the presence of very peculiar volcanic clasts whose geochemical features are compatible with Etna activity occurred during the last ten years. Within the sample there are metamorphic clasts, too; they are widespread in the crystalline basements of the Internal Zones of the Alpine belt and could therefore derive from the Calabria-Peloritani Arc. Finally, the sample contained fossils and marly-clayey aggregates, which are generally recorded in Pleistocene to Recent formations that crop out along the Ionian and Tyrrhenian sides of the Calabria-Peloritani Arc. Consequently the studied forensic soil could geographically derive from the Calabria-Peloritani Arc, in an area not too far from the coast and where Mount Etna volcanic ashes could also be present.

Romeo M., Maugeri G., Riccitelli W., Petruzzelli D., Schiavone S., Dugo G., Maniscalco R., Mottese A., Pollicino G.M., Sabatino G., Salvo A., Somma R. 2013. Murder: from victim identification to crime reconstruction. Forensic Science Society Summer Workshop, Lancaster Hall Hotel London, 27th-28th July 2013.

***In vitro* transformations of mineral fibers: a transmission electron microscopy investigation**

Vigliaturo R.*¹, Langenhorst F.², Pollok K.², Harries D.², Capella S.¹, Pugnali A.⁴ & Belluso E.¹⁻³

1. Dipartimento di Scienze della Terra, Università di Torino. 2. Department of Analytical Mineralogy of Micro and Nanostructures, Friedrich-Schiller University, Jena, Germany. 3. Istituto di Geoscienze e Georisorse, C.N.R. Torino. 4. Dipartimento di Scienze Cliniche e Molecolari, Università Politecnica delle Marche.

Corresponding email: ruggero.vigliaturo@unito.it

Keywords: Asbestos, Transmission Electron Microscopy, *in vitro*.

The biological interaction of several mineral fibers with cells and tissue can generate fibrosis, lung cancer and mesothelioma and represent an important interdisciplinary issue. These minerals are recognized as primary factor in the generation of reactive oxygen species (ROS). The thought that only fiber morphology and dimension represent the carcinogenic factors sounds like naive at the today level of consciousness: it is evident that other aspects such as the availability of metallic cations, structural defects and surface characteristics have to be considered, as well.

The target of this work is to study the possible chemical and physical transformations of mineral fibers (chrysotile, crocidolite and asbestiform erionite) in an “*in-vitro*” environment. To explore the possibility of different behaviour of mineral fibers, two biological environments (mesothelial and bronchoalveolar cells) representing their first target have been used. Investigations were carried out through high-resolution transmission electron microscopy, on the non-interacted fibers, after 48 hours and 96 hours interaction with cell cultures. This sheds light on transformations at the three levels of investigations (morphology, chemistry and crystallinity degree).

The most intense morphological and crystalline modification happens in chrysotile fibers, whilst higher chemical variation occurs in asbestiform erionite. Crocidolite is the most resistant in the biological environment, showing mainly a loss of non-tetrahedral coordinated cations.

This innovative approach allows to model interaction dynamics and collect information in the mineralogical, medical and biological fields.

The exhumation history of upper mantle rocks from the Sila unit, northern Calabria

Caparelli S.¹, Scicchitano M.R.² & Piluso E.¹

¹ Dipartimento di Biologia, Ecologia e Scienze della Terra, Università della Calabria, Italy.

² Research School of Earth Sciences, The Australian National University, Canberra, Australia.

Corresponding email: s.caparelli@libero.it

Upper mantle rocks occur in the northern sector of the Calabria-Peloritani Arc. They represent the deepest parts of the Sila Unit that is interpreted as a continuous section of continental lithosphere. The main lithologies consist of serpentinites and subordinate pyroxenites. Serpentinites formed after Amph-peridotites and have the mineral assemblage Ol+Opx±Amph±Spl. Pyroxenites are distinguished into: (i) tectonitic, and (ii) magmatic pyroxenites. The first occur as centimetric to metric layers deformed along the main mantle foliation and show porphyroclastic textures. The mineral assemblage is given by Opx±Cpx±Amph±Ol±Spl. Magmatic pyroxenites occur as centimetric to decimetric dykes cutting the main mantle foliation. They have a medium grain size and preserve typical magmatic textures. The mineral assemblage is given by Opx±Cpx±Amph±Spl. The subsolidus evolution of ultramafic rocks under investigation can be described by four main stages. Mineral assemblages in peridotites as well as temperatures estimated using the Opx-Cpx geothermometer in tectonitic pyroxenites (*i. e.*, ca. 820°C) suggest a first equilibration in the Spl-lherzolite facies. The transition to the Amph-lherzolite facies is documented by crystallization of amphibole, spinel, and olivine at the expenses of pyroxene. A third equilibration in the Chl-lherzolite facies ($T < 770^{\circ}\text{C}$) is documented by formation of chlorite after spinel. Lastly, late serpentine veins suggest hydration at $T < 500^{\circ}\text{C}$. This later event occurred during extensional tectonics as documented by the geometrical relationships of serpentine veins and by the growth textures of serpentine minerals in the fractures. These features suggest gradual decompression and cooling of upper mantle rocks related to lithospheric thinning associated with Permo-Triassic gabbroic magmatism (Liberi et al., 2011). Gabbros can be observed either at the crust-mantle boundary or as centimetric to metric dykes in ultramafic rocks. Petrographic analyses allowed to identify metasomatic textures in ultramafic rocks related to gabbros intrusion. Melt-rock interaction processes determined locally the transformation of amphibole-peridotites into hercynite-bearing peridotites as well as of tectonitic pyroxenites into websterites. Gabbroic magmatism occurred at $P \approx 0.55$ GPa (Liberi et al., 2011), while ultramafic rocks were equilibrating in the Amph-lherzolite facies. Therefore, ultramafic rocks in northern Calabria are fragments of subcontinental mantle exhumed during the Permo-Triassic rifting responsible for the breakup of Pangaea, and they record subsolidus equilibration as well as evidences for melt-rock interaction processes.

Liberi F., Piluso E. & Langone A. 2011. Permo-Triassic thermal events in the lower Variscan continental crust section of the Northern Calabrian Arc, Southern Italy: insights from petrological data and in situ U-Pb zircon geochronology on gabbros. *Lithos*, 124, 291-307.

Contents

Plenary lectures

Bodnar R.J.: The Metamorphosis of Melt Inclusions from Interesting Artifact to Valuable Geochemical Tool	5
Bonadonna C.: Volcanic ash and civil aviation: a new perspective	6
Doglionio C.: Plate tectonics: a polarized self-organized chaotic system	8
Nancy L. Ross : Mineralogy and Crystal Chemistry: Past, Present and Future	11

S1 - Mountain building processes: from surface to deep Earth

Balestro G., Borghi A., Compagnoni R., Cossio R., Gattiglio M. & Ghignone S.: Metamorphic and structural constrains for the exhumation of (U) HP - metaophiolites from the Susa Valley, Western Alps	13
Bartoli O., AcostaVigil A., Cesare B., Remusat L., Tajcmanova L., Walle M., Heinrich C. & Poli S.: Crustal melting from amphibolite- to granulite-facies conditions: the perspective of melt inclusions	14
Beltrando M., Manatschal G., Mohn G., Dal Piaz G.V., Vitale Brovarone A. & Masini E.: From rift-inherited hyper-extension to orogenesis: De-coding the axial zone of the Alpine belt	15
Bistacchi A., Gouffon Y., Monopoli B., Massironi M., Sartori M. & Dal Piaz G.V.: 3D modelling and balancing of post-metamorphic brittle deformation in the Austroalpine-Penninic collisional wedge of the NW Alps	16
Bolognesi F., Vinciguerra S., Bistacchi A. & Dobbs M.: The role of the mechanical anisotropy on deformation and failure mode of phyllosilicate-rich mylonitic fabric: new insights from rock deformation laboratory experiments	17
Carmignani L., Massa G., Salvini R., Pieruccioni D., Tufarolo E., Conti P., Mancini S. & Lorenzoni V.: Acquisition of morpho-structural data by the use of aerial lidar and proximal sensing in the southern end of Monte Altissimo syncline (Apuan Alps, Italy)	18
Carosi R., Montomoli C. & Iaccarino S.: In-sequence shearing within the Greater Himalayan Sequence in Central Himalaya: deformation and metamorphism by crustal accretion from the Indian plate	19
Garofalo P.S., Crispini L., GundlachGraham A., Günther D. & Capponi G.: The Au-transporting hydrothermal fluid of the shear syntectonic vein of Dorn, northern Victoria Land (Antarctica)	20
Iaccarino S., Montomoli C., Carosi R., Massonne H.J., Langone A. & Visonà D.: Pressure-temperature-time-deformation path of kyanite-bearing migmatitic paragneiss in the Kali Gandaki valley (Central Nepal): Evidence for Late Eocene-Early Oligocene melting	21
Iaccarino S., Montomoli C. & Papeschi S. : Tectonometamorphic evolution of the Massa Unit in Punta Bianca area (Northern Apennines, Italy)	22
Lo Pò D., Braga R. & Massonne H.J.: Unusual interpretation of the compositional heterogeneity of potassic white mica in low-grade metapsammopelites from Punta Bianca, Tuscany, by integrating petrography, mineral chemistry and thermodynamic modeling	23
Malatesta C., Gerya T., Crispini L., Federico L. & Capponi G.: Mountain building processes at oblique subduction zones: clue from 3D numerical models	24
Martin S., Tumiati S., Godard G., Toffolo L. & Nestola F.: The high-pressure Fe-Mn metacherts of the Aosta valley: a key to the metamorphic evolution of the Piemonte Nappe	25
Mosca P., Groppo C., Rapa G. & Rolfo F.: Structural and petrological features of the central-eastern Nepalese Himalaya	26
Nirta G., Montanari D., Moratti G., Papini M., Piccardi L., Carras N., Catanzariti R., Moraiti E. & Valleri G.: Preliminary	27

new stratigraphic, biostratigraphic and structural data on the Boeotian Flysch (Boeotia and Parnassus, central Greece).....	
Palmeri R., Di Vincenzo G., Godard G., Sandroni S., Talarico F. & Ricci C.A.: High-pressure metamorphism in Antarctica as marker of different palaeo-subduction zones: a review between history and scientific research.....	28
Rebay G., Zanoni D. & Spalla M.I.: HP/UHP metamorphic and structural evolution of subducted rodingites from the upper Valtouranche, Western Alps, Italy	29
Rolfo F., Groppo C., Sachan H.K. & Rai S.K.: Cold subduction processes in the western Himalaya (Ladakh, NW India): petrological constraints from lawsonite-blueschist facies metasediments	30
Scarsi M. & Malatesta C.: Lawsonite-bearing HP metabasite associated with eclogite in the Voltri Massif (Ligurian Alps, Italy): constraints for the geodynamic evolution	31
Somma R., NavasParejo P., MartínAlgarra A., RodríguezCañero R., SanchezNavas A., Cambeses A., Scarrow J.H. & Perrone V.: The Silurian beds of the Calabria-Peloritani Southern Subterranean (southern Italy).....	32
Tartarotti P., Festa A., Benciolini L. & Balestro G.: Mantle-cover sequence in the Western Alps metaophiolites: a key to recognize remnants of an exhumed Oceanic Core Complex (OCC)	33
Toffolo L., Martin S. & Nimis P.: The Cogne magnetite-bearing ultramafic body (NW Italian Alps): a metasomatized slice of oceanic lithosphere.....	34

S2 - Mantle processes and crustal genesis in extensional environments

Agostini S., Ronca S., Bellon H., Luciani N. & Lustrino M.: The Oligo-Miocene alkaline volcanism of Bahariya (Western Desert, Egypt)	36
Armienti P. & Gasperini D.: Rethinking mantle heterogeneity: insights into mantle geology	37
Basch V., Ferrando C., Rampone E., Ildefonse B., Crispini L. & Godard M.: Microstructural variations in lower crustal oceanic troctolites: an indicator of melt-rock interactions (Erro Tobbio, Ligurian ophiolites, Italy)	38
Berno D., Sanfilippo A., Tribuzio R. & Zanetti A.: Major and trace element variability within the troctolite-olivine gabbro association of the Pineto ophiolite (Corsica)	39
Borghini G., Fumagalli P. & Rampone E.: Partial melting experiments on a natural pyroxenite at 1 and 1.5 GPa: insights on the role of secondary-type pyroxenite in basalt generation	40
Borghini G.: Multiple origins of pyroxenites in the upper mantle: from nature to experiments	41
Callegaro S., Marzoli A., Bertrand H., BlichertToft J., Reisberg L., Cavazzini G., Zanetti A., Jourdan F., Davies J., Parisio L., Bouchet Bert Manoz R. & Schaltegger U.: Isotopic evidence for an enriched lithospheric component in the mantle source of the Freetown Layered Complex (Sierra Leone)	42
Francomme J.E., Fumagalli P. & Borghini G.: Olivine-gabbros and olivine-rich troctolites origin through melt-rock reaction in oceanic spreading lithosphere: an experimental study up to 0.7 GPa.....	43
Giovanardi T., Girardi V.A.V., Correia C.T., Sinigoi S., Tassinari C.C.G. & Mazzucchelli M.: Comparing the Cana Brava and Niquelândia complexes: different contamination and fractionation processes in coeval intrusions.....	44
Giovanardi T., Zanetti A., Morishita T., Langone A., Dallai L. & Mazzucchelli M.: Gabbroic dykes in the Finero Phlogopite-Peridotite Massif: evidence for melt-peridotite interactions at mantle conditions and igneous sapphirine formation by auto-metasomatism.....	45
Langone A., Zanetti A., Renna M.R., Tiepolo M., Mazzucchelli M. & Giovanardi T.: New insights into the evolution of the Finero Mafic Complex, north-eastern Ivrea-Verbano Zone	46
Ligi M., Bonatti E., Bosworth W., Cai Y., Cipriani A., Palmiotto P., Ronca S., Sanfilippo A. & Seyler M.: Oceanization starts from below during continental rifting in the Red Sea.....	47
Mazzeo F.C., Zanetti A., D'Antonio M., Petrosino P. & Aulinas M.: Melt/rock interaction: case study from Mt. Pollino ophiolites (Basilicata, Southern Italy)	48

Montanini A., Luguet A., Van Acken D. & Tribuzio R.: Highly siderophile elements and Os isotope compositions of recycled mantle pyroxenites in the Ligurian mantle section (N Apennine, Italy).....	49
Montanini A., Tribuzio R., Zanetti A. & Zibra I.: The lherzolite-pyroxenite-hornblendite association from St. Lucia (Corsica): evidence for refertilization of subcontinental mantle.....	50
Natali C., Beccaluva L., Bianchini G., Savo A. & Siena F.: Modelling the petrogenesis of the Ethiopian-Yemeni picrite-basalt CFB association: inferences on mantle heterogeneities and plume processes.....	51
Petriglieri J.R., Salvioli Mariani E., Costa S., Mantovani L., Tribaudino M., D'Alessio D., Bersani D. & Lottici P.P.: Preliminary study on polymorphs of serpentine present in the ophiolites from La Rocchetta (Taro Valley, Eastern Ligurian Apennines, Italy).....	52
Pinarelli L., Mattash M.A., Vaselli O., Minissale A. & Tassi F.: Geochemical evolution of mantle sources during continental rifting: the volcanism of the Red Sea.....	53
Sanfilippo A., Morishita T. & Senda R.: Role of melt-mantle interactions on the composition of MORB: the case of Re-Os isotopes.....	54
Sanfilippo A., Tribuzio R., Ottolini L. & Hamada M.: Olivine from replacive mantle bodies reveals modes of partial melting of the MORB mantle source.....	55
 S3 – The cycles of volatiles: fluxes and processes from the oceans, down to the mantle and backward to the Earth surface	
Barbieri R. & Cavalazzi B.: Microbial biogeomorphology in extreme surface environments fed by hot and cold springs and its implications.....	57
Bottini C. & Erba E.: Biogenic carbonate paleofluxes as proxy for $p\text{CO}_2$ during the Aptian.....	58
Calabrese S., D'Alessandro W., Aiuppa A. & Parello F.: Chemistry and fluxes of major and trace element from worldwide passive degassing volcanoes: a critical review.....	59
Callegaro S., Baker D.R., Marzoli A., De Min A. & Geraki K.: Sulfur degassing from LIPs estimated through clinopyroxene/melt S partition coefficient: synchrotron analyses and experimental constraints.....	60
Cardellini C., Chiodini G., Frondini F. & Caliro S.: Diffuse CO_2 Earth degassing in Italy: a globally relevant study case.....	61
Casellato C.E. & Erba E.: Tithonian Nannofossil Calcification Events and the Shatsky Rise Plateau emplacement: is there a relationship?.....	62
Casellato C.E. & Erba E.: The Toarcian Oceanic Anoxic Event and the emplacement of the Karoo-Ferrar Large Igneous Province: calcareous nannoplankton evidence trace major climate and paleoceanographic changes.....	63
D'Alessandro W., Yuce G., Italiano F., Bellomo S. & Gulbay A.H.: Geochemical characterization of the fluids circulating in the Kizildag ophiolitic body (Turkey).....	64
Daskalopoulou K., D'Alessandro W., Kyriakopoulos K., Calabrese S. & Parello F.: Gas manifestations of Greece: Catalogue, geochemical characterization and gas hazard definition.....	65
Erba E. & Bottini C.: Environmental consequences of Ontong Java Plateau and Kerguelen Plateau volcanism: Climate and ocean variability under excess CO_2	66
Faucher G., Erba E. & Bottini C.: The effects of excess CO_2 on calcareous nannoplankton biocalcification: the case history of the latest Cenomanian Oceanic Anoxic Event 2.....	67
Frigo C. & Stalder R.: OH incorporation in quartz in lithium-bearing systems at high pressure.....	68
Gagliano A.L., D'Alessandro W., Tagliavia M., Franzetti A., Parello P. & Quatrini P.: Interaction between geosphere and biosphere in geothermal soil at Pantelleria Island, Italy.....	69
Giacomoni P.P., Coltorti M., Bonadiman C., Ferlito C., Pelorosso B. & Ottolini L.: Inside the volatile content of Antarctic mantle responsible for the Cenozoic basic alkaline magmatism of Northern Victoria Land (Antarctica).....	70

Mair P., Zöll K. & Tropper P.: Electron microprobe U-Th-Pb dating of monazite inclusions in apatite: geochronological clues to fluid-rock interaction during Permian hornfels formation in the Monte Sabiona contact aureole	71
Minissale S. & Ferlito C.: Geochemical and petrographic characterization of basalts and rhyolites of Fantale's area (Ethiopia)	72
Sanna L., Arca A., Casula M. & Duce P.: Preliminary data on natural CO ₂ emissions from Nurra karst terrain (NW Sardinia, Italy).....	73
Scambelluri M.: The role of altered ultramafic rocks in subduction-zone volatile recycling	74
Scicchitano M.R., Rubatto D., Hermann J., PadrónNavarta J.A. & Shen T.: Oxygen isotope analysis of serpentine minerals by SHRIMP: analytical developments and geological applications	75
Tumiati S., Tiraboschi C., Pettko T., Recchia S., Ulmer P. & Poli S.: Silicate dissolution boosts the CO ₂ content of deep fluids	76
Vitale Brovarone A., Chu X., Martin L.A.J. & Ague J.J.: On the complexity of volatile fluxes in subducting oceanic slabs	77

S4 – The subduction factory - a key element in the Earth's dynamics

Avanzinelli R., Casalini M., Elliott T. & Conticelli S.: Constraining slab recycling under Vesuvius volcano from combined U-series and non-traditional stable isotope (Mo, ²³⁸ U/ ²³⁵ U) data	79
Bianchini G. & Natali C.: Carbon budget in Calatrava and Tallante xenoliths: insights on sources and petrogenetic processes	80
Borghini A., Ferrando S. & Groppo C.: Geologic and petrographic study of the veins in the metabasites of the ultra-high pressure Lago di Cignana Unit (upper Valtourneche, western Alps)	81
Cannaò E., Scambelluri M., Agostini S. & Tonarini S.: As, Sb and B-Sr-Pb isotopes in Voltri serpentinites: evidences of fluid-mediated mass transfer in subduction zones.....	82
Casalini M., Avanzinelli R., Elliott T., Tommasini S. & Conticelli S.: Non-traditional isotope tracers (²³⁸ U/ ²³⁵ U and ⁹⁸ Mo/ ⁹⁵ Mo) of subduction processes in the Central-Mediterranean magmatism.....	83
Castelli D., Groppo C., Ferrando S., Elia D., Meirano V. & Facchinetti L.: Is there a new UHP unit in the Southern Dora-Maira Massif? Insights from metasomatic Coe-Ctd-Gln-Grt-talcschists used for ancient quern-stones (III c. AD)	84
Colombi F., Chalal Y., Agostini S. & Lustrino M.: Late Miocene ultrapotassic rocks from NE Algeria (Constantine) in the framework of the circum-Mediterranean lamproites	85
Conte A.M., Perinelli C., Bianchini G., Natale C., Martorelli E. & Chiocci F.L.: New geochemical data on submarine volcanics from the Pontine Archipelago (Tyrrhenian Sea, Italy)	86
Förster B., Bianchini G., Natali C., Aulbach S. & Braga R.: Tracing carbon sources and mobility in subduction zones: an approach using carbon contents and isotopes in orogenic Ulten Zone peridotites.....	87
Ferrando S., Groppo C., Frezzotti M.L., Castelli D., Compagnoni R. & Proyer A.: Dolomite evolution from HP to UHP conditions: the impure Cal-Dol marbles from Dora-Maira Massif (Italian Western Alps)	88
Gilotti J.A., Petrie M.B. & McClelland W.C.: Ultrahigh-pressure metamorphism in accretionary orogens – the contribution of tectonic erosion to the subduction factory	89
Malatesta C., Federico L., Crispini L. & Capponi G.: Blueschist-facies boudinage and veining: implications for deformation processes and fluid flow in subduction zones.....	90
Martelli M. & Bianchini G.: Noble gases isotope composition of mantle-derived peridotite xenoliths from Sardinia.....	91
Mattioli M., Renzulli A., Agostini S. & Lucidi R.: Magmas with slab fluid and decompression melting signatures coexisting in the Gulf of Fonseca: evidence from Isla El Tigre volcano (Honduras, Central America).....	92
Mazzucchelli M.L., Angel R.J., Alvaro M., Nimis P., Domeneghetti M.C. & Nestola F.: Host-inclusion geobarometry for ultra high pressure metamorphic (UHPM) rocks.....	93
Moratti G., Santo A.P., Benvenuti M., Laurenzi M.A., Braschi E. & Tommasini S.: Genesis and evolution of the Late	94

Mesozoic magmatism of the High Atlas (Morocco).....	
Moretti H.C., Blundy J.D. & Gottsmann J.H.: The contributions of oxidised crustal carbonates to the modification of the explosive, aluminium depleted magmas of the Pollara eruptions of Salina, Italy.....	95
Pinarelli L., Christofides G., Pipera K., Soldatos T., Koroneos A. & Peckay Z.: Mantle heterogeneity and crustal contamination in Tertiary extensive magmatism in Southern Rhodopes: geochemical and isotope evidence from Evros volcanic rocks (Greece).....	96
Poli S.: The subduction of carbonated rocks and Earth degassing at warm convergent margins.....	97
Tiepolo M. & Vannucci R.: The contribution of amphibole from deep arc crust to the Silicate Earth's Nb budget.....	98
Tiraboschi C., Tumiati S., Ulmer P., Pettko T. & Poli S.: Solubility of forsterite, enstatite and magnesite in high-pressure COH fluids.....	99
Tumiati S., Godard G., Martin S., Malaspina N. & Poli S.: Are the Mn-rich subduction metasediments of Praborna (Zermatt-Saas Unit) really ultra-oxidized?.....	100
 S5 – Subduction and exhumation of continental lithosphere: implications on orogenic architecture, environment and climate	
Brandmayr E., Raykova R., Romanelli F. & Panza G.: A geophysical perspective on the lithosphere-asthenosphere system of the Periadriatic region.....	102
Clarke A.P., Vannucchi P. & Vinciguerra S.: Mechanics of Variably Deformed Basalt in the Osa Mélangé, Costa Rica: implications for seismogenesis in the erosive Middle America subduction zone.....	103
Cocetta F., Peresan A. & Panza G.F.: Competing/collaborative effect between snow-ice load and tectonic forces modulates large earthquakes occurrence.....	104
Ferraccioli F., Armadillo E., Crispini L. & Capponi G.: The Ross orogen in northern Victoria Land (Antarctica): new aeromagnetic and gravity perspectives for its geodynamic evolution and crustal architecture.....	105
Ferrando S. & Frezzotti M.L.: Petrological and geochemical role of fluid phases in orogenic settings.....	106
Gropo C., Rolfo F., Castelli D., Mosca P. & Rapa G.: Metamorphic CO ₂ -producing processes in collisional orogens: case studies from the Himalayas.....	107
Iaccarino S., Montomoli C., Carosi R., Massonne H.J., Langone A. & Visonà D.: Geology and tectono-metamorphic evolution of the Himalayan Metamorphic Core along the Mugu Karnali transect, Western Nepal (Central Himalaya).....	108
Montomoli C., Carosi R., Langone A., Iaccarino S. & Visonà D.: Relations between South Tibetan Detachment System, Tethyan Sedimentary Sequence and High Himalayan granite: a new perspective.....	109
Nunziata C., Costanzo M.R. & Mandara R.: Lithospheric V _s models in the Campanian volcanic area.....	110
Orešković J., Šumanovac F., Hegedüs E., Kolar S. & Kovács A.C.: Receiver functions analysis to determine crustal structure at the contact of the northern Dinarides and southwestern Pannonian Basin.....	111
Piana Agostinetti N. & Rosenbaum G.: An incipient lithospheric tear fault beneath Northern Apennines? Insights from geophysical and geological data.....	112
Piccolo A., Faccenda M., Carosi R., Visonà D. & Montomoli C.: Post collisional evolution in hot orogens and influence of surface processes.....	113
Rapa G., Gropo C., Rolfo F., Mosca P. & Neupane P.K.: Metamorphic CO ₂ -source rocks in collisional orogens: a petrographic journey through not-(always) obvious CO ₂ -producing lithologies in central Himalaya.....	114
Romanelli F.: The subduction of continental lithosphere: insights from multiscale geophysical modeling.....	115
Rossetti P., Barale L., Bertok C., d'Atri A., Gerdes A., Martire L., Piana F. & Scarrone F.: Metamorphic recrystallization related to the circulation of CO ₂ -rich hydrothermal fluids: the case of the Valdieri marbles (Maritime Alps).....	116
Spalla M.I., Delleani F., Gosso G., Marotta A.M., Rebay G., Regorda A., Roda M., Zanoni D. & Zucali M.: Exploitation	117

methods of the metamorphic rock memory in the continental crust of orogenic belts to infer subduction history.....	
Zanetti A., Giovanardi T., Mazzucchelli M., Langone A., Tiepolo T. & Wu F.Y.: LAM U-Pb zircon Early Jurassic exhumation age of the Finero Phlogopite Peridotite (Ivrea-Verbanò Zone, Western Alps) and its geodynamic consequences	118
S6 – Experimental and Computational Methods in Mineralogy and Geochemistry	
Benisek A., Dachs E. & Kroll H.: A comparison of ternary feldspar-mixing models	120
Campione M.: Nanotribological analysis of frictional anisotropy of crystalline surfaces and its relationship with surface structure studied through atomic force microscopy.....	121
Capizzi L.S., Fumagalli P., Poli S. & Tumiati S.: The mobility of hydrous carbonate liquids in the mantle: an experimental model.....	122
Carroll M.R.: Crystallization kinetics and time-scales of magmatic processes	123
Cavazzini G.: Determining isotopic composition of elements by linearization of exponential instrumental isotope fractionation	124
Dachs E., Benisek A. & Geiger C.A.: The way from estimated to measured thermodynamic properties: The impact of relaxation calorimetry on petrological calculations.....	125
Gatti E., Coleman M. & Bustos D.: Quantifying groundwater changes in evaporitic basins using stable isotopes experimental approaches on hydrated minerals	126
Mair P., Tropper P., Manning C. & Harlov D.: Solubility of F-Cl-apatites in KCl-H ₂ O brines at 800 °C and 1 GPa: Implications for REE transport during high-grade metamorphism.....	127
Malaspina N.: Forward modelling of redox equilibria in the Earth mantle: simple versus complex systems.....	128
Merli M., Bonadiman C., Diella V. & Pavese A.: Lower mantle hydrogen partitioning between periclase and perovskite: a quantum chemical modeling.....	129
Merlini M., Sciascia L., Merli M., Gatta G.D., Pavese A., Hanfland M., Lausi A. & Plaisier J.: Complexity of CaCO ₃ polymorphism	130
Miozzi F., Tumiati S., Recchia S., Tiraboschi C. & Poli S.: A new methodology to analyse COH fluids in experimental capsules.....	131
Moro D., Ulian G. & Valdrè G.: Cross-correlated Scanning Probe Microscopy and Quantum Mechanics investigation of chlorite-glycine interaction at the single molecule level	132
Orlando A., Ruggieri G., Chiarantini L., Rimondi V. & Borrini D.: Fluid-rock interaction experiments at supercritical conditions: a tool to investigate geothermal systems.....	133
Ortolano G., Visalli R. & Cirrincione R.: Timescale of relaxation of garnet growth zoning via multi-component diffusion modeling: the example of Mammola Paragneiss Complex (Serre Massif-Southern Calabria).....	134
Poli S. & Da Mommio A.: Liquids from CaCO ₃ in the presence of H ₂ O and the mobility of carbon in subduction zones.....	135
Russo C., Bianchi S., Protano G. & Salleolini M.: Multivariate statistical characterization of groundwater chemistry: a case study in a zone affected by hydrothermal circulation (southern Tuscany, Italy)	136
Rustioni G., Angel R.J., Milani S., Mazzucchelli M.L., Nimis P., Domeneghetti M.C., Marone F., Alvaro M., Harris J.W. & Nestola F.: Elastic geobarometry for host-inclusion systems: Pressure release and the role of brittle failure	137
Stabile P., Giuli G., Behrens H., Knipping J., Webb S., Cicconi M.R. & Paris E.: Experimental study on the effect of alkali ratio and oxygen fugacity on Fe redox and viscosity in pantelleritic glasses	138
Stangarone C., Tribaudino M., Lottici P.P. & Prencipe M.: Analysing the Raman vibrational pattern of Mg ₂ Si ₂ O ₆ <i>Pbca</i> enstatite: a quantum mechanical approach	139
Tiraboschi C., Tumiati S., Recchia S. & Poli S.: Carbon-saturated COH fluids speciation at 1 GPa: experimental data versus	140

thermodynamic modeling.....	
Ulian G., Moro D. & Valdrè G.: Quantum mechanics simulations of structural and physico-chemical properties of apatites and layer silicates	141
Vitale Brovarone A.: Limits in modeling organic carbon-bearing rocks at upper crust and forearc slab conditions.....	142
Zaffiro G., Angel R.J., Alvaro M., Nestola F., Domeneghetti M.C., Scandolo L., Mazzucchelli M.L., Milani S., Rustioni G. & Marciano C.: New micro-furnace for “in situ” high-temperature single crystal X-ray diffraction measurements.....	143
Ziberna L., Green E.C.R., Schumacher J. & Blundy J.D.: Geobarometry of igneous cumulates and the depth of magma storage zones	144

S7 – Microstructures: key to the interpretation of processes

Aretusini S., Mittempergher S., Gualtieri A.F. & Di Toro G.: Frictional processes in smectite-rich gouges sheared at low to high slip rates	146
Cirrincone R., Ortolano G., Pezzino A., Sacco V., Visalli R., Fiannacca P., Punturo R. & Mengel K.: Alpine re-activation of a late post - Variscan shear-zone: microstructural and petrological investigations (Sila, northern Calabria).....	147
Collettini C., Carpenter B.M., De Paola N., Giorgetti C., Mollo S., Scuderi M.M., Tesei T., Trippetta F. & Viti C.: Timing of microstructure development along carbonate-bearing faults	148
Fazio E., Ortolano G., Cirrincone R., Pezzino A. & Visalli R.: Microstructures and quartz c-axis patterns of mylonites at the ductile-brittle transition: insights from a crustal scale shear zone (Southern Calabria, Italy).....	149
Fiannacca P., Lombardo R., Militello G.M. & Cirrincone R.: Insights on the relationships between felsic granitoids in the Serre Batholith (Calabria, southern Italy) from plagioclase microstructures and compositions	150
Giorgetti C., Carpenter B.M. & Collettini C.: Fault zone microstructures from laboratory experiments on calcite/talc binary mixtures.....	151
Hassan B., Butt S. & Hurich C.: Control of saturant’s state upon intergranular adhesion affecting seismic and aseismic near surface site strength response inferred by combined V_p/V_s and Poisson’s ratios examination	152
Hassan B., Butt S. & Hurich C.: Understanding scale and direction dependent strength susceptibility of fault systems to seismic and aseismic effects by examining lateral and dilatational displacements characteristics using S-waves	153
Mittempergher S., Cerchiari A. & Remitti F.: Deformation mechanisms of the shallow subduction plate interface of the Sestola Vidiciatico unit, Northern Apennines (Italy)	154
Montomoli C., Iaccarino S., Carosi R., Nania L. & Lezzerini M.: Strain softening mechanisms in a regional scale shear zone: the Main Central Thrust Zone in the Mt. Makalu area (Eastern Nepal)	155
Punturo R., Cirrincone R., Fazio E., Fiannacca P., Kern H., Mengel K., Ortolano G. & Pezzino A.: Development of petrofabric within the Kavala syn-tectonic pluton (NE Greece) and insights for the seismic behaviour of extensional shear zones	156
Smeraglia L., Billi A., Carminati E. & Cavallo A.: Carbonate-clay mixing in cataclasite during fault activity	157
Tesei T., Viti C., Mugnaioli E. & Collettini C.: Frictional strength and deformation microstructures of mineralogically controlled Serpentinities.....	158
Zambrano M., Tondi E., Mancini L., Dinolfo G., Aibibula N., Arzilli F. & Napoli G.: 3D image analysis of deformation bands in porous carbonate grainstones	159
Zucali M., Spalla I., Gosso G., Chateigner D., Ouladdiaf B., Tartarotti P., Fontana E., Mancini L. & Barberini V.: Quantitative microstructural analysis of naturally deformed rocks as tool to understand tectono-metamorphic evolution.....	160

S8 – Magma chamber dynamics and timescales of volcanic processes

Bardeglinu I., Cioni R. & Scaillet B.: Experimental constraints on pre-eruption conditions of the 1631 Vesuvius eruption.....	162
---	-----

Braschi E., Francalanci L. & Vougioukalakis G.: Investigating heterogeneous magma systems by detailed characterization of the juvenile products: example from the Upper Pumiceeruption at Nisyros Volcano (Greece)	163
Campagnola S., Vona A., Romano C. & Giordano G.: Rheology and crystallization kinetics of the Pozzolane Nere tephriphonolite from Colli Albani volcano (Italy).....	164
D’Oriano C., Landi P., Pimentel A. & Zanon V.: Magmatic Processes Revealed by Textural and Compositional Features of Large Anorthoclase Crystals from the Lajes-Angra Ignimbrite (Terceira Island, Azores).....	165
De Rosa R., Di Salvo S., Donato P., Francalanci L., Gioncada A., Nicotra E., Pistolesi M., Viccaro M., Barca D. & Braschi E.: The Lipari-Vulcano volcanic complex: insights into the plumbing system of the last 1000 years.....	166
Di Salvo S., Francalanci L., Braschi E., Avanzinelli R. & Druitt T.H.: Understanding the last 3600 years plumbing system evolution of Santorini volcano: contributions by <i>in-situ</i> micro-Sr isotope data	167
Fantozzi I., Petrone C.M., Vougioukalakis G., Braschi E. & Francalanci L.: Pre-eruptive magmatic processes associated with the historic explosive activity of Kolumbo submarine volcano, Santorini, Greece: a petro-chemical study on the emitted products.....	168
Garozzo I., Romano C., Giordano G., Geshi N. & Vona A.: Magma dynamics of the 2000 Miyakejima eruption inferred from textural analysis of erupted products	169
Giacomoni P.P., Coltorti M., Ferlito C. & Mollo S.: Textural and chemical zoning of clinopyroxene and plagioclase as a tool to calculate the thermobarometric constraints of Mt. Etna feeding system	170
Giordano G. & Cashman K.: Calderas and magma reservoirs.....	171
GonzálezGarcía D., Zezza A., Vetere F., Behrens H., Morgavi D., Petrelli M. & Perugini D.: Experimental determination of major and trace element diffusivities in natural silicate melts: application to magma mixing and determination of timescales of volcanic eruptions	172
Laeger K., Petrelli M., Andronico D., Scarlato P., Cimarelli C., Del Bello E., Misiti V., Taddeucci J. & Perugini D.: High-resolution geochemical mapping of volcanic ash: Constraining of end-member proportions for syn-eruptive magma mixing of 2010 Eyjafjallajökull eruption.....	173
Mari N.: Temporal evolution of magma mixing related to the explosivity of volcanic eruptions	174
Mazzeo F.C., Fedele L., Iovine R., Aienzo I., Cavallo A. & D’Antonio M.: Timescales of mixing from diffusion chronometry on alkali feldspar phenocrysts from the Agnano-Monte Spina Eruption (4.7 ka), Campi Flegrei (southern Italy)	175
Morgavi D., Perugini D., De Campos C., ErtlIngrisch W. & Dingwell D.B.: Morphochemistry of Structures Produced by Mixing of Rhyolitic and Basaltic Melts: Volcano-Petrological Implications	176
Pensa A., Jowitt S.M., Giordano G. & Cas R.A.F.: The geochemical evolution of the Fogo A eruptive sequence: timing of development of anti-rapakivi textures and implications for dual magma source or zoned magma chamber models	177
Pensa A., Porreca M., Corrado S., Giordano G. & Cas R.A.F.: The thermal state of pyroclastic flow deposits of the 4.6 ka Fogo A plinian eruption sequence, São Miguel, Azores, using pTRM analysis and charcoal reflectance data, and implications for eruption and flow processes	178
Petrelli M., El Omari K., Le Guer Y. & Perugini D.: Timescales of Magma Mixing Unraveled by Numerical Simulations.....	179
Petrone C.M., Bugatti G., Braschi E. & Tommasini S.: NIDIS: Non-Isothermal Diffusion Incremental Step model. A new approach to elemental diffusion in volcanic rocks	180
Pompilio M., Bertagnini A., Pistolesi M., Di Roberto A., Isaia R., Cioni R., Francalanci L., Romano C., Campagnola S., Di Salvo S., Voloschina M. & Mazzone F.: Magma dynamics during Baia - Fondi di Baia eruption (Campi Flegrei) as inferred by microanalysis of juvenile products	181
Redi D., Danyushevsky L., Lima A., Cannatelli C., Esposito E. & De Vivo B.: Somma-Vesuvius’s activity over the last 33 ka years: a mineral chemistry prospective.....	182
Rocchi S., Paoli G., Jacobs J. & Ksienzyk A.: Inherited and antecrystic zircons as time markers for magma ascent/storage.....	183
Vetere F., Iezzi G., Behrens H., Holtz F., Ventura G., Misiti V., Cavallo A., Mollo S., Dietrich M. & Perugini D.: Glass	

forming ability of sub-alkaline silicate melts	184
Vona A., Giordano G., De Benedetti A.A., Romano C. & Manga M.: Ascent velocity and dynamics of a mud eruption: an analogue for volcanological studies	185
S9 – The role of GMPV disciplines in the definition of volcanic hazards	
Battaglia A., D’Aleo R., Tamburello G., Bitetto M., Delle Donne D., Coltelli M., Patanè D., Cannata A. & Aiuppa A.: SO ₂ degassing during the summer 2014 Etna eruption: a comparison between OMI satellite and ground-based SO ₂ flux measurements.....	187
Brancato A., Coltelli M., Tusa G., Proietti C. & Branca S.: Vents Pattern Analysis at Mount Etna volcano (Sicily)	188
D’Aleo R., Battaglia A., Tamburello G., Bitetto M., Delle Donne D., Coltelli M., Patanè D., Cannata A. & Aiuppa A.: Correlation between geochemical and geophysical data on Etna eruption of summer 2014	189
Dioguardi F. & Mele D.: A new shape dependent drag correlation formula for non-spherical rough particles.....	190
Elissondo M., Baumann V., Bonadonna C., Pistolesi M., Cioni R., Bertagnini A., Biass S., Herrero J.C. & Gonzalez R.: Chronology, dynamics and impact of the 2011 Puyehue-Cordón Caulle eruption, Chile	191
Mele D., Dellino P., Dioguardi F., Doronzo D.M., Isaia R. & Sulpizio R.: Hazard assessment of pyroclastic density currents at Mount Somma-Vesuvius: inference from the 79 AD eruption	192
Nazzaro I., Bruno P.P., Maraio S. & Festa G.: Analysis of high resolution 2D seismic reflection profiles for the determination of the structure of the Solfatara Volcano	193
Paredes J., Morgavi D., Di Vito M., de Vita S., Sansivero F. & Perugini D.: Fractal fragmentation theory on pyroclastic deposits from Vesuvius and Campi Flegrei: Determining explosive eruptions energy	194
Tadini A., Bevilacqua A., Neri A., Cioni R., Aspinall W.P., Bisson M., Isaia R., Valentine G.A., Vitale S., Baxter P.J., Bertagnini A., Cerminara M., De Michieli Vitturi M., Di Roberto A., Engwell S., Esposti Ongaro T., Mazzarini F., Pistolesi M., Todde A. & Russo A.: Towards a background probability map for vent opening position in a future Plinian-subPlinian eruption of Somma-Vesuvius, with structured uncertainty assessment.....	195
Valade S., Pistolesi M., Allocca C., Colò L., Coppola D., Delle Donne D., Genco R., Lacanna G., Laiolo M., Marchetti E., Olivieri G. & Ripepe M.: Effusive dynamics at Stromboli volcano (Aeolian Islands) and implications to volcanic hazard.....	196
S10 – Field studies in modern volcanology	
Baldoni E., Lucchi F., Sulpizio R., Forni F., Massaro S. & Tranne C.A.: Geological reconstruction of the cone building and alternating explosive and effusive activity of Monte dei Porri, Salina Island (Italy).....	198
Ciarcia S., Iannuzzi E., Isaia R., Prinzi E.P., Tramparulo F.D.A. & Vitale S.: Field evidences of last 5.5 ka ground deformation at Campi Flegrei caldera	199
Dellino P.: The importance of fieldwork in volcanology.....	200
Di Traglia F., Pistolesi M., Fusillo R., Rosi M. & Gioncada A.: The volcanological evolution of the Island of Vulcano in the last 1000 years.....	201
Fusillo R., Brooker R.A., Di Traglia F. & Blundy J.D.: Stratigraphic reconstruction of the Corbetti caldera (Main Ethiopian Rift).....	202
Gatti E., Leszczynska K., Durant A., Jeans C., Boreham S., Gibbard P.L. & Oppenheimer C.: Short-term environmental impact of the Youngest Toba Tuff, ~ 75 ka.....	203
Laurenzi M.A., Braschi E., Casalini M. & Conticelli S.: Timing of the shift from leucite-free (Tuscan Magmatic Province) to leucite-bearing (Roman Magmatic Province) magmas in Italy	204
Lucchi F.: Stratigraphic approach to fieldwork and mapping in volcanic areas: examples from Stromboli and the Aeolian Islands	205

Massaro S., Costa A. & Sulpizio R.: Stratigraphic data highlight the conduit erosion behavior during Plinian eruptions: the example of the Pomici di Avellino eruption of Somma-Vesuvius	206
Mussetti G., Corti G., van Wyk de Vries B. & Hagos M.: Volcanic rifts bracketing volcanoes: an analogue answer to an old unsolved problem	207
Ort M.H., de Vita S., Marotta E. & Sansivero F.: The use of AMS in the reconstruction of resurgent blocks kinematics: the Ischia island (Italy) case study	208
Pistolesi M., Bertagnini A., Di Roberto A., Isaia R., Cioni R., Vona A., Mazzone F. & Voloschina M.: The Baia - Fondi di Baia eruptions (Campi Flegrei): from fieldwork to physical volcanology	209
Principe C., GropPELLI G., Gottardi I., Faoro S., Antonelli A., BrogginI R. & MartI Molist J.: A new debris avalanche deposits on Tenerife (Canary Islands)	210
Ruberti D., Vigliotti M., Ermice A., Rolandi G. & Rolandi R.: Stratigraphic architecture of the Campania Plain, southern Italy. A key to understand evolution and impact of volcanic activity.....	211
Sulpizio R., Sarocchi D., Dellino P. & RodriguezSedano L.A.: Insights on volcanic granular flow dynamics from laboratory experiments and comparison with natural deposits	212
Todde A., Cioni R., Andronico D. & Mundula F.: Proximal products of the 16 March, 2013 eruption of Mt. Etna: dynamics and significance of large ejecta	213
Tramparulo F.D.A., Isaia R. & Vitale S.: Structural analysis of fractures, faults and dykes in the Somma-Vesuvio volcano	214
 S11 – Mineralogy	
Alvaro M., Angel R.J., Mazzucchelli M.L., Domeneghetti M.C. & Nestola F.: Elastic geobarometry for UHPM rocks: A link between mineralogy and petrology.....	216
Ardit M., Martucci A., Rodeghero E. & Cruciani G.: Spontaneous strain variations through the monoclinic-orthorhombic phase transition of ZSM-5 zeolite: effect of adsorbed organic molecules	217
Balassone G., Bellatreccia F., Ottolini L., Mormone A., Petti C., Della Ventura G. & Ghiara M.R.: Sodalite-group minerals from Somma-Vesuvius volcano (southern Italy): an EPMA, SIMS and FTIR study	218
Ballirano P., Pacella A., Cremisini C., Nardi E., Montereali M.R., Fantauzzi M., Atzei D., Rossi A. & Cametti G.: An insight into the mechanism of Fe (III) acquisition by erionite fibres: a first step toward the comprehension of the mechanisms inducing their carcinogenicity	219
Barucca S., Bellatreccia F., Della Ventura G., Butini F., Casanova Municchia A., Ricci M.A. & Sodo A.: Multi-methodological characterization of opals: Defining origin, structure, composition and gemological properties	220
Bellatreccia F., Della Ventura G., Cestelli Guidi M., VentruTI G., Schingaro E., Capitelli F. & Grita S.: FTIR spectroscopy of phosphate minerals with complex H-bonds network.....	221
Bernardini S., Bellatreccia F., Casanova Municchia A., Della Ventura G. & Sodo A.: Applications of Raman spectroscopy to the study of natural manganese oxides	222
Biagioni C., Bindi L. & Moëlo Y.: Structural complexity in sulfosalts – “Cu-sterryite” and meerschautite: two new expanded derivative of owyheeite from Italy	223
Biagioni C., Moëlo Y. & GuillotDeudon C.: Structural complexity in sulfosalts – Chovanite: two new occurrences from the Apuan Alps and its 8 Å crystal structure.....	224
Biagioni C., Mauro D. & Pasero M.: Crystal structure refinement of römerite and melanterite, two hydrated iron sulfates with complex hydrogen bond systems.....	225
Bonazzi P., Lepore G.O. & Bindi L.: Expanding the number of arsenic sulphides having a layered structure: duranusite, a new structural type related to arsenolamprite	226
Boni P., Balassone G., Mondillo N. & Boni M.: An unusual occurrence of gahnite in lower Cambrian dolostones of southwest Sardinia (Italy): chemical characterization and genetic hypotheses.....	227

Cesare B., Viti C., Mugnaioli E., Schmidt M.W. & Remusat L.: Progressive thermal deprotonation of staurolite during crustal anatexis: NanoSIMS, TEM and experimental constraints.....	228
D'Alessio D., Tribaudino M., Gaboardi M., Magnani G., Pontiroli D. & Riccò M.: New data on melanophlogite (type I clathrate) from Fortullino (Livorno, Italy).....	229
D'Ippolito V., Andreozzi G.B., Bersani D. & Lottici P.P.: Raman study of MgAl ₂ O ₄ -CoAl ₂ O ₄ and MgAl ₂ O ₄ -MgCr ₂ O ₄ solid solutions.....	230
De Grisogono F., Giuli G. & Paris E.: Si-P substitution mechanisms in olivines: Rietveld characterization of the LiMgPO ₄ -Mg ₂ SiO ₄ solid solution.....	231
Della Ventura G., Susta U., Bellatreccia F., Cavallo A. & Oberti R.: Synthetic potassic-ferro-richterite: HT behavior and deprotonation process by single-crystal FTIR spectroscopy and structure refinement.....	232
Garavelli A., Balić-Žunić T., Pinto D., Mitolo D., Jakobsson S.P. & Leonardsen E.: Na ₂ Ca ₃ Al ₂ F ₁₄ - A new fluoride phase from fumaroles on Eldfell, Hekla and Vesuvius.....	233
Giaccherini A., Di Benedetto F., Cinotti S., Montegrossi G., Guerri A., Carlà F., Felici R. & Innocenti M.: Structural characterization of Cu _{2-x} S ultra thin films obtained by electrodeposition.....	234
Giordani M. & Mattioli M.: Morphology and chemistry of erionite and offretite: increasing data of carcinogenic fibrous zeolites.....	235
Guastoni A., Pozzi G., Secco L., Fioretti A.M. & Pennacchioni G.: Xenotime-(Y) from LCT and NYF Tertiary pegmatites of the Central Alps.....	236
IannicelliZubiani E.M., Cristiani C., Dotelli G., Gallo Stampino P., Pelosato R., Lacalamita M., Mesto E. & Schingaro E.: Characterization of natural clays for rare earth ions recovery from WEEE.....	237
Lenaz D. & Schmitz B.: Crystal-structure determination of chromites from NWA6077 and NWA725 achondrites.....	238
Lepore G.O., Bindi L., Bonazzi P., Ciriotti M.E., Di Benedetto F., Mugnaioli E., Viti C. & Zanetti A.: A multimethodic approach to the characterization of a Mn-rich celadonite from Cerchiara mine, Eastern Liguria, Italy.....	239
Lepore G.O., Bindi L., Bonazzi P., Pedrazzi G. & Conticelli S.: Structural and chemical variations in phlogopites from lamproitic rocks of the Western Mediterranean Region.....	240
Lotti P., Gatta G.D., Arletti R., Merlini M., Pastero L. & Liermann H.P.: Large-channels zeolites at high pressure: the case of Na-mordenite and AlPO ₄ -5.....	241
Mesto E., Kaneva E., Lacalamita M., Schingaro E., Scordari F. & Vladykin N.: Structural disorders in narsarsukite structure..	242
Mugnaioli E., Capitani G.C. & Viti C.: Electron diffraction tomography for the characterization of sub-micrometric minerals: application to metamict phases.....	243
Nazzareni S., Comodi P. & Hanfland M.: High-pressure single-crystal X-ray synchrotron diffraction of pentahydrate.....	244
Oberti R., Boiocchi M. & Hawthorne F.C.: Impossible or unusual solid-solutions in oxo-amphiboles: mangano-mangani-ungarettiite vs. "oxo-mangani-leakeite" and potassic-fluoro-richterite vs. "oxo-potassic-richterite".....	245
Radica F., Della Ventura G., Bellatreccia F., Cinque G., Marcelli A. & Cestelli Guidi M.: HT-FTIR micro-spectroscopy of CO ₂ in cordierite: temperature dependence of the absorption and diffusion kinetics.....	246
Radica F., Della Ventura G., Bellatreccia F., Freda C., Marcelli A. & Cestelli Guidi M.: The diffusion of CO ₂ in cordierite and beryl: an FTIR-FPA spectroscopy study.....	247
Rinaldi R. & Llovet X.: The first 50 years of Electron Probe Micro-Analysis applications to the Geosciences: developments and perspectives.....	248
Scandolo L., Alvaro M., McCammon C., Milani S., Di Prima M., Domeneghetti M.C. & Nestola F.: The role of oxidation on the high-temperature behavior of Almandine.....	249
Schingaro E., Lacalamita M., Mesto E., Ventrucci G., Pedrazzi G., Ottolini L. & Scordari F.: Ti-rich garnets: an EPMA, SIMS, MÖSSBAUER, XRPD and SCXRD investigation.....	250

Stelluti I., Ioli P., Mura F. & Gianfagna A.: Analysis of the mineralogical content of incoherent lava portions containing fibrous minerals from volcanic products found in localities around S. Maria di Licodia town (CT), Italy	251
Susta U., Della Ventura G., Bellatreccia F., Hawthorne F.C., Boiocchi M. & Oberti R.: Crystal chemistry and HT behavior of riebeckite from Malawi: a combined XRD and FTIR study.....	252
Zaccarini F., Bindi L., Garuti G. & Bakker R.J.: The importance of a multimethodic approach for the characterization of platinum group minerals (PGM) and associated phases: some cases of study.....	253
 S12 – Mantle mineralogy	
Belmonte D., Ottonello G., De La Pierre M. & Vetuschi Zuccolini M.: Majorite stability and melting relations in the mantle transition zone: new constraints from first-principles thermodynamics	255
Boffa Ballaran T., Kurnosov A., Frost D.J. & Marquardt H.: The influence of cation substitution on the elastic behaviour of MgSiO ₃ bridgmanite in the lower mantle.....	256
Del Vecchio A., Poe B.T., Misiti V. & Cestelli Guidi M.: Hydrogen diffusion in nominally anhydrous minerals: implications for mass and charge transport.....	257
Gemmi M., Merlini M., Palatinus L., Fumagalli P., Fischer J. & Poli S.: Two new high pressure hydrated phases in the MASH system discovered with fast electron diffraction tomography: bringing water beyond the chlorite breakdown.....	258
Gentili S., Bonadiman C., Biagioni C., Comodi P., Coltorti M., Zucchini A. & Ottolini L.: Oxo-amphiboles in mantle xenoliths: a key to understand the hydrous rich metasomatic melts circulating beneath Harrow Peaks, Victoria Land, Antarctica	259
Guidoni F., Comodi P., BalicZunic T., Nazzareni S., Bini R., Fanetti S. & Brizi E.: Structural and photoelectric properties of chalcostibite at high pressure.....	260
Lenaz D., De Min A., Hålenius U., Kristiansson P., Musco M.E., Nilsson C., Perugini D., Petrelli M., Princivalle F., Ros L., Skogby H., Caldeira R., Grillo B., Marzoli A., Mata J., Boumehdi M.A., Idris Ali A.B. & Youbi N.: Mantle xenoliths of Cameroon, Morocco and Libya: A structural and chemical (major oxides, trace elements, REE, OH and B) study of their mineral assemblage	261
Milani S., Scandolo L., Zaffiro G., Di Prima M., Mazzucchelli M.L., Alvaro M., Domeneghetti M.C. & Nestola F.: On the determination of the entrapment pressure for garnet inclusions in diamonds.....	262
Zibera L. & Klemme S.: The effect of spinel-to-garnet peridotite transition on density variations in the upper mantle	263
 S13 – Characterization and use of geomaterials for sustainable industry and the environment	
Ardit M., Cruciani G. & Dondi M.: V-doped zircon: new diffraction and optical spectroscopy data on industrial pigments	265
Barone G., Mazzoleni P., Di Benedetto F., Giuffrida A., Capilleri P., Massimino M.R., Motta E., Genovese C. & Raccuia S.A.: Geotechnical and environmental aspects of the use of Mt. Etna volcanic tephra in embankment structures.....	266
Belviso C., Cavalcante F. & Lettino A.: Comparison between ultrasonic treatment and hydrothermal method for waste material transformation into useful secondary products.....	267
Clausi M., Tarantino S.C., Tedeschi C., Riccardi M.P., Zema M.: Microstructural features of geopolymer-based mortars: insights from high resolution SEM.....	268
Coletti C., Maritan L., Mazzoli C. & Cultrone G.: Assessment for the use of waste of trachyte in the brick production	269
Diella V., Marinoni N., Pavese A. & Francescon F.: The influence of quartz and waste glass particle size distribution on the evolution of sanitary-ware vitreous body	270
Gatta G.D., Brundu A., Cappelletti P., Cerri G., de Gennaro B., Farina M., Fumagalli P., Guaschino L. & Mercurio M.: The Cs-cycle in nuclear processes: From Cs-nanosponges to ceramic Cs-bearing materials	271
Ghizzardi V., Mantovani L., Romeo E., Tribaudino M. & Montepara A.: Fly-ash as a filler in environmentally-friendly hot	

mix asphalt	272
Gori C., Tribaudino M., Mantovani L., Skogby H., Hålenius U., Delmonte D., Mezzadri F., Gilioli E. & Calestani G.: Synthesis and color performance of $\text{CaCo}_x\text{Mg}_{1-x}\text{Si}_2\text{O}_6$ pyroxenes as ceramic pigments	273
Graziano S.F., D'Amore M., Correggia C., Dondi M., Zanelli C., Cappelletti P., Langella A. & de Gennaro R.: Manufacturing of high efficiency concretes: potential production of lightweight aggregates (LWA) from glass recycling	274
Graziano S.F., D'Amore M., Dondi M., Zanelli C., Cappelletti P., Langella A., Mercurio M. & de Gennaro R.: Secondary raw materials for the production of lightweight aggregates: some case studies	275
Lotti P., Gatta G.D., Arletti R., Quartieri S., Vezzalini G. & Merlini M.: The use of pressure to tailor the “sponge-like” behavior of zeolites: the case of SiO_2 -ferrierite	276
Martucci A., Blasioli S., Marchese L., Buscaroli E., Mzini L.L. & Braschi I.: High silica zeolites used to clean-up water polluted with sulfonamide antibiotics: from multidisciplinary model studies to real applications and regeneration techniques	277
Novembre D., Pace C., Gimeno D., d'Alessandro N. & Tonucci L.: Hydrothermal synthesis and characterization of kalsilite by using a kaolinitic rock (Sardinia, Italy) and its application in the production of biodiesel	278
Randazzo L. & Montana G.: Effects of compositional and textural characteristics of clay based plasters on the control of indoor relative humidity	279
Salviulo G., Strumendo M., Zorzi F. & Biasin A.: Thermal decomposition of calcite: CaO properties and growth model	280
Scrivano S., Gaggero L., Cnudde V., De Kock T., Derluyn H. & Gisbert Aguilar J.: Multiscale approach to rock porosity and its distribution	281
Tarantino S.C., Occhipinti R., Gasparini E., Riccardi M.P. & Zema M.: Sulfate-bearing kaolins: an unexploited resource. Implications for their use as alkali activated materials precursors	282
Zucchini A., Comodi P., Di Michele A., Blasi P., Gentili S., Santinelli F. & Neri A.: Nanomaterials addition to raw mixtures for portland clinker production. A way to decrease clinkerization temperature	283
 S14 – Environmental mineralogy and geochemistry: natural environment versus human activities	
Agrosì G., Tempesta G., Lisco S., Moretti M., Scardino G., Cotecchia F., Sollecito F., Vitone C., Lacalamita M., Mesto E., Schingaro E. & Mastronuzzi G.: Heavy metal analyses on core of polluted submarine sediments from Taranto: preliminary results	285
Atzori R., Ardaù C., Podda F., Agrosì G. & Frau F.: Removal of divalent metals by inducing precipitation of Layered Double Hydroxides from mine-waste drainages (Iglesias, Italy)	286
Bardi U.: The End of the Anthropocene and Beyond	287
Barone G., Mazzoleni P., Acquafredda P., Costagliola P., Barchitta M., Quattrocchi A., Maugeri A. & Agodi A.: Particulate matter exposure influencing the global DNA methylation in women: a cross-sectional study in Catania, Italy	288
Bernardini S., Armiento G., Bellatreccia F., Cavallo A., Della Ventura G., Proposito M. & Sodo A.: Enrichment of toxic elements in a Mn deposits associated with the Santa Severa (Latium, Italy) travertine quarry	289
Biddau R., Cidu R., Lorrain M. & Mulas G.: Lead and arsenic concentrations in groundwater from Sardinia (Italy). Natural background and influence of mining activities	290
Capecchiacci F., Zoppi M., Cabassi J., Marchionni S., Tassi F., Vaselli O., Pratesi G., Giannini L., Venturi S., Ulivi M., Forni F., Scodellini R. & Tommasini S.: Geochemical and mineralogical tracers of geothermal power plants input into the atmosphere: the case study of the Mt. Amiata geothermal field	291
Capella S., Fioretti E. & Belluso E.: Airborne inorganic fibers in Turin: identification and quantification by SEM-EDS	292
Capella S., Bellis D. & Belluso E.: Forensic mineralogy and pathology: a case-control study	293
Carbone C., Consani S., Dinelli E., Cutroneo L., Capello M., Salviulo G., Zorzi F. & Lucchetti G.: PTE (Potential ecotoxic Element) mobility in stream and marine sediments: the case of Gromolo Torrent (eastern Liguria, Italy)	294

Cibella F., Falcone E.E., Latteo V., Saiano F., Marcenò C. & Censi P.: Effect of the atmospheric fallout on the Rare Earths distribution in leaves	295
Colica A., Chiarantini L., Rimondi V., Benvenuti M., Costagliola P., Lattanzi P., Paolieri M. & Rinaldi M.: Toxic metal dispersion in mining areas: from point source to diffusion pollution. The case of Mt. Amiata Hg mining district (southern Tuscany - Italy): first results.....	296
Consani S., Carbone C., Salviulo G., Zorzi F., Dinelli E. & Lucchetti G.: Temperature-induced phase transition and remobilization of potential ecotoxic elements (PTE) in AMD colloidal precipitates	297
D’Orazio M., Biagioni C., Vezzoni S. & Dini A.: Inside the mine: interactions between hydrosphere, atmosphere, biosphere and the thallium-rich pyrite ores from southern Apuan Alps	298
Da Pelo S., Mulas G., Ghiglieri G., Ardaù C., Cidu R., Frau F. & Porcheddu A.: Origin of manganese, sulphates and trichloromethane in groundwater at Portoscuso (Sardinia-Italy).....	299
Di Benedetto F., Gazzano E., Tomatis M., Turci F., Pardi L.A., Bronco S., Fornaciai G., Innocenti M., Montegrossi G., Muniz Miranda M., Zoleo A., Capacci F., Fubini B., Ghigo D. & Romanelli M.: Physico-chemical properties of quartz from industrial manufacturing and its cytotoxic effects on alveolar macrophages: the case of green sand mould casting for iron production	300
Dore E., Cidu R. & Frau F.: Antimony removal from polluted mining water using Layered Double Hydroxides.....	301
Franceschini F., D’Orazio M., Biagioni C., Vezzoni S., Petrini R. & Giannecchini R.: Severe contamination of waters and stream sediments in an abandoned mine land from Alta Versilia (Southern Apuan Alps, Italy).....	302
Frau F., Da Pelo S., Atzori R. & Cidu R.: Environmental impact of a near-neutral mine drainage on surface waters and dissolved metal load to the Mediterranean Sea	303
Marescotti P., Crispini L., Fornasaro S., Beccaris G., Scotti E., Poggi E. & Lucchetti G.: Chromium and nickel distribution in ultrabasic soils of the Voltri Massif (Ligurian Alps).....	304
Marescotti P., Solimano M., Marin V., Salmona P., Vassallo P., Brancucci M. & Lucchetti G.: Mineralogical and geochemical spatial analyses of waste-rock dumps: a case study from the abandoned Rio Bansigo sulphide mine (eastern Liguria, Italy)	305
Medas D., Cidu R., De Giudici G. & Podda F.: Rare earth elements fractionation processes during mine waste weathering and secondary phases precipitation under near-neutral conditions.....	306
Medas D., De Giudici G., Podda F., Meneghini C. & Lattanzi P.: Apparent solubility constant of hydrozincite: effect of crystal size and surface energy	307
Monteali M.R., Angelone M., Manojlovic M., Armiento G., & #;abilovski R., Crovato C., De Cassan M., Massanisso P. & Vidojević D.: Mobility of potentially toxic elements in urban soils: a comparison between Rome and Novi Sad.....	308
Nannoni F., Protano G. & Rossi S.: Heavy element contamination in soil and accumulation in earthworms in the urban area of Siena (Italy).....	309
Nigro A., Barbieri M. & Sappa G.: Rare earth elements and Heavy metals in soils of an open landfill.....	310
Nigro A., Barbieri M. & Sappa G.: Rare earths elements and ⁸⁷ Sr/ ⁸⁶ Sr in groundwater landfill	311
Petrini R., D’Orazio M., Giannecchini R. & Bramanti E.: Thallium ecosystem diseases in dismissed mine sites as a threat for public health: the Valdicastello-Pietrasanta (Italy) case history	312
Pugnali A., Tiano L., Capella S., Vigliaturo R. & Belluso E.: Chrysotile, crocidolite, asbestiform erionite: mineralogical characterization and citotoxic effects	313
Pusceddu C., Medas D., Podda F., Cidu R., Lattanzi P., Wanty R., Kimball B. & De Giudici G.: Hydrological and Biogeochemical processes in the critical hyporheic zone along a mine-polluted-river (Rio San Giorgio – SW Sardinia-Italy)	314
Rossi M., Nestola F., Ghiara M.R. & Capitelli F.: Fibrous minerals from Somma-Vesuvio volcanic complex.....	315
Salviulo G., Magro M., Baratella D., Bonaiuto E., Carbone C., Dinelli E. & Vianello F.: Removal of Cr(VI) in contaminated water of Stoppani S.p.a. site (Liguria, Italy) by surface active maghemite nanoparticles	316

Tamburo E., Varrica D. & Dongarrà G.: Coverage intervals for trace elements in human scalp hair are site and also gender-specific	317
Tiepolo M., Langone A., Sacchi E., Nola P., Ficocelli S. & Giua R.: Historical reconstruction of heavy metal pollution in the Taranto area with dendrochemistry	318
Varrica D., Tamburo E. & Dongarrà G.: Influence of industrial activity on metal and metalloid contents in scalp hair of adolescents	319
Venturi S., Cabassi J., Tassi F., Capecchiacci F., Vaselli O., Bellomo S. & Calabrese S.: Active real-time analyzers vs. passive/diffusive samplers for hydrogen sulfide (H ₂ S) in air: a critical comparison	320
Vigliaturo R., Giorcelli M., Tagliaferro A. & Belluso E.: Tremolite asbestos: characterization by analytical electron microscopy, Raman spectroscopy and PCA data elaboration.....	321
Zoppi M., Pratesi G., Capecchiacci F., Cabassi J., Marchionni S., Tassi F., Vaselli O., Giannini L., Venturi S., Ulivi M., Forni F., Scodellini R. & Tommasini S.: PM ₁₀ emission near the Mt. Amiata geothermal field	322
 S15 – The geosciences for Cultural Heritage and Archeometry: consolidated and innovative approaches	
Artioli G.: Geosciences and the Cultural Heritage: the time line of human activities	324
Balassone G., Cicala L., D’Orazio L., De Bonis A., De Rosa F., Guarino V., Morra V. & Tardugno M.L.: Preliminary archaeometric investigations on ancient mortars from archaeological site of Velia (Salerno, Southern Italy).....	325
Barca D., PerezMonserat E.M., Török A., Aly N., GomezHeras M., Fort R., Varas-Muriel M.J., Alvarez de Buergo M., Valeria C. & Ruffolo S.: Heavy metals in black crusts on limestones as markers of environmental conditions influencing human health.....	326
Belfiore C.M., Fichera G.V., Ortolano G., Pezzino A. & Visalli R.: Element distribution within the cementitious matrix of pozzolanitic roman mortars: a new approach using image processing via x-ray map analyser	327
Belfiore C.M., Fichera G.V., Pezzino A., Ruffolo S., Calabrò C., Maniscalco R. & Malagodi M.: The carbonate building stone of the Ortygia Island (Syracuse, Italy): characterization and decay processes	328
Bianchi G., Mitchell J., Agresti J., Osticioli I., Siano S., Memmi Turbanti I. & Pacini A.: Preliminary chemical and mineralogical characterization by non-invasive analytical techniques of the <i>fibula di Montieri</i> from the archaeological site of the Canonica di S.Niccolò (Montieri, GR).....	329
Comite V., La Russa M.F., Ricca M., Rovella N., Ruffolo S.A., Urzi C., Arcudi A. & Silvestri C.: Innovative conservative strategies applied in Herculaneum archaeological site (Naples, Italy): the case of <i>Villa dei Papiri</i>	330
Comite V., Ricca M., Rovella N., Ruffolo S.A., Bonazza A., Sardella A., Urzi C., Arcudi A. & Silvestri C.: Multidisciplinary approach to characterize degradation products and archaeological materials from Roman <i>Thermae</i> of Reggio Calabria (Calabria, South Italy)	331
Crupi V., Majolino D., Pezzino A., Ruffolo S. & Venuti V.: Multi-technique spectroscopic investigation in Cultural Heritage	332
Dal Sasso G., Maritan L., Angelini I., Usai D., Salvatori S., Zerboni A. & Artioli G.: Radiocarbon dating of heavily altered bone apatite from the Al Khiday archaeological site (Central Sudan): is pristine apatite carbonate preserved?	333
De Bonis A., D’Angelo M., Guarino V., Massa S., Saiedi Anaraki F., Genito B. & Morra V.: Technology and Provenance of the Unglazed Pottery from the masjed-i jom‘e of Isfahan (Iran)	334
De Francesco A.M., Scarpelli R., Mastandrea A., Guido A. & Marino D.A.M.: UV fluorescence as tool to evaluate the biotic encrustation pervasiveness on underwater medieval amphorae near Crotona (Calabria - Italy).....	335
De Luca R., Gigliotti V., Panarello M., Bloise A., Crisci G.M. & Miriello D.: Characterization and provenance of plasters from residential buildings of 18 th century in Lamezia Terme (Calabria, Southern Italy)	336
Eramo G. & Giuliani R.: Building stratification in tower area of Montecorvino (Foggia, 11 th -15 th century): evidences of norman masonry techniques.....	337
Eramo G., Muntoni I.M., Gallo S. & De Siena A.: Early Greek Colonization in Southern Italy: archaeometric analyses of	338

ceramic local production and Greek imports in the Siris area (Basilicata)	
Fornacelli C., Mugnaioli E., Colomban P. & Memmi I.: Spectroscopy and electron microscopy for the characterization of CdSxSe1-x Quantum Dots in a Glass Matrix	339
FreireLista D.M. & Fort R.: Decay in heritage granite ashlar. Its dependence with exfoliation microcracks	340
Garavelli A., Marsico A., Pinto D., Monno A., Andriani G., Germinario G., Laganara C., Albrizio P., Piepoli L., Depalo M.R., Longobardi F. & Simonetti A.: The sanctuary of Sant'Angelo in Criptis at Santeramo in Colle, Apulian region, Italy: a multi-disciplinary approach for the conservation	341
Germinario L., Cossio R., Mazzoli C., Maritan L. & Borghi A.: Combining μ -XRF and SEM-EDS mapping in low and high resolution for determining the provenance quarry of volcanic porphyritic stones	342
Giustetto R., Perrone U. & Compagnoni R.: Neolithic polished greenstone implements from Castello di Annone (Italy): minero-petrographic and archaeometric aspects.....	343
Grifa C., Germinario C., Mercurio M., Langella A., Cucciniello C., Cappelletti P., Zollo D., Izzo F., De Bonis A., Monetti V. & Morra V.: Traditional ceramic production in central and southern Madagascar: first insights from mineralogy and petrology of bricks	344
Guarino V., De Bonis A., Grifa C., Langella A., Munzi P. & Morra V.: The Archaic cooking ware and <i>instrumenta</i> in Cuma: Italic and Greek traditions	345
Manca R.P, Pagliantini L., Pecchioni E., Benvenuti M., Chiarantini L., Cambi F., Corretti A., Costagliola P., Orlando A. & Santo A.P.: Archaeometric study of ceramic materials from archaeological excavations at the roman iron-working site of San Giovanni (Portoferraio, Elba island).....	346
Mantovani L., Tribaudino M. & Facchinetti M.: A mineralogical approach to the authentication of an archaeological artifact: real ancient bronze from Roman Age or fake?	347
Marengo A., Borghi A. & Costa E.: Multi-disciplinary approach to the characterization of <i>an ornamental stone</i> : the case study of "Busca Onyx"	348
Marinangeli L., Agostini S., Antonelli S., Baliva A., Cardinale M., Colantuono L., La Salvia V., Menozzi O., Moderato M., Pompilio L., Santoro S. & Somma M.C.: A multidisciplinary geo-archaeological approach to reconstruct the evolution of the Corfinio site (AQ)	349
Montana G., Randazzo L. & Cerniglia M.R.: Mineralogical and petrographic analysis of early-Hellenistic mortars from a Punic-Roman residential area discovered at Palermo (Sicily).....	350
Pecchioni E., Fratini F., Cantisani E., Vettori S. & Ricci M.: Chromatism and the chromatic alteration of the florentine sandstone pietra serena.....	351
Pinto D., Garavelli A., Muntoni I.M., Bellizzi F. & Lamacchia A.: Archaeometrical investigations of painted wall plasters from an Hellenistic <i>domus</i> at Arpi (Foggia, III sec. a.C.).....	352
Poretti G., De Vito C., Conte A.M., Borghi A., Brilli M., Gunter D. & Zanetti A.: <i>In-situ</i> LA-ICP-MS analysis of white marble for provenance purpose: application on Carrara quarry district and Musei Capitolini artifacts.....	353
Ricca M., La Russa M.F., Belfiore C.M., Ruffolo S.A., Barca D. & Crisci G.M.: Provenance study of marbles used as covering slabs in the archaeological submerged site of Baia (Naples, Italy): the case of the "Villa con ingresso a protiro"	354
Rispoli C., Esposito R., Cappelletti P., Morra V. & Talamo P.: <i>Piscina Mirabilis</i> : preliminary characterization of geomaterials	355
Ruffolo S.A. & Crisci G.M.: The use of nano particles in Cultural Heritage: examples of application on stone materials	356
Santello L., Maritan L., Mazzoli C., Germinario L., Nestola F., Hanchar J.M. & Usai D.: Multi-analytical characterisation of Egyptian Flint as a means for understanding seasonality in the Nile valley and Western Desert (Egypt).....	357
Santo A.P., Pecchioni E.P., Piccini L., Di Fazio L., Garzonio C.A. & Fratini F.: The " <i>Vie Cave</i> " archaeological and geologica	358
Silvestri A., Fioretti A.M. & Zanetti A.: Trace element analysis of archaeological glasses: comparison between LA-ICPMS and Electron Microprobe analysis	359

S16 – Fluid geochemistry in volcanic, geothermal and seismic areas

Beddini G. & Frondini F.: Geochemistry of groundwater from Parrano and Fonti di Tiberio (TR), a tool for evaluating the geothermal potential of southern-western Umbria	361
Bonzi L., Capaccioni B., Castaldini D., Coltorti M., Cremonini S., Di Giuseppe D., Ferrari V., Severi P., Sciarra A., Vaccaro C. & Todesco M.: Surface phenomena witnessed during and after the 2012 Emilia earthquakes: Fact or Fiction? A response from water and gas geochemistry	362
Capecchiacci F., Tassi F., Liegler A., Fentrees S., Deering C., Vaselli O., Martinez M. & Taylor Castillo W.: Geochemistry of water and gas discharges from the Tenorio volcanic system (Costa Rica)	363
Caponi C., Tassi F., Vaselli O., Fiebig J., Agosto M., Caselli A. & Liccioli C.: Carbon isotope fractionation of light hydrocarbons in hydrothermal fluids from Copahue volcano, Argentina	364
Cardellini C., Chiodini G., Rosiello A., Bagnato E., Avino R., Frondini F., Donnini M. & Caliro S.: Soil CO ₂ flux degassing at Solfatara of Pozzuoli (Campi Flegrei, Italy): 1998-2015, sixteen years of measurement	365
Chiodini G., Avino R., Caliro S., Cardellini C., Mangiacapra A. & Minopoli L.: Episodes of magmatic fluid injections into the Hydrothermal system of Campi Flegrei: geochemical evidences and physical simulations	366
Di Martino R.M.R., Camarda M. & Capasso G.: <i>In situ</i> determination of the carbon isotopologues of the CO ₂ emitted by soils	367
Di Martino R.M.R., Camarda M., Gurrieri S. & Valenza M.: The concentration transients of CO ₂ , H ₂ , and He in the volcanic gases: theoretical model and experimental results	368
Ricci A., Tassi F., Vaselli O., Fiebig J. & Viveiros F.M.: Carbon isotopic signature of light hydrocarbons (C ₁ –C ₄) in fluids emitted from fumarolic discharges at São Miguel Island (Azores Archipelago, Portugal)	369
Sortino F., Barberi F., Carapezza M.L., Gattuso A., Ranaldi M., Tarchini L., Zanolin F., Cosenza P., Foresta Martin L., Francofonte V., Mastrolia A. & Melián G.: Chromatography Monitoring Station. Potential and applications	370
Vaselli O., Tassi F., Fernandez E., Duarte E., Fischer T., De Moor M., Tardani D. & Martinez M.: Seventeen years (1998-2014) of geochemical observations at the Poás volcano (Costa Rica) fumarolic system	371
Venturi S., Tassi F., Gould I.R., Shock E.L., Lorance E.D., Bockisch C. & Fecteau K.: Experimental studies of mineral-catalyzed dehydrogenation of C ₆ cyclic hydrocarbons under hydrothermal conditions	372

S17 – From Rocks to Stars (The Nuclear History of the Galaxy as Written in Solar System Solids)

Agrosi G., Manzari P., Melone N. & Tempesta G.: Nano-mineralogical study of mesostases in enstatite chondrite	374
Aliatis I., Tribaudino M., Lambruschi E., Mantovani L., Bersani D., Lottici P.P. & Gatta G.D.: Plagioclase composition by Raman spectroscopy: a new tool in the analysis of extraterrestrial samples	375
Capaccioni F. & the VIRTIS Team : The comet 67P/Churyumov-Gerasimenko, a primitive Kuiper Belt body: results from the Rosetta mission	376
Caporali S., Grazi F., Scherillo A. & Pratesi G.: New data about the early stages of asteroidal accretion by neutron diffraction studies of iron meteorites	377
Caporali S., Loglio F., Pratesi G. & Folco L.: Effects of shock loading on ordinary chondrites: an X-ray microtomography study	378
Carli C., Pratesi G., Capaccioni F., Santoro S. & Moggi Cecchi V.: Reflectance spectra of hed, analogues of 4Vesta	379
Collareta A., D’Orazio M., Gemelli M., Pack A. & Folco L.: The diversity of the lunar crust as told by the new polymict regolith breccia Mount DeWitt 12007 (Antarctica)	380
Ferrari S., Alvaro M., Nestola F., Maturilli A., Helbert J., Domeneghetti M.C., Massironi M. & Zorzi F.: Thermal Expansion of C2/c Pyroxenes: Implications for the Thermal Infrared Spectroscopy of Solar System Bodies	381
Fioretti A.M., Mattiuz A. & Goodrich C.A.: A new Enstatite chondrite found in Italy	382

Folco L. & Cordier C.: Oxygen isotopes in cosmic spherules and the composition of the near Earth interplanetary dust complex.....	383
Gemelli M., Mugnaioli E., Di Rocco T. & Boschi C.: High precision d ¹⁷ O isotope analyses for micro-volumes: development of a new strategic resource for the Italian Planetary Sciences community.....	384
Marinangeli L., Pompilio L., Tangari A.C., Cardinale M., Piluso E. & Baliva A.: Mapping the sedimentary rocks on Mars and implications for planet evolution.....	385
Massironi M., Simioni E., Marzari F., Cremonese G., Giacomini L., Pajola M., Jorda L., Naletto G., Lowry S., Ramy ElMaarry M., Preusker F., Scholten F. & the OSIRIS team : Strata and the inner structure of 67P Churyomov-Gerasimenko comet.....	386
Meyzen C.M., Massironi M. & Pozzobon R.: Are magmatic processes at volcanoes from motionless plates analogues to those of the giant shield volcanoes on Mars?.....	387
Moggi Cecchi V., Caporali S. & Pratesi G.: Acapulcoites, winonaites and lodranites: new evidences on petrologic and minerochemical trends from X-ray maps and EMP analyses.....	388
Murri M., Scandolo L., Alvaro M., Domeneghetti M.C. & Fioretti A.M.: Clinopyroxene Fe-Mg exchange reaction applied to Martian nakhlites.....	389
Palmerini S.: Meteorite grains of red giant origins: when rocks help in modelling stars.....	390
Pozzobon R., De Toffoli B., Cremonese G. & Massironi M.: Cracks associated to mud-volcanic fields on Mars: clues for recent methane degassing?.....	391
Stangarone C., Tribaudino M., Prencipe M. & Helbert J.: How to study Mercury's surface in remote sensing: experimentally acquired and <i>ab initio</i> calculated HT-IR vibrational frequencies.....	392
Trippella O., Palmerini S., Busso M.M. & Wasserburg G.J.: Slow neutron captures contribution for isotope anomalies in the Fe-group elements of meteorites.....	393
 S18 – Geological, geophysical and geochemical prospection for economic geology and geothermal resources	
Arfè G., Boni M., Mondillo N., Aiello R. & Arseneau V.: Secondary enrichment of the Capricornio (Chile) epithermal Au-Ag-Cu mineralization and implications for the exploration.....	395
Bernardinetti S., Colonna T., Pieruccioni D., Abbigliati M., Trotta M., Algeri G., Tufarolo E., Minucci S., Mugnaioli E., Talarico F.M., Viti C., Harroud A., Guernouche M. & Cinà A.: A pilot study to test the reliability of the ERT method in the identification of mixed sulphides bearing dykes: the example of Skoura mine (Morocco).....	396
Boni M.: Supergene nonsulfide zinc ores: from exploration to processing.....	397
Botteghi S., Montanari D., Del Ventisette C. & Moretti S.: Persistent Scatterer Interferometry (PSI) to detect surface deformation in the Larderello-Travale geothermal area (Tuscany, Italy).....	398
Capecchiacci F., Eyjólfssdóttir E.I., Tassi F., Vaselli O. & Ruggieri G.: Geochemistry of Volatile Organic Compounds (VOCs) in fluids from the Krafla and Reykjanes geothermal systems, Iceland.....	399
Colucci F., Moia F., Guandalini R. & Agate G.: Geological and numerical modeling to support electric production in geothermal fields: a case test in Central Italy.....	400
Della Vedova B. & Cimolino A.: Geothermal heating and cooling in the FVG Region: the realization of the Grado District Heating Pilot Plant and the Pontebba Ice Rink.....	401
Fadda S., Fiori M., Matzuzzi C., Naitza S. & Secchi F.: Redox state of magmas and granite-related Mo mineralization: evidences from Late Variscan F-bearing granites from Southern Sardinia (Italy).....	402
Fedi M. & La Manna M.: The complex task of inverting gravity data for the estimation of the depth to the carbonate basement.....	403
Fusari A., Invernizzi C. & Carroll M.: Seismic, structural and geochemical prospectons for characterization of a medium-	404

enthalpy geothermal system within the Laga Basin (Central Italy): the Acquasanta Terme case study	
Granitzio F., Naitza S., Oggiano G. & Secchi F.: The Jibal Qutman deposit: first notes on a new gold discovery in the Arabian Shield (Kingdom of Saudi Arabia)	405
Lattanzi P., Ruggieri G., Benvenuti M., Costagliola P., Chiarantini L. & Rimondi L.: The mercury deposits of the Monte Amiata district: a review of existing data	406
Magi F., Pandeli E. & Vaselli O.: Geological, hydrogeochemical and isotopic features of the thermal system between Montalcino and Monte Amiata-Scalo (South-eastern Tuscany)	407
Maimaiti M. & Carroll M.R.: Geochemical behavior of Rare earth elements in magmas	408
Mondillo N., Mathur R. & Boni M.: Significant Zn isotope fractionation in the supergene environment from Yanque, Peru: implications for exploration	409
Montanari D., Minissale A., Doveri M., Trumpy E., Gola G. & Manzella A.: A multidisciplinary approach to unravel the geothermal fluid circulation within a –regional scale- carbonate reservoir	410
Nimis P. & Omenetto P.: Does subduction polarity control metallogeny?	411
Pastore Z., Mondillo N., Boni M. & Fedi M.: The magnetic method applied to the exploration of porphyry-cu deposits: the case of the Dolores Prospect (Peru)	412
Rimondi V., Fregola R.A., Ruggieri G., Zucchi M., Chiarantini L., Orlando A., Brogi A. & Liotta D.: Investigating fossil geothermal systems: the case of Elba Island (Tuscany, Italy)	413
Santilano A., Gola G., Castaldo R., De Novellis V., Pepe S., Tizzani P., Donato A., Trumpy E., Botteghi S. & Manzella A.: 3D geological, thermo-physical and rheological modelling for geothermal exploration: the case study of Ischia Island, Southern Italy	414
Santoro L. & Boni M.: The use of QEMSCAN® automated mineralogy in exploration for supergene Zn(Pb) nonsulfides characterization: a few examples	415
Tempesti L., Tassi F., Caselli A., Liccioli C., Vaselli O., Chiodini G., Agosto M. & Caliro S.: A geochemical conceptual model for the hydrothermal system of the Domuyo volcanic complex (Argentina)	416
Trumpy E., Botteghi S., Caiozzi F., Donato A., Gianelli G., Gola G., Minissale A., Montanari D., Santilano A. & Manzella A.: Geothermal data integration and favourability maps: a tool for discovering geothermal systems in Sicily, southern Italy	417
Vezzoni S., Dini A. & Rocchi S.: Campiglia Marittima skarn deposit: shifting paradigm from exoskarn to reverse telescoping	418
 S19 – Global pollutants: from mercury to POPs	
Acquavita A., Pasquon M., Skert N., Tamberlich F. & Mattassi G.: Total gaseous mercury concentrations and lichens bioaccumulation in the Northern Adriatic coastal area (Gulf of Trieste, Italy)	420
Bagnato E., Sprovieri M., Barra M., Cardellini C. & Tamburello G.: The role of Earth degassing in the global atmospheric mercury budget	421
Cabassi J., Tassi F., Vaselli O., Capecchiacci F., Venturi S., Calabrese S., Nisi B. & Rappuoli D.: Real-time measurements of Hg ⁰ in volcanic, geothermal and anthropogenic systems: a multi-methodological approach using Lumex® instrumentation	422
Cabassi J., Venturi S., Tassi F., Calabrese S., Capecchiacci F., D’Alessandro W. & Vaselli O.: A new geochemical approach to estimate the distribution of air pollutants from natural and anthropogenic sources: examples from Solfatara Crater (Campi Flegrei, Southern Italy) and Mt. Amiata Volcano (Siena, Central Italy)	423
Calabrese S., Cabassi J., Tassi F., Vaselli O., Capecchiacci F., Brusca L., Bellomo S., Daskalopoulou K., D’Alessandro W., Parello F., Niccolini M. & Rappuoli D.: Active Moss biomonitoring of mercury in the mine-polluted area of Mt. Amiata (Central Italy)	424
Chiarantini L., Rimondi V., Benvenuti M., Beutel M.W., Costagliola P. & Lattanzi P.: Are tree barks a suitable tool for Hg air pollution biomonitoring? Preliminary investigation from the Mt. Amiata region	425

Daskalopoulou K., Cabassi J., Calabrese S., D'Alessandro W., Grassa F., Parello F. & Tassi F.: Origin and distribution of methane and C ₂ -C ₆ hydrocarbons in hydrothermal and cold gaseous emissions in Greece.....	426
GarciaOrdiales E., Loredó J., Covelli S., Higuera P., Esbri J.M. & LopezBerdonces M.A.: Heavy metal speciation and risk assessment in freshwater sediments of an artificial reservoir in the Almadén mining district, Spain.....	427
Gozzi C., Menichetti S. & Bucciati A.: Partitioning of geochemical populations on cumulative probability plots: critical comparison of different graphical-numerical methods	428
Pavoni E., Covelli S., Emili A., Lenaz D., Petranich E., Crosera M., Adami G., Cattelan R. & Higuera P.: Geochemical characterization of drainage waters after closure of sulphides extraction activity (Salafossa, Northeastern Italian Alps)	429
Pavoni E., Petranich E., Crosera M., Adami G., Baracchini E., Lenaz D., Emili A., Higuera P. & Covelli S.: Bioaccumulation of Thallium and other heavy metals in <i>Biscutella laevigata</i> nearby a decommissioned Zn-Pb mine (Salafossa, Northeastern Italian Alps).....	430
Petranich E., Covelli S., Contin M., Faganeli J., Acquavita A. & De Vittor C.: Critical factors affecting mercury biogeochemical cycle in fish farm contaminated sediments (Grado Lagoon, Adriatic Sea).....	431
Tassi F., Cabassi J., Calabrese S., Nisi B., Venturi S., Capecchiacci F., Vaselli O. & Giannini L.: Measurements of gaseous elemental mercury (GEM) in diffuse soil emission using the static closed-chamber method	432
Tassi F., Venturi S., Cabassi J., Vaselli O., Gelli I., Cinti D. & Capecchiacci F.: Effects of microbial activity on C-bearing volatile compounds in interstitial soil gases from the Vicano-Cimino volcanic system (central Italy)	433
Vaselli O., Rappuoli D., Bianchi F., Nisi B., Higuera P.L., Cabassi J. & Tassi F.: Mercury pollution in the former mining area of Abbadia San Salvatore (Siena, Tuscany Region, central Italy): actions, criticalities and perspectives for the remediation process.....	434

S20 – Multidisciplinary contributes to the understanding of active geodynamic processes

Antonielli B., Monserrat O., Bonini M., Sani F. & Righini G.: Ground deformation of the Po-Plain detected through satellite radar interferometry (PSInSAR).....	436
Barreca G., Monaco C. & Pepe F.: High-resolution seismic exploration in the Mt. Etna offshore: preliminary results and implications with regional tectonics	437
Bosio G., Gariboldi K., Di Celma C., Gioncada A., Malinverno E., Tinelli C., Villa I.M., Cantalamessa G., Collareta A., Lambert O., Landini W., Urbina M. & Bianucci G.: Tephrochronology and biostratigraphy of two exceptional fossil localities in the Pisco Formation (Peru).....	438
Chiariotti L., Bresciani I. & Perotti C. : Salt diapirism in the Persian Gulf.....	439
Crispini L., Cianfarra P., Salvini F., Federico L. & Capponi G.: Geodynamics of northern Victoria Land (Antarctica): the role of the paleozoic lithospheric discontinuities and their reactivation	440
Cuffaro M. & Ligi M.: Thermal modelling of an oceanic transform domain: implications on rheology and friction along the fault	441
Cultrera F., Burrato P., Ferranti L., Monaco C., Morelli D., Passaro S. & Pepe F.: Active faulting in the Gulf of Patti (south-eastern Tyrrhenian Sea, Italy): evidences from high resolution seismic profiles and swath bathymetry data	442
Da Prato S., Catanzariti R., Ellero A. & Masetti G.: Subsoil geological model of the Leghorn area (Ligurian sea coast, Italy): a stratigraphic approach.....	443
De Matteo A., Castaldo R., D'Auria L., James M.R., Lane S., Massa B., Pepe S. & Tizzani P.: Modelling of volcanoes: the Mt. Vesuvius	444
Dogliani C., Carminati E., Petricca P. & Riguzzi F.: Graviquakes	445
Lirer F., Foresi L.M., Vallefucio M., Baldassini N., Correggia C., Di Stefano A., Ferraro L., Pelosi N., Russo B. & Sagnotti L.: Stable isotope stratigraphy and chronology of Langhian marine records from St. Peter's Pool section (central Mediterranean, Malta Island).....	446

Maestrelli D., Bonini M. & Sani F.: Quaternary slip rates along the frontal thrust system of the Pede-Apennine margin, between the Enza and Panaro valleys, Emilia Romagna, Italy	447
Mantovani A., AbuZeid N., Bignardi S., Caputo R., Palmieri F. & Santarato G.: Multidisciplinary geophysical approach for investigating the recent activity of blind tectonic structures in the eastern sector of the Po Plain (North Italy).....	448
Marchi A., Pandolfi L. & Catanzariti R.: Sandstone provenance and biostratigraphy of Modino Unit stratigraphic succession (Lutetian-Aquiutanian): a key stage of the Northern Apennine foreland basin	449
Meccariello M., Ferranti L. & Pepe F.: Active deformation in the NW sector of the Sicily Channel based on multiscale seismic profile analysis	450
Nestola Y., Balsamo F., Storti F., Ligi M., Bezzerra F.H.R. & Nogueira F.C.: Neogene re-activation of the Pernambuco Lineament (NE-Brazil): onshore and offshore evidence	451
Pagli C., Ebinger C., Keir D. & Wang H.: Diverse pattern of strain at the Afar Triple Junction.....	452
Pellegrino A., Maniscalco R., Speranza F., HernandezMoreno C. & Sturiale G.: Paleomagnetism of the Hyblean Plateau, Sicily: A review of the existing data set and new evidence from the Scicli-Ragusa Fault System.....	453
Piccardi L., Dobrev N., Moratti G., Corti G., Vannucci G. & Matova M.: Towards a seismotectonic map of Bulgaria.....	454
Piccardi L.: Active tectonics of Northern Apennines from digital and high resolution topography	455
Poli M.E., Monegato G., Zanferrari A. & Falcucci E.: Active tectonics at the front of the Eastern Southern Alps in the Carnic Prealps (NE Italy, Friuli).....	456
Salocchi A., Nereo P., Fontana D., Conti S., Grillenzoni C. & Argentino C.: History of Miocene temperate-type carbonate shelf in a compressive setting (northern Apennines), constrained by a chemostratigraphical, microfacies and compositional study.....	457
Scalera G.: Cause of East-West Earth Asymmetry.....	458
Scribano V., Manuella F.C.,Carbone S. & Brancato A.: The Tethyan roots of the Hyblean-Pelagian foreland domain (Sicily): geodynamic implications and possible modern analogues	459
 S21 – Open Poster Session	
Barfucci G., Ripepe M., Delle Donne D. & Lacanna G.: Geophysical signature of the 11 February 2010 dome collapse at Soufrière Hills Volcano, Montserrat, West Indies.....	461
Bello M., Carroll M.R. & Scipioni M.: Volatile metals and municipal waste incineration: a comparison with volcanic melting	462
Bonaccorsi E., Biagioni C. & D’Orazio M.: Minerals, rocks and meteorites on display: the new exhibition at the Pisa University’s Natural History Museum.....	463
Boniello A. & Paris E. : Geoscience education: teaching and learning Earth Sciences using the virtual worlds (Muves)	464
Fiannacca P., Militello G.M., Lombardo R. & Cirrincione R.: I- and S-type granites in the late Variscan Serre Batholith (Central Calabria, Italy) and applicability of the Restite and Peritectic Assemblage Entrainment models	465
Granieri D., Salerno G., Liuzzo M., La Spina A., Giuffrida G., Caltabiano T., Giudice G., Gutierrez G., Montalvo F. & Papale P.: Emission of gas and atmospheric dispersion of SO ₂ during the December 2013 eruption at San Miguel volcano (El Salvador).....	466
Maraio S., Pazzaglia F.J., Bruno P.P.G., Picotti V. & Brardinoni F.: Comparison between catchment geomorphology and alluvial fan seismic stratigraphy in defining the geomorphic process domains in the Val Venosta (Eastern Alps, Italy)	467
Marengo A. & Vigliaturo R.: Principal component analysis as a tool in the study of a mineral population. Muscovite case study.....	468
Pieraccioni F.: The research of active and inquiry based learning in Earth sciences in the school.....	469
Rashed H., Rovere M., Pecchioni E., Gamberi F. & Vaselli O.: Geochemical and mineraloical characterization of marine sediments in the mud diapir province of the Paola basin (Southern Tyrrhenian Sea).....	470

Scalera G.: Variable radius cartography - Birth and perspectives of a new experimental discipline	471
Somma R., Maniscalco R., Sabatino G. & Schiavone S.: Volcanic sands and benthic Foraminifers in a forensic soil related to a murder case: Can these particles support intelligence for establishing soil provenance?	472
Vigliaturo R., Langenhorst F., Pollok K., Harries D., Capella S., Pugnali A. & Belluso E.: <i>In vitro</i> transformations of mineral fibers: a transmission electron microscopy investigation	473
Caparelli S., Scicchitano M.R. & Piluso E.: The exhumation history of upper mantle rocks from the Sila unit, northern Calabria	474

Elenco alfabetico degli autori

A

Abbigliati M. 396
 Abu-Zeid N. 448
 Acosta-Vigil A. 14
 Acquafredda P. 288
 Acquavita A. 420, 431
 Acquavita A. 429, 430
 Adami G. 400
 Agate G. 288
 Agodi A. 36, 82,
 Agostini S. 85, 92
 Agostini S. 349
 Agresti J. 329
 Agrosi G. 285, 286,
 374
 Ague J.J. 77
 Agosto M. 364, 416
 Aibibula N. 159
 Aiello R. 395
 Aienzo I. 175
 Aiuppa A. 59, 187,
 189
 Albrizio P. 341
 Algeri G. 396
 Aliatis I. 375
 Allocca C. 196
 Alvarez de Buergo M. 326
 Alvaro M. 93, 137,
 143, 216,
 249, 262,
 381, 389
 Aly N. 326
 Andreozzi G.B. 230
 Andriani G. 341
 Andronico D. 173, 213
 Angel R.J. 93, 137,
 143, 216
 Angelini I. 333
 Angelone M. 308
 Antonelli A. 210
 Antonelli S. 349
 Antonielli B. 436
 Arca A. 73
 Arcudi A. 330, 331
 Ardau C. 286, 299
 Ardit M. 217, 265
 Aretusini S. 146
 Arfé G. 395
 Argentino C. 457
 Arletti R. 241, 276
 Armadillo E. 105
 Armienti P. 37
 Armiento G. 289, 308
 Arseneau V. 395
 Artioli G. 324, 333
 Arzilli F. 159
 Aspinall W.P. 195
 Atzei D. 219
 Atzori R. 286, 303
 Aulbach S. 87
 Aulinas M. 48
 Avanzinelli R. 79, 83,
 167
 Avino R. 365, 366

B

Bagnato E. 365, 421
 Baker D.R. 60
 Bakker R.J. 253
 Balassone G. 218, 227,
 325
 Baldassini N. 446
 Baldoni E. 198
 Balestro G. 13, 33
 Balic-Zunic T. 233, 260
 Baliva A. 349, 385
 Ballirano P. 219
 Balsamo F. 451
 Baracchini E. 430
 Barale L. 116
 Baratella D. 316
 Barberi F. 370
 Barberini V. 160
 Barbieri M. 310, 311
 Barbieri R. 57
 Barca D. 166, 326,
 354
 Barchitta M. 288
 Bardeglinu I. 162
 Bardi U. 287
 Barfucci G. 461
 Barone G. 266, 288
 Barra M. 421
 Barreca G. 437
 Bartoli O. 14
 Barucca S. 220
 Basch V. 38
 Battaglia A. 187, 189
 Baumann V. 191
 Baxter P.J. 195
 Beccaluva L. 51
 Beccaris G. 304
 Beddini G. 361
 Behrens H. 138, 172,
 184
 Belfiore C.M. 327, 328,
 354
 Bellatreccia F. 218, 220,
 221, 222,
 232, 246,
 247, 252,
 289
 Bellis D. 293
 Bellizzi F. 352
 Bello M. 462
 Bellomo S. 64, 320,
 424
 Bellon H. 36
 Belluso E. 292, 293,
 313, 321,
 473
 Belmonte D. 255
 Beltrando M. 15
 Belviso C. 267
 Benciolini L. 33
 Benisek A. 120, 125
 Benvenuti M. 94, 296,
 346, 406,
 425
 Bernardinetti S. 396
 Bernardini S. 222, 289
 Berno D. 39

Bersani D. 52, 230,
 375
 Bertagnini A. 181, 191,
 195, 209
 Bertok C. 116
 Bertrand H. 42
 Beutel M.W. 425
 Bevilacqua A. 195
 Bezzerra F.H.R. 451
 Biagioni C. 223, 224,
 225, 259,
 298, 302,
 463
 Bianchi F. 434
 Bianchi G. 329
 Bianchi S. 136
 Bianchini G. 51, 80,
 86, 87, 91
 Bianucci G. 438
 Biasin A. 280
 Biass S. 191
 Biddau R. 290
 Bignardi S. 448
 Billi A. 157
 Bindi L. 223, 226,
 239, 240,
 253
 Bini R. 260
 Bisson M. 195
 Bistacchi A. 16, 17
 Bitetto M. 187, 189
 Blasi P. 283
 Blasioli S. 277
 Blichert-Toft J. 42
 Bloise A. 336
 Blundy J.D. 95, 144,
 202
 Bockisch C. 372
 Bodnar R.J. 5
 Boffa Ballaran T. 256
 Boiocchi M. 245, 252
 Bolognesi F. 17
 Bonaccorsi E. 463
 Bonadiman C. 70, 129,
 259
 Bonadonna C. 6, 191
 Bonaiuto E. 316
 Bonatti E. 47
 Bonazza A. 331
 Bonazzi P. 226, 239,
 240
 Boni M. 227, 395,
 397, 409,
 412, 415
 Boni P. 227
 Boniello A. 464
 Bonini M. 436, 447
 Bonzi L. 362
 Boreham S. 203
 Borghi A. 13, 342,
 348, 353
 Borghini A. 81
 Borghini G. 40, 41, 43
 Borrini D. 133
 Boschi C. 384
 Bosio G. 438
 Bosworth W. 47
 Botteghi S. 398, 414,
 417

Bottini C.	58, 66, 67	Capaccioni F.	376, 379	Cerri G.	271
Bouchet Bert Manoz R.	42	Caparelli S.	474	Cesare B.	14, 228
Boumehti M.A.	261	Capasso G.	367	Cestelli Guidi M.	221, 246, 247, 257
Braga R.	23, 87	Capecchiacci F.	291, 320, 322, 363, 399, 422, 423, 424, 432, 433	Chalal Y.	85
Bramanti E.	312			Chateigner D.	160
Branca S.	188	Capella S.	292, 293, 313, 473	Chiarantini L.	133, 296, 346, 406, 413, 425
Brancato A.	188, 459			Chiariotti L.	439
Brancucci M.	305	Capello M.	294	Chiocci F.L.	86
Brandmayr E.	102	Capilleri P.	266	Chiodini G.	61, 365, 366, 416
Brardinoni F.	467	Capitani G.C.	243	Christofides G.	96
Braschi E.	94, 163, 166, 167, 168, 180, 204	Capitelli F.	221, 315	Chu X.	77
Braschi I.	277	Capizzi L.S.	122	Cianfarra P.	440
Bresciani I.	439	Caponi C.	364	Ciarcia S.	199
Brilli M.	353	Caporali S.	377, 378, 388	Cibella F.	295
Brizi E.	260			Cicala L.	325
Broggini R.	210	Cappelletti P.	271, 274, 275, 344, 355	Cicconi M.R.	138
Broggi A.	413			Cidu R.	290, 299, 301, 303, 306, 314
Bronco S.	300	Capponi G.	20, 24, 90, 105, 440	Cimarelli C.	173
Brooker R.A.	202			Cimolino A.	401
Brundu A.	271	Caputo R.	448	Cinà A.	396
Bruno P.P.	193	Carapezza M.L.	370	Cinotti S.	234
Bruno P.P.G.	467	Carbone C.	294, 297, 316	Cinque G.	246
Brusca L.	424			Cinti D.	433
Buccianti A.	428	Carbone S.	459	Cioni R.	162, 181, 191, 195, 209, 213
Bugatti G.	180	Cardellini C.	61, 365, 366, 421	Cipriani A.	47
Burrato P.	442	Cardinale M.	349, 385	Ciriotti M.E.	239
Buscaroli E.	277	Carlà F.	234	Cirriuncione R.	134, 147, 149, 150, 156, 465
Busso M.M.	393	Carli C.	379		
Bustos D.	126	Carmignani L.	18	Clarke A.P.	103
Butini F.	220	Carminati E.	157, 445	Clausi M.	268
Butt S.	152, 153	Carosi R.	19, 21, 108, 109, 113, 155	Cnudde V.	281
C				Cocetta F.	104
Cabassi J.	291, 320, 322, 422, 423, 424, 426, 432, 433, 434	Carpenter B.M.	148, 149, 151	Colantuono L.	349
Čabilovski R.	308	Carras N.	27	Coleman M.	126
Cai Y.	47	Carroll M.	404, 462	Coletti C.	269
Caiozzi F.	417	Carroll M.R.	123, 408	Colica A.	296
Calabrese S.	59, 65, 320, 422, 423, 424, 426, 432	Cas R.A.F.	177, 178	Collareta A.	380, 438
Calabrò C.	328	Casalini M.	79, 83, 204	Collettini C.	148, 151, 158
Caldeira R.	261	Casanova Municchia A.	220, 222	Colò L.	196
Calestani G.	273	Casellato C.E.	62, 63	Colomban P.	339
Caliro S.	61, 365, 366, 416	Caselli A.	364, 416	Colombi F.	85
Callegaro S.	42, 60	Cashman K.	171	Colonna T.	396
Caltabiano T.	466	Castaldini D.	362	Coltelli M.	187, 188, 189
Camarda M.	367, 368	Castaldo R.	414, 444	Coltorti M.	70, 170, 259, 362
Cambeses A.	32	Castelli D.	84, 88, 107	Colucci F.	400
Cambi F.	346	Casula M.	73	Comite V.	330, 331
Cametti G.	219	Catanzariti R.	27, 443, 449	Comodi P.	244, 259, 260, 283
Campagnola S.	164, 181	Cattelan R.	429	Compagnoni R.	13, 88, 343
Campione M.	121	Cavalazzi B.	57	Consani S.	294, 297
Cannaò E.	82	Cavalcante F.	267	Conte A.M.	86, 353
Cannata A.	187, 189	Cavallo A.	157, 175, 184, 232, 289	Conti P.	18
Cannatelli C.	182			Conti S.	457
Cantalamesa G.	438	Cavazzini G.	42, 124	Conticelli S.	79, 83, 204, 240
Cantisani E.	351	Censi P.	295	Contin M.	431
Capacci F.	300	Cerchiari A.	154		
Capaccioni B.	362	Cerminara M.	195		
		Cerniglia M.R.	350		

Coppola D.	196	De Benedetti A.A.	185	Dini A.	298, 418
Cordier C.	383	De Bonis A.	325, 334, 344, 345	Dinolfo G.	159
Corrado S.	178	De Campos C.	176	Dioguardi F.	190, 192
Correggia C.	274, 446	De Cassan M.	308	Dobbs M.	17
Correia C.T.	44	De Francesco A.M.	335	Dobrev N.	454
Corretti A.	346	de Gennaro B.	271	Dogliani C.	8, 445
Corti G.	207, 454	de Gennaro R.	274, 275	Domeneghetti M.C.	93, 137, 143, 216, 249, 262, 381, 389
Cosenza P.	370	De Giudici G.	306, 307, 314	Donato A.	414, 417
Cossio R.	13, 342	De Grisogono F.	231	Donato P.	166
Costa A.	206	De Kock T.	281	Dondi M.	265, 274, 275
Costa E.	348	De La Pierre M.	255	Dongarrà G.	317, 319
Costa S.	52	De Luca R.	336	Donnini M.	365
Costagliola P.	288, 296, 346, 406, 425	De Matteo A.	444	Dore E.	301
Costanzo M.R.	110	De Michieli Vitturi M.	195	D’Oriano C.	165
Cotecchia F.	285	De Min A.	60, 261	Doronzio D.M.	192
Covelli S.	427, 429, 430, 431	De Moor M.	371	Dotelli G.	237
Creminini C.	219	De Novellis V.	414	Doveri M.	410
Cremonese G.	386, 391	De Paola N.	148	Druitt T.H.	167
Cremonini S.	362	De Rosa F.	325	Duarte E.	371
Crisci G.M.	336, 354, 356	De Rosa R.	166	Duce P.	73
Crispini L.	20, 24, 38, 90, 105, 304, 440	De Siena A.	338	Durant A.	203
Cristiani C.	237	De Toffoli B.	391		
Crosera M.	429, 430	de Vita S.	194, 208	E	
Crovato C.	308	De Vito C.	353	Ebinger C.	452
Cruciani G.	217, 265	De Vittor C.	431	El Omari K.	179
Crupi V.	332	De Vivo B.	182	Elia D.	84
Cucciniello C.	344	Deering C.	363	Elissondo M.	191
Cuffaro M.	441	Del Bello E.	173	Ellero A.	443
Cultrera F.	442	Del Vecchio A.	257	Elliott T.	79, 83
Cultrone G.	269	Del Ventisette C.	398	Emili A.	429, 430
Cutroneo L.	294	Della Vedova B.	401	Engwell S.	195
		Della Ventura G.	218, 220, 221, 222, 232, 246, 247, 252, 289	Eramo G.	337, 338
D		Delle Donne D.	187, 189, 196, 461	Erba E.	58, 62, 63, 66, 67
D’Alessandro W.	59, 64, 65, 69, 423, 424, 426	Delleani F.	117	Ermice A.	211
D’Alessio D.	52, 229	Dellino P.	192, 200, 212	Ertl-Ingrisch W.	176
D’Amore M.	274, 275	Delmonte D.	273	Esbrì J.M.	427
D’Angelo M.	334	Depalo M.R.	341	Esposito E.	182
d’Atri A.	116	Derluyn H.	281	Esposito R.	355
D’Auria L.	444	Di Benedetto F.	234, 239, 266, 300	Esposti Ongaro T.	195
D’Ippolito V.	230	Di Celma C.	438	Eyjólfsdóttir E.I.	399
D’Orazio L.	325	Di Fazio L.	357		
D’Orazio M.	298, 302, 312, 380, 463	Di Giuseppe D.	362	F	
Da Mommio A.	135	Di Martino R.M.R.	367, 368	Faccenda M.	113
Da Pelo S.	299, 303	Di Michele A.	283	Facchinetti L.	84
Da Prato S.	443	Di Prima M.	249, 262	Facchinetti M.	347
Dachs E.	120, 125	Di Roberto A.	181, 195, 209	Fadda S.	402
Dal Piaz G.V.	15, 16	Di Rocco T.	384	Faganeli J.	431
Dal Sasso G.	333	Di Salvo S.	166, 167, 181	Falcone E.E.	295
D’Aleo R.	187, 189	Di Stefano A.	446	Falcucci E.	456
d’Alessandro N.	278	Di Toro G.	146	Fanetti S.	260
Dallai L.	45	Di Traglia F.	201, 202	Fantauzzi M.	219
D’Antonio M.	48, 175	Di Vincenzo G.	28	Fantozzi I.	168
Danyushevsky L.	182	Di Vito M.	194	Faoro S.	210
Daskalopoulou K.	65, 424, 426	Diella V.	129, 270	Farina M.	271
Davies J.	42	Dietrich M.	184	Faucher G.	67
		Dinelli E.	294, 297, 316	Fazio E.	149, 156
		Dingwell D.B.	176	Fecteau K.	372
				Fedele L.	175
				Federico L.	24, 90, 440
				Fedi M.	403, 412
				Felici R.	234

Fentrees S.	363	Gallo S.	338	Giuliani R.	337
Ferlito C.	70, 72, 170	Gallo Stampino P.	237	Giustetto R.	343
Fernandez E.	371	Gamberi F.	470	Godard G.	25, 28, 100
Ferraccioli F.	105	Garavelli A.	233, 341, 352	Godard M.	38
Ferrando C.	38	Garcia-Ordiales E.	427	Gola G.	410, 414, 417
Ferrando S.	81, 84, 88, 106	Gariboldi K.	438	Gomez-Heras M.	326
Ferranti L.	442, 450	Garofalo P.S.	20	Gonzalez R.	191
Ferrari S.	381	Garozzo I.	169	González-García D.	172
Ferrari V.	362	Garuti G.	253	Goodrich C.A.	382
Ferraro L.	446	Garzonio C.A.	357	Gori C.	273
Festa A.	33	Gasparini E.	282	Gosso G.	117, 160
Festa G.	193	Gasperini D.	37	Gottardi I.	210
Fiannacca P.	147, 150, 156, 465	Gatta G.D.	130, 241, 271, 276, 375	Gottsmann J.H.	95
Fichera G.V.	327, 328	Gatti E.	126, 203	Gouffon Y.	16
Ficocelli S.	318	Gattiglio M.	13	Gould I.R.	372
Fiebig J.	364, 369	Gattuso A.	370	Gozzi C.	428
Fioretti A.M.	236, 359, 382, 389	Gazzano E.	300	Granieri D.	466
Fioretti E.	292	Geiger C.A.	125	Granitzio F.	405
Fiori M.	402	Gelli I.	433	Grassa F.	426
Fischer J.	258	Gemelli M.	380, 384,	Graziano S.F.	274, 275
Fischer T.	371	Gemmi M.	258	Grazzi F.	377
Folco L.	378, 380, 383	Genco R.,	196	Green E.C.R.	144
Fontana D.	457	Genito B.	334	Grifa C.	344, 345
Fontana E.	160	Genovese C.	266	Grillenzoni C.	457
Foresi L.M.	446	Gentili S.	259, 283	Grillo B.	261
Foresta Martin L.	370	Geraki K.	60	Grita S.	221
Fornacelli C.	339	Gerdes A.	116	Groppelli G.	210
Fornaciai G.	300	Germinario C.	344, 357	Grosso C.	26, 30, 81, 84, 88, 107, 114
Fornasaro S.	304	Germinario L.	342	Gualtieri A.F.	146
Forni F.	198, 291, 322	Gerya T.	24	Guandalini R.	400
Förster B.	87	Geshi N.	169	Guarino V.	325, 334, 345
Fort R.	326, 340	Ghiara M.R.	218, 315	Guaschino L.	271
Francalanci L.	163, 166, 167, 168, 181	Ghiglieri G.	299	Guastoni A.	236
Franceschini F.	302	Ghignone S.	13	Guernouche M.	396
Francescon F.	270	Ghigo D.	300	Guerra A.	234
Francofonte V.	370	Ghizzardi V.	272	Guido A.	335
Francomme J.E.	43	Giaccherini A.	234	Guidoni F.	260
Franzetti A.	69	Giacomini L.	386	Guillot-Deudon C.	224
Fratini F.	351, 358	Giacomoni P.P.	70, 170	Gulbay A.H.	64
Frau F.	286, 299, 301, 303	Gianelli G.	417	Gundlach-Graham A.	20
Freda C.	247	Gianfagna A.	251	Gunter D.	353
Fregola R.A.	413	Giannechini R.	302, 312	Günther D.	20
Freire-Lista D.M.	340	Giannini L.	291, 322, 432	Gurrieri S.	368
Frezzotti M.L.	88, 106	Gibbard P.L.	203	Gutierrez G.	466
Friego C.	68	Gigliotti V.	336		
Froncini F.	61, 361, 365	Gilioli E.	273	H	
Frost D.J.	256	Gilotti J.A.	89	Hagos M.	207
Fubini B.	300	Gimeno D.	278	Hålenius U.	261, 273
Fumagalli P.	40, 43, 122, 258, 271	Gioncada A.	166, 201, 438	Hamada M.	55
Fusari A.	404	Giorcelli M.	321	Hanchar J.M.	357
Fusillo R.	201, 202	Giordani M.	235	Hanfland M.	130, 244
G		Giordano G.	164, 169, 171, 177, 178, 185	Harlov D.	127
Gaboardi M.	229	Giorgetti C.	148, 151	Harries D.	473
Gaggero L.	281	Giovanardi T.	44, 45, 46, 118	Harris J.W.	137
Gagliano A.L.	69	Girardi V.A.V.	44	Harroud A.	396
		Gisbert Aguilar J.	281	Hassan B.	152, 153
		Giua R.	318	Hawthorne F.C.	245, 252
		Giudice G.	466	Hawthorne F.C.	
		Giuffrida A.	266	Hegedús E.	111
		Giuffrida G.	466	Heinrich C.	14
		Giuli G.	138, 231	Helbert J.	381, 392
				Hermann J.	75

Hernandez-Moreno C.	453	Landi P.	165	Malatesta C.	24, 31, 90
Herrero J.C.	191	Landini W.	438	Malinverno E.	438
Higueras P.	427, 429, 430, 434	Lane S.	444	Manatschal G.	15
Higueras P.L.		Langella A.	274, 275, 344, 345	Manca R.P.	346
Holtz F.	184	Langenhorst F.	473	Mancini L.	159, 160
Hurich C.	152, 153	Langone A.	21, 45, 46, 108, 109, 118, 318	Mancini S.	18
I				Mandara R.	110
Iaccarino S.	19, 21, 22, 108, 109, 155	Lattanzi P.	296, 307, 314, 406, 425	Manga M.	185
Iannicelli-Zubiani E.M.	237			Mangiacapra A.	366
Iannuzzi E.	199	Latte V.	295	Maniscalco R.	328, 453, 472
Idris Ali A.B.	261	Laurenzi M.A.	94, 204	Manning C.	127
Iezzi G.	184	Lausi A.	130	Manojlovic M.	308
Ildefonse B.	38	Le Guer Y.	179	Mantovani A.	448
Innocenti M.	234, 300	Lenaz D.	238, 261, 429, 430	Mantovani L.	52, 272, 273, 347, 375
Invernizzi C.	404	Leonardsen E.	233	Manuella F.C.	459
Ioli P.	251	Lepore G.O.	226, 239, 240	Manzari P.	374
Iovine R.	175			Manzella A.	410, 414, 417
Isaia R.	181, 192, 195, 199, 209, 214	Leszczynska K.	203	Maraio S.	193, 467
Italiano F.	64	Lettino A.	267	Marcelli A.	246, 247
Izzo F.	344	Lezzerini M.	155	Marcenò C.	295
J		Liccioli C.	364, 416	Marchese L.	277
Jacobs J.	183	Liegler A.	363	Marchetti E.	196
Jakobsson S.P.	233	Liermann H.-P.	241	Marchi A.	449
James M.R.	444	Ligi M.	47, 441, 451	Marchionni S.	291, 322
Jeans C.	203			Marciano C.	143
Jorda L.	386	Lima A.	182	Marengo A.	348, 468
Jourdan F.	42	Liotta D.	413	Marescotti P.	304, 305
Jowitt S.M.	177	Lirer F.	446	Mari N.	174
K		Lisco S.	285	Marin V.	305
Kaneva E.	242	Liuzzo M.	466	Marinangeli L.	349, 385
Keir D.	452	Llovet X.	248	Marino D.A.M.	335
Kern H.	156	Lo Pò D.	23	Marinoni N.	270
Kimball B.	314	Loglio F.	378	Maritan L.	269, 333, 342,357
Klemme S.	263	Lombardo R.	150, 465	Marone F.	137
Knipping J.		Longobardi F.	341	Marotta A.M.	117
Kolar S.	111	Lopez-Berdonces M.A.	427	Marotta E.	208
Koroneos A.	96	Lorance E.D.	372	Marquardt H.	256
Kovács A.C.	111	Loredo J.	427	Marsico A.	341
Kristiansson P.	261	Lorenzoni V.	18	Martelli M.	91
Kroll H.	120	Lorrai M.	290	Martí Molist J.	210
Ksienzyk A.	183	Lotti P.	241, 276	Martin L.A.J.	77
Kurnosov A.	256	Lottici P.P.	52, 139,230, 375	Martin S.	25, 34, 100
Kyriakopoulos K.	65			Martín-Algarra A.	32
L		Lowry S.	386	Martinez M.	363, 371
La Manna M.	403	Lucchetti G.	294, 297, 304, 305	Martire L.	116
La Russa M.F.	330, 354			Martorelli E.	86
La Salvia V.	349	Lucchi F.	198, 205	Martucci A.	217, 277
La Spina A.	466	Luciani N.	36	Marzari F.	386
Lacalamita M.	237, 242, 250, 285	Lucidi R.	92	Marzoli A.	42, 60, 261
Lacanna G.	196, 461	Luguet A.	49	Masetti G.	443
Laeger K.	173	Lustrino M.	36, 85	Masini E.	15
Laganara C.	341	M		Massa B.	444
Laiolo M.	196	Maestrelli D.	447	Massa G.	18
Lamacchia A.	352	Magi F.	407	Massa S.	334
Lambert O.	438	Magnani G.	229	Massaniso P.	308
Lambruschi E.	375	Magro M.	316	Massaro S.	198, 206
		Maimaiti M.	408	Massimino M.R.	266
		Mair P.	71, 127	Massironi M.	16, 381, 386, 387, 391
		Majolino D.	332		
		Malagodi M.	328	Massonne H.-J.	21, 23, 108
		Malaspina N.	100, 128		

Mastandrea A.	335	Mollo S.	148, 170,	Navas-Parejo P.	32
Mastrolia A.	370		184	Nazzareni S.	244, 260
Mastronuzzi G.	285	Monaco C.	437, 442	Nazzaro I.	193
Mata J.	261	Mondillo N.	227, 395,	Neri A.	195, 283
Mathur R.	409		409, 412	Neri A.	
Matova M.	454	Monegato G.	456	Nestola F.	25, 93,
Mattash M.A.	53	Monetti V.	344		137, 143,
Mattassi G.	420	Monno A.	341		216, 249,
Mattioli M.	92, 235	Monopoli B.	16		262, 315,
Mattiuz A.	382	Montserrat O.	436		357, 381
Maturilli A.	381	Montalvo F.	466	Nestola Y.	451
Matzuzzi C.	402	Montana G.	279, 350	Neupane P.K.	114
Maugeri A.	288	Montanari D.	27, 398,	Niccolini M.	424
Mauro D.	225		410, 417	Nicotra E.	166
Mazzarini F.	195	Montanini A.	49, 50	Nigro A.	310, 311
Mazzeo F.C.	48, 175	Montegrossi G.	234, 300	Nilsson C.	261
Mazzoleni P.	266, 288	Montepara A.	272	Nimis P.	34, 93,
Mazzoli C.	269, 342,	Montereali M.R.	219, 308		137, 411
	357	Montomoli C.	19, 21,		
Mazzone F.	181, 209		22, 108,	Nirta G.	27
Mazzucchelli M.	44, 45,		109, 113,	Nisi B.	422, 432,
	46, 118,		155		434
	216	Moraiti E.	27	Nogueira F.C.	451
Mazzucchelli M.L.	93, 137,	Moratti G.	27, 94,	Nola P.	318
	143, 262		454	Novembre D.	278
McCammon C.	249	Morelli D.	442	Nunziata C.	110
McClelland W.C.	89	Moretti H.C.	95		
Meccariello M.	450	Moretti M.	285	O	
Medas D.	306, 307,	Moretti S.	398	Oberti R.	232, 245,
	314	Morgavi D.	172, 176,		252
Meirano V.	84		194	Occhipinti R.	282
Mele D.	190, 192	Morishita T.	45, 54	Oggiano G.	405
Melián G.	370	Mormone A.	218	Omenetto P.	411
Melone N.	374	Moro D.	132, 141	Oppenheimer C.	203
Memmi I.	339	Morra V.	325, 334,	Orešković J.	111
Memmi Turbanti I.	329		344, 345,	Orlando A.	133, 346,
Meneghini C.	307		355		413
Mengel K.	147, 156	Mosca P.	26, 107,	Ort M.H.	208
Menichetti S.	428		114	Ortolano G.	134, 147,
Menozzi O.	349	Motta E.	266		149, 156,
Mercurio M.	271, 275,	Mugnaioli E.	158, 228,		327
	344		239, 243,	Osticioli I.	329
Merli M.	129, 130		339, 384,	Ottolini L.	55, 70,
Merlini M.	130, 241,	Mulas G.	396		218, 250,
	258, 276	Mundula F.	290, 299		259
Mesto E.	237, 242,	Muniz Miranda M.	213	Ottonello G.	255
	250, 285	Muntoni I.M.	300	Ouladdiaf B.	160
Meyzen C.M.	387	Munzi P.	338, 352		
Mezzadri F.	273	Mura F.	345	P	
Milani S.	143, 249,	Murri M.	251	Pace C.	278
	262	Musco M.E.	389	Pacella A.	219
Militello G.M.	150, 465	Mussetti G.	261	Pacini A.	329
Minissale A.	53, 72,	Mzini L.L.	207	Pack A.	380
	410, 417		277	Padrón-Navarta J.A.	75
Minissale S.	72			Pagli C.	452
Minopoli L.	366	N		Pagliantini L.	346
Minucci S.	396	Naitza S.	402, 405	Pajola M.	386
Miozzi F.	131	Naletto G.	386	Palatinus L.	258
Miriello D.	336			Palmeri R.	28
Misiti V.	173, 184,	Nancy L.Ross	11	Palmerini S.	390, 393
	257	Nania L.	155	Palmieri F.	448
Mitchell J.	329	Nannoni F.	309	Palmiotto P.	47
Mitolo D.	233	Napoli G.	159	Panarello M.	336
Mittempergher S.	146, 154	Nardi E.	219	Pandeli E.	407
Moderato M.	349	Natale C.	86	Pandolfi L.	449
Moëlo Y.	223, 224	Natali C.	51, 80, 87	Panza G.	102
Moggi Cecchi V.	379, 388	Natali C.		Panza G.F.	104
Mohn G.	15				
Moia F.	400				

Paoli G.	183	Pieraccioni F.	469	Rappuoli D.	422, 424,
Paolieri M.	296	Pieruccioni D.	18, 396		434
Papale P.	466	Piluso E.	385, 474	Rashed H.	470
Papeschi S.	22	Pimentel A.	165	Raykova R.	102
Papini M.	27	Pinarelli L.	53, 96	Rebay G.	29, 117
Pardi L.A.	300	Pinarelli L.		Recchia S.	76, 131,
Paredes J.	194	Pinto D.	233, 341,		140
Parello F.	59, 65,		352	Redi D.	182
	424, 426	Pipera K.	96	Regorda A.	117
Parello P.	69	Pistolesi M.	166, 181,	Reisberg L.	42
Paris E.	138, 231,		191, 195,	Remitti F.	154
	464		196, 201,	Remusat L.	14, 228
			209	Renna M.R.	46
Parisio L.	42	Plaisier J.	130	Renzulli A.	92
Pasero M.	225	Podda F.	286, 306,	Ricca M.	330, 331,
Pasquon M.	420		307, 314		354
Passaro S.	442	Poe B.T.	257	Riccardi M.P.	268, 282
Pastero L.	241	Poggi E.	304	Ricci A.	369
Pastore Z.	412	Poli M.E.	456	Ricci C.A.	28
Patanè D.	187, 189	Poli S.	14, 76,	Ricci M.	351
Pavese A.	129, 130,		97, 99,	Ricci M.A.	220
	270		100, 122,	Riccò M.	229
Pavoni E.	429, 430		131, 140,	Righini G.	436
Pazzaglia F.J.	467	Pollok K.	258	Riguzzi F.	445
Pecchioni E.	346, 351,	Pompilio L.	473	Rimondi L.	406
	358, 470	Pompilio M.	349, 385	Rimondi V.	133, 296,
Pecskay Z.	96	Pontiroli D.	181		413, 425
Pedrazzi G.	240, 250	Porcheddu A.	229	Rinaldi M.	296
Pellegrino A.	453	Poretti G.	299	Rinaldi R.	248
Pelorusso B.	70	Porreca M.	353	Ripepe M.	196, 461
Pelosato R.	237	Pozzi G.	178	Rispoli C.	355
Pelosi N.	446	Pozzobon R.	236	Rocchi S.	183, 418
Pennacchioni G.	236	Pratesi G.	387, 391	Roda M.	117
Pensa A.	177, 178		291, 322,	Rodeghero E.	217
Pepe F.	437, 442,		377, 378,	Rodríguez-Cañero R.	32
	450		379, 388	Rodríguez-Sedano L.A.	212
Pepe S.	414, 444	Prencipe M.	139, 392	Rolandi G.	211
Peresan A.	104	Preto N.	457	Rolandi R.	211
Perez-Monserrat E.M.	326	Preusker F.	386	Rolfo F.	26, 30,
Perinelli C.	86	Principe C.	210		107, 114
Perotti C.	439	Princivalle F.	261	Romanelli F.	102, 115
Perrone U.	343	Prinzi E.P.	199	Romanelli M.	300
Perrone V.	32	Proietti C.	188	Romano C.	164, 169,
Perugini D.	172, 173,	Proposito M.	289		181, 185
	176, 179,	Protano G.	136, 309	Romeo E.	272
	184, 194,	Proyer A.	88	Ronca S.	36, 47
	261	Pugnaloni A.	313, 473	Ros L.	261
Petranich E.	429, 430,	Punturo R.	147, 156	Rosenbaum G.	112
	431	Punturo R.		Rosi M.	201
Petrelli M.	172, 173,	Pusceddu C.	314	Rosiello A.	365
	179, 261			Rossetti P.	116
Petricca P.	445	Q		Rossi A.	219
Petrie M.B.	89	Quartieri S.	276	Rossi M.	315
Petriglieri J.R.	52	Quatrini P.	69	Rossi S.	309
Petrini R.	302, 312	Quattrocchi A.	288	Rovella N.	330, 331
Petrone C.M.	168, 180			Rovere M.	470
Petrosino P.	48	R		Rubatto D.	75
Petti C.	218	Raccuia S.A.	266	Ruberti D.	211
Pettke T.	76, 99	Radica F.	246, 247	Ruffolo S.	326, 328,
Pezzino A.	147, 149,	Rai S.K.	30		330, 331,
	156, 327,	Rampone E.	38, 40		332, 354,
	328, 332	Ramy El-Maarry M.	386	Ruggieri G.	356
		Ranaldi M.	370		133, 399,
Piana Agostinetti N.	112	Randazzo L.	279, 350	Russo A.	406, 413
Piana F.	116	Rapa G.	26, 107,	Russo B.	195
Piccardi L.	27, 454,		114	Russo C.	446
	455			Rustioni G.	136
Piccini L.	357				137, 143
Piccolo A.	113				
Picotti V.	467				
Piepoli L.	341				

S

Sabatino G.	472	Scuderi M.M.	148		423, 424,
Sacchi E.	318	Secchi F.	402, 405		426, 432,
Sacco V.	147	Secco L.	236		433, 434
Sachan H.K.	30	Senda R.	54	Tassinari C.C.G.	44
Sagnotti L.	446	Severi P.	362	Taylor Castillo W.	363
Saiano F.	295	Seyler M.	47	Tedeschi C.	268
Saiedi Anaraki F.	334	Shen T.	75	Tempesta G.	285, 374
Salerno G.	466	Shock E.L.	372	Tempesta G.	
Salleolini M.	136	Siano S.	329	Tempesti L.	416
Salmona P.	305	Siena F.	51	Tesei T.	148, 158
Salocchi A.	457	Silvestri A.	359	the OSIRIS team	386
Salvatori S.	333	Silvestri C.	330, 331	the VIRTIS Team	376
Salvini F.	440	Simioni E.	386	Tiano L.	313
Salvini R.	18	Simonetti A.	341	Tiepolo M.	46, 98,
Salvioli-Mariani E.	52	Sinigoì S.	44		318
Salviulo G.	280, 294,	Skert N.	420	Tiepolo T.	118
	297, 316	Skogby H.	261, 273	Tinelli C.	438
Sanchez-Navas A.	32	Skogby H.		Tiraboschi C.	76, 99,
Sandroni S.	28	Smeraglia L.	157		131, 140
Sanfilippo A.	39, 47,	Sodo A.	220, 222,	Tizzani P.	414, 444
	54, 55		289	Todde A.	195, 213
Sani F.	436, 447	Soldatos T.	96	Todesco M.	362
Sanna L.	73	Solimano M.	305	Toffolo L.	25, 34
Sansivero F.	194, 208	Sollecito F.	285	Tomatis M.	300
Santarato G.	448	Somma M.C.	349	Tommasini S.	83, 94,
Santello L.	357	Somma R.	32, 472		180, 291,
Santilano A.	414, 417	Sortino F.	370		322
Santinelli F.	283	Spalla M.I.	29, 117,	Tonarini S.	82
Santo A.P.	94, 346,		160	Tondi E.	159
	357	Speranza F.	453	Tonucci L.	278
Santoro L.	415	Sprovieri M.	421	Török A.	326
Santoro S.	349, 379	Stabile P.	138	Tramparulo F.D.A.	199, 214
Sappa G.	310, 311	Stalder R.	68	Tranne C.A.	198
Sardella A.	331	Stangarone C.	139, 392	Tribaudino M.	52, 139,
Sarocchi D.	212	Stelluti I.	251		229, 272,
Sartori M.	16	Storti F.	451		273, 347,
Savo A.	51	Strumendo M.	280		375, 392
Scaillet B.	162	Sturiale G.	453	Tribuzio R.	39, 49,
Scalera G.	458, 471	Sulpizio R.	192, 198,		50, 55
Scambelluri M.	74, 82		206, 212	Trippella O.	393
Scandolo L.	143, 249,	Šumanovac F.	111	Trippetta F.	148
	262, 389	Susta U.	232, 252	Tropper P.	71, 127
Scardino G.	285			Trotta M.	396
Scarlato P.	173	T		Trumpy E.	410, 414,
Scarpelli R.	335	Taddeucci J.	173		417
Scarrone F.	116	Tadini A.	195	Tufarolo E.	18, 396
Scarrow J.H.	32	Tagliaferro A.	321	Tumiati S.	25, 76,
Scarsi M.	31	Tagliavia M.	69		99, 100,
Schaltegger U.	42	Tajcmanova L.	14		122, 131,
Scherillo A.	377	Talamo P.	355		140
Schiavone S.	472	Talarico F.	28, 396	Turci F.	300
Schingarò E.	221, 237,	Tamberlich F.	420	Tusa G.	188
	242, 250,	Tamburello G.	187, 189,	U	
	285		421	Ulian G.	132, 141
Schmidt M.W.	228	Tamburo E.	317, 319	Ulivi M.	291, 322
Schmitz B.	238	Tangari A.C.	385	Ulivieri G.	196
Scholten F.	386	Tarantino S.C.	268, 282	Ulmer P.	76, 99
Schumacher J.	144	Tarchini L.	370	Urbina M.	438
Sciarra A.	362	Tardani D.	371	Urzi C.	330, 331
Sciascia L.	130	Tardugno M.L.	325	Usai D.	333, 357
Scicchitano M.R.	75, 474	Tartarotti P.	33, 160		
Scipioni M.	462	Tartarotti P.		V	
Scodellini R.	291, 322	Tassi F.	53, 291,	Vaccaro C.	362
Scordari F.	242, 250		320, 322,	Valade S.	196
Scotti E.	304		363, 364,	Valdrè G.	132, 141
Scribano V.	459		369, 371,		
Scrivano S.	281		372, 399,		
			416, 422,		

Valentine G.A.	195	Webb S.	138
Valenza M.	368	Wu F.-Y.	118
Valeria C.	326		
Vallefuoco M.	446	Y	
Valleri G.	27	Youbi N.	261
Van Acken D.	49	Yuce G.	64
van Wyk de Vries B.	207		
Vannucchi P.	103	Z	
Vannucci G.	454	Zaccarini F.	253
Vannucci R.	98	Zaffiro G.	143, 262
Varas-Muriel M.J.	326	Zambrano M.	159
Varrica D.	317, 319	Zanelli C.	274, 275,
Vaselli O.	53, 291,	Zanetti A.	39, 42,
	320, 322,		45, 46,
	363, 364,		48, 50,
	369, 371,		118, 239,
	399, 407,		353, 359
	416, 422,	Zanferrari A.	456
	423, 424,	Zanolin F.	370
	432, 433,	Zanon V.	165
	434, 470	Zanoni D.	29, 117
Vassallo P.	305	Zema M.	268, 282
Ventruti G.	221, 250	Zerboni A.	333
Ventura G.	184	Zeza A.	172
Venturi S.	291, 320,	Zibera L.	144, 263
	322, 372,	Zibra I.	50
	422, 423,	Zoleo A.	300
	432, 433	Zöll K.	71
Venuti V.	332	Zollo D.	344
Vetere F.	172, 184	Zoppi M.	291, 322
Vettori S.	351	Zorzi F.	280, 294,
Vetuschi Zuccolini M.	255		297, 381
Vezzalini G.	276	Zucali M.	117, 160
Vezzoni S.	298, 302,	Zucchi M.	413
	418	Zucchini A.	259, 283
Vianello F.	316		
Viccaro M.	166		
Vidojević D.	308		
Vigliaturo R.	313, 321,		
	468, 473		
Vigliotti M.	211		
Villa I.M.	438		
Vinciguerra S.	17, 103		
Visalli R.	134, 147,		
	149, 327		
Visonà D.	21, 108,		
	109, 113		
Vitale Brovarone A.	15, 77,		
	142		
Vitale S.	195, 199,		
	214		
Viti C.	148, 158,		
	228, 239,		
	243, 396		
Vitone C.	285		
Viveiros F.M.	369		
Vladykin N.	242		
Voloschina M.	181, 209		
Vona A.	164, 169,		
	185, 209		
Vougioukalakis G.	163, 168		
W			
Walle M.	14		
Wang H.	452		
Wanty R.	314		
Wasserburg G.J.	393		

RENDICONTI *Online*
della Società Geologica Italiana

Instructions for authors

The “Rendiconti Online della Società Geologica Italiana” are published in quarterly volumes. The size of each volume is 21 × 29,7 cm (A4) and the printed portion is 18,5 × 24,4 cm, in two columns of 9 × 24,4 cm.

All Authors may submit to the journal original scientific contributions, both in Italian and English, concerning all aspects of geosciences. The instructions described below should be strictly followed by the authors. The non-compliance with these instructions may delay or prevent publication. Text and figures accepted for publication are copyright of the journal.

Types of contributions published in the Rendiconti Online della Società Geologica Italiana

The Rendiconti Online host three types of contributions: “abstracts”, “short notes”, and “articles”.

Abstracts - These are very short contributions (up to 3000 characters, without figures or tables) submitted to national or international conferences. Abstracts will be included in supplements to ordinary volumes.

Short notes - These are short reports (up to 3-4 pages, plus three figures or tables and no more than 15 references). Short notes, if accepted following a peer-reviewing process, will be published faster than articles.

Articles - These are original research peer-reviewed papers. They should not exceed 15 printed pages, including references and figure captions. There are no limits for the number of figures, even if it should be in due proportion with the length of the text.

Manuscript formatting

Manuscripts must be submitted in digital format, using the ROL template.

The text may be in English or Italian. It is, however, recommended to adopt English language to enable and promote a wider dissemination of the articles. Title of the manuscript, abstract, key words and figure captions must be bilingual. Manuscripts written in English should have an extended abstract in Italian and viceversa.

The manuscript, including references and figure captions, must be double spaced.

Submit the text in the following order: Title, authors' names and addresses, telephone, fax and e-mail of the corresponding author. Below abstract/riassunto, key words/parole chiave, text, acknowledgements, references. Figures, captions and tables should be inserted using the format provided by the editorial office.

References and quotations in the text

References should be inserted in parentheses in the text in full for single- and dual-authored papers (e.g. Lyell & Bertrand, 1987), but using first author and “et al.” for multiple authored papers (e.g. Lyell et al., 1988). Authors should be written with uppercase initials. The order in the text should be chronological, then alphabetical. List all references cited in alphabetical order at the end of the article in the following standard form:

Journal article

Baker V.R. (2006) - Water and the evolutionary geological history of Mars. *Boll. Soc. Geol. It.*, 125, 357-369.

Article in volume

Martini I.P., Sagri M. & Colella A. (2001) - Neogene-Quaternary basins of the inner Apennines and Calabrian arc. In: Vai G.B. & Martini I.P. (eds.), *Anatomy of an Orogen: The Apennines and Adjacent Mediterranean Basins*. Kluwer Academic Publisher, 375-400.

Volume

Ramsay J.G. & Huber M. (1987) - *The techniques of Modern Structural geology*. Volume 2: *Folds and Fractures*. Academic Press, London, 500 pp.

Thesis

Ghinassi M. (2000) - Il passaggio tra la prima e la seconda fase fluvio-lacustre del bacino del Valdarno Superiore nei pressi di S. Giovanni Valdarno. Unpublished Master thesis, University of Florence, 110 pp.

Headings

Please use a maximum of three levels of headings, hierarchically arranged as outlined below.

FIRST ORDER HEADINGS

Capital letters, centered, bold.

The first sentence after the heading begins after a blank line.

SECOND ORDER HEADINGS

Capital letters, left margin.

The first sentence after the heading begins after a blank line.

Third order headings

Italic, left margin. The first sentence after the heading begins after a blank line.

Footnotes

Footnotes are not allowed.

Abbreviations

All abbreviations used in the text must be clearly explained the first time they appear.

Illustrations

The maximum available space for an illustration is 185×244 mm (full page) or 90×244 mm (column). Figures should be prepared with lettering and symbols of sufficient size and clarity to be reduced (Arial, 6-8 pt. minimum). After reduction the smallest lettering should be a minimum of 2 mm high. Figures should be provided as .tif or .jpg format (at least with a resolution of 500dpi). Tables can be submitted as .xls or .doc files. Figures in the text must be quoted as fig. or figs., plates as pl. and tables as tab. (tabs). It is the responsibility of the authors to ensure that permission is granted for reproduction of any copyright material (reproduced figures, tables, text passages) and that this permission is acknowledged in their articles.

Proofs

The corresponding author will receive a single copy of the proof in PDF format. PDF proofs can be annotated using Adobe Reader version 11. The proof must be sent after correction to the Editors within five days. Text or figure changes can be also listed in a .doc file.

Manuscript submission

Manuscripts must be sent to the Editorial Board of the “Rendiconti Online della Società Geologica Italiana”, to the following e-mail addresses: domcalca@unina.it and fabio.petti@socgeol.it.

RENDICONTI *Online* della Società Geologica Italiana

Volume 35, Supplemento n. 2 - Luglio 2015



Il Pianeta Dinamico

Congresso congiunto SIMP-SGI-So.Ge.I-AIV

Firenze, 2-4 settembre 2015

PRESIDENTI DEL CONGRESSO

Bernardo Cesare (SIMP) - Guido Giordano (AIV) - Carmelo Monaco (SGI) - Orlando Vaselli (SoGeI)

COMITATO SCIENTIFICO

Riccardo Avanzinelli (Firenze) - Paola Bonazzi (Firenze) - Piergiulio Cappelletti (Federico II, Napoli) - Rodolfo Carosi (Torino) - Bernardo Cesare (Padova) - Rosa Cidu (Cagliari) - Raffaello Cioni (Firenze) - Domenico Cosentino (Roma Tre) - Francesco Frondini (Perugia) - Francesco Princivalle (Trieste) - Orlando Vaselli (Firenze) - Marco Viccaro (Catania)

COMITATO ORGANIZZATORE e LOGISTICA

Maria Laura Balestrieri (IGG-CNR, Firenze) - Luca Bindi (UniFI) - Eleonora Braschi (IGG-CNR, Firenze) - Marco Bonini (IGG-CNR, Firenze) - Francesco Capecciacci (UniFI) - Bernardo Carmina (UniPI) - Sandro Conticelli (UniFI - IGG-CNR, Firenze) - Giacomo Corti (IGG-CNR, Firenze) - Francesco Di Benedetto (UniFI) - Lorenza Fascio (SIMP) - Lorella Francalanci (UniFI - IGG-CNR, Firenze) - Giovanna Moratti (IGG-CNR, Firenze) - Fabio Petti (SGI) - Marco Pistolesi (UniFI) - Giovanni Pratesi (UniFI) - Alba Patrizia Santo (UniFI) - Franco Tassi (UniFI) - Simone Tommasini (UniFI) - Orlando Vaselli (UniFI - IGG-CNR, Firenze) - Alessandro Zuccari (SGI)

PLATINUM SPONSORS



GOLD SPONSORS



SILVER SPONSORS



Editing a cura di: Carmina B., Fascio L., Petti F.M., Zuccari A.

main partner



RENDICONTI ONLINE DELLA SOCIETÀ GEOLOGICA ITALIANA

Direttore responsabile: DOMENICO CALCATERRA

Iscrizione ROC 18414.

Pubblicato online il 30 Luglio 2015.